





STATE OF CALIFORNIA
GOODWIN J. KNIGHT, Governor
DEPARTMENT OF NATURAL RESOURCES

DeWITT NELSON, Director

DIVISION OF MINES
FERRY BUILDING, SAN FRANCISCO 11
OLAF P. JENKINS, Chief

SAN FRANCISCO

BULLETIN 171

NOVEMBER 1955

EARTHQUAKES IN KERN COUNTY CALIFORNIA DURING 1952

(A symposium on the stratigraphy, structural geology, and origin of the earthquakes; their geologic effects; seismologic measurements, application of seismology to petroleum exploration; structural damage and design of earthquake-resistant structures.)

Prepared Under the Direction of
OLAF P. JENKINS
GORDON B. OAKESHOTT, Editor



Price \$4.00

UCD LIBRARY
UNIVERSITY OF CALIFORNIA
DAVIS

CONTRIBUTING AUTHORS

Hugo Benioff	G. A. Peers
Revoe C. Briggs	O. W. Perry
J. P. Buwalda	Dorothy H. Radbrueh
William K. Cloud	C. F. Richter
G. H. Davis	Pierre St. Amand
T. W. Dibblee, Jr.	J. Schlocker
Beno Gutenberg	Maurice Sklar
H. B. Hemborg	George I. Smith
Mason L. Hill	J. L. Soske
G. W. Housner	Karl V. Steinbrugge
Robert L. Johnston	Harold C. Troxell
Donald H. Kupfer	V. L. VanderHoof
Stewart Mitchell	Archer H. Warne
Donald F. Moran	Robert W. Webb
Samuel B. Morris	George N. White
Siegfried Muessig	C. A. Whitten
Frank Neumann	H. D. Wilson, Jr.
Gordon B. Oakeshott	G. F. Worts, Jr.

COOPERATING AGENCIES

American Society of Civil Engineers
California Division of Highways
California Division of Water Resources
California Institute of Technology
Department of Water and Power, City of Los Angeles
Intex Oil Company
Pacific Fire Rating Bureau
Pacific Gas and Electric Company
Richfield Oil Corporation
Southern Pacific Company
Stanford University
Union Oil Company
United States Coast and Geodetic Survey
United States Geological Survey
University of California at Santa Barbara
Western Gulf Oil Company

LETTER OF TRANSMITTAL

To THE HONORABLE GOODWIN J. KNIGHT
Governor of the State of California

DEAR SIR: I have the honor to transmit herewith Bulletin 171, *Earthquakes in Kern County California during 1952*, prepared under the direction of Olaf P. Jenkins, Chief of the Division of Mines. The Arvin-Tehachapi earthquake of July 21 and its aftershocks, second most destructive earthquake in California history, violently disrupted the ground surface and man-made structures, killed 14 people and did an estimated \$60,000,000 damage in the heart of California's second greatest mineral-producing county. The volume contains numerous maps showing geologic features, earthquake intensities, surface ground effects, and structural damage, a large number of photographs, and papers generously contributed by 36 authorities and 16 cooperating agencies.

Bulletin 171 is not only of great interest because of its thorough account of the most completely investigated earthquake in our country's history but because the detailed information it contains will be widely applied in the location and construction of engineering structures such as railroads, highways, dams, schools, buildings of all kinds, tanks, canals, and power installations, in exploration for petroleum, natural gas, and other mineral resources, and as basic information useful in establishing building codes and insurance rates.

Respectfully submitted,

DEWITT NELSON, Director
Department of Natural Resources

July 1, 1954



Sycamore Canyon, near Arvin, Kern County, just before the aftershock of July 25, 1952. *Photo by Robert C. Frampton.*



Dust rising in Sycamore Canyon during the aftershock of the noon hour, July 25, 1952. *Photo by Robert C. Frampton.*

CONTENTS

	Page
PART I—GEOLOGY	13
1. The Kern County earthquakes in California's geologic history, by Gordon B. Oakeshott	15
2. Geology of the southeastern margin of the San Joaquin Valley, California, by T. W. Dibblee, Jr.	23
3. Kern Canyon lineament, by Robert W. Webb	35
4. Nature of movements on active faults in southern California, by Mason L. Hill	37
5. Geological effects of the Arvin-Tehachapi earthquake, by J. P. Buwalda and Pierre St. Amand	41
6. Ground fracture patterns in the southern San Joaquin Valley resulting from the Arvin-Tehachapi earthquake, by Archer H. Warne	57
7. Arvin-Tehachapi earthquake damage along the Southern Pacific Railroad near Bealville, California, by Donald H. Kupfer, Siegfried Muessig, George I. Smith, and George N. White	67
8. Measurements of earth movements in California, by C. A. Whitten ..	75
9. Effect of Arvin-Tehachapi earthquake on spring and stream flow, by Revoc C. Briggs and Harold C. Troxell	81
10. Water-level fluctuations in wells, by G. H. Davis, G. F. Worts, Jr., and H. D. Wilson, Jr.	99
11. Seismic prospecting for petroleum and natural gas in the Great Valley of California, by J. L. Soske	107
12. Application of seismic methods to petroleum exploration in the San Joaquin Valley, by Maurice Sklar	119
 PART II—SEISMOLOGY	 129
1. General introduction to seismology, by H. Benioff and B. Gutenberg ..	131
2. The major earthquakes of California: a historical summary, by V. L. VanderHoof	137
3. Seismic history in the San Joaquin Valley, California, by C. F. Richter	143
4. Seismograph development in California, by H. Benioff ..	147
5. Seismograph stations in California, by B. Gutenberg	153
6. Epicenter and origin time of the main shock on July 21 and travel time of major phases, by B. Gutenberg	157
7. The first motion in longitudinal and transverse waves of the main shock and the direction of slip, by B. Gutenberg	165
8. Magnitude determination for larger Kern County shocks, 1952; effects of station azimuth and calculation methods, by B. Gutenberg	171
9. Foreshocks and aftershocks, by C. F. Richter	177
10. Mechanism and strain characteristics of the White Wolf fault as indicated by aftershock sequence, by H. Benioff	199
11. Relation of the White Wolf fault, to the regional tectonic pattern, by H. Benioff	203
12. Strong-motion records of the Kern County earthquakes, by Frank Neumann and William K. Cloud	205

CONTENTS—Continued

	Page
PART III—STRUCTURAL DAMAGE	211
1. Arvin-Tehachapi earthquake—structural damage as related to geology, by J. Schlocker and Dorothy H. Radbruch.....	213
2. Earthquake damage to oil fields and to the Paloma cycling plant in the San Joaquin Valley, by Robert L. Johnston.....	221
3. Highway damage resulting from the Kern County earthquakes, by O. W. Perry, with supplement, Bridge earthquake report, Arvin-Tehachapi earthquake, by Stewart Mitchell.....	227
4. Damage to water works systems, Arvin-Tehachapi earthquake, by H. B. Hemborg.....	235
5. Damage to electrical equipment caused by Arvin-Tehachapi earthquake, by G. A. Peers.....	237
6. Earthquake damage to railroads in Tehachapi Pass, by Southern Pacific Company.....	241
7. Earthquake damage to elevated water tanks, by Karl V. Steinbrugge and Donald F. Moran.....	249
8. Earthquake damage to California crops, by Karl V. Steinbrugge and Donald F. Moran.....	257
9. Structural damage to buildings, by Karl V. Steinbrugge and Donald F. Moran.....	259
10. The design of structures to resist earthquakes, by G. W. Housner.....	271

PLATES

Plate 1. Geologic map and sections of southern Sierra Nevada, Tehachapi, and San Joaquin Valley.....	In pocket
2. Map of the White Wolf fault zone.....	In pocket

References cited in Bulletin 171.....	279
Finding list of authors.....	283
Finding list of titles.....	283

PREFACE

The major Arvin-Tehachapi earthquake of July 21, 1952, and the series of related earthquakes and aftershocks that followed, are but the latest of a succession of earthquakes demonstrating the position of California in the seismically active belt of geologically young, developing mountain ranges and valleys that rims the Pacific Ocean. The Kern County earthquakes of 1952 accounted for the loss of 14 lives and damage of over \$60,000,000 in Kern and Los Angeles Counties.

Californians are becoming more earthquake-conscious, and rightly so, as California and Nevada have had over 90 percent of the earthquakes recorded in the United States and there is no evidence of any early decline in earthquake frequency in this area.

It behooves us, then, to be informed on earthquakes: their origin and geologic causes, their characteristics and behavior, where they are most likely to occur, their probable effects in disrupting the land surface and on engineering structures of all types, their effects on surface and subsurface water supply, the bearing of earthquakes and their causative faults on location of dams, canals, highways, and similar structures, and—through better understanding—how future losses in life and property can be reduced. The principal objective of Bulletin 171 is the presentation of information on all these things.

Probably no earthquake in history has received as intensive field study by as many scientifically trained people as the Arvin-Tehachapi earthquake and the related aftershocks. Epicenter of the earthquake was in the southern San Joaquin Valley, a great petroleum-producing area, where many geologists are based. Within a few hours hundreds of geologists from the oil companies, the United States Geological Survey, California Division of Mines, Division of Highways, Division of Water Resources, and the universities, were making observations of surface ground effects along the White Wolf fault, which was responsible for the earthquake. Just as quickly, field parties from the Seismological Laboratory of California Institute of Technology, Pasadena, were in the area setting up a group of portable seismographs, augmenting the records obtained at their permanent stations and obtaining unprecedented coverage of the aftershocks of a major earthquake. Engineering coverage was also complete, with hundred of engineers and builders assessing damage to buildings, highways, railroads, and other engineering structures, and directing repair and reconstruction.

In effect, the Division of Mines acted as a coordinating agency for compilation, editing, and publication of this series of papers dealing with the principal results of observations and data, from many sources, in three main categories: *Geology* (Part I), *Seismology* (Part II), and *Structural Damage* (Part III). Field work of the Division of Mines consisted in reconnaissance of the geology of the earthquake area and observations along the White Wolf fault zone. Through arrangement with the division, T. W. Dibblee, Jr., mapped the basic geology of over 1,000 square miles of the area as the basis for his paper on *Geology of the Southeastern Margin of the San Joaquin Valley* (Part I, Contribution 2). Drs. J. P.

Buwalda and Pierre St. Amand did several weeks of intensive detailed field mapping along the White Wolf fault zone gathering data for their map and paper on *Geological Effects of the Arvin-Tehachapi Earthquake*. Other papers in Part I comprise discussions of the geologic setting of the earthquakes (Part I, Contribution 1), fault patterns and characteristics (Part I, Contributions 3, 4, 6, 8), geologic effects along the railroad (Part I, Contribution 7), effects on water levels and flow (Part I, Contributions 9, 10), and the uses of seismic methods in petroleum exploration (Part I, Contributions 11, 12). Part II presents the results of the extensive seismological observations, computations and conclusions of the Seismological Laboratory, headed by Dr. Beno Gutenberg, and includes papers by H. Benioff, B. Gutenberg, and C. F. Richter. Other papers in Part II include a general introduction to the science of seismology (Part II, Contribution 1), earthquake history (Part II, Contributions 2, 3) and the results of strong-motion records obtained by the United States Coast and Geodetic Survey. K. V. Steinbrugge and Donald F. Moran, both structural engineers with the Pacific Fire Rating Bureau, contributed the results of their extensive study of building damage to Part III. That part opens with a paper calling attention to the relation of structural damage to geology and closes with a technical paper dealing with the design of structures to resist earthquakes; other papers in Part III summarize damage to specific types of structure and installation.

In enlisting contributions from the 16 different agencies, selecting the 36 authors, suggesting the subject matter for the 34 papers, field checking, compiling, and editing manuscripts to produce this bulletin, we have kept in mind the place of the Division of Mines as a public information bureau on matters directly related to the mineral resources and basic geology of the State. The earthquake is a geological phenomenon and the extensive, disruptive, and complex events that occurred during and following the Arvin-Tehachapi earthquake are effects of a geological cause—an abrupt displacement along the White Wolf fault at a depth of a few miles below the ground surface near Wheeler Ridge at 4:52 PDT on the morning of July 21, 1952. Mining and petroleum geologists know faults for their importance in localizing mineral deposits, for displacing such deposits after their formation, and recognize their extreme importance to mineral exploration. Hence, the series of papers in Part I (*Geology*) deals with faults, fault patterns, and fault history. Many of the major oil fields in the earthquake-affected area of Kern County are in structural traps with one or more faults playing a major role in forming the oil pool. Recognition of a fault system or pattern, then, may be of great importance in judging the location and characteristics of faults on the alluvium-covered valley floor and therefore the possible location of an oil field. Similarly, the principles of the science of seismology and results of study of the seismograph records discussed in Part II (*Seismology*) has great economic importance, particularly as applied to petroleum exploration (Part I, Contributions 11, 12) on the floor of the valley, and have been responsible for the discovery of major

oil fields. Part III (*Structural Damage*), an account of earthquake damage to buildings, oil fields, a refinery, highways, bridges, water works, electrical installations, the railroad, water tanks, and to agriculture, brings to the mind of the engineer the importance of a knowledge of the nature and behavior of the materials on which his structures are based—the soil and rocks. Those who find themselves responsible for the design of earthquake-resistant buildings, for setting up building codes, and for fixing insurance rates find that some knowledge of the geologic causes and measurement of earthquakes is neces-

sary. For all of these economically interested scientists and engineers, and also the many people of our State who have a great curiosity about earthquakes, this volume has been compiled.

GORDON B. OAKESHOTT
Supervising Mining Geologist
Division of Mines

Ferry Building
San Francisco
July 1, 1954

PART I—GEOLOGY

INTRODUCTION

PART ONE provides the geologic setting and background for understanding of the great succession of earthquakes that disturbed the southern San Joaquin Valley area for over a year, beginning with the Arvin-Tehachapi earthquake of July 21, 1952. It also discusses those effects of the earthquakes which might be considered primarily *geologic* and which required geological investigation in the field. Maps are provided showing rock formations, folds, and faults, covering an area of over 1000 square miles, and the geologic history of the region is discussed, from the earliest evidences hundreds of millions of years ago to development of the present landscape. The earth movements produced striking geologic effects, including ground ruptures in the White Wolf fault zone, landslides, rock falls, ground fractures

in the Valley floor, and interruption of ground water and stream flow. These effects are described and shown in numerous maps, diagrams, and photographs in this section, and results of quantitative measurements, where available, are included. The extensive, disrupting, and complex surface effects of the Kern County earthquakes are viewed in proper relationship to their geologic origins as traced through the vast periods of geologic history. The discussions of seismic prospecting call attention to the application of this modern method of locating subsurface geologic structures, so successfully combined with geologic interpretation in location of oil and gas fields on the floor of the Great Valley in the past 20 years.

CONTENTS

	Page
1. The Kern County earthquakes in California's geologic history, by Gordon B. Oakeshott	15
2. Geology of the southeastern margin of the San Joaquin Valley, California, by T. W. Dibblee, Jr.	23
3. Kern Canyon lineament, by Robert W. Webb	35
4. Nature of movements on active faults in southern California, by Mason L. Hill	37
5. Geological effects of the Arvin-Tehachapi earthquake, by J. P. Buwalda and Pierre St. Amand	41
6. Ground fracture patterns in the southern San Joaquin Valley resulting from the Arvin-Tehachapi earthquake, by Archer H. Warne	57
7. Arvin-Tehachapi earthquake damage along the Southern Pacific Railroad near Bealville, California, by Donald H. Kupfer, Siegfried Muessig, George I. Smith, and George N. White	67
8. Measurements of earth movements in California, by C. A. Whitten	75
9. Effect of Arvin-Tehachapi earthquake on spring and stream flow, by Revoe C. Briggs and Harold C. Troxell	81
10. Water-level fluctuations in wells, by G. H. Davis, G. F. Worts, Jr., and H. D. Wilson, Jr.	99
11. Seismic prospecting for petroleum and natural gas in the Great Valley of California, by J. L. Soske	107
12. Application of seismic methods to petroleum exploration in the San Joaquin Valley, by Maurice Sklar	119

PLATES

Plate 1. Geologic map and sections of southern Sierra Nevada, Tehachapi, and San Joaquin Valley	In pocket
2. Map of the White Wolf fault zone	In pocket

1. THE KERN COUNTY EARTHQUAKES IN CALIFORNIA'S GEOLOGIC HISTORY

BY GORDON B. OAKESHOTT •

The recent series of earthquakes in the southern San Joaquin Valley, initiated by the severe Arvin-Tehachapi earthquake of July 21, 1952 and followed by a succession of lesser aftershocks, is part of the continuing evidence of the position of California in a seismically active belt of geologically young, developing mountain ranges, valleys, and abrupt continental margins that rim the Pacific Ocean. No part of the surface of the earth is free from earthquakes but even the short period of seismograph records (about 50 years) has been long enough to show that certain areas on the earth's surface have many times more earthquakes than others. These areas of greatest earthquake frequency are the regions of high, actively building mountain ranges, steep continental slopes, and deep oceanic belts, one such belt rimming the entire Pacific Ocean and the other extending discontinuously from west to east through the West Indies, Mediterranean Sea, and Himalaya Mountains, and turning southeastward to join the Pacific belt in the East Indies. California and Nevada, located in the great circum-Pacific seismic belt, have had about 95 percent of the earthquakes in the United States.

FAULTS AND THE CAUSES OF EARTHQUAKES

Causes of Earthquakes. Since earthquakes are vibrations transmitted as waves in the materials of the earth, they may originate from a variety of causes, including landslides, explosive volcanic activity, movements of molten rock at depth, natural and artificial explosions, and abrupt movements of masses of rock along breaks in the outer part (crust) of the earth. Seismograph records show that there are deep-focus earthquakes originating at depths as great as 400 miles, shocks of intermediate origin at depths of 27 to 150 miles, and shallow earthquakes whose foci are at depths of less than 27 miles. All destructive earthquakes come within the last group and nearly all have been the result of sudden movements of blocks of the earth's crust along breaks called faults. Rock, which makes up the material of the earth, is elastic and is known to yield to stresses by slow creep over extended periods of time. Measurements across the great San Andreas fault in California, for example, show that the block on the east side of that fault is moving southward with respect to the west block at a rate of about 2 inches per year. When the elastic limit of the rock material is exceeded at any point or friction along an old fault surface is overcome, an abrupt movement—similar to the 21-foot horizontal displacement which took place along the San Andreas fault to cause the San Francisco earthquake of 1906—may take place. The fundamental causes of accumulation of such stresses are not thoroughly understood but they are known to occur at the unstable margins of continental platforms and ocean deeps. The number of variables involved, the lack of long-recorded data, and incomplete measurements of all observed phenomena mean that predictions of specific earthquakes in time and place are impossible.

• Supervising mining geologist, California Division of Mines.

Faults and Fault Types. Since nearly all destructive earthquakes result from movements along faults, the locations and characteristics of faults in an earthquake belt are of particular interest. This is especially true of active faults, that is, those that have either a historical record of earthquake foci along their courses or show evidence of geologically Recent (last few thousand years) movement. Any fault should be considered active which has displaced Recent alluvium and whose surface effects have not been modified to an appreciable extent by erosion.

Faulting takes place in all kinds of rock and displacement occurring at any one time may be anything from a fraction of an inch to several feet. Along the course of a major fault, repeated small displacements, with resulting earthquakes, may take place at irregular intervals over long periods of geologic time until the cumulative relative displacement may amount to many miles. In such situations the fault becomes a fault zone of shattered and broken rock that may be more than a mile in width, often with rock formations of widely different type, structure, and age brought into contact. The surface along which movement takes place may approach a plane but is usually highly irregular and marked by the development of slickensides, breccia (broken rock), and gouge (clay-like powdered rock). The fault surface may dip (incline) at any angle from the horizontal to vertical, but most faults approach the vertical. Relative displacement of the opposite blocks along the fault surface may be horizontal, vertical, or any combination of these. In some faults the character of displacement may change along the strike (direction) and may change in geological time. These characteristics may all differ along a major fault as it displaces rocks of varying type and structure.

OUTLINE OF THE GEOLOGIC HISTORY OF CALIFORNIA

Geologically, the long and complex history of California properly starts with the origin of the earth some 4 billion years ago and progresses through the geologic eras and periods, culminating in the development of the present-day landscape. Each division of geologic time is represented in some part of the state by rock units deposited or formed in that time. The generalized geologic map herewith shows the broad distribution of rock types. Intensive study and careful mapping of the rock formations by hundreds of geologists working in California, particularly in the past 50 years, has gradually brought some understanding of the salient features of the state's history. The last period of geologic time—the Quaternary—is so recent that features of the present landscape, in addition to the rock formations, reflect the events of that period.

Having developed the close relationship between earthquakes and faulting, it is apparent that the epochs of most active mountain building, when faulting, as well as folding and volcanism, are going on most intensively, are the times of greatest earthquake activity.

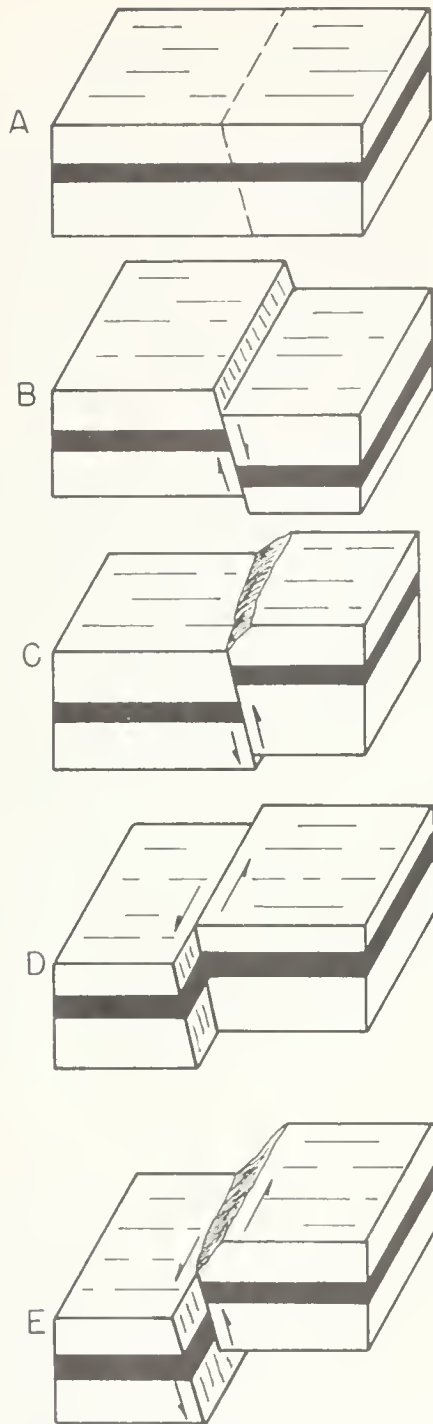


FIGURE 1. Fault types common in California; A, Incipient fault, before movement; B, Normal fault; fault surface dips toward down-dropped block; similar to Kern River fault; C, Reverse ("thrust" if inclination to horizontal less than 45°) fault; fault surface dips away from down-dropped block; similar to Pleito thrust fault; D, Horizontal, strike-slip fault; left lateral movement (block opposite observer has moved to left); similar to Garlock fault (San Andreas fault is horizontal, but with right lateral movement); E, Left lateral reverse fault (combination of movements of C and D); similar to White Wolf fault.

Consequently, in summarizing California's history by eras and periods, particular attention must be paid to the epochs of mountain-building (orogenic periods), including the last—that of the Quaternary period—in which we live.

Pre-Cambrian Eras. The events of pre-Cambrian time, covering about three-fourths of the record found in the rocks, are very little known in California. It is only in parts of the Basin-Ranges and Mojave Desert provinces in California that rocks of undoubted pre-Cambrian age are exposed. There the oldest pre-Cambrian rocks (Archean) are gneiss, marble, schist, and quartzite which are metamorphosed types developed during great mountain building at the close of Archean time. The areal extent of that orogenic period is unknown but it was certainly of world-wide importance. The overlying rock formations of the later pre-Cambrian (Algonkian) are little metamorphosed.

Paleozoic Era. Rock formations of possible Paleozoic age are widely distributed in the mountainous regions of California, but in only a few localities are they well dated. Marine Cambrian and Ordovician rocks are best exposed in southeastern California where they include sandstone, shale, limestone, and dolomite, indicating widespread seas. Rocks of Silurian age, also marine limestone, dolomite and shale, are exposed in southeastern California, in the northern Sierra Nevada, and in the Klamath Mountains.

Marine Carboniferous and Permian limestone, shale, dolomite, and conglomerate, with some interbedded volcanic rocks, are exposed in southeastern California, in the Klamath region, and in the western slopes of the Sierra Nevada. In the Mojave Desert, in the Coast Ranges, in the Peninsular Ranges, and in the Transverse Ranges are many remnants of more or less metamorphosed rock formations which may be Paleozoic in age; their dating as such has not been final.

In the Sierra Nevada it is probable that mountain building took place at the close of the Paleozoic era, as rock formations of the Upper Paleozoic Calaveras group were folded and faulted before the later Mesozoic formations were deposited. Less certain evidence of orogeny about this time in the Coast, Transverse, and Peninsular Ranges has been noted by geologists.

Mesozoic Era. Triassic and Jurassic marine sedimentary rocks, with abundant interbedded volcanic rocks, are widely distributed in California. The close of Jurassic time and, in some parts of the State, early Cretaceous time, was one of the most important periods of mountain building recognized. It is known as the Nevadan orogeny and is best dated in the northern Sierra Nevada. Comparable mountain building in the Coast Ranges region was probably less extensive, but there is evidence of widespread mountain building about that time throughout the Peninsular and Transverse Ranges and in the desert basins and ranges.

The long Cretaceous period was a time of extensive erosion in the Sierra Nevada, during which removal of a large cover of the older rock formations, which had been intruded by the Sierran granite, took place. The shoreline of the Cretaceous seas lay west of the newly elevated Sierra Nevada and in the Coast Ranges area

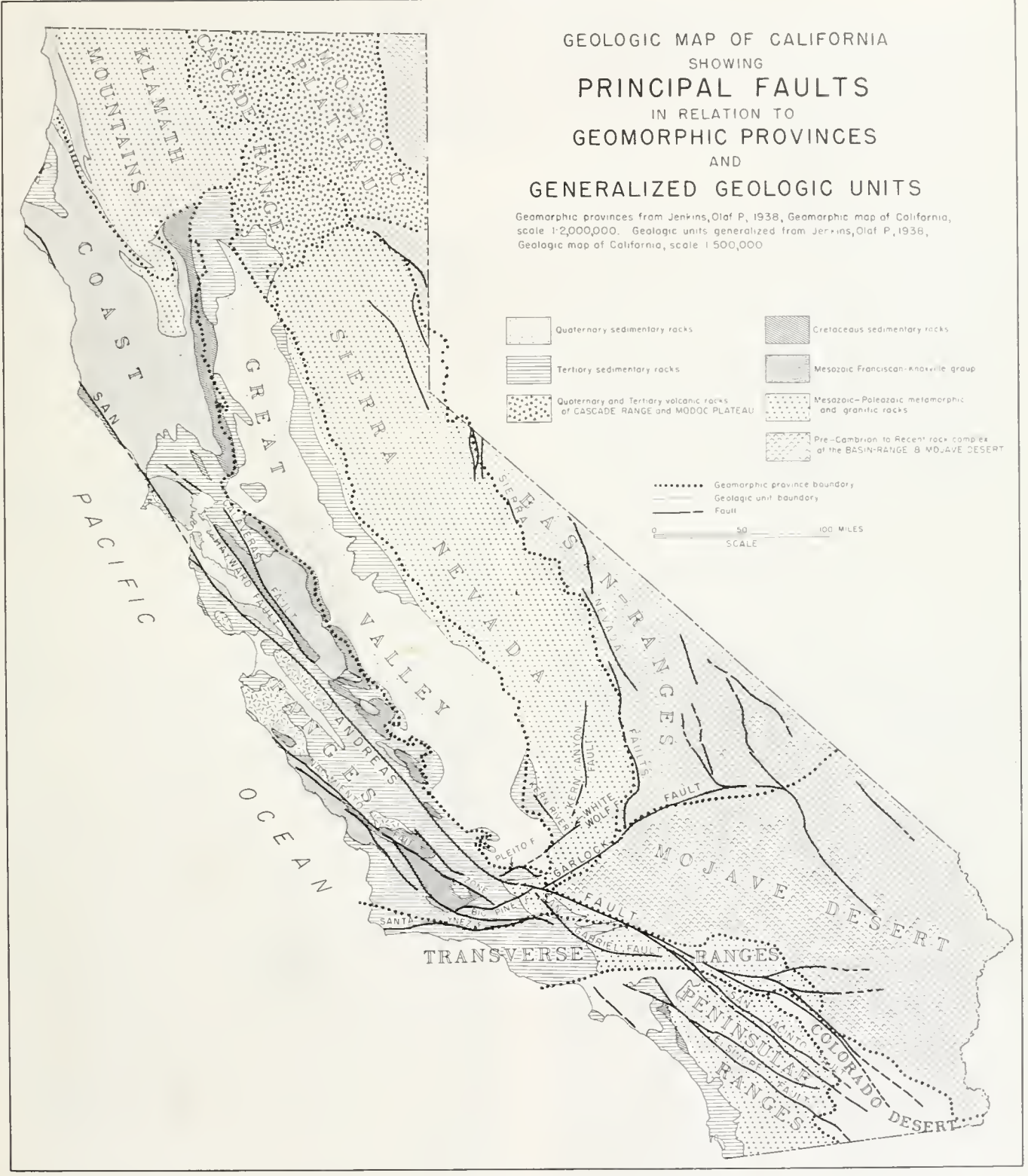


FIGURE 2

Geologic time scale and epochs of mountain building in California.

Era	Period	Epoch	Approximate age in millions of years	Mountain building
CENOZOIC	Quaternary	Recent	0—0.02	Local uplift and continued active faulting. Major epoch of folding, faulting, and uplift, particularly in the Coast Ranges, Transverse Ranges, and northern Peninsular Ranges. Principally elevation, tilting, and faulting in Sierra Nevada, Klamath Mountains, Basin Ranges, and Mojave. Crustal disturbances building Rocky Mountains may have extended into southeastern California. Great period of mountain building known as the Nevadan orogeny; folding, faulting and uplift to form Sierra Nevada, Klamath Mountains, Transverse Ranges, Peninsular Ranges, and many Desert and Basin Ranges. Milder mountain building in the Coast Ranges. Probable initiation of major fault zones.
		Pleistocene	0.02—1.	
	Tertiary	Pliocene	1—9	
		Miocene	9—28	
		Oligocene	28—38	
MESOZOIC	Cretaceous	Eocene	38—58	
		Paleocene	58—75	
	Jurassic	75—130		
	Triassic	130—155		
PALEOZOIC			155—185	
		Permian	185—210	
		Carboniferous	210—265	
		Devonian	265—320	
		Silurian	320—360	
		Ordovician	360—440	
PRE-CAMBRIAN			440—520	
			550—2100	

Origin of earth.

4000±

and over part of the Klamath Mountain province great quantities of mud, sand, and gravel were deposited. In southeastern California there is some evidence that the Laramide mountain-building period, during which the Rocky Mountains received their initial uplift in late Cretaceous and early Tertiary time, extended into California.

Tertiary Period. Rock formations of the Tertiary period in the Coast Ranges, western Great Valley, Transverse Ranges, western margin of the Peninsular Ranges, and the intervening basins indicate the Tertiary was a time of intermittent advances of seas from the west with local elevation and folding of different parts of this large area at irregular intervals. In general, the Eocene was the epoch of most widespread seas in the area, Paleocene and Miocene seas were more limited, and the Oligocene and Pliocene epochs were times of restricted seas. The Klamath Mountains, Sierra Nevada, Peninsular Ranges, and desert basins and ranges were land areas elevated at times in some places to considerable relief; they were the areas which, in general, furnished sediments to the Tertiary seas which lay to the west. The Miocene epoch was a time of intensive volcanic activity accompanying deposition of chert and shale in the Coast Ranges and western San Joaquin Valley provinces; volcanism also extended into the Coast Ranges and Transverse Ranges, in some places taking place below sea level. The Pliocene was a time of more or less restricted seas, with rapid accumulation of sediments deposited in localized basins and intermittent volcanic activity occurring widely throughout the State. The

Ventura and Los Angeles basins contain the thickest series of marine Pliocene sediments known in the world.

In late Pliocene time the crustal unrest began that culminated about middle Pleistocene with the great Coast Ranges-Transverse Ranges orogeny.

Quaternary Period. The Quaternary period, the last million years of geologic time, has been a time of great mountain building, including extensive folding, faulting and uplift, accompanied by intense local volcanic activity in certain parts of the State. This mountain building culminated about mid-Pleistocene time and is especially well-dated in the Santa Barbara-Ventura region where it has been called the Santa Barbara orogeny. While the Coast Ranges, Transverse Ranges and marginal areas were undergoing great folding, faulting, and elevation, the Sierra Nevada was being re-elevated along the series of great fault zones on its east front and tilted westward with minor folding and faulting along the western slopes. Volcanoes in the Cascade Range, Modoc Plateau, and desert basins and ranges were active in Pleistocene time. The higher ranges, including the Sierra Nevada, Cascade and Klamath Mountains, were subjected to periodic glaciation during the Pleistocene.

Recent time, the last few thousand years since the general melting and retreat of Pleistocene glaciers, has been a time of continued active faulting, as shown by the frequency of earthquakes, of local uplift demonstrated by marine terraces along the coast and in some places by river terraces inland, flooding of the lowest parts of the coastal areas because of the rise in sea level

on melting of the Pleistocene glaciers, and of the development of San Francisco Bay and lesser drowned valleys along the California coast. The development of California's present landscape has taken place during this epoch. A necessary and normal accompaniment of the latter stage of this great orogenic epoch is continued faulting and frequent earthquakes, with the probability of gradual decline of this type of activity over the next many thousands of years.

GEOLOGIC SETTING OF THE KERN COUNTY EARTHQUAKES*

Fault Pattern in Southern California. The pattern of known active faults in southern California comprises right lateral, left lateral, normal, and reverse faults in large number and great complexity. It has been developed over long periods of geologic time by great north-south and northeast-southwest-directed stresses of unknown origin. Geologic evidence suggests some of the faulting may have begun as long ago as the Jurassic period; modern earthquakes prove that accumulating strains are still being periodically relieved.

The fault pattern is dominated by the northwest-trending San Andreas fault, essentially right lateral, with the east block moving relatively south on the order of 2 inches a year. Total accumulative movement in this sense since late Jurassic time may be on the order of 300 miles, according to some geologists. The San Gabriel fault, trending southeast from Frazier Mountain, is of similar type. Good geologic evidence indicates right lateral movement on the San Gabriel fault since upper Miocene time has been possibly as much as 15 to 20 miles, and since middle Pleistocene time 2 to 2½ miles. Other major north- and northwest-trending faults, including the Kern Canyon, Sierra Nevada, Nacimiento, and Inglewood, are normal or right-lateral normal and all have been responsible for many earthquakes in historic times. The northwest-trending Kern River fault, just east of Bakersfield, is of comparatively limited extent and may be a simple normal type.

The Garlock-Big Pine fault zone, offset about 6 miles by the San Andreas fault, is the most prominent example of the northeast-trending fault system in which left lateral displacement is characteristic. Displacement along these faults is also measurable in miles. The White Wolf fault probably had a major component of movement in the reverse sense (south block elevated) with some left lateral displacement. Although recognized by geologists as having had geologically recent movements, the potential earthquake threat of these northeast-trending faults was not fully appreciated until the recent series of Kern County earthquakes initiated by movement on the White Wolf fault.

The system of reverse faults comprises a large number of east-west-trending faults which are shorter and much less continuous than the right lateral and left lateral systems. A fault in this system usually changes radically in strike along its course, often varies in dip of fault surface from less than 45° (thrust fault) to nearly vertical, and can rarely be traced continuously for more than a few miles. Prominent examples are the Pleito thrust in the San Emigdio Mountains area south of

Bakersfield, the San Cayetano thrust on the south side of the eastern Santa Ynez Mountains, the Santa Susana thrust in the Santa Susana Mountains, and the Sierra Madre zone of reverse and thrust faults along the south side of the western San Gabriel Mountains. Although recent movement on many of these faults is quite evident, no earthquakes have been definitely traced to displacement on any one of the thrusts.

Rock Formations in the Earthquake Area. The major Arvin-Tehachapi earthquake of July 21, 1952, had its epicenter near the eastern end of Wheeler Ridge and the hundreds of aftershocks, continuing more than a year later, centered chiefly in the area north of the Garlock and San Andreas faults, south of the Kern River and from Maricopa as far east as the longitude of Tehachapi. This area includes the southern part of the San Joaquin Valley, the adjacent southern end of the Sierra Nevada, Tehachapi Mountains, and the east-trending Wheeler Ridge-San Emigdio Mountains.

The Sierra Nevada, Tehachapi Mountains and the central part of the San Emigdio Mountains are made up of a complex of crystalline rocks composed largely of dark hornblende-biotite quartz diorite (a coarse-grained rock closely related to granite) of Jurassic or early Cretaceous age with inclusions of rocks derived from ancient sedimentary series (Triassic or older) which have been thoroughly metamorphosed to schist, quartzite, and marble.

The crystalline complex is overlain by a series of marine and continental sedimentary rocks of the Tertiary and Quaternary periods cropping out along the foothill areas and underlying the San Joaquin Valley. This series of stratified sandstone, conglomerate, shale, and related rocks is thin in the marginal mountain areas but thickens generally southwestward to an estimated total of about 28,000 feet just north of Wheeler Ridge. The Tertiary series dips under San Joaquin Valley with its contact with the underlying crystalline rock sloping southwest at an average angle of about 6°, steepening to about 20° immediately northwest of the White Wolf fault. The valley floor is covered by alluvium, including some lake beds and quantities of sand and gravel deposited by the Kern River and lesser streams.

The exposed 17-mile portion of the White Wolf fault, extending from the vicinity of Caliente to a point about 3 miles southeast of Arvin, is entirely within the area of granitic rock, but the fault extends at least an equal distance southwest under the valley alluvium to Wheeler Ridge.

Structure in the Earthquake Area. The southern Sierra Nevada-Great Valley makes up a more or less rigid block of crystalline rocks which was intermittently tilted westward during Tertiary and Quaternary time, with the eastern part of the block elevated to form the Sierra Nevada and the western part depressed to form the Great Valley. The eastern base of the Sierran block is marked by the Sierra Nevada fault zone; it is paralleled about 15 miles to the west by the Kern Canyon fault zone. Both these great faults appear to be of the normal type. The area southeast of the White Wolf fault (left lateral reverse type) was elevated to form

* Basic data in this section are taken largely from the papers following in Parts I and II of this bulletin.

Bear Mountain as a southwesterly extension of the Sierra Nevada. The northwest-trending Kern River fault is a normal fault locally separating the crystalline block of the Sierra Nevada from Tertiary-Quaternary sedimentary rocks at the western base of the range. Except for minor complexities, the sedimentary formations dip southwestward off the Sierra Nevada block.

The Tehachapi Range is an elevated block, continuous with the southern Sierra Nevada, which swings westward into the San Emigdio Mountains which in turn trend north of west into the Coast Ranges. The Tehachapi is followed by the great northeast-trending left lateral Garlock fault. The southern margin of the San Emigdio has been cut by repeated horizontal movements along the San Andreas fault with right lateral displacements totaling many miles. This has moved the northeastern block in an easterly direction with respect to the southwestern block. The horizontal shearing movements have been accompanied by intense compression in a north-south direction, shattering the basement crystalline-rock block of the San Emigdio Range, intensely folding the overlying Tertiary sedimentary rocks at their northern margin and thrusting them strongly northward along the Pleito thrust fault toward the San Joaquin Valley.

Numerous wells drilled for oil in the San Joaquin Valley have revealed some of the structural features of the sedimentary formations which are obscured by overlying alluvium. They show that the generally southwest-dipping Tertiary-Quaternary sedimentary strata are displaced by numerous faults. It is interesting to note that the fault pattern on the valley floor is similar to that in the marginal mountains; i.e., northwest-trending normal, or right lateral, faults and northeast-trending cross faults (left lateral?).

The pattern of faulting in the earthquake area appears to be genetically related to joints, shear zones, and planes of weakness in the ancient crystalline rocks which underlie the entire region and crop out in the mountains.

GEOLOGIC EFFECTS OF THE ARVIN-TEHACHAPI EARTHQUAKE *

White Wolf Fault Zone. According to records of the Seismological Laboratory of the California Institute of Technology, the major Arvin-Tehachapi earthquake originated at a depth of about 10 miles at 4:52 a.m. PDT on July 21, 1952, at latitude 35° 00' N, longitude 119° 02' W near Wheeler Ridge. It had a magnitude of 7.7 on the Richter scale, making it one of California's greatest earthquakes. Rupture, originating at that focus, progressed N. 50° E. along the White Wolf fault plane, or surface, at a rate approximating 2 miles per second. Calculations based on seismological records indicate the fault dips 60° to 66° toward the southeast and that the major relative movement along the fault plane was southeast block (Bear Mountain) up, with a lesser horizontal component of movement toward the northeast. Thus the White Wolf fault is a left lateral reverse type with oblique slip movement.

Existence of the White Wolf fault had been known by geologists for many years; its general trace was plotted on a geological map as early as 1906. It had been recognized as having movement in late geological

time but was not considered active in the sense of constituting an earthquake threat. The very steep northwest face of Bear Mountain, the succession of old landslides along that slope, and minor topographic features made it possible to plot the approximate location of the fault but its characteristics were unknown. Initial rupturing on July 21, originating at depth in solid crystalline rock, extended rapidly toward the surface and reached the surface through altered weathered rock, soil, and old landslide material to form a series of more or less discontinuous ground cracks, slides, scarplets, small pressure ridges, ground offsets, and "mole-track" effects generally along the trace of the White Wolf fault zone. These features were best developed near the base of Bear Mountain close to the fault trace from the base of the Tejon Hills, south of Arvin, to Caliente Creek. Subsequent aftershocks had little effect on the features which were developed along the fault trace on July 21.

The absence of fractures and other surface effects along the probable southwestern extension of the White Wolf fault under Valley alluvium between Comanche Point (Tejon Hills) and Wheeler Ridge suggests rupturing was absorbed by the deep alluvium in this area and did not reach the surface. Fractures developed along the base of the hills at Comanche Point and at the mouth of Little Sycamore Canyon were near-vertical and formed northwest-facing scarplets (steps) up to a foot high. Off the fault zone in the mouth of Comanche Canyon, numerous small mud volcanoes were developed as a result of lurching in moist alluvium. A prominent fracture zone follows the edge of the alluvium 1½ miles northeastward from the mouth of Little Sycamore Canyon, with foot-high fractures vertical or dipping steeply southeast, and left lateral movement up to 8 inches.

The greatest and most continuous zone of fracturing developed along the fault zone for 5 miles from a point 4 miles due east of Arvin to the White Wolf Ranch. It is here marked by thrust-fault scarplets facing northwest and the peculiar series of pressure ridges (mole tracks) up to 3 feet high. These are overthrusts, with the plane of thrusting dipping southeast at low angles and with movement toward the northwest over the Valley. In some places a series of parallel mole tracks replaces the single ridge and northwest-trending tension cracks developed. In general, the plane of movement dips 5° to 20° southeastward into Bear Mountain.

The zone of fracturing for 6 miles along the fault northeastward from the White Wolf Ranch to the Southern Pacific Railroad tunnels east of Bealville shows a different type of rupturing. Fractures in this zone are not exactly on the fault trace, but are an echelon vertical ruptures with a more northerly trend than the fault. There are two or three series of north-trending vertical fractures 1 mile to 3 miles long in the soil with left lateral offsets (west block moved south) up to one foot, but without the formation of scarplets.

Between the Bealville Road—U. S. Highway 466 intersection and Tehachapi Creek, fractures developed in the shattered dark granitic rock just north of the apparent trace of the fault. Trend of these fractures is northeast and evidence of left lateral movement and compression is found along the fractures and in the contortion of rails and shortening of the tunnels. On the hill through

* Basic data in this section are taken largely from the papers following in Parts I and II of this bulletin.

which tunnel 5 passes, there are four parallel fractures trending west of north for half a mile and dipping steeply north. The uphill side slipped down in each case so that an open fissure was formed with a scarp up to 2 feet high facing upslope.

There is no geologic evidence that the White Wolf fault extends north of Tehachapi Creek but a large north-trending crack 1,000 feet long developed across the divide between Tehachapi and Caliente Creeks along the contact between the dark granitic rock and Tertiary conglomerate; the crack dips steeply west with a 3-foot west-facing scarp.

Fractures and Landsliding in the Region. Ground ruptures, distortions, and fractures were developed very widely in the region, apart from those features closely associated with the White Wolf fault zone. Such features, in general, appear with greater frequency and prominence near the fault zone. Hundreds of rock falls and landslides of all sizes took place during the earthquake of July 21 and more occurred with each aftershock. The most damaging landslides were those affecting the highways. The Ridge Route (U. S. Highway 99) was blocked at several points between Castaic and Grapevine and rock falls as far from the fault as the San Gabriel Mountains partly blocked the Angeles Forest highway between Pasadena and Vincent. The Caliente Creek road and the Kern River highway were closed by rock slides for several weeks. The northwest face of Bear Mountain and canyon walls, like those of Sycamore Canyon, were major sites of rock and land slides. Evidence of very large landslides and the hummocks, depressions, and shattered rock associated with such slides present before the late series of earthquakes shows the northwest slopes of Bear Mountain have been subjected to repeated movements in the past.

Boulders up to 10 feet or more in diameter were dislodged from the slopes of Bear Mountain, Bear Valley, Cummings Valley, and steep slopes a few miles from the White Wolf fault zone. Some hopped and skipped down slope for several hundred feet, gouging the surface and leaving very characteristic boulder trails.

Cracking of highway pavement and barriers, and slumping of shoulders for miles away from the epicenters were particularly damaging. Cracks affecting pavement, and other stationary structures, had a tendency to be oriented parallel to or perpendicular to the length of the structure.

Fractures in Alluvium on the Valley Floor. Fractures and cracks in great variety developed on the floor of the San Joaquin Valley, principally the result of lurching in the deep water-saturated alluvium. Many formed scarps up to a foot or so in height and showed lateral displacement. However, such fractures were discontinuous and many showed no consistent direction or amount of displacement.

Faint surface lines, oriented northwest and northeast, had been noticed on aerial photographs by petroleum geologists for years previous to the Kern County earthquakes. The Arvin-Tehachapi earthquake produced a large number of minor cracks in the alluvium, often marked by swirls and loops at their ends, and oriented in the same patterns as the older features appearing on photos. It seems likely that these originated through

recurring small movements on an ancient system of faults in the basement crystalline rocks which underlie the alluvium and that settling and adjustments of the alluvium were reflected in the oriented cracks, lateral offset features, and minor sloughs that appear at the surface.

Movements Measured by U. S. Coast and Geodetic Survey. After the July 21, 1952, earthquake, the U. S. Coast and Geodetic Survey made repeat surveys of their triangulation and level schemes. Preliminary results of these surveys indicate that horizontal movements at the triangulation stations were small but suggest the Bear Mountain block moved northeast about 2 feet, while leveling indicates differences in elevation of 3 to 4 feet at points approximately 15 miles south of Bakersfield 6 to 8 miles south of Arvin. The area to the south has been uplifted and the area to the north lowered. The sharpest break appears about 6 miles south of Arvin. This is approximately on the White Wolf fault at Comanche Point.

Effects on Spring and Stream Flow. Studies by the U. S. Geological Survey show that the flow of many of the streams and springs in a wide area increased as a result of the Arvin-Tehachapi earthquake, but it is doubtful that the effect on the recharge areas or on the permeability of aquifers is permanent. The temporary increase was probably due to disturbance of unconsolidated materials in the discharge areas, resulting in the clearing of existing outlets and opening of new ones.

One of the most spectacular increases was in Caliente Creek. This increased from completely dry at the town of Caliente to 25 cubic feet per second within a few days. As far away as Sespe Creek in Ventura County, that drainage increased from 17 cubic feet per second on July 20, 1952, to 37 cubic feet per second on July 31. However, 88 percent of the Survey's observation points in the Santa Ynez Mountains indicated no change in flow. Streams in Los Angeles County showed little effect. Radical differences in flow characteristics were noted, even in short distances.

Water-Level Fluctuations in Wells. Well records of the U. S. Geological Survey from San Diego County to Butte County show the earthquake of July 21 reflected as oscillations of water surfaces. The amplitude of fluctuations ranged from 7.34 feet in a well near the White Wolf fault about 20 miles northeast of the epicenter to 0.012 feet in a well near Twentynine Palms about 180 miles southeast of the epicenter. Fluctuations did not vary regularly with distance from the epicenter. Most of the residual changes in wells in the San Joaquin Valley were upward; elsewhere many were downward. The records suggest major factors in the fluctuations were compressibility and elasticity of the aquifers; factors which, in turn, are closely related to the lithologic features of the materials.

UNUSUAL GEOLOGIC ASPECTS OF THE KERN COUNTY EARTHQUAKES

Probably no earthquake in history has been studied in the field as intensively or by as many geologists and seismologists as the Arvin-Tehachapi shock of July 21, 1952, and its aftershocks. Accessibility of the area, the

damage done, the striking land surface effects, the speed with which the Seismological Laboratory of the California Institute of Technology focused the attention of its staff and equipment on the area, and the large number of professional geologists in the state who visited the earthquake area have all contributed to the store of information on the earthquake series and its causes. Some of the unusual aspects are:

1. The fault responsible for the major earthquake trends northeast. Nearly all California's great earthquakes have been associated with movements on north-west-trending faults, usually the San Andreas or faults related to it.

2. The fault is of left lateral reverse type; the principal component of movement was reverse, with lesser left lateral movement. Most of California's great earthquakes have probably been caused by strike slip movements on right lateral faults.

3. Actual surface ruptures along a fault responsible for an earthquake are rare. The mole-track pressure ridges, linear ruptures with both vertical and horizontal offset, up-bowing of ground, and track-shortening in the railroad tunnels constitute a unique complex series of surface effects in this fault zone.

4. The White Wolf fault, traceable for about 34 miles, is one of the shortest known to have been responsible for a major earthquake in California.

5. Magnitude of the Arvin-Tehachapi shock (7.7) makes it one of the three greatest in California history.

6. Distribution of the large number of aftershocks shows not only that readjustments took place along the White Wolf fault, but also that movements were triggered on numerous other faults in the area. The destructive Bakersfield earthquake of August 22, 1952, is an example of this.

2. GEOLOGY OF THE SOUTHEASTERN MARGIN OF THE SAN JOAQUIN VALLEY CALIFORNIA

BY T. W. DIBBLEE, JR.*

ABSTRACT

The southern Sierra Nevada and Tehachapi Mountains are made up of a pre-Cretaceous crystalline complex composed of Jurassic (?) plutonic rocks with hornblende-biotite quartz diorite predominating, and linear inclusions of Paleozoic (?) schists, quartzite, and marble. The crystalline complex is overlain by a Tertiary-Quaternary marine and continental sedimentary series cropping out along the foothill areas and underlying the San Joaquin Valley where the series thickens southwestward to an estimated total of about 25,000 feet just north of Wheeler Ridge. The Tertiary series dips under San Joaquin Valley with the crystalline-rock contact sloping southwest at an average angle of about 6°, steepening to about 20° immediately northwest of the White Wolf fault.

The White Wolf fault, nearly parallel to the Garlock fault and about 18 miles northwest of it, is a major fault traceable from Tehachapi Canyon southwest along the base of the steep northwest slope of Bear Mountain for 17 miles, and probably extends under San Joaquin Valley toward Wheeler Ridge. The southeastern block has been elevated on this fault to a maximum displacement of at least 10,000 feet as indicated by surface and subsurface data, with the maximum displacement near the mouth of Sycamore Canyon.

Surface effects along the White Wolf fault zone produced on July 21, 1952, including overthrusting in the mole-track scarplets formed, shortening of fences and the railroad tracks crossing the fault, and dips of the more continuous fault-trace ruptures, strongly suggest thrusting. Seismographic evidence favors a high-angle reverse fault at depth. Ground cracks and small pressure ridges oblique to the fault trace, and small ground offsets indicate some left lateral movement.

The White Wolf fault is essentially a reverse fault, locally a thrust, elevated in the southeast block, with a small left lateral component of movement. It is more closely related to the Garlock and Pleito faults than to faults in the northern part of the area mapped.

INTRODUCTION

The southeastern margin of the San Joaquin Valley and the adjacent mountain area was the scene of the violent earthquake of July 21, 1952, which severely damaged the small towns of Arvin and Tehachapi in Kern County. The cause of this major earthquake was found to be a movement on the White Wolf fault at the base of the steep northwest slope of Bear Mountain as indicated by ground ruptures formed along the supposed course of this fault.

The topographic base map which most adequately covers the area which the White Wolf fault traverses is the 30-minute Caliente quadrangle, scale 1 inch = 2 miles, issued by the U. S. Geological Survey in 1914.

The geology of the northeastern quarter of the Caliente quadrangle was taken from previous detailed mapping done by the writer in 1950 (Dibblee, 1953). The geology of the northwestern quarter of the quadrangle is based on mapping by the writer during several week-ends in 1950, accompanied several days by A. H. Warne. The geology of the southern portion of the quadrangle and northernmost portion of the adjoining Tejon quadrangle is based on published maps and reports by Hoots (1930), Marks (1938), and Wiese (1949), although a week was spent in remapping critical portions of these areas. Two weeks of the present investigation were spent in the southeastern quarter of the Caliente quadrangle in the vicinity of Bear Mountain and southwest into the

Tejon Hills; as time was limited, the mapping is largely of reconnaissance nature.

Acknowledgments are due the geological staff of Richfield Oil Corporation for access to well logs used to determine the subsurface structure of the top of the basement complex buried under the San Joaquin Valley.

STRATIGRAPHY

Basement Complex

The pre-Cretaceous basement complex exposed throughout the southern Sierra Nevada, Tehachapi and San Emigdio Mountains, and buried under Tertiary strata in the San Joaquin Valley, is composed of granitic igneous rocks that form the Sierra Nevada granitic batholith. They range from granite to gabbro; quartz diorite predominates. The metamorphic rocks occur within the granitic batholith as roof-pendants or linear remnants of a once tremendous thickness of gneiss, schist, quartzite and limestone. The age of the metamorphic and igneous rocks is not definitely known, although the former are believed to range from pre-Cambrian to early Mesozoic, and the latter are directly traceable into the granitic rocks of late Jurassic age in the north central Sierra Nevada where they intrude the Upper Jurassic Mariposa slate and are unconformably overlain by Cretaceous sandstones and shales. Brief descriptions of the principal mapped units of the basement complex follow.

Pelona Schist. The pre-Cambrian (?) Pelona schist, as mapped by Wiese (1950, pp. 12-13), occurs only between the two branches of the Garlock fault in the Tehachapi Range where about 5,000 feet is exposed. The formation is highly foliated, with prominent cleavage, and is composed predominantly of dark greenish-gray mica-chlorite-albite-quartz schist which was probably metamorphosed from tuffaceous shale.

Biotite Gneiss. A large mass of gneiss of unknown but probable pre-Cambrian age is exposed on the north flank of the Tehachapi Mountains in the vicinity of El Paso Canyon. This formation is a complex of well banded biotite-hornblende-quartz-feldspar gneiss, and numerous injections of massive quartz diorite.

Pampa Schist. In the Cottonwood Canyon area of the western slope of the Sierra Nevada are several lenticular and linear pendants of mica schist within quartz diorite. The schist, of unknown age, mapped as the Pampa schist (Dibblee, 1953) and named after Pampa Peak, is dark gray and prominently foliated parallel to bedding. It is a biotite-quartz-feldspar schist similar to that of the Kernville series. The most southwesterly exposures of the schist in Cottonwood Canyon contain numerous large crystals of andalusite (chiastolite) elongated parallel to foliation planes. The Pampa schist is of sedimentary origin, having been metamorphosed from clay shale.

Kernville Series. The linear inclusions of metasediments exposed in the Sierra Nevada from Walker Basin southward to Keene and again on Bear Mountain ridge and Brite Valley were mapped as the Kernville series, because they are similar to the Kernville series mapped

* Consulting geologist. Manuscript submitted for publication June, 1953.



FIGURE 1. Mole-track scarp extending northeastward, close to trace of White Wolf fault. View northeast toward Bear Mountain. Photo by Lauren A. Wright.

by Miller and Webb (1940, pp. 349-353, map) in the Kernville quadrangle. The Kernville series is a sequence of metamorphosed marine sediments composed predominantly of biotite-feldspar schist with prominent platy foliation parallel to bedding. Interbedded with the schist are layers of gray-white quartzite and fine textured gray to white limestone. The maximum exposed thickness of the Kernville series within the mapped area is about 6000 feet, but the original thickness was no doubt many times that amount. The age of the Kernville series is unknown, as no diagnostic fossils have been found in it.

Limestone of Tehachapi Range. On the southeast slope of the Tehachapi range are several isolated exposures, within and south of the Garlock fault zone, of metamorphic blue-gray to white limestone containing minor interbeds of gray-white quartzite, lime-silicate hornfels and black schistose biotite hornfels. This formation is probably the same as the Bean Canyon schist-limestone series described by Simpson (1934, pp. 381-383) exposed 8 miles beyond the east border of the mapped area, and may be also the equivalent of the Kernville series north of the Garlock fault.

Schist of the San Joaquin Valley. Schist underlies the Tertiary sediments under a large portion of the east side of San Joaquin Valley, being encountered in wells throughout the Arvin-Mountain View-Edison oil field area, northward to the Ant Hill field, and southward nearly to the White Wolf fault. This buried schist is probably continuous with the outcrops of the Pampa schist exposed in Cottonwood Canyon to the northeast.

The schist immediately underlying the Tertiary sediments was shattered or rendered porous by weathering

prior to deposition of the sediments; and in portions of the Edison and Mountain View-Arvin oil fields, it is a reservoir rock for oil derived from the Tertiary strata where they buttress against the schist up dip. Basement cores from many wells in and near these fields have been examined by May and Hewitt (1948, pp. 129-158), who have determined the character and distribution of the schist under this part of the valley.

Diorite-Gabbro. In the western Sierra Nevada foothills there are three small exposures of a dark intrusive rock ranging from diorite-gabbro to gabbro. One of these occurs in Kern Gorge, another in Rattlesnake Canyon and one in the foothills east of the Rockpile. A large exposure of gabbro crops out east of Pastoria Canyon in the Tehachapi Mountains. These exposures are composed of dark-gray to nearly black medium-textured, equigranular rock composed almost entirely of calcic plagioclase feldspar and hornblende.

Quartz Diorite. The granitic rock so extensively exposed throughout the southern Sierra Nevada within Caliente quadrangle has been determined petrographically as quartz diorite (C. W. Chesterman, in Dibblee 1953). This rock, predominant in the vicinity of the White Wolf fault, is composed of quartz and white orthoclase and plagioclase feldspars with plagioclase predominating, and biotite mica and hornblende in varying amounts, but the dark minerals seldom exceed 30 percent of the total rock mass. The rock is light to medium-gray, depending on the amount of dark minerals present, is medium-textured, equigranular. Two facies of quartz diorite are developed in the southern Sierra Nevada and appear to have intruded the pre-existing rocks at different times or in different modes.

In the San Joaquin Valley the basement complex underlying the Tertiary sediments is made up largely of quartz diorite. From the foothill area between Caliente Canyon and the White Wolf Ranch the quartz diorite extends westward under the adjacent portion of the valley where it has been found below the Tertiary in all well cores. Well logs indicate the quartz diorite-schist contact exposed 2 miles north of Bena extends southwestward 6 miles to the Edison oil field, through which it curves southward passing just east of Arvin probably to the White Wolf fault. In the vicinity of the Kern River and Bakersfield most wells that penetrated to the basement complex cored quartz diorite.

Granite. A nearly white massive plutonic rock mapped as true granite by Wiese (1950, pp. 24-25) crops out on the south side of the Tehachapi Range south of the Garlock fault. Numerous dikes of pegmatite and aplite cut the foliated quartz diorite, especially at or near the borders of the massive facies from which the dikes may have originated. The pegmatite is composed of very coarse textured quartz and white feldspar, with gradations to fine textured aplite of the same minerals. The dikes range from less than an inch to 10 feet thick, and are especially numerous east of Caliente and in Rattlesnake Canyon where they trend northeast parallel to the contacts of the massive quartz diorite and dip steeply toward it.

Hypabyssal Intrusives. Fine textured intrusive igneous rocks have been cored in the basement complex by many wells that have reached it in the Bakersfield, Edison, and Mountain View areas, as reported by May and Hewitt (1948, pp. 141-3). These rocks are hard, massive to slightly schistose, light to dark gray or greenish gray, and are composed of aplite, malchite (microdiorite), andesite, diorite-aplite, diorite porphyry, and lamprophyre.

Intrusive rhyolite of probable Cenozoic age crops out 1 mile east of Keene as several small dikes up to 12 feet thick cutting quartz diorite. The rhyolite is a dense cream-white rock weathering tan, with small phenocrysts of quartz and feldspar. Associated with one of the rhyolite dikes is a small deposit of cinnabar at the Walibu mine.



FIGURE 2. Detail of mole-track scarp (pressure ridge) about 4 miles due east of Arvin. Bear Mountain in background. *Photo by Lauren A. Wright.*

Tertiary-Quaternary Series

The basement complex of the Sierra Nevada and Tehachapi-San Emigdio Mountains is unconformably overlain by the Tertiary and Quaternary sequence of sediments ranging in age from Eocene to Recent. Where the series is buried under the San Joaquin Valley the stratigraphy has been determined from numerous well logs. The series crops out as a strip along the Sierra Nevada foothills as far southeast as Caliente Canyon where the outcrop section is terminated by the Edison fault. Between this fault and the White Wolf fault to the southeast the Tertiary is not exposed. South of the latter fault the series again crops out in the Tejon Hills and along the foothills around the southeast end of the valley into the San Emigdio Mountains.

The Tertiary series within the mapped area is a continuous succession characterized by numerous and rapid changes of facies and thicknesses. In general the series thickens from east to west, absent along the foothills between the Edison and White Wolf faults and as thick as 25,000 feet just north of Wheeler Ridge. This westerly thickening is accompanied by gradation from coarse detrital material along the eastern margin to fine-grained argillaceous, thin-bedded sediments as the series thickens toward the deeper portion of the San Joaquin depositional basin. The general stratigraphic succession is as summarized below.

Marine sediments of Eocene age, the Tejon formation, overlie the basement complex and crop out only at the southern end of the San Joaquin Valley. This formation, which lies deeply buried under the westerly portion of the valley and does not extend as far east as the overlying strata, was deposited in a sea which transgressed from the west.

The Tejon formation and the basement complex are overlain by the nonmarine Tecuya formation of the San Emigdio-Tehachapi foothills, and the Walker formation and Bealville fanglomerate of the Sierra Nevada foothills, all of Oligocene (?) - lower Miocene age. These are made up of coarse, land-laid sediments containing some volcanic lavas and tuffs, deposited after regression of the Eocene sea. These sediments eventually grade westward into marine strata of the Pleito formation and its equivalents.



FIGURE 3. Broken fence, suggesting compression, across White Wolf fault east of Highway 466, at base of Bear Mountain east of Arvin. *Photo by Lauren A. Wright.*

The Tecuya and Walker formations are overlain by marine sandstones and clay shales of the Temblor (or Vaqueros) formation, lower Miocene age, deposited as the Miocene sea transgressed eastward to the present site of the Tehachapi and Sierra Nevada foothills. The Temblor formation crops out in the San Emigdio Mountains, and on the east margin of the San Joaquin Valley where it is represented by the Pyramid Hill, Vedder, and Jewett sands, Freeman silt, and Olcese sand. The Temblor formation is followed by the Maricopa (or Monterey) shale, a series of organic shales of middle and upper Miocene age deposited in the Miocene sea when it reached its maximum extent and depth. This formation extends eastward under the valley to the Tejon Hills and Sierra Nevada foothills where it is represented by the Round Mountain silt, Fruitvale shale, and marginal sand lenses. Overlying the Maricopa shale and its equivalents is the Santa Margarita sand, which is fairly persistent throughout the mapped area and represents the final stage of marine deposition as the Miocene sea regressed.

All of the above Miocene marine formations grade eastward into terrestrial facies mapped as the Bena gravels, which crop out in the Sierra Nevada foothills, Tejon Hills and Tehachapi foothills. There coarse detrital sediments were deposited as piedmont alluvial fans on the coastal plain bordering the Miocene sea whose strandline persisted along the present site of the southeastern margin of the San Joaquin Valley.

The Miocene strata are overlain by terrestrial sediments of the Chanac and Kern River formations, of Pliocene age, the latter ranging into Pleistocene. These coarse alluvial sediments crop out in the lowest portions of the Sierra Nevada foothills, Tejon Hills, Tehachapi foothills and Wheeler Ridge, and underlie San Joaquin Valley where the series attains a maximum thickness of 14,000 feet just north of Wheeler Ridge. The Chanac, and perhaps the lower part of the Kern River formation, eventually grade westward into the brackish-marine Etehegoi formation; the first definite marine beds appear in the outcrop section about 8 miles west of Wheeler Ridge, beyond the mapped area.

Summary of Geologic History

Pre-Cambrian (?). Accumulation of muds, volcanic ash, and minor amounts of sand and lime, probably in an open sea, now the gneiss and Pelona schist in the Tehachapi Mountains.

Paleozoic (?) to Jurassic (?). Accumulation of muds, sands, limestones and some lavas of the Kernville and Pampa series under an open sea to a tremendous thickness, resulting in a very deep burial of the lower strata and of the underlying strata.

Late (?) Jurassic Nevadan Orogeny. Strata deposited during pre-Cambrian (?) to Jurassic (?) time subsided to such great depth (10 miles or deeper) that they became subject to regional thermodynamic metamorphism. Pre-Cambrian (?) formations altered to gneiss and the Pelona schist, and Paleozoic (?) or early Mesozoic (?) strata to schist, quartzite, marble and meta-igneous rocks of the Pampa and Kernville series. At this great depth metamorphosed rocks were intruded by molten magmas which crystallized into granitic rocks, chiefly quartz diorite.

Cretaceous. Long interval of erosion; mountainous terrain built up during Nevadan orogeny deeply eroded to surface of low relief; westward tilt initiated, causing continued or renewed uplift of Sierra Nevada-Great Basin region and downward tilt of area to west under Pacific ocean.

Eocene. Continuation of last event; Sierra Nevada probably blocked out during this time by faulting; down-tilted area to west submerged under waters of ocean that transgressed from west;

deposition of sands and clays of Tejon and equivalent formations on deeply eroded and peneplaned surface of metamorphic and granitic basement complex.

Oligocene (?). Continued westward tilting; Sierra Nevada underwent renewed uplift and erosion; eroded debris deposited along western base as alluvial fans of the Bealville, Walker and Tecuya formations, causing partial regression of Eocene sea; local volcanic eruptions of pumiceous ash and some basaltic lavas.

Miocene. Continued westward tilt with some renewed uplift and erosion of ancestral Sierra Nevada; eroded debris deposited along western base as alluvial fans of the Bena gravel; down-tilted area continued to submerge under a great open sea transgressing from the west, with ancestral shoreline along base of Sierra Nevada uplift from site of mouth of Kern Gorge southward through Edison-Mountain View-Arvin oil fields, Tejon Hills, and across Tehachapi Mountains; sands deposited in shallow waters near shore, clays and siliceous muds in deeper waters farther to west. Sea transgressed from west in early Miocene time, regressed at end of Miocene; Edison fault developed during Miocene deposition, with uplift of south block.

Pliocene. Continued westward tilt; renewed uplift and erosion of Sierra Nevada; Tehachapi and San Emigdio ranges formed by compressive uplift against Garlock and San Andreas faults respectively; San Joaquin embayment thus formed with deposition of Etehegoi formation at southeast extremity of this lingering embayment; debris eroded from mountains deposited as alluvial sediments of Chanac and Kern River series, thus filling embayment to form San Joaquin Valley; major and some minor faults in area may have been initiated.

Pleistocene-Recent. Recurrent uplift of Sierra Nevada, involving adjacent foothill area, causing partial uplift and erosion of Tertiary sediments deposited along western base; development of Kern River fault and numerous other faults in foothill area and eastern San Joaquin Valley; Kern Canyon fault; uplift of Breckenridge Mountain block on Breckenridge fault and consequent filling of upper Walker Basin Canyon to form Walker Basin; development of Garlock and White Wolf faults with uplift of Bear Mountain, Bear-Brite-Cummings-Tehachapi Valley and Tejon Hills area as a single block between them; recurrent compressive uplift of Tehachapi-San Emigdio Range against Garlock and San Andreas faults; compressive northward movement and elevation of San Emigdio uplift on Pleito thrust fault and rise of Wheeler Ridge anticline and foothills in front of San Emigdio overthrust; material derived from erosion of all elevated areas deposited as alluvial fill in San Joaquin Valley.

GEOLOGIC STRUCTURE

Structural Setting of the Southeastern San Joaquin Valley Region. The southern Sierra-Great Valley province of California constitutes a regional structural block about 120 miles wide and roughly 600 miles long, made up of a complex of crystalline metamorphic and intrusive granitic rocks stabilized to a comparatively rigid mass during the great Nevadan orogeny at the end of Jurassic time. During Cretaceous and Cenozoic time this huge structural block was tilted westward almost continuously, with the eastern portion elevated to form the Sierra Nevada, and the western portion tipped downward to form the Great Valley. As this block was tilted, material eroded from the rising Sierra Nevada was carried westward and deposited to form an enormous thickness of Cretaceous-Cenozoic sediments in the sinking Great Valley area which was submerged under marine waters until late Tertiary time when it became filled with sediments. Westerly tilting caused progressively more rapid subsidence of the west side of the Great Valley so that the basement complex is progressively more deeply buried from east to west, being buried many miles deep on the western margin.

The Sierra Nevada has been uplifted as a huge west-tilted block on the north-trending Sierra Nevada fault zone along its eastern base. In this zone faulting is of the normal type with fault planes dipping steeply east-

ward. The northern and central portions are made up of several en echelon north-trending faults, while the southern portion is a single fault along which the mountain block was elevated to great heights to form the imposing front of the high Sierra. The southern Sierra Nevada fault is paralleled about 15 miles west by the Kern Canyon-Breckenridge fault along which the western portion of the southern Sierra Nevada was elevated.

The pivotal area of the continuously westward tilted Sierra Nevada-Great Valley block follows the present margin between the Sierra Nevada and the Great Valley, as topographic and stratigraphic evidence indicates this marginal area to have been neither elevated nor depressed to any great extent during Cretaceous or Cenozoic time. During that long interval of time this 600-mile long pivotal area has been remarkably stable and free from tectonic movements. Only in the extreme southeastern portion in the vicinity of Bakersfield have tectonic disturbances occurred and these have been in the form of faulting. The largest of these faults is the White Wolf fault trending northeast directly across the pivotal margin between the Sierra Nevada and the San Joaquin Valley. The area southeast of this fault was elevated as a block to form the great westward protrusion of the Sierra Nevada or the Bear Mountain uplift. Geologic and seismic evidence indicate this fault to be a southeast-dipping reverse fault with lesser left lateral movement.

The Sierra Nevada-Great Valley province is terminated on the southeast by the northeast-trending Tehachapi Range and uplift, traversed along its crestal portion by the Garlock fault. This is a master fault extending 150 miles north of east from its juncture at Lebec with the San Andreas fault, and separates the Sierra Nevada and Basin-Range provinces on the north from the Mojave Desert province on the south. This fault is a great active shear zone of a type similar to the San Andreas, although movement on the Garlock has been left lateral, with the north block having moved westward relative to the south block.

The Tehachapi Range merges westward with the San Emigdio Range which trends north of west and forms the southernmost of the inner Coast Ranges bordering the San Joaquin Valley on the southwest. These ranges have been formed by compressive uplifts recurring during Cenozoic time along or near the northwest trending San Andreas fault, largest and most vigorously active crustal break in California. Movement on this 600-mile-long vertical shear zone has been largely horizontal, right lateral, with the southwestern block having moved northwest relative to the northeastern block. This fault has been recurrently, if not continuously, active throughout Cenozoic time, and cumulative right lateral displacement has amounted to many tens of miles. The horizontal shear movement has been accompanied by crustal shortening, which in the San Emigdio Range on the northeast side of this great shear zone has been so severe that the once deeply buried rigid basement complex has been shattered and squeezed up to form the high crest of the mountains. The overlying thick Tertiary series has been folded and thrust northward toward the San Joaquin Valley on the Pleito fault along the foothills to form the San Emigdio overthrust.

It is noteworthy that the San Emigdio overthrust lies north of the intersection of the San Andreas and Garlock faults, two master shear zones with opposite horizontal movement. There is suggestive evidence that the White Wolf fault may extend at depth southwest to the San Andreas, and that it may have some left lateral component of movement like the Garlock fault. The White Wolf and Pleito faults are probably genetically related to the Garlock and San Andreas shear faults and not to any of the faults to the north.

The White Wolf Fault

Geologic Evidence. The steep northwest slope of the high westward protrusion of the Sierra Nevada between Tehachapi Canyon and the Tejon Hills has long been recognized as the scarp of a major fault. Such a fault was first recognized by Lawson (1906), and was mapped by Hoots (1930, p. 314), as the White Wolf fault, named after the White Wolf Ranch through which it passes.

The White Wolf fault trends from lower Tehachapi Canyon S 50° W for 17 miles along the base of the steep northwest slope of Bear Mountain to Comanche Point, and probably extends at least an equal distance across the San Joaquin Valley toward Wheeler Ridge. This fault is nowhere clearly exposed and is thereby difficult to trace as the northeastern portion is within quartz diorite, the central portion is covered by numerous landslides from the elevated block, and the southwestern portion is concealed by alluvium. Prior to July 21, 1952, practically nothing was known about this fault. Knowledge of its existence was based entirely on topography and was later substantiated by deep drilling in the valley area north of the fault and at Comanche Point. The steep, abrupt slope of Bear Mountain indicates the fault to have been active in very late Pleistocene and Recent time. Its generally straight base line might lead to the interpretation that the White Wolf fault is a normal fault, but the presence of numerous landslides and earth flows from the elevated mountain block suggests the fault to be of the reverse or thrust type. Left lateral movement on this fault might be inferred from its parallel trend with the left lateral Garlock fault, but this is not conclusively indicated by topographic or stratigraphic evidence.

Surface Ruptures Developed on July 21, 1952. The surface ruptures developed in the ground along the course of the White Wolf fault during the earthquake of July 21, 1952, if these represent the actual movement on the fault, serve to determine its exact location at the surface and indicate its probable direction of dip and nature of movement. Surface cracks formed along almost the entire 17-mile known course of the White Wolf fault, and most of these occurred on or very near its trace. The fracturing occurred mainly along the northeastern, central and southwestern portions of the fault, with gaps in between. The type of rupturing in each portion varies greatly and there is some doubt as to whether these all represent actual tectonic fault movements which caused earthquakes or gravitational earth settling movements which resulted from the earthquakes. For reasons stated in the following paragraphs, these large cracks along the White Wolf fault are believed to be primary features of fault movement on July 21, 1952, as expressed at the surface.



FIGURE 4. Northwestern slope of Bear Mountain, showing landslide topography. Two earthquake cracks, roughly at right angles, are near center of photo. The more prominent crack trends northeast and is close to the trace of White Wolf fault. *Official photograph, U. S. Air Forces, Edwards Air Force Base, Edwards, California.*

In areas upslope from the White Wolf fault there are many small ruptures on the steep slopes of Bear Mountain and on both sides of Sycamore Canyon up to the 4,000 foot contour. These ruptures are 10 to about 200 feet long and either follow a contour or in most cases are concave down slope. They are always gaping and dip steeply downhill with the hanging block having always slid downhill one or several feet. One of these on the south slope of Bear Mountain slid down as much as 30 feet. These are small shallow landslide features which developed only in the soil or in weathered or shattered quartz diorite on steep slopes, and were produced by gravitational settling of this material by lurching resulting from the main shock; they are therefore not faults.

The ruptures developed along the trace of the White Wolf fault are the largest and most extensive, and are believed to be true faults. The greatest and most continuous zone of fracturing exists along the central 5 miles of the White Wolf fault or that portion following the base of the steep 5,000-foot-high granitic scarp of Bear Mountain beginning at a point 4 miles east of Arvin and extending continuously for 3 miles northeastward, then intermittently for another 2 miles to the canyon south of the White Wolf ranch house. The entire mountain block on the southeast side of this zone of fracture was elevated 1 or 2 feet, and thrust toward the northwest. The fracturing along this 5-mile portion of

the White Wolf fault is consequently characterized by thrust fault scarplets usually facing northwest, and associated pressure ridges or mole tracks. In most places the upthrust block formed a single scarplet a foot or two high and traceable for several hundred feet. All the scarplets along this portion of the fault were miniature overthrusts with the plane of movement dipping southeast at low angles and with displacements toward the northwest or west of north. There was no evidence of oblique movement except where the scarplet deviated from the usual northeast trend, in which case the movement was always toward the northwest. In places where a scarplet was not developed, the same amount of shortening was taken up by a series of parallel pressure ridges or mole tracks. The hard dry soil was always broken up into small irregular blocks along the scarplets and ridges. However, in some places where they trend obliquely to the normal northeast trend, oblique tension fissures trending northwestward were developed along each scarplet. The scarplets and bucklings pass around spurs and extend up gullies or small canyons where they indicate an attitude of the plane of movement of about 5° to 20° southeastward toward the mountain mass with a probable average dip of about 15° . Throughout most of its extent, the zone of scarplets and bucklings follows the exact base of the steep mountain front along the contact between quartz diorite above and alluvium below. Only at the west end do the scarplets appear to

die out into alluvium, but mapping indicates that here also the elevated southeastern block is underlain either on the surface or at shallow depths by quartz diorite.

It seems clear that a thrust fault is indicated by the 5-mile-long zone of scarplets and pressure ridges at the base of the granitic scarp of Bear Mountain. Crustal shortening is definitely indicated, not only by the pressure ridges and miniature overthrusts, but in one instance by a fence crossing this zone of buckling in which several posts were pushed several inches toward each other, leaving the wires sagging. There is some doubt as to whether this zone of surface thrusting is an actual thrust movement on the White Wolf fault, or whether it is the result of landslide or earthflow movement of shattered material from the steep slope of Bear Mountain, as it was interpreted by Buwalda (1952, p. 5). Support for the latter interpretation is found in the generally shattered condition of the quartz diorite and resulting landslide topography of the steep northwest slope of Bear Mountain, and by the occurrence of this zone of thrusting only at the base of this high, steep slope. However, the following evidence seems to indicate thrust rather than landslide movement:

- (1) Not all of the lower northwest slope of Bear Mountain is characterized by landslide topography, but much of this slope rises abruptly from the base and is intact.
- (2) There is no large scale rupturing or separation of material upslope on Bear Mountain from the zone of buckling as would be expected if the buckling at the base of the steep slope resulted from downward movement of material from upslope.
- (3) The quartz diorite is shattered only on the lower slopes of Bear Mountain and is generally intact elsewhere.
- (4) The plane of movement is not horizontal nor does it dip downslope, but dips into the mountain throughout its course at an average angle of about 15°.
- (5) The White Wolf fault at the base of Bear Mountain has all the characteristics of a reverse or thrust fault, similar to the Pleito thrust, and not of a normal fault, as its course is irregular—the bedrock immediately above it is highly shattered and the scarp is characterized by numerous landslides as is always true of thrust fault scarps.
- (6) The July 21 earthquake failed to move any of the large landslides on the steep northwest slope of Bear Mountain, a fact indicating that even large landslides are superficial features developed only during or following periods of heavy rainfall.

It is concluded that the zone of surface thrusting at the base of Bear Mountain is most likely the result of actual thrust movement on this portion of the White Wolf fault along which the mountain block was thrust upward and toward the San Joaquin Valley about 3 feet on July 21, 1952.

The zone of rupturing along the northeastern 6 miles of the White Wolf fault between the White Wolf ranch house and the railroad tunnels east of Bealville is characterized by ruptures quite different from those of the central portion. The fractures of the northeast portion did not follow the exact trace of the fault, but occurred as vertical ruptures en echelon along and oblique to it with a more northerly trend. Between the White Wolf ranch house and the Bealville road there are two or three series of north-trending vertical fractures 1 mile to 3 miles long. These fractures developed as small pressure ridges or ruptures in the soil indicating left lateral movement (west block moved south relative to east block) in every case, with fences and highways offset a foot or two. These fractures did not form scarplets except in irregular topography, in which the scarplets

faced either direction, depending on the direction of slope, and always indicated left lateral displacement. The consistent left lateral offsets on these ruptures show them to be true fault cracks formed by tectonic movements rather than landslide cracks formed by earth settling movements.

Between the Bealville road-U. S. Highway 466 intersection and Tehachapi Creek, the White Wolf fault is within quartz diorite and the steep northwest-facing scarp gradually disappears rendering this portion of the fault difficult to locate. Its position is believed determined by an alignment of saddles and small canyons extending north of east from the road intersection, and also by the highly sheared, crushed and shattered condition of the quartz diorite on the north side of this alignment. In the July 21 earthquake fractures developed in the shattered quartz diorite immediately north of this supposed fault trace. The fractures between the road intersection and Southern Pacific Railroad Tunnel 5 trended generally northeast and showed evidence of left-lateral displacement and strong compressive movement indicated by contortion of the rails into S-shaped curves and shortening at tunnel 3 east of Bealville. On the south slope and crestal portion of the large hill through which tunnel 5 passes there were four parallel fractures trending west of north for half a mile and dipping steeply north (see photographs, Part III, Contribution 6). On each of these fractures the northern or uphill side slipped down so that movement on each one formed a gaping fissure up to 6 inches wide and a scarplet up to 2 feet high facing northward upslope. There was no evidence of lateral slip. These are probably minor tensional cross faults to the main course of the White Wolf fault, or might be the result of gravitational settling or lurching of shattered quartz diorite northward toward Tehachapi Canyon.

There is no topographic or structural evidence that the White Wolf fault extends beyond Tehachapi Creek although one small northeast-trending crack formed on the lower northeast slope of the canyon. One large north-trending crack extending about 1000 feet developed across the Tehachapi-Caliente divide, along the contact between quartz diorite and the Bealville conglomerate. This crack dips steeply west and formed a 3-foot scarp facing west.

In Caliente Canyon many very small north-trending cracks formed across the road in shattered quartz diorite for about a mile east of Harper Canyon. These appear to be fractures along jointing in the quartz diorite with no movement indicated.

On the southwestern portion of the White Wolf fault fractures developed along the northwestern base of the hills at Comanche Point and again at the mouth of Little Sycamore Canyon. Others developed about a mile south of the White Wolf fault near the mouth of Comanche Creek and in the foothills to the east. All these fractures were vertical or steep and produced northwest-facing scarplets up to a foot high.

At Comanche Point the alignment of scarplets followed the northwest base of the hills for a mile and the scarplets were vertical and up to 8 inches high. Some showed a small lateral component of movement of several inches.



FIGURE 5. Severe cracking in water-saturated low terrace in lower Comanche Creek; apparently east of White Wolf fault. Photo by Gordon B. Oakeshott.

The scarplets at the mouth of Comanche Canyon and in the foothills to the east were vertical and up to 8 inches high with no lateral motion indicated. These cracks did not seem to follow any definite alignment, but tended to be parallel to the northeast strike of the Chanac formation here. They may have been secondary effects produced by settling movements. At the springs near the mouth of Comanche Canyon, the alluvium was broken by numerous cracks, some of which produced small mud volcanoes of fine sand. These cracks could not be traced into the hills on either side of the canyon; they were obviously produced by lurching of the water soaked alluvium.

At the mouth of Little Sycamore Canyon a continuous zone of rupturing up to 70 feet wide was strongly developed on the White Wolf fault for a mile and a half along the base of the foothills. On the side-hill to the southwest a series of pressure ridges formed in the soil. From the mouth of the canyon northeastward the fracture zone followed the edge of the valley alluvium and was developed as a series of northwest-facing scarplets up to a foot high indicating an overall uplift of the southeastern block of $1\frac{1}{2}$ or 2 feet. The fractures were vertical or dipped steeply southeast, and nearly all showed left-lateral offsets up to 8 inches. In places where no defined scarplets were formed, especially where the fracture zone was dying out northeastward, the hard dry soil was broken by a series of an echelon north-trending gaping ruptures. These were tension ruptures

produced by left lateral motion (southeast block moved northeastward) along this portion of the White Wolf fault.

The fracturing of both Comanche Point and at the mouth of Little Sycamore Canyon was no doubt developed along the trace of the White Wolf fault, and indicated oblique movement on this portion along which the southeastern block was elevated up to 2 feet and displaced northeastward about half a foot. There is some doubt as to whether these fractures represent actual movement on the fault or gravitational settling of the thick valley alluvium, but the generally consistent left lateral displacement on so many of these fractures is difficult to explain by movements other than tectonic or fault movements.

The ruptures along the course of the White Wolf indicate a displacement of as much as 3 feet on July 21, on which the southeastern block was elevated and shoved laterally to the northeast. However the displacement at depth at and near the focus was probably much greater than that at the surface, as indicated by the fractures, as the displacement probably decreased upward and in many places failed to reach the surface. In the valley area southwest of Comanche Point past which the fault is believed to extend, the displacement may have been completely absorbed by the thick sedimentary fill; this could account for the total absence of fractures there.

Total Displacement. The amount of total vertical displacement on the White Wolf fault is indicated by the height of the Bear Mountain scarp on the elevated block plus the depth to the basement complex of the relatively depressed block, or the difference of the depth to the basement complex of each block where covered by Tertiary sediments. Depth to the basement complex under the alluviated valley floor is indicated by subsurface contours on the geologic map, based on points on the top of the basement complex as encountered in all wells that reached it. From a study of the geologic map, it may be seen that the total upward displacement of the southeast block of the White Wolf fault increases rapidly from none at Tehachapi Canyon to 5,000 feet or more at the base of Bear Mountain, and 10,000 feet between the mouth of Little Sycamore Canyon and Comanche Point. Southwest of Comanche Point the displacement is unknown, but it probably decreases.

Some left lateral displacement on the White Wolf fault is indicated by movement on the fault fractures as mentioned. However, the total overall lateral displacement must be small, probably not over 2000 feet. The easterly pinchout of the Santa Margarita sand is in about the same position on either side of the fault and therefore is not appreciably offset. There are no definitely offset streams along the course of the fault.

Dip of Fault Plane. The dip of the White Wolf fault plane is to the southeast as indicated by both the surface ruptures and by the physiographic expression of the landslide-covered Bear Mountain escarpment. The amount, as indicated by the ruptures, ranges from 10° to 90° . The ruptures indicate a low dip for the central portion and a high dip for the southwestern and northeastern portions. Perhaps the overall dip may best be indicated by the location of the epicenter—if accu-



FIGURE 6. Mud volcanoes along cracks in water-saturated low terrace in lower Comanche Creek; apparently east of White Wolf fault. Photo by Gordon B. Oakeshott.

rately determined. According to St. Amand (oral communication, November 1952), one important epicenter was located almost directly under Bear Mountain at about 12 miles below sea level. Projecting this position up to the nearest surface trace would determine a dip of about 70° southeast.

From the foregoing it appears that the only surface fractures that represent the true dip of the White Wolf fault are those at and near the mouth of Little Sycamore Canyon. The low angle thrust feature at the base of Bear Mountain must then be a local flattening of the fault at the surface where the elevated mountain block partially overrode the San Joaquin Valley area. The north-trending left lateral fault cracks along the northeastern portion of the White Wolf fault probably branch off from the main fault below the surface and were produced by upward and northeastward movement of the southeastern block.

Type of Fault and Movement. The foregoing data indicate the White Wolf fault to be a high angle reverse fault dipping southeast along which the southeastern block was elevated to a maximum displacement of some 10,000 feet and displaced a much lesser distance to the northeast—relative to the stationary northwestern block. The low-dipping thrust fault rupture along the central portion of the fault indicates that the northwestern or footwall block is stationary and that the southeastern block was actively elevated and thrust northwestward. This is further suggested by the intensity of the earthquake of July 21, 1952, which was more violent in the area southeast of the White Wolf fault than in the area to the northwest.

Possible Northeastward Extension. There is neither physiographic nor geologic evidence that the White Wolf fault extends northeast of Tehachapi Canyon and there is no evidence that the White Wolf fault ties to the Breckenridge Mountain fault. However, between the Tehachapi and Caliente Canyons several isolated ruptures trending nearly northward did develop in shattered quartz diorite. These may have formed along one

or several north-trending branches of the White Wolf fault that might extend at depth as far northward as Caliente Canyon.

Possible Southwest Extension. The extent of the White Wolf fault southwesterly from Comanche Point is unknown as there is no direct surface indication of this fault beyond that point, and no surface ruptures were formed during the earthquake of July 21, 1952. The White Wolf fault apparently does not reach the surface anywhere southwest of Comanche Point. However, stratigraphic, structural, subsurface, geophysical and seismic evidence indicate or suggest that the White Wolf fault does extend southwestward across the San Joaquin Valley and at depth under Wheeler Ridge and the San Emigdio foothills, possibly to the San Andreas fault. The exact location of this buried portion of the White Wolf fault is as yet unknown, but available evidence indicates it to maintain the same $S 50^\circ W$ trend as does the exposed portion between Tehachapi Canyon and Comanche Point.

Evidence that the White Wolf fault extends southwest from Comanche Point across the southeastern San Joaquin Valley to Wheeler Ridge is—(1) the 10,000 foot displacement at Comanche Point, indicating the fault to extend far beyond that point; (2) the abrupt change of the water table at the supposed trace of the fault across the valley; (3) differences in depth of geophysical reflections on either side of this buried fault; and, (4) the much greater depth to the base of the Plio-Pleistocene continental sediments in the valley area on the northwest side of the buried fault as encountered in deep wells in which the maximum drilled depth to this horizon is 14,000 feet on the northwest side of the fault and 4,000 feet on the southeast side. Although no well has reached the basement complex in the deeper portion of the valley area on either side of the fault, the marine formations underlying the continental Pliocene strata are consequently much more deeply buried under the valley area on the northwest side of the supposed extension of the White Wolf fault than on the southeast side. The great difference in thickness of the

Plio-Pleistocene continental series on opposite sides of this fault indicates it to have been active during deposition of those sediments.

Evidence that the White Wolf fault extends under Wheeler Ridge is as follows: (1) seismic—the occurrence of the main epicenter (St. Amand and Buwalda, 1953) of the July 21 earthquake, under the southwestern portion of the Wheeler Ridge anticline (latitude $35^{\circ} 00'$, longitude $119^{\circ} 02'$), at a depth of about 10 miles indicates that the White Wolf fault plane must pass through that point; (2) stratigraphic—the White Wolf fault probably passes under the northwestern portion of the Wheeler Ridge anticlinal uplift as the thickness of the Plio-Pleistocene series is about 4,000 feet on this structure, or about the same as in the adjacent valley area to the east, while it is over 12,000 feet thick in the valley area to the north; also a well drilled at the west portion of the Wheeler Ridge anticline reached the basement complex at a depth of about 12,000 feet while the basement complex is probably more than twice as deep in the valley area to the north; (3) structural—faulting under the north flank of the Wheeler Ridge anticline is suggested by its steep dip, and also by the occurrence of southward-dipping minor reverse faults under this asymmetric fold as encountered in deep drilling; faulting under the southward-plunging portion of this anticline is suggested by the northeast-trending alignment of small sharp east-trending subsidiary folds, which appear to be the result of left lateral movement on the White Wolf fault, or one aligned with it, at depth in the basement complex.

Evidence that the White Wolf fault may extend from Wheeler Ridge southwestward under the San Emigdio foothills at depth is suggested by the sharp upturning and intense folding of the Cenozoic sediments along these foothills. This disturbed zone is joined by the Pleito fault from the southeast, which here curves south of west to follow this zone of disturbance for some 12 miles nearly to the San Andreas fault, as mapped by Hoots (1930, map). Along this trend the Pleito fault steepens to over 50° as indicated by a well drilled in Pleito Canyon, and the basement complex is brought to the surface on the elevated southern block west of San Emigdio Canyon. This portion of the Pleito fault and the adjacent zone of sharp folding on the footwall block are aligned with the White Wolf fault, suggesting this zone of disturbance to have formed along or over the deeply buried White Wolf fault zone in the basement complex below.

While detailed mapping indicates that the Pleito fault zone does not extend to the San Andreas fault, nevertheless a distinct bend or curve concave northeast is developed in the San Andreas where the Pleito fault, or the underlying White Wolf fault zone, would intersect it if projected to it. Northwest from that point the San Andreas fault trends consistently $N 45^{\circ} W$, and to the southeast it trends $N 60^{\circ} W$. Although this bend is not sharp it is noteworthy in being the greatest deviation of trend in the San Andreas and suggests that this rift zone is intersected by the White Wolf fault at depth, that the bend may have resulted from left lateral movement on the buried White Wolf fault, and that the Pleito



FIGURE 7. Cracks and scarplets in White Wolf fault zone, Tejon Hills, just northeast of Comanche Creek. Photo by Gordon B. Oakeshott.

fault zone developed partly from uplift of the southeastern block on the White Wolf fault below.

Age of the White Wolf Fault. The White Wolf fault appears to have been most active during Pleistocene and Recent times. It may have been active during most, if not all, of Pliocene time as indicated by the much greater thickness of the Pliocene sediments of the San Joaquin Valley throughout the northwest block as compared to the southeast block as encountered in deep drilling. The fault may have been initiated in Miocene time, although there is as yet no definite evidence.

Regional Tectonics

The tectonic movements active in this area are the result of constant regional strain in this part of the earth's crust. The mapped area lies at the juncture of three great physiographic provinces—the Sierra Nevada, Great Valley, and Coast Ranges provinces. Adjacent ones are the Basin Ranges province to the east, Mojave Desert province to the southeast, and Transverse Ranges province to the south. Each one of these physiographic provinces is also a tectonic province, characterized by a well defined strain pattern, so that within the mapped area several related strain patterns exist.

Sierra Nevada-Great Valley Provinces. The Sierra Nevada-Great Valley province is made up of crystalline rocks stabilized during the Jurassic Nevadan orog-

eny to a comparatively rigid, compact mass and is overlain by a generally little disturbed Cretaceous-Cenozoic sedimentary series under the Great Valley. This large, rigid segment of the earth's crust has resisted tectonic movements; only in the extreme southern portion, where tectonic movements have been more severe, has it yielded by faulting.

The southern Sierra Nevada, bounded on the east by the Sierra Nevada normal fault zone, is partly broken into two major north-trending blocks by the normal Kern Canyon-Breckenridge fault zone.

Southeastern San Joaquin Valley. The mountainous areas surrounding the southeastern San Joaquin Valley are undergoing active uplift. These are rising portions of the earth's crust caused by constant, deep seated compressive and shear movements active throughout Quaternary time on the San Andreas, Garlock, and related faults. Earthquake-producing displacements have occurred on these faults several times in a century, and an earthquake produced by slippage on one may set off movement on another. This apparently happened during the recent earthquake in which the movement on the White Wolf fault that produced the shock of July 21, 1952, may have set off movement on a minor buried fault southeast of Bakersfield that caused the Bakersfield earthquake of August 22, 1952. It is also possible that many of the aftershocks of the first earthquake may have been caused by movements on minor faults in the vicinity of the White Wolf fault.

The southern Sierra Nevada foothills and eastern San Joaquin Valley northward from the White Wolf fault are cut by many parallel faults trending northwest to north. In the area south of the Kern River the faults trend generally northwest, and north of the river, tend to swing north. They trend due north in the Kern Front oil field area north of Bakersfield. This makes a broadly arcuate pattern. The great majority of these faults are of normal type although some are probably vertical or even steep reverse. Many of the northeast-dipping normal faults bound southwest-tilted blocks as indicated by the steepened southwesterly dip of the Tertiary sediments involved. These faults are of the same type as the major faults of the Sierra Nevada and displacements are probably mostly if not entirely vertical, although there are evidences of some lateral movements.

The southern Sierra Nevada is broken by only two widely spaced major normal faults—the Sierra Nevada and Kern Canyon-Breckenridge; while the adjoining foothill area is broken by moderately spaced normal faults of moderate displacement, the largest being the Kern River and Edison faults. The eastern margin of the adjacent San Joaquin Valley is broken by faults more closely spaced and with very small vertical displacements. From northeast to southwest the faults become progressively more closely spaced and their vertical displacements appear to decrease outward into the San Joaquin Valley.

The extreme southeastern portion of the Sierra Nevada-San Joaquin Valley provinces was elevated as a block on the northeast-trending White Wolf fault to form the Bear Mountain-Tejon Hills uplift. The Tehachapi Mountains are in part a compressive uplift formed against the northeast-trending Garlock fault, a

master shear zone separating the Sierra Nevada from the Mojave Desert province to the southeast. Nearly all of the movement on the Garlock fault has been left lateral, along which the Mojave Desert block has moved relatively northeastward. This would indicate a great north-east-southwest counterclockwise torsional stress. The Garlock fault took up nearly all this stress between these two provinces of crystalline rocks. However, a small part of this stress was taken up on the White Wolf fault as indicated by the small left lateral component of movement on it.

The area between the White Wolf and Garlock faults has undergone some northwest-southeast crustal shortening, as indicated by the northerly or northwesterly movement of the Bear Mountain uplift on the southeastward-dipping White Wolf fault, by east-west folding in the Tejon Hills, and by the compressive uplift of the Tehachapi Mountains against the Garlock shear zone. This would suggest a north-south compressive stress.

The pattern of slightly to moderately tilted north-northwest-trending fault blocks is similar to that of the Basin Ranges province so that both areas are apparently under the same stress. However, too little is known to determine what stress formed this pattern. The normal faults indicate, at least near the surface, an east-west tensional stress yet the mountain blocks seem to be actually rising as if heaved up from below while some of the valleys (such as Death Valley) are apparently sinking. The most plausible hypothesis that can be offered is that the entire combined Sierra Nevada-Basin Ranges province constitutes a thick segment of the earth's crust which was arched upward probably by a very deep-seated east-west compressive stress; and that the upper portion of this thick segment became broken into north-south trending blocks, some of which failed to rise, or even sank. During this arching process, the western margin became compressed downward to form the Great Valley. In the eastern San Joaquin Valley, the arcuate pattern of faults with the trends gradually swinging from south to southeastward suggests that southward the subterranean stress was directed progressively more from an east-west to a northeast-southwest direction.

The extreme southeastern portion of the Sierra Nevada-Great Valley province is thus affected by three stresses: (1), a deep subterranean east-west and/or northeast-southwest compressive (?) stress; (2), a north-east-southwest counterclockwise torsional stress; and (3), a relatively shallow north-south compressive stress.

Coast and Transverse Ranges Provinces. In the San Emigdio Mountains, the strain pattern is one of extensive north-south crustal shortening as indicated by northward movement of the San Emigdio uplift on the southward-dipping Pleito thrust fault and by the strongly compressed folds in Cenozoic strata with axes trending slightly north of west. The crustal shortening developed in the Tehachapi Mountains progressively increases westward into the San Emigdio Range as indicated by the increasing amount of movement on the Pleito fault and increasing deformation of the Cenozoic strata westward. This pattern is obviously the result of a severe compressive stress directed from the south or slightly west of south, and is progressively more intense west of that active in the Tehachapi Mountains.



FIGURE 8. View west toward Jones ranch house, showing cracks in alluvium. These cracks are not parallel to the fault trace but are in an area of extensive lurch cracking on the valley floor. At Edison Road about 4 miles southwest of Arvin. *Photo by Lawrence W. Chasteen.*

The San Emigdio Range, the southeasternmost member of the Coast Ranges province, is a compressive uplift built up against the San Andreas fault, as are all of the Coast Ranges adjacent to this great right lateral shear zone. The strain pattern of the San Emigdio Range is thus typical of that throughout the Coast Ranges province.

In marked contrast to the rigid Sierra Nevada-Great Valley province, the Coast and Transverse Ranges provinces together are a great zone of weakness in the earth's crust. It is an unstable zone of intense crustal shortening and shearing in which the San Andreas fault is the greatest single rupture.

In the Coast Ranges province the strain pattern is composed of several faults of the San Andreas type, that is, northwest-trending vertical or high angle shear faults with right lateral displacements of which the San Andreas is the largest and most active, and a series of tightly squeezed folds trending slightly west of north-west and some reverse or thrust faults with a similar trend. The San Andreas type faults are deep-seated ruptures originating many miles deep in the basement complex. Several of these faults were active throughout Cenozoic time with cumulative right lateral movements amounting to many tens of miles (Hill and

Dibblee, 1953, pp. 443-458). These great shear faults must be the result of a northwest-southeast clockwise torsional stress. The compressive folds and lesser reverse or thrust faults are comparatively shallow structures affecting the Cretaceous-Cenozoic strata and are most intense and numerous adjacent to or near the great shear faults and decrease outward away from them—as in the San Joaquin Valley. These compressive structures must therefore be subsidiary to the master shear type faults and were formed by an east-northeast west-southwest compressive force resulting in part from right lateral horizontal drag on the shear faults and in part from pressure and counterpressure of the opposing fault blocks.

In the Transverse Ranges province, the strain pattern is basically the same as that of the Coast Ranges province except that the folds and reverse or thrust faults trend more nearly east and in addition there are several major shear type of oblique slip faults trending slightly south of west with left lateral movements similar to the Garlock and White Wolf faults. This would indicate, in addition to the stresses active in the Coast Ranges province, that the northeast-southwest counter-clockwise torsional stress active along the Garlock shear zone across the San Andreas fault affected the Transverse Ranges province also.

Tectonic Implications of the Strain Patterns. Tectonic implications and relationships of the San Andreas, Garlock and other major strike-slip faults and related structures are discussed by Hill and Dibblee (1953), who suggest that they are genetically related and resulted from an overall single regional north-south stress.

It is concluded that the White Wolf fault is genetically related to the Pleito and Garlock faults and possibly in part to the San Andreas fault, but not to any of the faults to the north. Both the White Wolf and Pleito faults are in part the result of compressive stresses developed along both the Garlock and San Andreas shear zones. This is indicated by the southward dip of both faults toward the great shear zones and squeezing of the area between these faults and the shear zones. The White Wolf fault is believed to be closely related to the Garlock fault as indicated by its northeast trend parallel to it, southeast dip toward it, and by evidence of left lateral movements on both. The bending of the great San Andreas shear zone at both points where it is, or may be, intersected by the Garlock and White Wolf faults implies that both these northeast-trending faults are deep seated zones of weakness along which the rigid Sierra Nevada-Great Valley block is being pushed southwestward relative to the Mojave Desert block.

3. KERN CANYON LINEAMENT

BY ROBERT W. WEBB *

Introduction. The recent earthquakes in the Tehachapi area of the southern Sierra Nevada have refocused attention of geologists on this critical area of California structure. The recent summary of the Arvin-Tehachapi earthquake (California Division of Mines, 1952), calls attention to what may be a structural pattern in a series of faults (Jenkins, 1938; Nugent, 1942) whose geological relationships have never been established. The faults in question are known as the White Wolf, Breckenridge Mountain, Havilah Valley, Hot Springs, and Kern Canyon faults. The regional topographic pattern of these faults and the inter-segments between them will be referred to as the "Kern Canyon lineament." It seems pertinent to examine what is known currently about the structural pattern and to suggest a possible interpretation for the apparent pattern.

Geography of the Faults in the Lineament. The disconnected fault zones and inter-segments that appear to compose a structural lineament extend from the Tejon Hills in the southern San Joaquin Valley, northeastward and northward for more than 100 miles, beyond the headwaters of the Kern River. The faults have been studied, and evidence (Hoots, 1930, pp. 301-319; Lawson, 1906; 1904, pp. 291-376; Webb, 1936) for them presented. Between these are apparently unfaulted segments, none of which has been mapped in sufficient detail to prove positive connection, at least in the present-day structural pattern; other inter-segments are unmapped.

Historical Background. The first recognition of an important fault in the Kern River Canyon was by Lawson (1904), in the first of a series of three papers, discussing faulting in the upper Kern Basin. In a second paper (1906) he presents his observations made in the middle Kern Basin, the Havilah Valley, and Walker Basin, which suggested to him the apparent importance of faulting. A connection between the northern (Kern Canyon) faults and those in the Havilah and Walker regions was tentatively postulated. In his third paper on the Tehachapi Range (Lawson, 1906a) he recognized the important Tehachapi (White Wolf) fault, and raised the possibility of a connection between the earlier described faults and the White Wolf, although no connection between any of these faults was seriously implied, since he did not undertake geologic mapping. In 1922, the publication of a structural map of California (Seismological Society of America, 1922) showed the White Wolf fault, and that part of the Kern Canyon fault from the mouth of Golden Trout Creek nearly to Fairview, as "dead fault, well located;" the Breckenridge fault is symbolized as "probable fault, character and location uncertain." Additional geologic studies were not published until 1928, when faulting was mentioned incidental to other geologic problems (Hake, 1928; Miller, 1931). The White Wolf fault was mapped in 1930 (Hoots, 1930), and the Kern Canyon fault studied in 1936 (Webb, 1936). Interest in damsites along the Kern

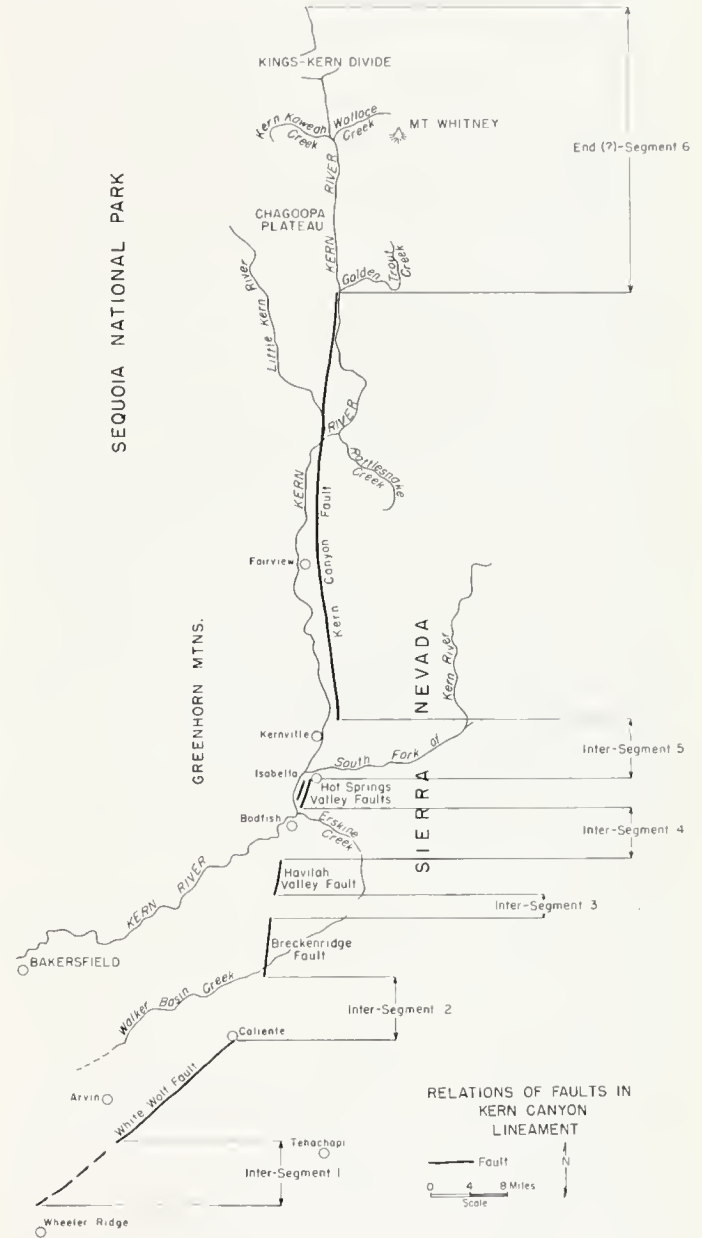


FIGURE 1.

River was revived, and several reports appeared¹ (Marliave, 1938; Treasher, 1949, 1949a). Significant information on faulting in Hot Springs Valley, at the site of the new Isabella Dam near the junction of Kern, and South Fork of Kern River will appear with the full publication of these studies. A geologic map of the Kernville quadrangle was published in 1940 (Miller and

* Professor of Geology, University of California, Santa Barbara. Manuscript received for publication December, 1952.

¹ Holdredge, Clair, Personal communications, July 19, 1949, and Oct. 7, 1949.

Webb), and included the southern part of the Kern Canyon fault and some observations on the Hot Springs fault; the influence of faulting in the mines in the vicinity of Kernville was discussed in a paper on the Big Blue mine (Prout, 1940); and the northern section of the Kern Canyon fault was mapped in 1946 (Webb, 1946). It is evident that no published work to date justifies the assertion of a single fault; nor of the connection of the separate faults into a master structure.

The map of California accompanying the text on the Arvin-Tehachapi earthquake (California Division of Mines, 1952, p. 2) is the first known to the writer since the 1922 map cited above that clearly shows the White Wolf fault as a separate and distinct structure, based on geologic mapping by Dibblee (Dibblee and Chesterman, 1953) in one of the critical inter-segments.

Interpretation of the Lineament. Although the relationship between the White Wolf, Breckenridge, Havi-lah Valley, Hot Springs Valley, and Kern Canyon faults is imperfectly known, the topographic patterns suggest a regional plan of the faults. The relation to the curving southern end of the Sierra, where the Sierra Nevada fault system and the Garlock fault system merge, seems significant. Also, if such superficial evidence as slickensides and epidotized joints is accepted, faulting can be demonstrated in segments between recognized faults. Reconnaissance in intersegments shows that the rocks involved are almost exclusively of the massive plutonic type, whereas faults are reflected in areas where the basement complex includes many pen-dants and residual areas of metamorphic rocks.

Faults arranged in a lineament, with evidence of ancient or recent movements on some faults and little or

no evidence of faulting in rocks of inter-segments might be explained by a geologically ancient continuity of the faults, with no necessary current relation of faults of a former continuous structure. An explanation of an ap-parent regional pattern might be found if the nature of fault decline with depth were understood.

The roots of a major fault of regional proportions originally continuous in a rock cover now stripped from an uplifted land mass, might be evidenced by residual segments, parts only of the original fault. The struc-tural effects of fault movement, such as measurable dis-placement and drag, slickensides, gouge, and brecciation, effective to differing depths and in differing degrees as the original fault descended into changing rock types of the block would thus be discontinuous.

The Sierra Nevada might be such a block, thus faulted and denuded.

The assumption so often repeated in map and text of a major continuous fault, extending from the head-waters of the Kern River on the north to the San Joa-quin Valley on the south through more than 100 miles will not easily be dispelled. Though the possibility of a direct present relationship between separate faults known in this regional lineament must be admitted, the concept of a single structure important in today's geol-ogy should be abandoned. The suggestion that the faults known today may be remnants of an ancient, and origi-nally continuous, fault, developed in the cover rocks of the ancient Sierra Nevada, is advanced as a plausible explanation of the topographic lineament. Understand-ing of this lineament, like so many of the faults of re-gional geologic maps, rests, like all other geologic prob-lems, on completion of detailed geologic mapping.

4. NATURE OF MOVEMENTS ON ACTIVE FAULTS IN SOUTHERN CALIFORNIA

BY MASON L. HILL *

Abstract. The principal fault types of southern California are right lateral, left lateral, reverse, and thrust faults. Some of the northwest-trending right lateral and east-northeast-trending left lateral faults are known to have strike-slip movement. Some of the reverse and thrust faults are likewise known to have mainly dip-slip movement. Many of the faults are probably characterized by oblique-slip movements where both the dip-slip and strike-slip components are relatively substantial.

Most, if not all, faults in southern California are potentially active. Movements on the large lateral faults, which have substantial strike-slip components of movement, are possibly responsible for much of the strong seismic activity in this region. Many of the reverse and thrust faults of outcrop, especially those associated with folded sediments, probably die out before reaching the focal depths of important southern California earthquakes.

The active White Wolf fault, being parallel to the left lateral-slip Garlock fault and conjugate to the right lateral-slip San Andreas fault and being steep and deep, is probably characterized by a substantial left lateral component of movement.

Introduction. The Arvin-Tehachapi earthquake of July 21, 1952, resulted from a movement of uncertain nature on the supposedly inactive White Wolf fault. Thus we were shockingly challenged with important tectonic problems. In this case: what was the nature of the movement and why did it cause a major earthquake? In the general case: which other faults in southern California could develop similarly surprising seismicity?

The principal objectives of this discussion are to indicate that the true nature of movements on, and the current activity of, faults are difficult to determine, and that lateral faults, with substantial strike-slip components of displacement, are possibly the most important breeders of major earthquakes in this region.

The writer acknowledges the use of considerable Richfield Oil Corporation field mapping, mainly by T. W. Dibblee, Jr., and the advice of Hugo Benioff, Marie Clark and Rollin Eckis, who have read the manuscript.

Fault Terminology and Classification. A fault is a fracture in the earth along which movement has occurred. Faults are more or less planar with strikes in any direction and dips from horizontal to vertical. The prime criterion for recognition of a fault is offset (separation) of geologic features. Although the orientation is rarely ascertained, relative displacement is described as dip-slip, strike-slip, or oblique-slip with reference to the attitude of the fault plane (zone). For faults other than vertical, the block above the plane is called the hanging wall and below the plane, the foot wall. Faults are caused by rock-rupturing stresses but the nature (tensional, compressional, etc.) and origin (gravity, contraction, etc.) of these stresses is very rarely known.

A purely geometric classification (more practical than genetic or slip classifications) based on apparent relative displacement (separation), is as follows (Hill, 1947):

Normal: In vertical section, hanging wall is relatively and apparently down—including vertical faults.

Reverse: In vertical section, hanging wall is relatively and apparently up—restricted to faults that dip more than 45° .

Right lateral: In horizontal section, side opposite observer is relatively and apparently to the right.

Left lateral: In horizontal section, side opposite observer is relatively and apparently to the left.

Thrust: Any fault which dips less than 45° and evidences dip-separation and horizontal shortening.

Right (or left) lateral normal (or reverse or thrust): These names for the six combination types are recommended when both strike and dip separations are known.

Because of the scope of this paper, which deals with the relative sense of movements on active faults, and because there is evidence of the nature of the movements on some of the discussed faults, it might appear advisable to use here a relative movement classification (dip-slip, strike-slip and oblique-slip faults). However, since in the usual case there is no definite evidence of the nature of movement, and since in some of the cases discussed the evidence is not conclusive, the geometric classification (based on separation) is used, with the addition of the relative movement (slip) terms where possible.

Faults in Southern California. The major fault of the region is the San Andreas. This is, however, only one of a set of northwest-trending right lateral-slip faults present. Other principal sets are east-northeast-trending left lateral-slip faults (e. g., Garlock fault), and east-west-trending reverse (e. g., the Oak Ridge fault), and thrust (e. g., the Santa Susana fault) faults of dip-slip movement. This grouping is believed to be significant with the right and left lateral faults of east-west relief¹ resulting from north-south shortening as the primary strain system² of the region. The east-west reverse and thrust faults of upward relief result from the same north-south shortening. Other classes and trends of faults occur, but in southern California they do not appear to be major or primary³ structures.

Obviously the above grouping is tentative because data on significant fault characteristics are woefully incomplete, especially orientations of displacement and even locations, extents, and dips of the faults themselves. Also inadequate are data on ages and cumulative displacements on important faults. Other complicating situations comprise the determination of the relative importance of dip-slip and strike-slip components on faults of oblique-slip movement, and the gradation of a fault, along either strike or dip, from one geometric type to another.

A noteworthy aspect of some of the faults in southern California is their transection of geologic provinces. For example, the San Andreas fault cuts through the Coast Ranges, Transverse Ranges and the Colorado Desert without being importantly influenced by diverse rock types and structures. It appears significant that, although most of the faults are confined to separate prov-

* Geologist, Richfield Oil Corporation, Los Angeles, California. Manuscript submitted for publication August, 1953. Published by permission of the Richfield Oil Corporation.

¹ Orientation of maximum relative elongation of the deformed unit.

² The strain system is the unit of deformation which is caused by a single but less readily determined, stress system.

³ Primary structures are those faults which are considered to be caused directly by the regional stress system.

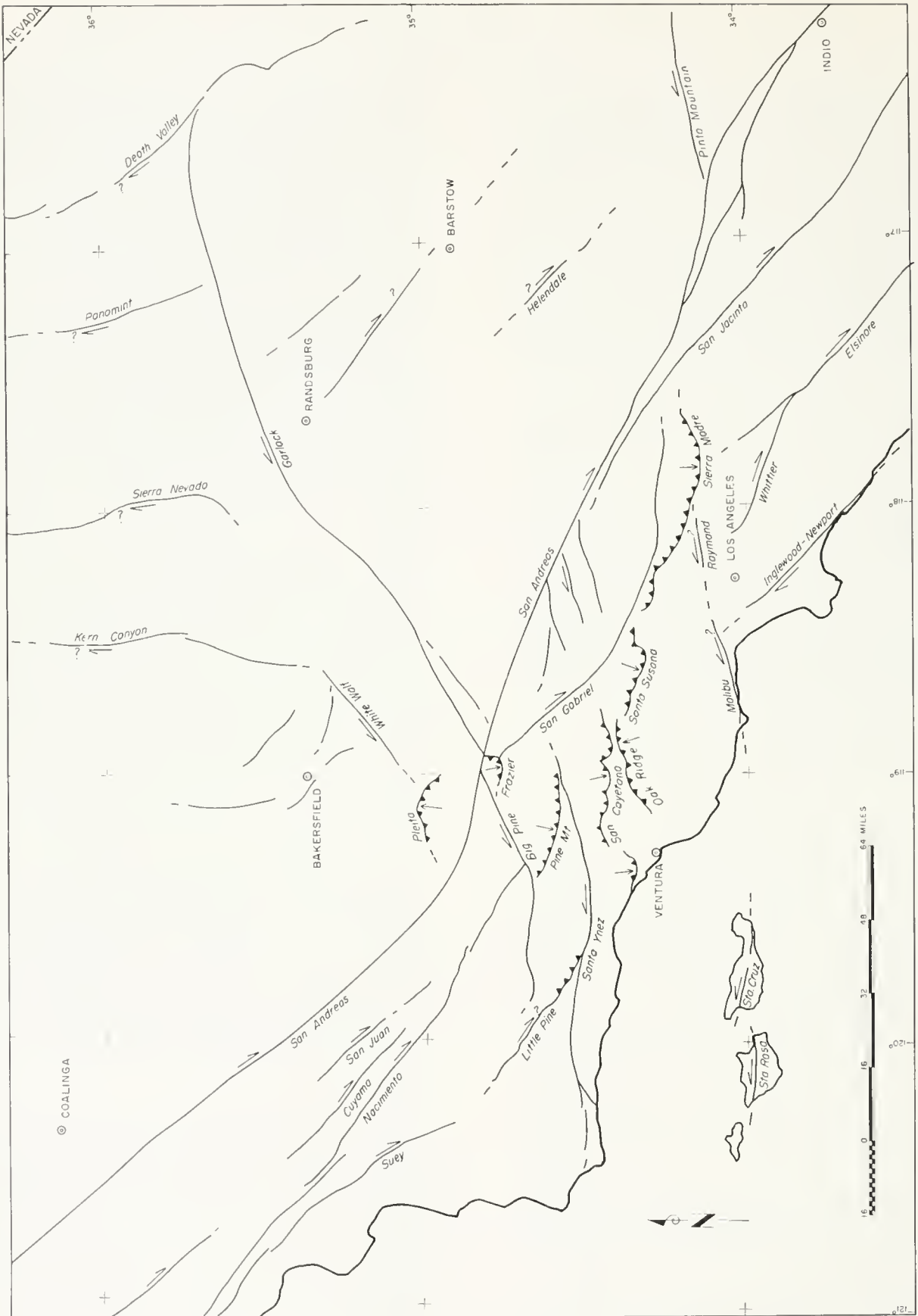


FIGURE 1. Fault map of southern California. Arrows tentatively indicate principal component of relative movement.

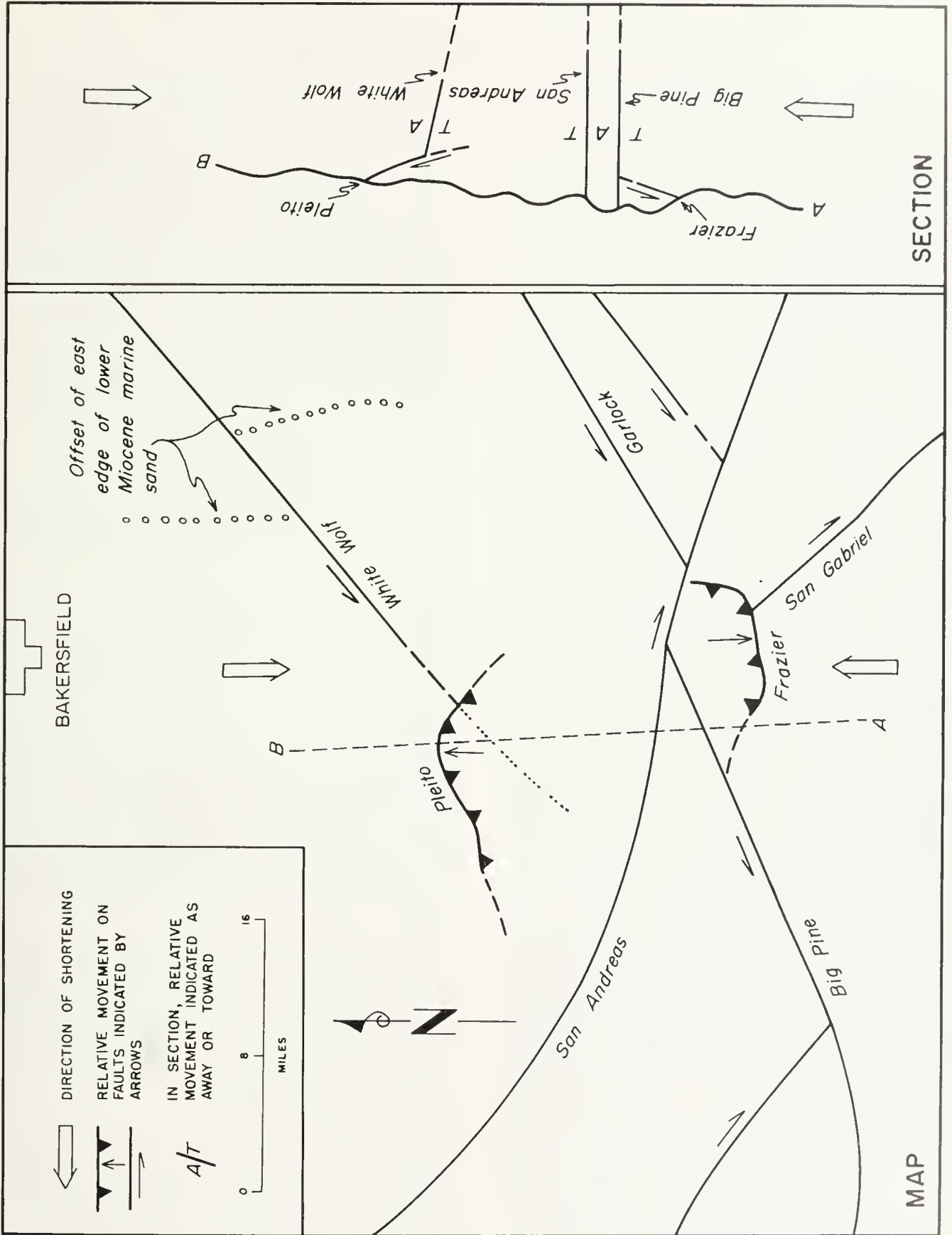


FIGURE 2. Strain pattern map and section.

inces, only the laterals extend through more than one geologic province.

Nature of Movements on the Faults. The orientation and especially the cumulative amount of movement are obviously the most critical geologic aspects of faulting but, unfortunately, the most difficult to determine. Direct evidence of orientation is occasionally manifest at the time of earthquakes. Examples are the right lateral movements of 21 feet (1906) and 10 feet (1940) on the San Andreas fault. Recent movements are also sometimes shown by topographic anomalies, such as scarps and offset drainage lines. Contrarily the sense of movement along the White Wolf fault was not definitely revealed by surface displacements at the time of the Arvin-Tehachapi earthquake nor is the movement clearly revealed by topographic features.

Geologic evidences of orientation are occasionally shown by fault zone features such as striations, fracture cleavage, etc., and adjacent drag folds, feather joints, etc. Other indirect evidences of the nature and amount of movement on faults comprise offsets of rock or structural units. These offsets ordinarily show only the apparent relative displacement and they are usually described in terms of the vertical component (throw). In the case of some lateral faulting, however, indications of sense and amount of strike-slip displacement may be shown by sidewise offsets of the following: basement rock facies, sedimentary facies, stratigraphic thicknesses or sequences, unconformities, faunal facies, deposits from source areas, and offsets of structures.

Recently these criteria have been used to indicate $20 \pm$ miles of right lateral movement on the San Gabriel fault during late Miocene-early Pliocene time (Crowell, 1952a) and possibly several hundred miles of right lateral movement on the San Andreas fault since Jurassic time (Hill and Dibblee, 1953).

As described elsewhere in this bulletin, the minor (2 feet, plus or minus) displacements along and adjacent to the trace of the White Wolf fault at the time of the earthquake indicated, although not clear and consistent, thrust and left lateral movements. However, since the epicenter plot for the 10-mile deep focus is near the southwestern projection of the surface trace, it is obvious that the fault zone is steep. Therefore thrusting is probably only a surface manifestation, possibly developed as a creep effect by the sharp topographic relief between Bear Mountain and the floor of the San Joaquin Valley.

Some topographic evidences of late activity on the White Wolf fault are present, although apparently no worker had suspected it as a seismic threat. The obvious topographic feature along the fault is the northwest-facing Bear Mountain scarp. Also present are saddles and sag ponds (common on lateral-slip faults) and sharp left lateral bends of Sycamore and Little Sycamore Canyons at their mouths.

The prominent topographic and geologic offset is the relatively upward throw of thousands of feet of the southeast (hanging wall) block. This throw, however, may be a relatively surficial component of mainly strike-slip movement at depth and/or the result of the juxtaposition of topographically high and low blocks by such

sidewise movement. In fact, the eastern edge of lower Miocene marine sands appears to be offset several miles in a left lateral sense by the White Wolf fault (see fig. 2). Eocene sediments may have been shifted even further and the upper Miocene Santa Margarita sand can easily be offset by movement which comprises a greater lateral than vertical component. Because of the above, and since this deep and steep fault is essentially parallel to the left lateral-slip Garlock fault, it is here tentatively classified as a left lateral reverse (oblique-slip) fault with the cumulative amounts of strike-slip and dip-slip components as yet undetermined. Furthermore, since the White Wolf fault is nearly perpendicular to the right lateral-slip San Andreas, to which it may extend under the south-dipping thrust faults of the San Emigdio Mountains, it is probably conjugate to it.

Activity of the Faults. Now that we know that the White Wolf fault is active, whereas it had generally been placed in the inactive category, a new inquiry into the locations of potentially active faults seems appropriate. Faults in this region commonly show physiographic evidences of geologically late movements by scarps, trenches, ridges, offset drainage lines, etc. Furthermore, since southern California is tectonically active, nearly all faults are subject to a possible renewal of movement and still other faults could be developed. It appears, however, that movement on certain classes of faults may be responsible for most of the sizeable earthquakes in this region.

Major lateral-slip faults are characterized by great length and steepness and probably extend to depths of at least 10 miles. The reverse and thrust (dip-slip) faults, the other principal types of the region, are relatively restricted in length, are most common in areas of thick sedimentary sections and may ordinarily extend only to relatively shallow depths. Therefore, in this region lateral-slip faults, of which the White Wolf is possibly a member, are perhaps the best candidates for the generation of major earthquakes (above 6 on the Richter magnitude scale and instigated at a depth of approximately 10 miles). However, even if these are the likely earthquake faults, there are so many of them (without including the probable many others which do not reach the surface) that there is no tangible reason for suspecting earthquakes from movement on any particular fault, or in any specific area, in southern California.

Conclusions. Tentative answers to the questions of the first paragraph of this discussion are: (1) a component of left lateral movement probably occurred on the White Wolf fault, and being a deep fault, such movement occurred at the correct depth and involved sufficient energy to cause a major earthquake; and (2) nearly all of the major right and left lateral-slip faults of the region are seismic threats.

A further conclusion is that the determination of sense and cumulative displacement on lateral-slip faults, combined with seismic and geodetic data, are likely to reveal important facts and concepts regarding the geologic history and present tectonic status of the region.

5. GEOLOGICAL EFFECTS OF THE ARVIN-TEHACHAPI EARTHQUAKE

BY JOHN P. BUWALDA * AND PIERRE ST. AMAND *

ABSTRACT

The Arvin-Tehachapi earthquake of July 21, 1952, originated on the White Wolf fault. This fault runs from west of Wheeler Ridge to the vicinity of Harper Peak. The strike is roughly N 50° E; the length is at least 32 miles and it appears to be a steep reverse fault or a thrust. The overall movement seems to be oblique slip, up dip, with a left lateral component of motion. The vertical offset is greater than 10,000 feet.

The geologic effects included landslides, rock falls, changes in ground water and stream flow, lurches and fault trace development. A series of ground ruptures extended intermittently along the length of the fault, except across the alluvium of the San Joaquin Valley, where lurching was developed. At the foot of Bear Mountain the traces were compressional, indicating thrusting of the southeastern block over the valley, coupled with a small component of right lateral movement. Near the White Wolf Ranch a left lateral tear fault crossed the upper and lower blocks of the White Wolf fault. To the northeast of this the fresh displacements on the White Wolf fault were primarily left lateral and tensional. There are, in places, minor exceptions to the general displacements and nearly all the traces are complicated by landsliding.

INTRODUCTION

The Arvin-Tehachapi disturbance was the strongest in California since the San Francisco earthquake of 1906 and in southern California since the Fort Tejon shock of 1857. Because some of the stronger earthquakes in California and Nevada during the past century were accompanied by surface displacements and other geologic and physiographic changes along the faults on which the shocks originated, it was hoped that similar features would be found along the White Wolf fault. This expectation was realized only in part, and the features developed were quite different from those produced in the San Francisco earthquake of 1906, Imperial Valley in 1940, Owens Valley in 1872, and Pleasant Valley, Nevada, in 1915.

Immediately after the earthquake, instrumental parties, under instructions from Dr. Beno Gutenberg, Director, and Dr. C. F. Richter, Seismologist, of the Seismological Laboratory of the California Institute of Technology, located mobile seismographic units at different and changing points in the earthquake area to record aftershocks with a view to securing evidence on exact location, extent, and mechanism of the faulting, depth of foci, and other problems. The authors, at the same time, started an intensive, systematic field investigation of all the geologic and physiographic changes that occurred at the time of the earthquake along the causative fault. This work continued intermittently for 2 months, and was concentrated along the fault zone. Rupture and other phenomena were abundant for several miles on either side of the fault and some attention was given to them, but field work was terminated when it was realized that all of the myriads of surface evidences of ground disturbance could not be studied—the effort had reached the stage of decreasing returns for time invested.

A brief field examination was also made along the trace of the northwest-trending Kern River fault after a rather strong shock, magnitude about 6.5, apparently

occurred on it on July 29, 1952. No evidence of surface fault displacement was found. All the phenomena recorded in this paper are believed to relate to the Arvin-Tehachapi earthquake of July 21, 1952 and possibly to aftershocks centered near the White Wolf fault zone.

Hundreds of ruptures cut the alluvium on the floor of the entire southern end of the San Joaquin Valley at least as far north as points west of Pixley, which is some 45 miles north-northwest of Bakersfield. The authors did not attempt to map these, but other geologists have made careful studies of them in some areas (Warne, Part I, Contribution 6, this bulletin).

In the field study the ground ruptures along the White Wolf fault were traced and mapped carefully from Tejon Hills to Centennial Ridge, 4 miles northeast of Caliente.

Similar features were examined on Wheeler Ridge, toward the south end of the fault, and on Harper Peak, which is 9.5 miles northeast of Caliente and possibly near a northeastern extension of the fault. Attention was also given to a number of localities showing other unusually interesting ground fractures, among them the south end of Walker Basin, the west side of Breckenridge Mountain, the higher parts of Bear Mountain, and a short section on the Garlock fault where the Oak Creek Pass road crosses it.

Two preliminary papers relating to the 1952 Kern County earthquakes were published (Benioff, et al., 1952; Buwalda and St. Amand, 1952).

LOCATION AND EXTENT OF WHITE WOLF FAULT

The Arvin-Tehachapi earthquake originated on the White Wolf fault, at the south end of the San Joaquin Valley. This crustal fracture is known to extend from Wheeler Ridge, in the middle of the south end of the Valley, on a course N. 50° E., to cross the eastern margin of the valley to or beyond a point on Caliente Creek 1.0 mile northeast of Caliente. Its known length is therefore about 32 miles. The White Wolf fault was first shown on a map by A. C. Lawson (1906a, facing p. 432) but not mentioned or named by him. It was named and described briefly by H. W. Hoots (1930) and its position was indicated on his geologic map for about 5 miles northeastward from Comanche Point. Previous to the earthquake the surface geologic evidence for the existence, location, and attitude of this fault was rather general. From Comanche Point northeastward, in the Tejon Hills, the inferred fault is roughly a boundary between valley alluvium and the Tertiary formations. Farther northeast it is either a boundary between valley alluvium and the old crystalline rocks of Bear Mountain or lies with old crystalline rocks on both sides. The one possible exception is a fault contact between Tertiary strata to the northwest and the old crystalline rocks on Caliente Creek 1.0 mile northeast of Caliente, but this point may be northwest of the fault. From the Tejon Hills northeastward the zone of the fault trace has nearly everywhere suffered enormous and widespread landsliding from Bear Mountain scarp. The usual types of geologic evidence for tracing a fault between Tejon

* Division of Geological Sciences, California Institute of Technology. Ed. note: This paper was set in type after Dr. Buwalda's death in August, 1954.

Hills and Caliente Creek, some 16 miles, are therefore missing or have been obscured. The existence and general location of the White Wolf fault was inferred originally from the bold scarp forming the northwest face of Bear Mountain, rising 4,000-5,000 feet above the floor of the San Joaquin Valley, and the depression along its base in which the White Wolf Ranch is located. Since the base of the bold northwest face of Bear Mountain is not a straight regular line, such as marks many steep fault scarps, mainly because of landsliding, and there is little contrast in rock types in the scarp and in the foothills, the exact location and course of the fault trace has not been, and is not now, determinable so far as the writers are aware. It has been located only roughly, and northeast of Comanche Point entirely or almost entirely on physiographic evidence.

Geologists have long suspected that the White Wolf fault is a southwest-trending terminal segment of the important Kern Canyon fault or fault zone which is followed for over 70 miles by the south-flowing main fork of Kern River from north of Mount Whitney to Kernville and which then, with a more westerly branch (Breckenridge fault) as shown on Dibblee's map, forms the high scarp bounding Walker Basin on the west. It is not yet certain that this is not the true relation but it appears from the distribution of aftershocks and of ground ruptures that the White Wolf fault probably continues northeastward beyond the point where the Kern River or Breckenridge fault projected southward would meet it. Although it has not been possible to trace the Breckenridge fault to the White Wolf it is improbable that such a long and important fault zone would terminate only a few miles from an intersection with another important fault.

While it has not been possible to trace the White Wolf fault northeastward by ordinary geologic or physiographic evidence beyond Tehachapi Creek, it may be more than a coincidence that a quite strong earthquake, magnitude $6\frac{1}{4}$, occurred on 15 March, 1946 north of Walker Pass, about 44 miles to the northeast and on or close to its projection. No fault is known at the epicenter of the Walker Pass earthquake.

Reverting now to the southwest 12 miles of the White Wolf fault, from Comanche Point to Wheeler Ridge, it is not indicated by surface evidence. This deeply alluviated plain at the south end of the San Joaquin Valley showed no scarp or warped surface, so far as known, to mark the course of this important fracture, either previous or subsequent to the earthquake. But geophysical studies demonstrate the existence and general location of the fault very clearly. Its position as plotted on the map (plate 2) is based on seismic reflection data and was kindly furnished by Mr. Rollin Eckis, Chief Geologist, and Dr. Mason Hill, Senior Geologist, of the Richfield Oil Corporation of Los Angeles. The line shown is not the surface outcrop of the fault but its approximate trace, within the limits of geophysical accuracy of location, on the surface of the granitic basement. The fault in all probability dips southeastward and the line shown is therefore presumably the northwestern overhanging edge of the granitic block southeast of the fault. From the surface near the mouth of Sycamore Canyon, northeast of Comanche Point, the trace descends to an elevation of nearly 8,000 feet below sea level at a point about

3.5 miles southwest of the point. The bedrock trace has apparently veered to a position roughly three-quarters of a mile southeast of the southwestward projection of the nearly straight section of the fault as inferentially traced from Sycamore Canyon northeastward past White Wolf Ranch to the neighborhood of the railroad; since it dips south this is expectable. In the next 6 or 7 miles southwestward the bedrock trace, in approaching the northeast face of Wheeler Ridge, rises from about —8,000 feet to about —3,000 feet. While the geophysical data here are less exact the trace does not appear to return toward the southwestward projection of the surface trace of the fault, but continues sub-parallel to it. If a fact, this is explicable either by a change to a slightly more southerly strike, as it proceeds southwestward, or to a slight flattening of the dip of the fault. The course of the surface trace of the fault as inferred northeast of Sycamore Canyon, projected southwestward, would pass slightly north of the highest point on Wheeler Ridge, and the projected bedrock or seismic trace would pass a bit south of it. It is interesting that a zone of surface ruptures occurs on Wheeler Ridge on the southwestward projection of the bedrock trace; the zone also has about the same trend as the strike of the fault. Presumably the steeper White Wolf fault passes southwestward under the lower, south-dipping Wheeler Ridge overthrust and the Pleito thrust south of it, both of which trend more nearly east-west than the White Wolf. At any rate, in spite of the fact that the epicenters of the main shock and of the one foreshock were somewhat south of the highest part of Wheeler Ridge, no evidence of the White Wolf fault southwest of the ridge was found. From the point where the bedrock trace of the White Wolf fault passes under the northeast face of Wheeler Ridge it is about 17 miles measured along its southwestern projection to the San Andreas fault. One might well suspect that a fault with as large displacement as the White Wolf would continue at depth to an intersection with the San Andreas, which it would meet at an angle of about 60° , but this can apparently only be speculation at present.

It is interesting that the White Wolf fault trends roughly at right angles to the Kern River, Bena, Tejon, and other northwest-striking faults of the eastern part of the southern end of the San Joaquin Valley.

Although the magnificent northwest face of Bear Mountain obviously resulted from relatively recent vertical fault movement at its base, the White Wolf fault had not generally been considered one of the State's active fractures, and an expected source of earthquakes, by geologists in the past. No scarplets due to late displacement along the base of the scarp, such as occur at numerous points along the south base of the San Gabriel Mountains, had been noted so far as is known, and the course of the fault under or through the alluvium between Comanche Point and Wheeler Ridge is not known to be marked by such evidences of recent disturbance as scarplets, sagponds, trenches, and drainage derangement so common along the San Andreas and other major active faults.

GEOLOGICAL EFFECTS OF THE EARTHQUAKE

When movement on the White Wolf fault occurred on the morning of July 21, 1952, an interesting expression

of that movement developed along the fault trace. For nearly 40 miles, a succession of features ranging from lurch cracks to actual fault displacement marked the position of the fault zone. In many places the features were obscured and complicated by landsliding and slumping and in others cross faulting developed on an impressive scale. The following account is a detailed description of the phenomena developed along the surface expression of the White Wolf fault.

Chronologically, attention was first attracted to the fault zone in the region of Bealville where damage was done to the railway tunnels and along the Arvin cutoff road where conspicuous scarpets were developed. This account presents the observations in a geographic sequence, beginning in the epicentral region and continuing in a northeasterly direction to where the fault zone dies out in the region of Caliente. The reader may find the map of the fault trace (plate 2 in pocket) helpful as references, by number, are made to specific localities thereon.

San Emigdio Ranch. The shaking at the San Emigdio Ranch, near the western end of Wheeler Ridge was severe, causing damage to structures and developing a number of gaping furrows 6 inches wide and 200 feet long near the ranch house. The cracks were sub-parallel to the contour lines and were best developed in irrigated, filled land. A number of 1- and 2-inch water pipes lying on flat alluvium were ruptured; similar pipes on nearby hillsides were not. The fissures were deemed to be lurch cracks caused by severe shaking rather than by actual fault displacement.

Wheeler Ridge. The most southwesterly ground ruptures that are probably more or less directly related to the movement on the White Wolf fault during the Arvin-Tehachapi earthquake, rather than merely to the lurching which presumably produced most or all of the cracks on the floor of the San Joaquin Valley, lie in a narrow northeast-southwest zone obliquely across the upper half of the highest part of the east-west Wheeler Ridge. This ridge is a more or less isolated feature rising 1000-1500 feet above the flat floor of the south end of the San Joaquin Valley; it lies immediately west of the main Los Angeles-Bakersfield highway—the Ridge Route. The ruptures are of particular interest for several reasons. Ground distortions and fractures, more or less directly related to the fault movement, which are so conspicuous from Caliente to Tejon Hills, are apparently absent from the 12 miles of flat San Joaquin Valley floor southwest of the Tejon Hills, but apparently reappear in Wheeler Ridge. They occur on the part of the Ridge which is on the southwestward projection of the fault as plotted from geophysical data, and very few ruptures occur on other parts of the Ridge. Their trend is that of the fault. Their trend projected southwestward passes close to the instrumental epicenter of the main shock.

As in the Tejon Hills-Caliente section of the fault zone there are at least three types of ruptures on Wheeler Ridge. The most numerous are soil cracks; these are often tens of feet long, occasionally one or two hundred feet long, and tend to be parallel to the contour lines. They are often rather widely open and are clearly due to a thin layer of soil, not over a few feet in thickness in most cases, slipping directly down the hill slope on the firmer rock surface on which it rested. Some of these cracks developed in other parts of Wheeler Ridge also. A second type occurs around the upper end of old or new landslides; it is more curved, the horns of the arc pointing down hill. These ruptures are clearly the result of movement or resumption of movement of landslide masses, the upper parts pulling away from the stationary ground above. The landslide ruptures were most numerous near the main northeast-southwest zone of ruptures; the local direction of slope of ground determining the direction of landslide movement and hence the trend of the ruptures.

The third and most important of the breaks were the long straight ones which crossed the crest of the hills obliquely on the projection and trend of the fault. Unlike the two previous types they were independent of topography, traversing hills and depressions indifferently. There were three of these cracks. One began in the deep canyon draining northward next east of the main group of Standard Oil Co. wells, at a point perhaps one third of the way from the crest of the ridge down to the north base. This

crack climbs the hillside with a strike of S. 55° W., and crosses a road at a point 250 feet S. 20° E. of KCL well No. 29. At this point the crack is clearly an old fracture or fault dipping 50° northwest. A layer of gouge about a sixteenth of an inch thick occurs on it. The grooves and striations indicate about equal dip-slip and strike-slip movement, right lateral in direction. The crack continues to the crest of Wheeler Ridge and ends in the second gulch east of the main oiled road leading to the Standard Oil camp from the south. It is roughly $\frac{3}{4}$ mile in length. Near its southwestern end it crossed a tight east-west wire fence at an angle of 30-40 degrees; movement on the crack did not break or slacken the wires but offset the alignment about 4 inches. This could have resulted from the 1 foot of dip slip on the fracture. The crack is nearly straight in general plan but quite crooked in detail and apparently did not experience much horizontal movement. Usually the northwest side of the crack had dropped down 1 to 4 feet and the opening between walls was 6 to 12 inches wide. The rupture clearly cut the Pliocene Etchegoin formation and was not due to soil slippage or to ordinary landsliding. The southwest end of the crack is roughly an eighth of a mile southeast of the superintendent's house.

A second long crack ends northeastward at the same second gulch, about 1500 feet east of the oiled road, at which the first crack ends southwestward, and about 300 feet north of its end. Crossing the main oiled road 100 feet south of the east-west fence line and cattle guard about $\frac{1}{2}$ mile south of the camp, it continues with the same S. 50° W. strike across the canyon and beyond the crest of the next north-south spur which leads south from the tree-enclosed superintendent's house on the hilltop. It passes about 50 feet north of a huge boulder which lies about 650 feet south of the superintendent's house. This crack shows no horizontal offset; the oiled road surface north of it dropped a few inches relatively. It is also about three-eighths of a mile long.

A third crack crosses the road about 25 feet north of the east-west fence line and cattle guard. It is short, and extends only about 200 feet northeastward from the oiled road. The pavement was dropped a few inches on the south side of it.

The third or short crack overlaps on the second, but the two long cracks do not overlap—they are not en echelon. The second or southwestern long crack lies northwest of the southwestern projection of the first one and begins where it terminates. Altogether they are over half a mile in length and cross the crest of Wheeler Ridge. The dominant vertical movement on the cracks is down on the northwest side, as much as 4 feet; the horizontal movement is so small as to be rather uncertain in direction, but it is probably right lateral.

While the cracks do not extend southwest of the spur leading south from the superintendent's house, it is an interesting fact that the Richfield oil pipeline was ruptured during the earthquake roughly a quarter to three-eighths mile farther southwest and approximately on the projection of the zone of cracks. The pipeline here lies just west of the paved road ascending the south slope of Wheeler Ridge and leading to the new Richfield wells; it is the paved road next west of the one leading northward to the Standard Oil Co. wells and crossed by the zone of cracks. The break in the Richfield Oil Corporation pipeline was about 100 feet north of the telephone box on a pole along the road. Search failed to reveal any ground ruptures hereabouts or in the territory to the southwest.

The zone of cracks and the pipeline rupture presumably are the surface expression of fractures and sharp distortion which have extended steeply upward through the Wheeler Ridge overthrust plate from the trace of the White Wolf fault below it.

San Joaquin Valley. There were many cracks in the San Joaquin Valley floor that were distributed over a distance on either side of the fault. Most of them were lurch cracks and were not actual fault displacements. Offsets in cotton rows were common but as often in one direction as in another, and after a few hundred feet, the displacement on a particular crack sometimes reversed. At a spot on the Arvin-Wheeler Ridge road about 3 miles north of the fault the shaking was especially severe. Large lurch cracks abounded and a reservoir on the west side of the road was ruined by them.

Comanche Point. There are at least six prominent cracks between Comanche Point and Little Sycamore Canyon, numbered from 1 to 6. The crack at point 1 trends N. 40° E. for 500 feet. The northwestern side was dropped down 15 inches. There are en echelon cracks associated with it indicating a possible, but small, right lateral offset. The soil here is thin and gopher holes are surrounded by fragments of Tertiary shales and red sand-

stone. The crack lies 100 feet above the margin of the valley alluvium.

A 300-foot fracture at point 2, trending N. 40° E., consisting of an echelon cracks indicative of a small left lateral motion, shows a consistent upthrow of 15 inches on the southeast side. This crack is located 100 feet northwest of the base of the hills.

At 3, the crack lies to the southeast of, and overlaps, the one described at point 2. This is not a continuous break but consists of an echelon cracks indicative of a small left lateral strike slip displacement and was accompanied by an upthrow of 17 inches on the southeast side. This crack lies at the base of the hills and is partly in alluvium and partly in bedrock. The down dropping appeared as if the alluvium had settled. In spite of the indicated left lateral motion, there is but little other evidence of horizontal movement as the irregularities in the individual cracks fit together. The trace is curved, and along the base of the hills the rupture developed into a compressive moletrack 30 to 40 feet wide and appeared to dip towards the hills at angles of 30 to 60 degrees. This crack does not follow the base of the hills faithfully, but cuts across the base of promontories and then over alluvium-filled valleys and again over the bases of the hills. The trace dies out in the alluvium of the Comanche Creek fan.

The crack at point 4 is a few hundred feet long, down on the southern side a fraction of a foot and trends N. 30° E. It is in the alluvium, about three-quarters of a mile from the fault line.

At the base of the hills, at point 5, is a rupture 200 feet long, downthrown on the southerly side. Its trend is parallel to the base of the hills, N. 50° E. and there is some indication of compressive movement.

At 6, to the east of the fault trace, is a rupture that appeared to be the result of landsliding. It is 1,000 feet long, trends N. 30° E., was downthrown on the southwest 17 inches, and is usually continuous. In places however, it developed an en echelon habit with a right lateral pattern. It lies at the base of a face which is apparently the back of a landslide mass. This crack is of interest because it was probably of landslide origin, but resembled those near the fault trace.

Little Sycamore Canyon. The northwest end of the smooth, broadly rounded spur southwest of Little Sycamore Canyon (point 7) is traversed by about two dozen cracks. Most of these are parallel and sub-parallel to the contours of the hillside. The spur is a promontory due to landsliding. Most of the cracks are irregular and crooked, the average length being 200 to 300 feet with several up to 900 feet in length. The whole series covers a zone a mile wide and had the appearance of landslide fractures. This area was not easily accessible and was examined with binoculars from a distance of three-eighths of a mile.

Trace Along the Foot of Bear Mountain, East of Arrin. Although this portion of the fault trace is the most continuous and impressive of all, it is of different character in different places along its length and at times demonstrates a differing offset. It will be described in detail beginning from the southwest end. This trace was first noticeable at point 8, approximately half a mile south of Bear Mountain Boulevard. Here the trace lies in the alluvium of the San Joaquin Valley. It is distinguished by a series of pressure ridges from 2 to 10 feet in length with little or no evidence for other movement. There was no perceptible change in elevation across the trace. It was difficult to follow in this section because of grass, cultivation and trampling by cattle. Where the moletrack crosses north-south fences it demonstrates right lateral offsets of a fraction of a foot. The trend of the trace in this section varies from N. 22° E. to N. 35° E. Between 8 and 12, the traces form a gradually curving track which turns more and more eastward until it becomes almost east-west at the foot of Bear Mountain. As it nears the mountain it crosses a road not shown on the map and in so doing develops a compression crack 6 inches high and 60 feet long which indicates a right lateral offset.

At point 9 and southwest, the trace is a series of pressure ridges with a small amount of right lateral movement. At point 10, the trace developed a clear vertical uplift of 3 to 4 feet on the southeast side, probably indicating uplift of the mountain. Here the trace is a single pressure ridge with a few cracks on the southeast side. The ridge is essentially a buckle, or a broken warp, without great evidence of shortening. There was some evidence of right lateral strike slip movement at this point.

In the vicinity of 11, the trace developed into a series of pressure ridges at the base of a low hill. The total shortening over four of these ridges was estimated as 2 feet. The vertical uplift was of the order of 2 or 3 feet. The evidence of horizontal movement was not clear, of the order of an inch or so, and indeterminate

as to sense. The low hill at this point is of some interest, having a lobate shape something like a debris tongue; it forms a mesa-like platform at the foot of the mountain. On the western side it shows evidence of having been trimmed back by washes coming from the face of Bear Mountain. Near the west end a gulch in one of these washes has exposed a section aligned northwest-southeast. Near the base of this 40-foot section is a 5-foot layer of gray sand intercalated in the conglomerate which has boulders as much as 3 feet in diameter. The sand layer is more nearly horizontal than the present stream bed and may even dip back toward the mountain, due to rise of the north edge of this terrace-like feature. The mole track in general follows the north edge of this feature in this region and it seems as if the feature had been formed by previous uplift along the fault, or at least along the moletrack.

In places there were multiple fractures; these follow along berm-like platforms on the edge of the so-called terrace.

At 12, the trace makes a 50° turn. Southeast of the turn the pressure ridges are weaker, the cracks stronger and indicative of right lateral motion. West of the turn the pressure ridges are stronger and the cracks absent. The vertical offset in the pressure ridges amounted to as much as 4 feet. Conjugate sets of tension cracks and pressure ridges were well developed along this section of the scarplet, the pieces lying between them forming triangles of sod so that the cracks were behind the part that move forward and the compression ridges before.

The trace follows the contours at the base of the low hill previously described and is some distance out from the face of the mountain proper. The ridge is here 10 to 15 feet above the general fan surface.

At 13 the trace is single and is situated on a very gentle slope near the base of the low flat ridge. Strong cracks are superimposed on the pressure ridges in such a manner as to indicate right lateral motion. The vertical offset here is 15 inches over a zone comprising seven cracks. The strike of the zone is N. 45° W. as the trace follows along the foot of the hill and enters each reentrant. A few hundred yards up the hill from point 14 is a water tank some 10 feet across and about 30 inches high from which a great deal of water was flung during the earthquake. At point 14 the trace is subdued and there was very little vertical displacement. Two or three pressure ridges run parallel to the course of the trace and several 1- to 2-inch cracks indicate a feeble right lateral offset.

At 15, the trace is well developed with a zone of cracks about 100 feet wide, composed of as many as 12 separate pressure ridges. The shortening of the original hillside at right angles to the pressure ridges must have been several feet. The trace at this point may have been complicated by creep of a surficial layer of sod and soil which had slipped down slope as indicated by many plates of the material which had slip surfaces parallel to the hill slope. Oldham reports a similar effect in the Indian Earthquake Report, page 111. Approaching point 16 from the west, the trace swings up and back out of a canyon and in doing so encloses a portion of a fence set across the canyon. The enclosed portion of the fence was moved southward up the canyon about 2 feet with



FIGURE 1. Fence offset by thrusting of hill toward valley. View northeast near point 16.

respect to the other portion, indicating that the mountain had moved northwestward with respect to the valley block.

At point 16, the trace is still mainly a compressive moletrack and is accompanied by a vertical offset of 4 feet in the profile of the hill. A combination of open cracks and pressure ridges is present which indicated some right lateral shearing movement.

At point 17, the trace consists of pressure ridges 4 to 5 feet in height over a zone 100 feet wide. The largest ridge is just above the base of the hill and appears to have a dip of 15° or less to the southeast and to offset the profile 2 to 3 feet vertically. It is impossible to determine the nature of the lateral movement at this point, or even if it exists, because of the complicated moletracks and the surficial slumping and sliding which appears to have taken place. At each canyon hereabouts the soil slid down the sides of the canyons into the trough and the whole mass had migrated down hill as well. Between point 16 and point 17, a branch trace ran up a canyon as shown on the map. There are several of these features and they show the same characteristics as the parent moletrack to a large extent but are not as well developed. Between 16 and 17, the trail has been crumpled by the moletrack and little platelets of dried soil were pushed up to form overthrust ridges. A broken $\frac{3}{4}$ -inch water pipe crossed the trace near here and the ends were offset a fraction of a foot in a right lateral sense.

At point 18 the overthrust character of the moletrack was best developed. Here a pressure ridge composed of a series of soil plates was found lumped up between 6 and 10 feet. The whole movement must have taken place during or since the earthquake because the blades of dried grass when observed, were standing at an angle of 25 to 30 degrees to the vertical, away from the hill side. It was not possible to judge the amount or sense of lateral movement at this point. Just to the northeast, there were tensional cracks developed which indicated a feeble right lateral movement.

The trace continues, mainly as a pressure ridge, or moletrack, with no well defined evidence of shear movement, until a left lateral displacement may be noted at point 19. Here it loses its primarily compressional characteristics and demonstrates a 23-foot left lateral offset of a fence. This is contrary to the displacement of all the traces to the southwest where the lateral movement was primarily right lateral in sense and very feeble.

Eastward of 19, the trace continues over the nose of the spur on which 19 is located and then turns up the next canyon to the east. The shaking must have been severe, because boulders near here, both on spurs and in valleys, have been rocked out of their nests and vigorously jostled. This was especially noticeable between points 19 and 23.

The trace makes a sharp turn and proceeds up the canyon, following it faithfully, although changing at times from one side to the other. The trace here is double part of the way, and as it climbs the canyon shows increasing signs of becoming tensional in nature. At point 20, the trace bounds the east side of a swale perhaps 100 feet across. Here the trace is an open fissure, down on the west side on both parts, 3 feet on the easterly part and one foot or less on the westerly part. Broken roots in the trace have displaced ends which showed that the westerly side moved south 6 inches to a foot. A fence stretched across the swale at this point, and formerly occupying the bottom of it, has been



FIGURE 3. Stretched fence at point 20; tensional trace in middle ground.

stretched so that the lower ends of the posts in the middle of the swale were 7 feet in the air. The posts were formerly buried for about 2 feet of this length and this makes the uplift of the bottom of the fence posts at least 9 feet.

Beyond this point, the trace turns south and begins to double back as if it were ringing a huge landslide mass. The trace dies out at the point shown on the map, showing tensional qualities and having stretched another fence at 21, going over a nose so tightly that it lies upon the ground. Other ruptures at about the 3500 foot level were mostly tensional in nature.

In a number of localities, noted on the map, tensional features may be seen on the tops of ridges above the moletrack which winds along the base of hills.

A search near 19 failed to produce any evidence that there was a moletrack, or fault trace of any sort, going northeasterly to connect with those farther along the scarp in the vicinity of the White Wolf Ranch. There was landsliding in this area, one or two small springs were developed in canyons, and some boulders rocked out of their nests; near the highway, the fills and cuts of which showed considerable mass movement, a large boulder had been rolled down hill and lay partially blocking a small canyon.

Another trace begins at Point 22 and winds along the base of a low scarp, up the White Wolf grade, rounding the edge of the little valley in which the White Wolf Ranch is located and climbs gently toward the hills. This trace is primarily a compressive moletrack with some indication of right lateral strike slip movement. The trace goes over several noses and the compression is enhanced where it climbs their western sides. Near its north-easterly end, the trace begins to climb and soon dies out on the steep slopes of Bear Mountain. It could not be followed northeast of point 23.

North-South Fault Near White Wolf Ranch. The next trace is of considerable interest and trends at a large angle to the others. It is a cross fault with a generalized trend of N. 10°E. The break is continuous and was easily followed for 3½ miles. The predominant displacement was left lateral and varies from imperceptible amounts to several feet. The trace could first be discerned at point 24 near the 3600 foot contour on Bear Mountain. The whole mountain face in the vicinity of the fault is shattered; locally, sliding and mass movement obscure the trace. The whole mass of the mountain appears to be crushed and nowhere are any extensive bodies of solid rock visible. Above the end of the trace, the ground at about the 4000 foot contour, at an excellent spring, suffered severe lurching and sliding. There are perhaps 25 tension cracks between the end of the trace and the spring. Pipes running down hill from the spring were stretched, but not broken, and many of them have been pulled so that they are no longer in contact with the ground. Near 25 the trace offset fences and wheel ruts in a left lateral manner.

At point 25, the trace bifurcates and the two branches continue down the mountain to rejoin at point 26. At the 2800 foot level, the westernmost branch is a crack which is up on the west from 1 to 4 feet. The crack is often a foot to a foot and a half wide and an echelon cracks indicate left lateral movement. Many of the trees here have had branches broken off and one live oak



FIGURE 2. Tensional fracturing. View east near point 20.



FIGURE 4. Looking north at left lateral offset of fence by north-striking cross fault at point 27.

tree with a defective 15-inch trunk was snapped off at the base. Boulders were rotated by slippage on the moletrack. The material between the two branches appeared to have slid down hill. The trace itself seems to be related to minor topographic features, such as small swales, cols and large terraces.

The feature persists as a strong left lateral moletrack to the north of 26 and at a point near 27 it leaves the hill and enters the alluvium of the little valley containing the White Wolf Ranch. At point 27 it offset a north-south fence in a left lateral direction some 10 inches, indicating a considerable displacement, even through some depth of alluvium. The trace was easily followed northward as a zone of en echelon fractures, and where it crossed the Arvin road it developed an excellent set of en echelon fractures in the asphalt. The total opening in the cracks, measured along the center line of the road the day following the earthquake was 1.1 feet; the white line was offset 3 inches. Later the road was patched and on 11 August it was noted that the same set of cracks had again opened, indicating that movement on this fault continued for some time after the main shock. The fence wires on both sides of the road were stretched inordinately tight and the barbs were dragged across the fence posts, scratching them deeply and even pulling out some of the staples.

North of 28 the trace closely follows a small stream course as it crosses the next field. It appears that the stream course had been determined by previous movement on this fault, as its course was very straight and ran across the regular drainage pattern. A former crack had been utilized by the rill in the past and was reopened by the earthquake. Where the trace crosses highway 466 at 29, the pavement had been patched and no measure of offset could be taken. The trace crossed 466 at a culvert, still following the water course. North of this point the trace was still distinct and could be followed as a set of en echelon left



FIGURE 5. En echelon cracks in Arvin road at point 28, indicating left lateral movement.

lateral cracks which continued to point 30, located in a col between two hills.

This cross fault is an important structure and appears to exist in both the upper and lower blocks of the White Wolf system. Perhaps it is primarily a lower block feature and was extended into the upper block by frictional forces but it may actually cut the White Wolf fault in a primary sense, dividing both blocks into two parts.

Between the White Wolf Ranch and Rogers Ranch. The trace at 31 appeared to be greatly complicated by landsliding, the sliding utilizing the trace as an upper boundary and modifying it. Here two ruptures run around the nose of the spur above the edge of valley alluvium. The ruptures are sub-parallel to the contours. The upper one is an open vertical fissure, the lower one an overthrust, flat fracture in the soil. The two ruptures gradually die out toward the canyons on either side. There is an indication of left lateral shear along the upper, or tensional feature, the north edge of which dropped down a fraction of a foot.

Farther up the same slope near 32, the whole slope is shattered and there are a number of features, primarily tensional, upon which no left or right lateral movement was noted. There may have been some lateral movement, but the features appear to be the result of landsliding.

A trace heading northeastward was noted near the end of this fracture; it continues to the next mole track to the north, at 33, and beyond. There is some evidence that this crack, which also looks like a landslide feature, but which shows left lateral and extensional movement near 33, extends farther to the north, as the road in the col 34 between the sawmill and the White Wolf Ranch was fractured, as was the Arvin road, 35, one quarter mile west of the junction with highway 466, and 466 itself was fractured at a point N. 5° W. of this point. The indication is that a zone of fracturing of considerably less, and indeterminate, offset crosses the roads and perhaps joins with the north-trending cross fault that passes near the White Wolf Ranch. This trace is dotted on the map to indicate that it is not definitely connectable throughout the whole distance.

The fracture at 36 is primarily a compressional feature with some evidence of left lateral displacement. Pipes crossing the trace are bent and show a general shortening of the area. The edges of the cracks, and occasional en echelon cracks and pressure ridges indicate left lateral movement. The trace is confused near point 33 and terminated in the vicinity of the northeast-trending fracture at that point. To the east, the trace reached a maximum displacement and development in the center of the ridge it transected.

Farther up the mountain face at 37, is another trace, removed a considerable distance from the general zone of fracturing. The north side of this rupture was uplifted 6 inches to a foot. There is a spring at both ends and in the middle of it. This extensional trace was first noted by C. R. Allen on 13 September and may not have been made by the main shock, as it was not noticed earlier, when the area was examined, although it is quite possible that it was overlooked. This feature disappears in the detritus in the canyon at both ends.

From 38 eastward the rupture shows left lateral movement all along its length, and the trace it makes on the hill sides suggests that it dips to the southeast under Bear Mountain at angles varying from vertical to 45°. Where the trace of this rupture makes a sharp turn as it does at 39, and the tendency would be for a left lateral fault to pull apart, it developed grabens and extensional fracturing on an impressive scale, some of the cracks being wide enough to admit a man and up to 10 feet deep. West of 39 the trace runs up and down over ridges and was at times hard to follow, but east of 39, the left lateral offset attains several feet and was clearly indicated by offset foot paths, wheel ruts, fences and the sides of a turkey pen. The vertical offset was variable, the south side being uplifted in some cases, the north in others. Where the trace passes near the easternmost house of the Rogers Ranch, a frame building occupied by Mr. and Mrs. C. V. Thompson, it transects a fence, the posts of which were offset in an interesting manner. The post directly above, and seated in the moletrack was vertical, the posts on either side sloped away from the moletrack. The trace of the fence was also surprising in that it simply bulged or bowed a foot downhill in plan over a distance of 60 feet, to the northeast, along the trace of the moletrack. There was no apparent right or left lateral offset on this fence. The wires were very tight and some were broken. There is no simple way to explain this odd distortion, as the road is offset just northeast of here and there is abundant evidence of a left lateral offset to the southwest of this point. Oldham described a similar feature which

he called the Bordwar fracture on page 149 et seq. of his report on the 1897 Indian earthquake.

The trace forks at 40, within 100 feet of this point and one branch, the Bealville fault, departs from the general zone of fracturing and strikes N. 10° E. as does the cross fault in the region of the White Wolf Ranch. The other branch roughly parallels the fence just described, and eventually reaches the railway tunnels which were damaged by the earthquake. The fact that this trace runs parallel to the fence for a distance may have altered the offset of the fence somewhat and perhaps is responsible for the peculiar fence displacement.

Bealville Fault. After branching off at point 40, the Bealville fault passes through a field and crosses the road at the intersection of the Bealville road and highway 466; here it offset the fence in a left lateral manner and proceeds as a moletrack around the northwest side of the hill, locally known as "Shaking Mountain." It then crosses the Bealville road, displacing fences on both sides of it by about 1 foot and snapping fence wires. Where the trace crossed the railway tracks 800 feet west of Bealville 8 inches of rail were removed by workers to correct the shortening. The trace crosses a field and ends at 41, a quarter of a mile north of the railway tracks. In places the trace is marked by open cracks with 6 inch gaps; in others the ground surface was humped up. The vertical movement varied, being alternately down on one side and then on the other. Left lateral en echelon cracks mark the course of this fracture.

South of Sawmill. Returning for a moment to the region south of the sawmill, there are several rupture traces parallel to the main moletrack. Near 43 is a spring, serving the sawmill, opened by a tunnel driven into the mountain. The roof of the tunnel had caved in about 20 feet from the entrance. A typical compressional moletrack passes parallel to the front of the hill just below the spring; to the west it bifurcates, one branch going up the hill, the other following the base. The upper trace soon ends, but the lower goes around the hill and up into a canyon where the upper trace reappears and joins the lower trace. It then crosses the canyon and enters it again as the canyon swings right. Beyond this point the trace fades out but it reappears in a short distance and continues up the hill parallel to the longer track above it. The indication of movement on this feature is predominantly left lateral with alternating compression and extension along it, but in general there was more extension; it, however, did not amount to more than a few inches.

To the east, the trace has developed characteristics of a landslide or slump feature and continues with interruptions until a trace with a N. 25° E. trend was found at 43 leading eventually to the Bealville fault which it joins. The predominant movement on both was left lateral.

Railway Tunnel Faults. Returning to point 40, the southerly branch of the fault may be traced easterly. This branch swings off within 100 feet of the bulged fence near the easternmost Rogers Ranch building, runs subparallel to it for a matter of a few hundred feet, and then strikes across a field displaying a fine set of left lateral en echelon fractures. Where it crossed fences, posts were tilted and wires broken. It then goes over a low ridge just west of highway 466 without changing trend and crosses the high-



FIGURE 6. Normal faulting at point 44. This trace, or branch of it, passed through tunnel 4. T. R. Fahy photo.

way under a marker post designated KER58E. The pavement was cracked and broken and the moletrack emerges on the northeast side of the highway as a fissure open 6 inches to a foot and displaying signs of small left lateral movement. The northwest side of this fissure went up. This means that the upthrow was, locally at least, on the uphill side and on the block north of the fault. These traces on "Shaking Mountain" at 44 were visited by many people in the weeks following the earthquake. The cracks continued to open after the earthquake. They were first observed the morning following the earthquake and then again 2 days later; in the intervening time they had opened an additional 3 or 4 inches.

As this trace continues eastward it frays into several branches which die out and into two important branches at 45, which pass over the brink of the hill above tunnels 3 and 4 of the Southern Pacific and Santa Fe railroads. One branch passes into a gully just south of tunnel 3 and the other through tunnel 4.



FIGURE 7. Detail of normal faulting near point 44. T. R. Fahy photo.

Tunnel Area. The fault zone crossed the Southern Pacific Railroad tracks like the bar in a dollar sign and the three tunnels at two of these crossings suffered severely. Huge excavations and fills were made immediately to reopen the railroad. The tunnel offsets and the high and costly cut faces afforded the best information to be found anywhere along the fault zone bearing on the nature of the fault movement. Only here were cross sections of the ruptures brought to view. These exposures shed considerable light on the true nature of the ruptures or moletracks followed on the surface for miles to the southwest and northeast. Much more detailed information was gathered in the field than can be set forth here.

The southern part of the 700-foot north-south Tunnel 3 was so badly damaged that the southern 206 feet of it was converted to open cut. At the south end the arch or upper part of the tunnel moved relatively 10 inches south with reference to the lower part along a nearly horizontal fracture at the spring line. This was shown by the offset of the portal face and by the bent reinforcing steel. The lower part of the tunnel walls or lining was shoved inward toward the center about 3 feet. The steel rails of the single track were thrown into letter-S figures both inside the south end and south of the tunnel and pushed sidewise through the concrete lining to the rock walls. The deformation of the rails has been described in another section of this bulletin (Kupfer, Muessig, Smith, and White). The movement of the crown portion of the tunnel with reference to the lower part and the kinking of the steel rails indicate or strongly suggest horizontal shortening in a north-south direction such as might result from reverse movement on a southeast-dipping fault.

The clean-walled open cut made south of the south portal at 47 displays beautifully a reverse or thrust fault dipping 20-30 degrees southeast and striking about N. 45° E. It rises northward from below track level on both the east and west sides of the cut from a point about 100 feet south of the new portal to an elevation slightly above the cap of the concrete portal face and hence was exposed on three sides of the cut. On the east side of the cut the rock above the thrust surface is shattered diorite; below it are beds of somewhat compacted sand and boulders



FIGURE 8. View west toward fault trace just east of south portal of tunnel 4. *T. R. Fahy photo.*

dipping about 3° northerly. They are probably old Quaternary sediments and not less than 30 feet thick. These brown and yellow beds enclose the south end of the present concrete tunnel barrel. Ten feet west of the portal face, before being covered by concrete, they could be seen terminating and abutting against a diorite surface sloping 40° E.; this was quite certainly not a fault but a depositional contact. The trace of the thrust fault above the sediments can be followed just over the top of the tunnel; where the sediments end west of the portal it enters diorite and descends southward to track level on the west face of the cut. The diorite above the thrust is badly shattered and is cut by numerous northwest-trending steep minor faults, marked by gouge layers $\frac{1}{2}$ - $\frac{3}{4}$ inch in width. The trace of the thrust dips about 30° at track level but is convex upward and practically horizontal above the tunnel portal. It is clearly an old fault, for there is commonly half an inch of gouge along it, and in some places as much as 10 inches in pocket-like accumulations. In a cut 50 feet east of and at the same elevation as the portal cap, the striations on the fault surface strike about N. 35° E., suggesting mainly left lateral displacement.

One of the interesting features of this thrust fault is that while movement presumably occurred on it during the main or July 21, 1952, shock which severely damaged the tunnel, which it cut, displacement continued on it after the earthquake. The cut was made about August 1 and a photograph of the west face of the cut made on September 1, 1952. The hanging wall had moved eastward over $2\frac{1}{2}$ inches during August. On an unascertained date, nails had been driven into the gouge above and below the slip surface, their heads originally in contact. Their separation indicated that the direction of movement of the upper block was about N. 45° E., or almost entirely strike slip with left lateral displacement. From dated pencil marks on the underside of the hanging wall it is clear that the movement did not occur at any one time but was distributed, irregularly or regularly, between August 1 and September 15. Oddly, the trace of the thrust fault on the clean east face of the cut showed no offset whatsoever. This raises the question whether the post-earthquake offset on the west face of the cut was the result of aftershocks or fault creep on the one hand or of merely settlement and plastic spreading of the shattered rock in the hill mass above the fault, on the other.

Tunnel 4, now abandoned, was a few hundred feet south of Tunnel 3, trended northwest, and was 334 feet in length. The tunnel was so badly damaged by fault offset, collapse of roof at several places, and shattering of lining that the Southern Pacific Company, instead of repairing it, cut a shelf at tunnel floor level across the hill spur through which the tunnel passed, immediately east of the tunnel, and re-located its track on it. The uncovered barrel of the abandoned tunnel remains. Rising above it to the southwest is a huge cut face, some 400 feet long, roughly 200 feet high, with perhaps 1:1 slope and several berms; an

unfortunate necessity, it is a magnificent geological exposure in the fault zone.

The most severe damage in the tunnel was about 80 feet from the south portal, where a fault crossed it and caused uplift of about 3 feet, and a shift of about 2 feet eastward, of the block north of it. This fracture continues downhill to Clear Creek and is probably the same break that is so well exposed at 48, at the south portal of Tunnel 5. Westward from the tunnel it rises obliquely up the 200 foot face of the cut with a dip of about 30° southward, and a strike roughly east. The gouge along it is as much as 3 inches wide. The diorite above the fault is gray in color, less shattered and weathered than the diorite below it, which is brown and badly broken and decomposed. The crushed zone along the fault is about 3 feet wide and contains good spherical fault-rolled pebbles, "rollers," 1 inch-3 inches in diameter. Striations on the footwall on the berm at the top of the tunnel indicate dip slip movement; on the next higher berm, 50 feet above the tunnel, the striations slope 30° eastward on the footwall, suggesting mainly right lateral movement. Below the fault there is a brown weathered zone some 50 feet wide, parallel to it, and northwest of it is more gray, less shattered and weathered diorite. Viewed from a distance the brown weathered zone seems to be steeper than the fault.

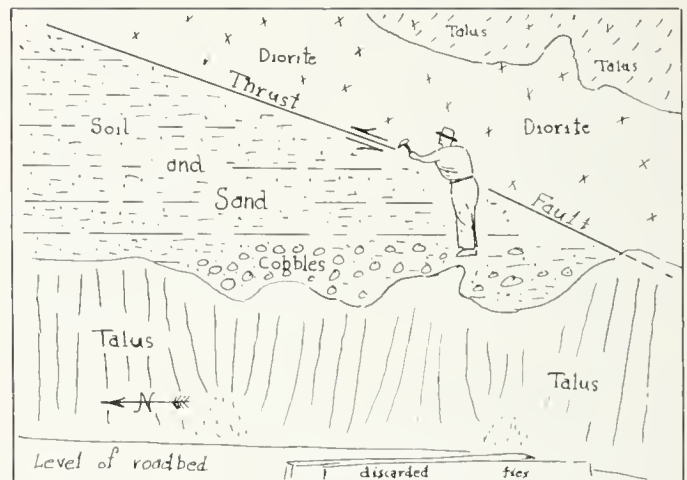


FIGURE 9. Thrust fault that cut tunnel 3; view east. Sketched from photo.

The rupture or zone of ruptures which crosses Highway 466 at 44 forks on top of the hill at 45, above and west of the tunnels and one branch goes down a gulch to the south end of the original Tunnel 3 at 47, where so much damage was done. The more southerly branch goes to the top of the 200-foot high face above Tunnel 4 at 46, and after itself forking, connects with the fault above described which goes through the south end of Tunnel 4. We have the dilemma that the faults indicated at the tunnels show displacements of at least several feet while the moletracks which are presumably their continuation on the hill above show relatively small offsets both horizontally and vertically.

A slice of bedrock remaining along the northeast side of the tunnel barrel consists of brown somewhat weathered diorite cut by a number of roughly east-west faults dipping southward 45 - 75° . One minor fault dips about 45° N. The main fault which offset the tunnel is steep in this cross section, still strikes approximately east, and shows about 3 feet of breccia and several inches of brown gouge.

Below the track and roughly opposite the northwest end of Tunnel 4 conspicuous rock outcrops existed, now largely buried by fill. A striking fault cut this outcrop; it dipped about 60° S., with strike of about N. 60° E. It has somewhat the same trend as the main fault which cut the south end of Tunnel 4 but must have been some 300-500 feet north of it.

Another fault cuts the upper part of the south end of the 200-foot cut face above Tunnel 4; it dips roughly 30° S. and strikes approximately east-west.



FIGURE 10. Fault and gouge in west side of railroad cut. Hanging-wall block (upper) probably moved upward during earthquake, but displaced nail heads show downward landslide-type movement following earthquake.

Longest of the tunnels (1169.6 feet), under the most cover (over 200 feet), and through badly shattered rock, Tunnel 5 was very severely damaged and required months for repair. It is on the east or opposite side of Clear Creek from Tunnels 3 and 4, is northeast of them, and hence also in the fault zone. Collapse of the tunnel roof and failure of the disintegrated dioritic rock resulted in three or four glory holes on the hill surface above the tunnel. Long sections of the bore were filled with material which flowed in from the roof. Mr. Mehrwein reported that in one section of 100 feet in the tunnel the track was shortened 2.33 feet.

For train operation a shoofly was built around the end of the spur pierced by the tunnel and along it a face over 1,000 feet long was cut nearly normal to the fault zone, all in shattered diorite. Only one fault was found cutting this face; it is near its south end. It dips about 45° S., and strikes about N. 75° E. It is accompanied by a crushed zone about 1 foot wide, with breccia and gray gouge. Traced eastward up the crest of the spur this fracture probably connected with the southern of four long cracks above the tunnel.

The cracks above the tunnel form a zone some hundreds of feet wide trending N. 65° E. and therefore roughly at right angles to the tunnel. They extend from somewhat west of the tunnel line for many hundreds of feet northeastward across the spurs extending southward from the crest of the ridge pierced by the tunnel. The cracks are most conspicuous in a large landslide basin just south of the crest and east of the tunnel line. They are up to 12 inches wide and roughly vertical, widest in thick soil, narrowest in thin soil. They are crooked and showed very little horizontal displacement. The total widening across the cracks must have been over 5 feet. The most northwesterly crack of the four showed left lateral displacement in its southwestern portion, right lateral in its northeastern part; the southeast side was down about 12 inches. The other three cracks showed downthrow of 6-10 inches on the northwest side. There are numerous shorter cracks south of this more conspicuous zone, both east and west of the tunnel; one of these, in rising up the ridges east of the landslide basin, showed strong left lateral displacement.

A rather conspicuous fault crosses the south portal cut; it dips about 80° N. and strikes roughly east. Its trend is quite irregular. It may well be the fault which crosses the south portion of Tunnel 4. At Tunnel 5 it connects with a moletrack on the natural land surface both east and west of the cut. Eastward the moletrack goes half a mile to a saddle in the crest of the ridge and ends near a striking old landslide basin. This is clearly an old fault; the gouge zone along it is quite wide. It continued to creep on both sides of the portal cut after the earthquake.

Ground ruptures are virtually absent north of Tunnel 5. Tunnel 6 was not badly damaged but the railroad company deemed it advisable to convert it to open cut.

Around the curve to the east of Tunnel 6, on the slope into Tehachapi Creek, at Cliff Siding, the track was on a fill resting on the hillside. It was lengthened by a gap of about 18 inches, with shearing of the rail bolts. This was not due to faulting, however,



FIGURE 11. View west toward remains of tunnel 4, crossed by the White Wolf fault zone, and destroyed by the earthquake. The right portion of the tunnel was elevated about 3 feet and moved eastward approximately 1 foot with respect to the left end. The shear zone is of darker color and is marked by gouge and rounded rock fragments.

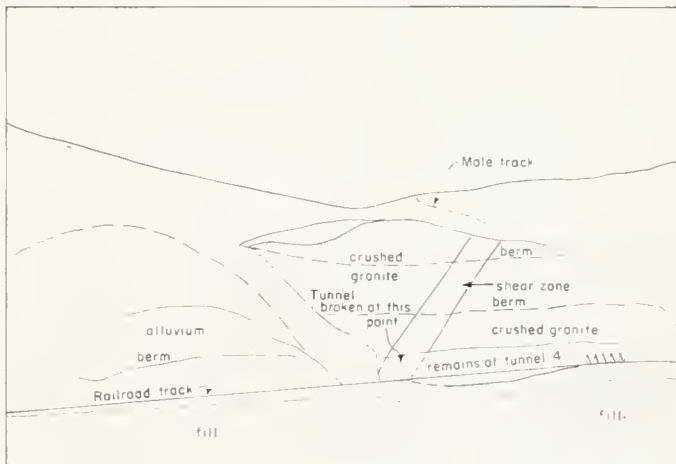


FIGURE 12. Sketch from photo, figure 11.

but to shaking; the fill convex to the northeast, slid northeastward and downhill, several feet in places. There were no ground ruptures hereabouts and Cliff was presumably somewhat northwest of the zone of most acute deformation.

Tunnels 7 and 8 are a mile to a mile and a half to the southeast and were only slightly damaged. They are apparently southeast of the fault zone. Along the railroad between Cliff and these tunnels there was virtually no ground rupturing and no evidence of sharp deformation.

Resuming the discussion of the ground cracks and traces, the hill lying between Clear Creek and Tehachapi Creek was fractured in a complex and bewildering way. The cracks have the generalized trend of the White Wolf fault zone, but are irregular in plan, both on small and large scale. The predominant movement on these features was that of northwest-southeast extension. When lateral movement could be discerned it was usually left, but there are exceptions; there is occasional vertical displacement. The direction of uplift is fairly consistent on any one crack but not necessarily on two adjacent cracks. Frequently the downhill slide of a crack will be uplifted from 6 inches to a foot. The cracks cut across features of the topography without being influenced much by them, several cutting across gulleys and ridges without changing trend, but at the same time tending to favor small cols. This suggests that they are old fractures. The cracks reveal that the underlying rock is so badly crumbled that it resembles alluvium. The cracks did not in general lie above the seriously damaged areas in Tunnel 5. There was some offsetting of the tube in the tunnel, but most of the damage resulted from collapse of the tunnel roof.

Summary of data regarding ground rupture.

Trace or location (map numbers, pl. 1)	Trend	Dip	Length (ft.)	Vertical		Extension or compression		Lateral movement			Comments
				Side up	Amount (ft.)	Sense	Amount (ft.)	Sense	Amount (ft.)	Evidence	
San Enigdio R.	--	--	200	--	--	E	½	--	--	----	Lurches, parallel to contours.
Wheeler Ridge.....	N45 to 55° E	Steep	3,000±	S	1-4	E	0 to ½	--	--	----	

COMANCHE POINT

1.....	N40E	--	500	SE	0-¼	--	--	R	Small	En echelon cracks	Crooked, 30' wide. Alluvium. Landslide crack? Zone ¼ mile wide.
2.....	N40E	--	300	SE	0-¼	--	--	L	Small	En echelon cracks	
3.....	N55-60E	SE30	--	SE	0-½	C	?	L	Small	En echelon cracks	
4.....	N30W	--	200±	N	Small	--	--	--	--	----	
5.....	N50E	--	200	NW	--	C	?	--	--	----	
6.....	N30E	--	1,000	W	0-½	--	--	R	--	En echelon cracks	
7.....	--	--	200-900	E	0-1	--	--	R	--	En echelon cracks	

MAIN MOLETRACK, EAST OF ARVIN

8.....	N30E	--	--	--	0	C	Small	R	Small	En echelon cracks	Zone up to 50 feet. From here on to 14. Overthrust zone. 100' wide zone, soil slip. Soil slip accompanies moletrack. 4-5' high ridges, 100' zone. Fence pulled up tight. Fence pulled down.
9.....	N50±E	--	--	--	Small	C	Small	R	Small	En echelon cracks	
10.....	--	--	--	SE	3-4	C	1-2	R	Small	En echelon cracks	
11.....	--	--	--	SE	2-3	C	2	I	Small	----	
12.....	--	--	--	SE	4	C	Feet	R	Small	----	
13.....	N45W	Low	--	SE	1½	C	?	R	Small	En echelon cracks	
14.....	Curving	Low	--	SE	Small	C	?	R	Small	En echelon cracks	
15.....	--	Low	--	SE	Small	C	Several	I	Small	En echelon cracks	
16.....	--	Low	--	SE	4?	C	Several	R	Small	En echelon cracks	
17.....	--	--	--	SE	?	C	Several	I	?	----	
18.....	--	--	--	SE	?	C	6?	R?	Small	----	
19.....	--	V	--	--	--	C	<1	L	2½	Fence	
20.....	N45W±	V	--	E	4	E	3-5	L	½	Roots	
21.....	N20E±	V	--	?	--	E	>1	?	--	----	

TRACE AT TOP WHITE WOLF GRADE

22.....	--	V	--	?	?	C	>1	R	>1	En echelon cracks	Nothing between 19 and 22. Nothing between 19 and 22
23.....	--	S?	--	?	?	C	>1	R	>1	En echelon cracks	

CROSS FAULT NEAR WHITE WOLF RANCH HOUSE

24-25.....	N10E	V?	--	--	--	--	--	L	>1	En echelon cracks; path & fences.	Fence trace splits. Fences Road, fences. En echelon cracks
26.....	N10E	V?	--	W	1-4	E	1-1½	L	>1	Fence trace splits.	
27.....	N10E	?	--	--	0	--	--	L	>1	Fences	
28.....	N10E±	--	--	--	0	--	--	L	<1	Road, fences.	
29.....	--	--	--	--	--	--	--	L	>1	En echelon cracks	

Summary of data regarding ground rupture—Continued.

Trace or location (map numbers, pl. 1)	Trend	Dip	Length (ft.)	Vertical		Extension or compression		Lateral movement			Comments
				Side up	Amount (ft.)	Sense	Amount (ft.)	Sense	Amount (ft.)	Evidence	
BETWEEN WHITE WOLF RANCH AND CLEAR CREEK											
31.....	Curved	--	--	--	--	E	1	?	--	----	Landslide?
33.....	N-S	--	--	--	0	E	?	L	Small	En echelon cracks	Landslide?
34-35.....	N-S	--	--	--	--	--	--	I	Small	----	Fractures in road.
36.....	N45E	SE?	--	--	--	C	1±	L	1±	En echelon cracks	
37.....	N70W	V	--	N	½-1	E	0-¼	I	--	----	Allen's.
38.....	N45-50E	SE?	--	--	--	C	--	L	>1	En echelon cracks	
39.....	--	--	--	NW	½	E	2-3	L	>1	En echelon cracks	Paths, fences, en echelon cracks.
39-40.....	--	--	--	--	--	C	1±	L	>1	En echelon cracks	
40-41.....	N10E	--	--	--	--	C	Small?	L	1±	En echelon cracks	Fences, rails, en echelon cracks.
42.....	N45-50E	SE	--	--	--	C	Small?	L	>1	En echelon cracks	
43.....	N20E	V	--	--	--	C	Small?	L	>1	En echelon cracks	Joins 40 to 41, fences.
44.....	N50E	?	--	N	½-1	E	½-1	L	Small	En echelon cracks	
45-46.....	--	?	--	?	0	E	Small	L?	Small	En echelon cracks	
48.....	E-W	?	2,000	S	½	E	0-½	L	Small	En echelon cracks	

BETWEEN TEHACHAPI AND CALIENTE CREEKS

49.....	N40E	--	1,500	E	1¾	C	Small	I	--	----	Fence
50.....	S80E	--	700	S	2	C	foot ±	I	1±	----	
51.....	N80E	S75°	3,000	S	1	C	--	I	--	----	
52.....	N80E	--	?	--	--	C	?	--	--	----	
54.....	N15E	--	2,500	E	3-4	E	1±	L	?	En echelon cracks	
55.....	N30W	--	500	N	½	--	--	I	--	----	
56.....	N40W	--	500±	S	¼	--	--	I	--	----	
57.....	N10-20E	--	3-4,000	E	1-1½	E	2 to 4	L	½	En echelon cracks	
58.....	N70E	--	1,000±	E	½-¾	--	--	--	--	----	
59-60.....	N30E	--	2,500±	E	0-¼	--	--	L	2-3	En echelon cracks	Total L movement over 200' zone.
61.....	N40W	--	500±	--	0	E	0-¼	--	0	----	
62.....	--	--	400±	--	<1	E	<1	--	0	----	Three cracks.

LEGEND:

Column	Symbol	Meaning
Dip	V	Vertical
Extension or compression	E	Extension
	C	Compression
	I	Indeterminate
Lateral movement	L	Left lateral
	R	Right lateral
	I	Indeterminate

Tunnel 5 has been the scene of considerable trouble in the past. The roof had collapsed before, following a derailment and fire in the tunnel. The rock flowed down producing a glory hole high on the hill. Four of these glory holes revealed a foot of brown soil and several feet of badly weathered diorite, grading into fresher, but crushed rock.

Between Tehachapi and Caliente Creeks. Some of the largest cracks and fissures produced by the earthquake were found on the ridge separating Tehachapi and Caliente creeks.

At 49 a trace with a trend N. 40° E. went up the stream bluff. The east side of this fracture was elevated 20 inches. The crack crosses the stream.

A compressional moletrack at 50 ran N. 80° E. for at least 700 feet; the south side was elevated 2 feet. In crossing an east-west fence, the moletrack slackened the wires about a foot, indicating a combination right lateral and compressional movement.

Beginning at 51 and trending N. 80° E. is a strong compressional crack. The south side was elevated one foot and the trace when crossing a canyon indicates that the feature dips to the south 75°. There seemed to be little if any horizontal motion and the feature cuts across spurs and swales independently of topography.

The rupture at 52 was compressional and trends N. 80° E.

Farther up Caliente Creek at 53 an exposed fault dips 80° SE. strikes N. 40° E. It appears from the exposure on the stream bluff that the igneous bedrock crops out on the upstream side and the sedimentary material on the lower side. The rock is so badly macerated, however, that a decision was not possible.

There is a gigantic crack at 54 trending N. 15° E., the east side of which was uplifted 3 to 4 feet. The crack was extensional and at places developed a graben 50 feet wide and 4 feet deep. This crack itself seemed to show no horizontal displacement, but associated en echelon cracks indicated a left lateral habit.



FIGURE 13. View east toward ground rupture between Caliente and Tehachapi Creeks. Surfaces are jagged, demonstrating lack of appreciable strike-slip movement.

At 55 is a crack a few hundred feet long, downthrown 6 inches on the south side and exhibiting no lateral movement. Parallel to the crack at 55 is a similar one at 56. This is situated on the crest of the ridge and like 55 passes through a col between two knobs. Its trend is N. 40° W., the south side was elevated 4 inches and there was no indication of lateral movement over the several hundred feet of its length.

One of the largest displacements found during the field work was the big crack at 57 which crosses the ridge obliquely and ends on the north side. In its midlength and near the top of the ridge, it is 24 to 40 inches wide, 6 feet deep; the east side was uplifted 12 to 18 inches and there was about 6 inches of left lateral movement. Northward this feature runs parallel to the contours, passing through a saddle at a point where the slope of ridge sud-

denly steepens. The material downhill from it appears to be sedimentary, that uphill appears to be igneous, but it is difficult to decide.

A moletrack at 58 was uplifted 6 to 10 inches on the uphill or southeast side, showed some left hand en echelon cracking and trends N. 70° E. for a considerable distance, about 100 feet east of the ridge.

There are two parallel cracks at 59, each 200 feet long, consisting of beautifully developed shear patterns showing left lateral displacement. The en echelon fractures are 3 inches wide, 20 feet long, and trend north. The cracks at 59 proceed intermittently to the region of 60 where there is a zone 200 feet wide consisting of about 9 cracks, all of left lateral en echelon habit and each having a horizontal displacement between 2 and 6 inches. The total displacement was perhaps 2 to 3 feet. There are in this zone some parallel cracks each open about 2 inches. Some show uplift of 1 to 4 inches on the east or downhill side.

At 61 is a 4-inch vertical crack trending N. 40° W. with no vertical or horizontal movement.

At 62 there is a group of cracks, all extensional, with a fraction of a foot vertical displacement and with no strike slip movement.

Between 62 and 63 the ground is broken by innumerable small cracks. Southward from 63 the cracks decrease rapidly and no significant break was visible between 63 and 64.

The fissures on this ridge were primarily extensional in nature, but showed compression as they approached stream bottoms; they are disposed to pass through cols or saddles and yet run along the sides of ridges and across canyons disregarding topographic features; they are long and comparatively straight. The trends seemed to fall into two groups, one about N. 45° E., the other more nearly north-south. Almost all the lateral movement was left.

No large or continuous fractures were found to the northeast of Caliente Creek, but there were some smaller ones.

Centennial Ridge. North of Caliente Creek and east of Harper Canyon, the northwestern part of this ridge lies approximately on the northeastern projection of the White Wolf fault zone. It trends more nearly east-west than the fault. Harper Canyon, straight in plan but crooked in detail, has the trend of the fault and may well be an expression of part of it, although it appears to be somewhat northwest of its projection. Centennial Ridge was examined for about 2 miles from its northwest end. Huge landslides which occurred during the main earthquake and its aftershocks produced great scars on its lower south side and its west end.

There are numerous ground ruptures along the crest of Centennial Ridge from its northwest end to about the 3,000-foot elevation, near 65, a distance of about a mile and a half. They are steep cracks striking from N. 50-80° E., and always roughly parallel to the crest of the ridge. They are rather straight, not en echelon, and showed no lateral movement. They were usually open $\frac{1}{2}$ -1 $\frac{1}{2}$ inches, sometimes 2-4 inches. Where the ridge is rather sharp-crested the cracks are in one zone along the top; where the crest is nearly flat there are usually two sets of cracks, one set near each rim of the flat area where it drops off to the steep flanks. Virtually no ruptures cross the ridge obliquely with the strike of the fault zone. This fact, the tensional nature of the cracks, and their location along the sharp crest or along the rims of the flat upper surface of the ridge, lead to the inference that they are primarily due to movement of soil down the slope during the shaking rather than to faulting. However, their abundance and their limitation to the portion of the ridge lying approximately across the projection of the fault zone, suggest strongly that the fault passes beneath the northwest end of the ridge.

From Centennial Ridge one could see scattered landslide cracks along the north side of Harper Canyon and on hill slopes along Caliente Creek to the east.

Harper Peak. Ground ruptures on Harper Peak (elevation 5,700 feet), about 10 miles northeast of the railroad tunnels, are of interest because they are the most northeasterly cracks found and they are roughly on the northeasterly projection of the fault zone. Mr. Weatherwax, a Walker Basin rancher who discovered them, kindly drove the authors to them by jeep. They are on the east and south sides of the top of the peak. Although curved they strike about N. 50° E. Of the several cracks the largest was 1 inch wide and the northwest side was raised 1 inch to 2 inches, and it continued for several hundred feet. There was no en echelon pattern, and no suggestion of horizontal offset. The nests in which individual boulders lie hereabouts show no enlargement and it is clear the shaking was much less severe than at the railroad tunnels and at White Wolf Ranch.

Walker Basin. Because the Breckenridge fault, named by Dibblee, which created the imposing scarp west of Walker Basin, has sometimes been thought to be the continuation of the White Wolf fault, this region was examined carefully for ground ruptures. Practically no ground disturbance was noted along the Oiler Canyon road into Walker Basin. The ridge leading eastward from the summit on this road toward Harper Peak displayed no cracks.

In a borrow pit at 67, on the west side of the highway $\frac{1}{2}$ mile south of the Rankin Ranch, which is at the south end of Walker Basin, several ruptures were found. This is at the south end of the Walker Basin scarp. One about 125 feet long crossed the east edge of the quarry; the south part of it is on a rock cut surface and the north part on an east-sloping grassy hillside. It is crooked and a quarter to half an inch wide. About 400 feet east of the highway there is a crack about 40 feet long on the top of the next little north-south ridge east of the quarry. It is about $\frac{1}{4}$ inch wide and trends N. 5° E. There are a number of other small north-south cracks hereabouts. All seemed to be tension cracks; there was no suggestion of vertical or horizontal offset.

No ground ruptures attributable to the recent earthquake or scarplets in the alluvium produced by geologically late movements on the Breckenridge fault were found at the base of the Walker Basin scarp.

At the Joe Walker mine, on the northeast side of Walker Basin, a long irregular crack in soft wet earth marks the end of what appears to be a landslide mass. A spring near the crack was flowing vigorously on August 31, 1952, 6 weeks after the earthquake, and we were informed by Mr. Cannon that at the time of the 1946 Walker Pass earthquake the discharge of this spring was roughly quadrupled.

Breckenridge Mountain. This 7,000-foot north-south ridge lies along the west side of Walker Basin and is apparently a block tilted toward the west along the Breckenridge fault. On its south-west slope a crack was formed at the time of the earthquake, about $\frac{1}{2}$ mile long and striking N. 40-60° W. It passes through a col at the 4,400-foot level about 1 mile southeast of the junction of Central Fork of Cottonwood Creek and Weiss Canyon, at 35° 24' 30" north latitude and 118° 36' 30" west longitude, on the divide between Cottonwood and Walker Basin creeks. The crack is about 4 inches wide, with downthrow of 4-5 inches on the southwest side. The manner in which it crosses ridges and valleys suggests that it dips 60-70° to the southwest. It seems to have been displaced in a right lateral manner in some places, left lateral in others. There is a landslide basin downhill from the crack in some places, but not in others. There was a spring near the southeast end of the crack. The rupture was discovered during range riding by Mr. Charlton, who kindly led the authors to it at the request of Mr. Leroy Rankin of Rankin's Ranch in Walker Basin. Mr. Charlton reported that he did not notice any other cracks on the west slopes of Breckenridge Mountain. This long crack is of interest because it is about 9 miles due north of the White Wolf fault zone at the railroad tunnels; it presumably cuts bedrock and is not merely a soil phenomenon; it has approximately the same trend and seems to lie on the southeastward projection of a line of scarps extending northwestward from Allen Ranch through Hoosier Flat to Kern River with a strike of N. 45° W.

Garlock Fault

On the day following the earthquake the senior author, through the courtesy of Mr. Hearst of White Oak Lodge, examined the Garlock fault for about 18 miles, from Cottonwood Creek west of the Lodge to Cameron. Numerous short lurch cracks were found crossing the road at different places and with various trends; they were attributed to shaking. At one locality the ground ruptures seemed to have more significance. The paved Oak Creek Pass road to Tehachapi, 0.8 mile northwest of its junction with the Oak Creek road, is crossed nearly at right angles by a zone of cracks; it is 4 feet wide and the roadbed was dropped 6 inches between the two outside cracks, necessitating a detour, regrading, and repaving before the road could be put into use again. This is exactly where the Garlock fault crosses the road. The cracks extend 100 feet west and 300 feet east of the road. Neither side was appreciably uplifted with ref-

erence to the other, nor could any lateral displacement be discerned. The trend of the zone of cracks is that of the fault. While the low and damp meadow west of the road approaches a sagpond in form the area east of the road does not appear to be deeply alluviated, so the area should not be particularly susceptible to lurching. It may be that the ruptures merely resulted from shaking, but their length, their position exactly on the fault (and yet no other long cracks found anywhere else in that territory), and the coincidence in strike of the zone of cracks and the fault, cannot but cause one to suspect that some slight local movement or other change in the Garlock fault, presumably triggered by the main Arvin-Tehachapi earthquake of July 21, 1952, may have produced the cracks.

Landslides

Landslides, a common phenomenon on steep slopes in all strong earthquakes, developed on a huge scale in the Arvin-Tehachapi disturbance and its aftershocks. There are two aspects of this subject. One comprises the slides that occurred during this earthquake; the other relates to downhill mass movements of earlier decades and centuries along the White Wolf fault zone.

There were many hundreds of large and small slides on the morning of the main earthquake. They were of course most numerous near the causative fault but many occurred 50-60 miles from it. The main Los Angeles-San Francisco highway, the Ridge Route (U.S. Route 99), was blocked at a number of places between Grapevine and Castaic. Large quantities of rock came down onto the Pasadena-Vincent highway over the San Gabriel Mountains. The road along Caliente Creek between Harper Canyon and Loraine was closed by rock slides for weeks, as was the road up the Kern River gorge east of Bakersfield. In nearly all the deeper canyons on the northwest face of Bear Mountain slides occurred. The steep slopes around Sycamore Canyon, and even some of the gentler areas high on the mountain around the head of this deep cleft, suffered severely and spectacularly from landsliding. Canyons were dammed with rock debris and some small lakes were formed.



FIGURE 14. Ground ruptures forming small graben in trace of Garlock fault. View westward across Oak Creek Pass road.

Dependent upon topography and rock type the slides took quite diverse forms. Some were types of slides found both under ordinary conditions and after earthquakes: rock falls; avalanches or rock slides; long but narrow shallow soil flows; and old deep and massive landslides which resumed movement for a few feet, opening up cracks at their heads and buckling the ground at their toes. A type unique to strong shocks consists of the movement of the soil as a sheet over the bedrock over quite a large area, sometimes several acres, with roughly subparallel ruptures distributed over the entire area. This was well developed around Sycamore Canyon. In other cases the soil sheet slid down one or both steep sides of a ridge with tension cracks along the crest, or along the two edges or rims of the crest where rounded or nearly flat.

Landsliding on the northwest face of Bear Mountain continued for at least two months after the main shock, probably mainly under the stimulus of aftershocks. Whenever one of the numerous aftershocks was felt, clouds of dust from landslides would be seen rising out of the canyons shortly afterward.

The second aspect of the landsliding related to the White Wolf fault is that along the whole lower northwest face of Bear Mountain and in the flat upland valley lying northwest of and parallel to it landsliding on an enormous scale has apparently been going on for centuries in the past. A large part of a strip from half a mile to a mile wide from Little Sycamore Canyon to the railroad tunnels presents striking landslide topography. It is quite certain that many or most of the small hills in this zone, probably many of the large ones, are the tops of landslide masses. A considerable area northwest of the White Wolf grade, 5 to 9 miles east of Arvin, and a much larger tract south of it, reaching up on the mountain slopes and extending eastward to White Wolf Ranch and beyond, shows convincing landslide topography and macerated rock material. Equally striking subsidence topography lies between the railroad tunnels and the Tehachapi-Bakersfield highway. These landslide masses are mostly large ones, up to hundreds of feet long and wide. Many of them showed little or no effects of movement during this earthquake period. Their unique and characteristic features are that they form ridges or long rounded hills that parallel the mountain front instead of running down the slope as normal ridges between canyons; they often have steep faces toward the mountain front as well as away from it; they often have abnormally flat depressions behind them on the side toward the mountain, some depressions resemble or actually are closed basins; the ridges sometimes divert drainage so that it runs nearly parallel to the mountain face for hundreds of feet; the topography as a whole is the hummocky type so typical of landslide areas; and the material of which the ridges and hummocks are made is completely shattered and much of it is a jumbled mass of rock fragments and fine material.

Landslide topography is so widespread and so marked along the northwest base of Bear Mountain that the authors were very dubious during much of the field investigation whether all of the ground ruptures traced and mapped were not merely landslide features. Unquestionably a large fraction of the total number are of that origin, especially the curved and short ones and

the ruptures that trend in directions quite different from the strike of the fault zone. But the long straight ones trending northeast are in all probability the surface expressions of branches of the White Wolf fault that experienced displacement at the time of the earthquake.

It would appear from the authors' observations that an active reverse fault with numerous branches, creating a high scarp, is a very favorable zone for landsliding on a large scale. It creates a wide zone of crushed, pulverized and jumbled rock readily amenable to weathering and open to surface waters; the block above the fault is shattered and weakened; the fault movements produce over-steepened slopes and a tendency to overhang by repeated uplift of the scarp side of the fault; and violent shaking from time to time resulting from the movements aids the constant downward pull of gravity. This seems to the authors to be the explanation of the extreme amount of landslide activity that has occurred along the northwest lower portion of Bear Mountain.

Dislodged Boulders

At many places within a few miles from the fault large boulders resting on hillsides were dislodged by the earthquake and rolled down hill varying distances. In one of the canyons on the face of Bear Mountain south of White Wolf Ranch a sub-spherical boulder about 10 feet in diameter rolled down a long steep hillside, bounding 200-300 feet at a time and cutting trenches 2-3 feet deep at each contact; it finally stopped after mowing down some quite large trees. On the north slope south of the sharp switchback curve half a mile west of the junction of the east-west Caliente road with the main highway, at 71, several large boulders rolled down the hill and one of them jumped the highway. All left spectacular curved dribble paths. At an elevation of about 1400 feet on the White Wolf grade, at 72, a rock about the size of an automobile rolled down against a highway fill near a culvert. About 10 miles from the fault, on the southeastern extremity of Bear Mountain, on the northeast sides of Cummings and Brites valleys and about a mile and a half northeast of the former California Institution for Women, many rocks rolled down the hillside into the canyons and left interesting dribble trails. This is the greatest distance from the fault that extensive rolling of boulders was noted. Landsliding seems to have occurred at much greater distances from the fault than the rolling of boulders.

It is interesting that, as might be expected, it was the large boulders that rolled down the hillsides; the small ones either were not dislodged or were soon trapped. The smaller ones apparently could roll down only the steepest slopes.

Some large rock masses in outcrops or still resting in their nests seemed to have been elevated a fraction of an inch by the shaking and presumed rocking, which permitted smaller rock fragments to roll or slide under them.

In places within the White Wolf fault zone the shaking apparently actually jostled some of the larger boulders at least partly out of their nests, so that they were rotated a bit when they came to rest.

Within one or two hundred feet, and only at that short distance, from any one of the long straight ruptures considered to be actual fault traces, boulders rest-

ing in soil often enlarged their nests in horizontal diameter by 5-10 percent. This appeared to be an inertia effect rather than due to rocking, but it could be both.

INTERESTING OR UNIQUE FEATURES OF THE FAULT AND EARTHQUAKE

While no two strong earthquakes are alike with reference to the nature of the shocks and the character of the faulting which causes them, the Arvin-Tehachapi earthquake and the White Wolf fault presented some interesting and unusual features when compared with other California earthquakes and earthquake-producing faults.

1. The shock was the strongest in southern California in nearly a century—since the 1857 Fort Tejon earthquake, which occurred on the nearest portion of the San Andreas fault.

2. The White Wolf fault on which the Arvin-Tehachapi earthquake occurred is surprisingly short for a shock of this magnitude; its known length is only about 32 miles. However, the area of the fault surface is in all probability large enough to make up for the shortness.

3. The majority of strong earthquakes which have occurred west of the Sierra Nevada have originated in the Coast Ranges west of the Great Valley, but this series of shocks centered at the south end and along the east side of the southern San Joaquin Valley.

4. The fault on which the main shock originated does not trend west of north, like the San Andreas and the other faults on which so many earlier strong earthquakes have had their sources, but rather strikes at right angles to the San Andreas—roughly northeast—and subparallel to the Garlock fault.

5. The White Wolf fault is apparently not a typical strike-slip fault like the vertical San Andreas fault or the vertical Garlock fault, but is mainly a reverse fault, or perhaps even a thrust fault, which has experienced a very large vertical component of displacement in the past.

6. While generally oblique-slip, the movement on the fault in the Arvin-Tehachapi earthquake was apparently more dip-slip than strike-slip; it apparently differed somewhat along the fault, and involved other complexities—all in contrast to the relatively simpler strike-slip movement on the San Andreas fault during the 1906 San Francisco earthquake and the 1940 Imperial Valley shock.

7. The maximum intensity of this earthquake, which is related to the vigor of the shaking and therefore to its destructiveness, seems to have been lower than usual for a shock of this magnitude.

8. There is some reason to think that the intensity was higher on the southeast side of the White Wolf fault than on the northwest. To judge from the damage at Tehachapi, the California Institution for Women, and Monolith, the vigor of shaking was nearly or quite as great in that territory as it was at Arvin on the opposite, or northwestern, side of the fault but only about a quarter the distance from it ($4\frac{1}{2}$ miles). To be sure the damage at Tehachapi was mainly to old buildings, but those at the women's prison and at Monolith were not weak structures; also, Arvin is located on the deep allu-

gium of the San Joaquin Valley, in which the vigor of shaking would expectably be accentuated. A plausible explanation for the unsymmetrical distribution of intensity on the two sides of the fault might be that it is due to the fault's southeast dip, toward and under the Tehachapi region. Perhaps the actual permanent displacement of the initial fling enhanced the intensity on the upper block.

9. The White Wolf fault, on which the main earthquake originated, was not regarded by geologists as one of those more active faults of the state along which most of our stronger shocks develop. It was recognized as a young fault because of the age of the youngest (Upper Tertiary) strata which it cuts and the high, bold, and relatively little-dissected scarp on the end of Bear Mountain which it created; but the fault lacked such evidences of recent activity as fresh scarps in alluvium, old moletracks, sagponds and fault trenches—so common along the principal active Coast Ranges faults.

10. Though east- and northeast-trending faults in southern California have for a long time been recognized as active, and though the Santa Barbara earthquake of 1925 presumably originated on an east-trending fracture, most or nearly all of the historic strong shocks in the western part of the state have come from the northwest-trending faults; these have strikingly restless fault physiography, like the San Andreas. Geologists and seismologists have come to expect that future strong shocks will emanate from these long northwest faults. The Arvin-Tehachapi earthquake should modify judgment somewhat on this score. Apparently shocks must be expected in the future from faults not in the old orthodox category. Strong shocks are likely to originate on relatively short faults as well as on long ones; on east- and northeast-trending fractures and perhaps still other trends, as well as on the traditional northwest-southeast Coast Ranges directions; and on faults which do not exhibit striking indications of recent activity and which on the basis of other geologic considerations would not be regarded as being active faults. Since moderately strong earthquakes (Bakersfield August 22, 1952 and others) have now occurred along the eastern margin of the San Joaquin Valley and the floor of the valley is known to be folded and faulted more or less like the Coast Ranges to the west, it is clear that strong shocks will not always be limited in future entirely to the Coast Ranges. They may be expected from foci beneath the San Joaquin Valley and probably from beneath the Sacramento Valley. This probability takes on added importance because of the thickness of alluvium beneath these valleys.

11. The earthquake did not develop a simple clean-cut trace along the fault, like the strike-slip ruptures on the San Andreas fault near San Francisco in 1906 and in Imperial Valley in 1940, or like the dip-slip scarps on the Sierra Nevada fault along the Alabama Hills in Owens Valley in 1872 or the fault along the east side of Pleasant Valley south of Winnemucca, Nevada, in 1915. Instead, a complex pattern of ruptures in a zone along the fault, a half mile or more in width, were formed.

12. The ruptures have quite different trends and the displacements on them are in diverse directions. There are quite long minor faults meeting and crossing the

zone of ruptures at angles approximating 45 degrees. From these facts and from the results of U.S. Coast and Survey re-triangulation and re-levelling, it appears that the movement on the fault may have been quite complicated.

13. While the zone of ruptures marking the north-eastern 20-24 miles of the White Wolf fault ends southwestward at the Tejon Hills and the alluvial surface of the San Joaquin Valley between the Hills and Wheeler Ridge, for some 12 miles, does not indicate the existence or the location of the fault, it is a very interesting fact that another series of ruptures appears on the higher part of Wheeler Ridge. The epicenter of the main shock has been located by Dr. Gutenberg and Dr. Richter somewhat south of the highest part of the ridge. The east-trending ridge is an anticlinal structure pushed northward toward the San Joaquin Valley on a rather flat south-dipping thrust fault whose trace would lie near the north base of the ridge. Presumably the White Wolf fault passes beneath the thrust. The ruptures in the upper half of Wheeler Ridge occur where the White Wolf fault would pass under it, and their trend is the same as that of the White Wolf. Careful search and inquiry revealed no ruptures in any other parts of the ridge. It would be an odd coincidence if the only ruptures on the ridge, occurring on the projection of the White Wolf fault and parallel to it in trend, were not related to it.

14. It is interesting and rather odd that, huge as the vertical offsets have been on the White Wolf fault, it does not appear to continue southwestward from Wheeler Ridge, and the epicenter of the main shock, to the San Andreas fault, a distance of some 15 miles, or less than half of its own known length. It is also odd that the surface geology does not more clearly indicate whether the White Wolf fault turns gradually northward at its northeast end near Caliente and merges into the south end of the long Kern Canyon fault zone—into that en echelon southern member of it mapped along the west side of Walker Basin by Dibblee as the Breckenridge fault—or whether the White Wolf continues northeast-

ward from Caliente and whether the Breckenridge does not continue southward to intersect or join it. Possibly the White Wolf connects with both the San Andreas and the Breckenridge faults at depth.

15. The epicenter of the main shock is even southwest of the known southwest end of the White Wolf fault and from the fact that all the aftershocks occurred northeast of the epicenter it is believed that the slip on the fault that caused the earthquake progressed in only one direction from the point of initial rupture. Only the single foreshock, which occurred about 2 hours before the main shock, originated southwest of the main shock epicenter.

16. The many aftershocks, a number of them actually moderately strong earthquakes, did not all originate in the fault which caused the main shock; a large fraction of them apparently had their source in the block above and the block below the sloping fault surface and at a distance of some miles from it.

17. From the initial shock at 4:52 on the morning of July 21 until the afternoon of July 22, the aftershocks all originated in the block above and southeast of the fault; later the aftershocks occurred in both blocks.

18. The sequence of events in connection with many strong earthquakes has been thought to be the occurrence of the main shock, preceded by some or no foreshocks, and followed by a long train of aftershocks in or close to the fault surface, decreasing in general both in frequency and in magnitude during the ensuing months or a few years. In the case of the Arvin-Tehachapi earthquake, in addition to the long train of aftershocks, a series of quite independent earthquakes developed in the months following the main shock, some of them presumably on faults roughly at right angles to the White Wolf and with epicenters up to 20 miles distant from it. Each of these shocks had its own train of aftershocks. Some of the shocks were moderately strong earthquakes which did damage at nearby points, as for instance the one which struck Bakersfield August 22, 1952, a month after the Arvin-Tehachapi earthquake, and caused major damage at Bakersfield.

6. GROUND FRACTURE PATTERNS IN THE SOUTHERN SAN JOAQUIN VALLEY RESULTING FROM THE ARVIN-TEHACHAPI EARTHQUAKE

BY ARCHER H. WARNE *

Abstract. A series of faint surface lines observed on aerial photos in the vicinity of Bakersfield have long been thought by the writer to be a clue to the existence of a system of closely spaced lateral faults traversing the area in a northwesterly direction. The remarkable broad parallelism of these surface features, together with their highly interrupted aspect and their frequent looped shapes, has led to much speculation regarding their significance and manner of origin. Although no positive relationship can be established, it has long been assumed that the steep horizontally slickensided fractures cored in widely scattered deep wells in this area, were of the same trend and system as the surface lines.

The initial earthquake of July 21, 1952, produced in the Bakersfield-Arvin area a number of surface features which compare so favorably with the older series of lines that there can be little doubt regarding their identical manner of origin. It is believed that during most of the Cenozoic there has been a recurrence of slight shifts on an ancient system of basement faults, with individual adjustments reflected at the ground surface as oriented shallow sloughs and lateral offsets.

Introduction. As a result of the initial earthquake shock on July 21, 1952 numerous small areas in the cotton fields in the southern end of the San Joaquin Valley were intensely fractured. A study of observed effects in the portion of this area lying between Arvin and Bakersfield forms the basis for the first half of this report. Attention was directed to these ground disturbances by the appearance of cracks and slumps crossing roads and highways in several dozen localities, often rendering them impassable. Other effects related to ground-cracking included failure of levees and reservoir embankments, offsetting and breaking of concrete standpipes and buried irrigation pipe, and dislocation of concrete foundations of houses and other structures. Not only was buried pipe widely damaged, but the ground in many fields was so badly fractured that water, when finally obtained, could not be prevented from entirely disappearing into the cracks crossing the cultivated rows.

Although the areas where earthquake fracturing was observed are somewhat irregularly scattered through the Bakersfield-Arvin area, they show a tendency to fall into several belts trending in a northwesterly direction. Despite the large number of varied and often strong aftershocks occurring over a period of many days following July 21st, the fracturing in the flat area (fig. 12) is believed to have been entirely the result of the initial and strongest earthquake.

Jones Ranch Area. A farm house located about 5 miles southwest of Arvin unluckily happened to lie within one of the fractured areas. Although the wooden structure of the house remained standing, the foundation was broken and offset in a number of places, and the concrete walls of the small square basement were pushed

to the shape of a parallelogram 10° (degrees) off square. The ground cracks seemed to approach the house from all directions, some showing a vertical offset of up to 1 foot, and open as much as 6 inches, while others appeared merely as belts of cracks which opened only slightly.

During an inspection tour of this area a set of these fractures was found which lay in an open 80 acre field immediately to the southeast of the farm house just described. The field contained no cotton crop and therefore offered an unobstructed view of the pattern assumed by a group of fractures. The fractures were found to be preserved clearly and in great variety of trend and spacing. They were mapped July 27-30 by subdividing the field into square plots of 100 feet on a side and sketching in the individual cracks in each.

On the map (fig. 4) each individual fracture is shown, the heavier lines representing those on which there has been more than 6 inches of vertical offset. The soil in this field was loose, silty, and sandy, but was sufficiently coherent to retain a clear record of the intense ground dislocation. The cracks in the predominating looser soil areas were V-shaped in profile, indicating that a wedge of loose material had disappeared into the space created when the crack developed. Scarps, also generally beveled, were occasionally sharp where irrigation had earlier formed surface mud.

The zone of surface rupture exposed in this open field continued into cotton fields for some distance to the northwest and southeast of this locality. Their mapping was prevented or made impractical by both lack of available time and by poor exposure due to the presence of rows of cotton reaching 6 inches to 3 feet in height. The presence of hardened surface mud, or even of a packed dry dirt road cake seems to have had a marked effect on both spacing and in some cases direction of the surface fractures.

It was found that almost without exception each group or belt of fractures had resulted in the formation of a shallow depression, without any perceptible uplift of its margins. The fracture patterns seem at first to consist chiefly of hooked shapes having little or no consistent direction. It may readily be seen that those groups not actually constituting part of a hooked shape show a predominant northwesterly trend.

Several surface profiles (fig. 6) were measured during mapping, where maximum slumps of approximately a foot and a half were found. These individual fractures have a nearly vertical attitude and show no offsets or offsets smaller than 1 foot. There is no noticeable uplift around the fracture groups or in any part of the area shown on this map (fig. 5). The fracture depressions being distinctly limited, both in lateral as well as longitudinal extent, it is not difficult to perceive that, if left undisturbed, they would without a doubt eventually become shallow sloughs.

The development of the thick swampy vegetation which characterizes undrained sloughs would inevitably create a thick dark soil body which would stand out in contrast

* Geologist, Richfield Oil Corporation. Manuscript submitted February, 1953.

Thanks and appreciation are extended for the generous assistance of many friends and associates, including particularly the following: to Mason Hill, who gave critical suggestions; to Rollin Eckis, Irving Schwade, J. W. Mathews, and Marie Clark, who made helpful suggestions; to Elmer Marlave, who furnished all air photos made since the earthquake, and to Clifton Johnson, who also assisted in obtaining them; to Edward M. Bien, who loaned photographs; to Ray Arnette and R. L. Bowman, who assisted in obtaining additional photographs; to Warren Stoddard and Gordon Dolton, who gave valuable cooperation in mapping of ground fractures. Acknowledgment is tendered to the Richfield Oil Corporation for permission to publish this report.

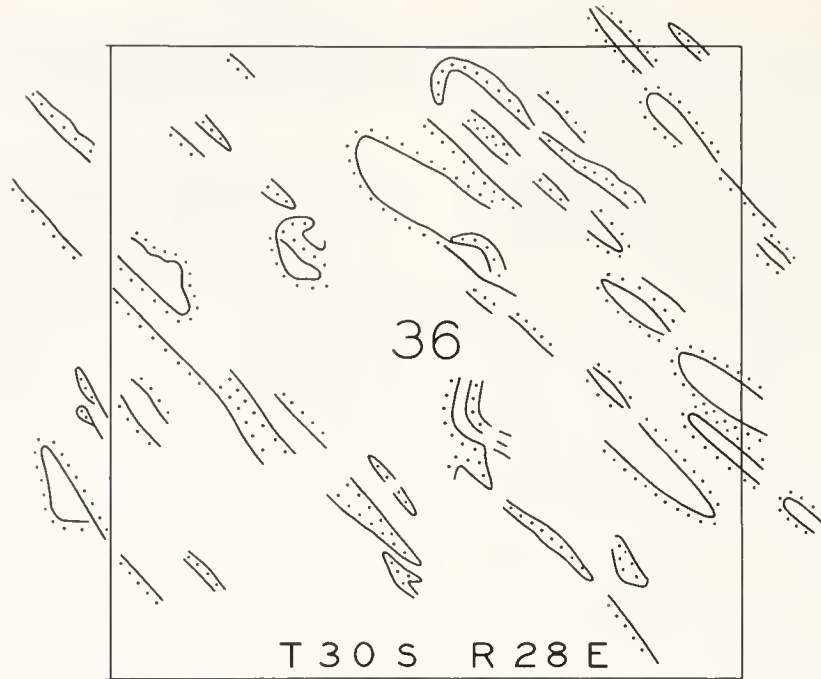


FIGURE 1. Typical group of linear surface markings.

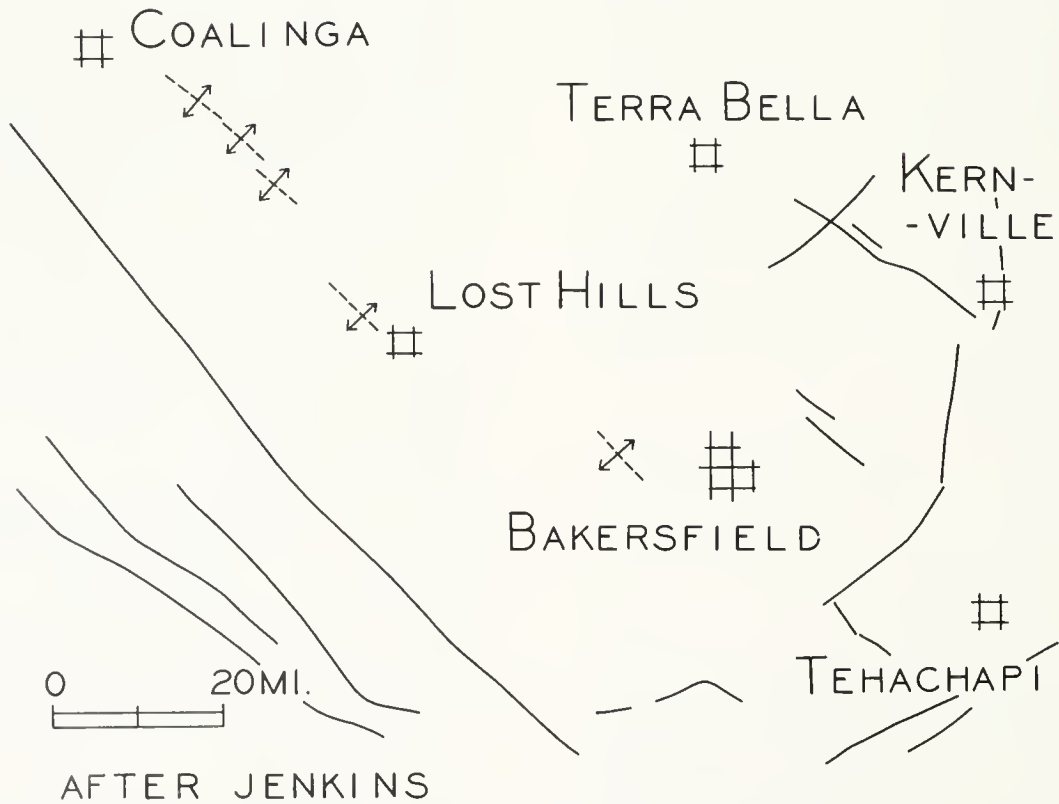


FIGURE 2. Fault pattern in southern San Joaquin Valley area.

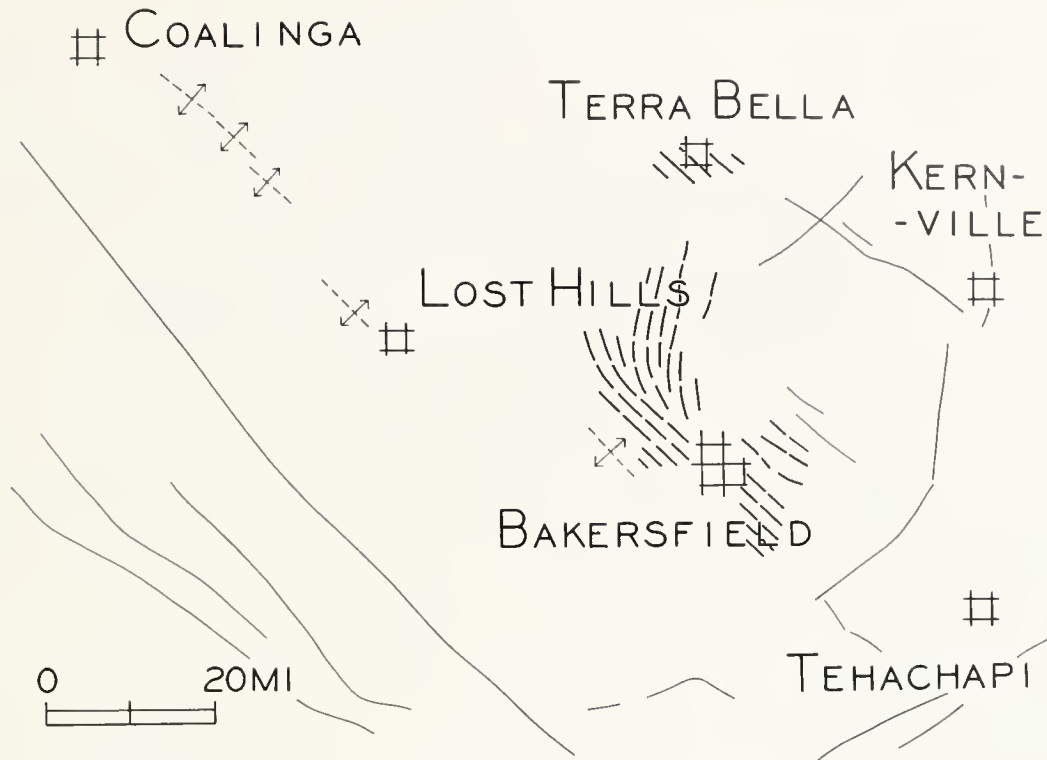


FIGURE 3. Location of linear surface markings in relation to fault pattern in southern San Joaquin Valley area.



FIGURE 4. Map showing linear surface markings in the southern San Joaquin Valley.

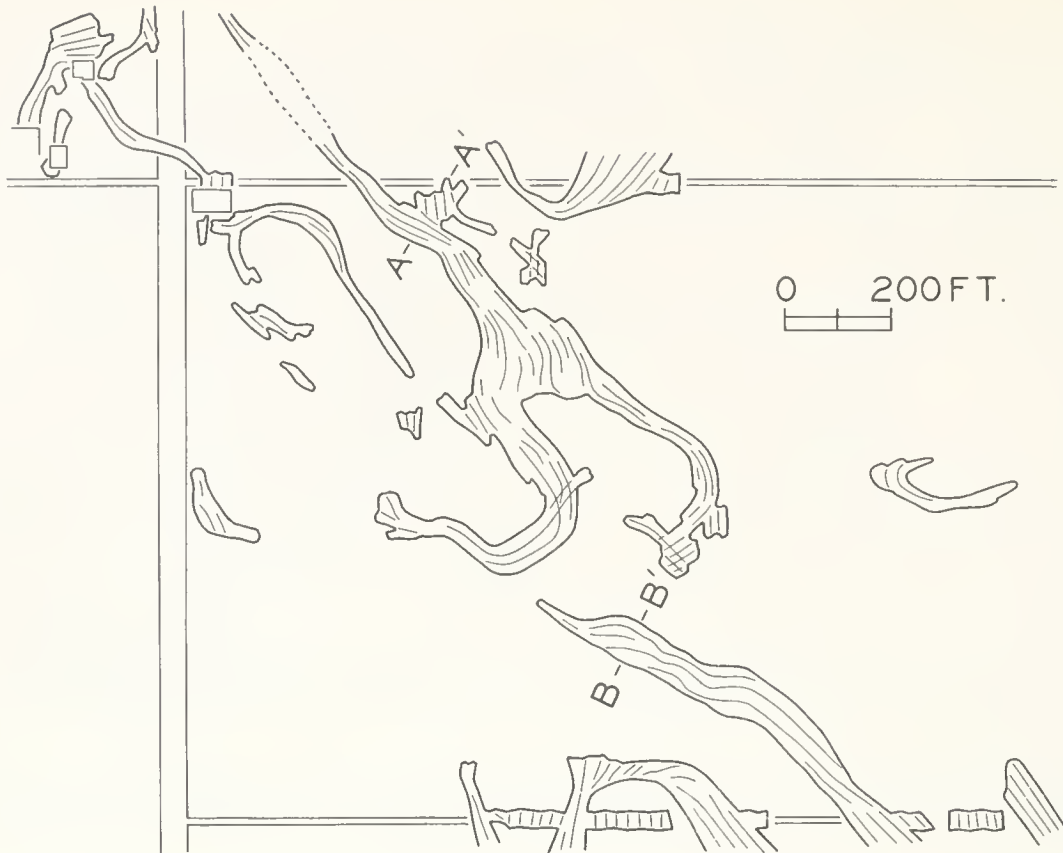


FIGURE 5. Generalized outlines of groups of fractures.

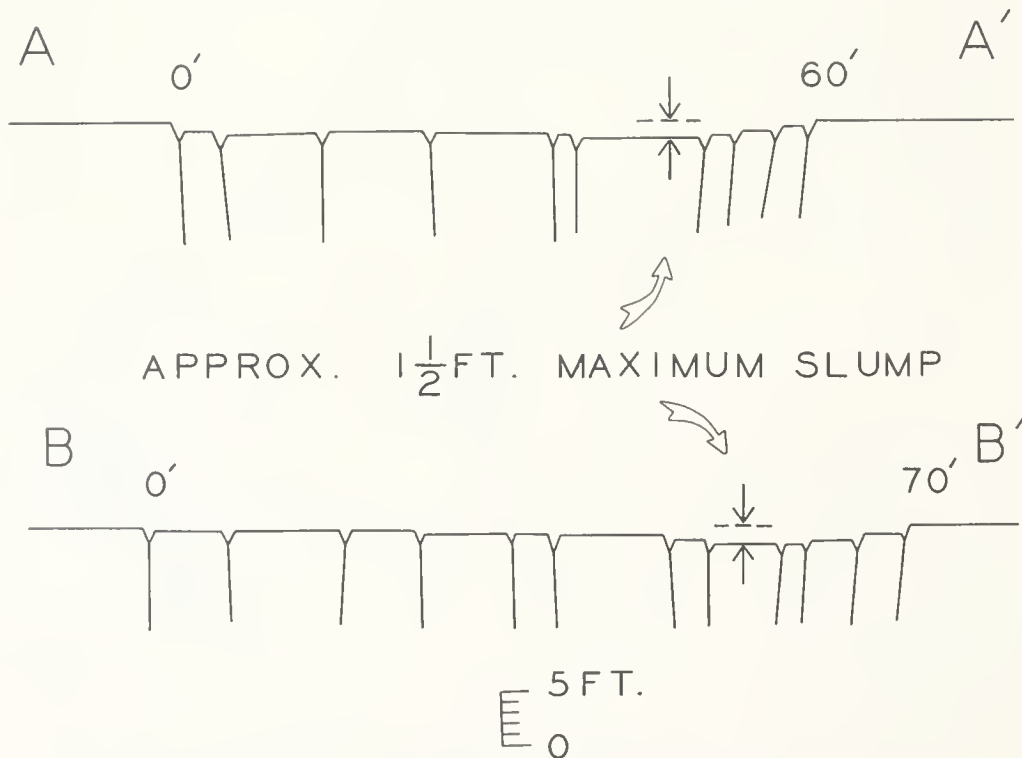


FIGURE 6. Cross sections A-A' and B-B' from figure 5.

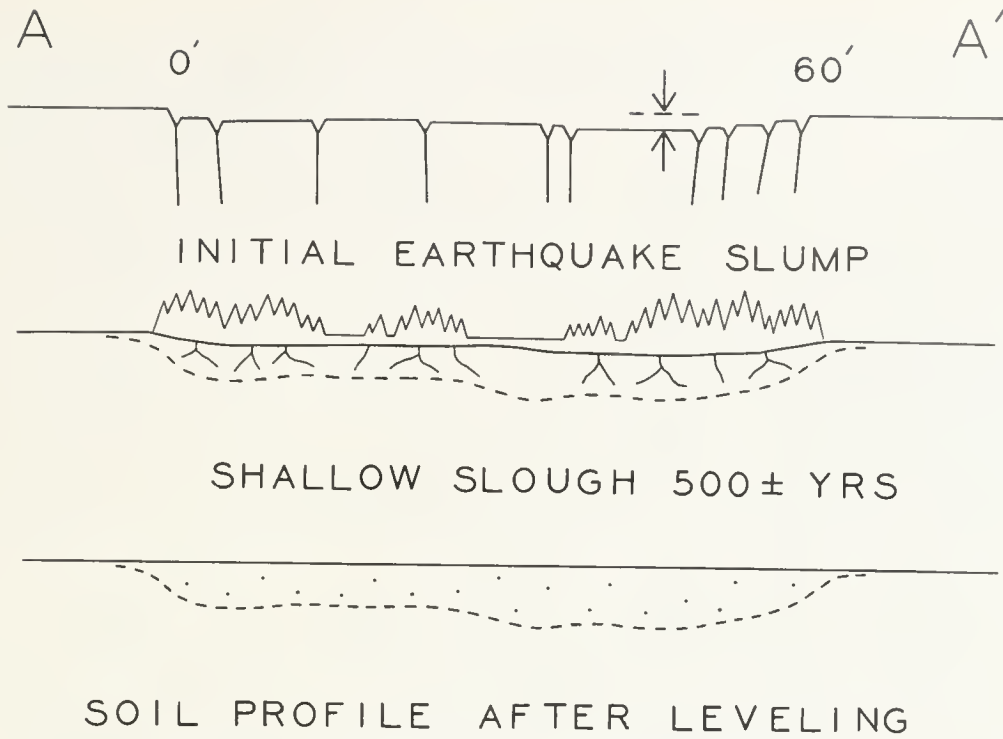


FIGURE 7. Process of development of sloughs from fracture groups.

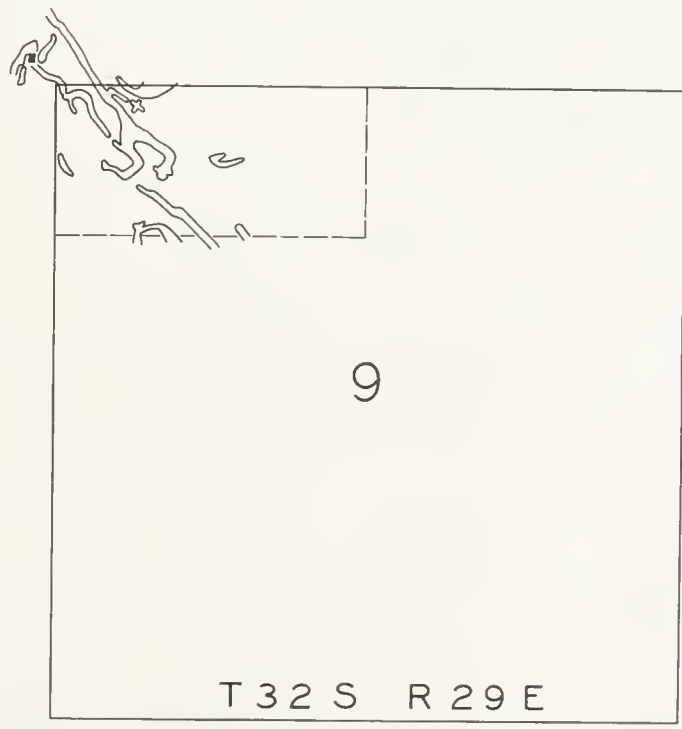


FIGURE 8. Jones Ranch group of fractures in relation to a square-mile grid.

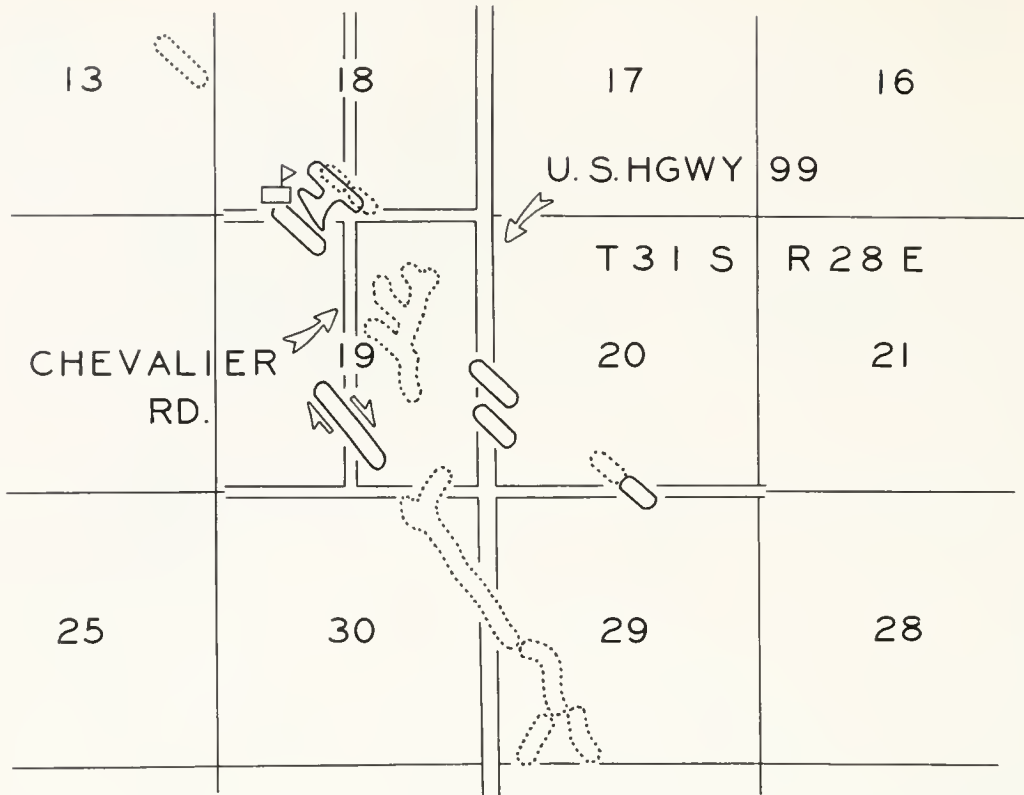


FIGURE 9. Fracture zones crossing U. S. Highway 99 and Chevalier Road.

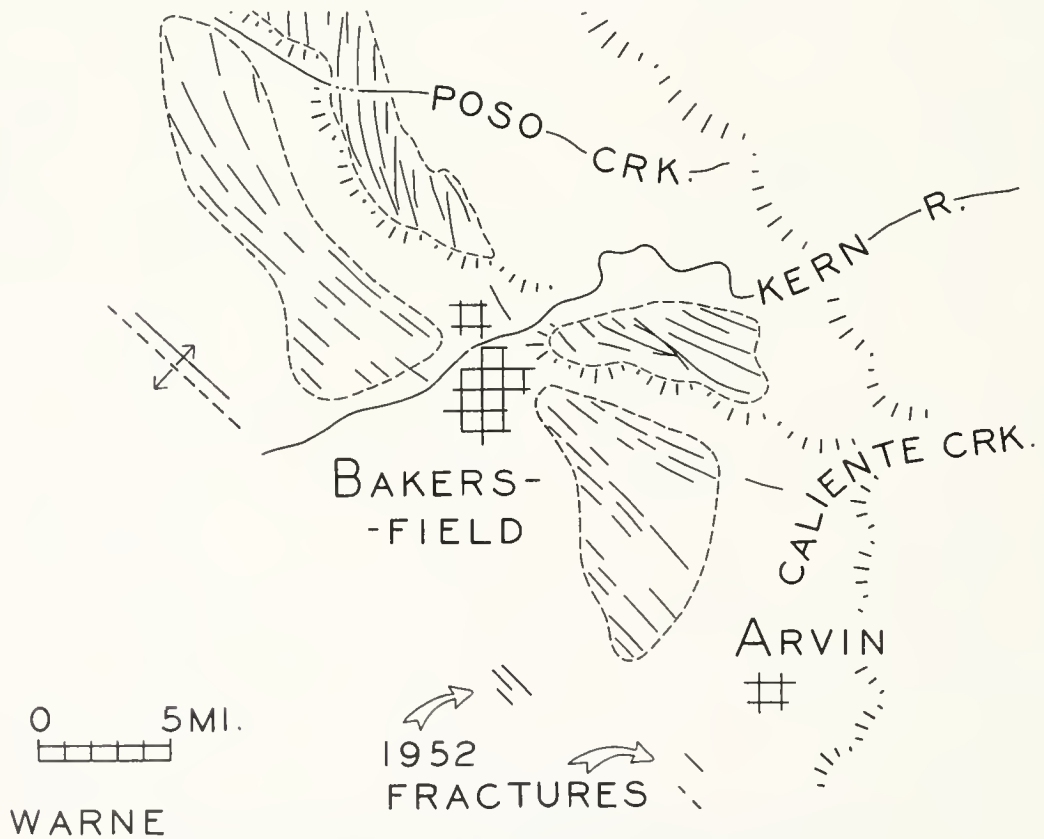


FIGURE 10. Relationship of 1952 fractures to ancient fracture pattern.

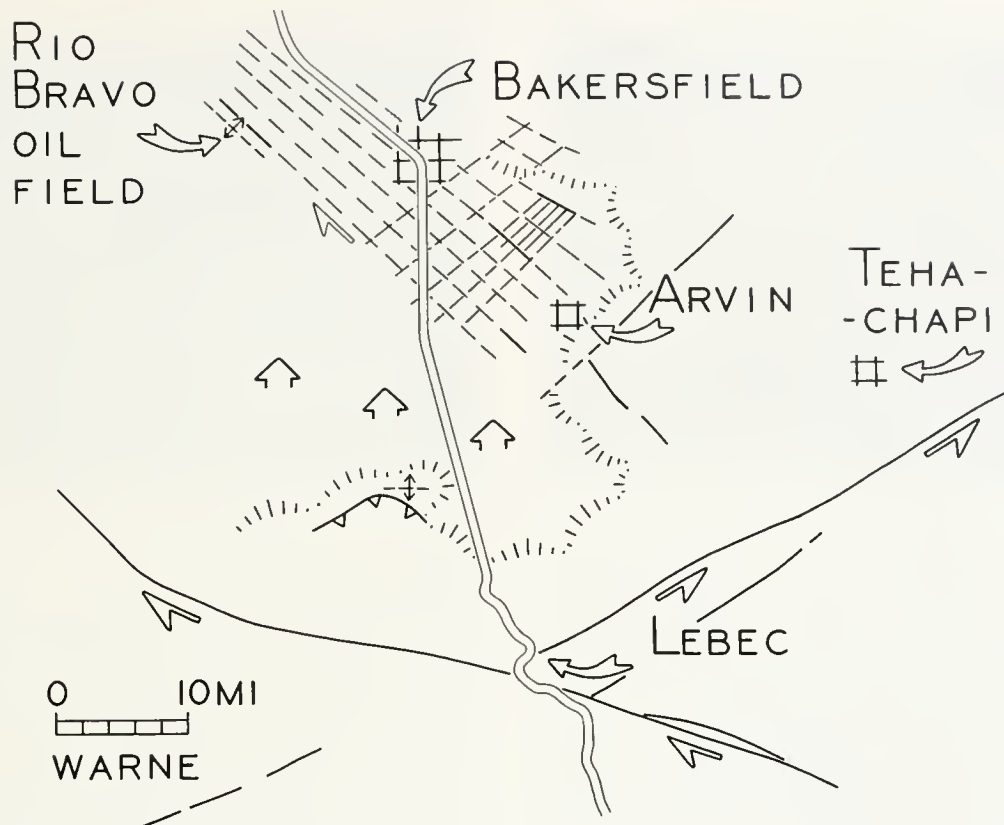


FIGURE 11. Hypothetical primary joint pattern relative to movements on Garlock and San Andreas faults.



FIGURE 12. Belts of earthquake fracturing in the Bakersfield area.

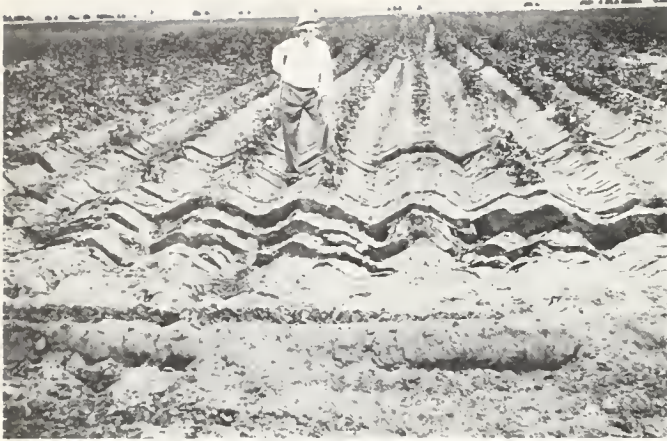


FIGURE 13. Intense fracturing in irrigated cotton fields. Photo by E. M. Bien.

to adjoining soils upon removal of the slough or its site by later grading and plowing.

U. S. Highway 99 and Chevalier Road. Slumps which suddenly appeared across U. S. Highway 99, 11 miles south of Bakersfield, at the time of the first shock interrupted bus, truck, and tourist traffic. Two areas on that highway, where the pavement dropped nearly a foot, are only a part of a group of intense fracture zones. The recent breaks lie within the areas bounded by solid lines (fig. 9). The east wing of the school building in section 18 was lowered nearly a foot by the slump outlined nearest to it.

The break in Chevalier Road showed a horizontal offset of about 1 foot, combined with over 1 foot of slump development. A most interesting and significant fact is that this offset is exactly aligned with a much earlier and perhaps ancient tree-filled slough extending for half a mile to the southeast. Shown in dotted lines (fig. 9), the former full extent of this slough, as mapped by the U. S. Geological Survey in the early 1930's, included a one-time distinct hook-shaped slough in section 29. The remaining dotted outlines are in each case the position of former sloughs present at the time the topography was mapped, but since then leveled out and planted in cotton and alfalfa.

It is of interest to note that 7 months after their formation several of the road slumps are still growing deeper. This is true of those crossing U. S. Highway 99 at the locality just described, and also one on Shafter Road and one on McKittrick Road. This may be mainly due to the weight of vehicles.

Ancient Linear Surface Markings. These observations and events take on special significance when viewed in the light of what has been learned in the past decade from a study of ancient linear surface markings in the Bakersfield area (fig. 10). The discovery on aerial photos in the middle 1930's of some rather indistinct dark lines traversing plowed fields in the Bakersfield area led to the conclusion that these were possible surface traces of faults. The lines seemed to be rather broad for single fault traces, and appeared much too interrupted along their courses. But they could be seen to have a pre-



FIGURE 14. Fracturing along road marking south border of mapped field. Photo by E. M. Bien.

dominant northwesterly trend, and were found to lie roughly parallel to one another.

The examination of several hundred aerial photos covering an area extending from Wasco and Porterville to Elk Hills, San Emidio Ranch and Arvin revealed hundreds of such markings. The lines were so faint that their detection in most cases depended on careful study. When the lines are all plotted on a regional map they show a broad parallelism, and it is easily seen that they must belong to some sort of a system. The extreme faintness of the lines, as well as their interrupted habit, has probably been largely responsible for their having been rarely recognized or for having been considered of no significance. Generally there is little more clue to their position than a line or band of contrasting soil colors on newly plowed farm land. The dots in the illustration (fig. 1) represent in each case the darker side of a line of color contrast.

Speculation as to what might have been the manner of origin of these lines led to a consideration of old wagon roads, ancient game or livestock trails, and even successive old lake shore lines, but each failed to provide an adequate explanation. The frequent appearance of hooked or looped shapes only served to increase the mystery of their origin.



FIGURE 15. Buckling of roads in Arvin area. Photo by E. M. Bien.



FIGURE 16. Detail of intense fracturing along road marking south border of mapped fields. Photo by E. M. Bien.

It is noteworthy that these lines may have been recently anticipated without their presence having been known. In the paper *Structural Relation of Tehachapi Mountains to the Sierra Nevada and the Coast Ranges* presented by J. P. Buwalda in 1946 at the Berkeley meeting of the Geological Society of America, a series of northwest-trending fractures in the Tehachapi Mountains was described and their relation to the well-known southern San Joaquin Valley structures suggested. In this paper it was indicated that these Tehachapi fractures are only a part of a great system of faults and folds which extends beneath the San Joaquin Valley floor across to the Coast Ranges beyond Coalinga.

The index map (fig. 3) serves as a key to the general location of the system of markings found on aerial photos and shows their relation to well-known outcropping faults in the southern San Joaquin Valley area. The surface markings fall approximately within a 15 by 35 mile rectangle enclosing the city of Bakersfield. It must be emphasized that the lines on the index are a greatly simplified version of the detailed map, and offer no idea of the actual number and close spacing of the lines.

Relation of the Markings to Lateral Faulting. The appearance of these lines on a map and their parallelism

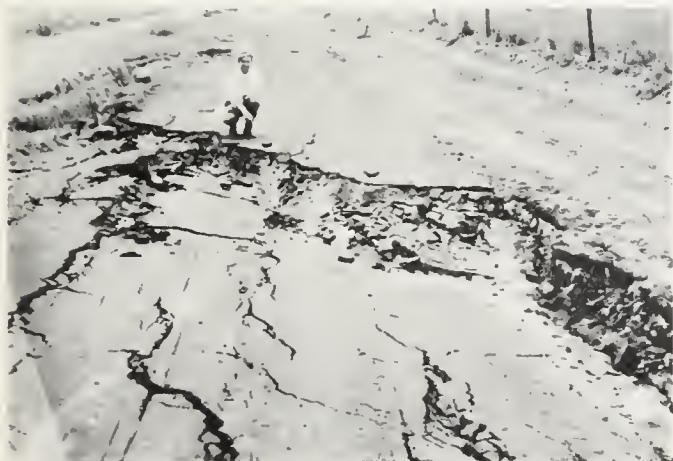


FIGURE 17. Chevalier Road slump, which has a measured 1-foot right lateral offset (note rim marks). Photo by E. M. Bien.



FIGURE 18. Ground fractures in cotton fields near Arvin.

with regional fault trends as well as within their own group immediately suggested lateral faulting. This fact combined with the frequent appearance of lateral fault evidence cored in wells led to a review of all the core descriptions from wells located in the area of interest. This survey revealed a large number and wide distribution of cored steep fractures bearing horizontal slickensides. Several incomplete and rather detailed subsurface electric log studies of oil-field-structure problem areas have yielded strong evidence of a close-spaced lateral fault system in older formations.*

It is also found that most evidence of lateral slippage comes from cores of strata underlying the upper Miocene, and that this evidence usually shows a downward increase in abundance. This may represent the accumulation of lateral shifting in older beds, to be expected if adjustments have occurred throughout the Tertiary.

In an early attempt to prove that the surface markings were the result of lateral faulting, a trench in the Famoso area was excavated 6 feet in depth and 30 feet in length across one of the better defined surface lines. The result of this effort was negative, and consequently the significance of the surface markings remained obscure until the 1952 earthquake. No proof turned up during a ten-year interval that the surface lines and the subsurface lateral slippage planes were of the same origin and trend, or that they had anything to do with one another. The map (fig. 10) of distribution of the old surface markings shows the relationship of the lines seen in aerial photos to the two described groups of earthquake fractures, and the striking parallelism is at once evident. The outlines shown here and the lines within them are again extremely simplified and generalized.

The apparent absence of the surface markings in the alluvial fan areas of the Kern River and the Caliente and Poso Creeks led to extensive re-checking of photos, but was finally accepted as a fact. It is readily seen on the map that this absence is simply due to removal by flood processes of features once present there. The great number of ancient lines found in the areas protected from effects of stream and river floods, when compared

* Unpublished report, *Evidence of Extensive Lateral Faulting in the Bakersfield Area, Kern County, California*, by A. H. Warner; 60 pp., with critical summary by Mason L. Hill. 1945.



FIGURE 19. Lurch cracks in irrigated field near Arvin.



FIGURE 20. Lurch cracks in irrigated field.

with the relatively few potential features formed during the major 1952 shock suggests that this is a cumulative record of many earthquakes like the recent one. The significance of this gap in the surface features depends to a large extent upon the time involved in the processes of formation of the individual lines. It could be taken as an indication that the shifting and fracturing forces have been inactive for sufficient time to permit seasonal floods to remove all traces resulting from the last period of activity. This would suggest that perhaps the normal frequency of recurrence of shocks causing surface fracturing is actually once in several hundred years and that we have only inhabited this area long enough to experience one. On the other hand, the extent to which the old features resemble one another would lead us to believe that they were all formed in a relatively short time, and that after a quiet period, somewhat greater than the two centuries of local recorded history, another cycle of frequent adjustments has commenced. In either case we may be fairly certain that these slump-forming adjustments are not the first of their kind in this area, even though no such events are known from the local recorded history.

In considering the significance of the looped and hooked shapes seen in fracture patterns (figs. 1, 4, 5) it is important that all the small component fractures, with rare exceptions, show purely vertical offsetting or tensional opening. Their appearance therefore suggests initial lurching and subsequent differential resettling to form the commonly observed slumps. The confinement of these slump features to belts having a definite trend and the occasional appearance of strong lateral shifting

such as the Chevalier Road offset suggest that lateral movements at great depth, and possibly considerable age, have been transmitted as a variety of strains set up in the shallow less consolidated strata. Activated by a shock wave from a nearby earthquake, a number of these strains would then convert to very local and varied adjustments, some lateral, but each, in turn, functioning as a small earthquake center, and producing its own effects at the surface. The fact that the looped patterns are independent and may even be seen to intersect in places, indicates that they are the effect of energy derived from various secondary sources lying in a belt rather than from a single point or along a single fault plane.

Much of the subsurface structure encountered in studying the oil fields in the area lying to the east and southeast of Bakersfield suggests, in addition to the common normal faulting, a set of northwest-trending steep faults having a varying degree of lateral movement, and intersected by a similar but lesser northeasterly set. In the final illustration (fig. 11) a joint system was drawn representing a hypothetical primary jointing of the regional basement rocks as a result of the overall initial strain set up by early movements on the San Andreas and Garlock faults. Subsequent movements, both horizontal and vertical, on this set of basement joints could easily account for much of the structural complexity observed, for example, in the Mountain View and Edison oil fields, as well as in the Racetrack Hill and Ant Hill oil fields. The influence of such a fault system is suspected in a dozen other oil fields lying in an area of wider radius.

7. ARVIN-TEHACHAPI EARTHQUAKE DAMAGE ALONG THE SOUTHERN PACIFIC RAILROAD NEAR BEALVILLE, CALIFORNIA†

BY DONALD H. KUPFER,* SIEGFRIED MUESSIG,* GEORGE I. SMITH,* AND GEORGE N. WHITE*

ABSTRACT

The Arvin-Tehachapi earthquake occurred in south-central California on July 21, 1952, on the White Wolf fault. Where the fault zone crosses the Southern Pacific Railroad, four tunnels were destroyed, rails were twisted and buckled, and in one area about 10 feet of crustal shortening was measured. The types of damage associated with the earthquake, and their distribution relative to each other, seem to have been caused by movement in a reverse- or thrust-fault zone that dips south. The damage resulted from compression and from subsequent relaxation along normal faults.

INTRODUCTION

Surface displacement during the Arvin-Tehachapi earthquake of July 21, 1952 took place principally along the White Wolf fault, the trace of which lies along the base of a pronounced escarpment that forms the northwest slope of Bear Mountain, Kern County, California (California Division of Mines, 1952; Benioff, et al., 1952; Buwalda, 1952). Severe damage occurred where a fault zone, presumably an extension of the White Wolf fault, crosses the Southern Pacific Railroad tracks 1,500 feet southeast of Bealville Railroad Station. Before the earthquake the tracks here made an S-shaped curve and passed through four tunnels; all three limbs of the curve and three of the four tunnels were intersected by the fault zone.

The authors visited the area on the day of the earthquake. On that day and the two days following, they examined the fault trace at several points between Bealville and the bend in the road east of Arvin.

As bulldozers were about to destroy much of the evidence of earth movement along the railroad, the plane-table map was made by the authors on July 22, 1952. On August 14 and 15 Kupfer and Smith revisited the area and examined the damage in tunnel 5, which had been impassable during the previous visit. The purpose of this report is to present the authors' observations—most of which can not be made again—and their conclusions.

Acknowledgments. The authors wish to thank Mr. D. J. Russell, president of the Southern Pacific Railroad Co., for the courtesy and cooperation that he and his men extended during the investigation; Messrs. E. E. Earl, G. F. Mehrwein, D. P. Boykin, F. M. Misch, W. Jaekle, W. E. Bussey, and S. T. Moore, all officials of the company, were particularly helpful. The Kern County Land Co. loaned the plane-table equipment.

Terminology. The tunnels on the Southern Pacific Railroad are numbered consecutively from Bakersfield to Mojave. In local railroad parlance, the directions on the track are referred to as "west" toward Bakersfield and "east" toward Mojave, without regard to actual compass direction. This terminology is used in this report only when referring to location of tunnel portals. Distances are given from the west portals of tunnels, and "left" and "right" refer to the left and right side of a train heading toward Mojave or Los Angeles. Figure 1 shows the general relations of the area affected; figure

2 represents in more detail two of the tunnels and the part of the tracks that were disturbed; and the photograph in figure 4 shows their relation to local topography.

GENERAL GEOLOGY

In the area of the railroad tracks and tunnels, the bedrock is predominantly granular intrusive rock, cut by small pegmatite dikes. No microscopic examination of the rock was made, but it seems to range in composition from a quartz diorite to a gabbro. It has been altered and decomposed to an undetermined depth, and bulldozers were therefore able to make sloping cuts 100 feet or more into the bedrock without the use of explosives.

During the reconstruction of tunnel 3, an exposure of nonintrusive bedrock, which is now partly concealed by the finished tunnel, was found. It is a wedge of arkosic material that was exposed from the arch of the tunnel to a point 50 feet along the left (east) embankment. Most of this rock is unbedded, compact, and fine-grained, but it contains a few rounded cobbles up to a foot in diameter. The top of this mass is in horizontal contact with intrusive rock; in some places the contact is indistinct, in others it is sharply defined by a zone of gouge 1 inch to 2 inches thick. The lower contact was not exposed. No further information was collected about this rock and it is now concealed. For this reason its structural relations are doubtful.

DISPLACEMENT ALONG THE WHITE WOLF FAULT DURING THE EARTHQUAKE

The general trend of the trace of the White Wolf fault is N. 55° E., subparallel to the Garlock fault, which lies 18 miles southeast. The trace of the recent offset was generally represented by several minor but conspicuous fractures that cut the surface in an echelon, parallel, or braided patterns along a zone up to 1,000 feet in width. The relative displacement of the surface along most of these fractures was less than a foot, but locally was up to 4 feet. Fractures of the normal, reverse, thrust, and strike-slip types were observed.

Along the base of the Bear Mountain scarp due east of Arvin the movements apparently took place on a thrust fault; the southeast block was thrust relatively over the northwest block. Two tear faults were observed.

In the vicinity of U. S. Highway 466 and the railroad the surface fractures appeared to be on normal faults with downthrow on the southeast. The average displacement was 6 to 8 inches and included a strike-slip component.

DAMAGE ALONG THE SOUTHERN PACIFIC RAILROAD TRACKS

The railroad tracks between Bakersfield and Mojave were damaged by the earthquake in many places. Bulldozers and large rock masses slumped onto the tracks and most of the larger fills settled slightly, so that much of the track had to be cleared, leveled, and straightened. In the S-curve area near Bealville, the track and tunnels

* Geologist, U. S. Geological Survey, Claremont, California.

† Publication authorized by the Director, U. S. Geological Survey.

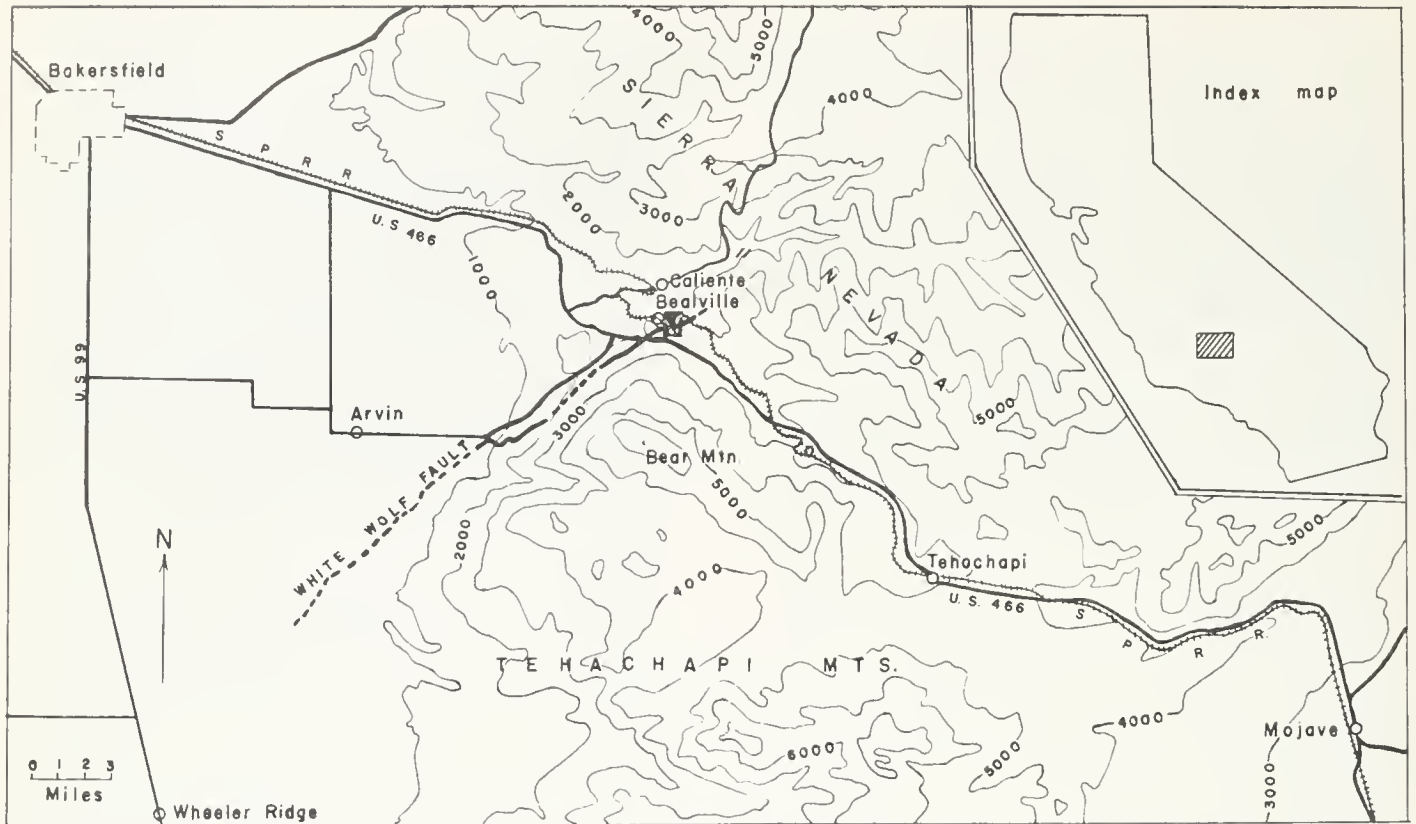


FIGURE 1. Trace of White Wolf fault, partially from data from T. W. Dibblee Jr. (this bulletin). Location of Map of railroad route east of Bealville (fig. 2) is shown by solid rectangle. Topography from U. S. Geological Survey Caliente quadrangle. Contour interval 1000 feet. Datum mean sea level.

were so severely damaged that all traffic on the line was suspended for 25 days.

The tunnels in this area are lined with steel-reinforced concrete walls from 12 to 24 inches thick. Large slabs of concrete that broke away from all other adjacent support were held in place by the reinforcing steel for several days, but continued aftershocks finally broke them loose.

Tunnel 3. Tunnel 3, originally 700 feet long, actually runs a little west of south from the "west" portal. It was undamaged from this portal to a point 548 feet south, where a displacement approximately at right angles to the centerline of the tunnel fractured both walls from floor to arch. When examined on the morning of July 22, both concrete walls of the tunnel were displaced about 2 feet horizontally, the south side to the east. By the time the plane-table map was made that afternoon, the left (east) wall had collapsed inward. From this fracture to the "east" portal, a distance of 152 feet, the walls of the tunnel were broken and large slabs of concrete were loosened but kept from falling by the steel reinforcement. In the last 70 to 90 feet of the tunnel, the concrete was thoroughly shattered; the arch was broken, and the tunnel was caved in.

In repairing this tunnel, 206 feet of the damaged end was converted into an open cut, or "daylighted." After daylighting, the west wall of the new cut was examined and two zones of broken and crushed rock were observed, one 605 feet and the other 620 feet from the west portal.

At a point 570 feet from the west portal (76 feet south of the new east portal) a fracture was observed on which movement had occurred after the daylighting, and by August 15 this movement had amounted to about an inch. On November 1, when Smith visited the area, the displacement had increased to several inches. This fracture strikes N. 15° E. and dips 35° SE. at waist height but flattens out upward. At the top of the new tunnel portal the fracture is nearly flat. The arkosic material described in the section on "General Geology" occurs under this fault.

Between Tunnels 3 and 4. Between tunnels 3 and 4 the track was laid mostly on fill. The rails between the north side of this fill and the south end of tunnel 3 had been contorted into bends with radii of 20 feet or more, as if the ground under the track had been shortened.

No fractures were observed under the tracks, but a small normal fault was observed in the bedrock about 300 feet east of the fill between tunnels 3 and 4. The vertical displacement on the fault appeared to be about 2 feet. On July 22, its strike was N. 80° W. and its dip 50° SW—into the hill. On August 14 it had a similar strike, but the dip had flattened to 37° SW, probably by slumping.

Tunnel 4. Tunnel 4, originally 334.4 feet long, runs about east southeast. Its walls were cracked or broken from the west portal to a point about 85 feet from the east portal. Midway between the portals, in a zone about 50 feet wide, large breaks had occurred and the walls

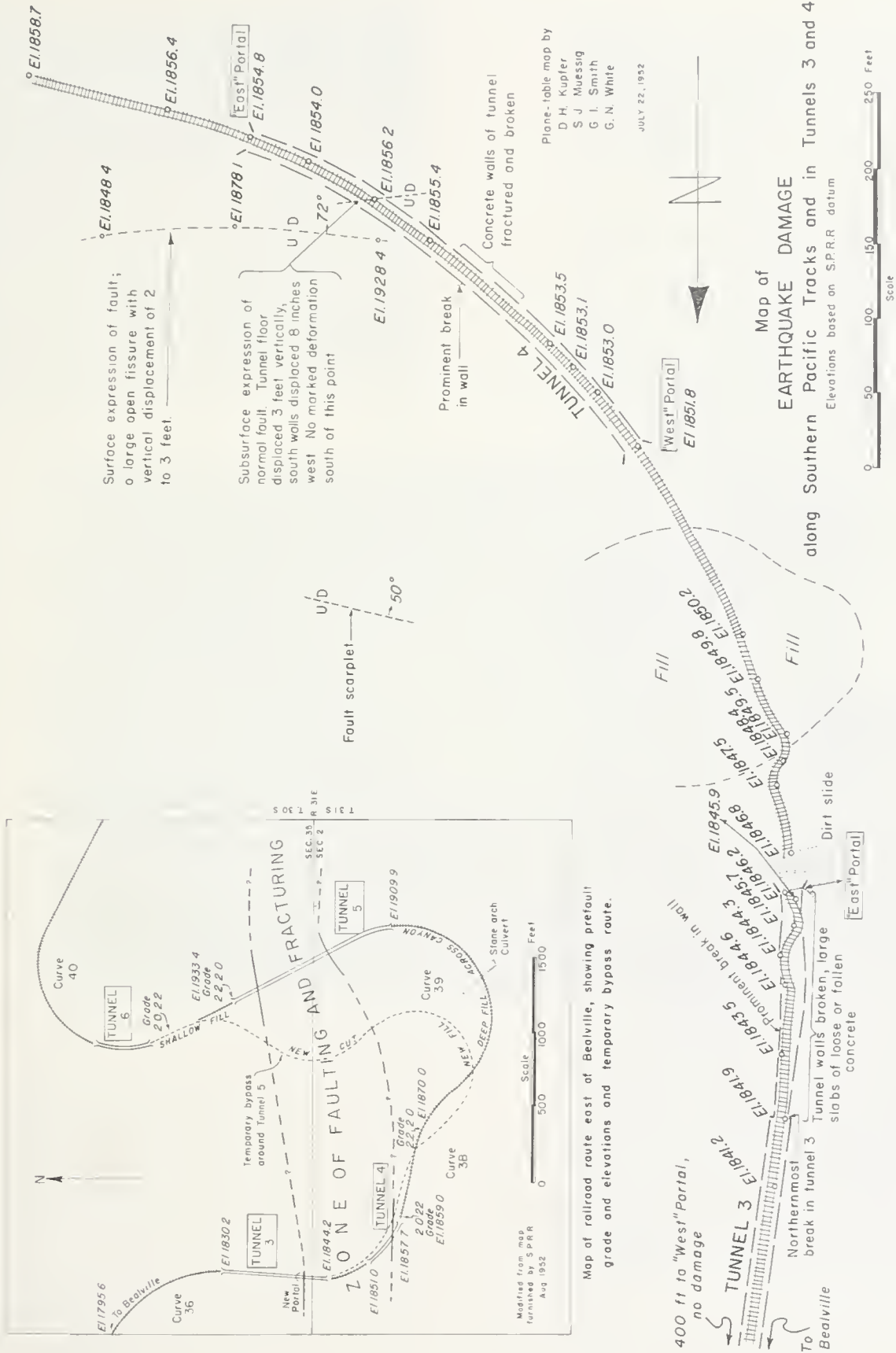


FIGURE 2.

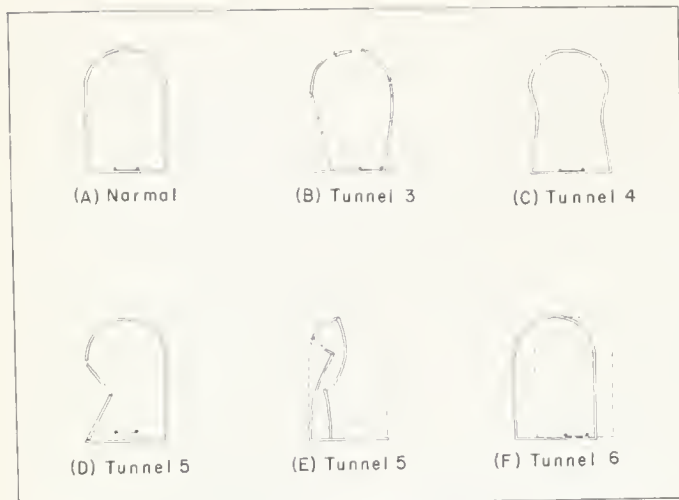


FIGURE 3. Typical tunnel cross sections to show results of earthquake damage. All sections drawn looking along track toward Tehachapi.

the bulldozers had made the extensive excavations around the tunnel, the fault was visible in the bedrock from the top of the cut to track level, a vertical distance of more than 100 feet. Fifty feet above the track level in this cut the fault strikes N. 67° E. and dips 72° SE.; it is marked there by a gouge zone 1 foot to 3 feet wide and a much wider breccia zone. On the south (hanging-wall) side the rock is a hard and relatively unaltered gabbro. On the north side it is highly altered and light-colored; the amphibole is altered to pale green epidote(?) and only the subordinate biotite is unaltered. The rock in the two walls appears to be identical except for the alteration. It seems probable that at the time of alteration both walls were affected equally. As the degree of alteration is now very unequal, previous movements on the fault are suggested. If the alteration is assumed to result from surface weathering, then the fresh rock must have come from depth, and the older movements must have been of the reverse type, and current movement on the fault is but a renewed action along the old line of weakness.



FIGURE 4. Air view of the S-curve in the Southern Pacific Railroad tracks east of Bealville, California. View south. The main valley separates tunnels 3 and 4 on the extreme right side from tunnels 5 and 6 left of center. Portal of tunnel 6 is distorted. Photo by John Shelton.

had buckled inward, giving the tunnel a cross section resembling a keyhole.

The largest vertical displacement observed in any of the tunnels occurred on a fracture about 95 feet from the east portal of tunnel 4; the floor and walls were displaced about 3 feet vertically and 8 inches horizontally. The fracture trends east, dips 72° S., and is a normal fault along which the rocks on the south side moved relatively down and west. The track remained unsevered and was left suspended in the air above the downdropped block.

This normal fault was visible on the surface above the tunnel where it could be traced for about 500 feet. After

Between Tunnels 4 and 5. On curve 38, south of tunnel 4, the damage consisted of small landslides and fill shifting. On curve 39, between tunnels 4 and 5, the track was laid on a deep fill across the main valley. After the earthquake the track and ties were a foot and a half south of their original east marks in the fill. Apparently the fill under the track shifted during the earthquake, while the arc of track, firmly tied to bedrock at each end, did not.

Tunnel 5. Tunnel 5, which runs northwestward from the west portal, caved in at three places and was inaccessible for many days after the earthquake. When visited



FIGURE 5. Damage near the east portal of tunnel 3. Apparently the wall was raised just as the track bent, and the wall then came down on top of the rail. View northwest.

on August 14 it had been reopened enough for a man to walk or crawl through. The principal damage was in a zone 833 to 974 feet from the west portal. The following notes describe the tunnel damage as observed on August 14. The intervals (in feet) refer to postearthquake distances from the west portal. The right wall is the northeast wall.

Feet	
0 to 220	Minor breaks in concrete at base of tunnel walls.
220 to 270	No damage.
270 to 290	Minor breaks in concrete of left wall.
290 to 450	No damage.
450 to 475	Minor breaks in concrete walls.
475 to 500	Major breaks. A fault marked by a 14-inch gouge zone crosses tunnel in this interval from right wall (475 feet) to left wall (500 feet). It strikes about N. 60° W. and dips 65° NE. Reinforcing bars in the concrete were bent into a "U" indicating shortening of 6 inches, and the ceiling arch is 6 inches lower in the northeast block than in the southwest block. This is a normal fault, yet seems to have resulted in horizontal compression.
500 to 598	Concrete cracked.
598 to 632	Roof collapsed and tunnel originally closed but now opened.
632 to 833	Tunnel open but walls badly damaged. Center of left wall buckled inward 3 to 5 feet. Track bowed up from floor in a broad arch whose center is 1½ feet above grade. Maximum distortion of walls at 700 feet.
833 to 850	Roof collapsed and tunnel completely closed. Small passageway reopened.
850 to 960	Very badly damaged. The arch of the roof had not completely collapsed, so section is not closed. Right wall, however, is pushed over against the left wall, leaving only tall narrow opening. In a typical cross section the lower part of the tunnel is only 1 foot to 4 feet wide, but just under the roof arch the opening widens to 8 feet. Normal tunnel width is 16 feet.
960 to 974	Roof collapsed and tunnel completely closed. Small passageway reopened.
974 to 1170	No damage.
1170	East portal (actually west of other portal).

Between Tunnels 5 and 6. Between tunnels 5 and 6 the track was mostly on fill, which settled and moved downhill slightly and carried the track with it. In the middle of the fill zone the track both slumped and moved laterally a foot or two.



FIGURE 6. Sharp bend in the tracks south of tunnel 3 strikingly demonstrates that the ground had been shortened in this area. A landslide blocks the east portion of tunnel 3.



FIGURE 7. View in tunnel 4. Normal fault dipping 72° toward the camera has offset the walls and lifted the track 3 feet. The slender curved rods are steel reinforcement.



FIGURE 8. Surface expression of the normal fault shown in figure 7. The fault was traced several hundred feet to the right of the area shown in the photograph. View north.

Tunnel 6. Tunnel 6 was not on the main fault zone. Its walls were shattered and broken, mainly by longitudinal cracks in the arch, and the tunnel was displaced to the left with respect to the tracks. In the hillside above the tunnel there were fractures roughly parallel to the tunnel, suggesting that the ground through which the tunnel passed slumped downhill a few feet as a result of the earthquake, while the track moved somewhat less. Tunnel 6 has been daylighted.

Beyond Tunnel 6. Beyond tunnel 6, in the east arm of the S-curve, the track was warped by settling of fills and covered in places by landslides; otherwise it was not seriously damaged. Where the fault zone crosses the track, the rails were slightly buckled and the fills had slumped 2 feet. Thirteen inches of rail were removed from the tracks during realignment. There are fractures trending N. 53° E. on both sides of the track in this area.

As tunnel 7 lies southeast of the general area described above and is not on the main fault zone, it was not visited. The concrete walls of the tunnel are said to have been cracked by the initial shock, but not broken. Later shocks, however, worked some of the concrete loose and necessitated repairs.



FIGURE 9. Cracked and buckled walls in tunnel 5. Camera is on the cave-in at 833 feet from the west portal; looking toward the cave-in at 632 feet. The tracks are bowed up about 1½ feet.

EVIDENCE OF SHORTENING AND VERTICAL DISPLACEMENT IN THE FAULT ZONE

The major fault damage in the vicinity of the Southern Pacific tracks near Bealville was confined to an east-west zone about 500 feet wide. The fault zone was well delimited where it cut tunnels 3 and 4, and also where it cut tunnel 5, though at the surface its boundaries were obscure.

Tunnels 3 and 4. The most spectacular evidence of crustal shortening was that afforded by twisted and contorted rails found near the east portal of tunnel 3, where measurements made by the Southern Pacific engineers the day after the earthquake indicate that the earth's crust was shortened by 10.9 feet.

Measured shortening near tunnels 3 and 4.

	S.P.R.R. (tape)	U.S.G.S. (stadia)
Tunnel 3	2.3 feet	2.0 feet
Between tunnels 3 and 4	8.6 feet	9.6 feet
Tunnel 4	0	-1.7 feet
Total shortening	10.9 feet	9.9 feet

All this shortening occurred between the northernmost break in tunnel 3 and the west portal of tunnel 4; outside of this zone neither the rails nor the ties had

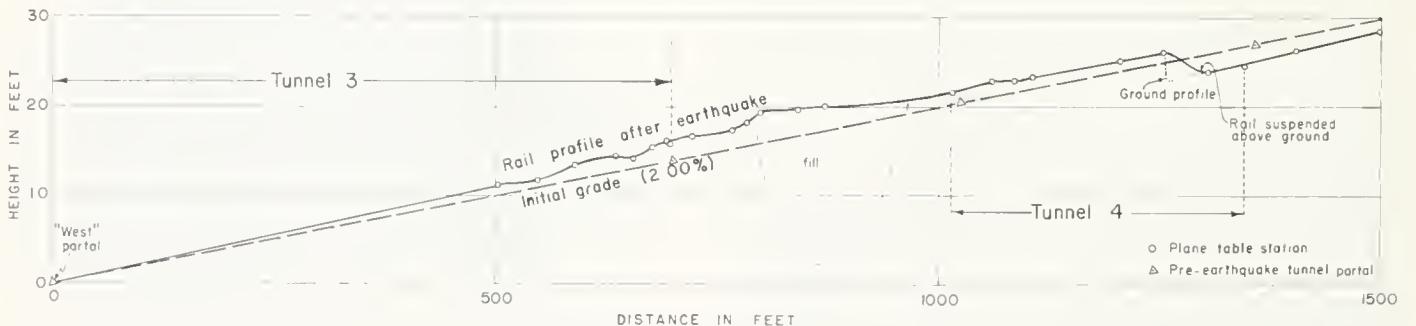


FIGURE 10. Profile along the tracks showing grade before and after earthquake. Datum is west portal of tunnel 3. Tunnel positions indicated are those immediately following earthquake. Vertical exaggeration x10.

shifted in relation to the ground or to each other. About 75 percent of this shortening occurred in a section less than 150 feet long, just outside the east portal of tunnel 3. South of this section, the shifting and deformation of the rails was minor; north of it, tunnel 3 was shortened only about 2 feet. In spite of the concentration of shortening in this narrow zone, however, no significant fractures were observed, even though half of the section is underlain by bedrock.

The observed vertical displacement of 3 feet on the normal fault in tunnel 4 should have caused an extension of 0.6 foot along the line of the track. The Southern Pacific Company's measurements, however, show no change in the total length of tunnel 4, so this extension in one part of the tunnel was apparently balanced by shortening in other parts.

Figure 10 illustrates the relative vertical displacements along the track line of tunnels 3 and 4. The dashed line represents the theoretical prefault grade of 2 percent, and the solid line represents the postfault grade as determined with the plane table. The elevation of the west portal of tunnel 3 was assumed to have been unchanged and was used as a datum for the horizontal and vertical measurements. Any actual change in the elevations of these portals will be determined when the U. S. Coast and Geodetic Survey completes its present resurvey of the first-order-level line through the area (Whitten, this bulletin).

Apart from the displacement on the normal fault at the south end of the disturbed zone, the principal effect of the earthquake on the track profile was to warp the track into an arch, whose crest was about $3\frac{1}{2}$ feet high and coincided with the contact of the fill and the bedrock.

Tunnel 5. No complete resurvey of tunnel 5 had been made at the time of the authors' last visit, but enough work had been done by the Southern Pacific engineers to indicate some horizontal and vertical shifting. The centerline of the tunnel was displaced horizontally about 1 foot. The bent reinforcing bars at 486 feet and some bowed-up track between 632 and 833 feet indicated local shortening, but the overall length of the tunnel was reported to be unchanged.

According to a preliminary survey, the arch of the tunnel dropped 6 inches at one point and 3 inches at another. In one zone the grade of the arch, which was formerly 2 percent, had changed to 0.5 percent for 50 feet and to 4 percent for 90 feet, perhaps because of slumping.

Other Areas. There is a marked contrast between the observed characteristics of the fault zone in the tunnels and on the surface. In the tunnels the zone was about 500 feet wide and the damage was severe. On the surface, except along the normal fault over tunnel 4, the fractures were few and small and the displacements were less than a foot.

Where the fault zone crosses U. S. Highway 466, it is about 300 feet wide, but the only visible damage consisted of 5 or 10 minor fractures in the asphalt. Many small normal faults were seen between the highway and the railroad, and the displacement on each was less than a foot.

In the east arm of the S-curve in the railroad, where there are no tunnels, the faulting caused only a single minor fracture and a 13-inch shortening of the rails.

SUMMARY AND CONCLUSIONS

In the preceding pages the writers have outlined and described in detail the earthquake damage along the Southern Pacific tracks and have presented a minimum of interpretation. In the following section this damage is grouped first according to type and then according to distribution; each grouping, in turn, leads to suggestions of geologic causes. In the concluding statement, all these data and the deductions drawn from them are synthesized to produce an interpretation of the process that caused all the observed features.

Evidence Given by Types of Damage. 1. Damage by landslides was widespread. Tunnel 6, north of the fault zone, was damaged by a landslide, and many stretches of track in other areas were covered or dislocated. Some of the wall buckling in tunnel 5 may have been caused by the pressure of sliding earth. The prime cause of this damage was undoubtedly the dislodging of masses of regolith and decomposed rock by the earthquake.

2. Damage clearly related to a single fracture was found in only two places: at 239 feet in tunnel 4, and at 475 feet in tunnel 5. Both fractures are normal faults. In view of the evidence that the net result of motion in the fault zone was shortening, it is believed that normal faulting was a late and minor phase of the total movement; reverse faulting occurred first, and normal faulting occurred slightly later as a result of settling.

3. The most extensive damage to tunnels consisted of buckling and cracking walls. As this type of damage was confined almost exclusively to the fault zone, it probably was not caused directly by earth shaking, but rather by displacements along a multitude of small fractures, which may have been the distributaries of larger movements at depth.

4. The most striking damage, and the most significant tectonically, was the buckling of the track between tunnels 3 and 4. The ground beneath the track had not only been shortened over 10 feet but had been bowed up. Both of these features prove that there was at least local compression.

Evidence Given by Distribution of Damage. 1. The principal shortening in the vicinity of tunnels 3 and 4 took place in a strip 150 feet wide, located in the northern part of the 500-foot-wide fault zone. In tunnel 5, also, the major damage took place in the northern part of the fault zone. This asymmetrical distribution of damage could be explained by one of the following hypotheses: (a) The stress was most intense along the north boundary of the fault zone, and diminished southward as if the shock had been instantaneously relieved along numerous fractures. This hypothesis hinges on the premise that faulting had occurred in this zone previously and that the renewed stress was relieved mainly in the northern part of the fault zone. (b) The major shortening may have occurred in the first instant of shock over a zone about 150 feet wide. In the next few moments the fault zone may have widened southward to the 500-

foot width later observed, giving the appearance of asymmetrical destruction in the final zone.

2. The fault zone as exposed in the tunnels was about 500 feet wide, but on the surface it was apparently much narrower. This narrowing of the fault zone upward probably was more apparent than real, for minor fractures in rigid concrete would be seen and recorded, whereas many of these fractures might pass unnoticed when they cut the overlying regolith. Near the surface, movement was dissipated along numerous fractures, and part of it may have been absorbed by intergranular shifting in the regolith and decomposed bedrock.

3. Large-scale shortening was found in the vicinity of tunnels 3 and 4 but nowhere else along the strike of the fault zone in this area. Compression may have been concentrated in the vicinity of tunnels 3 and 4, and have been dispersed to the east and west, because of lateral variations in the competency of the bedrock. The

presence of fill between the two tunnels may have made the effects of compression more apparent.

Conclusions. The earthquake that occurred in the vicinity of Bealville on July 21, 1952, was the result of compression that was relieved by reverse faulting in the White Wolf fault zone. Because the south block moved up relative to the north block (fig. 12), the fault zone dips south. Seismologic and other data * published after this paper was written corroborate this dip and movement. The compression was immediately followed by relaxation and settling along normal faults.

* Buwalda, J. P., and St. Amand, Pierre, 1953, Arvin-Tehachapi and Bakersfield earthquakes of July-August 1952: Bull. Geol. Soc. America (abstract p. 1500, Dec. 1953); Richter, C. F., 1953, Kern County aftershocks: Progress Report: Geol. Soc. America (abstract in press); and Dibblee, T. W., Jr., and Oakeshott, G. B., White Wolf fault in relation to geology of the southeastern margin of San Joaquin Valley, California: Bull. Geol. Soc. America (abstract p. 1502-03, Dec. 1953).

8. MEASUREMENTS OF EARTH MOVEMENTS IN CALIFORNIA*

BY C. A. WHITTEN †

Abstracts. Resurveys by the United States Coast and Geodetic Survey across parts of the San Andreas fault are consistent in showing a slow drift to the northwest at a rate of about 2 inches per year, west of the fault. Reobservation, in 1941, of the triangulation system crossing the San Andreas fault in Imperial Valley, where the earthquake of 1940 occurred, established the fact that the area on the east side of the fault shifted to the southeast and that the area on the west shifted to the northwest. Preliminary results of repeat surveys of triangulation and level schemes in Kern County, in September 1953, suggest that the Bear Mountain block, southeast of the White Wolf fault, moved north-northeast a distance on the order of one to 2 feet and the valley block a similar distance in a west-southwest direction. The Bear Mountain block was also elevated, and the valley side was depressed on the order of a foot and a half near Arvin.

The large relative displacements in the earth's crust which were noted after the San Francisco earthquake of 1906 suggested the repetition of surveys for determining the amount and extent of these horizontal movements. Reports from residents indicated relative displacements from 5 to 20 feet at many points along the San Andreas fault (fig. 1). These relative displacements were noted along 185 miles of the fault and averaged about 10 feet.

Because of the changes in geographic positions of points near the fault, it was necessary for the Coast and Geodetic Survey to reobserve the existing triangulation in that locality. The first surveys in the area had been made in 1851. The basic first-order scheme had been completed in 1885. By noting the differences in the geographic positions of the triangulation stations as determined by the resurvey, it was possible to measure these displacements.

The report of the Superintendent of the Coast and Geodetic Survey for 1907 contains a detailed description of these resurveys with tabulations, maps, and sketches showing the differences of the geographic positions as determined by the various surveys. The studies made in 1907 produced unexpected evidence of earlier displacements, probably the result of the earthquake of 1868.

In 1922, at the request of Dr. Arthur L. Day, director of the Geophysical Laboratory of the Carnegie Institution, and chairman of the Committee on Seismology of that Institution, the Coast and Geodetic Survey made plans to reobserve the first-order triangulation scheme along the coast between San Francisco and Los Angeles. These resurveys were more extensive than those made immediately after the earthquake of 1906 and were completed in 1924. The results showed very conclusively that there had been relatively large displacements. Because of the length of the scheme and the possible accumulation of errors, it was not possible to determine the absolute amount and direction of the movement for the points in the middle of the arc.

In 1929, the Committee on Seismology recommended the establishment of a series of arcs of triangulation crossing the San Andreas fault at right angles, with repeat observations at 5- to 10-year intervals. Each

arc was to consist of a primary scheme, 40 to 50 miles in length, supplemented with a secondary scheme of closely spaced points inside and extending the full length of the primary scheme. This pattern of survey will aid in measuring two types of earth movement. The primary scheme when reobserved will indicate the presence of any movement or drift of the area on one side of the fault relative to the area on the other side. If this movement is continuous over a long period of time, the repeated observations will show the rate of movement. The repetition of the survey with the secondary scheme of closely spaced points will measure these smaller movements.

The first two of these special surveys were established from Newport Beach to Bear Lake (1) and from Point Reyes to Petaluma (2). This work was completed in 1929 and 1930. During the next 3 years four similar projects were extended from Monterey Bay to Mariposa Peak (3), from San Fernando to Bakersfield (4), in the vicinity of the San Luis Obispo (5), and in the vicinity of Taft (6).** In 1934 the scheme between Newport Beach and Bear Lake was reobserved. An investigation of these reobservations made at that time indicated there had been no displacement of any significance.

The arc of triangulation between Point Reyes and Petaluma was reobserved in 1938. The results of this resurvey were not conclusive, although some interpretations gave evidence of a northwesterly drift for the stations in the vicinity of Point Reyes.

The Committee on Seismology made further recommendations in 1935 to modify the pattern of the surveys. The new plans specified lines of traverse and leveling crossing the fault at right angles. The marks were to be spaced at intervals of 100 feet for the first mile from each side of the fault, at 200 feet for the second mile, and at 300, 400, and 500 feet for the third, fourth, and fifth miles, respectively. Eight areas located along the San Andreas fault in southern California were selected for these special studies. The areas were near Maricopa (7), Gorman (8), Palmdale (9), Inglewood (10), Brea (11), Cajon Pass (12), Moreno (13), and White Water (14). The surveys for the Maricopa, Gorman, and Palmdale zones were completed in 1938.

The traverse in the vicinity of Palmdale was remeasured in 1947. A comparison of these measurements with those of 1938 disclosed no changes indicative of earth movement. The small differences which were noted were either the result of accidental errors of observation or due to local settlement of marks.

The surveys in the vicinity of Maricopa and Gorman were reobserved in 1948-49. It is planned to continue this project of establishing and repeating these special traverses until the eight zones are completed.

Imperial Valley Earthquake. On May 18, 1940, a severe earthquake occurred in the Imperial Valley. Although no triangulation had been established in that area for the particular purpose of studying earth movements, an extensive net covering the area had been

* Modified from Whitten, C. A., *Horizontal Earth Movement*, in the *Journal of the Coast and Geodetic Survey*, April 1949, no. 2, pp. 84-88. Later data relating to the Kern County earthquakes were furnished by Mr. Whitten in September 1953.

† Mathematician, U. S. Coast and Geodetic Survey.

** Note: The numbers in parentheses refer to the areas correspondingly numbered in fig. 1.

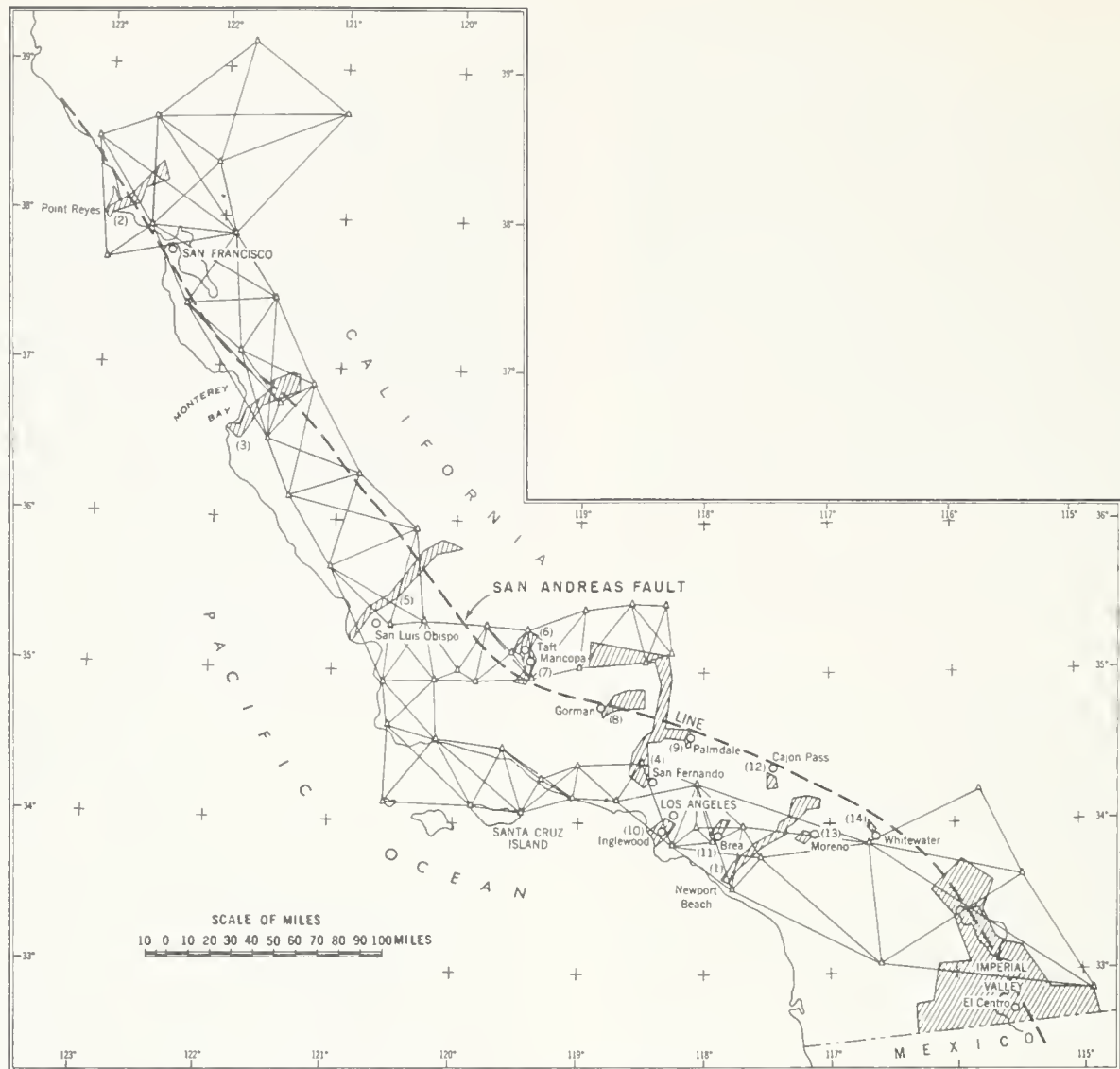


FIGURE 1. Hatched areas show planned control across San Andreas fault to determine crustal changes. Numerals in parentheses refer to corresponding numbers in text. *Reprinted from U. S. Coast & Geodetic Survey Journal, April 1949, p. 84.*

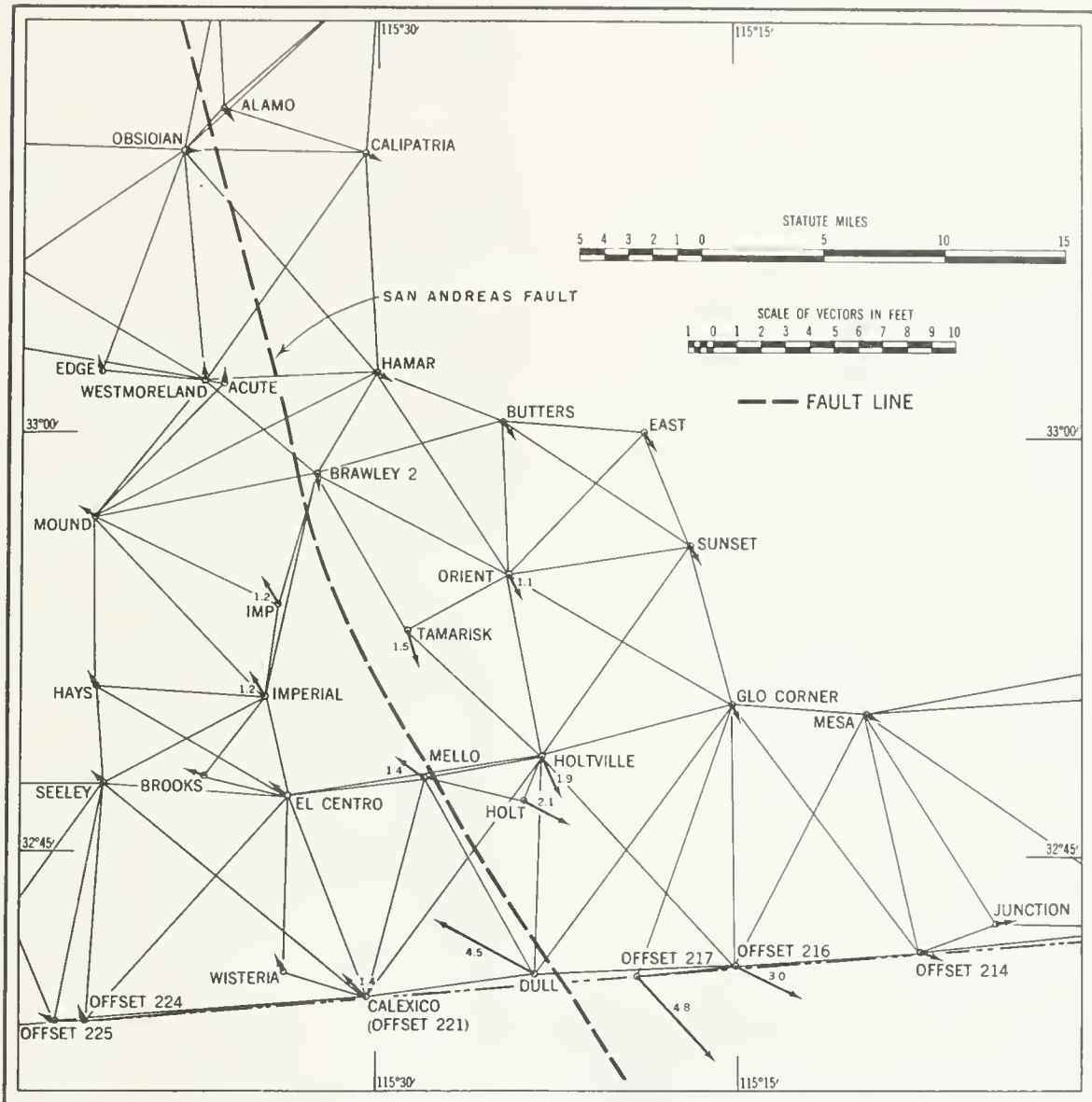


FIGURE 2. Earthquake investigation in Imperial Valley, California, 1941. Reprinted from *U. S. Coast & Geodetic Survey Journal*, April 1949, p. 86.

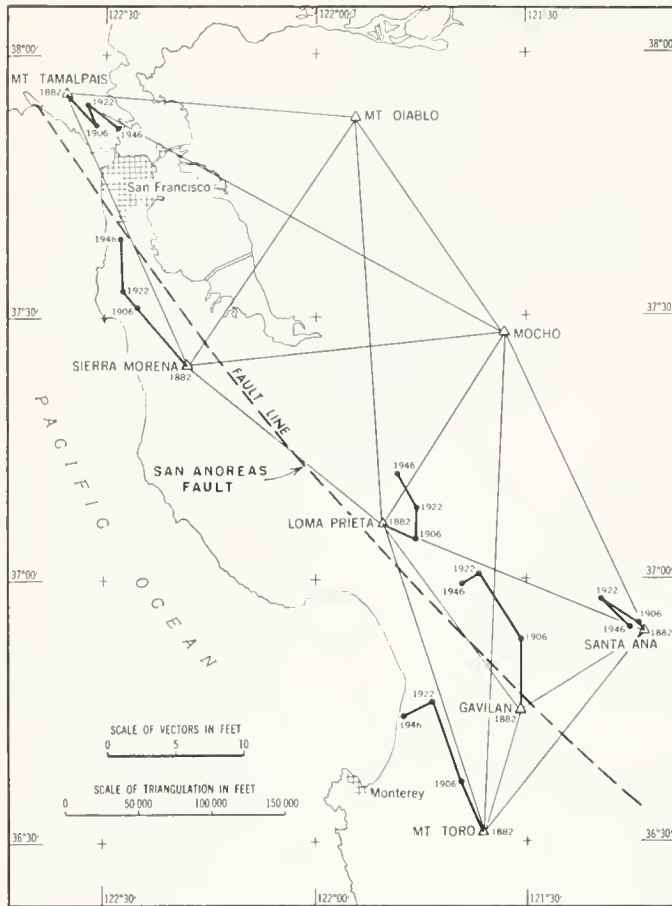


FIGURE 3. Results obtained from four triangulation adjustments between 1882 and 1946 showing displacements as vectors. Reprinted from *U. S. Coast & Geodetic Survey Journal*, April 1949, p. 87.

established in 1935, with supplemental surveys in 1939. A part of this triangulation was reobserved in the spring of 1941. After the work was completed, a preliminary investigation indicated that the resurveys should have been extended over a larger area so that the problems of adjustment would be simplified. No further field work, however, was done at that time.

At the conclusion of the war the data from the surveys in this area were given further study. Comparisons of the final geographic positions of the two adjustments sharply defined the location of the fault line, the direction and magnitude of the horizontal movement, and the extent of the area that was affected by these movements. The vectors in figure 2 show the direction and magnitude of the displacements. The region of maximum shift was near the southern limit of the survey. Reports from Mexico stated that the amount of displacement decreased along the fault south toward the Gulf of California. It can be seen from the figure that the area on the east side of the fault shifted to the southeast and that the area on the west shifted to the northwest. At distances of 15 to 20 miles east or west of the fault the magnitude of the shifts is reduced to a small fraction of a foot. The data from this investigation are more consistent in showing these displacements than are the results of any previous resurvey. This study brought out

the great value in having an extensive triangulation network over all of the area of the fault, so that if an earthquake did occur, the basic surveys will have been made.

Slow Drift Along Coast. In 1946 basic triangulation networks were executed in the San Francisco Bay area and in the Santa Clara Valley with rigid connections made to the old primary scheme. A comparison of the lists of the directions from the various surveys spaced over a period of more than 60 years shows that there has been a progressive change in the azimuths of the lines crossing the fault at approximately right angles. The azimuths are increasing in a clockwise direction. Astronomic azimuths observed in 1885, 1906, 1923, and 1947 on one of the lines crossing the fault also show this progressive change. Since azimuths determined by triangulation and those determined astronomically are independent of each other with regard to observation and computation, the similarity of results strengthens the evidence supporting a slow drift of the area to the west of the fault. Knowing the lengths of the lines crossing the fault, the displacements needed to produce the changes in azimuth were computed. The results of these computations are very consistent and show a slow drift to the northwest at a rate of about 2 inches per year, west of the San Andreas fault. The width of the area varies from 30 to 40 miles. This rate is based on the results of the four different surveys spaced at intervals of approximately 20 years. (See fig. 3.)

The results of these studies showed the need for more extensive surveys so that the geographical limits of the areas affected by this movement could be determined. In 1948 the triangulation scheme north of San Francisco was reobserved as well as the scheme extending along the coast as far south as San Luis Obispo and then east to Bakersfield. The same slow movement is indicated throughout the full length of the scheme. The section near Bakersfield was originally observed in 1926. The other surveys which have been repeated date back to 1880. The longer span of years of course will give a more accurate rate. However, even the more recent work near Bakersfield shows a rate for this movement of an inch and a half per year (the area east of San Andreas fault is moving south). It will be necessary to repeat these surveys after an interval of a few years to verify this rate.

Kern County Earthquakes of 1952. After the Arvin-Tehachapi earthquake of July 21, 1952 and numerous aftershocks, including the Bakersfield earthquake of August 22, the U. S. Coast and Geodetic Survey made repeat surveys of triangulation and level schemes in Kern County. Field work was started in October 1952 and completed in January 1953; adjustments of the surveys were in progress in September 1953 when this section was written. Some of the final results of the triangulation adjustment and preliminary results from the leveling are shown graphically in figure 4. The line marked "White Wolf fault" is the trace of the fault based on geological field evidence and has been added to the map by the Division of Mines. The horizontal displacement, as determined from adjustment of the 1951-52 and 1952-53 surveys, is shown by means of vectors. The

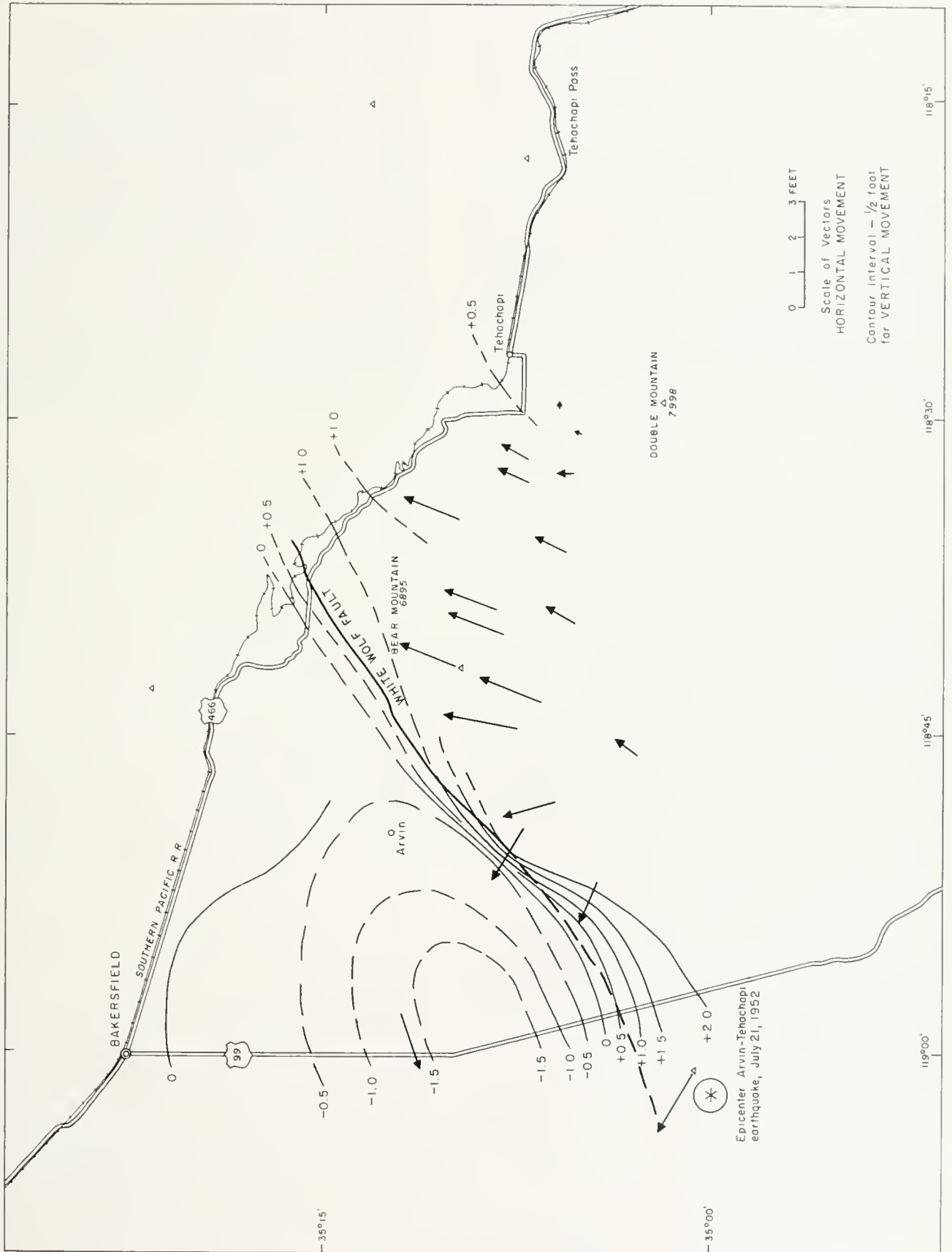


FIGURE 4. Measurements of earth movements in Arvin-Tehachapi earthquake area.

vectors might be expected to have errors equivalent to half a foot or possibly a foot. The relationship between two adjacent points where the shifts are shown by the vectors may be considered to be accurate to a quarter of a foot. The triangulation stations on Double Mountain and on the high point about 2 miles north of Tehachapi Pass were used as fixed or stationary points in the adjustment.

The differences of elevation are the result of the comparison of the two surveys without an adjustment of closures. The sharp break about 6 miles south of Arvin has been accurately determined as well as the more gradual uplift southwest of that point. The area of subsidence south of Bakersfield is not definitely determined with respect to its geographical extent, but the magnitude of the settlement is accurate to a small fraction of a foot. The vertical changes occurring through the mountains between Bakersfield and Tehachapi are not as sharply defined.

As may be seen in figure 4, the data show that the Bear Mountain block, southeast of the fault, moved toward the north-northeast a distance on the order of one to two feet, but the southwest segment of that block, as shown by triangulation stations, appears to have moved upward and toward the northwest over the valley. The one triangulation station on the valley floor suggests movement of the valley block a similar distance in a west-southwest direction.

Greatest vertical movement, an elevation of 2 feet, appears to have taken place in the epicentral region of the Arvin-Tehachapi earthquake of July 21, with the Bear Mountain block elevated and tilted toward the southeast, but moved northwest. Depression of the valley side was on the order of a foot and a half, centering in a basin-shaped area southwest of Arvin.*

* Ed. Note. It is significant that these measured movements of the land surface, showing the southeast (Bear Mountain) block moved relatively up and in a northerly direction, are thoroughly consistent with geologic data indicating the White Wolf as a left lateral reverse fault, and with seismologic data supporting oblique-slip movement in the same sense on that fault.

9. EFFECT OF ARVIN-TEHACHAPI EARTHQUAKE ON SPRING AND STREAM FLOW *

BY REVOC C. BRIGGS † AND HAROLD C. TROXELL †

ABSTRACT

Flow in many of the streams and springs in the area covered by this report increased as a result of the Arvin-Tehachapi earthquake. Although this increase in flow appears to have been temporary, there was still evidence of it in some of the streams and springs as late as June 1953, when this report was prepared. It is doubtful if the earthquake had any permanent effect on the recharge areas or on the permeability of the aquifers. This temporary increase in some cases is probably due to the mere disturbance of the unconsolidated material in the discharge areas, resulting in the clearing of the existing outlets and opening of new ones.

INTRODUCTION

In arid and semiarid localities where water supply is always in the public mind, any event which affects natural water resources is of interest. The Arvin-Tehachapi earthquake proved to be no exception. Immediately after the earthquake local newspapers reported marked increase or decrease in the flow of several springs and streams.

From time to time data on the flow of springs affected by earthquakes have been obtained by private and public agencies. Usually these individuals or agencies do not have an opportunity for placing such data in public records and consequently much information is unavailable for use by the general public.

This analysis represents an attempt at reporting all data available at this time reflecting the change in flow of the mountain streams and springs in Kern, Santa Barbara, Ventura and Los Angeles Counties as a result of the Arvin-Tehachapi earthquake. However, neither the degree of coverage nor the type of data is identical throughout this entire area.

A special effort was made to obtain factual data in Kern County near areas of greatest disturbance. However, the available data consisted primarily of eye-witness accounts of changes in spring or stream flow. These accounts were supported by continuous records of discharge for a number of streams at gaging stations maintained by the U. S. Geological Survey or the U. S. Bureau of Reclamation. The points of observation and reference numbers for data in Kern County are shown on figure 1. In addition, this map indicates by symbol whether the flow of the spring or stream (a) increased, (b) decreased, or (c) remained unchanged, as a result of the Arvin-Tehachapi earthquake.

By far the predominant effect of the earthquake on these streams and springs in eastern Kern County was to increase the flow. Probably the most noteworthy evidence of this increase was in Caliente Creek basin. Before the earthquake the stream channel of Caliente Creek (25) was completely dry below its confluence with Tehachapi Creek at the town of Caliente. Immediately after the earthquake, the flow from springs in the headwaters increased so that within a few days the flow of Caliente Creek at Caliente reached about 25 cubic feet per second and remained near that value until winter precipitation increased and sustained a still larger flow.

In Santa Barbara, Ventura, and Los Angeles Counties, it was impractical to engage in a complete field examination. As a result this study was restricted to the mountain areas of these counties. The data used were obtained from a well distributed network of gaging stations operated cooperatively by the U. S. Geological Survey and the State of California, supplemented by stations operated by Los Angeles County Flood Control District and Ventura County Water Survey. This network was further supplemented by an intense investigation of stream and spring flow already under way in one area. In the Santa Ynez Mountains just west of the city of Santa Barbara, the U. S. Geological Survey, in cooperation with the Santa Barbara County Water Agency, measures monthly the flow in about 130 springs and small mountain streams. A portion of these networks is shown on figure 2. The sites indicated on figure 2 include all the gaging stations at which there was a measurable increase in discharge attributable to the Arvin-Tehachapi earthquake. Also shown is a limited group of stations at which there was no measurable increase in flow attributable to the earthquake. Inclusion of this latter group of stations was largely for the purpose of delineating or defining the general area in which stream or spring flow was affected by the earthquake.

In the mountain areas of these three counties, the most significant increase in runoff attributable to the Arvin-Tehachapi earthquake occurred in Ventura County. In the 254-square-mile mountain drainage area of Sespe Creek near Fillmore (90), the daily discharge increased from 17 cubic feet per second on July 20 and 21, 1952, to 37 cubic feet per second on July 31, an increase which apparently was entirely a result of the earthquake. This increase in runoff amounted to 2,160 acre-feet between July 21 and September 30, 1952, and was equivalent to 61 percent of the entire runoff for the preceding dry water year of 1951.

The change in flow in many of the smaller springs was even more spectacular. In one of the smaller springs (67) on the Juan Y Lolita Rancho in the Santa Ynez Mountains, the flow following the earthquake was about three or four times as great as that during the fairly wet water year of 1952.

Notwithstanding this noteworthy increase in flow, almost 88 percent of the points of observation in the Santa Ynez Mountains indicated no change in flow as a result of the earthquake. Moreover, even in short distances there were often radical differences in flow characteristics attributed to the earthquake.

The principal mountain ranges and major fault systems have been indicated on figure 2 as a suggestion of geologic structure. Those gaging stations showing an increase in flow are mostly located in the Santa Ynez Mountains or minor ranges between the San Rafael Mountains on the west and the San Gabriel Mountains on the east. However, had coverage been as intense in the San Rafael and San Gabriel Mountains as in the middle Santa Ynez Mountains, evidence of increased runoff attributable to the Arvin-Tehachapi earthquake may have been more widespread.

* Published by permission of the Director, U. S. Geological Survey.
† District Engineer and Hydraulic Engineer, U. S. Geological Survey.

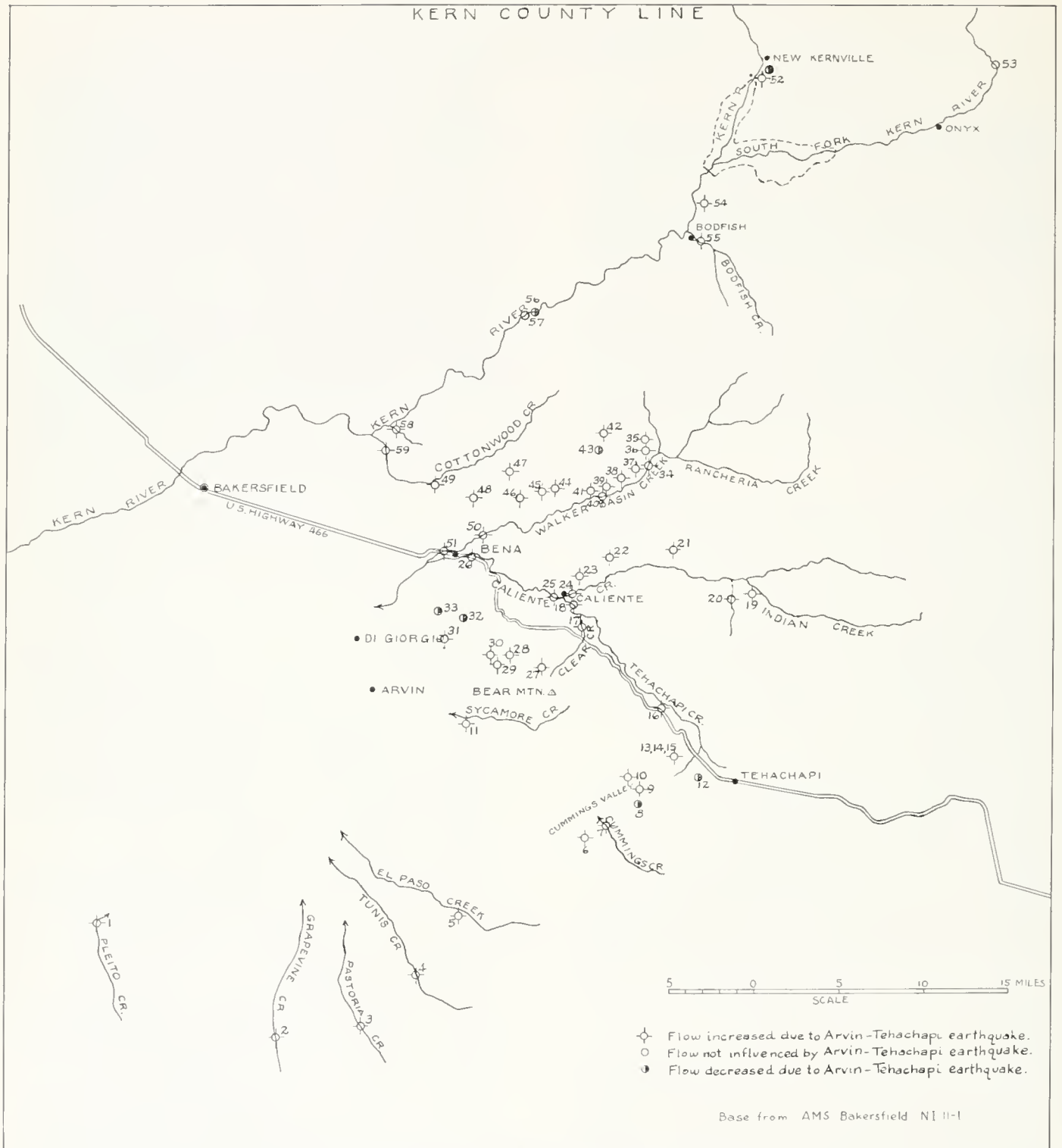


FIGURE 1. Location of selected gaging stations in Kern County.

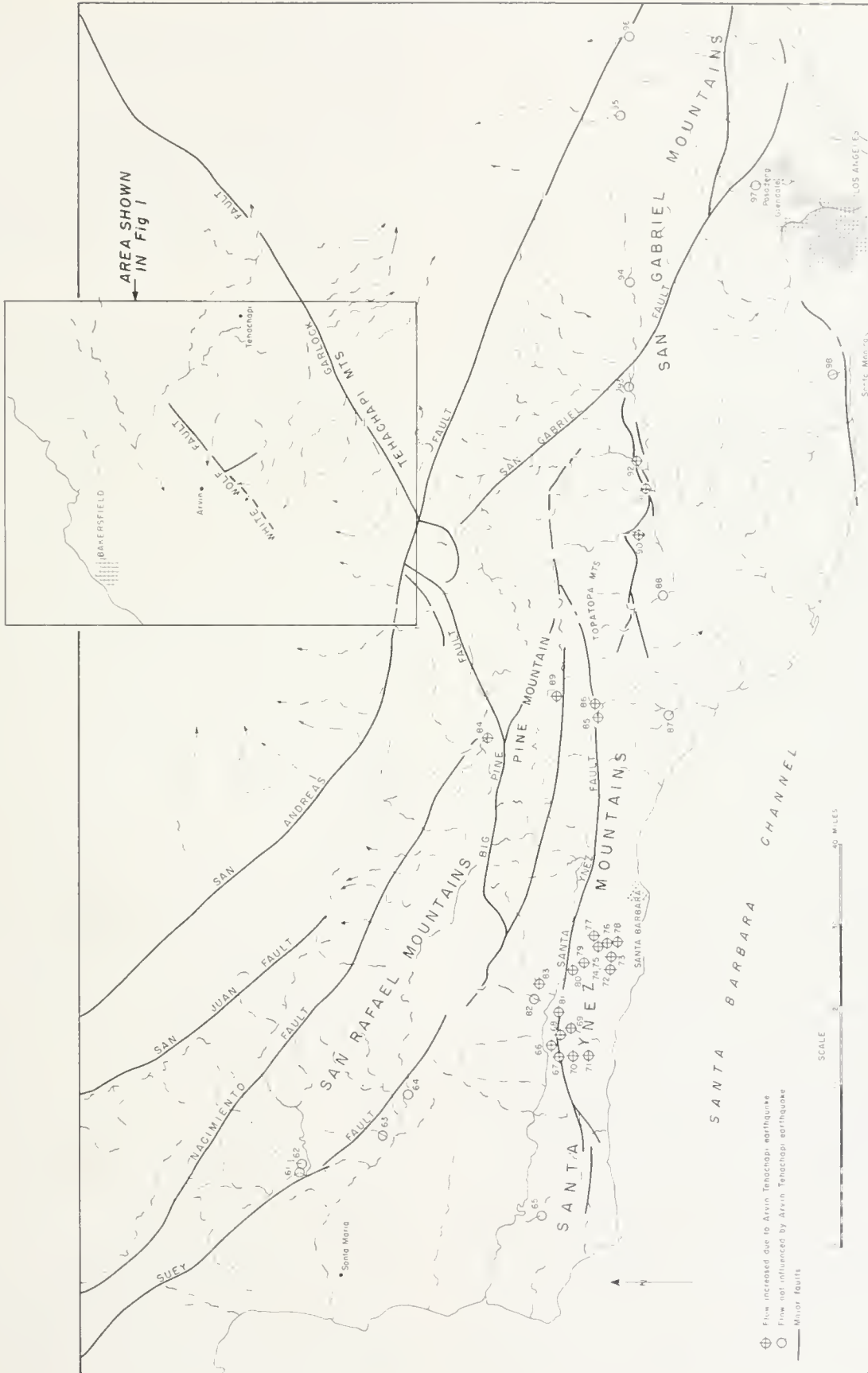


FIGURE 2. Location of selected gaging stations in Santa Barbara, Ventura, and Los Angeles Counties.

Streams investigated in Los Angeles County did not show any noticeable increase in flow following the earthquake.

ACKNOWLEDGMENTS

The authors wish to thank their fellow workers in the U. S. Geological Survey for suggestions and assistance in preparing this report, particularly T. A. Cooper, field engineer at Visalia, who obtained many useful data. Also they wish to thank the many local people in the earthquake area who furnished information, especially Leroy Rankin of Walker Basin, C. W. Poole of Lorraine, and Brad Krauter of Tehachapi.

Although it is impracticable to name all who gave assistance, the following people should be mentioned: W. M. Jaekle, Eng. Dept., Southern Pacific Railroad, San Francisco; J. G. Sinclair, Eng. Dept., Southern Pacific Railroad, San Francisco; H. Cole, Southern Pacific section foreman, Bena; Roy Ballard, U. S. Soil Conservation Service, Tehachapi; Elmer Lyne, U. S. Soil Conservation Service, Tehachapi; L. E. Williams, Caliente; A. F. Nenmarkel, near Arvin; Lawrence Brown, Caliente; W. T. Blackburn, Wrigley Ranch, Tehachapi; F. W. Nighbert, Bakersfield (White Wolf Ranch); Jack Shepard, Humble Oil Co., Bakersfield; Joe Prowell, Kern Rock Co., near Bakersfield; Frank Lawrence, Bodfish. The offices of the U. S. Bureau of Reclamation at Fresno and Visalia furnished records of discharge of several streams in the Kern County area.

CHANGES IN SPRING AND STREAM FLOW ATTRIBUTABLE TO THE EARTHQUAKE

The Arvin-Tehachapi earthquake is known to have affected the flow in many springs and streams over a sizeable area in the counties of Kern, Santa Barbara, and Ventura. The earthquake, on the morning of July 21, 1952, occurred in that part of the year characterized by minimum runoff and precipitation. During these warm summer months, practically all flow from springs and runoff in mountain canyons has its immediate origin in perennial ground-water storage.

This storage is periodically recharged by the excessive precipitation during the wetter years. For example, in the San Bernardino Mountain drainage area of Mill Creek, as a result of a very wet 1921-22 winter, there was a large recharge to mountain ground-water storage equivalent to 21 inches over the entire area. The next measurable replenishment to ground-water storage did not occur until 5 years later when a recharge equivalent to 9.2 inches over the area resulted from the 1925-26 winter precipitation. As a result of these periodic sizeable contributions, seepage has been sustained, in the form of perennial flow, even during such extended droughts as those of 1893-1904, 1923-34, and 1944-51.

Earth tremors such as those experienced on July 21, 1952 may cause some change in the ability of these fractured mountain blocks to store ground water, and frequently disturb existing conditions of permeability in the discharge areas. For many years those closely associated with water supply have known that seepage from these mountain ground-water sources has been disturbed at times by earthquakes. However, seldom is this change in flow sufficiently documented to appear in scientific literature. Consequently, it is the primary

purpose of this report to record all available data on the change in flow of springs and streams in the nearby mountain areas as a result of the Arvin-Tehachapi earthquake.

These factual data are presented in the form of a brief description of the point of observation and a statement indicating the effect of the earthquake on seepage from springs and flow in streams. These data are given in numerical sequence, segregated into two parts, (a) Kern County area, and (b) Santa Barbara, Ventura, and Los Angeles County areas. This segregation is largely associated with the differences in types of available basic data.

General Interpretation of Spring and Stream Flow Data

Before analyzing records of spring and stream flow it is necessary to develop criteria whereby effects of the Arvin-Tehachapi earthquake can be identified. Discharge of springs and streams in these California areas can be extremely variable. This variability is of two distinct types and is the result of a complicated interrelationship between many of the physiographic and hydrologic factors.

First, there is the general annual cyclic-like pattern of runoff distribution. Maximum discharge usually occurs during the winter rainy season, due to the larger rates of rainfall, the recharge to mountain ground-water storage with immediate seepage therefrom, and early snowmelt. With the conclusion of the runoff resulting from the rainy season, discharge tends to follow a fairly well-defined recession during the warm, dry summer months, with minimum discharge occurring in late summer or early fall. This recession in discharge seldom changes in pattern and can usually be readily established after a number of years of observation.

The second type of variability in discharge is far more difficult to evaluate. This fluctuation varies from hour to hour and day to day, reflecting changes in the evapotranspiration opportunity and the occasional summer precipitation. This summer precipitation is generally light and the runoff attributable to it is minor and readily definable. The effect of the more significant evapotranspiration opportunity on flow of springs and streams is harder to recognize. The influence of these water losses is more generally recognized in streams or springs where the discharge is small. Under these conditions, changes in evapotranspiration opportunity may cause tremendous percentage differences in day-to-day flow.

Consequently, certain data have been assembled on figure 3 to illustrate the effect of some of these influences on spring and stream flow. The upper portion of this diagram indicates days on which daily precipitation exceeded 0.1 inch at a group of mountain, or near-mountain, stations for the period of June through September 1952. These records indicate the storms to be of the usual summer convectional type and to be of limited distribution, and are furthermore confined to the latter part of July, August and September.

The second part of figure 3 shows daily evaporation at the standard Weather Bureau station on the Baekus Ranch near the town of Mojave. In addition to indicating evaporation from a water surface, this record becomes an index of the amount of water required to support native and domestic plant life. Variability of

- Station
 Kern River P. H. 3
 Kernville
 Tehochopi
 Mojave
 Tejon Rancho
 Pattiway
 Cuyoma
 Ozena
 Ojai
 Sandberg
 Mt. Wilson
 Squirrel Inn No. 2

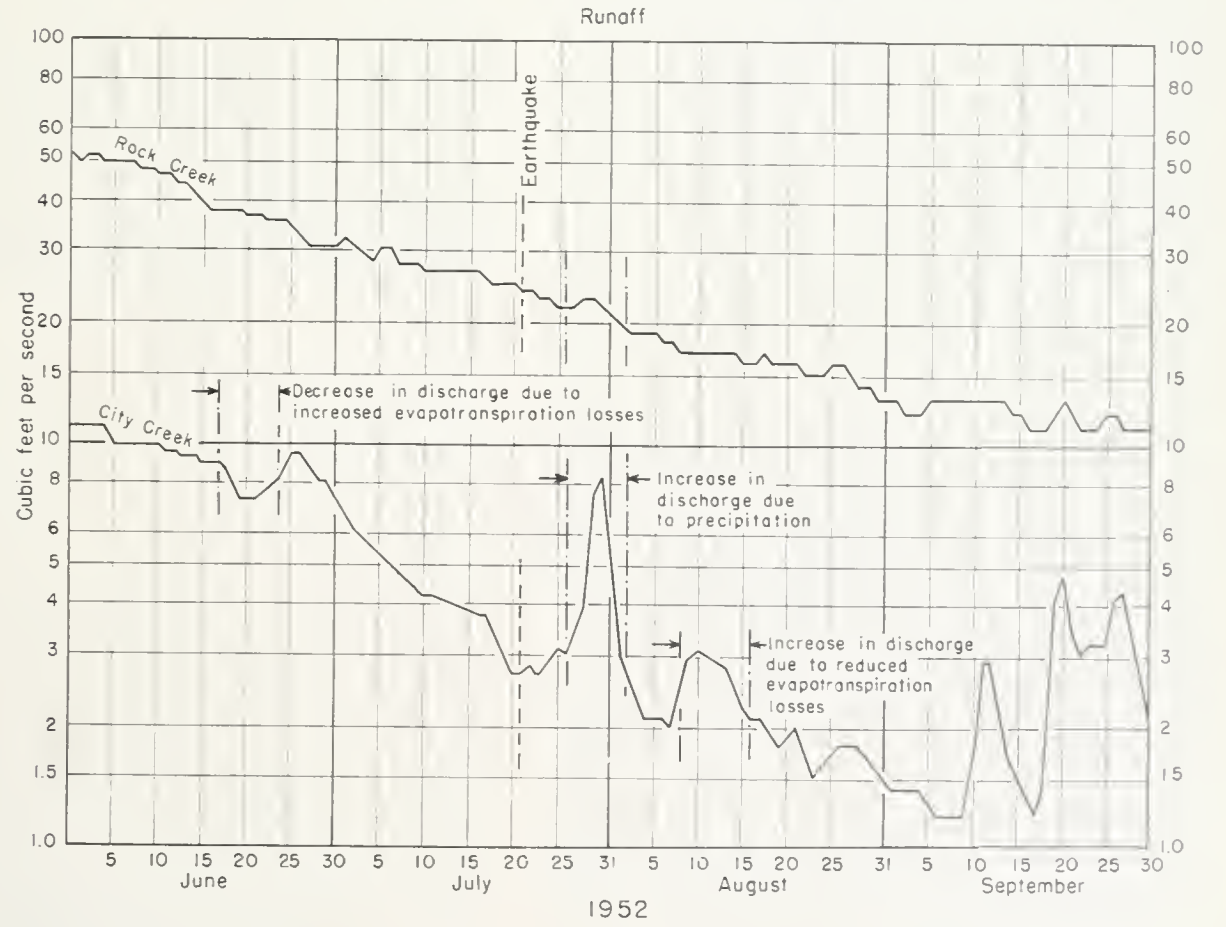
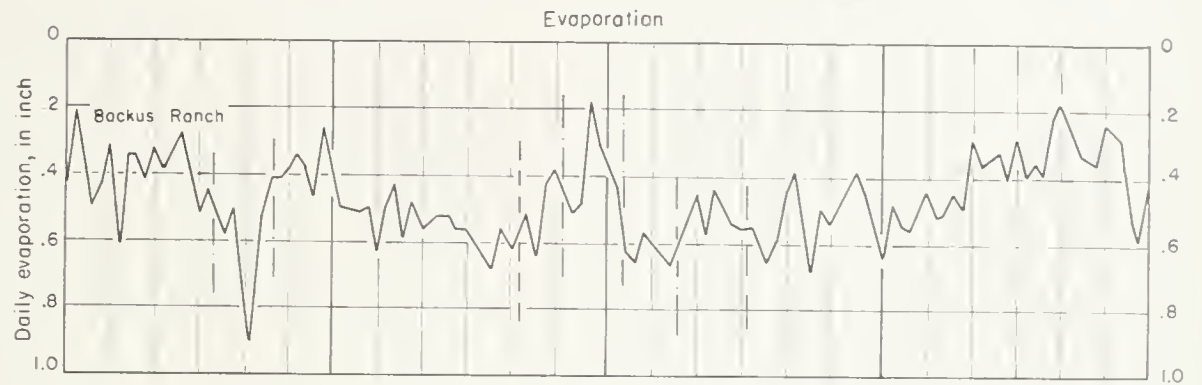
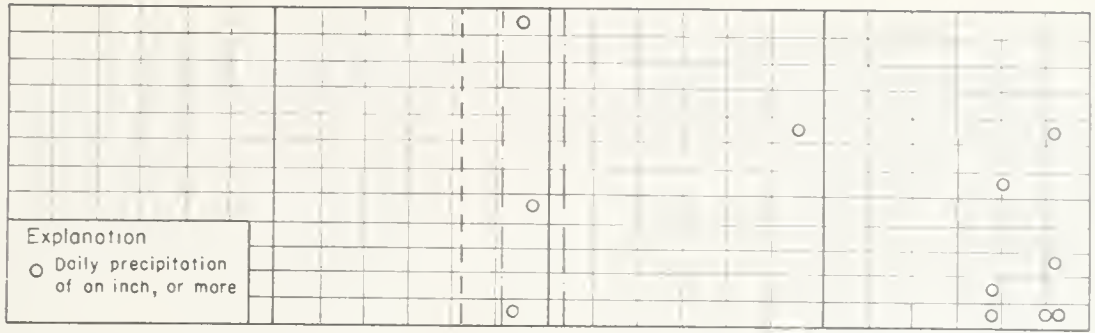


FIGURE 3. Precipitation, evaporation, and runoff at selected stations.

this water requirement is indicated by the fact that daily evaporation at this station ranged from 0.18 to 0.91 inch with a daily mean of 0.48 inch during the 4-month period of June through September 1952. This record is included on figure 3 as an index of changes in the evapotranspiration opportunity during this 4-month period. This record is shown in an inverted form in order to indicate parallelism with changes in discharge.

The lower part of this diagram gives the record of daily discharge for two gaging stations along the San Andreas fault zone in the San Gabriel and San Bernardino Mountains, presumably on stream flow outside the area of influence of the Arvin-Tehachapi earthquake. The runoff from the first of these drainage areas, Rock Creek (96) on the north side of the mountain range, shows the typical summer recession, and the hydrograph of this flow when plotted on semilogarithmic projection, such as used in this analysis, tends to approach a straight line. In this rugged mountain drainage area the mantle rock was sufficiently absorptive and retentive to retain all the limited summer precipitation and also to subdue the effects of daily changes in evapotranspiration.

The second stream, City Creek, is located on the southern face of the San Bernardino Mountains near San Bernardino. In this instance daily runoff fails to reflect the smooth recession of Rock Creek. Here, due to a less absorptive and retentive mantle rock, the recession hydrograph is quite irregular, responding to rainfall during each period of summer precipitation and reflecting significant changes in evapotranspiration opportunity.

It will be noted on figure 3 that on the date of the Arvin-Tehachapi earthquake there was no immediate change in discharge at either station. However, less than ten days after the earthquake, on July 30, daily discharge of City Creek increased to 8.5 cubic feet per second from 2.7 cubic feet per second on July 21. The records in the upper part of figure 3 indicate that this increase in discharge was due primarily to precipitation and secondly to a reduction in evapotranspiration opportunity. During the same period, changes in discharge from these two causes are very much more subdued in the Rock Creek drainage area.

Shortly after this storm period, daily discharge of City Creek increased from 2 to 3 cubic feet per second during a period of no precipitation. In this instance the increase in discharge must have been due to a reduction of evapotranspiration opportunity as suggested by the record obtained at the Backus Ranch. Again the influence of this change in evapotranspiration opportunity was not reflected in the discharge of Rock Creek.

On an earlier occasion, daily discharge of City Creek decreased from 9 cubic feet per second on June 17 to 7.3 cubic feet per second on June 19. This decline in discharge is largely attributable to increase in evapotranspiration opportunity as suggested by the evaporation period at Backus Ranch.

In view of this variability of discharge during the summer recession period in some streams, it is often difficult to properly credit changes in flow to a single event, such as the Arvin-Tehachapi earthquake.

Hydrographs of daily discharge have been included as part of the analysis, when the data warrant it, in order to show better the effects of the Arvin-Tehachapi

earthquake on spring and stream flow. In general these hydrographs consist of two parts. The upper portion of the diagram gives the hydrograph of daily discharge plotted on a semilogarithmic projection similar to that shown on figure 3. The advantages of this type of projection are that the hydrograph of the summer recession tends to approach a straight line, and secondly, small changes in discharge can be readily identified where these changes are large in percentage of discharge. When available, typical antecedent records are included in order to develop the trend of the 1952 runoff had the earthquake not occurred.

The lower part of most diagrams shows the change in flow attributable to the earthquake. This portion of the diagram is plotted on an arithmetical scale, so that the change in discharge and its time distribution is more readily discernible. Then for purpose of emphasis, increase in discharge due to the Arvin-Tehachapi earthquake has been cross-hatched on both parts of the diagram.

Passing mention should be made of a seismograph type of record nearly always found on the charts of recording stream-gages in an area affected by earthquakes. At the time of each large shock a vertical line is found on the gage-height chart, and there is a rough relation between the severity of the shock and the length of the line.

The line is caused by the vertical movement of the float in the stilling-well when the shock sloshes the water from side to side. Vertical movements indicating surges of more than a foot have been recorded.

Following the shock, if the gage-height graph continues at the same stage as before the earthquake, the event has no immediate significance so far as the discharge of the stream is concerned.

Occasionally the change in the discharge at the gaging station might be the result of the making or breaking of a small dam in the stream channel upstream from the recording gage.

Kern County Area

In this mountain area where the Arvin-Tehachapi earthquake damage was most significant, the effect on flow in springs and streams was most prompt and pronounced. Good evidence is available to show that the flow appreciably increased in some 15 streams and 32 springs within about 35 miles of Caliente as shown on figure 1. This same map indicates eight springs where the flow is known to have decreased.

Previous mention has been made of summer precipitation and the fact that generally its effect could be separated from that of evapotranspiration and from the effect of the earthquake. So far as eastern Kern County is concerned, it seems quite certain that precipitation in late July and early August was almost insignificant in its effect upon spring and stream flow. Records of the U. S. Weather Bureau, as well as testimony of local residents, showed that scattered thunderstorms visited some parts of eastern Kern and Tulare Counties during the period July 24-31. However, such moisture was generally small in quantity and fell on relatively small, widely separated areas. Table 1 shows daily precipitation for the period July 23 to August 2 at eight representative precipitation stations in eastern Kern and Tulare Counties.

Table 1

Precipitation station	Daily precipitation in inches 1952										
	July									August	
	23	24	25	26	27	28	29	30	31	1	2
Tejon Rancho.....	0	T	0	0	T	0	T	0	0	0	0
Tehachapi.....	0	.05	T	0	0	.06	.03	T	0	0	0
Weldon*.....	0	0	0	0	0	0	0	0	0	0	0
Southern California Edison Co. Kern River No. 3 Powerhouse.....	0	0	0	0	0	.43	.01	0	0	0	0
California Hot Springs*.....	0	0	0	0	.03	0	.12	0	0	0	0
Springville, Tule Headworks dam*.....	0	0	0	0	.01	.01	.30	.15	0	0	0
Glennville Fulton Ranger Station*.....	0	0	0	0	0	0	0	0	0	0	0
Lorraine*.....	0	0	0	0	0	0	0	0	0	0	0

* Recording gage.

Detailed topography of eastern Kern County is shown on the topographic maps of the U. S. Geological Survey. The respective maps are named in the following text which gives a brief description of each spring and stream. The numbers following the names of springs and streams are those used on figure 1.

Pleito Creek at San Emigdio Ranch (1). Pleito Creek drains the north side of Wheeler Ridge, at the southernmost part of the San Joaquin Valley, about 26 miles south of Bakersfield (Buena Vista Lake quadrangle).

Jack Shepard of the Humble Oil Company, Bakersfield, stated that Pleito Creek was dammed by a slide which resulted from the earthquake, and for about 2 weeks thereafter did not flow at all in the lower reaches. The creek normally goes dry in summer and had almost ceased flowing on July 21, 1952. The earthquake apparently caused flow to start upstream from the slide-dam because water appeared downstream from the dam about August 4 and continued to flow throughout the summer and winter.

Grapevine Creek above Richfield Pumping Station (2). Grapevine Creek drains the north and west slopes of the Tehachapi Mountains at the extreme southern end of the San Joaquin Valley (Tejon quadrangle). Prior to the Arvin-Tehachapi earthquake, the U. S. Bureau of Reclamation established a temporary gaging station on this creek above the Richfield pumping station. A hydrograph of daily discharge at this site for the period July through September 1952 is given on figure 4.

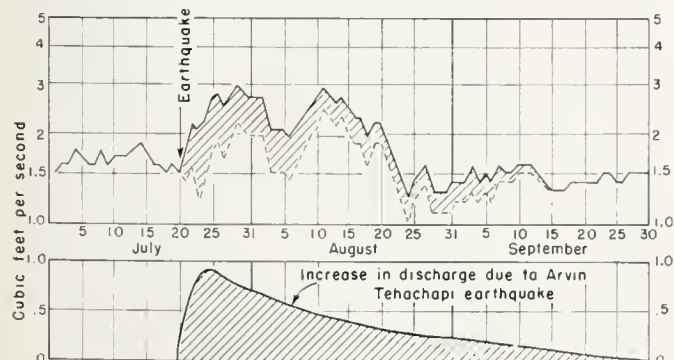


FIGURE 4. Hydrographs of daily discharge for Grapevine Creek.

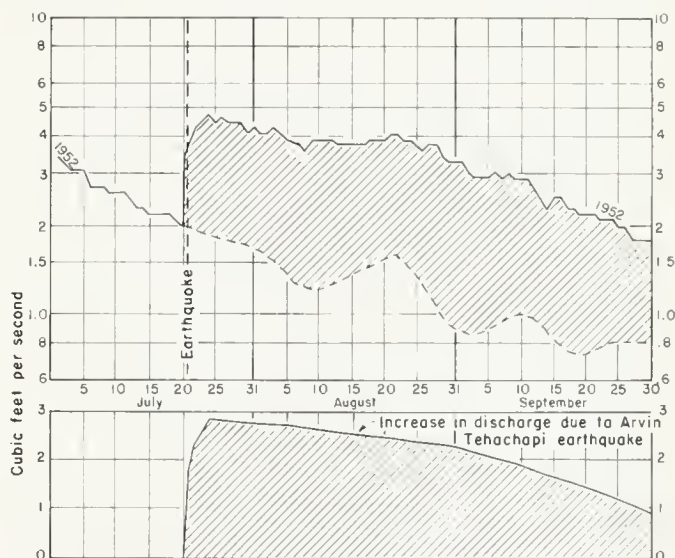


FIGURE 5. Hydrographs of daily discharge for Tunis Creek.

This hydrograph shows two characteristic periods of high discharge centered around July 29 and August 11. These maxima are probably associated with reduced evapotranspiration opportunity, and possibly a little precipitation, as indicated for City Creek. Consequently it becomes difficult to define accurately any change in flow in this stream due to the Arvin-Tehachapi earthquake.

The second graph on figure 4 represents an estimate of the increase in discharge due to the Arvin-Tehachapi earthquake. This increase in flow, credited to the earthquake, has been indicated on the upper graph also. The increase in flow has been emphasized by cross-hatching both diagrams.

As indicated on figure 4, this estimated increase in flow, July 21 to September 30, 1952, due to the earthquake, amounts to about 48 acre-feet, or the quantity of water required to cover 48 acres a foot deep.

Pastoria Creek above Cable Corral, El Tejon Rancho (3). Pastoria Creek is also at the southern tip of the San Joaquin Valley, a few miles east of Grapevine Creek (Tejon quadrangle). A record of the flow in this stream was obtained by the U. S. Bureau of Reclamation on the El Tejon Rancho above Cable Corral, and indicates that discharge increased from less than 1 cubic foot per second just prior to the earthquake to about 7 cubic feet per second by July 26. The flow then gradually decreased to the pre-earthquake flow of October. The increased runoff July 22 to September 30, as a result of the earthquake, is estimated at about 200 acre-feet.

Tunis Creek above El Tejon Rancho Diversion (4). Also draining the northwest slope of the Tehachapi Mountains, and northeastward of Pastoria Creek, is the Tunis Creek drainage area

(Tejon quadrangle). The runoff from this creek above El Tejon Rancho diversion, has been recently measured by the U. S. Bureau of Reclamation. A record of daily discharge is given on figure 5 in the form of a hydrograph. This hydrograph shows in a most spectacular manner the increase in flow due to the Arvin-Tehachapi earthquake. Within a few days after the earthquake flow of the stream increased from 2.0 cubic feet per second to 4.8 cubic feet per second and then maintained the normal recession slope throughout the remainder of the period.

The lower diagram on figure 5 indicates the estimated increase in runoff attributable to the earthquake. The cross-hatched areas show that the increase amounted to 310 acre-feet, July 22 to September 30, 1952.

El Paso Creek above El Tejon Rancho Headquarters (5). The El Paso Creek drainage area is north of the Tunis Creek drainage area in the Tehachapi Mountains and tributary to the south San Joaquin Valley (Caliente quadrangle). Runoff from that portion of the drainage area above the El Tejon Rancho Headquarters has been measured recently by the U. S. Bureau of Reclamation. The daily discharge of this stream for the period of July through September 1952 is given in hydrographic form on figure 6. The effect of the Arvin-Tehachapi earthquake on the flow was very similar

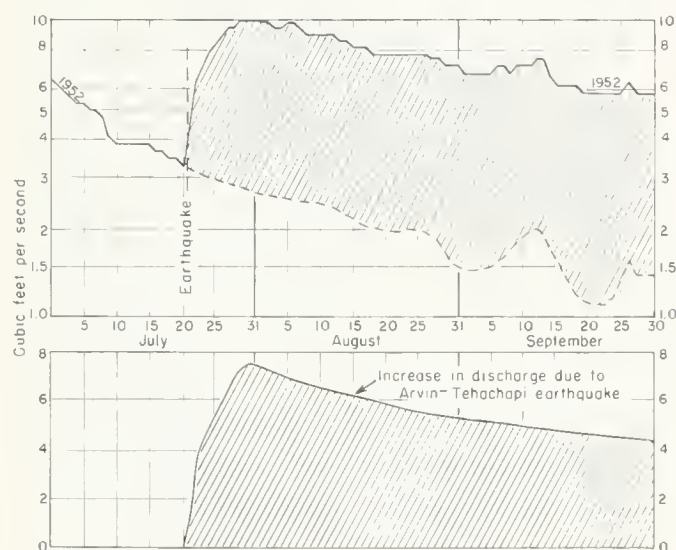


FIGURE 6. Hydrographs of daily discharge for El Paso Creek.

to that shown on figure 5 for Tunis Creek. The increase in runoff attributable to the earthquake is believed to be well defined. As a result of the Arvin-Tehachapi earthquake the runoff of this stream was increased by about 800 acre-feet for the period July 22 to September 30, 1952.

Banducci Ranch Spring (6). At the Banducci Ranch, a mile and three-quarters southwest of Cummings Valley School (Caliente quadrangle), a dry well-hole started to flow about 35 gallons per minutes about August 5, 1952, and was still flowing approximately that amount on February 17, 1953.

Cummings Creek at Cummings Valley (7). Elmer Lyne, engineer of the U. S. Soil Conservation Service at Tehachapi, observed Cummings Creek (Caliente quadrangle) in September, 1952, and estimated that its flow was about 30 percent greater than normal for that time of year.

Institution Spring in Cummings Valley (8). The spring which was the main source of water supply for the California Institution for Women, on the east side of Cummings Valley (Caliente quadrangle) decreased greatly in flow following the quake. The spring was located near the top of the ridge between Cummings Valley and Brite Valley.

Spring in Brite Valley (9). Alongside the road at the west edge of Brite Valley (Caliente quadrangle) a new spring broke out shortly after the quake. This probably is tied in with the decrease in flow, at the same time, of the spring which had previously been the main water supply for the California Institution for Women, just over the hill to the southwest.

Spring in Cummings Valley (10). Several persons reported an increase in flow of this spring at the upper end of Cummings Valley (Caliente quadrangle).

Sycamore Canyon Creek, West Side of Bear Mountain near Arvin (11). David J. Leeds, Geophysicist, U. S. Coast and Geodetic Survey, noted an increase in the flow of Sycamore Creek (Caliente quadrangle) and the same fact was reported by employees of the Albert Angus Ranch near Arvin where Sycamore Creek water is used for irrigation.

Meadowbrook Farm Spring (12). At the Meadowbrook Farm (dairy), 2 miles west of Tehachapi (Mojave quadrangle), springs dried up following the earthquake and sub-irrigated alfalfa died.

Wrigley Ranch Springs (13, 14, 15). At Wrigley Ranch (formerly Hall Ranch) 1 mile north of Old Town (Mojave quadrangle), manager W. T. Blackburn reported that their large spring had decreased over the years until it was just a trickle prior to the quake. Almost immediately afterwards it increased to "fill a 4-inch pipe," and two new springs appeared north of the original.

Unnamed Stream near Walong (16). Unnamed small creek about half a mile southeast of Walong (Caliente quadrangle), on the Southern Pacific Railroad, was reported by Elmer Lyne of Tehachapi to have been flowing about 10 gallons per minute prior to the quake and some 100 gallons per minute about the middle of August.

Clear Creek near Bealville (17). It appears that the headwaters of Tehachapi Creek did not show an increase in the same proportions as the downstream area. By contrast, Clear Creek, a lower tributary, dry before the earthquake, started to flow within about 36 hours and was estimated at 3 to 4 cubic feet per second by W. M. Jaekle of the engineering department of the Southern Pacific Company. On January 19, 1953, a current meter measurement by T. A. Cooper of the U. S. Geological Survey showed 2.6 cubic feet per second in Clear Creek, just upstream from the Southern Pacific Railroad high fill near Bealville (Caliente quadrangle). On July 21, 1953, the flow of Clear Creek at the same point was estimated as 0.5 cubic foot per second.

Tehachapi Creek near Caliente (18). L. E. Williams of Caliente reported that water of Tehachapi Creek, reinforced by Clear Creek, reached the confluence with Caliente Creek at Caliente (Caliente quadrangle), about July 26 and that both Caliente Creek and Tehachapi Creek reached their maximum summer flow at Caliente about August 10. Since the record of the U. S. Bureau of Reclamation shows the flow holding steady at 21 second-feet below the confluence, August 26-29, it seems reasonable to estimate the flow of each stream, reported as similar in size, above the confluence, at about 12 second-feet on August 10. Tehachapi Creek was down to 0.5 cubic foot per second on July 21, 1953, as measured by T. A. Cooper.

Indian Creek at Lorraine (19). C. W. Poole, the U. S. Weather Bureau observer at Lorraine (Mojave quadrangle), at the confluence of Indian and Caliente Creeks, reported as follows: Both creeks had been dry July 1-20, 1952, preceding the earthquake. During the latter part of the preceding winter (1951-52) Caliente Creek above Lorraine had flowed for the first time in four years. Indian Creek had flowed as usual during the same winter (1951-52). Indian Creek started to flow at Lorraine 1 week after the earthquake. Most of the water originated in a southeast fork of the creek, on the southwest shoulder of Cache Peak. By the latter part of August, Indian Creek was carrying an estimated 3 cubic feet per second. It is notable that Caliente Creek did not start to flow upstream from Indian Creek at Lorraine until after the rains of November 1952. Mr. Poole offered as an explanation that there are large areas of sand in the upper Caliente Creek channel, and that percolation slowed the advance of surface flow.

Mr. Poole reported no rainfall at Lorraine from April 1952 until early in November 1952. However, there were thunderstorms in some neighboring areas late in July and in August.

Studhorse Creek (20). Mr. Poole stated that Studhorse Creek (Mojave quadrangle), first tributary to Caliente Creek downstream from Indian Creek, started to flow immediately after the quake.

Unnamed Stream near Caliente (21). An unnamed small creek nearly opposite Devil Canyon (Caliente quadrangle), tributary to Caliente Creek, started to flow soon after the earthquake. It is believed that a small flow also appeared in Devil Canyon.

Oiler Canyon Spring (22). A spring appeared alongside the road in Oiler Canyon (Caliente quadrangle), immediately after the quake, and was still running in January and February 1953.

Rock Spring (23). Rock Spring, about 1 mile northeast of Caliente (Caliente quadrangle), on the L. E. Williams Ranch, was reported to have increased in flow from 3 gallons per minute before the quake to 6 afterwards.

Caliente Creek above and below Tehachapi Creek at Caliente (24 and 25). Tehachapi Creek joins Caliente Creek at the small town of Caliente (Caliente quadrangle), and in the words of the local people, "dry as popcorn" described both creeks for at least several weeks preceding the earthquake. Springs in the headwaters of the creeks started to flow immediately after the quake on July 21 and Caliente Creek water reached the point of confluence about July 25, followed by Tehachapi Creek water about a day later. The flow in both creeks continued to increase as water from newly flowing tributaries saturated the channels and came through. Caliente Creek below the confluence is believed to have reached its maximum about August 10 with a flow estimated at about 25 cubic feet per second, and then held fairly constant until the November rains increased it.

Slightly more than a month after the Arvin-Tehachapi earthquake the U. S. Bureau of Reclamation, on August 26, 1952, established a gaging station on Caliente Creek below its confluence with Tehachapi Creek. The tributary drainage area is about 340 square miles. The record obtained at this station, together with the estimate made by local residents, has been plotted on figure 7 to form a hydrograph for the period of July through

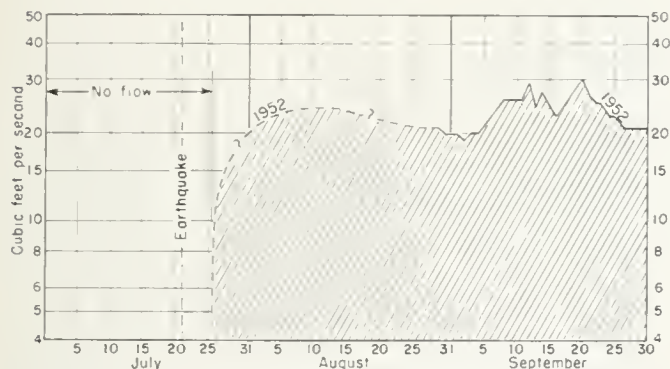


FIGURE 7. Hydrographs of daily discharge for Caliente Creek at Caliente.

September 1952. All of the runoff occurring subsequent to July 21, 1952, as shown on figure 7, is assumed to have originated from the earthquake since there is insufficient data to develop a clear-cut delineation between the flow originating because of the earthquake and that due to reduced evapotranspiration losses and precipitation. The estimated runoff for the period July 26 to September 30, 1952 amounts to about 3,000 acre-feet for Caliente Creek below the confluence with Tehachapi Creek.

On July 21, 1953, exactly 1 year after the major earthquake, T. A. Cooper measured 3.3 cubic feet per second in Caliente Creek at Caliente. Of this amount only 0.5 cubic foot per second was contributed by Tehachapi Creek. Since there is normally no flow at Caliente at this time of year it appears that the flow in Caliente Creek and especially in the main stem above the confluence with Tehachapi Creek is still showing notable results of the 1952 earthquake. In fact, the increase in runoff, due to the earthquake, for Caliente Creek above Tehachapi Creek would be in the order of 5,000 acre-feet for the year following the quake.

Caliente Creek near Bena (26). Caliente Creek water advanced downstream from Caliente at a relatively slow rate since large quantities of water were required to wet the channel sufficiently to sustain surface flow. About 3 miles upstream from Bena (Caliente quadrangle), a railroad station alongside State Highway 466, there is a wide channel area that is normally swampy. Water was observed there in ponds during January and February 1953. This area was reported practically dry preceding the quake. Water is believed to have reached it about August 1, 1952 and to have saturated it sufficiently by the middle of the month to permit surface flow to proceed downstream.

Water reached the bridge on State Highway 466 near Bena on August 24, as shown by the water-stage recorder record of the

U. S. Bureau of Reclamation. From that point downstream, Caliente Creek channel widens out into a sand and gravel delta where percolation is extremely rapid. About 3 miles downstream from the bridge on State Highway 466, and downstream from the confluence of Walker Basin Creek and Caliente Creek, the creek is crossed by Neumarkel Road. The ford at this point is usually dry on the surface, and impassible on only very rare occasions.

A. F. Neumarkel stated that surface flow reached the ford about November 10, 1952, after fall rains began. The ford was impassable for automobiles for about a week following the heavy rains of November 14 and 15. Flow continued intermittently all winter and spring. For long periods there would be surface flow only during the night. Following the rains of May 27 and 28, 1953 the creek again was not fordable for two days. Flow then decreased rapidly and surface flow at the ford ceased entirely on June 1, 1953.

Surface flow at the highway crossing near Bena lasted until about June 12. T. A. Cooper reported that both Caliente Creek and Walker Basin Creek were dry at the highway bridges near Bena, on July 21, 1953.

Skunk Spring, White Wolf Ranch (27). Fred W. Nighbert stated that this spring, high up on the northwest side of Bear Mountain (Caliente quadrangle), practically doubled its flow immediately after the quake of July 21. He also stated that at a lower elevation he had been pumping water, since the earthquake, from a well originally drilled for oil.

Unnamed Streams at Bear Mountain (28 and 29). Two unnamed creeks on the northwest side of Bear Mountain (Caliente quadrangle), crossing the White Wolf fault, were observed to be flowing on February 17, 1953 and were reported by L. B. Krauter of Tehachapi to have started flowing early in August following the quake. It is probable that some of the water in No. 28 originated at or near Skunk Spring, No. 27.

White Wolf Springs (30). White Wolf Springs (Caliente quadrangle), about 2 miles west of White Wolf Ranch headquarters, is stated to have shown a definite increase in flow after the quake.

Rock Pile Spring (31). Rock Pile Spring, $4\frac{1}{2}$ miles west of White Wolf Ranch headquarters (Caliente quadrangle), was reported to have gone dry at the time of the July 21 quake but started to flow again following the heavy shock of August 22.

Berenda Spring (32). The Berenda Spring is located about 4 miles northwest of White Wolf Ranch headquarters (Caliente quadrangle). Arthur J. Neumarkel and Fred W. Nighbert agree that it flowed strongly until July 21, 1952 and was used for stock watering. There has been no flow since that date.

Neumarkel Spring (33). The Neumarkel Spring is about 7 miles northeast of Arvin (Caliente quadrangle). Arthur F. Neumarkel stated that it "flowed strong" until the earthquake of 1906 when it decreased so much that it required pumping. It was pumped until 1938 when the water was still "reachable" but pumping was discontinued. After the earthquake of July 21, 1952 the water "went out of sight."

Walker Basin Creek at Walker Basin (34). Leroy Rankin of the Rankin Ranch in Walker Basin (Caliente quadrangle), stated that the creek at the lower end of the basin is perennial but that within a few days after July 21 the flow increased from a trickle to some 2 or 3 cubic feet per second. This was a direct result of new and increased flow in tributary springs, especially along the west and north sides of the basin. Downstream from Walker Basin, in the canyon section, new springs also appeared and many old ones increased their flow.

Tributaries to Walker Basin Creek (35-41). These springs and small creeks along Walker Basin Creek (Caliente quadrangle), were all reported by Leroy Rankin to have started or increased their flow very shortly after July 21. Nos. 35, 37, and 38 were reported to be new springs. The largest was No. 40, Benninger (Castro) Canyon, for which the flow about the first of August 1952 was estimated at 700 gallons per minute.

Springs near Walker Basin (42-49). Increase in the flow of these springs (except No. 43) in the mountains between Walker Basin Creek and Kern River (Caliente quadrangle), was also reported by Leroy Rankin. No. 43 ceased to flow. No. 46 (Fig Tree Canyon) is distinctive because it dried up for a period of about 2 weeks following the quake and then opened up again with a flow greater than before. It was back to about normal in February 1953.

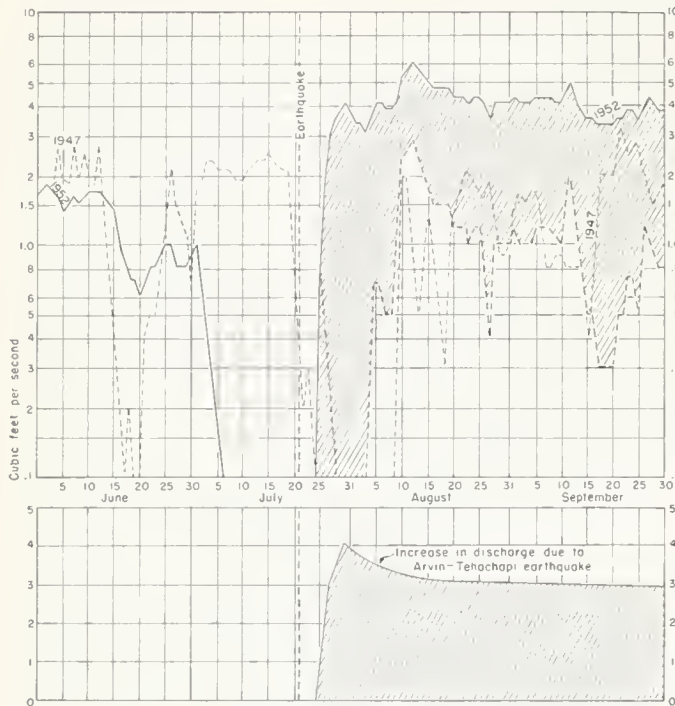


FIGURE 8. Hydrographs of daily discharge for Walker Basin Creek at Indian Mill Rock.

Walker Basin Creek at Indian Mill Rock (50). The U. S. Bureau of Reclamation has maintained, for several years, a gaging station on Walker Basin Creek near the lower end of the canyon at Indian Mill Rock about 2 miles northeast of Bena (Caliente quadrangle). Tributary drainage area is about 111 square miles. The record of daily discharge obtained at this site for the period of June through September 1952 is shown on figure 8. This record indicates that the stream channel became dry on July 8 and remained dry until about four days after the earthquake. Antecedent records show the streambed to be dry throughout most of the summer months. The records obtained in 1947, and also shown on figure 8, indicate that the daily discharge can change rapidly in short intervals of time for many reasons other than earthquake. Because of this extreme variability in discharge, it is difficult to attempt a segregation of the Arvin-Tehachapi earthquake's effect on the flow.

The lower part of figure 8 gives the best estimate available at this time of the increase in discharge due to the Arvin-Tehachapi earthquake. The maximum increase in discharge amounted to 4.1 cubic feet per second on July 30 and decreased to about 3 cubic feet per second on September 30. This total increase in flow attributable to the earthquake amounted to about 440 acre-feet, for the period July 25 to September 30, 1952.

Walker Basin Creek near Bena (51). The channel of Walker Basin Creek passes under State Highway 466 about 1 mile west of Bena (Caliente quadrangle) and perhaps 4 miles, by stream channel, downstream from Indian Mill Rock. This 4-mile reach lies in an absorptive gravel-and-sand formation and the advance of the surface water was very slow. Although no definite information is available it is believed that it was near the end of August before the flow reached the bridge on State Highway 466. Water was still flowing there in January and February 1953. It ceased flowing sometime before July 21, 1953.

Pascoe Spring (52). The Cecil Pascoe household spring was located in Caldwell Canyon about $2\frac{1}{2}$ miles northeast of the former Kernville (Kernville quadrangle), and about 1 mile southeast of New Kernville. It ceased flowing on July 21, 1952 and was still dry one year later. However, new small springs broke out in the vicinity, and the M. L. Crowder spring, half a mile west, increased its flow about 50 percent.

South Fork Kern River near Onyx (53). The discharge of the South Fork Kern River at the southern extreme of the Sierra Nevada has been measured for many years by the U. S. Geological Survey at a site 5 miles northeast of Onyx (Kernville quadrangle). The contributing drainage area is 531 square miles. The records have been published in the annual water-supply papers, and the hydrographs on figure 9 give daily discharge during 1938, 1941 and 1952 for the four-month period of June through September. Records for the 2 earlier years were selected for inclusion on figure 9 because of similarity in discharge at the beginning of the summer recession period. The slopes of the hydrographs for all 3 years are quite similar through June and July until modified by the summer rainfall.

In 1952 the normal recession was interrupted by a pronounced increase in discharge on July 26. This increase in flow is believed to be more closely associated with the summer rainfall occurring at that time, than the Arvin-Tehachapi earthquake. However, the well-sustained flow of 149 to 155 cubic feet per second between July 27 and August 1 suggests that the earthquake may have had some influence on the runoff.

Hot Springs near Bodfish (54). The Seavern Hot Springs, 2 miles northeast of Bodfish (Kernville quadrangle), spouted a considerable increase of flow at the time of the earthquake, July 21, 1952. A similar action occurred with the quake of March 15, 1933. On July 21, 1953, 1 year after the recent quake, the flow was estimated at 0.25 to 0.30 cubic foot per second, still somewhat more than normal flow.

Bodfish Creek at and near Bodfish (55). Frank Laurence of Bodfish reported that the creek at the town of Bodfish (Kernville quadrangle) was dry on July 21, 1952. At a point about 3 miles upstream it started to flow on July 22 or 23 but the flow did not reach town during the summer of 1952.

On March 17, 1953 T. A. Cooper of the U. S. Geological Survey measured 0.6 cubic foot per second in Bodfish Creek, three-quarters of a mile downstream from the town. It is concluded that the earthquake had little lasting effect upon the flow of this creek.

A small spring on the Laurence property in Bodfish almost doubled its flow within a few hours after the quake of July 21.

Democrat Springs (56). The hot spring which supplied the plunge at Democrat Springs in Kern River Canyon, 10.5 miles southwest of Bodfish (Tobias Peak quadrangle), ceased flowing entirely on July 21, 1952. During April 1953 it showed a slight trickle and by July 21, 1953 it was flowing 8.5 gallons per minute.

Kern River near Democrat Springs (57). A gaging station with a recording instrument has been maintained a mile downstream from Democrat Springs (Tobias Peak quadrangle) by the Southern California Edison Co. (under direction of the U. S. Geological Survey), since 1951. Tributary drainage area measures 2,264 square miles.

The record of daily discharge showed no unusual change on July 21-22 but did show an increase in discharge on July 26 and 27, 1952 similar to that shown by South Fork of Kern River near Onyx (No. 53 above). For the same reasons cited there, it is concluded that the increase was caused by precipitation and not by the earthquake.

Kern Canyon Creek (58). A small unnamed creek flows into the Kern River on the left (south) bank, just downstream from the mouth of Kern Canyon (Caliente quadrangle). Employees at the nearby power-plant reported that the creek started to flow soon after July 21, 1952. It was dry at the same point on March 16, 1953.

Cottonwood Creek near Kern Canyon (59). Leroy Rankin, who grazed cattle in the upper Cottonwood Creek area (Caliente quadrangle) reported that many tributary springs increased their flow shortly after the earthquake.

Joe Prowell, at the Kern Rock Co. plant on Cottonwood Creek, about 1 mile upstream from its confluence with Kern River, stated that the creek had stopped flowing prior to July 21, 1952. It normally ceases flowing at that point about June of each year and does not start again until after the onset of winter rains. However, the creek started to flow at the rock company plant about July 25, 1952, and continued throughout the balance of the summer and winter and on March 17, 1953 was carrying 1.4 cubic feet per second, as measured by T. A. Cooper of the U. S. Geological Survey. On July 21, 1953 he reported no flow.

White River near Ducor (60). A regular gaging station with a recording instrument has been maintained on this stream eight miles southeast of Ducor (White River quadrangle) since 1937.

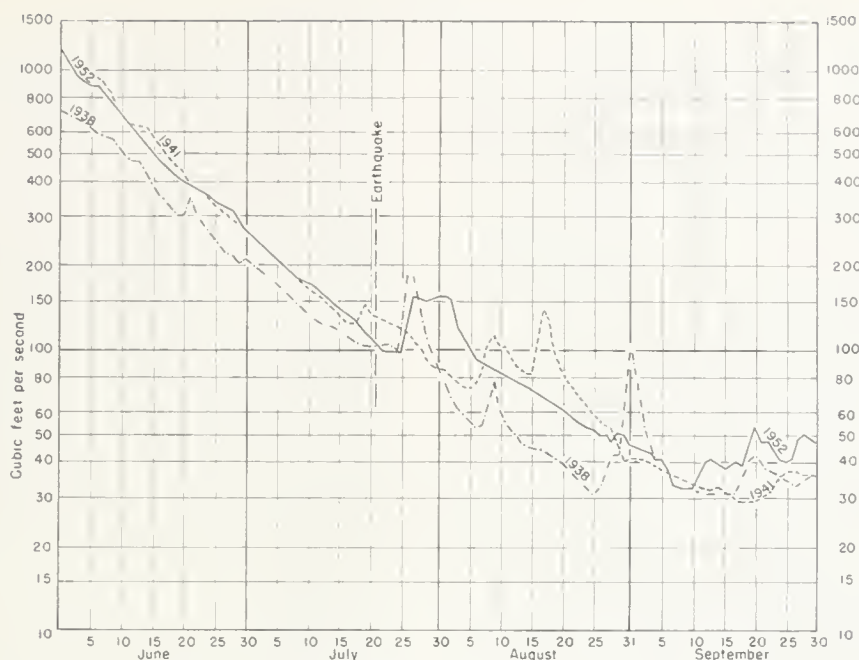


FIGURE 9. Hydrographs of daily discharge for South Fork Kern River near Onyx.

The drainage area is 120 square miles. Records of daily discharge are published in the U. S. Geological Survey annual water-supply papers. This record shows a sudden increase on July 29 and 30, followed by a rapid recession to no flow on August 5. Since the increase corresponds to the thunderstorm period in that area, it is concluded that it was due to the precipitation and not to the earlier earthquake.

Santa Barbara, Ventura and Los Angeles County Areas

The following text describes points of observation and the effect of the Arvin-Tehachapi earthquake on the flow in streams and springs of Santa Barbara, Ventura and Los Angeles Counties at stations indicated on figure 2. As already indicated, these data were obtained as a part of the overall program of the U. S. Geological Survey in cooperation with the State of California, the U. S. Bureau of Reclamation, Santa Barbara County Water Authority, Ventura County Water Survey and Los Angeles County Flood Control District.

Huasna River near Santa Maria (61). Huasna River, a tributary to Cuyama and Santa Maria Rivers, drains the south and west slopes of the Santa Lucia Range. The runoff is measured at an altitude of 600 feet at a site about 0.5 mile upstream from the stream's confluence with Cuyama River and 8 miles northeast of Santa Maria. The runoff from this 119-square-mile drainage area has been obtained since December 1929.

The runoff records at this site do not show any change in discharge, subsequent to July 21, 1952, that could be attributed to the Arvin-Tehachapi earthquake.

Alamo Creek near Santa Maria (62). Alamo Creek, a tributary of Cuyama River, drains the low mountain areas between the Santa Lucia Range and the San Rafael Mountains. The runoff from this 87.7-square-mile drainage area has been measured since October 1943 at a site about 580 feet above sea level and 1.2 miles above the confluence with Cuyama River, 9 miles northeast of Santa Maria.

The runoff observations indicate that the discharge of this stream was not affected by the Arvin-Tehachapi earthquake.

Tepusquet Creek near Sisquoc (63). Tepusquet Creek, a tributary to Sisquoc River and through it to Santa Maria River, drains the south face of the San Rafael Mountains. A gaging station was established in October 1943 to measure runoff at a site

about 500 feet above sea level, 3 miles east of Sisquoc. The stream has a drainage area of 28.9 square miles at this site.

The discharge records indicate that the Arvin-Tehachapi earthquake did not have any measurable influence on the runoff of this stream.

Sisquoc River near Sisquoc (64). Sisquoc River, a tributary of Santa Maria River is an east-west stream draining the interior areas of the San Rafael Mountains. The runoff from this stream system has been measured between December 1929 and September 1933, and since October 1943 at a site where the stream discharges onto the alluvial valley floor about 7 miles east of Sisquoc. The station is located at about 620 feet above sea level and measures the runoff from a 290-square-mile area.

Runoff measured at this station since July 21, 1952 does not indicate any noticeable change in discharge attributable to the Arvin-Tehachapi earthquake.

Salsipuedes Creek near Lompoc (65). Salsipuedes Creek, a tributary to Santa Ynez River, drains the interior regions of the westerly end of Santa Ynez Mountains. Runoff from this 46.6-square-mile drainage area has been measured since January 1941 at a site on the Jalama Road bridge, just downstream from El Jaro Creek and about 5 miles southeast of Lompoc. The altitude of the gage is about 340 feet above sea level.

Runoff records obtained at this site since July 21, 1952 do not indicate any measurable change in discharge attributable to the Arvin-Tehachapi earthquake.

Juan Y Lolita Rancho Spring (66). This spring is on the north side of the Santa Ynez Mountains at an altitude of about 1,150 feet, about 1 mile north of the Santa Ynez fault. It is on the Juan Y Lolita Rancho about 3 miles south of the town of Santa Ynez. Monthly observations from February 1, 1949 to January 9, 1952 indicate a range in discharge of 0.9 to 3.3 gallons per minute. As a result of a fairly wet winter, the flow from this spring increased to 50 gallons per minute on April 16, 1952, then decreased to 9 gallons per minute on July 3, the last observation prior to the Arvin-Tehachapi earthquake.

Immediately after the earthquake, the flow increased, reaching an observed maximum of 17 gallons per minute on October 21, 1952. Flow was then sustained at 13 to 18 gallons per minute throughout the dry 1952-53 winter, declining to a flow of 12 gallons per minute on June 1, 1953. This gain in flow attributable to the Arvin-Tehachapi earthquake amounted to about 16 acre-feet by June 1, 1953.

Juan Y Lolita Rancho Spring (67). A second and somewhat smaller spring on the Juan Y Lolita Rancho is located almost in



FIGURE 10. Hydrographs of discharge for Juan Y Lolita Rancho spring.

the Santa Ynez fault zone and about 1 mile south of station (66). This spring is also on the north side of the Santa Ynez Mountains at an altitude of about 1,150 feet. The very noticeable change in flow of this spring caused by the Arvin-Tehachapi earthquake is shown graphically on figure 10. This diagram gives the monthly observations of flow made at this station from February 1949 to June 1953. The hydrograph, developed by connecting successive points of measured discharge by straight lines, indicates a successively decreasing annual cycle till the winter of 1951 due to depleted mountain ground-water storage. Then, as a result of a substantial recharge during the fairly wet winter of 1951-52, the discharge increased to 3.5 gallons per minute on April 14, 1952. Subsequently the flow diminished to 1.25 gallons per minute on July 3, 1952 just prior to the earthquake.

The first measurement after the Arvin-Tehachapi earthquake indicated an increase to 9.0 gallons per minute on September 2, 1952, then a decrease to 3.0 gallons per minute in June 1953. Thus at the end of this period which followed the very dry 1952-53 winter, the observed flow was almost as great as that shown for April in the previous wet year.

It has been estimated that had the earthquake not occurred, the flow would have followed the pattern shown by the dashed line.



FIGURE 11. Hydrographs of discharge for Cañada del Refugio Creek.

The difference between these two hydrographs, shown by the cross-hatched area, represents the estimated increase in flow attributable to the Arvin-Tehachapi earthquake. This gain in runoff is shown to a much better advantage in the lower part of figure 10.

J. V. Crawford Spring (68). This spring, also located on the north side of the Santa Ynez Mountains at an altitude of about 1,750 feet, and close to the Santa Ynez fault, showed an appreciable increase in flow as a result of the Arvin-Tehachapi earthquake. The monthly observations showed about the same pattern of runoff distribution as that shown on figure 10. During the winter periods of 1949, 1950, and 1951 the flow ranged from about 0.4 to 0.8 gallons per minute. Then, due to the greater recharge during the 1951-52 winter, the flow increased to 1.5 gallons per minute. By July 14, 1952 it had declined to 1.03 gallons per minute.

With the advent of the Arvin-Tehachapi earthquake, flow increased to 1.50 gallons per minute on September 3, 1952 and remained in excess of 1.2 gallons per minute through June 1953.

Wons Creek at Walska Estate (69). Wons Creek also originates on the north side of the Santa Ynez Mountains and is tributary to the Santa Ynez River. The runoff from this very small drainage area of about half a square mile is measured at an altitude of 2,200 feet, about half a mile north of the divide. This highland area is south of the Santa Ynez fault.

Monthly observations at this site represent the composite runoff of many individual springs. The records show the same annual cycle as shown on figure 10 with greatest discharge in winter and spring, and minimum discharge in summer and fall. A substantial portion of this runoff depletion during summer and fall is due to evapotranspiration losses within the area. Due to lack of any substantial recharge to mountain ground-water storage, winter runoff showed the same progressive decrease from 1949 to 1951 as indicated on figure 10. Then as a result of the substantial ground-water recharge during the fairly wet winter of 1951-52, winter runoff increased to 200 gallons per minute from the usual winter runoff of 30 to 60 gallons per minute. By mid-June flow had decreased to 104 gallons per minute.

Following the Arvin-Tehachapi earthquake, flow increased to 132 gallons per minute on August 5, 1952 and remained in excess of 47 gallons per minute through June 1953. As a result, it has been estimated that the excessive runoff attributable to the earthquake will amount to 67 acre-feet or about 2.5 inches of water over the drainage area.

West Fork Quiota Creek at Forest Service Spring (70). West Fork Quiota Creek is another small highland drainage just north of the divide of the Santa Ynez Mountains and south of the Santa Ynez fault. Monthly observations of flow are made at an altitude of 2,040 feet.

Between the spring of 1949 and the fall of 1951 this stream channel was dry most of the time. However, as a result of the

ground water recharge in the 1951-52 rainy season, flow on June 18, 1952 was still 0.42 gallons per minute.

Immediately following the earthquake, flow increased to 15 gallons per minute on August 5, 1952, and the creek was not reported dry until October 20, 1952. This latter small increase in runoff is believed to be attributable to the Arvin-Tehachapi earthquake.

Cañada del Refugio Creek near Refugio Guard Station (71) Cañada del Refugio Creek drains a steep frontal mountain area on the south side of the Santa Ynez Mountains and is tributary to the Pacific Ocean. Monthly observations of flow are made at an altitude of 400 feet just below the confluence of the two principal forks.

The observations prior to the 1951-52 rainy season were plotted on figure 11 and indicate the same typical trend shown on figure 10. As a result of the fairly wet winter of 1951-52, flow increased to 560 gallons per minute, then diminished to 150 gallons per minute on June 18, 1952.

With the advent of the Arvin-Tehachapi earthquake, flow increased to 330 gallons per minute on August 5, 1952 as shown on figure 11. From that date until June 1953 the flow was substantially higher than normally to be expected during this year. That portion of the runoff attributable to the earthquake is indicated as in the preceding diagrams. This increase in the 11-month

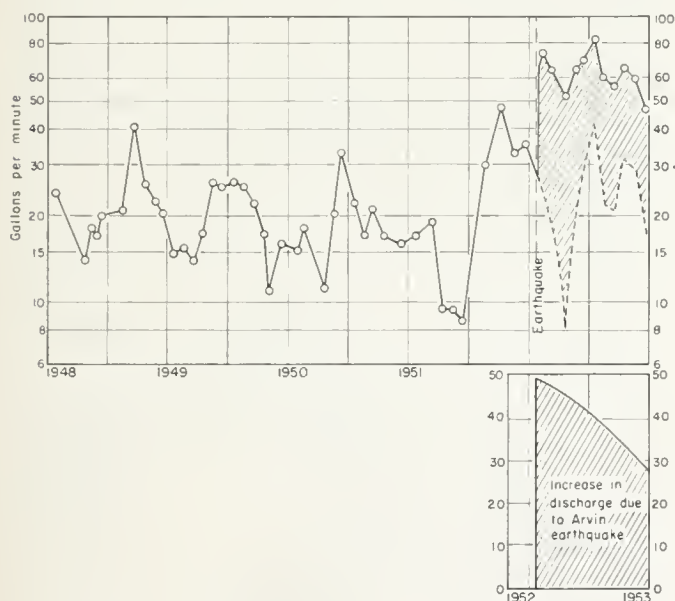


FIGURE 12. Hydrographs of discharge for Carneros Creek.

period of August 1952 through June 1953 amounted to 139 acre-feet. On an areal basis, this is equivalent to 1.2 inches of water over the drainage area.

Carneros Creek (Bartlett Canyon) near Goleta (72). Carneros Creek, like Cañada del Refugio Creek, is a frontal stream on the south side of the Santa Ynez Mountains. Monthly measurements are made in Bartlett Canyon about 500 feet above sea level, 3 miles northeast of Goleta, and 5 miles upstream from the ocean.

All observations since July 1948 are plotted on figure 12. The hydrograph developed from these observations shows the typical general decline in flow due to a depleted ground-water storage prior to the winter of 1951-52. The greater recharge resulting from the 1951-52 precipitation caused an increase in runoff which continued until the time of the Arvin-Tehachapi earthquake.

As a sequence to the earthquake, the flow greatly increased and was sustained well above the 1951-52 winter runoff. The estimated increase in the flow attributable to the earthquake has been cross-hatched in the hydrograph and replotted in the lower part of the diagram. During the 11-month period subsequent to the earthquake this additional runoff is believed to be in the order of 60 acre-feet and is equivalent to 0.6 inch of water over the drainage area.

Canatsey-O'Bannon Spring (73). This spring consists of a seep from landslide material on the canyon wall. It is at an alti-

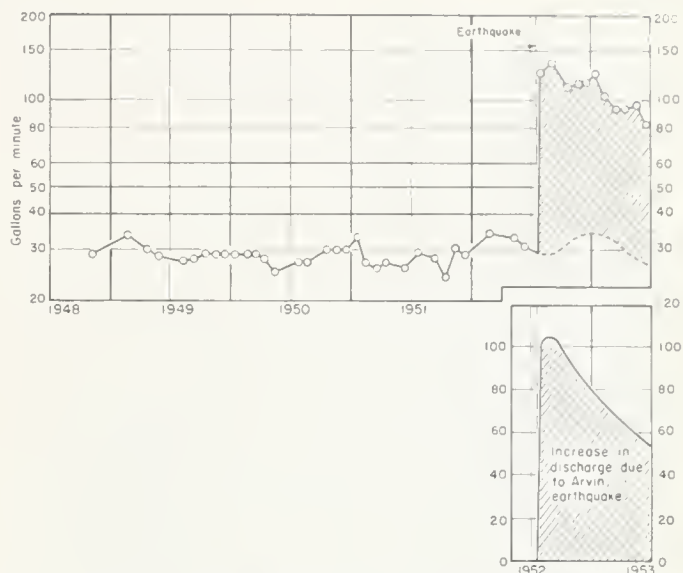


FIGURE 13. Hydrographs of discharge for Mrs. K. C. Canatsey and Mrs. B. O'Bannon spring.

tude of 425 feet in the basin of San Pedro (or San Piedro) Creek, a frontal stream on the south side of the Santa Ynez Mountains, and tributary to the Pacific Ocean. Monthly measurements are made about 3 miles north of Goleta and 4 miles upstream from the ocean.

The monthly observations shown on figure 13 indicate a remarkably constant flow prior to the Arvin-Tehachapi earthquake. This uniformity of flow was abruptly disrupted by the earthquake. In a very short interval of time flow increased from about 30 gallons per minute to 125 gallons per minute on July 30. Subsequent to this date, the flow declined steadily to 83 gallons per minute in June 1953.

The cross-hatched area on this hydrograph and the one plotted in the lower part of figure 13 indicate the estimated increase in runoff attributable to the earthquake. In the 11-month period of August 1952 through June 1953 this increased runoff has amounted to 116 acre-feet. This spectacular increase is more than 2.5 times the entire annual runoff prior to the earthquake.

Holmes Spring (74). This is the first of a series of springs in the frontal drainage area of San Jose Creek, on the south side of the Santa Ynez Mountains. This spring is in the form of a seep from the alluvial stream bed deposits at an altitude of about 1,900 feet.

Observations made prior to the occurrence of the Arvin-Tehachapi earthquake have the same general uniformity of flow shown on figure 13. A seepage of 2.4 gallons per minute on June 3, 1952 increased to 14 gallons per minute on August 4. Subsequently the flow diminished but remained above 6 gallons per minute prior to June 1953.

San Jose Creek at Holmes' Place near San Marcos Pass (75). Monthly observations are made in this small headwater drainage area at an altitude of 1,890 feet, about 5.5 miles north of the ocean. A hydrograph developed from these observations is given on figure 14. In general, the hydrograph prior to the Arvin-Tehachapi earthquake is similar to those shown in the preceding diagrams. Subsequent to the earthquake the discharge increased greatly and was sustained through June 1953. That portion of the runoff believed to be attributable to the earthquake is shown by cross-hatching and replotted for better definition in the lower part of figure 14. During the 11-month period subsequent to the earthquake and ending in June 1953, this excessive runoff has been estimated as 55 acre-feet or the equivalent of 0.86 inch of water over the drainage area.

San Marcos Trout Club Spring near San Marcos Pass (76). The San Marcos Trout Club Spring has its immediate origin in the alluvial deposits in San Jose Creek at an altitude of about 1,700 feet, about 1.5 miles southeast of San Marcos Pass. Monthly observations at this site since July 1948 indicate a flow that



FIGURE 14. Hydrographs of discharge for San Jose Creek at Holme's place near San Marcos Pass.

generally ranged from 2 to 6 gallons per minute, except for short winter periods, prior to the Arvin-Tehachapi earthquake. Subsequent to the earthquake the flow increased to 9 gallons per minute and remained in excess of 6 gallons per minute through June 1953, along a pattern very similar to that shown on figure 14.

Unnamed Tributary to San Jose Creek at Hobo Rock near San Marcos Pass (77). This unnamed tributary to San Jose Creek is measured monthly at a site having an altitude of about 1,700 feet, about 1 1/4 miles east of San Marcos Pass. During the earlier part of the record the distribution was quite similar to that shown on figure 11. The discharge reflected the depletion of the groundwater. Ground-water recharge in the 1951-52 rainy season increased the runoff and gave a sustained flow prior to the earthquake comparable to the earlier winter runoff. With the advent of the earthquake, the flow increased but was not as well sustained, as shown on figure 11.

San Jose Creek (78). San Jose Creek is measured monthly at a site 1 mile above Patterson Ave. Bridge, at an altitude of about 250 feet. Discharge followed a pattern very similar to that shown on figure 14 prior to the occurrence of the Arvin-Tehachapi earthquake. Subsequent to the earthquake, flow increased from about 80 gallons per minute to 280 gallons per minute. This increase in runoff attributable to the earthquake was not as well sustained as for some of the measuring points upstream.

Cold Spring Canyon Creek near San Marcos Pass (79). Cold Spring Canyon Creek is on the north side of the Santa Ynez Mountains and is tributary to the Santa Ynez River. Monthly observations of the flow in this headwater drainage area are made about 1,600 feet above sea level.

Like many of the preceding records, the flow indicated a gradual decreasing trend prior to the winter of 1951-52. During

that winter period there was an appreciable increase in discharge, followed by a recession that produced a runoff of 28 gallons per minute on July 15, 1952. With the advent of the Arvin-Tehachapi earthquake, flow increased to 64 gallons per minute on September 4, 1952 and was well sustained through June 1953.

Hot Springs Creek (80). Also located on the north side of the Santa Ynez Mountains is Hot Springs Creek. Monthly measurements are made about 950 feet above sea level and about 1 mile above the confluence with the Santa Ynez River. After a fairly wet winter the discharge had declined to 176 gallons per minute on July 15, 1952. Subsequent to the Arvin-Tehachapi earthquake it increased to 300 gallons per minute on September 4, 1952, declining to 128 gallons per minute on June 5, 1953.

Crown Eleven Ranch Spring (81). Crown Eleven Ranch Spring is also located on the north side of the Santa Ynez Mountains between Hilton and Tequepis Canyons, at an altitude of about 990 feet. Monthly observations between October 1948 and December 1951 showed a range in flow of 0.2 to 1.8 gallons per minute. As a result of the 1951-52 rainy season, flow increased to almost 3 gallons per minute and remained fairly well sustained, declining to 2.3 gallons per minute on July 14, 1952. Subsequent to the Arvin-Tehachapi earthquake, flow increased to 5.0 gallons per minute, the highest discharge recorded during the period of record, and remained sustained at this amount or more until February 1953. The latest observation on June 2, 1953 indicated a discharge of 3.6 gallons per minute.

Cachuma Creek near Santa Ynez (82). Cachuma Creek drains the southern slopes of the San Rafael Mountains and is tributary to the Santa Ynez River. A gaging station was established in October 1950 about 3.6 miles upstream from Santa Ynez River and 8.8 miles east of the town of Santa Ynez.

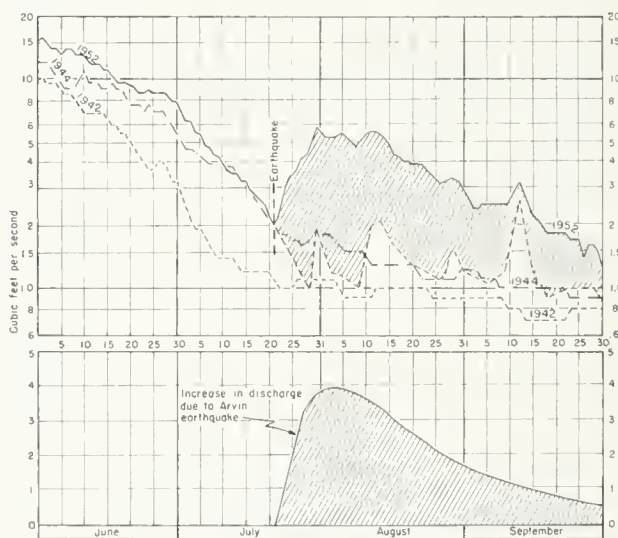


FIGURE 15. Hydrographs of daily discharge for Santa Cruz Creek near Santa Ynez.

The discharge at this station does not reflect any influence from the Arvin-Tehachapi earthquake.

Santa Cruz Creek (83). Santa Cruz Creek drainage area is also on the south and western slope of the San Rafael Mountains and is adjacent to the Cachuma Creek drainage area. The gaging station is about 0.5 mile above the stream's confluence with Santa Ynez River. Unlike Cachuma Creek, runoff from this 77-square-mile drainage area increased immediately following the Arvin-Tehachapi earthquake.

This station has a record of daily discharge beginning in October 1941. The daily record for the 4-month period of June through September is shown on figure 15 for 1952 as well as for the two antecedent years of 1942 and 1944. Discharge increased promptly after the earthquake, and reached a maximum in the first part of August.

On the basis of antecedent records, it has been possible to estimate the flow had there been no earthquake. The difference between the dashed line and the 1952 record shows the increase

attributable to the Arvin-Tehachapi earthquake. It reached a maximum of about 3.9 cubic feet per second on August 3, 1952 and then gradually decreased to about 0.6 cubic foot per second on September 30, 1952. This increase in runoff subsequent to the earthquake amounted to 297 acre-feet. On an areal basis, this is equivalent to 0.07 inch over the drainage area.

Cuyama River near Ventucopa (84). Some distance east and slightly north of Santa Cruz Creek drainage area, on the north side of Pine Mountain, is the headwater area of Cuyama River, a tributary to Santa Maria River. In November 1944 a gaging station was established at an altitude of about 3,500 feet at Ozena, about 12 miles southeast of Ventucopa.

The record of daily discharge shows the same pattern of distribution as that on figure 15. Discharge of 0.5 cubic foot per second on July 20, 1952 increased to 3.0 cubic feet per second three days later. The total increase in runoff attributable to the Arvin-Tehachapi earthquake amounted to about 300 acre-feet prior to October 1, 1952. This increase in runoff is equivalent to about 51 percent of the entire annual runoff during the dry 1951 water year. On an areal basis it is equivalent to about 0.07 inch of water over the drainage area.

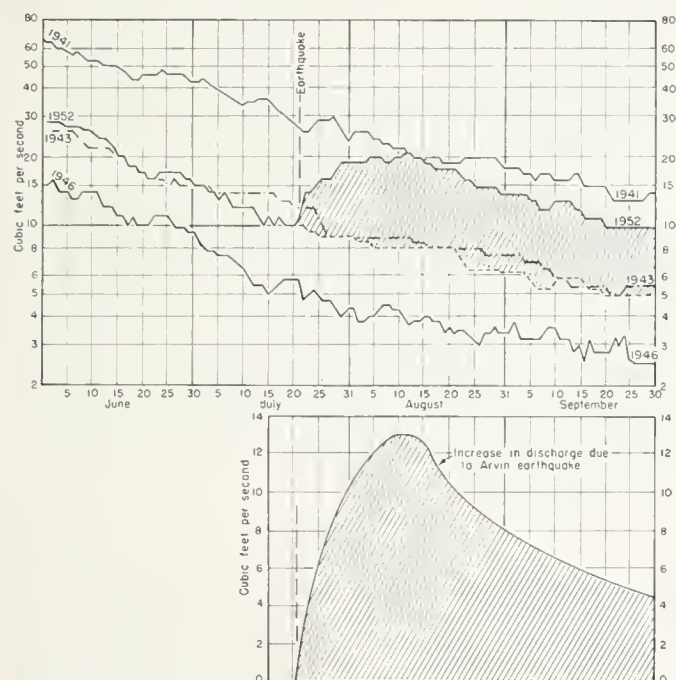


FIGURE 16. Hydrographs of daily discharge for Matilija Creek above Matilija Dam.

Matilija Creek above Reservoir (85). South of the Cuyama River headwater areas and across the upper Sespe Creek drainage area is Matilija Creek, a tributary of Ventura River. Matilija Creek drains the mountain plateau north of the Santa Ynez Mountains. The daily discharge is measured about 1,160 feet above sea level and about 2 miles upstream from Matilija Dam. Records are available since May 1948, and at a site 2.4 miles downstream since October 1927.

The effect of the Arvin-Tehachapi earthquake was to increase the runoff from many of the springs and streams in the area. As shown on figure 16, daily discharge progressively increased from 10 cubic feet per second on July 20, 1952 to 21 cubic feet per second on August 11 and 12, largely as a result of the earthquake.

The hydrographs on figure 16 include records obtained in 1941, 1943, and 1946 at the station downstream so that daily discharge could be estimated subsequent to July 20, 1952 had there been no earthquake. Flow under these conditions is shown by a dashed line and the cross-hatched area between these estimated and observed discharges represents the increase attributable to the earthquake.

This increase in runoff prior to October 1, 1952 amounted to 1,170 acre-feet or only slightly less than the total annual runoff during the preceding dry year of 1951. On an areal basis, it is equivalent to 0.43 inch of water over the drainage area.

North Fork Matilija Creek at Matilija (86). East of the Matilija Creek drainage area (85) is North Fork Matilija Creek. Records of daily discharge are available since 1928 at a site about 0.5 mile above its confluence with Matilija Creek. There was a pronounced increase in discharge immediately following the earthquake, along a pattern very similar to that shown on figures 15 and 16.

The increase attributable to the earthquake was about 560 acre-feet, or the equivalent of about 0.68 inch over the drainage area.

Coyote Creek near Ventura (87). Coyote Creek, a tributary to Ventura River, drains the south slopes of the Santa Ynez Mountains and the foothill areas on the ocean side of these mountains. A continuous record of discharge has been obtained for this stream since October 1927, except for the period of October 1932 to September 1933, at a point about 0.2 mile above its confluence with Ventura River and about 5.5 miles northwest of Ventura.

The records indicate that the discharge declined continuously throughout the 4-month period of June through September 1952 without modification as a result of the Arvin-Tehachapi earthquake.

Santa Paula Creek near Santa Paula (88). Santa Paula Creek, a tributary to Santa Clara River, originates on the south side of Topatopa Mountains and on the north side of Santa Paula Peak. A gaging station was established in October 1927 just upstream from the Santa Paula Water Works diversion dam, about 3 miles north of Santa Paula, to measure the runoff from this 39.8-square-mile mountain drainage area.

The records obtained before and after the Arvin-Tehachapi earthquake do not indicate any definite change in runoff as a result of this event.

Sespe Creek near Wheeler Springs (89). The headwater areas of Sespe Creek are on the southern slopes of Pine Mountain and northern slopes of Ortega Hill and adjacent mountains. Discharge is measured in Sespe Gorge at a site about 3,500 feet above sea level and about 5 miles northeast of Wheeler Springs. Runoff from this 50-square-mile drainage area has been measured continuously since July 1948.

Daily discharge showed a general increase due to the Arvin-Tehachapi earthquake. The runoff distribution was similar to that on figure 16, increasing from 1.5 cubic feet per second on July 20, 1952 to 3.6 cubic feet per second on August 1.

As a result of the earthquake, the runoff was increased by 204 acre-feet, or the equivalent of 0.08 inch of water over the drainage area.

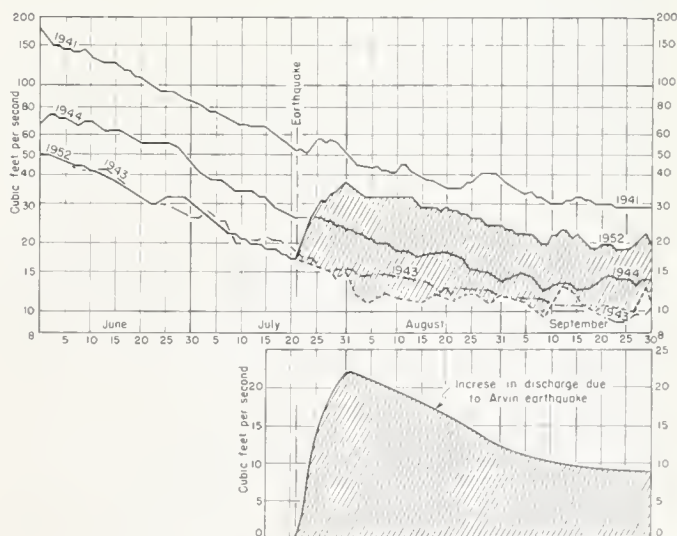


FIGURE 17. Hydrographs of daily discharge for Sespe Creek near Fillmore.

Sespe Creek near Fillmore (90). This gaging station, downstream from the Wheeler Springs station, is about 0.1 mile downstream from Little Sespe Creek and 3.5 miles north of Fillmore. At this site the stream channel has an altitude of only about 590 feet. Records of runoff from the 254-square-mile drainage area have been obtained continuously since 1934.

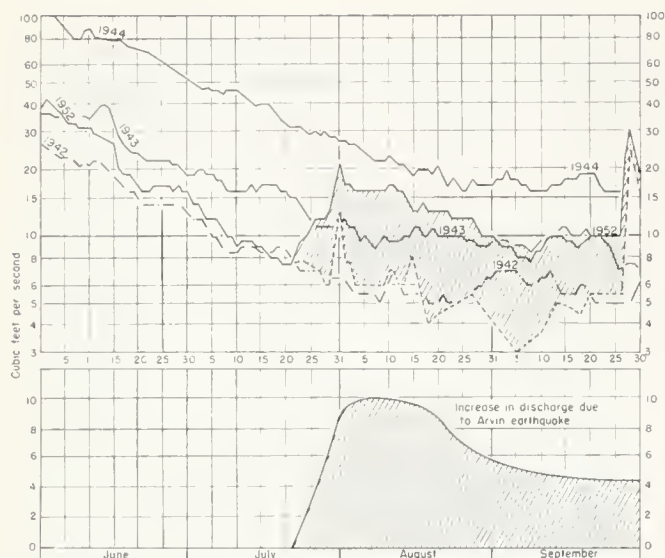


FIGURE 18. Hydrographs of daily discharge for Piru Creek near Piru.

The discharge was definitely affected by the Arvin-Tehachapi earthquake, as indicated on figure 17. Discharge of 17 cubic feet per second on July 20, 1952 increased to 37 cubic feet per second on July 31 largely as a result of the earthquake.

On the basis of records obtained in 1941, 1943, and 1944, it has been possible to estimate the probable discharge at this station had there been no earthquake. The cross-hatched area between the estimated hydrograph and the observed discharge represents the gain in discharges resulting from the earthquake.

This increase, plotted in the lower part of figure 17, ranged from zero on July 21, 1952 to 22 cubic feet per second on August 1, gradually decreasing to 9 cubic feet per second on September 30. Thus, as a result of the earthquake, Sespe Creek acquired an additional runoff of 2,160 acre-feet. This is equivalent to 61 percent of the entire annual runoff in the dry 1951 water year. On an areal basis, the additional runoff is equivalent to 0.16 inch of water over the entire drainage area.

Hopper Creek near Piru (91). East of Sespe Creek is the short frontal drainage area of Hopper Creek. The gaging station is at the bridge on U. S. Highway 126, 2 miles southwest of Piru. Records of daily discharge are available since 1930. Following a normal summer recession, the stream channel became dry early in July. Immediately following the Arvin-Tehachapi earthquake, the stream started to flow, increasing to over 3 cubic feet per second by mid-August along a pattern very similar to that shown on figure 16.

Piru Creek near Piru (92). East of Hopper and Sespe Creeks is the 432-square-mile mountain drainage area of Piru Creek. This stream originates on the northern slopes of Pine Mountain, and after following a generally easterly course through the interior mountain areas, turns sharply southward to join the Santa Clara River. A continuous record of discharge is available for a site 1.8 miles northeast of Piru where the stream channel has an altitude of about 780 feet.

As indicated on figure 18, daily discharge was noticeably affected by the Arvin-Tehachapi earthquake. The flow increased from 7.5 cubic feet per second prior to the earthquake to more than 16 cubic feet per second during the first part of August.

On the basis of the antecedent records obtained in 1942, 1943, and 1944, it was possible to estimate the probable discharge subsequent to July 21, 1952, had no earthquake occurred. The cross-hatched area between these estimated records and the observed data represents the gain in flow attributable to the earthquake.

This increase, as shown in the lower part of figure 18, amounts to 920 acre-feet, or the equivalent of 0.04 inch of water over the 432-square-mile drainage area.

Santa Clara River near Saugus (93). The headwater areas of the Santa Clara River lie east of Piru Creek in the San Gabriel

Mountains. Continuous records of discharge are available from the gaging station at U. S. Highway 99 crossing, about 3 miles west of Saugus, since September 1929. The altitude of the stream channel at this site is about 1,040 feet.

The records indicate that the Arvin-Tehachapi earthquake did not affect the flow at this point.

Santa Clara River near Lang (94). The gaging station is at an altitude of 1,735 feet in the headwater area of Santa Clara River about 0.7 mile east of Lang Railway Station. A continuous record of discharge exists since October 1949.

The data obtained at this site do not reflect any change in flow as a result of the Arvin-Tehachapi earthquake.

Little Rock Creek near Little Rock (95). Still further east, on the north side of the San Gabriel Mountains, is the Little Rock Creek drainage area. A continuous record of discharge is available for this stream at an altitude of 3,290 feet, about 5 miles south of Little Rock. This record is important because the station is located about 5 miles upstream from the San Andreas fault zone.

The records at this site do not indicate any change in flow as a result of the Arvin-Tehachapi earthquake.

Rock Creek near Valermo (96). The Rock Creek drainage area is just east of the Little Rock Creek drainage area and is also on the north side of the San Gabriel Mountains. An almost continuous record of discharge of this stream exists since January 1923 at the gaging station located about 1.8 miles southeast of Valermo, at an altitude of about 4,050 feet. The important San Andreas fault zone is within 1 mile of this station.

This record also failed to reflect any influence attributable to the Arvin-Tehachapi earthquake, as shown on figure 3.

Arroyo Seco near Pasadena (97). This drainage area is on the south side of the San Gabriel Mountains. The discharge of this stream has been measured continuously since December 1910 at an altitude of almost 1,400 feet, at a site 5.5 miles northwest of Pasadena.

The records failed to reflect any change in discharge attributable to the Arvin-Tehachapi earthquake.

Topanga Creek near Topanga Beach (98). The Topanga Creek drainage area is located on the south side of the coastal Santa Monica Mountains. A continuous record of discharge of this stream is available since January 1930, except for one year, at a site about 265 feet above sea level and 2 miles north of Topanga Beach.

This record does not show any change in discharge resulting from the Arvin-Tehachapi earthquake.

SUMMARY

The accelerated ground-water runoff resulting from the Arvin-Tehachapi earthquake represents at least a temporary depletion of the ground-water supply. In the 0.5-square-mile drainage area of Wons Creek in the Santa Ynez Mountains, this accelerated ground-water runoff amounted to 2.5 inches of water over the entire basin. The effect of this depletion could mean a reduction in runoff during subsequent years if not promptly replaced by precipitation. Also, the effect decreases as the size of the drainage area increases.

Evidence of the magnitude of the overall depletion of this ground-water supply is shown on figure 19. This diagram indicates the size of the drainage area and the increased runoff resulting from the earthquake in inches of water over the entire drainage area. The volume of ground-water runoff is for the limited 71-day period of July 21 to September 30, 1952 for all stations except those located in the Santa Ynez Mountains and part of the Teolote Investigation. In this latter instance the volume is for the period July 21, 1952 through June 30, 1953.

Superimposed on the diagram is an enveloping curve showing the maximum observed increase in runoff for the 71-day period as a result of the earthquake. On the

basis of this curve, the volume of ground-water runoff amounted to the equivalent of 2.2 inches over an entire 2-square-mile drainage area, 0.94 inch over a 10-square-

mile drainage area, 0.28 inch over a 100-square-mile drainage area, and 0.083 inch over a 1,000-square-mile drainage area.

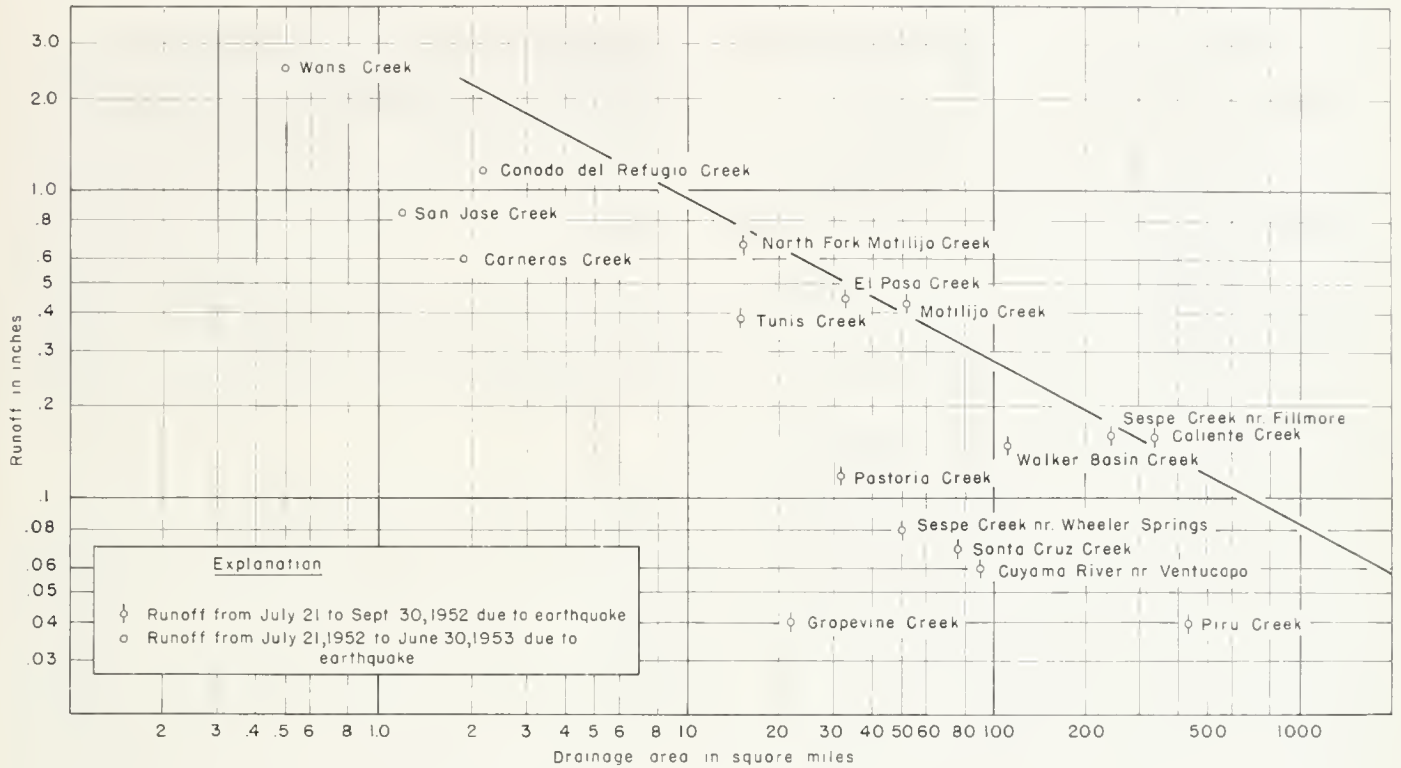


FIGURE 19. Volume of runoff due to earthquake.

10. WATER-LEVEL FLUCTUATIONS IN WELLS *

By G. H. DAVIS,† G. F. WORTS, JR.,† AND H. D. WILSON, JR.‡

ABSTRACT

Fluctuations of ground-water levels caused by the Arvin-Tehachapi earthquake were detected by automatic water-level recorders in wells as far north as Durham, Butte County, and as far south as Oceanside, San Diego County. The amplitude of recorded fluctuations ranged from 7.34 feet in a well about 20 miles northeast of the epicenter to 0.012 feet in a well about 180 miles southeast of the epicenter. Many records, especially from wells near the epicenter, show a small residual displacement of the water level above or below the level prior to the earthquake on the order of a few hundredths to a few tenths of a foot.

Water-surface fluctuations in wells penetrating unconfined aquifers were of small amplitude, but fluctuations in nearby wells penetrating partially confined or confined aquifers were many times greater. Although the water-surface movements in partially confined and confined aquifers tend to decrease in amplitude with distance from the epicenter, these fluctuations appear to be more directly related to the compressibility and elasticity of the aquifer materials than to the degree of confinement of the aquifer or the distance of the well from the epicenter.

INTRODUCTION

Water-level fluctuations resulting from earthquake shocks have been observed for many years and have been described in many reports (Leggette and Taylor, 1935; Blanchard and Byerly, 1935; Thomas, 1940; La Rocque, 1941; Parker and Stringfield, 1950). They are of special interest to hydrologists because of the possible relation between the magnitude of the fluctuations and the compressibility and elasticity of the water-bearing materials. The Arvin-Tehachapi earthquake of July 21, 1952, is unique because of its large magnitude, $7\frac{1}{2}$ on the Richter scale, and because of the large number of wells in diverse types of sediments in which water-level fluctuations were recorded. The principal damage—to buildings, oil pipelines, an oil refinery at Paloma, irrigation pipelines, and electric facilities—centered around Arvin, about 16 miles southeast of Bakersfield and Tehachapi, about 36 miles east-southeast of Bakersfield (Benioff, et al., 1952).

Automatic water-level recorders in California wells as far north as Durham, Butte County, and as far south as Oceanside, San Diego County, recorded the shock. The rapid oscillation of the water surface appears on standard water-level charts as a vertical trace of the pen above and below the point on the chart representing the water surface at the time of the shock (figs. 2 and 3).

Water-level recorders used in ground-water investigations were not designed for use as seismographs; because of their condensed time scale they do not record details of the various phases of the earthquake. Blanchard and Byerly (1935, p. 321) have shown that water-level recorders in wells are inferior seismographs even when fitted with expanded-time-scale instruments because of the damping effect caused by inertia in the system. The fluctuation of the water surface, however, is many times greater than comparable ground motion at the well because of hydraulic magnification. It is generally accepted that water-level fluctuations due to earthquakes are caused by successive dilation and compression of the water-bearing materials, and that volume change of the aquifer varies considerably, depending upon the elas-

ticity and compressibility of the water-bearing materials and the earth motion in the vicinity of the well. Thomas (1940, p. 96) reported that distant earthquakes cause water-surface fluctuations that differ in many respects from those caused by nearby shocks. Continuity of the trend of the hydrograph before and after the disturbance and equality of fluctuation above and below the general trend line are characteristic of distant earthquakes, whereas fluctuations caused by nearby disturbances commonly show more movement in one direction than in another, and permanent rearrangement of rock materials as the result of the shock is sometimes indicated by a change in water level. The foregoing appears to hold true with respect to the Arvin-Tehachapi earthquake. Water-level records from wells near the epicenter were characterized by inequality of fluctuations and residual change in water level, but wells in the northern Sacramento Valley, 300 to 400 miles from the epicenter, showed equal fluctuation and no residual change in water level (see table 1).

Ground water is generally thought of as existing either under confined (artesian) conditions or unconfined (water-table) conditions. Lack of confinement implies free movement of water downward from the land surface to the water surface within the containing deposit, whereas confinement implies lack of hydraulic continuity with the overlying land surface; that is, confining beds lie between the land surface and the aquifer and, because of their low permeability relative to that of the aquifer, prevent or impede vertical movement of water. In nature perfect examples of either type are rare. Even the least permeable aquicludes permit slow, perhaps imperceptible, movement into or out of confined aquifers. On the other hand, water bodies that normally appear to represent unconfined conditions may react to sudden stresses, such as seismic waves, in much the same manner as confined water bodies. Presumably this effect is due to the presence of local semiconfining lenses or layers of material of relatively low permeability which do not prevent water-table conditions from existing on an areal or regional scale, but which impede the movement of water in response to sudden dilational or compressive stresses acting upon the containing deposits. Wells should not fluctuate in response to earthquake shocks under true unconfined conditions. Apparent water-level fluctuations, however, may occur if the recorder is shaken severely enough to move relative to the water surface, or if the shock sets up a sloshing motion in the water in the casing, thereby causing a vertical movement of the float. These special conditions might exist near the epicenter of a strong earthquake but could hardly be expected to affect wells at any great distance.

Acknowledgments. We wish to express our thanks to our colleagues in the Geological Survey and in other federal, state, and local agencies who supplied helpful advice and comments. Special thanks are given to the following agencies which supplied records used in this study: The California Division of Water Resources, the U. S. Bureau of Reclamation, the Kern County Land Company, and the City of Long Beach.

* Publication authorized by the Director, U. S. Geological Survey.

† Geologist, U. S. Geological Survey.

‡ Engineer, U. S. Geological Survey.

Table 1. *Fluctuations of water level in 56 wells in California coincident in time with the Arrin-Tebuchapi earthquake, July 21, 1952.*
 (Data by U. S. Geol. Survey from charts of water-level recorders operated by Geological Survey and other agencies).

Well number	Location of well	Depth of well, feet	Perforated interval, feet	Casing diameter, inches	Depth to water below land surface before shock	Fluctuations				Type of occurrence
						Amplitude, feet	Rise, feet	Fall, feet	Residual rise (+) or fall (-), feet	
SACRAMENTO VALLEY										
M.D.B. & M. 21N/2E-30H1	About 5.6 miles southwest of Chico, Butte County Record from U. S. Bureau of Reclamation	375	84-375 open hole	--	23.16	0.12	0.06	0.06	none	Partially confined water in Pleistocene alluvium and Pliocene alluvial and volcanic deposits (Tuscan fm).
20N/2E-23A1	About 10.1 miles northwest of Oroville, Butte County Record from U. S. Bureau of Reclamation	196	--	12	48.41	0.15	0.08	0.08	none	Partially confined water in Pleistocene alluvium and Pliocene alluvial and volcanic deposits (Tuscan fm).
14N/3E-31J2	About 9 miles southwest of Yuba City, Sutter County Record from Calif. Div. of Water Resources	65	--	--	17.10	0.30	0.17	0.13	none	Partially confined water in Pleistocene alluvium.
14N/3E-31K1	About 9 miles southwest of Yuba City, Sutter County Record from Calif. Div. of Water Resources	213	126-213 open hole	14	15.22	0.18	0.10	0.08	none	Partially confined water in Pleistocene and Pliocene alluvium.
13N/3E-11F1	About 10.2 miles south of Yuba City, Sutter County Record from Calif. Div. of Water Resources	172	70-172 open hole	8	15.60	0.31	0.16	0.15	none	Partially confined water in Pleistocene and Pliocene alluvium.
13N/3E-14P2	About 11.7 miles south of Yuba City, Sutter County Record from Calif. Div. of Water Resources	83	--	--	10.65	0.60	0.37	0.23	none	Partially confined water in Pleistocene and Pliocene alluvium.
12N/2E-2R1	About 16.3 miles southwest of Yuba City, Sutter County Record from Calif. Div. of Water Resources	320	280-320 open hole	6	4.83	0.15	0.08	0.07	none	Partially confined water in alluvium of Recent to Pliocene (?) age.
9N/2E-35D1	About 3.2 miles north of Davis, Yolo County Record from Calif. Div. of Water Resources	175	--	--	36.75	0.25	0.0	0.25	-0.20	Partially confined water in alluvium of Recent to Pliocene (?) age.
7N/2E-1M1	About 6.4 miles east of Dixon, Solano County Record from Calif. Div. of Water Resources	302	--	--	28.61	0.61	0.29	0.32	none	Partially confined water in alluvium of Pleistocene to Pliocene (?) age.
SAN JOAQUIN VALLEY										
12S/18E-21H1	About 6.4 miles south of Madera, Madera County Record from U. S. Bureau of Reclamation	100	open bottom	12	78.78	1.75	0.83	0.92	none	Partially confined water in alluvium of Pleistocene to Pliocene (?) age.
13S/17E-10A	About 9.6 miles south of Madera, Madera County Record from U. S. Bureau of Reclamation	124	--	10	28.51	3.48	1.72	1.76	-0.03	Partially confined water in alluvium of Pleistocene to Pliocene (?) age.
13S/20E-7D	About 6.2 miles northwest of Fresno, Fresno County Record from U. S. Bureau of Reclamation	86	--	--	63.90	0.36	0.25	0.11	none	Partially confined water in Pleistocene and Pliocene alluvium.
14S/14E-28E2	About 6.6 miles southwest of Mendota, Fresno County Record from U. S. Bureau of Reclamation	437	--	16	101.74	110.86	0.34	10.52	-10.52	Partially confined water in alluvium of Recent to Pleistocene age.
15S/14E-7B2	About 9.6 miles southwest of Mendota, Fresno County Record from U. S. Bureau of Reclamation	--	--	16	252.64	1.02	0.64	0.38	pen off chart	Partially confined water in alluvium of Recent to Pleistocene age.
15S/16E-20R1	About 12.8 miles southeast of Mendota, Fresno County	356	--	16	52.60	1.72	0.91	0.81	+0.27	Partially confined water in alluvium of Recent to Pleistocene age.

Table 1. *Fluctuations of water level in 56 wells in California coincident in time with the Arvin-Tehachapi earthquake, July 21, 1952.—Continued.*
(Data by U. S. Geol. Survey from charts of water-level recorders operated by Geological Survey and other agencies).

Well number	Location of well	Depth of well, feet	Perforated interval, feet	Casing diameter, inches	Depth to water below land surface before shock	Fluctuations			Type of occurrence	
						Amplitude, feet	Rise, feet	Fall, feet		
SAN JOAQUIN VALLEY										
<i>Continued</i>										
M.D.B. & M. 15S/16E-34E1	About 15 miles southwest of Mendota, Fresno County	--	--	12	133.41	1.00	0.68	0.32	+0.10	Confined water in Pleistocene (?) alluvium.
19S/18E-27M1	About 20.8 miles east of Coalinga, Fresno County	2,105	730-2,105	18	338.02	2.51	0.55	1.96	+0.55	Confined water in Pleistocene (?) alluvium.
19S/18E-27N1	Record from U. S. Bureau of Reclamation	152	--	15½	81.53	0.25	0.22	0.03	+0.12	Partially confined water in alluvium of Recent to Pleistocene age.
27S/24E-32R1	About 20.8 miles east of Coalinga, Fresno County	80	--	--	75.81	0.40	0.20	0.20	none	Partially confined water in alluvium of Recent to Pleistocene age.
27S/25E-24R1	Record from U. S. Bureau of Reclamation	253	152-253	8	166.00	>5.0	--	--	+0.20	Partially confined water in Pleistocene and Pliocene (?) alluvium.
27S/25E-35C2	Record from Kern Co. Land Company	483	--	14	149.90	>5.0	--	--	none	Partially confined water in alluvium of Recent to Pliocene (?) age.
28S/26E-24P1	About 5.9 miles southeast of Wasco, Kern County	405	--	--	128.33	>5.0	--	--	-0.30	Partially confined water in Pleistocene and Pliocene (?) alluvium.
30S/26E-27C1	Record from Kern Co. Land Company	54	--	8	18.72	0.35	0.28	0.07	+0.20	Unconfined water in Recent (?) alluvium.
30S/26E-34R1	About 10.9 miles southwest of Bakersfield, Kern County	104	--	10	18.19	3.93	2.27	1.66	+0.20	Partially confined water in alluvium of Recent (?) to Pleistocene (?) age.
30S/27E-4Q1	About 11 miles southwest of Bakersfield, Kern County	98	48-98	14	17.50	1.45	3	1.45	none	Partially confined water in alluvium of Recent to Pleistocene age.
30S/27E-5H1	Record from Kern Co. Land Company	50	--	12	6.68	0.20	0.14	0.06	none	Unconfined water in Recent (?) alluvium.
30S/30E-3I1	About 4.8 miles west of Bakersfield, Kern County	505	300-482	--	371.75	7.34	2.34	5.00	+0.09	Partially confined water in Pleistocene and Pliocene (?) alluvium.
32S/27E-26J1	Record from U. S. Bureau of Reclamation	300	--	16	26.79	>5.00	--	--	mechanical failure	Partially confined water in Recent and Pleistocene (?) alluvium.
ANTELOPE VALLEY										
S.B.B. & M. 9N/10W-12R1	About 3.2 miles south of Muroc, Kern County	187	169-178	16	20.58	1.65	1.40	0.25	+1.40	Partially confined water in Pleistocene and Pliocene (?) alluvium.
9N/9W-7M1	About 2.6 miles south of Muroc, Kern County	245	--	12	24.82	>0.38	--	--	mechanical failure	Unconfined water in Pleistocene and Pliocene (?) alluvium.
9N/9W-8D1	About 1.9 miles south of Muroc, Kern County	32	--	12	25.97	0.61	0.58	0.03	+0.44	Partially confined water in Pleistocene alluvium.
SANTA YNEZ VALLEY										
7N/34W-9H3	About 5.0 miles north of Lompoc, Santa Barbara County	103	--	8	11.21	0.04	0.01	0.03	none	Unconfined water in Recent sand of Pleistocene age.
7N/34W-12E1	About 5.0 miles north of Lompoc, Santa Barbara County	385	345-385	8-6	303.53	>1.0	--	--	+0.01	Partially confined water in Caroga sand of Pliocene age.
7N/34W-21F1	About 2.4 miles north of Lompoc, Santa Barbara County	145	73-93	8	21.24	0.24	0.12	0.12	+0.08	Partially confined water in Orcutt sand of Pleistocene age.
6N/30W-20F4	About 4.2 miles east of Solvang, Santa Barbara County	65	--	16	14.82	0.73	0.30	0.43	none	Unconfined water in Recent alluvium.
6N/30W-20F51	About 4.5 miles southeast of Solvang, Santa Barbara County	52	--	10	12.55	0.21	0.05	0.16	-0.02	Unconfined water in Recent alluvium.

Table 1. Fluctuations of water level in 56 wells in California coincident in time with the Arvin-Tehachapi earthquake, July 21, 1952.—Continued.
(Data by U. S. Geol. Survey from charts of water-level recorders operated by Geological Survey and other agencies).

Well number	Location of well	Depth of well, feet	Perforated interval, feet	Casing diameter, inches	Depth to water below land surface before shock	Fluctuations				Type of occurrence	
						Amplitude, feet	Rise, feet	Fall, feet	Residual rise (+) or fall (-), feet		
S.B.B. & M. —Continued											
4S/10W-36A1	COASTAL PLAIN, ORANGE COUNTY About 4.2 miles east of Garden Grove, Orange County	200	--	8	149.82	1.80	0.94	0.86	+0.13	Unconfined water in undifferentiated Pleistocene alluvium.	
5S/11W-16D2	About 5.3 miles northwest of Huntington Beach, Orange County	400	--	16	42.38	1.02	0.74	0.28	+0.37	Confined water in undifferentiated Pleistocene alluvium.	
	SANTA MARGARITA RIVER VALLEY										
10S/4W-7J1	About 9.6 miles north of Oceanside, San Diego County	162	--	20	5.34	0.138	0.078	0.06	none	Unconfined water in Recent alluvium.	
10S/5W-23Q1	About 6.6 miles north of Oceanside, San Diego County	290	50-280	6	11.60	0.012	0.012	0	none	Confined water in La Jolla formation (Eocene).	
10S/5W-26L1	About 5.8 miles north of Oceanside, San Diego County	175	80-100	6	8.17	0.075	0.03	0.045	+0.005	Partially confined water in Recent alluvium and La Jolla fm. (Eocene).	
11S/5W-2N4	About 3.7 miles north of Oceanside, San Diego County	200	100-120 160-200	6	5.65	1.54	0.87	0.67	+0.065	Partially confined water in Recent alluvium within a narrow canyon closely surrounded by competent San Onofre breccia (Miocene).	

1 Large permanent decline of water level believed due to shaking of casing causing increased contribution to well from deep confined aquifer that has lower head than overlying partially confined aquifer.

2 Apparently part of record missing on chart.



FIGURE 1.

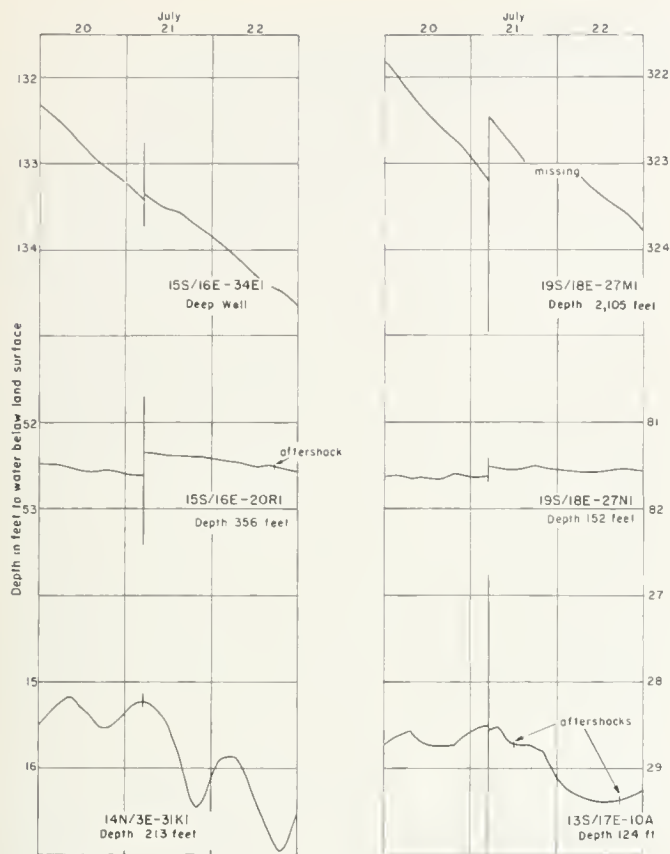


FIGURE 2. Hydrographs for six wells in the Central Valley, July 20-22, 1952.

WATER-LEVEL FLUCTUATIONS CAUSED BY THE ARVIN-TEHACHAPI EARTHQUAKE

*Amplitude * of Fluctuations and Residual Changes in Water Level.* Water-level graphs covering the period of the Arvin-Tehachapi earthquake were collected from 55 wells equipped with automatic float-type water-stage recorders and one well equipped with a pressure recording gage. These wells are distributed from the northern Sacramento Valley, about 370 miles north of the epicenter, to the Twentynine Palms area, about 180 miles southeast of the epicenter. Approximately half the wells are in the Central Valley and the remainder are in the Antelope Valley, the Santa Ynez River basin, the Santa Barbara basin, the Ojai Valley, the Santa Clara River valley, the upper Santa Ana Valley, the Twentynine Palms area, the Los Angeles coastal plain, and the Santa Margarita River valley. All the wells are in alluvial valleys, with the exception of those in the Santa Ynez River basin, several of which are on alluvial uplands adjoining the Santa Ynez River valley. Figure 1, a map of California, shows well numbers and locations for all wells listed in table 1 and gives the amplitude of water-level fluctuation for each well.

The amplitude of fluctuations ranged from 7.34 feet in well 30S/30E-31, near the White Wolf fault about 20 miles northeast of the epicenter, to 0.012 foot in a well

near Twentynine Palms, about 180 miles southeast of the epicenter, in the Mojave Desert. The distribution of fluctuations indicates that water-level fluctuations are not wholly dependent upon distance from the epicenter, but are governed also by other factors.

Residual displacement of water level above or below the level before the earthquake appeared on many charts, especially on records from wells near the epicenter. Well 9N/2E-35D1, approximately 300 miles northwest of the epicenter, was the most distant well in which a residual change occurred. Most of the residual changes were on the order of a few hundredths to a few tenths of a foot; the three records that show residual changes greater than a foot are all subject to question. Charts on wells 9N/10W-12R1 and 4S/12W-28H10 had both slipped partly off the recorder and it was not possible to check the apparent displacement of water level when the recorder chart was changed. The decline of 10.52 feet recorded in well 14S/14E-28E2 actually represented a drop in water level. The casing, however, is perforated opposite zones of different head and the water level in the well normally represents a compromise between the higher head in the shallow and lower head in the deep zone. It is assumed that the earthquake caused enough shaking in the casing to open the well more to water from the deep zone, thereby causing the compromise water level to adjust downward. In the San Joaquin Valley most of the residual changes were upward, but in the Santa Clara River valley three of the



FIGURE 3. Hydrographs for five wells in the San Joaquin Valley, Los Angeles coastal plain, and the upper Santa Ana Valley, July 20-22, 1952.

* As used here, "amplitude" is used to mean the maximum range of fluctuation recorded by a well from highest to lowest—that is, to be equivalent to the term "double amplitude" as commonly used in seismology and physics.

four changes were downward. Throughout the rest of the state residual rises occurred about twice as often as declines, but there appears to be no significance to their distribution. La Roeque (1941, p. 379) attributed residual water-level rise to reduction of porosity caused by rearrangement of granular material of the aquifer and residual decline to release of stress upon the aquifer with some deformation of the ground-water basin.

Relation to Hydrologic Conditions and Physical Character of the Aquifers. Figures 2 and 3, which show typical water-level fluctuations in 11 wells during the period July 20-22, were replotted on a uniform scale from the original recorder charts. Well 30S/26E-27C1 is believed to tap an unconfined water body, wells 15S/16E-34E1 and 19S/18E-27M1 are known to tap a confined water body, and the other seven wells shown are believed to tap bodies of water which are under some degree of confinement. Six of the records are from paired wells—that is, wells located close together that tap different water bodies. The paired wells are 15S/16E-34E1 and 15S/16E-20R1, 19S/18E-27M1 and 19S/18E-27N1, and 30S/26E-27C1 and 30S/26E-34B1.

Water-level fluctuations in the wells penetrating unconfined aquifers are of small amplitude. For example, wells 30S/26E-27C1 and 30S/27E-5H1, 54 and 50 feet deep, respectively, which both tap unconsolidated sandy alluvium of the Kern River alluvial fan, showed an amplitude of only 0.35 and 0.20 foot, respectively, in spite of the fact that the wells are within 30 miles of the epicenter.

Consideration of the fluctuations in wells known to penetrate partially confined and completely confined water bodies suggests that the degree of confinement does not necessarily control the amplitude of water-level fluctuation. For example, at paired wells 15S/16E-34E1 and 15S/16E-20R1, which tap a confined aquifer and a partially confined aquifer, respectively, the fluctuation in the partially confined water body was considerably larger than that in the confined water body. Conversely, at paired wells 19S/18E-27N1 and 19S/18E-27M1, which tap the same partially confined and confined water bodies as wells 15S/16E-20R1 and -34E1, the fluctuation in the well tapping the confined water body was 10 times greater than that in the well tapping the partially confined water body. The fluctuation in well 13S/17E-10A, which is believed to tap partially confined water, was

considerably greater than the water-level change in either well 15S/16E-34E1 or well 19S/18E-27M1, both of which tap an aquifer confined beneath a thick laterally extensive clay bed which underlies most of the western San Joaquin Valley. Well 30S/30E-31, which registered an amplitude of 7.34 feet, is believed to penetrate only partially confined water bodies. Several wells in Kern County reported to penetrate partially confined aquifers showed water-level surges in excess of 5 feet, which was the limit of fluctuation the particular instruments could record.

The records presented from the Arvin-Tehachapi earthquake suggest that water-level fluctuations are more directly related to the compressibility and elasticity of the aquifers than to the degree of confinement of the aquifers or even to distance from the epicenter. The compressibility and elasticity of aquifers, in turn, appear to be related to the lithologic features of the materials. Studies by foundation engineers (Terzaghi and Peck, 1948, pp. 57-61) have shown that fine-grained materials such as clay and silt are far more compressible than sand. However, because the water level fluctuations in question represent an instantaneous response to stresses on the aquifer, it seems unlikely that thick clay or silt lenses within an aquifer would yield much water, because of their low permeability; hence they would have little effect on the water-level fluctuation. Jacob (1941, p. 577) indicates, however, that if a sufficient number of clay laminae are interbedded with sand in an aquifer, the release of stored water from the clay is virtually instantaneous and the quantity of water yielded is related to the modulus of compression of the clay and the thickness, configuration, and distribution of intercalated clay beds. The mineralogy of the constituent sands also may exert an important effect upon the compressibility of an aquifer. Terzaghi (and Peck, 1948, pp. 57-60) has demonstrated that a mica content in excess of 10 percent can raise the compressibility of a sand to that of a soft clay. Alluvial fill in California basins, especially that derived from granitic source areas such as the Sierra Nevada, the San Gabriel and San Bernardino Mountains, and the Peninsular Range, might be expected to have an appreciable mica content, on the order of 10 percent or more. Hence, it is likely that this factor may influence the compressibility of the aquifers tapped by many of the wells considered herein.

11. SEISMIC PROSPECTING FOR PETROLEUM AND NATURAL GAS IN THE GREAT VALLEY OF CALIFORNIA

By JOSHUA L. SOSKE

ABSTRACT

The refraction seismograph was introduced as a method of investigating geologic structure in the Great Valley of California early in 1926. After several years of exhaustive testing it was found to be inadequate to solve the problems of the San Joaquin Valley and was discarded in 1929 as a routine method of study. The reflection seismograph was introduced for the study of the buried structure in the Delano-Bakersfield area by the Geophysical Research Corporation in 1928 and became the generally accepted method for oil and gas prospecting in the areas of no rock outcrops. The success of the reflection method in making locations for the discovery tests of Buena Vista Lake and Chowchilla gas fields in 1934 stimulated experimental work resulting in improvements applicable to the problems of the Great Valley. The limited applicability of correlation methods of reflection study led to the development and wide use of the dip method of analysis and the construction of maps of phantom horizons to represent the buried geologic structure. As a result of continued improvements in seismic instruments and techniques, many areas were resurveyed from time to time. The success of the reflection seismograph in the Great Valley is indicated by the discovery of 34 oil and gas pools in which the method contributed essential technical information in advance of drilling. If new oil and gas pools are to be found in the future at the rate established during the last 20 years, new geological approaches and technical improvements in suitable geophysical methods seem necessary.

INTRODUCTION

The seismograph was introduced in California in its early stages of development to aid in the search for oil and gas. Only in the Gulf Coast area and Oklahoma was the method used earlier. No attempt will be made here to discuss the technical aspects of the method involving the theory of elasticity, wave propagation or computations, but an attempt will be made to present a rather broad picture of the principles of the seismic method and how it has been applied in the search for gas and petroleum.

Oil and gas pools exist in various geological settings. Several prerequisites are necessary: (1) Sources for the generation of petroleum or natural gas. These are usually recognized as dark-colored carbonaceous shale beds. (2) A reservoir rock with sufficient porosity and permeability to allow for the accumulation and withdrawal of the oil and gas in sufficient quantities to be commercial. This rock is usually sandstone, fractured shale, or porous limestone. (3) A suitable geological trap to facilitate the gathering and storing of the oil and gas underground in sufficient volume to justify commercial extraction. Types of these structural traps include closed anticlines, domes, faulted anticlines, noses, wedgeouts, and lithological traps.

The problem of whether source beds and reservoir rocks are present is principally one for the geologist. The prospecting geophysicist using seismic methods is interested in mapping the underground geological structure in hopes of finding favorable oil or gas traps. The oil operator is also interested to a lesser degree in learning about unfavorable areas, i.e., synclinal areas.

Where geological exposures of the formations reveal the structure of the area the services of the geophysicist are not required by the geologist. But in those cases where the exposures are hidden from the view of the field geologist, he often needs the services of the geo-

physicist to map the structures of the buried rocks. Much of the Great Valley of California presents this problem of geology covered by alluvial deposits. To solve the problem the geophysicist often uses the refraction method to study the characteristics of the overburden and the reflection shooting method to determine the structure of the buried sedimentary rocks. The seismic method is not one that locates oil or gas directly. It is a method that investigates the existing geological conditions to determine whether they are favorable or unfavorable for the possible commercial production of oil or gas.

Acknowledgments. The writer wishes to acknowledge his indebtedness to many friends who have reported first hand experiences with seismic prospecting in California. If the writer could recall all their names, the list would be too long to include here. It is a pleasure to acknowledge the assistance of a number of individuals who supplied material and valuable suggestions used by the writer in the preparation of this paper.

Mr. Henry Salvatori furnished information concerning the early seismic work, Mr. Milton C. Born supplied data regarding early work of the Geophysical Research Corporation in California, Dr. H. B. Peacock supplied reproductions of early seismograms recorded in the San Joaquin Valley, Dr. Frank E. Vaughan supplied photographs and descriptions of early refraction work in California, Messrs. W. D. Gould and Downs McCloskey reported on Frank Rieber's early refraction experiments and supplied photographs, Mr. Carl H. Savit supplied photographs of Western Geophysical Company's early equipment and E. Fred Davis collaborated by supplying factual information on early refraction shooting in California.

ARTIFICIAL EARTHQUAKES

Both the refraction and reflection methods of seismic prospecting make use of artificial earthquakes. Charges of dynamite are placed in holes in the ground and then detonated, causing the ground to be agitated by the quick and sharp impact of the blast. This initiates the elastic waves which are propagated through the subsoil in every direction.

The terms refraction and reflection have been borrowed from optics and are used to describe the path of elastic waves in much the same manner that these terms are used to explain the wave paths of light rays. Variations of the velocity of light in substances cause refraction and reflection and similarly such variations in seismic wave velocities cause similar events to take place along the paths of the elastic waves.

Seismic waves obey Snell's law, Fermat's and Huygen's principles. The basic law of refraction, usually referred to as Snell's law, is actually a consequence of Fermat's principle. This law states that the ray follows the fastest path in traveling from a given point to a second point in a medium. If the medium through which the ray passes provides a constant velocity, then the path is a straight line; if, however, the second point on the path is in a second medium providing a velocity

different from the first, then the path is not a straight line and the bending of the path takes place at the point or points where the velocity changes.

THE REFRACTION SEISMOGRAPH METHOD

In using the refraction method, the bending of the ray path makes possible the penetration of the earth's crust by the seismic wave at one point and its reappearance back at the surface at a second point where it may be observed with seismographic instruments. The refraction method is based on the condition that if we can measure the seismic velocities, that is, the speed of an impulse through the various layers of the subsoil, then we can graphically plot the ray path in space.

As a general rule when high explosives are detonated in the ground the forces released in the rock far exceed the strength of the rock-forming materials. This leads to a zone of complete failure which extends outward in all directions from the center of a well-confined blast. At greater and greater distances from this destructive center the effective force on the rock decreases. Inspection of the results of a blast reveals that at the origin the rock is violently ruptured and crushed but the evidence of this great physical force decreases rapidly as the distance from the explosive center is increased. In brittle rock we find a more or less spherical zone of shattered materials completely enclosing the central space of total destruction.

Examination beyond the severely shattered zone demonstrates that the degree of shattering decreases until finally there is a gradation into rocks that have not suffered any visible rupture or permanent set as a result of the blast. In this zone the strength of the rocks exceeded the applied effective forces, and the reaction of the rock to the quick and sharp compressional forces was in the form of elastic deformation or strain. Here the compressional pulse wave is initiated by the elastic response of the formations. The initially disturbing pulse wave is propagated outward from the zone as a spherical wave front. The oscillatory nature of the origin may in

part be accounted for by the release of strain energy, which was momentarily stored during the very short period of the initial deformation caused by the sudden application of the compressional forces and transferred to the zone of no failure. The nearly unrestrained relief of this deformation of the rock causes a rarefaction effect to follow the release of compressional deformation. This disturbance is likewise propagated as a pulse wave front following the first. The rarefaction may exceed equilibrium conditions and thus initiate a second but less vigorous compressional pulse at the origin. In this manner the particle oscillation at the shot point is rapidly reduced to an insignificant amplitude thus giving rise to a short train of damped wave pulses.

Wave Front Diagram. Figure 1 is called a wave front diagram and represents successive positions of the traveling pulse front plotted at equal time intervals (10 milliseconds) following the instant of the origin. It illustrates how the ray paths and wave fronts propagate from the center of the blast space to deeper and higher speed layers, thence along the surface contacts of these layers and back to the ground surface. As the ray paths are always normal to the wave fronts this scale drawing of a vertical section through the wave fronts shows how the ray taking the detoured path through the higher speed beds may arrive at a point at the surface simultaneously with the pulse which takes a more direct route at a lower velocity through the surface layer. This point where the rays arrive simultaneously marks the so-called "critical distance" (x_c) from the shot point. Beyond this point the first arriving rays are those that have been refracted and thus indicate the presence of the higher speed layers at depth.

Above the vertical section the travel-time curve has been plotted. This graph represents the data measured in the field. The reciprocal of the slope of this curve is the apparent velocity of the seismic wave along the ground surface. When the boundaries of the layers are horizontal the apparent surface velocity is equal in magnitude to the actual velocity of the deeper layer penetrated by the observed wave. When the apparent velocities deviate from the true seismic wave velocities of the various layers, the geophysicist is given a clue to the attitude of the layers. This is illustrated by the portion of the travel-time curve showing the most distant arrivals of the refracted waves from the inclined boundary of the third layer of the diagram.

In this manner of making measurements of the apparent surface velocities the prospector can often obtain the depth to the various layers, the true seismic velocity of the various layers and in many places he can determine the attitude of the layers. The determination of the seismic velocity of the buried media gives a clue as to the physical properties of the subsurface materials because the seismic velocity is a consequence of the physical characters of the rock, i.e., density, bulk modulus and rigidity. Water saturated gravels, various types of bed-rocks, rock salt, sedimentary and igneous formations may be located and identified by this method of studying seismic travel-time data.

Despite the tremendous success attained (40 salt domes were found by this method 1924-32) through the use of the refraction method and the large number of

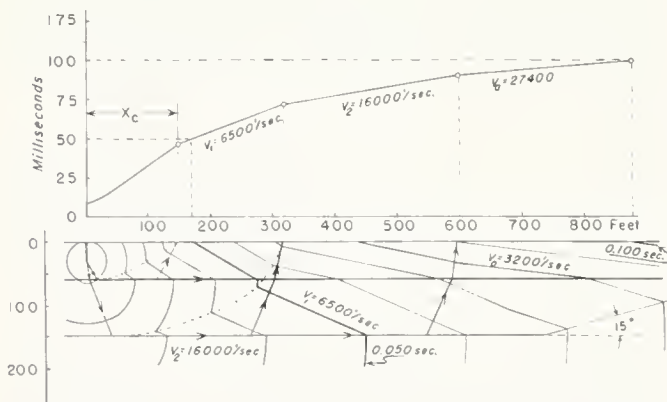


FIGURE 1. A refraction wave-front diagram sketched for a three-layer problem showing the effect of a change in slope of the buried surface of the third layer. The magnitudes of the seismic velocities were chosen to approximate those experienced where the uppermost layer consists of dry alluvial gravels, sands and clays, the intermediate layer the same as the uppermost except saturated with water, and the third and deepest layer of crystalline bed rock.

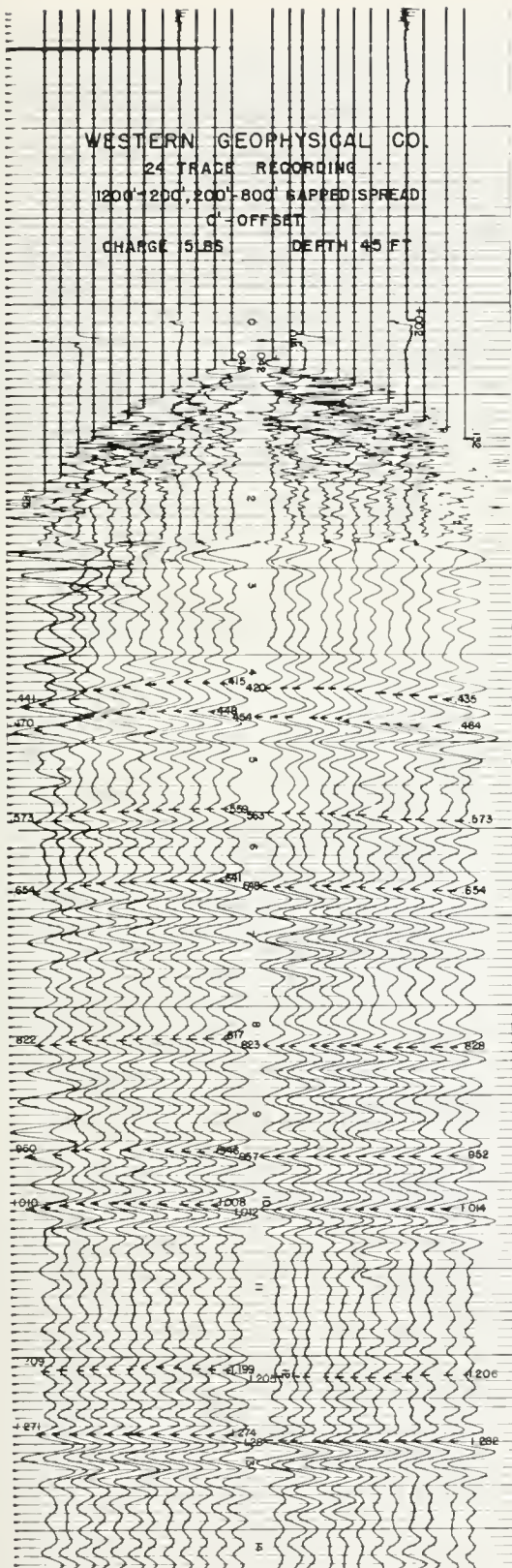


FIGURE 2. A 24-trace seismogram recorded in the San Joaquin Valley illustrating the arrivals of direct, refracted, and reflected pulses. Split spread spacing 1200 feet, 400-foot gap, 800 feet, no offset. *Courtesy Western Geophysical Company.*

prospects surveyed, such as dam sites, bedrock, and salt dome, only a few seismograms and travel-time curves have been published. Now that the refraction method has been largely superseded by the extensive employment of the reflection seismograph there is little hope that many of these will ever be published.

THE REFLECTION SEISMOGRAPH

In general, reflection seismograph prospecting requires much more elaborate instrumental apparatus and more field equipment, such as power driven shot hole drills and water trucks, than refraction prospecting. This wide difference in equipment stems from the fact that the two methods are concerned with the observations of pulses of very unlike characteristics. In reflection shooting we employ an echo method and, therefore, we are especially concerned with the recording of late arriving events on the seismogram. The time required for the round trip of the wave from the shot point down to the reflecting horizon and back to the surface is in general much greater than the time necessary for the direct or refracted wave to travel only one way from the shot point to the recording seismometer. The arrivals of the direct and refracted waves are usually the first events recorded on the seismogram. In refraction work nearly all the interpretation may be based on these first impulses recorded, often referred to as the "first breaks." In refraction studies only one seismometer may be used and the refracted pulses may be readily identified on a single trace seismogram. On the other hand, reflected pulses recorded on a single trace seismogram would be indeed difficult to identify. Several single trace seismograms involving different distances from the shot point to the recording seismometers would be necessary to identify a certain reflected pulse. One good reason for the use of multitrace seismograms in reflection seismograph work is that the later pulses recorded on the seismogram after the first breaks may be either direct, diffracted, refracted or reflected pulses. In general practice the reflections are identified on the seismogram by the distinct pattern in which the reflected pulses appear on a multitrace seismogram. The pattern is frequently referred to as the "line up." Early reflection equipment employed only four or six recording traces while current reflection seismographs employ 24 to 48 traces. Each trace represents a separate channel of recording consisting of three units, one or more seismometers, an amplifier and a recording galvanometer.

The patterns of the reflected pulses on the multitrace seismogram are distinctive because all of the reflected pulses, from a nearly horizontal reflecting interface, arrive at the ground surface almost simultaneously and in like phase, thus similarly activating all the seismometers almost at the same instant. Figure 2 is a reproduced reflection seismogram showing first break data and marked reflections. The fairly good line-ups of recorded pulses of similar characters are recognized by (a) similar wave form, (b) similar wave length, (c) similar groups of wavelets, (d) similar amplitudes. These criteria have been used to identify the reflections as marked on the reproduced seismogram of figure 2. The reflected wave fronts which arrive at the seismometers are usually much more nearly horizontal than are those representing refracted waves.

There are many specifications which must be met in the design of reflection recording equipment. Some of the more important of these are (a) great timing accuracy (one part in ten thousand), (b) high damping throughout the recording system, (c) suitable ranges of frequency responses (filter circuits), (d) an adequate method of automatic volume control, (e) high sensitivity, and (g) multiple seismometer arrangements. Only great timing accuracy and high sensitivity are critical specifications for refraction equipment.

The field procedure for the two methods is similar in that both require that the explosive charges be placed in that portion of the ground that is characterized by efficient elastic transmission characteristics. One exception to this statement is the procedure making use of explosions in the air for recording of reflections. When shooting in the ground the charges should be well-confined so as to avoid the transfer of the blast energy to the atmosphere. Water is usually used as the stemming material. Explosive charges range from half a pound to 5 pounds in routine reflection shooting; however, slightly larger charges are sometimes used. The charges are always detonated by electric type blasting caps.

Briefly, the function of seismic equipment is to amplify and make permanent recordings of the feeble displacements of the ground and to eliminate or decrease the influence of undesired impulses, i.e., wind, rain and other background noises, as much as possible. In practice it has been found that apparatus which is capable of a maximum magnification of about ten million (about ten millimeters displacement of the trace on the seismogram corresponding to one milli-micron displacement of the ground) is satisfactory.

In seismic work only two items are measured, time and distance. The disposition of the configuration of the seismometers is measured in feet and the elapse of time between successive events is measured in seconds. The distances are a matter of plane surveying in the field and the elapse of time is taken from the seismogram. If the round trip time for a certain reflection is obtained from the seismogram, then the distance traveled by the wave during this time is obtained as the product of the average velocity and the observed time. This gives the round trip distance. The depth is approximately half this distance. In precise work needed for detailed geological structure, adjustments are frequently made for the curved paths of the rays due to refraction and variations in seismic velocity. For example, if reflections traveling through the Tertiary sediments of the Great Valley of California, where the dip of the bedding planes is approximately horizontal, gave observed reflection times of 0.500, 1.000, 2.000, 3.000 and 4.000 seconds, then the reflections arise respectively from interfaces 1,530, 3,350, 8,020, 14,250 and 21,700 feet below the surface of the ground.

The reflection method is ideally suited to mapping of the attitudes of deeply buried sedimentary rocks. The effect of a dip as small as 50 feet per mile can be detected under favorable conditions. The various layers of shale, sandstone and limestone give good reflections as a general rule over most of the floor of the Great Valley of California. Some difficulties have been encountered in areas where the seismic wave transmitting qualities of the overburden are either too good or too poor. A portion

of the southernmost area of the San Joaquin Valley is a place in which the rather thick overburden is a poor transmitter of seismic waves and it is difficult to obtain good reflections consistently in this area. A few small areas in the Great Valley have overburden that is too good in its transmitting quality for the recording of good reflections. These handicaps are now being overcome in some degree by various patterns for the positions of seismometers, multiple seismometer arrangements, multiple shot holes, air shooting and new instrument designs.

THE NEW ERA IN PETROLEUM PROSPECTING

The First Oil Pool Found by Geophysical Methods.

A new era in petroleum prospecting was ushered in when geophysical methods were credited with the discovery of the Nash Salt Dome, Fort Bend County, Texas in 1924 by the Rycaide Oil Company. Actual oil production on the flank of the dome was not attained until 2 years later but the presence of the salt dome was confirmed by the very first test well. Long Point Salt Dome was also discovered the same year by the Gulf Oil Company making 1924 an important date in the history of geophysical prospecting for petroleum. These first successful investigations involved gravity studies and definitely demonstrated that conditions favorable for the subsurface occurrence of crude oil could be located deep within the earth's crust by means of instruments at the surface of the ground. The attention of the early oil prospectors immediately turned to reviewing the available knowledge on all natural phenomena that might lead to new geophysical methods.

There can be little doubt that this review led to a thorough examination of fundamentals and principles that had been applied by seismologists in their studies of earthquakes and large accidental explosions. These early studies indicated that information on the surface formations could be obtained by measuring the velocities, frequencies and energies of the seismic waves propagated through the earth's crust. The application of the principles used and the information gained by the earthquake seismologist led to the development of the seismic method of geophysical prospecting.

Acceptance of the Refraction Method. In 1924 the refraction seismographic method of prospecting was accepted as one of the important tools of the exploration geologist, a result of the discovery of the Orchard Salt Dome in Fort Bend County, Texas. The results obtained were possible because of the relatively uniformly low seismic velocity of the near surface rocks which was easily distinguished from the higher velocities of the salt or associated cap rock of the salt domes. This led to a rapid succession of oil pool discoveries in this type of geologic structure. During the following 8 years the refraction seismograph enjoyed a high place among the tools used by the oil prospectors in Texas and Louisiana. In this period the refraction method was credited with the finding of 40 salt domes.

Refraction Method Introduced in California. Only 2 years after the seismograph had been applied to geological problems in the Gulf Coast area it was tested in California. Mr. W. D. Gould of the Tide Water Associated Oil Company reports that he was a member of a refraction seismograph crew which began field tests west



FIGURE 3. Frank Rieber recording truck and crew operating in the San Joaquin Valley during 1926. Photo supplied by Downs McClosky.

of the Lost Hills oil field in June 1926. The experimental work was performed by Frank Rieber and jointly supported by the Standard Oil Company of California, the Associated Oil Company, and the General Petroleum Corporation.

The equipment used by the Rieber organization employed a new idea in seismometers in using the piezoelectric property of a quartz crystal. In use the crystal was loaded with a relatively large inertia reactor in such a way that the vertical motion of the earth imparted an acceleration of the inert mass which exerted varying pressures on the confined crystal. This pressure variation on the crystal caused electrical potential differences between opposite faces of the crystal. These potential differences were amplified by means of an electronic amplifier and then applied to a galvanometer, whose reaction was recorded on a moving strip of photographic film resulting in the seismogram.

Advantages claimed for this new seismometer were (a) that the seismometer contained no moving parts such as masses supported by springs, (b) that the generated voltages are proportional to the acceleration of the ground, whereas the outputs of most other seismometers were proportional to the velocity of the ground motion. The fragility of the crystals and the very low sensitivity of the Rieber refraction seismometer may have contributed to the general failure of these early tests. Relatively large charges of explosives were used. Gould describes one of the experimental tests as follows: "The single seismometer was placed at a distance of 1 mile from the shot point, which consisted of 30 holes 4 inches in diameter, drilled by hand into the earth to a depth of approximately 6 feet. A total charge of 1,500 half-pound sticks of 80 percent strength gelatin was distributed among the holes so as to fill them about half full with dynamite. All the holes were detonated simultaneously with the use of 'Cordeau' fuse. This resulted in a terrific explosion, a tremendous dust cloud and sometimes a seismogram."

Rieber's refraction crew made further tests in the vicinity of the present Coalinga Nose oil field during the early part of 1927. It is reported that this work demonstrated that the water table at a depth of about

300 feet could be successfully mapped as a high-speed marker layer. It seems that no hint of the presence of the Coalinga Nose Pool was obtained by this work. Figure 3 is a photograph of Rieber's seismogram recording truck and some of the crew.

In 1930, Frank Rieber published a report on some of his early experiments with the refraction method in which he pointed out the effects of the unconsolidated nature of the near surface formations on the refraction travel-time curves and recognized the increase of seismic velocity with increased depth of the sedimentary formations of California. In the opinion of the writer the results of Rieber's work would have been much more important had there been any possibility of finding salt domes in California.



FIGURE 4. Shell Oil Company refraction seismograph recording crews operating in the San Joaquin Valley in 1928. Photo supplied by Frank E. Vaughan.

Shell Oil Company Tests Refraction Methods. Following Rieber's experiments probably the next attempt to test the refraction method as a tool to assist in the study of buried geologic structure of the San Joaquin Valley was made by the Shell Oil Company. Shell began these tests in 1927, continued the work through 1928 and 1929. Dr. Frank E. Vaughan provided the general historical sketch of these early operations in California. Schweydar mechanical two-component seismographs were employed in these tests. Two complete seismometer mechanisms were built into a single instrument. In general the two systems consisted of two inertia masses mounted on leaf type springs in such a manner as to respond to vertical and horizontal components of the earth movements. The movement of each mass relative to the frame of the seismometer was first magnified by a long, light, stiff lever attached to the inertia mass. At the end of each lever a bow was attached which usually carried a human hair as a bow string wound around a slender spindle to which a small plane mirror was attached. Any slight movement of the bow caused a corresponding rotation of the mirror which reflected a beam of light that fell on a cylindrical lens at a distance of 1 meter. The beam of light was brought to a focus by the lens on a moving strip of photographic paper. The photographic paper was contained in a sep-



FIGURE 5. Adjusting mechanical seismograph, Shell Oil Company, 1928. Photo supplied by Frank E. Vaughan.

arate instrument called the camera which was driven by a clockwork type of mechanism. It is reported that only the registration of the vertical ground motion was of any actual value. The frequency of these instruments was about 15 cycles per second; the magnification of the ground motion, apart from any possible slipping between the bowstring and the spindle, has been estimated to range between 14,000 and 40,000. Little or no damping of the seismometer mechanism was provided in this work because a record of the first arrivals of the waves only were desired. Charges of explosives used in these studies ranged from 300 to 600 pounds of 60 percent nitro-gelatin powder; however, a few charges as large as 1200 pounds were used. Experiments with 10 percent ammonia powders are reported to have given good results in the absence of water.



FIGURE 6. Seismologist contacting shooter by radio, Shell Oil Company, 1928. Photo supplied by Frank E. Vaughan.

In spite of the general opinion that the results of the early refraction tests were conjectural, there is some evidence that the results of the Shell Oil Company work were useful to the petroleum prospector of that period. This work aided the Shell Company in the following ways: (1) The Shell Oil Company was apparently able to increase their knowledge of the general structure of the San Joaquin Valley by more mapping the basement complex along the eastern area as far out into the valley as Hanford. (2) Their refraction work afforded additional proof that the gravity anomalies detected by early torsion balance surveys along the eastern portion of the San Joaquin Valley were probably due to variations in density of the buried complex rocks, rather than to deformation of the basement surface or the overlying sediments. This idea was suggested by an earlier study of the comparison of magnetometer and torsion balance surveys. (3) There seems to be little question that this work supplied the Shell Oil Company with some information on local geologic structure in the southeastern portion of the valley. Moreover, if this rather expensive and hazardous procedure had not given some usable information the tests would not have been continued



FIGURE 7. Mushroom shaped refraction blast, San Joaquin Valley, Shell Oil Company, 1928. Photo supplied by Frank E. Vaughan.

for almost 2 years. In general it probably indicated displacements of faults in the shallow basement complex and may have suggested the structure in the overlying sediments as a consequence of the faulting.

Very little refraction work has been done in California since 1929 except for a few very special types of surveys. During 1937 and 1938 the Geophysical Engineering Corporation mapped the basement complex surface in the vicinity of Arvin, California using the refraction method. The problem of seismic wave penetration to the basement rocks was solved by the innovation of placing the shot point directly in the outcrop of the high-speed basement rocks. The seismometer spreads were placed along radial lines containing the shot point as a means of observing the travel-times for the wave to pass along the basement interface and up through the overlying sedimentary formations to the surface. Differences in observed travel-times were attributed to

either different horizontal distances from the shot point or different thicknesses of the sediments. When the horizontal distances were equal between the shot point and different recording stations then the differences in the travel-times were attributed to variations in the depth to the basement complex. This involves the reasonable assumption that the velocity of the seismic wave is nearly constant in the basement rocks over the distances recorded, which in this case varied from a few thousand feet to 8 and 10 miles from the shot point. In this manner it was a relatively easy matter to make a map of the surface of the basement rocks at depths in excess of 1 mile. The general purpose of the survey was to locate possible buried scarps, ridges and valleys in the basement rock surface of the area.

No discussion of early seismic work in California can ignore the activities of the Geophysical Research Corporation, a subsidiary of Amerada Petroleum Corporation. Mr. M. C. Born, Geophysical Supervisor for the Amerada Petroleum Corporation in California reports the following early activities of his company. Dr. H. B. Peacock was in charge of a Geophysical Research Corporation crew which operated in California during 1928



FIGURE 8. Dry rotary shot hole drill, Shell Oil Company, 1928. Photo supplied by Frank E. Vaughan.

and 1929 for a period of 21 months. This crew was operated jointly for the Amerada and the General Petroleum Corporations. The work was done in the Bakersfield-Delano area. Initial work comprised a refraction shooting program using three recording trucks, each equipped with a single channel recording system with radio code communication and a blast-phone detector for the purpose of measuring distance by using the velocity of the sound of the blast through the air. A dry rotary drill, similar to that used for present day telephone hole placements, drilled the shot holes to depths of about 15 feet. Charges up to 500 pounds of explosives were detonated. Analysis of these early records disclosed the basement complex reflection which in some places could be correlated over considerable distances. With this encouragement, a four-channel recording system was installed in a truck and one crew operated as a reflection crew.



FIGURE 9. Large refraction blast near a San Joaquin Valley orchard, Shell Oil Company, 1928. Photo supplied by Frank E. Vaughan.

First Seismic Reflections Observed in California by the Geophysical Research Corporation in 1928. There seems to be no doubt about the fact that the reflections recorded in 1928 were the first to be observed in California. Figure 13 is a photograph of one of GRC's early refraction units which operated in California. Figure 14 is a photographic reproduction of two California seismograms recorded by GRC in 1928 illustrating refraction pulse arrivals, reflections, ground roll, and blast-phone breaks. The last was used to compute the distance between the shot point and the receptor.

The Geophysical Research Corporation terminated their seismic work in California in 1929 but returned



FIGURE 10. Recording car and tent enclosing seismograph, Shell Oil Company, 1928. Photo supplied by Frank E. Vaughan.



FIGURE 11. Large refraction shot, San Joaquin Valley, Shell Oil Company, 1929. Photo supplied by Frank E. Vaughan.

early in 1932 with improved equipment. The first unit was soon joined by several others in the same year and this group began the routine seismic work which has been continued by the Amerada Oil Corporation in California up to the present time.

In 1925, the Seismos Company had four refraction crews operating in the Gulf Coast area, and was doing practically all of the commercial seismic work in the United States. The Seismos crews employed mechanical seismographs which were relatively low in sensitivity and efficiency. That same year, the Geophysical Research Corporation was organized, in the hope of improving seismograph technique and thereby widening the use of the instrument. GRC's first achievement was to introduce an effective electrical seismograph with a much improved sensitivity and to employ radio communications between the recording and shot point stations. The first GRC Refraction Crew was placed in the field under the direction of Dr. E. E. Rosaire in the Spring of 1926. At this

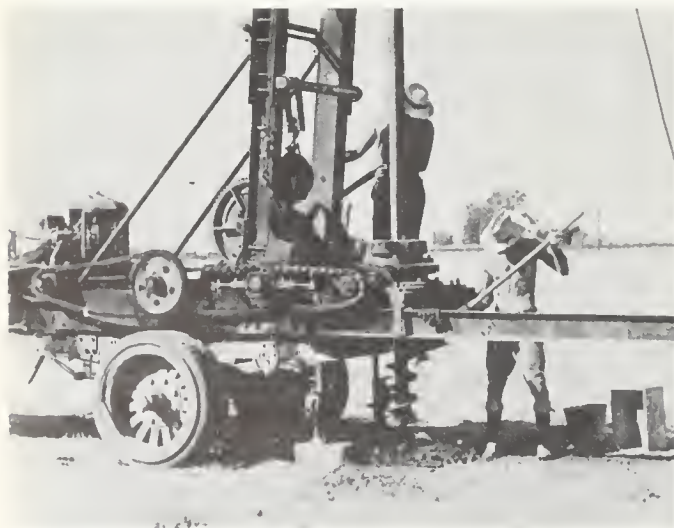


FIGURE 12. Dry rotary shot hole drill showing details of machine, Shell Oil Company, 1928. Photo supplied by Frank E. Vaughan.

early date the seismograph as a tool for exploration was in its infancy and the radio art had not progressed very far. The vacuum tubes of this period were not very efficient and it was not an easy problem to build a portable and stable audio type amplifier. By the end of 1926 GRC had five or six refraction crews working in the Gulf Coast area and one experimental crew testing the possibility of recording reflections. Messrs. J. E. Duncan and Henry Salvatori worked together on this GRC research project during December 1926 and by March 1927 they had succeeded in recording and identifying their first seismic reflections. This seems to have been the very beginning of the technique of using the reflection method. During the summer of 1927, GRC, in addition to maintaining their large number of refraction crews, increased the number of seismic reflection crews to four, and systematically prospected the Seminole Plateau of Oklahoma. It seems that the reflection method was not used commercially by any company other than GRC until 1929. The status of the now extensively used reflection shooting method is indicated by the remark of Donald Barton in his report before meeting of the Amer-



FIGURE 13. Early reflection and refraction recording equipment used by Geophysical Research Corporation near Bakersfield, California, 1928. Photo supplied by H. B. Peacock.

ican Association of Petroleum Geologists in 1929. He stated, "the reflection shooting being tested by the Geophysical Research Corporation has not been completely accepted as an acceptable method, though GRC seems to have confidence in it!"

With this experience, it is not surprising to find that GRC tested the reflection seismograph in California as early as 1928. However, it was not until the years 1931 and 1932 that the reflection method was persistently tried in California by other operators. The first year of this work was somewhat disappointing. The areas chosen for these initial tests were, on reworking with modern equipment, found to be rather unfavorable lands for the application of the reflection seismograph. Nevertheless the tests gave some slight encouragement for further testing of the method.

This minor encouragement was not considered sufficient to justify the supporting reflection seismograph crew by a single oil company. Consequently the opera-

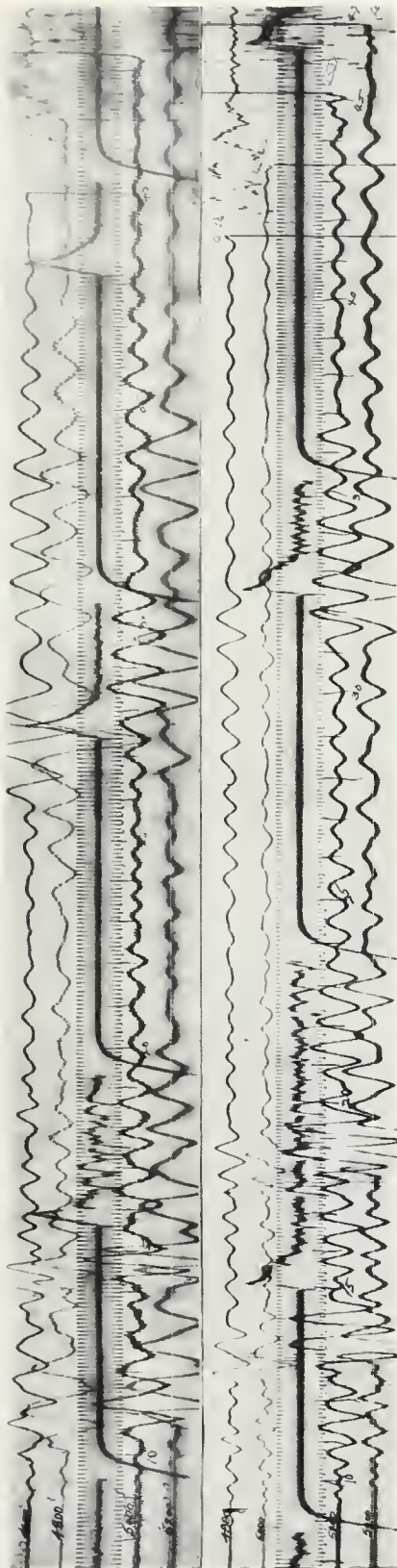


FIGURE 14. Reproduction of early seismograms recorded by Geophysical Research Corporation, 1928, near Delano, California. Shows timing trace, arrivals of refractions, reflection, ground roll, and air sound wave. Photostat supplied by M. C. Born.

tion of a Western Geophysical Company seismograph crew was supported jointly by several oil interests on a more or less experimental basis. The area chosen for this joint seismic study was in the vicinity of Merced, California, where the ground conditions were found to be more favorable to the problem of obtaining reflection seismograms. Almost from the very beginning of this joint operation, good reflections were obtained. At an early stage of the work the efforts of the pioneer reflection seismologists were rewarded with two and as many as four good reflections on a large percentage of the seismograms. It is reported that at least one of these reflections could be correlated over much of the area.

The seismographic results indicated a geologic structure about 16 miles south of the city of Merced. Pure Oil Company tested it with a well completed in November 1934 as the discovery well of the Chowehilla gas field. The principal interest in this discovery is probably an academic one: that is, it marks one of the very early natural gas discoveries as a result of systematic reflection seismograph work in California. As a natural gas producer the Chowehilla gas field has not been very important because of the low heating value of its gas.

There is some evidence that the first natural gas field discovered in California by the aid of the reflection seismograph was the Buena Vista gas field brought in by the Ohio Oil Company on July 11, 1934. It was completed four months in advance of the Chowehilla gas field discovery.

Amerada's discovery of the Tracy gas field in 1935 may be considered the second discovery of a commercial gas field in California found by the use of the reflection seismograph. This field is of importance because it was the first commercial gas field discovery to indicate that the northern portion of the Great Valley of California contained natural gas accumulations in significant quantities to interest the prospector. The geologic structure of this field is that of an elongated dome covering an area of about 600 acres. No hint of this field is discernible from the surface and no subsurface information from wells drilled in the area was available prior to the discovery. It is therefore concluded that this discovery was the direct result of reflection seismograph work.



FIGURE 15. Early multitrace reflection seismograph recording truck used in the San Joaquin Valley, 1933. Courtesy Western Geophysical Company.

The very first success in using the reflection seismograph to find an oil field in California was that of the Shell Oil Company (Waterman, 1948). They completed the first well in the Ten Section field for nearly 1,000 barrels of high gravity oil on June 2, 1936. This company conducted their reflection seismograph survey of the area during 1934-35 under the very competent direction of Dr. W. Hafner. As a result of the reflection shooting and a careful interpretation of the data, the location for the test well was made practically on the apex of the geologic structure. This was indeed an outstanding accomplishment when one considers that it was done in a period when the reflection seismograph was still in its infancy and that the closure of the structure was only about 200 feet. No surface indication of the structure exists. This discovery also established that it was commercially attractive to prospect the deeper zones for possible oil production in the floor of the San Joaquin Valley. It also marked the discovery of the productive Stevens sand zone of upper Miocene age and indicated that this sand might extend into adjacent areas. Following this discovery, all of the subsequent seismic work in the nearby areas was directed toward the making of contour maps of this geologic horizon.

Only 16 days after the completion of the first Ten Section well, The Amerada Petroleum Corporation discovered the Rio Vista gas field, which today is California's largest. This marked the second gas discovery for Amerada Petroleum Corporation and the sixth success for the reflection seismograph in the Great Valley of California. Shortly after the flow of the Rio Vista gas field discovery well was established at 81 million cubic feet of natural gas per day through a $\frac{3}{4}$ -inch orifice, the oil operators began a fervid exploration program in the Sacramento River valley.

The Shell Oil Company's success in Ten Section area was soon followed by a similar success by the Standard Oil Company of California when they completed the first well in the Greeley oil field on December 22, 1936 for more than 2000 barrels of crude oil per day. This discovery also was the direct result of reflection seismograph studies which the Standard Oil Company had made in the years 1935-36. The Stevens sand zone was found productive at Greeley thus enhancing the importance of the discovery of this zone at Ten Section oil field. The general structure of the Greeley oil field is that of an elongated anticline, about 1 mile in width and 4 miles in length. It was the first field found on the northwest-trending Wasco-Rio Bravo-Greeley trend. The discoveries of Ten Section and Greeley oil fields on the floor of the San Joaquin River valley stimulated use of the reflection method in many other parts of the area. Many of the reflection surveys made prior to Standard's discovery of the Greeley structure had been conducted in reconnaissance fashion. All possible structural reversals of these surveys were immediately re-examined and re-evaluated in the light of these first two oil discoveries. Many completely new detailed surveys were made, as well as the many older, widely spaced surveys reshot.

At the time the discovery well at Greeley was being drilled the Union Oil Company was studying the Rio Bravo area with the aid of a Western Geophysical reflection seismograph crew. The historical record indicates

that the Union Oil Company had considered this particular area favorable as early as 1925 when they drilled a deep test well on a slight topographic high located just west of the present Rio Bravo oil field. The discovery well was drilled to the equivalent of the Stevens sand zone established as an oil producer at Ten Section and Greeley oil pools. The zone was somewhat disappointing to the Union Oil Company in the test well because it was represented by a hard and dark brown shale containing a very thin unproductive silty oil sand lens at a depth of about 8,500 feet. However, the thin oil saturated sand was interpreted as confirmation that the test well was on a closed geologic structure as indicated by the reflection seismograph survey. With this in mind the Union Oil Company decided to drill ahead in search of a more favorable oil sand. They completed the Rio Bravo discovery well, flowing at the rate of 2400 barrels of oil per day, on November 3, 1937 at a depth of 11,300 feet. The producing zone consisted of two sands. The upper one was regarded as a new sand discovery while some geologists thought that the lower one was the geological equivalent of the Vedder sand, the main producing zone along the east side of the San Joaquin Valley. The upper sand was appropriately called the Rio Bravo sand. All geologists agreed that the sands were of lower Miocene age. This new well was at that time the deepest producing well in the world. The success of the well increased the demand for reflection seismograph surveys of still deeper geological structures. The new, deeper studies involved the identification and study of reflected waves that returned to the ground surface as late as 2.5 to 3.0 seconds after the blast in the shot hole. Up to this time reflections for these extreme depths had not been considered very important and little or no systematic effort had been made to obtain them. They are less distinct than earlier ones; the periods of the pulses are much longer and the amplitudes are less than those recorded earlier, resulting in broader and less sharp pulse recordings. These less well-defined reflected pulses do not permit extremely accurate determination of the reflection move out times, which are essential for the computation of the dip of the reflecting interfaces. However, with more effort being expended to obtain the deeper reflections, improvements were made that led to the re-shooting of some areas.

Very soon after the discovery of the production from the Rio Bravo and Vedder sands at Rio Bravo, the Standard Oil Company of California promptly tested for these sands at the Greeley oil field. The test well was completed in the Vedder sand for an established flow of 14,000 barrels of oil per day marking a considerable improvement over the original production found in the Stevens sand.

With the discovery of the Rio Bravo oil field and a second producing zone at the Greeley oil field, a new structural trend in the floor of the San Joaquin Valley was found and interested oil operators energetically focused their attention on it and on the possibility of finding other such trends. The conditions found at Greeley and Rio Bravo indicated that this structural trend was plunging northwest.

The next discovery well on the Greeley-Rio Bravo trend was drilled by the Continental Oil Company. The well penetrated an oil bearing cherty shale bed of upper

Miocene age—probably the equivalent of the upper portion of the Stevens sand—at a depth of 9,540 feet. The well was apparently completed under adverse mechanical conditions. Initial production was 35 barrels of crude oil per day. The Continental Oil Company, encouraged by this experience, promptly drilled another test well completed in 35 feet of oil sand encountered at a drill depth of 13,095 feet for a demonstrated flow of 3,385 barrels of oil per day on April 11, 1938. Before completion, this well was drilled to a total depth of 15,004 feet where it encountered Eocene formations (Erickson, 1948). It established new world records for deep drilling and deep production.

Subsequent wells drilled in the field indicated that the Wasco structure is an elongated dome of very low relief with approximately 60 feet of closure over a rather small area. In addition to having the deepest commercial production, the field also is an outstanding achievement in the application of the reflection seismograph, as it was located on a structure of low relief and small area at very great depth. The 35 feet of producing sand at Wasco was not the equivalent of either the Rio Bravo or the Vedder sands at the Rio Bravo oil field, but instead represented a geological zone slightly higher than the Rio Bravo sand.

The accomplishment of the Geophysical Department of the Continental Oil Company in delineating the Wasco oil field structure has frequently been referred to as a demonstration that the reflection method was the most important step in oil and gas exploration. It has given the oil prospector a means of securing information on buried geologic structure almost as definite as though human eyes had been given the power to look into the earth. For some time after the Wasco oil field discovery, no oil pool seemed to be too small or too deep for the reflection seismograph to find it. We now know this is not an exact statement because a combination of conditions may naturally exist which could make even larger structures if not impossible, improbable to detect with the reflection seismograph as the only source of information.

The history of the brilliant successes of the reflection seismograph in the San Joaquin and Sacramento Valleys, as it continued to unfold, is indicated by the accompanying list of oil and gas discoveries given in a chronological order. A complete story would require the interweaving of personal biographies of geologists and geophysicists and the stories of the seismograph scouts, who reported to their companies the operations of competitors. One could not exclude a treatment of the scout's trade secret as to how he knows where to catch the shooting crew in action. There is that often repeated story how the party chief had planned secretly to shoot a particularly important and confidential location on a Sunday at 4 A.M. only to find the seismograph scout of a competitor company waiting for them when the crew reached the spot at daybreak. This amiable fellow though always an uninvited guest was not completely unwelcome. He often furnished information about other crews in the area and frequently would break the startling news to the unofficial host crew as to where their next job would be and about how soon they would be moving to it.

Some important oil and gas fields of the Great Valley of California found with the aid of the reflection seismograph.

1.	Buena Vista Lake gas field	Ohio Oil Company	July 1934
2.	Chowchilla gas field	Pure Oil Company	November 1934
3.	Tracy gas field	Amerada Petroleum Corporation	August 1935
4.	McDonald Island gas field	Standard Oil Company of California	June 1936
5.	Ten Section oil field	Shell Oil Company	June 1936
6.	Rio Vista gas field	Amerada Petroleum Corporation	June 1936
7.	Greeley oil field	Standard Oil Company of California	December 1936
8.	Rio Bravo oil field	Union Oil Company	November 1937
9.	Fairfield Knolls gas fields	Standard Oil Company of California	November 1937
10.	Canal oil field	Ohio Oil Company	November 1937
11.	Willows gas field	Ohio Oil Company	January 1938
12.	Wasco oil field	Continental Oil Company	April 1938
13.	North Coles Levee oil field	Richfield Oil Corporation	November 1938
14.	Strand oil field	Tide Water Associated Oil Company	June 1939
15.	Paloma oil field	Western Gulf Oil Company	August 1939
16.	Veroalis gas field	Standard Oil Company of California	January 1941
17.	Raisin City oil field	Shell Oil Company	June 1941
18.	Helm oil field	Amerada Petroleum Corporation	October 1941
19.	Riverside oil field	Amerada Petroleum Corporation	December 1941
20.	Gill Ranch gas field	Texas Company	April 1943
21.	Lodi gas field	Amerada Petroleum Corporation	April 1943
22.	Thornton gas field	Amerada Petroleum Corporation	July 1943
23.	Ord Ben gas field	Superior Oil Company	September 1943
24.	Moffett gas field	Texas Company	September 1943
25.	McClung oil field	Continental Oil Company	September 1943
26.	Colusa gas field	General Petroleum Corporation	December 1943
27.	Chico gas field	Richfield Oil Corporation	January 1944
28.	Afton gas field	Richfield Oil Corporation	February 1944
29.	Millar (Dixon) gas field	Amerada Petroleum Corporation	August 1944
30.	Corning gas field	Superior Oil Company	September 1944
31.	San Joaquin oil field	Superior Oil Company	March 1947
32.	Cuyama oil field	Richfield Oil Corporation	May 1949
33.	Harvester gas field	Shell Oil Company	February 1950
34.	Wild Goose gas field	Humble Oil & Refining Company	August 1951

A study of this impressive list indicates that the rate of seismic oil and gas discoveries has varied considerably from time to time in the Great Valley of California. It is presumed that this rate depends on the ease with which the undiscovered pools are recognized by seismic means before drilling. As more and more fields are found, it becomes harder to find new pools. The time may come when no simple anticlinal type of structure remains to be discovered in the Great Valley. If discoveries are to continue the geologist and the geophysicist will find it necessary to look for new types of oil traps such as fault and lithological closures. Success along these lines may require marked improvements in geophysical prospecting techniques and probably some new ideas about the existing geology. Certainly, continued success in finding oil and gas in the Great Valley of California will make necessary close cooperation between the geologist and the geophysicist. The seismograph may be used to work out suspected extensions of known fields, the solutions of faulted structures and other associated problems but it seems the days of the older reconnaissance-type reflection seismograph surveys are rapidly coming to an end. It may be necessary

to develop and employ more sensitive methods in order to continue to find new oil pools in the Great Valley of California.

REFERENCES

Any more or less complete bibliography on seismic methods would be much too long to be given here. Publications on seismic prospecting have increased in number rapidly since 1929. A short list of the more recent publications is: (1) *Geophysical explora-*

tion, by C. A. Heiland, Publisher, Prentice-Hall, Inc.; (2) *Geophysical prospecting for oil*, by L. L. Nettleton, Publisher, McGraw-Hill Book Company, Inc.; (3) *Exploration geophysics*, by J. J. Jakosky, published by Trija Publishing Company; (4) *Practical seismology and seismic prospecting*, by L. D. Leet, Publisher, Appleton Century-Crofts, Inc.; (5) *Introduction to geophysical prospecting*, by M. B. Dobrin, Publisher, McGraw-Hill Book Company, Inc.; (6) *Seismic prospecting for oil*, by C. Hewitt Dix, Publisher, Harper & Brothers; (7) *Geophysical case histories*, vol. I, 1948, Society of Exploration Geophysicists.

12. APPLICATION OF SEISMIC METHODS TO PETROLEUM EXPLORATION IN THE SAN JOAQUIN VALLEY

BY MAURICE SKLAR

ABSTRACT

Seismic prospecting and earthquake seismology are both based on the laws of propagation of seismic waves in the earth. The first part of this paper ties in the two sciences, and discusses examples of earthquakes recorded by seismic parties exploring for petroleum. Three seismograms, recorded by a party working within a few miles of the White Wolf fault, in July, 1952, clearly show events which are aftershocks of the major Kern County earthquake. These events are analyzed and related to aftershocks recorded by earthquake stations.

The second part of the paper reviews the history and development of seismic exploration in California, from its beginning, in the 1920's, to the present day. The refraction and reflection methods have both been used, but the latter has proved to be the more effective in discovering petroleum. The earliest reflection technique employed the "correlation" method. This was replaced by the "dip" method, and later by "continuous profiling".

Those California oil and gas fields whose discovery can be credited at least in part to the seismograph are indicated. They are grouped in four periods, which are mainly chronological, but partly geographical. These are (1) Early gas discoveries (1931-1936); (2) Southern San Joaquin Valley oil discoveries (1936-1944); (3) Sacramento Valley gas discoveries (1937-present time); (4) Recent California oil discoveries (1946-present time).

Introduction. Earthquakes in California have been recorded for at least a century and a half (California Division of Mines, 1952, p. 1), and it is quite probable that they have occurred throughout most of geologic time. It is only during the last century that artificial earthquakes, produced by the controlled detonation of explosives under, on, or above the surface of the earth, have been employed as a means for exploring the subsurface structure, especially as applied to the search for petroleum and other minerals.

Seismic prospecting is therefore derived from earthquake seismology, both being based on the same fundamental physical laws. Moreover, there are close similarities in instruments and in methods of interpretation.

Acknowledgments. The writer wishes to express his thanks to the Union Oil Company of California for permission to publish this paper, and to John Sloat for many helpful suggestions and comments. The illustrations have been prepared by Robert Bowman, Taylor Moore, and Richard Huntley.

Geologists and geophysicists of many oil companies have contributed much information which has been used in assembling the lists of seismic discoveries. Appreciation is expressed for their help.

Thanks are extended to Dr. Beno Gutenberg of the California Institute of Technology Seismological Laboratory, who has given much information concerning the Kern County earthquakes of 1952 and interpretation of earthquakes recorded by seismic parties.

SEISMIC EXPLORATION AND EARTHQUAKES

In both seismic prospecting and earthquake seismology the original data for analysis and subsequent geological interpretation are the seismograms. Seismic waves originate at the point of detonation of an explosive charge, or at the origin of movement along a fault (focus), and are transmitted through or along the

boundaries of formations to the seismometer stations; by means of proper amplifiers and other electrical and optical equipment, they activate various traces on the seismograms.

Although earthquake seismographs are designed to record most effectively seismic waves produced by earthquakes and prospecting seismographs to record explosions in shot holes, each type could, if the disturbance were close enough or strong enough, record the other type of wave.

Earthquakes have been recorded many times by seismic parties engaged in exploration for petroleum. Several parties were working within 100 miles of the White Wolf fault on July 21, 1952. (Benioff, Buwalda, Gutenberg, and Richter, 1952, pp. 4-7). Figure 1, which has been prepared by the Seismological Laboratory of the California Institute of Technology, shows the locations of the White Wolf and other major faults of the Southern San Joaquin Valley area. In addition the positions of the permanent and temporary Institute seismological stations, and of the epicenters of recorded aftershocks are represented.

A Western Geophysical Company of America seismic party working for the Richfield Oil Corporation in the southern end of the San Joaquin Valley was within a few miles of the White Wolf fault during the latter part of July 1952. Figure 2 is a reproduction of portions of three seismograms recorded by this party on July 23 and 25; their locations are superimposed on figure 1. Each seismogram shows strong events which undoubtedly are produced by aftershocks.

Each illustration is the latter portion of a routine reflection type seismogram, and on each the earthquake events were recorded later than a time of about 3.0 seconds, measured from the time of detonation of the explosion for the particular seismograms. This is later than the deepest reflections to be expected from the shots, and therefore the events must have originated from other sources.

Dr. Beno Gutenberg, of the Seismological Laboratory, has examined the seismograms and states that no recorded aftershocks occurred at the approximate times given on figure 2. Because of the wide scattering of the epicenters of recorded aftershocks (figure 1), it is most unlikely that any two of the three seismograms would record earthquakes from the same origin. In fact, seismograms A and B, with the same ground location for the seismometers, indicate waves with opposite directions of movement, and therefore from different sources.

The best determination that can be made of amplitude of ground motion at the seismometers for the three seismograms of figure 2 is 10^{-6} cm for A and C, and 10^{-7} cm for B. These values, which have been supplied by the Laboratory of Western Geophysical Company of America, from a consideration of seismogram amplitudes, wave frequency, and sensitivity settings, must be considered approximations.

Since the distance from the epicenters for these aftershocks is not known, the magnitudes can only be esti-

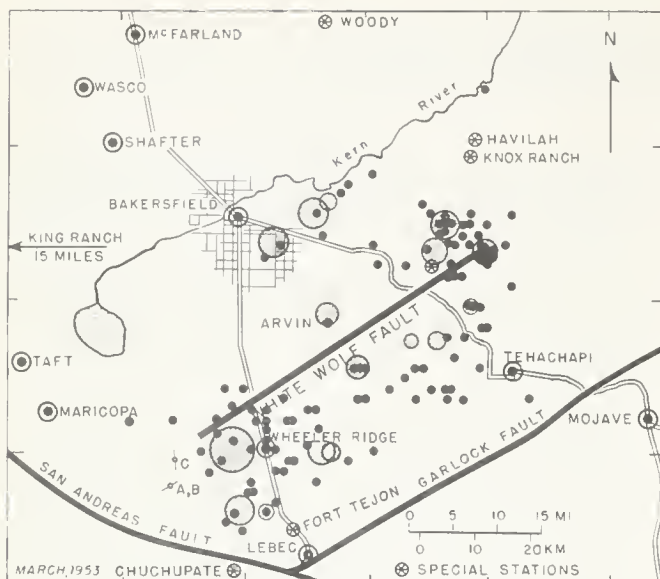


FIGURE 1. Epicenters of Kern County shocks, July 1952 to March 1953. A, B, and C, are locations for seismograms of figure 2. Map by permission of Seismological Laboratory, California Institute of Technology.

mated. They would be 3 to 4 for A and C, 2 to 3 for B. These are smaller than the magnitudes for figure 1, which, in general, are 4 or larger.

Present day reflection seismographs are extremely sensitive to low amplitude ground motion. On July 22, when the frequency of aftershocks reached a maximum, the ground disturbance caused by them in the area was so great that it was practically impossible to obtain usable reflection records, and operations were suspended for the day by the party.

The seismograms are susceptible to partial analysis only. If we speculate, in order to carry out the computations, that the events on seismograms A and C are from the same origin, the moveout times may be resolved, and a direction for the wave arriving at the seismometers determined. It is also assumed that the two spreads of seismometers are at about the same location. The graphical solution is shown on figure 3.

A resultant time moveout of .060 sec. is indicated, and the direction of arriving wave is from S 01° E to N 01° W. Referring again to figure 1, the arrival would either be from a fault south of the White Wolf, or would suggest that this fault may have a considerable hade to the south. The apparent velocity of the wave arriving at the seismometers is $1200/.060$, or $20,000'$ /sec. This value lies very close to that of the longitudinal velocity in granite, 6.34 km./sec. or $20,800'$ /sec.; thus, if the wave being recorded were longitudinal, the wave path in granite before entering the superjacent sediments would be about horizontal. No earlier phases of the arrivals on figure 2 are said by Richfield Oil Corporation to be visible on the earlier portions of the seismograms, and hence these arrivals are probably longitudinal waves.

The frequency of the waves is between 25 and 35 cycles per second. This is much higher than that of earthquake waves which have travelled long distances,

usually $\frac{1}{4}$ to 4 cycles per second. The absence of the low frequency components on the seismograms is caused by the electrical filtering used to transmit reflected energy, while attenuating frequencies outside of the frequency range of the reflections. Thus the filter used has a peak frequency between 20 and 30 cycles per second, and the much lower frequency components of the earthquake spectrum have been filtered out. On the other hand the higher frequencies registered on these seismograms are not recorded on the usual earthquake seismograms because they are more rapidly attenuated with long distances than the lower frequencies, and also because of seismograph characteristics.

A second example of an earthquake being recorded by a seismic party is one recorded by The Texas Company, in Ventura County, California, on June 25, 1947, 12:58 P. M. The earthquake was felt by the observer while taking a reflection seismogram, and he continued the recording for several additional seconds in order to record the earthquake. This seismogram has been described in a paper entitled *An earthquake recorded by reflection seismograph instruments* by Norman J. Lea (Geophysics, 1948, p. 656) and presented on June 18, 1948, at the first annual spring meeting of the Pacific Coast Section of the Society of Exploration Geophysicists, Bakersfield.

The seismogram showed many phases with different apparent velocities. Dr. Gutenberg has examined the seismogram, and has referred to two shocks felt at Carpinteria within 1 minute, on the same day, the second having a time of origin of 12:55:54 P. M., and probably the one recorded by the party. The waves with the smallest apparent velocity were probably transverse, while those with the largest were possibly reflections of longitudinal waves from deep layers (bottom of granite?).

One conclusion presented in the above paper was that transverse waves could be recorded by exploration seismograph equipment. This observation was used as a possible explanation of lagging reflections observed in the Salinas Valley.

Because oil-producing areas exist on both sides of the White Wolf fault, seismic waves, originating from explosions detonated by geophysical prospecting parties, have been observed after crossing the fault trace. A seismic line that crossed the trace is shown in figure 4. This section has a generally northwest-southeast bearing, and lies between Wheeler Ridge and Comanche Point. As is typical of much of this area, seismic data are only fair in quality. Nevertheless, the section shows the abrupt termination of the continuity of dips, which often is observed at a fault zone, especially if it comprises a width of several hundred feet or more. Some of the steeper dips may be refracted reflections from the fault; in this case the plotted dip would not be the dip of the fault surface.

DEVELOPMENT OF SEISMIC EXPLORATION IN SAN JOAQUIN VALLEY

General. Although the earliest use of artificially produced seismic waves dates back into the latter part of the 19th century, it was not until after 1920 that the practical development of both the refraction and the reflection seismograph was realized. The early history of the development of the methods is described in excellent

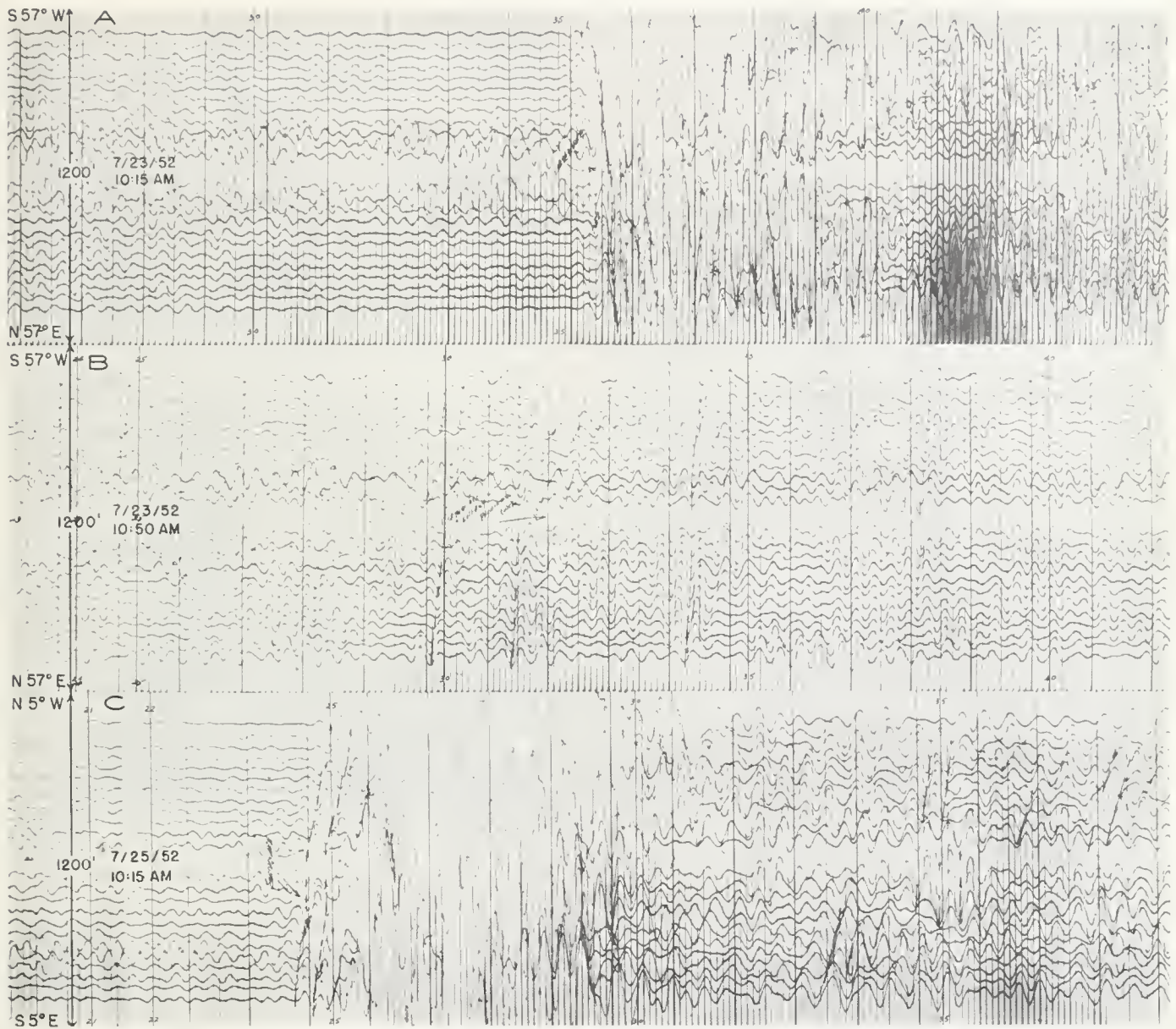


FIGURE 2. Earthquake events on reflection-type seismograms. *By permission of Richfield Oil Corporation.*

fashion by Weatherby (1948, 1948a), Salvatori (1948), and Schriever (1952).

Refraction Prospecting. Refraction was the first of the seismograph methods to be used to discover an oil field in the United States; Orchard Dome, Texas Gulf Coast, was discovered by this method in 1924. The first refraction work in California was probably done in 1925, on an experimental basis, and regular surveys were carried out by 1927.

The method had its greatest success in the Gulf Coast area, where it recorded the large time accelerations attained by seismic paths through high velocity (15,000'/sec.) salt domes intruded into low velocity sediments (5000-10,000'/sec.). Although the geological section underlying the San Joaquin Valley resembles that of the Gulf Coast in both age and lithology, the method did not

enjoy comparable success, because of the lack of such surfaces of large velocity contrast within the sedimentary section.

The refraction method was used to best advantage along the east side of the Valley, where it could trace the granitic basement surface from the western margin of the Sierra Nevada under the sediments of the Valley. Results in the vicinity of Hanford have been described (Vaughan, 1943, pp. 67-70).

Refraction shooting in this early period made a valuable contribution to our knowledge of the regional geology of the San Joaquin Valley. It showed that the syncline of the valley lay not in the center, but close to the western margin. A minimum depth (Vaughan, 1943) of 30,000 feet is quoted for the depth to basement in the deep trough immediately east of Coalinga Nose.

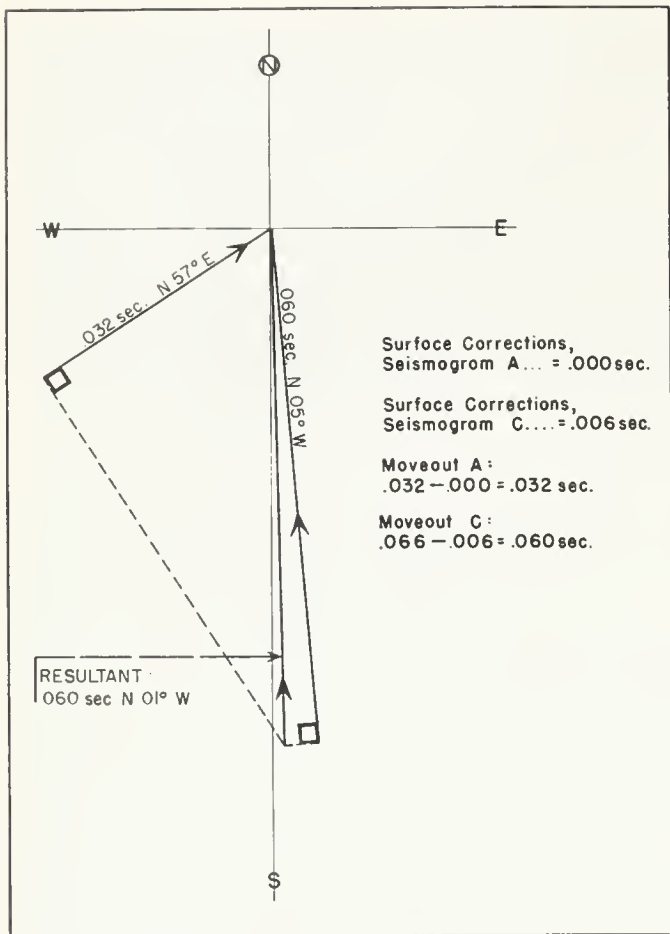


FIGURE 3. Resolutions of moveouts from seismograms A and C, figure 2, assuming same origin for shocks and same location for spreads of seismometers.

Reflection Prospecting. The reflection method of seismic prospecting originated in Oklahoma, where the first experimental profiles were observed in 1921 (Weatherby, 1948, 1948a, Schriever, 1952). By 1927 exploration for petroleum was in progress, and the first oil field discovered by this method, South Earlsboro, Oklahoma, was found in 1929.

The first use of the reflection method in California was in 1928, but the work was more or less experimental in nature. Salvatori (1948) mentions that the results were not very favorable, and that the work was soon discontinued.

In 1931, after the method had led to the discovery of several oil fields in Oklahoma, another attempt was made in California. Only a few seismic parties operated until about 1934. About this time the reflection method led to the discovery of several gas fields, and, beginning in 1936, of many oil fields.

This proof of the value of the method led, of course, to an increase in the number of parties throughout the state, and today the number remains high. Figure 5 shows graphically the number of seismic parties employed in California from the early 1930's to the present. In addition to these parties, there has been at least one offshore party in operation for most years since 1944.

Technique of Reflection Prospecting. As developed initially in Oklahoma the reflection method was by correlation. Shot points were spaced at $\frac{1}{4}$ to 1 mile intervals, and neighboring seismograms were correlated, or matched on reflections with similar appearance, or character. Depths computed from such correlated reflections would give the configuration of a given geologic horizon.

The method worked quite well in Oklahoma, where marked differences in lithology between successive formations exist, and continue for long lateral distances. The method still has an application in certain areas of the Mid-Continent and Canada, where the formations are of Mesozoic or Paleozoic age. In California, however, lithology often varies quite rapidly in short distances, and reflections do not always maintain their character for many successive stations.

The correlation method was succeeded by the dip method. This method was first developed on the Gulf Coast, where the geologic section resembles that of many basins of California, and lateral lithologic changes are also rapid. It was first employed in California in the early 1930's.

The dip method employs the moveout time of a reflection across a seismogram. By use of the proper mathematical equations, based on formation velocities and the geometry of the spread of seismometers and the shot, the

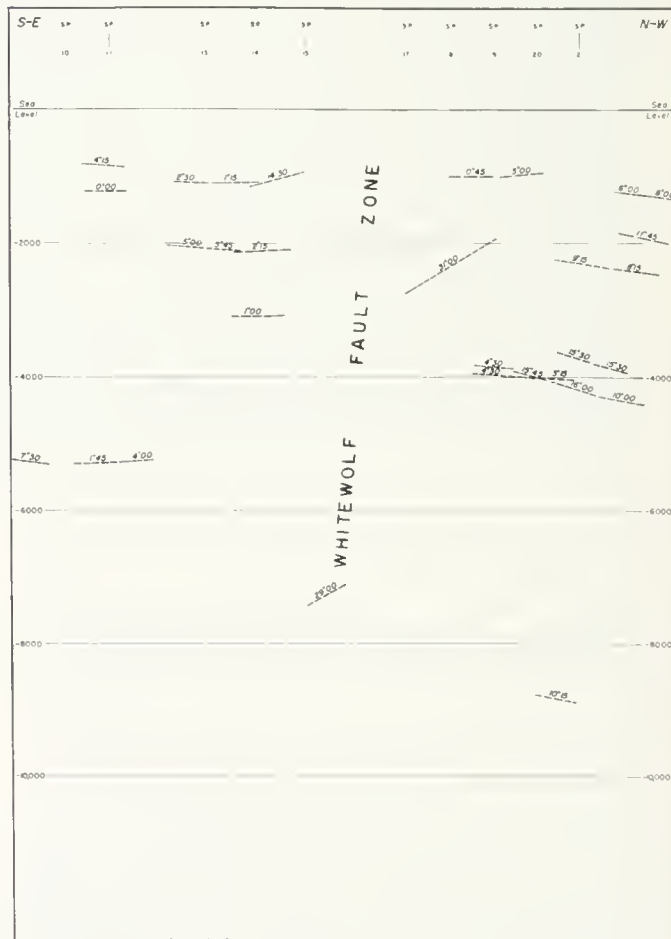


FIGURE 4. Reflection seismograph section across White Wolf fault.

dip of the reflecting bed at the point of incidence is computed. As actually used in California, the seismometer spreads were usually spaced along straight lines (either parallel or normal to the direction of regional dip), at intervals of a quarter to half a mile, with the shot points either in line or offset a few hundred feet.

Dips so computed were projected from one station to the next, and "phantom" horizons were carried from station to station, and from line to line. Where available, correlations were used to supplement the dips. The dip method, in use during most of the 1930's and 1940's, has led to the discovery of many oil and gas fields in the San Joaquin Valley.

A variation of the line method of laying out stations is the use of spreads in two different directions (preferably normal) at a given station. In this case the computed dip components are resolved into a total dip.

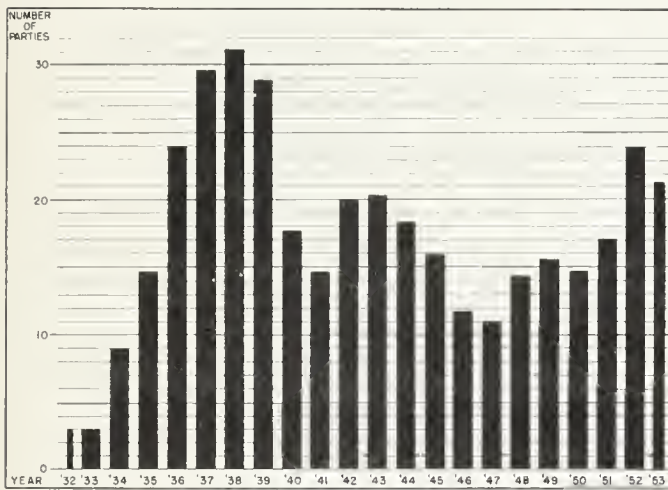


FIGURE 5. Reflection seismograph parties in California September 1932 to June 1953.

The relationship between the correlation and dip method can be readily seen by use of an analogy derived from a consideration of a series of electric logs from bore holes in an area. Let us suppose that at each bore hole the ordinary self-potential and resistivity log, and also a dipmeter survey is available. Logs of holes may be matched in two ways. If the ordinary logs are used, they are correlated on character, and the difference in elevation on a given marker horizon is given by the difference on the logs (correcting for variation in reference elevation). The alternative procedure would be to use the dips from the dipmeter survey at two bore holes, resolve each into the direction between the two holes, and project each dip halfway. These two systems are analogous to the correlation and dip methods of reflection prospecting.

During the 1940's, after the floor of the San Joaquin Valley had been covered in reconnaissance, and the most prominent structures had been found, the need arose for a more refined technique to discover the smaller anticlines, structural noses, faults, overlaps, and unconformities. This method, the one used almost entirely in California today, is that of *continuous profiling*. This system, with continuous spacing of seismometer stations on the ground, and with the stations between each two

successive shot points shot from both points, gives continuous subsurface coverage. The interval between adjacent shot points is usually between 400 and 1000 feet.

Figure 6 is a reproduction of six successive seismograms, with 4800 feet of continuous subsurface coverage, located on the west side of the San Joaquin Valley, between the valley syncline and the Kettleman Hills—Lost Hills anticlinal trend. Because of the continuity of coverage, and with the dip all in one direction, the series of seismograms is, in effect, a subsurface geologic section; the vertical scale is not uniform because of the increase of velocity with depth, and the steeper reflections are, of course, not migrated up-dip. The vertical depths and the positions of the top of the Pliocene and the top of the Miocene beds are only approximate.

The seismograms demonstrate the fact that the continuous profiling method employs both correlations and dips. Actually both methods are employed in the computations.

The above brief summary of the development of reflection shooting in California has been concerned with the evolution of the various types of surface patterns. This has been accompanied by a continuous improvement in instrument design, both in seismometers and in recording equipment. The number of stations per spread has increased from its early value of 4 to 6 to the present 20 to 24, with some 36 and 48 trace units in present day operation. Multiple seismometers have come into use, along with the procedure of mixing, both mechanical and electrical. Amplifiers and filters have been improved to increase sensitivity and to increase the reflection to extraneous energy ratio. Improvements in computing and interpreting methods have kept pace with advances in field procedures.

RESULTS OF SEISMIC EXPLORATION IN THE SAN JOAQUIN VALLEY

Introduction. The success of the seismic method as applied to the search for petroleum sources must be measured by the volume of reserves and production from fields whose discovery is credited to the method. The following paragraphs comprise a brief summary of those oil and gas fields whose discoveries are generally credited to the reflection seismograph, or towards whose discovery the method has made a substantial contribution.

Because of the fact that many of the fields here enumerated fall in the latter category, many of these fields are near the line which separates seismic discoveries from those discovered by other methods, mainly subsurface geology. Doubtless some readers would not place certain of these fields here; a few fields which are not mentioned here may be considered by some as seismic discoveries. In general, the fields listed here are those for which the company who made the discovery gives at least part credit to the seismograph. Size of the field, or volume of reserves or production is not a factor in the selection. Some of these fields are now abandoned; others may not yet have been placed on production, although the potential has been indicated.

The sources for the data were discussions with members of the exploration departments of the various companies concerned, and published records.

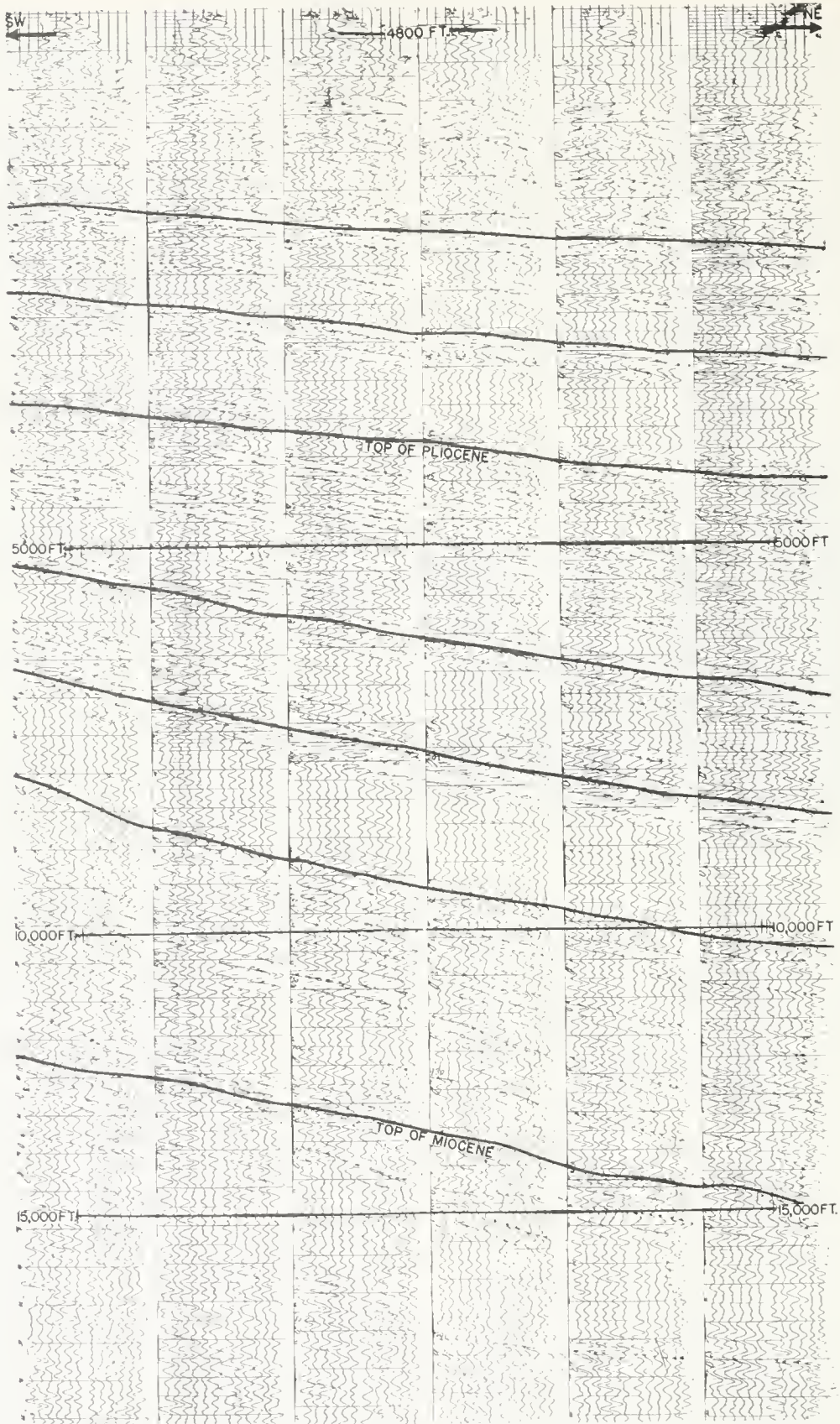


FIGURE 6. Continuous seismograph coverage, west side of San Joaquin Valley. Vertical depths and positions of top Pliocene and top Miocene approximate.

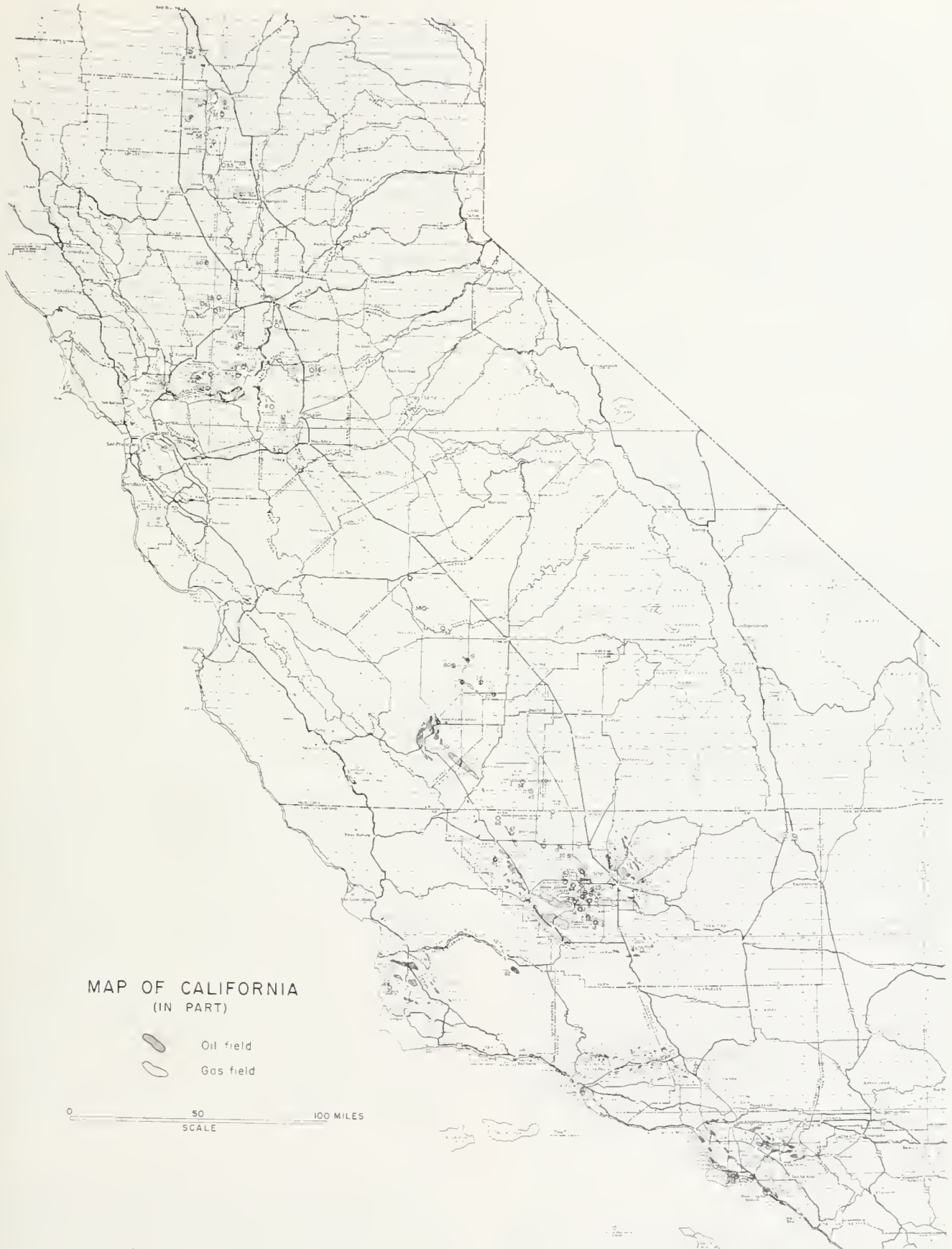


FIGURE 7. Location of oil and gas fields discovered by reflection seismograph. Numbers correspond to those used in text. *Base map by permission General Petroleum Corporation.*

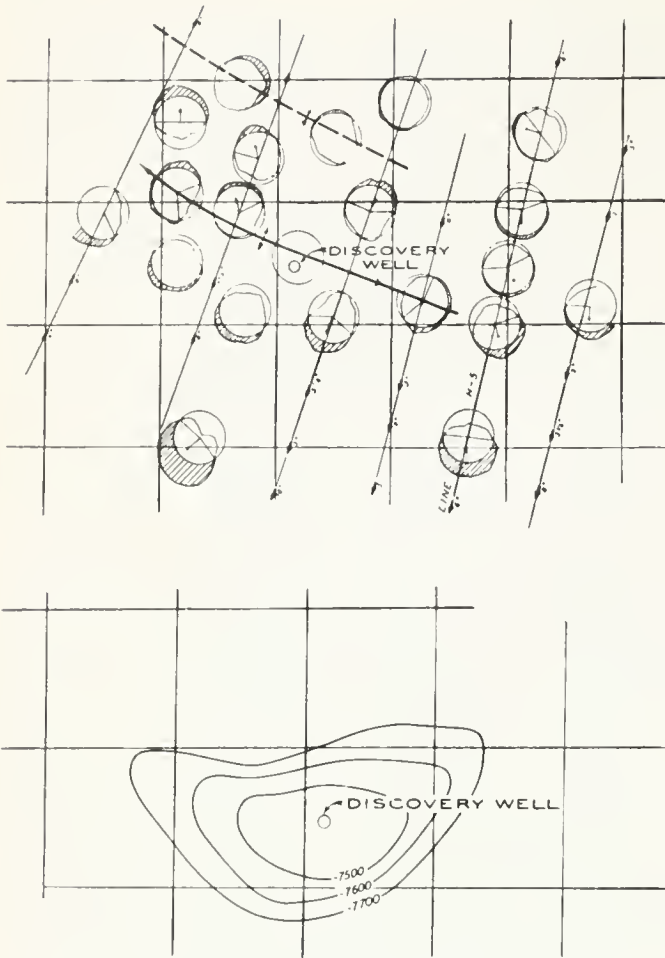


FIGURE 8. A (above) Pre-discovery seismic map of Ten Section oil field. Reproduced from "Geophysical Case Histories, vol. I," by permission of Society of Exploration Geophysicists. B (below) Contours on productive sand, Ten Section oil field. Reproduced from "Geophysical Case Histories, vol. I," by permission of Society of Exploration Geophysicists.

Seismic discoveries are here grouped in four divisions, which are partly chronological and partly geographical, so as to indicate the trend from the first discoveries to the present day. All of these fields are credited to the reflection method, none to refraction.

Early gas discoveries.

Name of field	County	Discovered by	Date	Producing zones
1. Chowchilla	Madera	Pure Oil Co.	November 1934	Miocene, Cretaceous
2. Paloma (Buena Vista Lake gas field)	Kern	Ohio Oil Co.	July 1934	San Joaquin (upper Pliocene)
**3. Trico*	Kern, Kings, Tulare	Trico Oil & Gas Co.	November 1934	San Joaquin
4. Semitropic*	Kern	Standard Oil Co.	March 1935	San Joaquin
5. Tracy	San Joaquin	Amerada Petroleum Corp.	August 1935	Cretaceous
6. McDonald Island	San Joaquin	Standard Oil Co.	April 1936	Paleocene
7. Rio Vista	Solano, Sacramento	Amerada Petroleum Corp.	June 1936	Eocene

** (Doell, 1943, p. 551) Trico is only partially a seismic discovery. Mr. Harry Magee became interested in the area because of gas shows in water wells, and because of the slight topographic expression. The location of the discovery well was based on seismic work of the Standard Oil Company.

Early Gas Discoveries (1931-36). The first fields in California to be discovered as a result of exploration by the reflection seismograph are a series of relatively shallow gas fields found between 1934 and 1936. That the first fields contained reservoirs of gas rather than oil is due mainly to the fact that in the earlier years of seismic exploration, information much deeper than about 5000 feet was not generally obtained. Moreover, under the floor of the San Joaquin Valley, the shallow formations (upper Pliocene in southern part, Eocene-Cretaceous in the northern) contain dry gas, rather than oil.

The field generally considered to have been discovered by the earliest reflection exploration in California is the Chowchilla gas field, Madera County. (See figure 7 for location of fields discovered by the seismograph.) As a result of reflection shooting carried out in 1931 and 1932 (Salvatori, 1948), the field was discovered by the Pure Oil Company in November, 1934. The seismic work was of the correlation type. Chowchilla field was not very important, economically, because of the low heating value of the gas.

In this and the following sections, an asterisk following the name of the field indicates that credit for the discovery is shared between the seismograph and other

Southern San Joaquin Valley oil discoveries.

Name of field	County	Discovered by	Date	Producing zones
8. Ten Section	Kern	Shell Oil Co.	June 1936	Stevens
9. Greeley	Kern	Standard Oil Co.	December 1936	Stevens, Vedder
10. Rio Bravo	Kern	Union Oil Co.	November 1937	Vedder
11. Canal	Kern	Ohio Oil Co.	November 1937	Stevens
12. Canfield Ranch	Kern	Standard Oil Co.	January 1938	Stevens
13. Wasco	Kern	Continental Oil Co.	April 1938	Vedder, Eocene
14. South Coles Levee	Kern	Ohio Oil Co.	November 1938	Stevens
15. North Coles Levee	Kern	Richfield Oil Corp.	November 1938	Stevens
16. East Coalinga Extension, Amerada area*	Fresno	Amerada Petroleum Corp.	April 1939	Eocene
17. Strand	Kern	Tide Water Associated Oil Co.	June 1939	Stevens
18. Paloma (Oil)	Kern	Western Gulf Oil Co.	September 1939	Stevens
19. Raisin City	Fresno	Shell Oil Co.	June 1941	Miocene, Eocene
20. Shafter	Kern	Continental Oil Co.	September 1941	Vedder
21. Helm	Fresno	Amerada Petroleum Corp.	October 1941	Miocene, Eocene, Paleocene, Cretaceous
22. Riverdale	Fresno	Amerada Petroleum Corp.	December 1941	Miocene
23. Antelope Hills*	Kern	Shell Oil Co.	May 1942	Miocene
24. East Strand*	Kern	Tide Water Associated Oil Co.	January 1943	Stevens
25. McClug*	Kern	Continental Oil Co.	September 1943	Stevens
26. Burrel	Fresno	General Petroleum Corp.	October 1943	Miocene
27. Ant Hill*	Kern	Amerada Petroleum Corp.	July 1944	Miocene
**28. Wilmington	Los Angeles	General Petroleum Corp.	December 1936	Pliocene, Miocene

** Located in Los Angeles basin.

methods. The number corresponds to its location on figure 7.

Southern San Joaquin Valley Oil Discoveries (1936-44). This period was ushered in by the discovery of Ten Section field, and, as used in this paper, carries to about 1944. It is overlapped somewhat by the next period, that of the Sacramento Valley gas discoveries.

Sacramento Valley gas discoveries.

Name of field	County	Discovered by	Date	Producing zones
29. Fairfield Knolls	Yolo	Standard Oil Co.	November 1937	Eocene
30. Willows	Glenn	Ohio Oil Co.	January 1938	Cretaceous
31. Vernalis	San Joaquin, Stanislaus	Standard Oil Co.	January 1941	Cretaceous
32. Bowerbank	Kern	The Texas Co.	January 1942	San Joaquin
33. Roberts Island	San Joaquin	Standard Oil Co.	August 1942	Eocene
31. Gill Rauch	Madera	The Texas Co.	April 1943	Eocene
35. Lodi*	San Joaquin	Amerada Petroleum Corp.	April 1943	Eocene
36. Ord Bend	Glenn	Superior Oil Co.	August 1943	Cretaceous
37. Thornton	Sacramento, San Joaquin	Amerada Petroleum Corp.	September 1943	Eocene
38. Moffat Ranch	Madera	The Texas Co.	September 1943	Eocene
39. Colusa	Colusa	General Petroleum Corp., Union Oil Co.	December 1943	Cretaceous
40. Chico	Butte	Richfield Oil Corp.	January 1944	Cretaceous
41. Afton	Glenn	Richfield Oil Corp.	February 1944	Eocene
42. Honker Bay	Solano	Standard Oil Co.	April 1944	Eocene
43. Millar (Dixon)	Solano	Amerada Petroleum Corp.	August 1944	Eocene
44. Suisun Bay*	Solano	Standard Oil Co.	September 1944	Eocene
45. Alpaugh*	Kings	Standard Oil Co.	September 1944	San Joaquin
46. Corning	Tehama	Superior Oil Co.	October 1944	Pliocene
47. Kirby Hills*	Solano	Shell Oil Co.	January 1945	Eocene
48. Maine Prairie	Solano	Amerada Petroleum Corp.	March 1945	Eocene
49. Caebe Slough*	Solano	Standard Oil Co.	March 1945	Eocene
50. Dunnigan Hills*	Yolo	The Texas Co.	February 1946	Cretaceous
51. Winters	Yolo, Solano	Shell Oil Co.	February 1946	Cretaceous
52. Durban	Butte	Standard Oil Co.	July 1946	Eocene
53. Pleasant Creek*	Yolo	Shell Oil Co.	December 1948	Cretaceous
54. Harvester*	Kings	Shell Oil Co.	February 1950	San Joaquin
55. Wild Goose	Butte	Honolulu Oil Corp., Humble Oil & Rfg. Co.	September 1951	Cretaceous
56. Freeport*	Sacramento	Standard Oil Co.	May 1952	Cretaceous
57. Sutter	Sutter	Richfield Oil Corp.	August 1952	Paleocene
58. Beehive Bend	Glenn	Suuray Oil Corp.	May 1953	Cretaceous

The correlation method of seismic prospecting had by 1936 been replaced by the dip method, since the correlation method was not successful in most areas. It has been the dip method which has led to the discovery of most of the fields described in this paper.

The first discovery of this period, and the first discovery of an oil field in California by the reflection seismograph, was of Ten Section field, Kern County, on June 2, 1936, by the Shell Oil Company (Waterman, 1948, pp. 551-553). Figures 8A and 8B are reproduced from Mr. Waterman's paper, and show a pre-discovery seismic map for comparison with contours on top of the productive sand.

The discovery of Ten Section was followed within the next few years by that of many other oil fields, principally in Kern County.

The Stevens and Rio Bravo—Vedder sand zones of Miocene age, have been the sources of much of the oil produced from beneath the San Joaquin Valley. The Stevens sand was first produced in the Ten Section field. The Rio Bravo—Vedder sand was first produced under the valley floor from Rio Bravo field (Sloat, 1948, p.

Recent California oil discoveries.

Name of field	County	Discovered by	Date	Producing zones
59. Leffingwell*	Los Angeles	Standard Oil Co.	February 1946	Pliocene
60. San Joaquin*	Fresno	Superior Oil Co.	March 1947	Eocene
61. West Montalvo*	Ventura	Standard Oil Co.	April 1947	Pliocene, Miocene
62. South Cuyama	Santa Barbara	Richfield Oil Corp.	May 1949	Miocene
63. Calder Corners*	Kern	General Petroleum Corp.	May 1949	Stevens
64. Goose Slough*	Kern	The Texas Co.	January 1952	Stevens
65. Lost Hills (government area)*	Kern	Superior Oil Co.	August 1952	Pliocene
66. Jesus Maria*	Santa Barbara	Union Oil Co.	September 1952	Miocene
67. Tejon Flats*	Kern	Union Oil Co.	March 1953	Miocene
68. Lost Hills*, Farnsworth area	Kern	Tide Water Associated Oil Co.	April 1953	Pliocene

569); this production, from below 11,000 feet, was at that time the deepest in the world.

Wilmington field, Los Angeles County, is included in the accompanying chart because of its early time of discovery. The discovery of this field, by far the largest found by the seismograph in California, with an estimated ultimate production valued around \$2,000,000,000, resulted from drilling a structure outlined by recordings from only four stations, and supplemented before drilling by 16 others (Salvatori, 1948).

Sacramento Valley Gas Discoveries (1937-June 1953). Gas had been discovered by the seismograph in the San Joaquin and southern Sacramento Valleys previous to this period. Discoveries in this period resulted in many gas fields, almost half of the total number of fields considered in this paper. Most of these are located in the Sacramento Valley, with a few in the San Joaquin. Whereas most of the early discoveries are credited almost entirely to the reflection seismograph, many of the more recent are shared between it and subsurface or stratigraphic methods.

The names assigned to the more recent of these discoveries are geographical descriptions, not the official field designations, which have not yet been assigned.

Recent Period of California Oil Discoveries (1946-June, 1953). This period is characterized by a lower frequency in the discovery rate, as discoveries become smaller in size and harder to find. On the other hand, two of these fields, West Montalvo and South Cuyama, are comparable in size to most fields discovered during the period of southern San Joaquin Valley exploration (1936-44).

The continuation of seismic discoveries in the San Joaquin Valley and in the other oil and gas provinces of California is definitely indicated by the fact that discoveries are being made practically up to the date of this paper, and by the maintenance of a high level of seismic exploration.

PART II—SEISMOLOGY

INTRODUCTION

PART II comprises the seismologic record of the Kern County earthquakes, computations using the voluminous data recorded by seismographs, and the conclusions of seismologists regarding the origin of the earthquakes, the mechanism of faulting, and relationships of the White Wolf fault to the regional fault pattern. This Part is the work of the Seismological Laboratory of the California Institute of Technology, with the exception of introductory statements on the history of earthquakes in California by Dr. VanderHoof (Part II-2) and a concluding paper on records obtained from strong-motion seismographs by the United States Coast and Geodetic Survey (Part II-12). Preliminary to a complete technical discussion of results obtained from instruments at the Seismological Laboratory (Part II-6, 7, 8, 9) are introductory chapters on principles of the science of seismology and definitions of its terms (Part II-1), history of earthquakes in the Valley (Part II-3), development of instruments used in recording earthquake waves (Part II-4), and the location of seismograph stations in California (Part II-5).

Probably no earthquake in history has had as complete seismological coverage as the Arvin-Tehachapi shock on July 21, 1952 and the hundreds of succeeding aftershocks. This was largely because of the Seismological Laboratory at Pasadena, which not only obtained seismograph records at the Pasadena station and semi-permanent stations in the southern Sierra Nevada, but also, within a few hours after the major earthquake, set up a series of portable seismographs in the earthquake area as basis for a special recording program on a scale never before undertaken. The instrumental records provided data for computation of magnitudes, locations of epicenters and foci "hitherto not available for any earthquake." The approximate distribution of

aftershock foci around a seismic source has been determined for the first time. The Arvin-Tehachapi is the "first major earthquake for which a sufficient number of highly sensitive seismographs with time good to the nearest tenth of a second were in operation at short distances in different directions." This permitted locating each shock within a few miles—in depth and in epicentral position—and times within a fraction of a second. The extraordinarily detailed local coverage was supplemented by data obtained from many distant seismograph stations in all parts of the world.

Drs. Gutenberg, Benioff, and Richter, as the result of evaluation of the data to mid-1953, have been able to develop new and revised concepts concerning such things as foreshocks in major earthquakes, characteristics of the release of strain in aftershocks, the radiation of energy in a shock, the relation of first motion of the ground to direction of slip on the causative fault, and the speed and direction of progression of faulting. They have arrived at quantitative values for the strike and dip of the plane of the White Wolf fault, the rate of progression of faulting, and direction of slip in the fault plane, from the instrumental data. These measurements and concepts have made it possible to derive additional conclusions as to the mechanism and strain characteristics of the White Wolf fault (Part II-10) and the relationship between activity on that fault and the pattern of faulting and other geologic structures in the region (Part II-11).

Part II-12 summarizes the conclusions of the United States Coast and Geodetic Survey based on records obtained from their strong-motion seismograph and includes a map showing intensities felt in California, according to the Modified Mercalli Intensity Scale.

CONTENTS

	Page
1. General introduction to seismology, by H. Benioff and B. Gutenberg.....	131
2. The major earthquakes of California: a historical summary, by V. L. VanderHoof.....	137
3. Seismic history in the San Joaquin Valley, by C. F. Richter.....	143
4. Seismograph development in California, by H. Benioff.....	147
5. Seismograph stations in California, by B. Gutenberg.....	153
6. Epicenter and origin time of the main shock on July 21 and travel times of major phases, by B. Gutenberg.....	
7. The first motion in longitudinal and transverse waves of the main shock and the direction of slip, by B. Gutenberg.....	165
8. Magnitude determination for larger Kern County shocks, 1952; effects of station azimuth and calculation methods, by B. Gutenberg.....	171
9. Foreshocks and aftershocks, by C. F. Richter.....	177
10. Mechanism and strain characteristics of the White Wolf fault as indicated by the aftershock sequence, by H. Benioff.....	199
11. Relation of the White Wolf fault to the regional tectonic pattern, by H. Benioff.....	203
12. Strong-motion records of the Kern County earthquakes, by Frank Neumann and William K. Cloud.....	205

1. GENERAL INTRODUCTION TO SEISMOLOGY

By H. BENIOFF AND B. GUTENBERG

ABSTRACT

This paper presents statements of the present status of some of the more important concepts in seismology. It includes discussions of the origin and mechanism of earthquakes, energy sources, distribution of earthquakes in space and time, characteristics of seismic waves, earthquake magnitude and intensity, nature of faulting, methods of locating foci, aftershocks, wave paths and tsunamis.

Earthquakes result from stresses which accumulate within the outer 400-mile shell of the earth. The origins of these stresses are still obscure both as to the source of energy and as to the mechanism by which this energy is converted to strain energy. The energy source is generally assumed to be of thermal origin (radioactivity, cooling, etc.) although other sources such as gravitational forces may also be active. The mechanisms which have been suggested for transferring thermal energy into mechanical energy or elastic strain are convection currents, change of phase or state, diffusion processes, expansion, or contraction. Gravitational return to equilibrium from disturbances produced in the past may also play a role. However, these mechanisms appear to the authors to be generally inadequate to explain all the known observations, so that other as yet unknown sources may also be active.

The large majority of earthquakes have a tectonic origin although, in the vicinity of volcanoes, shocks are produced by the processes of volcanism. These are classed as volcanic earthquakes and, in general, are small and shallow. Tectonic earthquakes are generally assumed to be generated by release of strain in crustal rocks, brought about by sudden slippage on faults in accordance with the elastic rebound theory of Reid (1910). Other mechanisms may also be involved. The number of earthquakes which have been definitely related to observed fault displacements is very small. According to C. F. Richter there are only about 20 instances throughout the world in which faulting in association with an earthquake has been adequately established by field observations. Four of these occurred in California—on the San Andreas fault in 1857 and 1906, in Owens Valley in 1872, and in the Imperial Valley in 1940. There are



LARGE INTERMEDIATE AND DEEP FOCUS EARTHQUAKES SINCE 1904

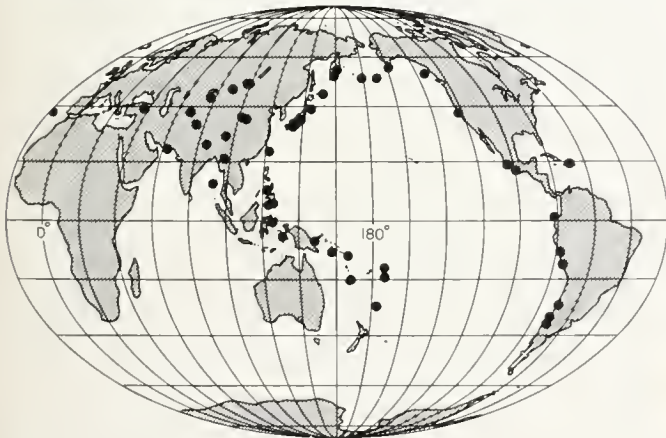
FIGURE 2. Distribution of deep-focus earthquakes.

many other instances, such as the Arvin-Tehachapi (Kern County) 1952 earthquake, in which the available evidence for faulting is not entirely convincing; and still others about which there is no information. Many, especially small earthquakes, such as the Long Beach 1933 and the Santa Barbara 1925, produced no visible surface evidence of faulting. Others occur beneath the ocean and in consequence the surface traces are not observable, if they exist.

The largest number of earthquakes and those with the greatest energy occur in the upper 40 kilometers of the earth's crust. Deeper earthquakes occur with decreasing frequency down to the 250 km level; below that level the frequency of occurrence per unit depth interval becomes approximately constant to a depth of 700 km.

Although earthquakes may occur anywhere on the earth, the great majority are concentrated in the circum-Pacific belt (fig. 1), which includes about 80 percent of the shallow shocks, 90 percent of shocks occurring at depths between 60 and 300 km, and nearly all of the deeper ones (fig. 2). Nearly all of the remaining large intermediate and shallow shocks occur in the Mediterranean and trans-Asiatic belt. In addition, only one deep earthquake (in southeastern Spain on March 29, 1954, depth 640 km, magnitude $7.1 \pm$) has ever been observed in this belt outside the area surrounding the Pacific Ocean. A smaller number of earthquakes including a few major shocks occurs along the principal ridges of the Atlantic, Arctic, and Indian Oceans. The Pacific basin and the continental shields are very nearly inactive. For further details see Gutenberg and Richter (1954).

Accurate information regarding the distribution of earthquakes in time and space has been available only for the last 50 years, since instrumental observations have been possible. Although this is a very short interval of geologic time the observations show that, in general, activity does not proceed at a uniform rate. Thus since 1904 earthquakes of magnitude 8 and larger have occurred in about five active periods (fig. 3) of decreasing



SHALLOW EARTHQUAKES MAGNITUDES ≥ 8.0 SINCE 1904.

FIGURE 1. Distribution of great shallow earthquakes.

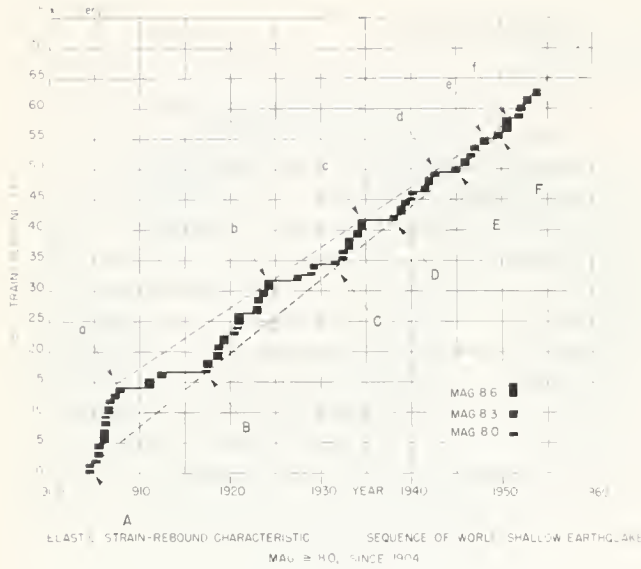


FIGURE 3. Strain release as a function of time for all great earthquakes since 1904.

amplitude and duration (Benioff, 1951). Moreover, there are different patterns of world activity for each of the three major depth classifications (Benioff, 1951).

Any disturbance at a point within a solid produces two principal wave types—longitudinal and transverse—(figs. 4, 5) which proceed with different speeds depending upon the physical properties of the rock. Longitudinal waves (P, push-pull) always travel faster than transverse waves (S, shear-displacement at right angles to direction of propagation) (fig. 6). The energy is not propagated uniformly in all directions and the directional pattern of longitudinal waves is not the same as that of transverse waves. The direction of maximum radiation for transverse waves is approximately at right angles to the plane of the fault, whereas the longitudinal radiation pattern has minima in the direction of the fault plane and at right angles to it. In earthquakes the amplitudes and periods of the transverse waves are usually greater than the amplitudes and periods of the

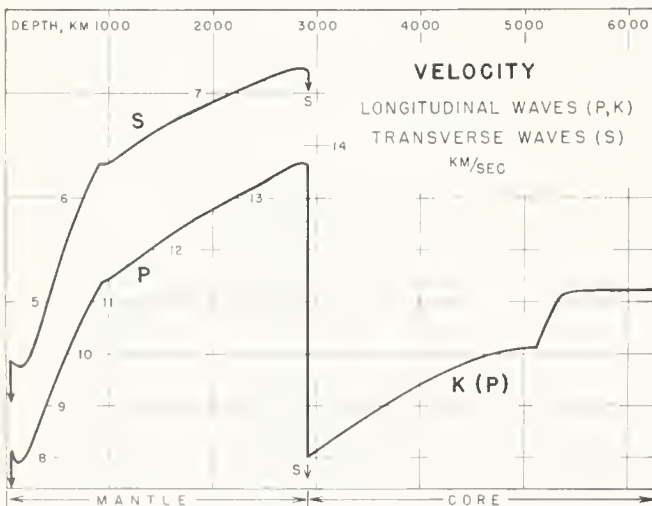


FIGURE 4. Wave velocity as function of depth in the earth.

longitudinal waves. Those P and S waves which arrive at the surface near the source produce two additional wave types known as Rayleigh waves and Love waves. These travel along the surface only. The energy released in the greatest earthquakes is very roughly equivalent to 10,000 of the original atomic bombs; the smallest earthquakes recorded near the source liberate approximately 10^{-14} times as much energy as the largest shocks. With the present available data it is not possible to calculate accurately the energy of earthquakes and consequently a magnitude scale has been devised by Professor Richter (1935) which is based on the maximum recorded ampli-

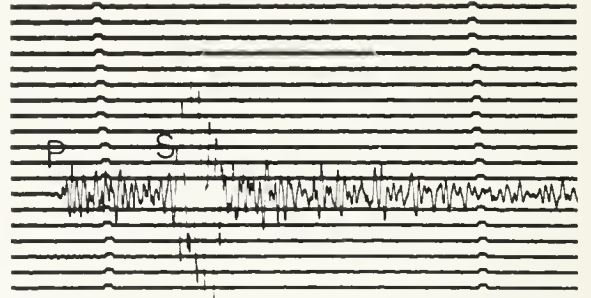


FIGURE 5. Seismogram of aftershock, August 11, 1952, 13:22:12, recorded by Benioff vertical capacity seismograph at Pasadena; distance $125 \pm$ km. Time marks are 1 minute apart, successive lines are 15 minutes apart.

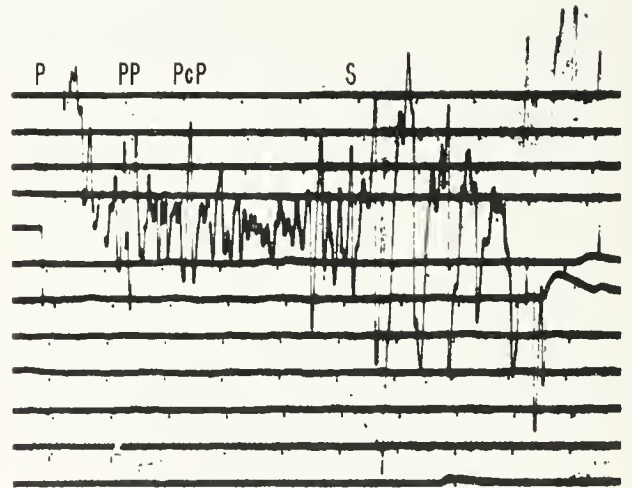


FIGURE 6. Record of main shock July 21, 1952, at Palisades, New York, distance 35.7° . Columbia University vertical seismograph, $T_0 = 10$ sec., $T_g = 75$ sec. Time marks every minute, successive lines are 1 hour apart. Motion down on record corresponds to motion up of the ground (compressions).

tude of a standard torsion seismograph located at a distance of 100 km from the source for shallow earthquakes. Tables have been constructed for calculation of the magnitude at all epicentral distances and for various focal depths and for several types of waves. An approximate relationship between the magnitude M and the energy E liberated as seismic waves has been given by Gutenberg and Richter (1942) in the form

$$\log E = A + BM.$$

The constants A and B have been revised a number of times. The values for the constants ($A = 12, B = 1.8$) given originally by Gutenberg and Richter (1942)

appear to lead to values of the energy which are excessive. For shocks of magnitude greater than perhaps 6½, $A = 7.5$, $B = 2.0$ are preferable. The constant B is not necessarily 2, as might be expected, because the period and duration of the wave trains both vary with the magnitude. Actually a better approximation to the relation between magnitude and energy would undoubtedly require terms of higher order, or different values of A and B for small and for large shocks.

Seismic intensity refers to the violence of shaking at any given point. On the other hand, the scales of intensity now in use, such as the modified Mercalli scale, are based on the effects or destructiveness produced by the ground vibration at particular points on available structures and thus are only roughly related to the actual intensity. Magnitude refers to the earthquake as a whole and is a constant for each shock, whereas Mercalli intensity varies from point to point depending on the distance from the source, the nature of the structures involved, and the density of population. The destructiveness of an earthquake depends upon the energy released, the focal depth, the distance from the source, the relative orientation of source and structure, the nature of the ground, the spectrum (distribution of energy with respect to period) of the source, the spectrum (distribution of vibration period) of the structures, as well as the type of structure.

Although the relationship between the magnitude M , the modified Mercalli intensity I_0 near the epicenter, the maximum acceleration a_0 and the radii r of isoseismals (assumed to be circular) are too complicated to be expressed exactly, it is possible to construct a rough tabulation of the way in which these quantities vary with the magnitude. Such an approximation is given in table 1 which is based on calculations by Gutenberg and Richter (1942) for average conditions in southern California. Actually, the isoseismals are quite irregular in shape, depending upon the ground conditions and underlying structures as well as the strike, dip, extent, and depth of faulting. Similarly, the other tabulated quantities are subject to large variations from the assumed averages.

Table 1. Modified Mercalli intensity I_0 near the epicenter, maximum acceleration a_0 in cm/sec^2 and its ratio to gravity g , and radii r in km for isoseismals corresponding to various intensities I , as function of magnitude M . After results of Gutenberg-Richter (1942) for average southern California earthquakes.

M	2.2	3	4	5	6	7	8	
I_0	1.5	2.8	4.5	6.2	7.8	9.5	11.2	
a_0	1	3	10	36	130	460	1670	cm/sec ²
a_0/g	0.001	0.003	0.01	0.04	0.13	0.5	1.7	
r for $I=1\frac{1}{2}$	0	25	50	110	200	400	750	km
r for $I=3$	--	--	30	60	120	220	400	km
r for $I=5$	--	--	--	20	60	100	200	km
r for $I=6$	--	--	--	5	30	60	130	km
r for $I=7$	--	--	--	--	15	40	80	km
r for $I=8$	--	--	--	--	--	25	60	km
r for $I=9$	--	--	--	--	--	10	40	km

The horizontal extent of faulting in a given earthquake varies from perhaps a few feet in the smallest earthquakes to at least 400 km, as observed in the San Francisco 1906 shock. The extent of faulting downward has never been determined but probably occasionally

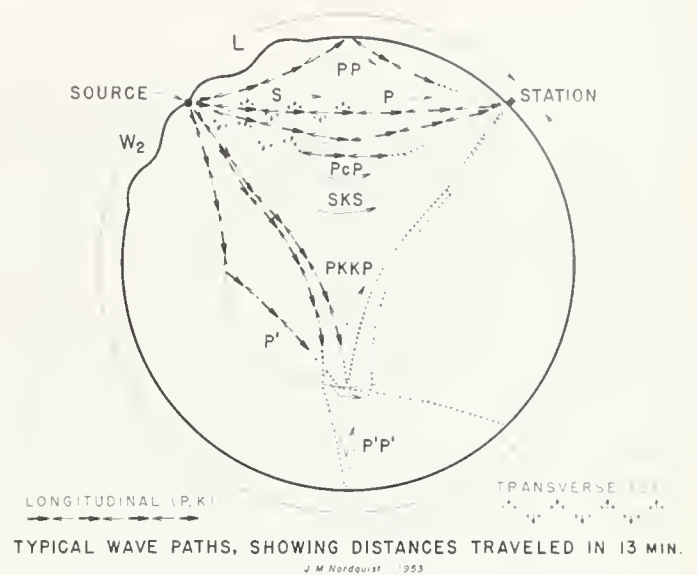


FIGURE 7. Some typical wave paths. L = surface waves, W2 = surface waves over the greater arc. Dotted lines are continuation of the wave paths after 13 minutes following the origin time of the earthquake.

amounts to more than 50 km since aftershocks have been observed to occur with a range of depth of this magnitude. The largest observed fault displacements occurred during the Yakutat Bay earthquakes in Alaska in 1899 when the vertical relative slip reached a maximum of 15 meters (47 feet).

Although some faults have very nearly vertical slip surfaces, nearly all orientations are observed. Wherever a fault intersects the surface of the earth the intersection produces a feature known as a fault trace.

Instrumental evidence indicates that faulting is initiated at depth at a point called the focus or hypocenter, from which it proceeds along the fault surface in two dimensions, presumably with different speeds. Faulting in the direction of slip must proceed with a speed less than that of the compressional wave and faulting perpendicular to the direction of slip must proceed with a speed less than that of the shear wave. The point vertically above the focus or hypocenter is designated the epicenter. It is usually not on the fault trace except when the fault surfaces are vertical. The point of origin calculated from seismograms always refers to the hypocenter and usually does not correspond with the region of maximum energy release. The direction of slip may be horizontal, vertical, or a combination of the two. Under favorable conditions the first motion of the ground at an observing station is directly related to the direction of slip.

Slipping of the fault produces the two principal types of body waves, longitudinal (P) and shear (S), as well as Rayleigh waves and surface shear (Love) waves mentioned earlier. The latter waves travel along the surface with amplitudes decreasing rapidly with depth and with speeds equal to or less than the S-wave speed. In most cases, destructiveness produced by shear waves is greater than that produced by other types of waves. Since all waves travel from the origin over minimum time paths and since for most of the earth the velocity

increases with depth, most of the paths within the earth are curved with the concave side up (fig. 7).

The precise determination of the location of the source involves triangulation based principally upon the time of arrival of the first waves at a number of observing stations. A rough determination at a single station can be made using the direction of the first motion of ground as exhibited by a three component seismograph assembly together with time interval between the arrival of the compressional (P) and shear (S) waves and other phases with established travel times. For exact determination of position and origin time, effects of local structure between source and station must be taken into account. With a dense distribution within 200 km of the epicenter of stations furnishing accurate data, the time of origin can be determined within ± 0.2 second and the position of the epicenter can be located within a radius of ± 3 km provided that there are no serious systematic errors. The depth is not so accurately determined. In shallow shocks the error may be quite large. Thus, for shocks at a depth of 16 km the error may well be ± 6 km in favorable cases. At a depth of 50 km it may be as high as ± 20 km.

According to the elastic rebound theory, an earthquake is initiated at a point where the gradually accumulating stress becomes equal to the strength of the rock and so produces a slip (fig. 8). The final increment of stress may be a result of some external force such as a tidal stress, a change in the barometric pressure, loading by precipitation, etc. Frequently large earthquakes are preceded at intervals of hours or days by foreshocks. Usually the foreshocks are small. They may be single or multiple. There is no way of knowing which of the many small shocks occurring in a region is a foreshock until after the occurrence of the principal shock. Clearly the occurrence of a foreshock increases the stress on the fault in its neighborhood and thus hastens the break of the main shock. Fairly frequently a large earthquake is followed within a few hours or days

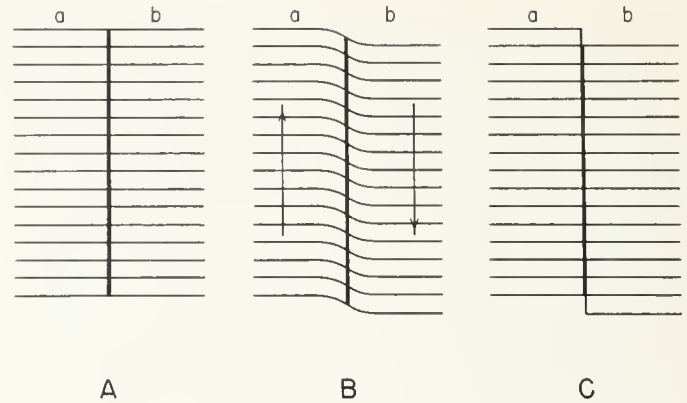
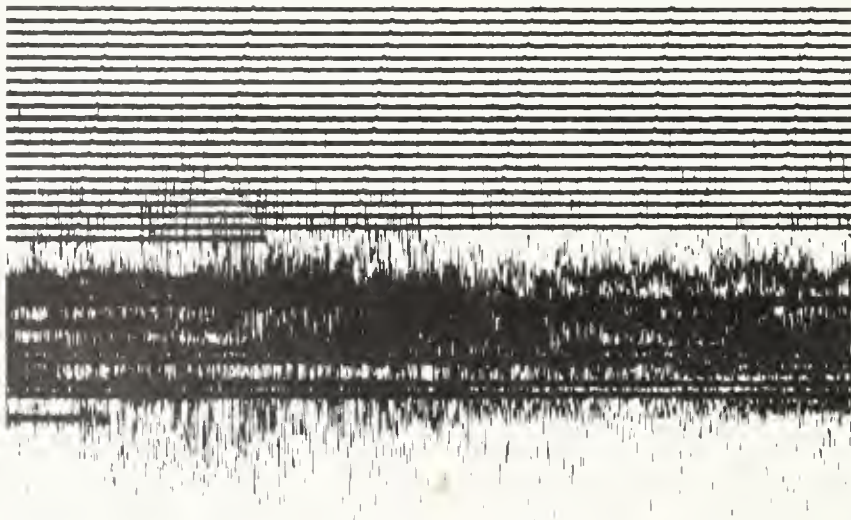


FIGURE 8. Schematic illustration of rebound theory. A, unstrained blocks; B, strain condition preceding earthquake; C, configuration just after earthquake.

or months by another of similar or greater magnitude in the same region. Every large shallow earthquake is followed by a great number (many thousands) of aftershocks (fig. 9). Occasionally swarms of small earthquakes occur without any principal large shock. In deep earthquakes the number of aftershocks appears to be much smaller than in shallow shocks although there may be a large number of small aftershocks which on account of their greater distance from sensitive instruments escape detection. The lack of surface waves in these earthquakes also makes their detection more difficult on seismograms written with older, long-period seismographs. The frequency of aftershocks is usually highest immediately following the principal shock and it falls off rapidly (fig. 10) with time so that usually the sequence ends within 1 or 2 years. Studies of aftershock sequences indicates that they are produced by elastic afterworking of the fault rock. With sensitive instruments located not too far from the epicenter, the ground is observed to be in continuous motion for intervals of one or more



PALOMAR SHORT PERIOD VERTICAL
1952 July 21, 11:52:51.8

FIGURE 9. Palomar high magnification seismogram covering first 4 hours after main shock. Successive lines are 15 minutes apart. Time marks are every 30 seconds.

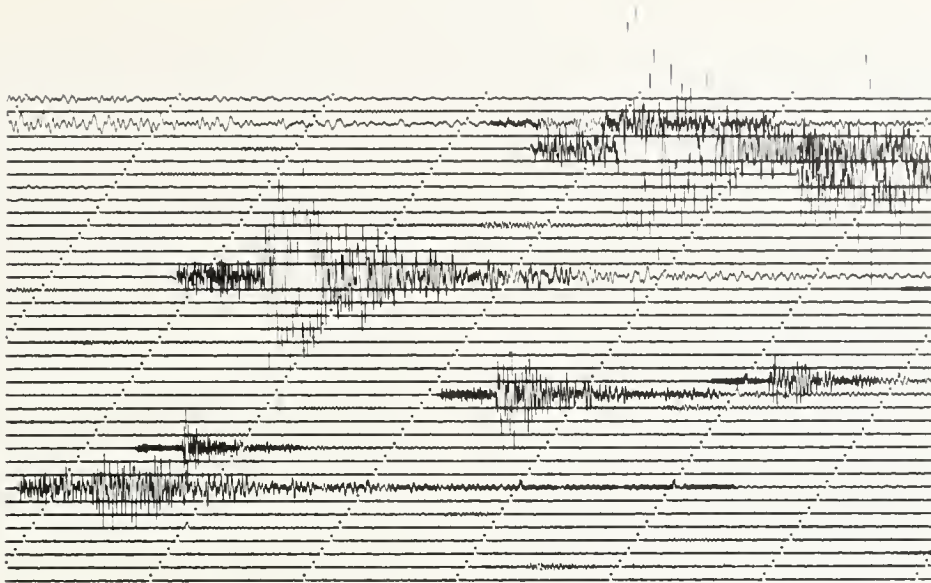


FIGURE 10. Portion of a seismogram written by NS torsion seismograph at Santa Barbara, July 23-24, 1952. Time marks are 30 seconds apart, successive lines are 15 minutes apart. Large phase in each shock is S. Surface waves are not yet well developed in these epicentral distances of about 100 to 150 km. Magnitude of largest shock is about $4\frac{1}{2}$.

days following a great earthquake as a result of the high frequency of aftershocks.

In great earthquakes the faulting movement may last for 1 minute or even more. The duration decreases rapidly with decreasing magnitude. With increasing distance from the source, the wave movement increases in duration so that at a distant station an earthquake which was generated by, say, 1 minute of faulting may record for 8 or more hours. Waves traveling within the earth and reflected from the various boundaries (fig. 7) including the surface of the earth have been observed to travel for more than one hour. Surface waves have been observed after seven complete circuits around the earth more than 12 hours after they started.

Observers in the vicinity of the epicenter of great earthquakes occasionally see large waves in the ground. However, these waves never leave any visible evidence of their movement such as failures in concrete, etc. and we are of the opinion they are an optical effect produced by the large fluctuations in atmospheric density with consequent variations in the index of refraction as a result of large vertical vibrations of the ground, particularly those connected with slow Rayleigh waves.

The frequency range of earthquake waves extends from some high frequency limit in the audible range to waves of at least 8 minutes and, perhaps, even nearly 1 hour period. The audio frequency components are often heard by many persons in the vicinity of the epicenter and can be very loud. These components however are rapidly

damped or scattered with distance from the source. Sound waves travel within the earth with speeds up to 20 times that of sound waves in the air.

Large earthquakes in the vicinity of coasts sometimes produce great ocean waves known as tsunamis. Usually the tsunamis occur only in regions adjacent to the great oceanic trenches. Several causes for the origin of tsunamis have been suggested. Since tsunamis have appeared with earthquakes whose epicenters lie up to 100 miles inland it has been assumed that these ocean waves were initiated by land slides on the steep slopes of the neighboring trench. Thus the source of the tsunami, on this hypothesis, is displaced both in space and time from that of the earthquake. In places where the fault slip extends to the ocean bottom in the region of a trench a dip-slip movement should produce a tsunami. If a trench lies within the epicentral region of a great earthquake it is possible that tsunamis may be generated by the long period surface waves. In the open ocean the distance from crest to crest of the tsunami waves may be several hundred kilometers. They travel at speeds ranging from about 70 meters per second in 500 meter deep water to 300 meters per second in 9 km deep water. Their periods usually range from about 15 to 30 minutes. Their amplitudes in the open ocean are small so that tsunamis are frequently missed by ships; upon approaching shore the amplitudes may rise to 20 meters or more.

2. THE MAJOR EARTHQUAKES OF CALIFORNIA: A HISTORICAL SUMMARY

BY V. L. VANDERHOOP

That portion of the earth's crust that has come to be known as California has been experiencing earthquakes since the beginning of time. At some periods in the geologic past, earthquakes were less frequent than at others. It may be that we are now living at a time of greater frequency, for it is likely that we are still witnessing mountain building of the episode which geologists call the Coast Range Revolution.

California (and the whole Pacific coast) is part of one of the great mobile belts of the earth, and relative turbulence and instability of the crustal rocks are characteristics only too plain during a major shock. It must be understood that this turbulence and instability cause changes in the landscape scarcely noticeable during the life span of a human being—probably less than effects produced by other concurrent geologic agents, such as erosion, volcanism and atmospheric circulation.

But the enormous forces (vastly greater than man-made nuclear explosions) released by a major earthquake do manifest themselves suddenly and the changes they often produce on the earth's surface are immediately apparent. This catastrophic aspect is seen in a few other geologic phenomena, notably volcanoes and landslides, and all have terrified man throughout the ages.

Much as science considers and evaluates earthquakes as normal natural phenomena capable of being recorded instrumentally with great precision, it is vitally necessary to consider them as another burden, when destructive, that man has to bear during his brief tenancy of the planet Earth. Literate people no longer impute supernatural causes to quakes, nor do they regard them as some sort of penance imposed for group sin. Rather they are looked upon as recurrent hazards, like fire and hurricanes, to be considered when a house is to be built. For after all, it is *man's* house that is shaken down. Lest we forget, he is the only earth inhabitant that constrains devices that unemotionally record the character of the quakes, and it is *he* that writes about them.

Scales of intensity reflect man's interest in what happens to him or his works: "destructive, generally felt, fall of chimneys," and the like are phrases useful in assessing the size of an earthquake where no instruments are located. But if we view quakes as a natural phenomenon, they are not destructive in the absolute sense; they merely cause a rearrangement, of greater or lesser degree, of certain components of the earth's crust, whether bricks, bric-a-brac, soil or bedrock.

In writing the history of an earthquake, as is done in the present volume, seismologists rely primarily on seismographic data to evaluate the fundamental nature of the shock, but it is very necessary to have also the testimony of eye (or sense) witnesses who are at or near areas of greatest intensity. For it is they who can describe the effects on the works of man, something the instruments cannot do. But in comparing numerous accounts of witnesses to the same event, we at once notice that there is disagreement over both major and minor details, as one would expect. This "phenomenon of uncertainty" is augmented in witnesses of an earthquake

because the witnesses' sense organs *are affected at the same time as his environment*. People, like structures, are affected differently, but nonetheless, the net impression is relative, not absolute.

Man's works are likewise affected according to their orientation and hence a witness is bound to be influenced by the behavior, during a quake, of any building he is in or near. One cannot help conjecturing that a person standing on a featureless plain could give a better account of an earthquake than one in a city! Professor Branner of Stanford University once looked into a phase of this matter and wrote an account which he entitled "The untrustworthiness of personal impressions of direction of vibrations in earthquakes." * Branner pointed out that "my own observations (of 23 years) of things overthrown lead me to attach very little or no importance to the direction in which they fall. In the California Earthquake of 1906, a vast amount of data was collected on this subject. Statues, monuments in cemeteries, chimneys and loose and unstable objects generally, were thrown in every conceivable direction. The direction in which such things fell was determined much more frequently by some accident of mounting, such as the shape of its base, than by the direction of any particular earthquake waves." And Branner concludes his account with this: "Instrumental records show that the directions are many and the movements complex. Out of such entangled movements it seems quite impossible for our uncertain impressions to gather trustworthy conclusions regarding the location of epicenters."

In the Hereford, England, earthquake of 1896, four hundred and sixty-nine observers made notes of their impressions of the direction of vibration. Dr. Charles Davison, who described this quake, noted that "when those directions are plotted on a map of the district, it is seen at once that they are either nearly parallel or perpendicular to the roads in which the observers were living; that is, the apparent direction of the shock was at right angles to one of the principal walls of the house. This, of course, is a result to be anticipated, for, whatever the direction of the earthquake motion, a house tends to oscillate in a plane perpendicular to one or the other of its walls."

The present writer happened to be at Saunders Ranch in Tejon Canyon during the Arvin-Tehachapi earthquake. This locality is about midway between the White Wolf and Garlock faults. Four of the five chimneys on the ranch house were thrown down in the direction of the Garlock fault and it was thereupon presumed that this fault was responsible for the shock. But further inspection revealed two cement sacks, once resting upon a low stone wall, thrown in the opposite direction, that is, west. If a conclusion can be drawn from this, it is that Branner and Davison are right.

In the 184 years since the first human record of an earth shock in California there have been about 5000 feelable quakes each year in the California-Nevada area, or about 2½ percent of those felt in the entire world and

* Bulletin Seis. Soc. America, vol. 5, No. 1, 1915

about 90 percent of those felt in the United States. 1200 were felt per year in southern California, or about one-half of 1 percent of the world's quakes. This means that there is an earthquake of sufficient intensity to be felt by a person somewhere in the California-Nevada area every hour and forty-five minutes, on an average, year in and year out. But of the 920,000 feelable earthquakes since the first record, only 43 can be classed as major shocks with a Rossi-Forel intensity of VII+ or greater. The incidence of major shocks averages only one every 4.3 years, which may offer comfort to some.

LIST OF MAJOR EARTHQUAKES, 1769-1952,
CALIFORNIA-NEVADA AREA

1769. July 28. Los Angeles region (near Olive). "On the 28th, when the governor (Portola) and his followers were on the Santa Ana River, four violent shocks of earthquake frightened the Indians into a kind of prayer to the four winds, and caused the stream to be also named Jesus de los Temblores. Many more shocks were felt during the following week; yet the foreigners were delighted with the region . . ." (Baneroft, Hist. Cal., vol. 1, p. 146, quoting from diaries of the expedition.) Both Holden and Townley rate this as a shock of R-F VI but Wood and Allen rate it as R-F VIII.

1790? Inyo County. Indian legends have it that a great earthquake similar to the one of 1872 occurred in the Owens Valley eighty years earlier. This quake is commonly assigned an intensity of R-F X. It would seem that a quake of this intensity would be widely felt and hence recorded in Spanish or Mission archives but it is not.

1800. October 11 to 31. R-F VIII or IX. San Juan Bautista.

"There were shocks of earthquake from the 11th to the 31st of October, sometimes six in a day, the most severe on the 18th. Friars were so terrified that they spent the nights out of doors in the mission carts. Several cracks appeared in the ground, one of considerable extent and depth on the banks of the Pajaro, and the adobe walls of all the buildings were cracked from top to bottom, and threatened to fall. The natives said that such shocks were not uncommon in that vicinity, and spoke of subterranean fissures, or caverns, caused by them, from which salt water had issued." (Baneroft, Hist. Cal., vol. 1, p. 559). On November 22 at San Diego, there was a shock of about R-F VIII. "The earthquake occurred at 1:30 p.m. and the soldiers' houses, warehouses, and the new dwelling of the volunteers (in the Presidio) were considerably cracked." (Baneroft, Hist. Cal., vol. 1, p. 654).

1812. May to December. R-F IX-X. San Juan Capistrano (December 8).

Forty lives lost by destruction of the mission, where Mass was being said. Damage also at San Gabriel. (December 21). Damage at San Fernando, San Buenaventura, Santa Barbara, Santa Ynez, and Purisima. Santa Barbara and Purisima Missions were completely wrecked and Santa Ynez was

damaged. A huge earthquake wave was reported at sea which broke along the Santa Barbara coast. A ship at Refugio was carried up a canyon and returned to sea. There was no record of loss of life at any of the missions. It has been suggested that this quake of December 21 had its origin on a submarine fault some miles offshore between Santa Barbara and Gaviota. The reported sea-wave resembled that of the other offshore quake of November 4, 1927 (q.v.). 1812 was recorded in mission archives as "el año de los temblores."

1836. ? June 9th or 10th. R-F VIII to X.

San Francisco Bay Region, possibly originating along Hayward fault, as did the great shock of 1868. Great fissures were said to have opened at the surface of the ground and aftershocks continued for a month.

1838. June and July. R-F VIII. San Francisco, San Jose, Santa Clara and Monterey.

Severe in San Francisco Harbor and damaging at Monterey and Redwood City. This shock has been ascribed by some writers as originating on Hayward fault but evidence seems to point properly to the San Andreas fault.

1852. November 9th. R-F VIII to X. Region of Ft. Yuma.

" . . . the camp was violently shaken by an earthquake, and the shocks continued almost daily for several months after, and were so frequent and expected as not to excite remark . . . the first shock threw down a portion of Chimney Peak (20 miles NE of Ft. Yuma) and opened fissures and cracks in the clay strata of the desert bordering the Colorado." Active mud volcanoes, with temperatures up to 170° F., were noted 40 miles southwest of the post. (Blake, Pac. R.R. Repts, vol. 5, p. 115-116, 1856).

November 26-30. R-F IX. Southern California.

1. Eleven strong shocks at San Simeon, Los Angeles and San Gabriel. Felt as far south as Guaymas, Mexico.
2. Long sequence of shocks felt from San Luis Obispo to the Colorado River and south to San Diego. Thirty-mile fissure reported in Lockwood Valley, Ventura County, near the San Andreas and Big Pine faults.
3. Two-minute shock at San Diego, followed by lighter ones for several days. Townley and Allen suggest that this epicenter may have been at Ft. Yuma with R-F IX owing to the long duration at San Diego.

1853. October 23. R-F VIII. Humboldt Bay.

Three heavy shocks. Houses were reported to have rolled like ships at sea and a wharf sank 4 feet.

1857. January 8 and 9. R-F IX-X. Fort Tejon.

One of the three or four strongest shocks in California since the advent of the white settlers. It was strongly felt from Ft. Yuma to Sacramento but was most violent at and near Ft. Tejon. Here all build-

ings and big trees were thrown down, and a fissure 20 feet wide and 40 miles long appeared, but closed with such force that a ridge 10 feet wide and several feet high was formed. Byerly says this ridge still exists at the head of Terwilliger Valley in Los Angeles County. Among the many things done by this shock were: caved in the roof of the Ventura mission, reversed the flow, temporarily, of the Kern River, threw the Los Angeles River out of its bed, formed new springs at Santa Barbara, changed part of the course of the San Gabriel River, and caused a great rumbling over most of the area of shock. This earthquake without doubt had its origin along the San Andreas fault from the Cholame Valley to San Bernardino and the epicentral region was perhaps in the Carrizo Plain with the Elkhorn scarp as the surface evidence remaining.

1858. November 26. R-F VII to IX. San Jose-San Francisco.

Very considerable damage to structures in San Jose, somewhat less in San Francisco where the daily papers described it as "a violent earthquake . . . consisted of two shocks, separated by an interval of a few seconds . . . at Musical Hall, where the Independent National Guard was having a ball, the shock was not noticed on the dancing floor, though the building was very much shaken" (!).

1860. March 15. R-F V-VI at Sacramento, VII at Carson City.

Felt as far east as Utah. A quake of large magnitude but with epicenter in sparsely populated areas, hence no reports of great damage.

1864. March 5. R-F VI to VII+. San Jose, Stockton, Santa Rosa, San Francisco, Santa Clara, Santa Cruz. Light at Visalia, strongest at San Francisco.

1865. October 1. R-F IX. Eureka and Fort Humboldt.

" . . . scarcely a house in town escaped fracture in its brickwork."

- October 8. R-F IX. San Francisco-Santa Cruz.

Two strong shocks close together. Structural damage in San Francisco largely confined to buildings on made ground and service mains in it. Some fissuring, especially in the Santa Cruz Mountains, and some rock slides. Brick structures overthrown at New Almaden mine. Epicenter probably on San Andreas Rift nearby.

1868. September 3-28. R-F IX. Headwaters of Kern River, Inyo County.

About a thousand shocks during this period, some very severe " . . . tall trees swayed and even the grass was observed to wave back and forth. Immense masses of boulders and earth were detached from the surrounding cliffs."

- October 21. R-F X. Hayward. IX San Francisco.

One of California's major earthquakes. Duration 42 seconds. 49 aftershocks, some heavy, reported to November 16. Most damage at Hayward and San Leandro, with 30 lives lost, mostly by falling

brick. San Francisco damage again largely to structures on made ground. Epicenter along Hayward fault, with horizontal surface displacement from San Leandro to Warm Springs (20 miles).

1871. March 2. R-F VII? Humboldt County.

Chimneys thrown down at Eureka, Petrolia, Rohnerville, Hydesville. Duration 20 seconds. "Severest for several years."

1872. March 26. R-F X. Owens Valley, Inyo County.

Commonly regarded as largest earthquake in California in historic time. Every masonry house in Lone Pine levelled. 27 fatalities, and 60 serious injuries. Few frame buildings but none seriously damaged. Ground disturbed for the 70 miles from Haiwee to Bishop along Owens Valley fault system. Maximum movements: horizontal, 20 feet; vertical, 23 feet. Shock felt in all of California and Nevada, parts of Utah and Arizona (about 125,000 square miles were sharply affected).

1873. November 22. R-F VII to X? Del Norte County and southern Oregon.

Felt from Portland to San Francisco but most severe in Crescent City, with reported damage to every brick building. Felt inland at Redding, Yreka, and Red Bluff.

1885. April 11. R-F VIII or higher. Central Coast Ranges.

Felt from Marysville to Ventura with probable epicenter on San Andreas Rift between Cholame and San Benito. A large quake but with small damage owing to unpopulated area of highest intensity.

1890. February 9. R-F VII? Southern California.

Three distinct shocks felt at Pomona, Los Angeles, San Diego. Character of waves and duration in above cities indicated a quake of large magnitude originating in the San Jacinto Mountains.

1892. February 23. R-F X? Southern California and Lower California.

Felt from Ensenada to Visalia. Plaster fell and walls were cracked in San Diego area. Epicenter probably in uninhabited region of Baja California east of Ensenada. This is perhaps the strongest shock reported in the period of 1873-1906.

- April 19-21. R-F IX-X. Solano County.

Extreme damage at Vacaville and Winters, especially to brick and stone structures. Fissures formed in bed of Putah Creek. Slight damage in San Francisco and Sacramento. Felt from Red Bluff to Fresno and as far east as Reno. The shock of April 21 may have been less intense than the one on April 19, but damage was just as severe owing to already weakened structures.

1893. April 14. R-F IX or X. Mendocino County Coast.

Mountain roads blocked by landslides and fallen trees, frame houses damaged at Greenwood, fall of chimneys and tombstones at Mendocino. Felt as far south as San Jose. Aftershocks continued for weeks.

1899. December 25. R-F IX or X. San Jacinto.

"Generally felt in southern California and Arizona. Brick and adobe structures were wrecked at San Jacinto and Hemet. Six Indians were killed and eight injured by collapsing adobe walls on the Coachella Reservation. A large-magnitude quake, felt over an area of 100,000 square miles."

1901. March 2. R-F IX. Stone Canyon, Monterey County.

"There were surface cracks in the ground, some of them hundreds of feet in length. . . . In some places there was a vertical displacement of one foot." Felt over an area of 40,000 square miles. Epicenter probably on San Andreas rift zone northwest of Cholame Valley.

1902. July 27, 31. R-F VIII to IX. Los Alamos, Santa Barbara County.

Severe locally, throwing down oil tanks near Lompoc and twisting and breaking surface oil pipes. At least one oil well (Lompoc Oil and Development Company #1) was lost by casing failure. Two more severe shocks occurred on July 31 and completed the total damage score at Los Alamos. Cracks, fissures and landslides contributed to the 5-day "reign of terror." Everybody left town.

1903. January 23. R-F X? (V or VI at San Diego). Imperial Valley.

This shock was recorded by seismographs all over the world and was no doubt of great intensity at its epicentral area, the uninhabited area south of Imperial Valley in Baja California.

1906. April 18. R-F X, Central California Coast.

"The San Francisco Earthquake." Probably the best known and certainly the most documented of the three great shocks of California history. Duration 40 seconds in San Francisco. 270 miles of surface rupture along San Andreas Rift from Fort Bragg to San Juan. Maximum horizontal displacement 21 feet near Olema. Vertical displacement small, and at north end. Perceptible over 375,000 square miles. Total damage to San Francisco by quake and resulting fire estimated from 350 million to 1 billion dollars. Total casualties in San Francisco between 500 and 1,000, 300 out of the city. All known quake effects observed on men, animals and things. $938 \pm$ aftershocks recorded from April 18 to June 10, 1907.

1909. October 28. R-F IX. Humboldt County.

Greatest damage at Rhonerville, with all brick and concrete structures reported damaged or destroyed. Lasted 22 seconds at Eureka. Felt over northwestern California and southwestern Oregon. Shaken area estimated at 100,000 square miles.

1915. June 22. R-F IX. Imperial Valley.

Two violent shocks, separated by 57 minutes, affected an area of over 50,000 square miles in southern California, western Arizona, and northwestern Mexico. Greatest damage (\$900,000) in El Centro, Calexico, and Mexicali. Epicenter along (?) San

Jacinto fault near latter two towns. Six casualties in Mexicali.

October 2. R-F X. Pleasant Valley, Nevada.

A very great earthquake with high intensity and large magnitude. Felt from Washington to the Mexican border and from the Pacific shore to Montana, Wyoming, Colorado, and Arizona, or an area of 500,000 square miles. Epicenter along great scarp which appeared suddenly at western pediment of the Sonoma Range south of Battle Mountain. Vertical displacement was 2 to 15 feet for 22 miles. After 38 years, this scarp still looks quite fresh. Damage slight, owing to lack of inhabitants. Very strongly felt in northeastern California (R-F IV-V).

November 20. R-F IX to X. Volcano Lake, Baja California.

Damage in Imperial Valley and Calexico. Intensity greatest at Volcano Lake near mouth of Colorado River. Seismograms indicate shaken area exceeded 120,000 square miles.

1918. April 21. R-F IX-X. San Jacinto and Hemet, Riverside County.

Ground cracked along San Jacinto fault, but no evidence of displacement. Chief damage to brick and artificial stone buildings. No loss of life. Felt over southern California from Taft to Mexico and east into Arizona. Area affected not less than 150,000 square miles.

1922. January 31. R-F X. Submarine, northwest of Cape Mendocino.

Intensity VI at Eureka. Recorded at 106 seismograph stations throughout the world. Shaken area at least 400,000 square miles. Magnitude probably as great as the shock of April 18, 1906.

March 10. R-F VIII+. Cholame Valley, Monterey, and San Luis Obispo Counties.

Cracks in ground along San Andreas fault. Chimney and house damage at Parkfield. Felt throughout central California and as far south as Los Angeles. Shaken area perhaps 100,000 square miles. Recorded at 43 stations, over most of the world.

1923. January 22. R-F IX. Submarine, near Cape Mendocino coast.

Damage at Petrolia, Dyerville, Ferndale, Alton, and other nearby towns. Recorded at 71 stations throughout the world.

1925. June 29. R-F IX-X. Santa Barbara and westward.

Nearly destroyed business district, especially poorly constructed buildings on made land in lower State Street. Felt from Watsonville through Mojave to Santa Ana. Total area affected at least 100,000 square miles. Recorded throughout the world and had an unusual number of aftershocks. Possible epicenters were Mesa Fault (submarine extension) and quickly triggered Santa Ynez fault, according

to Bailey Willis. Not a great shock, but of high intensity at a thickly populated area, resulting in several deaths.

1927. November 4. R-F IX-X. Submarine, west of Pt. Arguello, Santa Barbara County.

R-F IX near Surf with production of small sea wave of 6-foot rise. Probably R-F VIII at Lompoc, where chimneys fell and brick buildings damaged. Recorded over the world as a stronger shock than the Santa Barbara quake of 1925.

1932. June 6. R-F VIII+. Submarine, near Eureka. Much damage at Eureka and Arcata. One death from falling chimney.

1932. December 20. R-F X. Western Nevada near Cedar Mountain.

As strong as the 1915 Pleasant Valley shock. Surface rifts noted in belt of faulting 4 to 9 miles wide and 38 miles long. Felt over Pacific states. Little damage owing to lack of inhabitants.

1933. March 10. R-F IX. Long Beach and vicinity.

Not a great shock but as it occurred in a region of dense settlement with many buildings of poor construction, it ranks second only to the San Francisco quake of 1906 in destructive effect. Over 100 lives were lost and monetary damage reached an estimated 40 million dollars. Felt over a sea and land area of about 100,000 square miles. Epicenter just offshore along Inglewood fault.

1940. May 18. R-F X. Imperial Valley.

Eight deaths, 20 injuries. Damage to buildings, crops, canals, and railroads over six million dollars. Caused visible surface fault about 45 miles long from Imperial to Volcano Lake in Baja California. Maximum displacement was 14 feet, 10 inches, horizontally; apparently no vertical displacement. Felt over an area of 60,000 square miles in southern California and northern Baja California.

1952. July 21; August 22. Arvin-Tehachapi. Bakersfield.

See this volume for data.

While the earthquakes listed above have been very briefly treated, it is felt that the discussion is adequate to give the reader a fair appraisal of what is known of historic shocks in the California-Nevada region. For those who wish to inquire further into the matter, a list of definitive works is given below; from it this article was largely derived.

1. Holden, Edward S. Catalogue of earthquakes on the Pacific Coast, 1769-1897. Smithsonian Misc. Collections, No. 1087 (1898).
2. MeAdie, Alexander. Catalogue of earthquakes on the Pacific Coast, 1897-1906. Smithsonian Misc. Collections, Vol. XLIX, no. 1721 (1907).
3. Townley, Sidney D., and Allen, Maxwell W. Descriptive catalogue of earthquakes of the Pacific Coast of the United States, 1769 to 1928. Bull. Seismological Soc. America, vol. 29, no. 1, Jan. 1939. (This list is the most recent and complete catalog and offers many additions, corrections and emendations to the two previous lists.)
4. Wood, H. O., Allen, M. W., and Heck, N. H. Earthquake history of the United States, Part II—California and Nevada. U. S. Dept. Commerce, Coast & Geodetic Survey, Serial 609, 1939.

Two important papers must be mentioned here, for they throw much light on any inquiry into the field of earthquake study. One is the Report of the State Earthquake Investigation Commission (Carnegie Institution of Washington, 1908) on the San Francisco earthquake of 1906, without doubt the most comprehensive and detailed piece of research ever done in the field of seismology. The other paper is by George D. Louderback and is an account of the history of the University of California seismographic stations. It was published in the Bulletin of the Seismological Society of America for January 1941. Here Dr. Louderback has shown that the first earthquake-recording instruments ever used in North America were set up simultaneously at Berkeley and Mount Hamilton (Lick Observatory) in 1887 and the first shock ever instrumentally recorded in the United States was one on April 24, 1887, with an intensity of R-F II.

3. SEISMIC HISTORY IN THE SAN JOAQUIN VALLEY

BY C. F. RICHTER

The part of Kern County most affected by the earthquakes of 1952 has been shaken in the past about as hard and as frequently as most sections of California. Geologists and seismologists examining the historical record have attributed most of this disturbance to the great faults marginal to the area—the San Andreas fault, the Garlock fault, and the major Sierra Nevada fault. Instrumental records of recent years, in this area as in others, show that minor shocks originate at points rather generally peppered over the map, and only the larger shocks can be taken as related to the principal faults. Geological field evidence, in agreement with the imperfect historical record, indicates that no great earthquake is likely to have originated on the western part of the Garlock fault in historical time.

Most of the information obtained before 1927 is non-instrumental. The most complete account available is that by Townley and Allen (1939), from which most of the following list is abstracted.

1852 October 26. Strong at San Simeon, possibly related to the next or an error in date.

1852 November 26. (See VanderHoof, Part II, 1)

1853 February 1. Violent shocks at San Simeon.

1853 June 2. Plains of the San Joaquin. Two smart shocks. Similar shocks apparently on July 12 and September 2.

1857 January 9 (See VanderHoof, Part II, 1)

Several authors have considered that the shock of 1857 was larger than that of 1906; the present writer prefers the opposite opinion.

1868 September 4. A strong shock apparently originating near the headwaters of the Kern River, where a party was in camp. Numerous aftershocks, many of them felt at Lone Pine.

1872 March 26. The great Owens Valley earthquake, felt strongly in the San Joaquin Valley.

1882 December 19. Shock felt at Bakersfield and Visalia.

1885 April 11. Strong shock originating in the Coast Range, probably in Las Tablas district about 30 miles northwest of San Luis Obispo; more probably associated with the Nacimiento fault than with the San Andreas fault. Strong as far east as Visalia; plaster cracked at many places in the San Joaquin Valley.

1889 September 29. Strong near Bishop; felt as far as Bakersfield.

1890 February 13. Three light shocks felt at Tehachapi.

1890 July 24 or July 25. "Severe" at Bakersfield; felt at Porterville.

1894 July 29. Felt from Bakersfield to San Diego. Minor damage (goods off shelves, etc.) at Mojave and in the Los Angeles area.

1896 August 17. Plaster cracked at Hanford. Clocks stopped at Bakersfield and Merced. Felt at Fresno and Visalia.

1903 January 7. Alarmed persons into the streets at Bakersfield.

1905 January 5. Felt at Bakersfield and Wasco; apparently also reported at Lone Pine, Claremont and Riverside.

1905 March 18. Felt at Isabella and Wasco. Heavy at Bakersfield, still more so at McKittrick.

1905 December 23. At Bakersfield much plaster fell, goods were thrown off shelves, and wide cracks opened in buildings. Much alarm. Felt at Wasco and Tejon Ranch.

1906 April 18. San Francisco earthquake; affected most of California. In the southern San Joaquin Valley it was relatively light; at Bakersfield windows and doors rattled, and some clocks stopped. The shaking was noticed at Isabella.

1908 November 4. Strong shock in the Death Valley region, felt at least as far as Tehachapi.

1910 May 6. Strong at Bishop; rock slides in Rock Creek. Felt as far as Bakersfield.

1915 May 28. Earthquake in the southern Sierra Nevada, strong enough to record at distant seismograph stations; sharp shock at Lone Pine and Bakersfield; felt northwest as far as Merced; reported at Glennville and California Hot Springs.

1916 October 22. Strong shock centering at Tejon Pass, felt over wide area. Probably, but not certainly, on the San Andreas fault.

1919 February 16. A shock similar to the preceding but centered farther west; damage occurred at Maricopa, and the shaking was strong at Belridge, Lebec, Grapevine station, and Gorman. The epicenter cannot have been far from that of 1952, but may nevertheless have been on the San Andreas fault.

1920 November 20. Dishes off shelves at Taft. Felt at Maricopa.

1921 March 26. Felt at Maricopa.

1921 November 15. Slight shock at Bakersfield and Edison.

1922 March 10. Large shock centering on the San Andreas fault. Damage at Parkfield and Cholame. Felt across the San Joaquin Valley and into the Sierra as far as Springville.

1922 August 17. Strong aftershock of the preceding, felt at least as far as Bakersfield.

1926 June 30. Strong shock in Kern River Canyon, with rock slides; sleepers awakened at Bakersfield and California Hot Springs; abrupt shock at Glennville. Light shock felt at Porterville, Lindsay, Tulare, Visalia, and as far as Pasadena and San Luis Obispo. This incomplete information suggests an epicenter near that of 1952, July 29.

Beginning with 1927, seismograms from the Southern California stations are available, but for the first few years epicenters are located approximately only. The following data are from files at Pasadena.

1927 July 8. At Bakersfield, dishes rattled heavily; felt by motorists; one parked car shifted. Felt sharply in Kern River oil fields; one abandoned well returned to production. Noticed at Fellows but not at McKittrick.

1927 September 17. Damage at Bishop; shock felt in the Sierra Nevada and San Joaquin Valley, and as far as Palmdale.

1929 March 12. Felt from Delano to Ventura; rather generally noticed in the southern San Joaquin Valley.



FIGURE 1. Instrumentally located epicenters, 1932 and 1934 to June 30, 1952, listed in table 1.

Table 1. Instrumentally located epicenters (plotted in fig. 1). 1932 and 1934- June 30, 1952. Limits Lat. 34° 45' N to 35° 45' N. Long. 118° 15'-120° 00' W.

Date	Lat. Deg. Min.	Long. Deg. Min.	Mag.	Quality	Date	Lat. Deg. Min.	Long. Deg. Min.	Mag.	Quality
1932—Jan. 7.....	34 45	118 40	2	C	1941—Feb. 21.....	35 42	118 22	3.5	B
Feb. 14.....	34 58	119 00	2.5	C	Mar. 13.....	35 23	119 18	3.5	C
Apr. 19.....	35 41	118 28	3.5	B	Mar. 30.....	35 05	119 17	3	C
June 22.....	34 55	119 05	2.5	C	June 4.....	35 25	119 18	4	C
July 25.....	34 53	119 00	2	C	Sept. 21.....	34 52	118 56	5.2	A
1934—Apr. 30.....	35 15	119 10	2.5	C	Sept. 21.....	34 52	118 56	3	B
May 6.....	35 40	119 18	3.5	B	Sept. 21.....	34 52	118 56	3	B
July 6.....	35 15	118 15	2	C	Sept. 21.....	34 52	118 56	3	B
July 12.....	35 05	118 40	2.5	C	Sept. 29.....	34 52	118 56	3	C
Aug. 25.....	35 34	119 51	3	B	1942—Aug. 10.....	35 44	118 25	3	C
Sept. 27.....	34 59	118 35	2	B	Dec. 5.....	35 00	119 03	3	C
Oct. 13.....	34 49	119 00	2.5	B	1943—Jan. 15.....	35 07	119 00	3	C
Nov. 16.....	35 00	118 53	2.5	C	Feb. 17.....	35 01	118 56	3	C
Dec. 5.....	35 06	119 00	3	C	May 19.....	35 43	118 26	2.2	C
Dec. 21.....	34 59	118 35	2	B	Oct. 7.....	35 02	118 56	3	C
1935—Jan. 23.....	35 27	119 15	4	C	1944—Jan. 21.....	35 34	118 51	3.0	C
Mar. 4.....	35 01	118 23	3	B	Jan. 21.....	35 34	118 51	3.1	C
Mar. 5.....	34 59	118 35	2.5	C	Jan. 22.....	35 33	118 55	2.9	C
Mar. 17.....	35 22	118 50	4	B	Jan. 22.....	35 33	118 55	2.5	C
Mar. 18.....	35 22	118 50	2.5	B	Jan. 26.....	35 33	118 55	2.9	C
Apr. 13.....	35 00	118 53	3	C	Jan. 27.....	35 33	118 55	2.4	C
May 10.....	35 42	118 22	3.5±	B	Jan. 28.....	35 33	118 55	3.5	C
6 shocks + 35 others prior to midnight May 18/19					Jan. 30.....	35 33	118 55	3.2	C
June 9.....	35 20	119 50	3.5	C	Jan. 30.....	35 33	118 55	3.2	C
June 11.....	35 42	118 22	4	B	Jan. 31.....	35 33	118 55	2.3	C
June 11.....	35 42	118 22	3	C	Jan. 31.....	35 33	118 55	3.1	C
June 18.....	35 42	118 22	2.5	B	Feb. 3.....	35 33	118 55	2.6	C
July 6.....	35 42	118 22	3	C	Feb. 23.....	35 27	118 30	3.6	C
July 7.....	35 11	118 59	3	C	May 31.....	35 32	118 47	2.3	C
Sept. 10.....	35 05	119 10	3	C	May 31.....	35 32	118 47	2.0	C
Sept. 22.....	35 15	119 09	3	C	July 26.....	35 42	118 20	2.7	C
Oct. 27.....	35 00	118 53	2.5	C	Sept. 30.....	34 57	119 00	2.9	C
Nov. 23.....	35 00	119 17	2.5	C	1945—Feb. 5.....	35 09	118 53	2.8	C
1936—Feb. 3.....	34 45	119 45	2.5	C	Mar. 15.....	34 49	119 00	3.0	B
May 3.....	35 42	118 22	4	C	Mar. 21.....	35 09	118 53	2.9	B
May 6.....	35 42	118 22	3	C	June 16.....	35 03	118 55	2.7	C
May 30.....	34 53	119 08	3	B	July 21.....	34 58	118 53	2.7	C
Aug. 4.....	35 00	118 53	3	C	July 24.....	34 54	118 57	3.4	C
Aug. 20.....	35 00	118 53	3	C	Sept. 3.....	35 35	119 15	3.2	B
Sept. 26.....	35 15	118 50	3.5	B	Nov. 14.....	35 24	118 55	3.7	C
Oct. 5.....	34 58	118 51	3.5	C	Nov. 30.....	35 12	119 12	2.9	C
Oct. 9.....	35 15	118 50	3	B	1946—Jan. 17.....	34 48	118 58	3.4	B
Nov. 28.....	34 49	119 00	4	B	Feb. 13.....	34 48	119 12	2.7	C
Nov. 30.....	34 55	119 20	3	C	Feb. 15.....	35 18	118 38	2.7	C
Dec. 22.....	34 55	118 15	2.5	C	June 5.....	35 39	118 21	4.3	A
1937—Jan. 19.....	35 42	118 22	4	B	June 5.....	35 39	118 21	3.7	B
Apr. 22.....	34 53	119 08	2.5	C	July 23.....	35 06	119 05	4.0	B
June 8.....	34 55	118 50	3	C	July 23.....	35 05	119 04	3.0	C
Oct. 4.....	35 00	118 53	2.5	B	July 25.....	34 54	119 07	2.9	C
Nov. 27.....	35 42	118 22	3.5	C	Aug. 20.....	35 30	118 25	2.6	C
Nov. 27.....	35 42	118 22	3.5	C	Aug. 20.....	35 30	118 25	2.7	C
Dec. 11.....	35 20	119 26	3.5	C	Nov. 5.....	35 15	119 00	2.6	C
Dec. 19.....	34 49	119 00	3	B	Nov. 25.....	35 06	119 03	3.2	B
1938—July 1.....	34 59	118 35	2.5	C	Dec. 29.....	34 58	119 13	3.0	B
Oct. 15.....	34 53	119 08	2.5	C	1947—Feb. 1.....	35 12	118 21	3.5	B
Dec. 4.....	35 06	118 30	3	C	Feb. 1.....	35 12	118 21	2.4	C
1939—Feb. 23.....	34 52	119 01	4.6	A	Feb. 3.....	34 59	118 49	3.0	C
Feb. 23.....	34 52	119 01	3	B	Feb. 6.....	35 31	118 42	2.4	C
Feb. 23.....	34 54	119 00	4.8	A	Feb. 7.....	35 28	118 43	3.1	C
Feb. 23.....	34 54	119 00	3.5	B	Feb. 9.....	35 28	118 43	3.0	C
Feb. 23.....	34 54	119 00	3	B	Feb. 10.....	35 30	118 45	2.7	C
Feb. 23.....	34 54	119 00	3.5	B	Feb. 10.....	35 30	118 45	2.8	C
Mar. 7.....	34 49	119 00	4	B	Feb. 12.....	35 27	118 25	3.2	C
Apr. 14.....	34 50	119 00	2.5	C	Feb. 17.....	35 18	118 44	2.9	C
May 7.....	34 54	119 03	4.4	A	Feb. 25.....	35 32	119 05	2.9	C
June 20.....	35 42	118 22	3	C	Mar. 18.....	34 45	118 43	2.5	C
July 21.....	35 05	118 18	3	C	July 17.....	34 57	119 20	2.8	C
July 24.....	34 49	119 00	2.5	C	Sept. 18.....	34 55	119 05	2.7	C
Aug. 19.....	35 15	119 09	3	C	Oct. 19.....	35 33	118 38	2.8	C
Oct. 9.....	35.7	118.3	2.5	C	Oct. 27.....	34 53	118 55	2.9	C
Oct. 25.....	35 02	119 16	3.5	B	Nov. 26.....	35 36	118 24	2.8	C
Oct. 25.....	35 02	119 16	3	C	1948—Feb. 5.....	35 12	119 05	2.9	C
1940—Jan. 18.....	34 58	118 59	2.5	C	Mar. 14.....	35 05	118 29	2.6	C
July 12.....	34 59	118 35	3	C	Mar. 19.....	35 15	119 25	2.9	C
July 29.....	35 06	119 05	3.5	B	Mar. 20.....	35 15	119 25	3.2	C
Aug. 6.....	34 50	119 13	3.5	B	Mar. 23.....	35 15	119 25	3.3	C
Oct. 23.....	34 49	119 00	3	C	Apr. 3.....	34 53	119 01	3.4	C
Nov. 17.....	35 00	119 30	3	C	Apr. 20.....	35 18	118 58	2.9	C
1941—Jan. 20.....	35 20	119 15	4	C	May 6.....	34 59	118 25	2.7	C
Jan. 23.....	35 20	119 12	3	C	May 28.....	35 30	118 30	3.0	C
Feb. 9.....	34.9	119.1	2.5	C	May 31.....	35 30	118 30	2.9	C
					July 20.....	35 02	118 58	3.0	C

Table 1. Instrumentally located epicenters (plotted in fig. 1), 1932 and 1934—June 30, 1952. Limits Lat. 34° 45' N to 35° 45' N, Long. 118° 15'–120° 00' W.—Continued.

Date	Lat. Deg. Min.	Long. Deg. Min.	Mag.	Quality	Date	Lat. Deg. Min.	Long. Deg. Min.	Mag.	Quality
1948—Sept. 16	35 00	118 30	2.7	C	1950—Dec. 7	35 31	118 49	2.6	C
Sept. 16	35 00	118 30	3.0	C	Dec. 10	35 30	118 49	2.4	C
Sept. 28	35 30	118 58	4.2	C	Dec. 14	35 03	119 10	4.4	B
Oct. 27	35 01	119 02	2.8	D	Dec. 15	35 31	118 52	2.6	C
1949—Jan. 22	34 45	118 59	3.0	B	Dec. 17	34 54	118 52	2.5	C
Mar. 26	35 40	118 20	3.1	C	1951—Jan. 19 GCT	35 01	118 30	3.2	B
Apr. 20	34 59	119 12	3.0	C	Mar. 26	35 01	118 56	3.6	B
June 21	35 02	119 00	3.2	B	May 13	35 15	119 04	3.2	C
July 14	34 47	119 08	3.0	C	May 29	35 05	119 39	3.2	C
July 29	35 03	118 53	2.8	C	June 6	34 55	119 00	2.6	C
1950—Feb. 10	35 12	118 46	2.7	C	July 27	35 45	118 32	3.5	C
Mar. 12	34 58	118 23	2.6	B	Aug. 18	35 18	118 56	2.6	C
Mar. 18	35 31	118 21	2.9	B	Oct. 28	34 56	118 55	2.9	C
Mar. 23	35 05	118 20	3.0	B	Nov. 17	34 55	119 02	3.4	C
Apr. 15	35 45	119 37	4.6	C	Nov. 25	35 20	119 30	3.8	B
June 30	34 50	119 00	2.5	C	Dec. 15	35 15	119 07	2.9	C
July 11	35 23	119 15	3.6	C	Dec. 15	35 15	119 07	3.4	C
Aug. 10	35 43	118 15	3.6	C	Dec. 26	34 45	118 55	2.8	C
Sept. 10	35 44	118 20	3.2	B	Dec. 28	34 58	118 38	3.1	B
Sept. 22	35 41	118 19	3.0	C	1952—Jan. 1	35 16	119 08	2.9	C
Nov. 1	35 20	118 50	2.6	C	Mar. 7	35.0	119.2	2.5±	D
Nov. 3	35 13	118 45	2.5	B	Mar. 16	34 49	119 04	3.0	C
Nov. 28	34 56	119 19	2.8	C	Apr. 13	35 00	119 15	2.8	C
Dec. 6	35 29	118 49	2.9	C	Apr. 24	35 38	118 18	3.1	B
Dec. 7	35 31	118 49	3.0	B	June 14	34 55	118 50	2.7	C

The writer investigated this small earthquake in the field. Strongest apparent intensity appeared to be in the vicinity of Old River and Panama, where small objects were moved and old frame structures were slightly damaged. Seismograms at Santa Barbara and Pasadena indicate distances of 92 and 125 kilometers from those stations; these distances are within a few kilometers the same as for the major earthquake of 1952.

1930 October 30. Seismograms indicate a minor shock near Bakersfield.

1931 April 21. Shock similar to the preceding.

For 1932, and for 1934 to date, a bulletin on local earthquakes in southern California was issued from the Seismological Laboratory.

Table 1 is extracted from this bulletin, listing shocks in the area Lat. 34° 45'–35° 45' N, and Long. 118° 15'–120° 00' W. The epicenters are plotted in figure 1. Through 1950, records at Pasadena were kept in Pacific Standard Time, with no attention to the vagaries of daylight-saving time. This may occasionally affect the date of shocks near midnight when compared with other listing. Beginning in 1951, all records were kept in the universally standard Greenwich Civil Time (sometimes denoted G.M.T., but beginning the day at midnight); this is eight hours faster than Pacific Standard Time, or seven hours faster than the corresponding daylight-saving time. Shocks during the late afternoon according to either local time will hence appear as of the following day G.C.T.

In the earlier part of table 1, magnitudes are given to the nearest half unit; beginning 1943 they are given to the tenth. B indicates location believed trustworthy within about 5 kilometers (3 miles), C within about 15 kilometers (10 miles); A indicates that the shock is exceptionally well recorded and specially studied.

On July 25, 1932, a shock of magnitude 4.5 originated in the upper Kern River district. The epicenter was placed instrumentally (quality C) at 35° 48' N 118°

32' W, northwest of Kernville near the trace of the Kern Canyon fault. The shock was sharp, but caused no reported damage in the central area (but chimneys were reported cracked at Springville); it was felt across the Sierra Nevada from Owens Valley to San Joaquin Valley.

Table and map do not include the Walker Pass shocks of 1946. The principal shock of that group occurred on March 15, 1946; epicenter 35° 43' N 118° 02' W, magnitude 6½. The shock was felt over much of southern California. Weak structures were damaged at Weldon, Onyx, and some more distant points. Rock slides in Sand Canyon damaged the cover of the Los Angeles aqueduct. The epicenter named is that assigned by Chakrabarty and Richter (1949). This was based on the time-distance curves then being used as standard in southern California, but since revised. Mr. G. G. Shor finds that applying the later revision will not displace the epicenter more than a few kilometers.

Aftershocks of the Walker Pass earthquake tended to spread geographically in time; especially southwestward, into the Kern River area. One on June 5, 1946, included in the Chakrabarty-Richter study, has been placed by Mr. Shor at a revised location Lat. 35° 39' N., Long. 118° 21' W.

The shocks in 1939 and 1941 at Lat. 34° 52'–54' N., Long. 118° 56'–119° 01' W. are of particular consequence. They were included by Gutenberg (1943, 1944) in studies establishing standard travel times for the area. Reinterpretation since 1949 will not materially alter these epicenters, which are in the Wheeler Ridge block between the San Andreas and White Wolf faults. The times of these shocks were directly compared by Gutenberg with those of the major earthquake of 1952, in order to derive a preliminary epicenter for the latter (Lat. 35° 00' N., Long. 119° 00', only slightly modified since); the relative placing of these shocks to that epicenter is therefore unusually precise.

4. SEISMOGRAPH DEVELOPMENT IN CALIFORNIA

BY HUGO BENIOFF

ABSTRACT

A number of new forms of seismographs have been developed in California. These include the torsion seismograph, the variable reluctance transducer electromagnetic pendulum seismograph, the electromagnetic linear strain seismograph and the fused quartz secular strain gage.

As California is the most seismically active state of the Union, it is not surprising that the development of seismographs has been prosecuted vigorously here. However, up to about 1923, seismographs operating in California were few in number and for the most part of old or obsolete types. The impetus of the new program of development was given by H. O. Wood (1916), who was the first to point out that for the study of seismicity of a region such as California, a coordinated network of stations is required in which each station is provided with accurate time and seismographs of special characteristics. Although at that time there existed in Japan a large number of stations in a relatively small area, they were not provided with sufficiently accurate recording-drum drives and inter-station time, and the seismographs were of inadequate magnification to record the high frequencies observed in local earthquakes.

The first instrument to appear on the new program was the torsion seismograph, invented by Dr. J. A. Anderson and developed jointly by him and H. O. Wood (1925). Essentially, it consists of a horizontal pendulum in the form of a small copper mass eccentrically mounted on a vertical taut wire suspension as shown in figure 1. Damping of the pendulum motion is provided by the reaction of eddy currents generated in the mass with the field of a permanent magnet in which the mass is immersed. Horizontal vibration of the ground results in angular vibration of the pendulum mass about the suspension. A small mirror attached to the mass serves to deflect the recording light beam which comes to a point focus on the sensitive emulsion of a paper or film wrapped around the recording drum. For recording rapid earth movements, the pendulum mass is con-

structed in the form of a small cylinder, 2 millimeters in diameter and 25 millimeters long. The free period of vibration of the pendulum rotating about its suspension is 0.8 second. With this instrument the magnification, defined as the ratio of light spot displacement to ground displacement, has a maximum value of 2800.

For recording the slower wave movements which are generally observed in distant earthquakes the pendulum mass is built in the form of a rectangular plate of copper with dimensions approximately 25 x 8 x 1 millimeters. This pendulum has a free period of 6 seconds and a maximum magnification of 800.

The magnifications of these instruments were too high for recording the principal ground movements in large, nearby earthquakes and consequently a modified form of the torsion seismograph was developed for these movements by Dr. Sinclair Smith of the Mount Wilson Observatory staff. In this strong motion seismograph, the pendulum was made up of two masses of unequal size, mounted at opposite ends of a horizontal bar supported by a vertical torsion suspension through its center. This instrument has a period of 10 seconds and a maximum magnification of 4. It wrote satisfactory seismograms of the Long Beach earthquake of 1933 and the Kern County shock of 1952.

However, for most routine studies of local earthquakes the maximum obtainable magnification of the torsion seismograph was inadequate. In addition, a satisfactory instrument of this type for recording the vertical component of the ground motion was never made. To meet these limitations, a new form of electromagnetic pendulum seismograph was developed in 1931 (Benioff, 1932). In this instrument the movement of the pendulum generates electric power by means of a variable reluctance electromagnetic transducer. Recording is accomplished with a galvanometric photographic system. Earlier forms of electromagnetic instruments used moving conductor transducers and were constructed with long periods and relatively low magnification. With the magnetic materials available before 1931 it was not possible to construct instruments of the moving conductor type having sufficiently short periods and high magnifications for an adequate study either of local earthquakes or of the short period waves of distant earthquakes. The variable reluctance transducer represents an embodiment of the telephone receiver principle in which a permanent magnet supplies magnetic flux through an associated armature in series with one or more air gaps. In the latest model (fig. 2) movement of the seismometer pendulum varies the lengths of four air gaps in such a way that for a given direction of movement of the pendulum, two of the gaps increase in length while the other two decrease. The resulting changes in flux through the armatures generate emfs in the output coils surrounding them. In order to produce a large electrical output without recourse to amplifiers, the pendulum mass was made large—100 kilograms. In the vertical component instrument the mass is supported by a helical spring, as shown in figure 2, which in later models is made of an Elinvar-type alloy having a low temperature coefficient of elasticity. Six

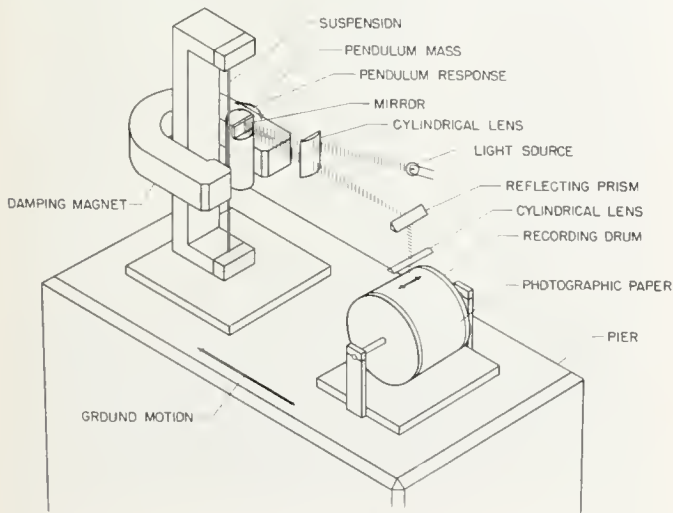
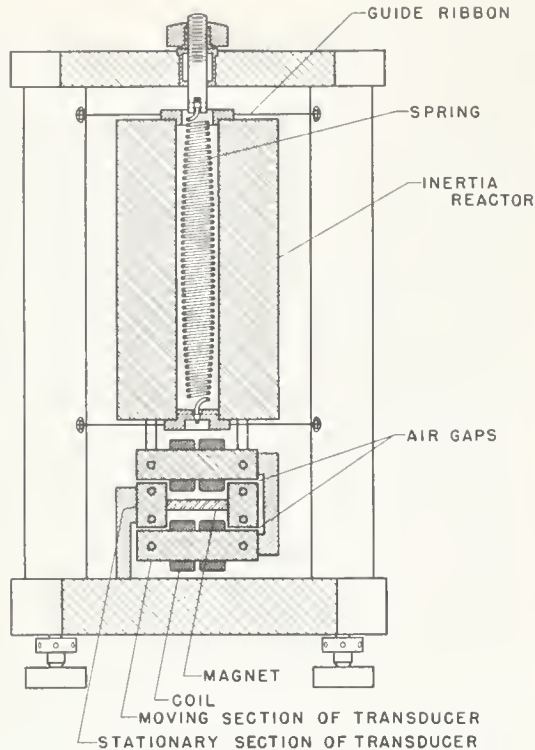


FIGURE 1. Schematic representation of torsion seismograph.

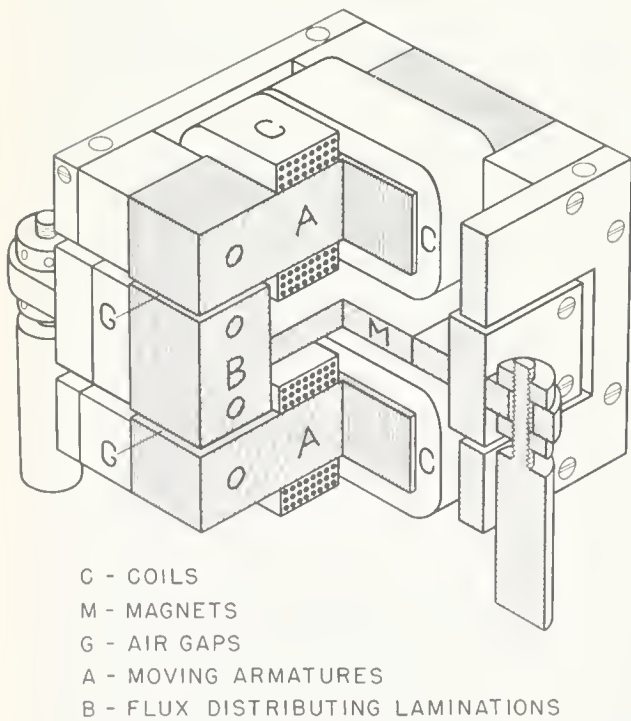


SCHEMATIC SECTION, VERTICAL COMPONENT VARIABLE RELUCTANCE SEISMOMETER H. BENIOFF - 1932

FIGURE 2.

steel ribbons stretched radially between the cylindrical mass and the three steel supports of the instrument serve to constrain the movement of the pendulum to the vertical direction only.

In the original form, damping was provided by a dashpot mechanism in which a perforated disc attached to the pendulum moved in a cylinder containing oil. Later in 1932 (Benioff, 1934) the transducer design was modified (fig. 2) to increase the efficiency to the point where damping of the pendulum was derived solely from the reaction of the output currents. The efficiency of the seismograph was thus raised to the maximum possible value. Referring to the cut-away transducer drawing (fig. 3), M is the magnet in the form of a 3-inch-square plate, $\frac{5}{8}$ inch thick; B is the flux distributing armature originally formed of laminations of silicon steel and later of nickel steel alloy; G, G are the air gaps; A, A are the laminated alloy armatures around which are wound the coils C, C. The portion of the structure including the magnet and distributing armatures B is attached to the frame of the instrument. The rest of the transducer structure moves with the pendulum. In addition to a greatly increased efficiency, this transducer also provides a negative restoring-force for overcoming approximately nine-tenths of the positive restoring-force of the spring. The whole seismometer can thus be made very much more rugged than would be possible without the negative restoring-force. Moreover, since the gaps are large (2 millimeters) close manufacturing tolerances are not required. In the latest model having an alloy spring, this pendulum remains stable and in operating condition over a temperature range of 55 degrees centigrade. The power



- C - COILS
- M - MAGNETS
- G - AIR GAPS
- A - MOVING ARMATURES
- B - FLUX DISTRIBUTING LAMINATIONS

VARIABLE RELUCTANCE TRANSDUCER

H. BENIOFF - 1932

FIGURE 3. Cut-away drawing of variable reluctance transducer.

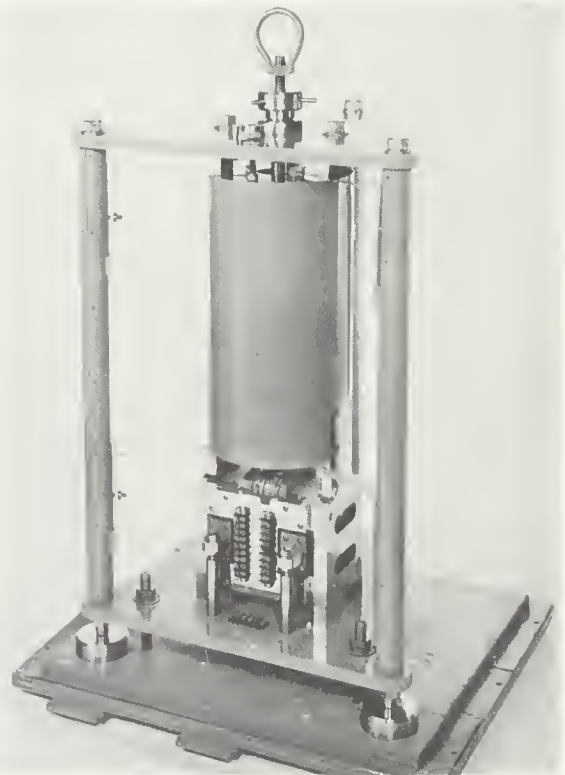


FIGURE 4. Vertical component variable reluctance electromagnetic seismometer.

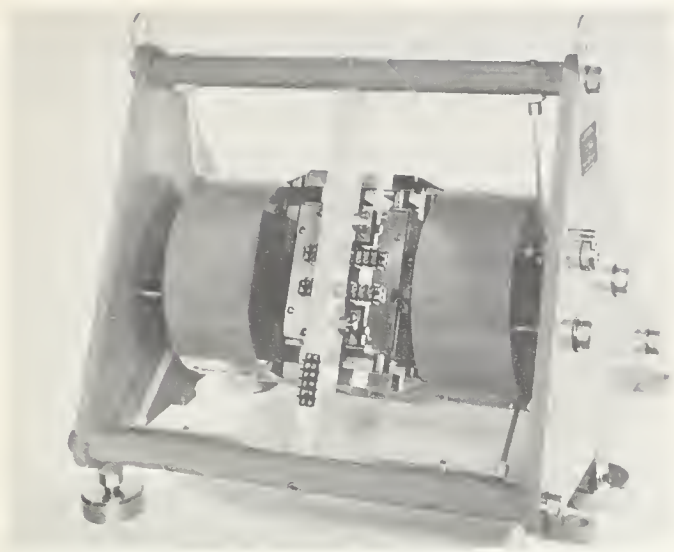


FIGURE 5. Horizontal component variable reluctance electromagnetic seismometer.

output of this seismometer, derived solely from the energy of the seismic waves, is sufficient to operate two galvanometers simultaneously. The transducer is provided with eight identical coils. In the standard form, four of the coils are connected in parallel to form a generator of 31 ohms resistance for operation of an 0.2 second period galvanometer and the other four are connected in series to form a 500 ohm generator for driving a 90 second period galvanometer. The latest model of the vertical component instrument as manufactured by the Geotechnical Corporation, Dallas, is shown in figure 4.

A similar design was developed for the horizontal component instrument shown in figure 5. In this component the steady mass is supported by two of the six constraining ribbons. Restoring-force is provided in part by gravity and in part by tension of the ribbons. In other respects the electrical and mechanical characteristics of the horizontal seismometer are identical with those of the vertical component. Both are operated with a free period of 1 second and with critical damping. With the two standard galvanometers these seismographs have recorded waves ranging in period from $\frac{1}{5}$ second in the case of small local earthquakes to 4 minutes in the surface waves of the Assam earthquake of August 15, 1950. The maximum effective magnification of these instruments is limited solely by the ground unrest, which is present everywhere on earth. In regions where the unrest is small, the maximum useful magnification approaches 500,000 for the short period galvanometer combination.

Another new type of seismograph was developed at the Seismological Laboratory in 1931 (Benioff, 1935). Up to this time all existing seismographs were of the pendulum type in which the response is derived from the relative motion of the pendulum mass and the vibrating ground. In this new form, known as the linear strain seismograph, the response is derived from the actual strain or distortion of the ground produced by the seismic waves. This strain is brought about as a result of the finite speed of propagation of seismic waves so that the phase of motion at a given point is different from that at another point along the line of propaga-



FIGURE 6. Schematic representation of linear strain seismometer.

tion. In the original form (figure 6 and figure 7) the instrument consisted of two steel piers set into the rock at points 20 meters apart. A two-inch iron pipe rigidly attached to one pier extends to within a short distance of the other pier. The pipe is suspended by 12 wire supports which are longitudinally compliant and relatively rigid in the transverse direction (figure 8). When a seismic wave traverses the site of the seismometer the two piers alternately approach and recede from each other. The free end of the pipe is thus displaced to and fro relative to the adjacent pier and this relative motion serves to actuate a variable-reluctance transducer similar to the one previously described for the pendulum instrument. The transducer output power is recorded galvanometrically as in the pendulum seismographs described above. Since the response of this instrument is derived



FIGURE 7. Original electromagnetic linear strain seismometer.

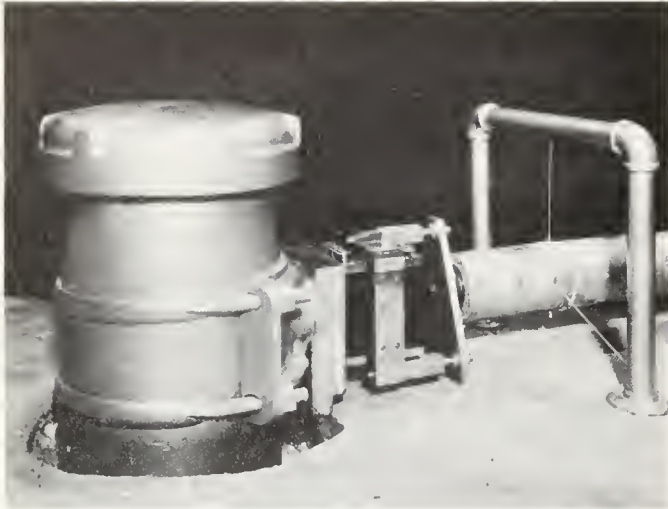


FIGURE 8. Transducer end of electromagnetic linear strain seismometer showing pier, transducer and one of the supports for the indicator tube.

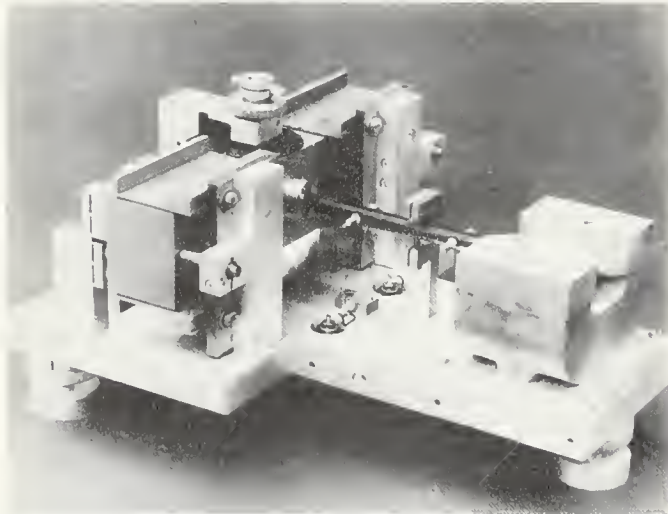


FIGURE 9. Vertical component variable capacity seismometer.

from ground strain rather than displacement, as is the case with the pendulum seismographs, its directional and frequency characteristics differ radically from those of the pendulum instruments. Observations made with this instrument taken by themselves and in combination with those of the pendulum instruments, provide information concerning seismic waves which cannot be had from pendulum instruments alone. The seismogram of the Kamchatka earthquake of November 4, 1952 written by this instrument with a recording galvanometer of 3 minutes period, contained waves of 51 minutes period—much longer than any waves that have been observed hitherto. The effectiveness of this instrument for very long period strains such as the secular strains which generate earthquakes, is limited by the thermal expansion characteristics of the indicator pipe. Thus with the steel pipe, changes of temperature of 1 degree centigrade produce movements of the free end corresponding to strains in the earth of 10^{-5} . In an attempt to measure secular strains and also tidal strains produced by the

sun and moon, a modified form of the linear strain instrument is being set up in a tunnel situated in the mountains north of Glendora. A tunnel such as this should exhibit very small temperature variations. Moreover, in order further to reduce the thermal response of the instrument, the indicator pipe is constructed of fused quartz—a substance having a thermal expansion of only five parts in ten million per degree centigrade. The instrument is nearing completion at the time of this writing. Should the preliminary experiments indicate that this instrument operates in accordance with expectations, it is hoped that a large number of instruments of this kind can be distributed throughout the state. With such a network it should be possible to determine the nature of the strain patterns which generate our earthquakes and from these learn something as to the origin of the forces which produce strains. Moreover, given enough time, possibly one or two centuries, a study of the strain pattern variations in relation to the sequence of earthquakes may provide a sufficient basis for approximate predictions of the times and locations of future earthquakes.

Another type of pendulum seismograph has been developed by the writer primarily for operation of visible writing recorders and magnetic tape recorders. This instrument is provided with a transducer of the variable discriminator type for operation with a high frequency oscillator of constant frequency (figure 9). The rectangular mass is positioned between two sets of fixed plates to form two condensers of equal capacity when the pendulum is in the rest position. The two condensers are each shunted by identical inductances. The two tuned circuits thus formed have the same resonant frequency. The inductances are coupled to the output circuit of a crystal oscillator operating at a frequency of 5.35 megacycles. When the pendulum is in its rest position the two circuits are each detuned 50 kc from the crystal frequency at which point they each have currents approximately 0.7 times their resonant value. Outputs from the two tuned circuits are rectified by two

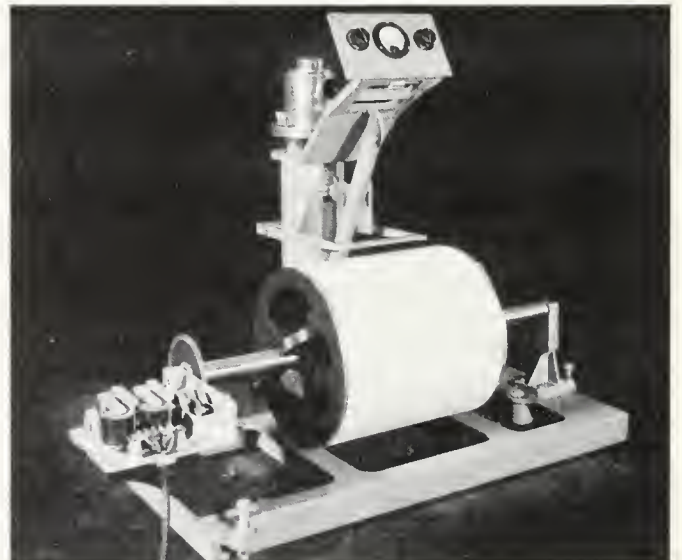


FIGURE 10. Short period galvanometer recorder using photographic paper.

germanium crystal diodes. The difference between the two rectified outputs is proportional to the movement of the pendulum. For recording directly with a galvanometer the diodes are connected through two high resistances to the galvanometer and a large series capacitor. The capacitor thus serves to eliminate the slow current drifts. For operation of other electronic devices, the outputs go to push-pull amplifiers. The amplifiers in turn may serve to operate visible writing and/or magnetic tape recorders. In the latter instrument, in use at the Seismological Laboratory in Pasadena, recording is effected at a tape speed of $\frac{1}{2}$ mm/sec. When played back at the normal 15 inches/sec, the seismic frequencies are accelerated approximately 750 times and are transformed into the audio range of frequencies in which form they can be analysed with audio frequency instruments.

Galvanometer Recorders. The galvanometer recorders use drums which accommodate photographic paper sheets 30 x 90 cm, or 90 cm lengths of 35 mm film. For local earthquakes the paper recorders operate with a writing

speed of 1.0 mm/sec and the film recorders 0.25mm/sec. Figure 10 shows one of the paper recorders operating with a short period (0.20 sec.) galvanometer. This drum was designed by Howell and Sherburne of Pasadena and has come to be known as the Henson drum. (Henson was one of the early manufacturers of seismographs described in this paper.) For each revolution the drum advances axially $2\frac{1}{2}$ mm by means of a screw located within the axis of the instrument. One standard sheet is thus covered in 24 hours with successive recording lines 15 minutes apart. The film recorders operate at one-fourth the speed of the paper recorders and the line spacing is also reduced. However, the increased resolution of film as contrasted with paper more than offsets the effects of the slower speed. In the early days the power line was not controlled in frequency and consequently in order to rotate the drums at a sufficiently uniform rate a tuning fork controlled drive was developed. However, at present most installations are driven by small synchronous motors operated by the 60 cycle power line.

5. SEISMOGRAPH STATIONS IN CALIFORNIA

BY B. GUTENBERG *

ABSTRACT

A short history of seismograph stations in California is given. Stations in neighboring states which contributed information to the study of the Kern County earthquakes in 1952 are listed. Detailed information is given for stations in California which recorded the shocks in 1952; this includes a list of installations with portable instruments in the epicentral area from July 21 to November 13, 1952.

The first instruments in the United States to record earthquakes seem to have been installed at Berkeley and at Lick Observatory in 1887 (Louderback, 1942). The equipment at each station included two horizontal Ewing seismographs and one seismograph to record the vertical motion. The recording was started by the earthquake, and the three traces were recorded on the same rotating disk. Minute marks were made by a clock. Similar instruments were operating temporarily at several other locations in the same area. The San Francisco earthquake of 1906 was recorded at Berkeley, Oakland, Yountville, Alameda, San Jose, Los Gatos, Lick Observatory in California, and at Carson City, Nevada; most of these instruments had magnifications of about 4. Records were discussed and reproduced by Reid (1910). In 1910 instruments with higher magnification were installed at Berkeley and Lick Observatory and later better instruments and other stations were added with Berkeley as central station.

The need for a network of seismic stations in southern California was emphasized by Wood (1916) and, as a result, a network with Pasadena as central station was inaugurated jointly by the Carnegie Institution of Washington and the California Institute of Technology in 1923 (Day, 1938). In 1936, the Carnegie Institution transferred their part to the California Institute of Technology which has maintained and expanded the network since.

The two networks provide the bulk of the stations in California. Another of the oldest stations is that inaugurated in 1909 by the University of Santa Clara at the Ricard Observatory. The U. S. Coast and Geodetic Survey, recognizing the need for additional data about earthquakes in California, has installed two stations there, one near Ukiah, the other at Shasta in cooperation with the Bureau of Reclamation. Records of the Shasta station are now measured at Berkeley. In addition, the U. S. Coast and Geodetic Survey is operating many strong-motion instruments throughout California (see Part II, 12).

For location and study of earthquakes in California, records or reports of a number of stations in neighboring states are frequently used. Among them are the following which have made available records of the Kern County shocks for the present investigation: the Dominion Observatory station at Victoria, B. C., with three auxiliary stations; the station of the Division of Seismology at the University of Washington at Seattle; the station at the Department of Physics, Oregon State College at Corvallis, Oregon; the seismological station at Mt. St. Michael's, Spokane, Washington; the following

five stations, operated by the U. S. Coast and Geodetic Survey, partly in cooperation with local institutions (as indicated): Boulder City, Nevada (Bureau of Reclamation), Bozeman, Montana (Montana State College), Butte, Montana (Montana School of Mines), Hungry Horse, Montana (Bureau of Reclamation), Tucson, Arizona; furthermore the following independent stations: the station at the University of Nevada, Reno, Nevada (records are measured at Berkeley); the seismological station at Regis College, Denver, Colorado; the seismological observatory of the Texas Technical College at Lubbock, Texas; several seismological stations in Mexico, operated by the Instituto de Geofísica, Universidad Nacional de Mexico.

The following data on California stations which furnished records for the investigation of the Kern County shocks include the location of the instruments, and (for general information only) the main characteristics of the instruments. Cooperating agencies and institutions are given in parentheses. However, correspondence should be directed to the respective central stations. (There have been many changes and additions since the time of writing.)

Abbreviations used:

N = North latitude

W = West longitude

H = elevation in meters

BS = Benioff seismograph with short-period galvanometer; period of pendulum about 1 second, galvanometer period about $\frac{1}{4}$ second.

BL = Benioff seismograph with long-period galvanometer; same pendulum as preceding, galvanometer period of the order of 1 minute.

TS = standard Wood-Anderson torsion seismograph, period 0.8 seconds; maximum magnification about 2800 (for waves with periods of less than $\frac{1}{2}$ second).

TL = similar instrument with period of about 6 seconds; maximum magnification about 800 (for waves with periods of less than 5 seconds).

G = Galitzin seismograph; period of pendulum and galvanometer roughly 12 seconds.

S = Sprengnether seismograph: periods of instruments and galvanometer about 2 seconds; maximum magnification (for periods of about $1\frac{1}{2}$ seconds) about 3500 for horizontal components and amount 5000 for vertical components.

V = order of magnitude of maximum magnification for continuous sinusoidal waves; these values change considerably with time and should not be used for calculations without consulting the respective central stations. Where possible, the approximate ground period (or range of periods) to which V applies is added in parenthesis. Recording on film is indicated by VF which then refers to the record as viewed on the screen of a standard projector with 8x magnification.

* Manuscript received for publication July 13, 1953.

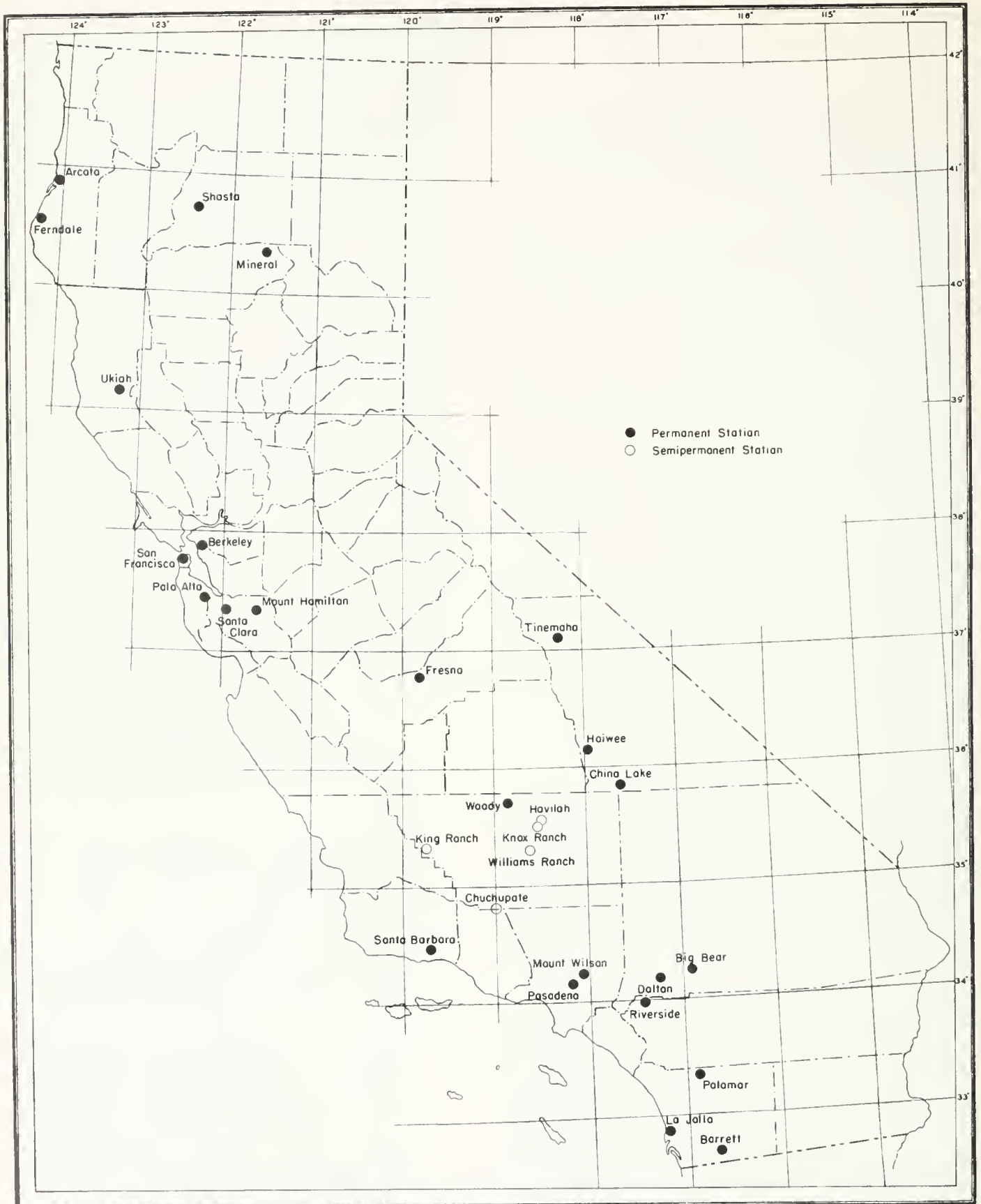


FIGURE 1. Map showing locations of permanent and semi-permanent seismological stations in California during 1952.

Z, EW, NS refer to vertical, east-west and north-south components respectively; the orientation of the horizontal instruments may deviate by $\pm 10^\circ$ from the given directions.

A. Instruments of the Pasadena group of stations:

Pasadena, Seismological Laboratory; N=34°08.9'; W=118°10.3'; H=295. Mailing address for all stations of this group: 220 North San Rafael Avenue, Pasadena 2, California.

BS, Z, EW, NS; V=30,000 (0.2 sec.)

BL, Z, EW, NS; V=2,000 (1 sec.)

Benioff capacity seismograph, Z, NS; V=8,000 (1 sec.)

Benioff strain seismograph, NS; V=300 ($\frac{1}{4}$ to 20 sec.); EW; V=100± ($\frac{1}{4}$ to 20 sec.)

TS, EW and NS TL, EW and NS.

Strong-motion seismograph, EW, NS; V=4 (0 to 5 sec.)

Mount Wilson; N=34°13.5'; W=118°03.4'; H=1742 (Mount Wilson Observatory, Carnegie Institution of Washington).

BS, Z; V=30,000 (0.2 sec.)

Riverside; N=33°59.6'; W=117°22.5'; H=250 (City of Riverside).

BS, Z; V=30,000 (0.2 sec.). TS EW and NS

Palamar; N=33°21.3'; W=116°51.6'; H=1700 (Palamar Observatory, California Institute of Technology).

BS, Z; V=30,000 (0.2 sec.). EW and NS; VF=30,000 (0.2 sec.)

La Jolla; N=32°51.8'; W=117°15.2'; H=8 (Scripps Institution of Oceanography, University of California).

TS, NS; V=2,800. Discontinued July 30, 1952.

Santa Barbara; N=34°26.5'; W=119°42.9'; H=100 (Santa Barbara Museum of Natural History).

BS, Z; VF=3000± (0.2 sec.)

TS, EW and NS; VF=2800 (0 to $\frac{1}{4}$ sec.)

TS, NS; V=2800 (0 to $\frac{1}{4}$ sec.). Discontinued on Dec. 23, 1952.

China Lake; N=35°49.0'; W=117°35.8'; H=766 (Naval Ordnance Test Station).

BS, Z; V=50,000± (0.3 sec.). BS, EW, NS; VF=30,000± (0.2 sec.)

BL, Z; VF=10,000± (1 sec.)

Haiwee; N=36°08.2'; W=117°57.9'; H=1100 (Bureau of Water and Power, City of Los Angeles).

BS, Z; V=6,000± (0.2 sec.)

TS, EW and NS.

Tinemaha; N=37°03.3'; W=118°13.7'; H=1180 (Bureau of Water and Power, City of Los Angeles).

BS, Z; V=30,000 (0.2 sec.)

BL, Z; V=1000± (1 sec.). NS; V=2000± (1 sec.)

TS, EW and NS.

Dalton; N=34°10.2'; W=117°14.0'; H=523 (Los Angeles County Flood Control District).

BS, Z; VF=30,000± (0.2 sec.); VF=2,000± (0.2 sec.)

Big Bear; N=34°14.3'; W=116°54.8'; H=2060 (Big Bear Lake Elementary School, Big Bear Lake, California).

BS, Z; V=30,000± (0.2 sec.)

Barrett; N=32°40.8'; W=116°40.3'; H=510 (Water Department, City of San Diego).

BS, Z; VF=40,000± (0.2 sec.) until December, 1952; V=40,000± (0.2 sec.) since February, 1953.

Benioff capacity seismograph, EW and NS; VF=8000± (1 sec.) since March, 1953.

Woody; N=35°42.0'; W=118°50.6'; H=500 (Kern County Forestry and Fire Department), installed on August 5, 1952.

BS, Z; V=30,000± (0.2 sec.)

Fort Tejon; N=34°52.4'; W=118°53.7'; H=980 (State Board of Beaches and Parks, Fort Tejon Historical Monument, State of California), installed on November 21, 1952.

BS, Z; V=30,000± (0.2 sec.)

The following are *temporary* installations; all were equipped with Benioff vertical seismographs and short-period galvanometers; constants were average and recording was on paper except for King Ranch, where recording is on film:

Chuchupate; N=34°48.5'; W=119°00.7'; H=1590; (Ranger Station, U. S. Forest Service), installed on July 21, 1952, discontinued on November 19, 1952.

Havilah; N=35°30.6'; W=118°31.0'; H=990; (Ranger Station, U. S. Forest Service), installed on July 25, discontinued on September 4, 1952.

Knox Ranch; N=35°29.0'; W=118°31.7'; H=1090; (Mr. and Mrs. Charles Knox), installed on September 4, discontinued on November 10, 1952.

King Ranch; N=35°19.7'; W=119°44.7'; H=670; (Elmer King Ranch, Mr. Charles Willis), installed on October 16, 1952.

Williams Ranch; N=35°17.9'; W=118°36.7'; H=430; (Mr. and Mrs. Boyd Williams), installed on November 10, 1952, discontinued on March 20, 1953.

In addition, for short intervals, portable instruments were set up in the epicentral area. Most of them consisted of a Benioff Vertical variable reluctance seismograph recording with a short-period galvanometer on photographic paper (indicated by *A* in Table 1). However, at two installations (indicated by *B*) a Benioff capacity horizontal seismograph was used recording on Sanborn heat sensitive paper by means of a hot stylus recorder, and at one location (*C*) this type of recorder was connected with a Benioff capacity vertical component.

Table 1. Installations with portable instruments.

Location	North Lat.	West Long.	Elevation meters	Instrument (see text)	Period (PDT) 1952
BED.....	35°05.7	118°24.7	1310	A	July 21
White Oak.....	34°59.1	118°31.0	1570	A	July 21-22
White Wolf.....	35°15.0	118°39.9	620	A	July 23-27
Shirley Meadow.....	35°42.5	118°33.8	2000	A	Aug. 13-14
Walker Dump.....	35°24.3	118°29.0	760	A	Aug. 14, 19-20
Piute Ranch.....	35°21.8	118°22.9	1150	A	Aug. 20-21;
				B	Sept. 3-5
Clear Creek.....	35°15.1	118°36.6	820	A	Aug. 21-22-
Kern Gorge.....	35°28.9	118°44.6	430	A	Aug. 27-28
Parker Creek.....	35°26.4	118°43.8	910	A	Aug. 28-29;
				B	Sept. 3-5
Clear Creek Ranch.....	35°14.8	118°36.5	825	C	Sept. 3-5
Elkhorn.....	35°09.3	119°28.2	720	A	Nov. 12-13
San Emigdio.....	34°59.6	119°11.0	435	B	Nov. 12-13

B. Instruments of the Berkeley group of stations (based mainly on information furnished by Mr. Charles E. Herriek, Berkeley).

Berkeley; N=37°52.3'; W=122°15.6'; H=81. Mailing address: Seismological Station, University of California, Berkeley 4, California.

G, EW and NS; V=1300 (6 sec.); Z; V=1000 (6 sec.)

BS, Z; V=30,000± (0.2 sec.)

TS, EW and NS

Bosch-Omori, EW and NS; V=40± (0 to 10 sec.)

Mount Hamilton; N=37°20.4'; W=121°38.6'; H=1282 (Lick Observatory).

BS, Z; V=30,000± (0.2 sec.)

TS, EW and NS

Palo Alto; N=37°25.1'; W=122°10.8'; H=83 (Stanford University).

BS, Z; V=20,000± (0.2 sec.)

TS, EW and NS

San Francisco; N=37°46.4'; W=122°27.2'; H=100 (University of San Francisco).

TS, EW and NS

Ferndale; N=40°34'; W=124°16'; H=17 (City of Ferndale) Bosch-Omori, EW and NS; V=40± (0 to 10 sec.)

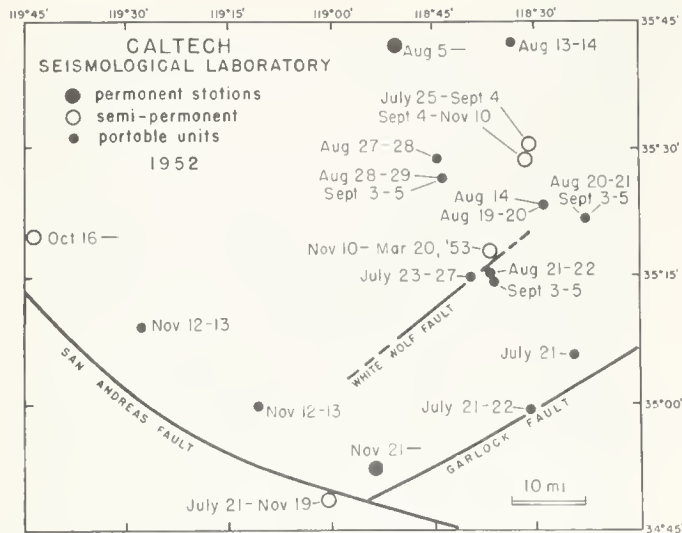


FIGURE 2. Map showing stations in the epicentral area.

Fresno; $N = 36^{\circ} 46.1'$; $W = 119^{\circ} 47.8'$; $H = 88$ (Fresno State College).

S; EW, NS and Z

Mineral; $N = 40^{\circ} 21'$; $W = 121^{\circ} 35'$; $H = 1495$ (National Park Service).

BS, Z; $V = 40,000 \pm (0.2 \text{ sec.})$

TS, EW and NS

Arcata; $N = 40^{\circ} 52.6'$; $W = 124^{\circ} 04.5'$; $H = 60$ (Humboldt State College).

S; EW, NS and Z

Shasta; $N = 40^{\circ} 41.7'$; $W = 122^{\circ} 23.3'$; $H = 312$ (U. S. Coast and Geodetic Survey in cooperation with the Bureau of Reclamation).

BS with galvanometer period of about $1\frac{1}{2}$ sec.; Z, EW, NS; $VF = 40,000 \pm (1 \text{ sec.})$

C. Other permanent stations

Santa Clara; $N = 37^{\circ} 21'$; $W = 121^{\circ} 57'$; $H = 27$ (University of Santa Clara).

G; Z, EW, NS; $V = 1000 \pm (6 \pm \text{sec.})$

Ukiah; $N = 39^{\circ} 08'$; $W = 123^{\circ} 13'$; $H = 27$ (U. S. Coast and Geodetic Survey in cooperation with the International Latitude Observatory).

McComb-Romberg seismograph; $V = 70$ (0 to 5 sec.)

Figure 1 shows the location of the permanent and semipermanent seismological stations in California during 1952. The locations of the portable installations in the epicentral area are shown in figure 2 in which also the permanent and semipermanent stations are marked.

The writers of Part II-6, 7, 8, and 9 wish to acknowledge their indebtedness to the Director of the United States Coast and Geodetic Survey and of many individual stations, who have lent their original seismograms or sent copies, and provided valuable data for interpretation; particularly to the staff at Berkeley, for a long series of seismograms of the University of California group of stations, as well as for magnitudes of aftershocks determined at Berkeley.

Our grateful thanks go to the organizations and individuals who have provided facilities for and helped maintain the special stations set up in Kern County, particularly to the United States Forest Service, the Kern County Forestry and Fire Department, the California State Division of Beaches and Parks, Mr. and Mrs. Charles Knox, Mr. and Mrs. L. E. Williams and Mr. Charles Willis (at King Ranch). Property owners and tenants who courteously provided sites for the portable recorder were: Mr. and Mrs. Glenn N. Hurst, Mr. Jim Rogers, Mr. and Mrs. Kermit Austin, Mr. N. Berry, E. Hales Ranch, San Emigdio Ranch. We are also indebted to the officers of the Monolith Portland Cement Company. Operators of the Pacific Telephone and Telegraph Company were extremely helpful during the emergency in keeping field parties in touch with Pasadena headquarters. Special service and many courtesies were provided by Mr. and Mrs. Orville House, at Clear Creek Cafe. A radio receiver for use in the special recording program was lent by the Gilman Scientific Instrument Company of Pasadena.

All members of the Seismological Laboratory staff made significant contributions to the extensive program of field recording, measurement and interpretation of seismograms.

Chief responsibility for setting up and maintaining stations was shared between Mr. F. E. Lehner and Mr. Ralph Gilman; the latter had charge of this during the important month of August.

Mr. G. G. Shor contributed heavily to all parts of the program, including working out preliminary epicenters.

The figures in Part II-6, 7, 8, and 9 have been drafted by Mr. Gilman and Mr. J. M. Nordquist.

6. EPICENTER AND ORIGIN TIME OF THE MAIN SHOCK ON JULY 21 AND TRAVEL TIMES OF MAJOR PHASES

BY B. GUTENBERG

The epicenter of the main earthquake on July 21, 1952, was determined a) from the arrival times of P at near-by stations; b) from comparison of these times with those found previously for shocks in the same region in which, contrasting with the present shock, the motion was not so large that the light spot left the paper shortly after the beginning and in which the onset of the transverse waves (S) could be found on records of several stations (mainly shocks no. 13-16, Gutenberg 1943, with origin times revised in 1951); c) from similar comparison with times in records of aftershocks originating near the main shock, but for which seismograms from portable or temporary stations at short distances furnished additional data. For details of the method see Gutenberg (1943, p. 502). If arrival times of Pn (longitudinal wave leaving the source downward and refracted twice at the Mohorovičić discontinuity; see fig. 1) at the stations near the Sierra Nevada (Haiwee, Tinemaha, Reno) are used, the effects of the difference in crustal structure at the station must be considered. For Pn , which has to go deeper down than usual as a consequence of the Sierra Nevada root, this may result in a delay of as much as 4 seconds.

Methods a) and b) give the following coordinates for the epicenter:

$$\text{Latitude } 35^{\circ}00' \text{ North; Longitude } 119^{\circ}02' \text{ West (1)}$$

Method c) was applied by C. F. Richter and confirmed the result within about 1 minute of arc (or about 1 mile). The origin time resulting from methods a) and b) is

$$\text{July 21, 1952, } 11^{\text{h}}52^{\text{m}}14.3^{\text{s}} \text{ GCT. (2)}$$

Values (1) and (2) are used in calculations. Another way to calculate the origin time when most stations are too distant to record the direct longitudinal wave p (fig. 1) leaving the focus upward, but have a clear Pn (distance Δ less than 6°), is to find the intercept time K (extrapolated travel time at $\Delta = 0^{\circ}$) of the travel time curve of Pn for each station in a number of aftershocks near the main epicenter (within a fraction of a degree) and assume that the focal depths and the values of K are the same in all these shocks. The travel time t of Pn is then given with very good approximation by

$$t = K + b\Delta. \quad (3)$$

From Dr. Richter's investigations of seven shocks originating close to the main shock the following values of K result with $b = 1.818 \text{ sec/km}$: Riverside 5.4 ± 0.1 , Big Bear 5.8 ± 0.2 , Palomar 5.6 ± 0.2 , Dalton 5.2 ± 0.1 , China Lake 5.5 ± 0.3 , Fresno 4.8 ± 0.3 , Haiwee $7.2 \pm 0.2 \text{ sec}$. For Boulder, Berkeley, Palo Alto and Lick, the data were not sufficient to find separate values of K and the average of 5.1 sec. (Gutenberg, 1951) was taken for each. Origin times of the main earthquake are calculated on the assumption that the average velocity of the direct longitudinal waves (p) is 6.34 km/sec and that of Pn (refracted at the Mohorovičić discontinuity) is 8.18 km/sec . The resulting individual times are listed in table 1. Their average is

$$O = 11:52:14.3 \pm 0.1 \text{ sec. (4)}$$

Finally, the method of least squares was applied to the residuals on the assumption that the values of K and the velocities of p and Pn are correct as given above. The result is:

$$\text{Latitude } 35^{\circ}00' \pm 3' \text{ North; Longitude } 119^{\circ}01' \pm 14' \text{ West (5)}$$

$$\text{Origin time } 11^{\text{h}}52^{\text{m}}14.2^{\text{s}} \pm 0.13^{\text{s}} \quad (6)$$

The systematic errors which depend on the assumptions are probably greater than the standard errors resulting from the calculation. It should be kept in mind that our knowledge of the velocity in the earth's crust is rather incomplete, especially near the low-velocity layer to be discussed later in this section, and that local effects of the sedimentary layers, batholiths, roots of mountains, etc. accumulate to several seconds as indicated by the differences in the value of K discussed above.

The depth of focus can not be found very accurately. From other data for southern California shocks and artificial explosions an approximate focal depth of 15 km was considered to fit best with an estimated uncertainty of about $\pm 6 \text{ km}$.

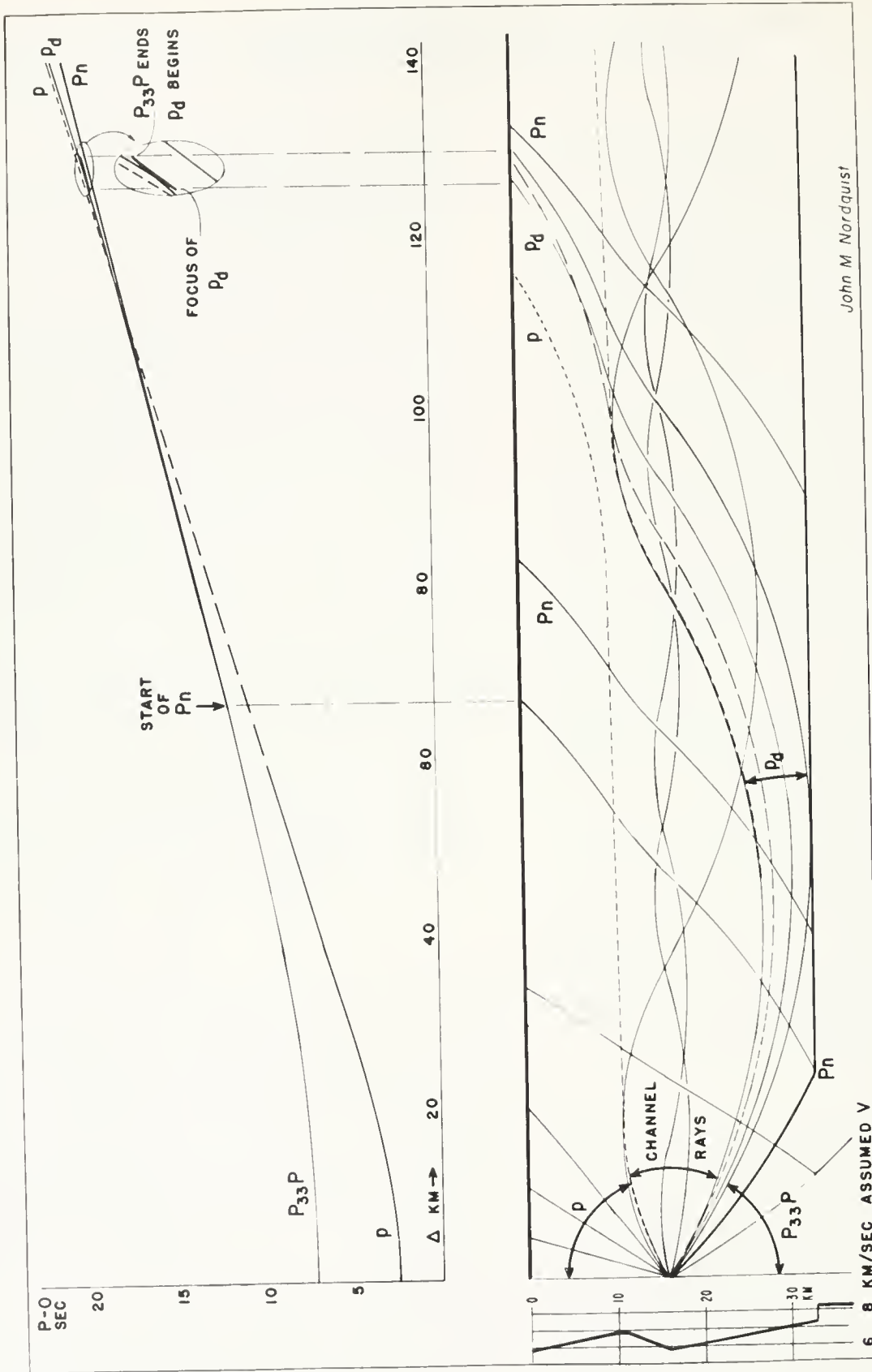
For a detailed study of the original records, all stations with which the Pasadena station exchanges bulletins were asked for their records of the main earthquake and some records of the aftershocks. Records of 165

Table 1. Calculated origin times of main shock, July 21, in seconds after $11^{\text{h}}52^{\text{m}}$ GCT.

From p :	Santa Barbara 14.8	Pasadena 14.0	Mount Wilson 14.5		
From Pn :	Haiwee 14.8	China Lake 14.4	Riverside 14.4	Fresno 14.2	Big Bear 14.3
	Palomar 13.7	Lick 13.8	Palo Alto 13.5	Boulder 15.1	Berkeley 14.1

stations have been received. Unfortunately, in quite a number of instances no instrumental constants are available, and in some the direction of ground motion corresponding to an upward motion of the trace on the record is not known. However, nearly all records can be used for the study of times, since at very few stations is the time correction in doubt by more than $\pm 1 \text{ second}$. At many stations it is given to 0.1 second and was changing by less than 1 second per day. Reports giving the time of P or S are available from 40 additional stations, either direct from the station or through the U. S. Coast and Geodetic Survey or the International Central Office at Strasbourg.

Arrival times and ground amplitudes of the major phases have been determined as far as possible. Arrival times of the main phases are given in table 2. Where the magnification of instruments is not known, ratio of amplitudes in aftershocks was determined. This made it possible to determine the magnitude of smaller aftershocks relative to one of the larger aftershocks usually



John M Nordquist

FIGURE 1. Travel times (top) and wave paths (below) of longitudinal waves to distances up to 140 km, if the source of an earthquake is in a low-velocity layer. Assumed velocities as a function of depth are given in the lower left of the figure. p are the direct longitudinal waves upward, P_n the waves refracted at the Mohorovičić discontinuity which is assumed to be at a depth of 33 km, $P_{33}P$ are waves which have started downward, have not reached the discontinuity, but have reached the surface of the earth, $P_{33}P$ are the waves reflected at a depth of 33 km (Mohorovičić discontinuity).

FIGURE 1. Travel times (top) and wave paths (below) of longitudinal waves to distances up to 140 km, if the source of an earthquake is in a low-velocity layer. Assumed velocities as a function of depth are given in the lower left of the figure. p are the direct longitudinal waves upward, P_n the waves refracted at the Mohorovičić discontinuity which is assumed to be at a depth of 33 km, $P_{33}P$ are waves which have started downward, have not reached the discontinuity, but have reached the surface of the earth, $P_{33}P$ are the waves reflected at a depth of 33 km (Mohorovičić discontinuity).

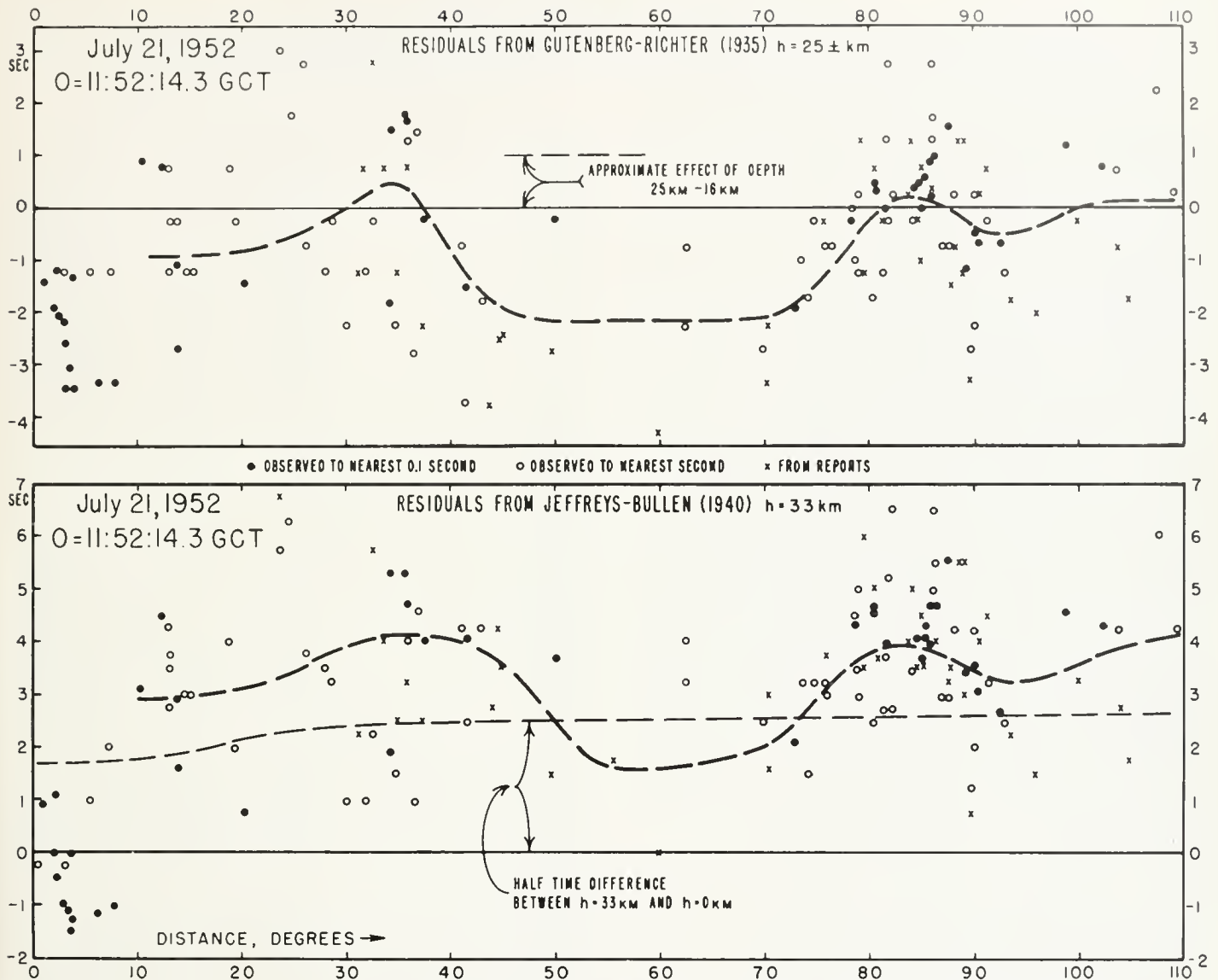


FIGURE 2. Residuals of observed travel times of longitudinal waves as function of epicentral distance.

that of July 23, 0^h or July 29, 7^h, for both of which the magnitude is well known. Resulting data are used together with those found from amplitudes which are calculated directly by use of the instrumental constants.

Records of the longitudinal waves in the main shock written at distances of less than 20° confirm conclusions drawn previously by the author concerning the structure of the upper 300 km of the earth's crust. Since discussion of these phenomena requires more space than is available here, a paper presenting data and results was prepared for publication elsewhere (Gutenberg, 1954); the following is a summary.

There are indications of at least two layers in the earth's mantle exhibiting lower wave velocity than the layers above or below, one at a depth between roughly 10 and at least 20 km, a second in the "ultrabasic material" from a depth of about 30 or 40 km down to roughly 150 km for *P* and 250 km for *S*, and possibly a third between these two in a different material (gabbro?). It is tenta-

tively suggested that the low-velocity channels are the effect of the increase in temperature with depth which, in the depth ranges involved, surpasses the effect of the pressure increase acting in the opposite direction (Gutenberg, 1955). Laboratory experiments by Hughes and Cross (1951) with various rock types indicate that in most the rate of increase in velocity with depth is getting smaller, and that at a depth of the order of 10 km the velocity increase stops altogether. In a few samples, for which the effect of still higher pressure and temperature could be observed, a decrease in velocity was found.

The deepest low-velocity channel occurs in the depth range in which the temperature approaches the melting point of the rocks and which frequently has been considered to be the upper part of the asthenosphere. This channel may well be the seat of viscous flow which has a tendency to restore equilibrium in tectonically disturbed areas with a time of relaxation of probably over a thousand years.

Table 2. Observed arrival times (min.:sec.) of longitudinal and transverse waves for main earthquake July 21, 1952. Hour (11 or 12 GCT) is omitted. An asterisk (*) indicates that times are taken from report of stations. Δ = distance in degrees.

Station	Δ	P	SKS	S	Station	Δ	P	SKS	S
Santa Barbara	0.78	52:28.7			Angra do Heroismo	70.4	30		35 ±
Pasadena	1.11	33.7		52:50 ±	Kiruna	73.1	44.9		13:12
Mount Wilson	1.12	34.3			Sapporo	73.3	03:47½		13:15
China Lake	1.42	39.2			Aberdeen	74.0	50		23
Haiwee	1.43	40.9			Edinburgh	74.3	53		31
Riverside	1.70	42.9			Rathfarnham	74.5	54.5		29
Fresno	1.87	44.4			Bergen	74.6	55		31
Big Bear	1.90	46.1			Mizusawa	75.5	04:00		48
Tinemaha	2.18	50.9			Durham	75.8	02*		46*
Palomar	2.45	52.2			Sendai	76.2	03.5		48
Barrett	3.04	53:00.1 ⁹			Tokyo CMO	78.3	17.0		14:18
Mt. Hamilton	3.15	01.7			Tokyo ERI	78.3	17½		21
Santa Clara	3.33	05			Kew	78.5	17½		12
Palo Alto	3.50	06.2			Uppsala	78.9	19		16
Boulder City	3.59	09.0			Matsushiro	78.9	21 ±		22
Berkeley	3.88	11.9			Jersey	79.2	21*		25*
San Francisco	3.89	12.9			Wajima	79.3	24*		26*
Reno	4.56	24.8			Nagoya	80.5	27		35
Ukiah	5.28	34			De Bilt	80.5	29.3		39
Mineral	5.72	40 ±			Witteveen	80.6	30*		
Shasta	6.30	45.9			Copenhagen	80.6	29.7		39
Ferndale	6.93	58 ±			Hamburg	81.4	32		48
Tucson	7.35	54:01.0			Kamigamo	81.4	33*		
Corvallis	10.10	43.2			Coimbra	81.6	34		45
Butte	12.05	55:11.1			Paris	81.7	34.8		42
Bozeman	12.29	14			Osaka	81.8	36.6		
Chihuahua	12.70	55:18 ±			Santa Lucia	81.8	34?		54
Spokane	12.78	20			Kobe	82.0	39?		57½*
Seattle	12.88	21			Lisbon	82.1	37		52
Hungry Horse	13.84	33.2			Koti	83.7	45*		15:10
Victoria	13.89	32.6			Jena	84.0	04:46	15:10	15:12
Lubbock	14.28	39			Clermont-Ferrand	84.1	48*	16*	26*
Albemi	14.89	47			Collmburg	84.3	48.0	(12)	12
Lincoln	18.61	56:35			Strasbourg	84.3	48.2	(15)	15
Saskatoon	19.30	41		00:14	Toledo	84.4	48		16
Guadalajara	19.85	42		30	Stuttgart	84.7	50.3		20
Fayetteville	20.22	50.2			Basel	85.0	51.2*		
Florissant	23.17	57:23*		01:36*	Cheb.	85.0	52*		23*
Saint Louis	23.32	24*		39*	Neuchatel	85.1	51.8		23
Cape Girardeau	23.9	30*		49*	Zurich	85.5	54.4		28
Tacubaya	23.45	27		44	Praha	85.8	56.2	18	26
Puebla	24.40	37		02:03 ±	Fukuoka	86.2	59	21	31?
Sitka	25.07	36		02	Miyazaki	86.3	59	26	35
Veracruz	25.7	50			Tortosa	86.3	58.7	29	38?
Whiting Field	27.3	58:01.6			Chur.	86.3	58*		
Cincinnati	27.7	05*			Malaga	86.4	05:01	22?	31
Ann Arbor	28.4	11			Cartuja	86.6	03.6	26	48?
Merida	29.4	24 ±		03:17	Averroes	86.6	04:59	31	43?
Cleveland	30.0	23		19?	Barcelona	86.7	05:00 ±	33	
Columbia	31.2	35		40	Milano	86.9	04.9	31	42
Pittsburgh	31.2	44		48	Pavia	87.4	00*	33*	
Kirkland Lake	31.7	38			Almeria	87.4	03*	25*	
Buffalo	32.0	43*			Alicante	87.5	03.3*	30	49*
Guatemala City	32.8	52*			Saló	87.7	07	30	55
State College	32.8	49		58	Wien	88.1	11*	42*	16:10*
Washington	33.5	57*		04:03	Skalnate Pleso	88.7	10 ±	47	15:55
Ottawa	34.3	59:01.5		28	Bologna	89.0	10.9	40	58
Miami	34.4	05.7			Trieste	89.1	13*	41*	56*
College	34.5	59:03		04:36	Hurbanovo	89.1	05*	47*	
Philadelphia	34.9	07*		39*	Padova	89.2	05:09½	15:40	16:01
Hawaii	35.5	14.6			Prato	89.3	10*		08*
Swan Island	35.6	15.0			Firenze-Ximeniano	89.7	14½	45	02?
New York C.C.	35.7	15*			Budapest	89.9	13	43	13
Palisades	35.7	16		51	Eva Perón	89.9	14.8		06
Fordham	35.8	11*		53*	Zagreb	89.9	18*		26*
Shawinigan Falls	36.4	18½		05:11	Kaloesa	90.5	17.6	52 ±	20
Honolulu	36.6	23.7		08	Alger-University	90.6		45*	
Harvard	37.4	28*			M' Bour	91.4	22	50	17 ±
Weston	37.5	31.1		18	Roma	91.7	24*		11*
Kingston	41.1	00:01		06:12	Rocca di Papa	92.5	26.0	16:01 ±	42
Resolute Bay	41.5	02		15 ±	Beograd	93.2	29		
Guantanamo Bay	41.5	03.8			Napoli	94.4	34*		
Halifax	42.9	15½		41	Tunis	94.8		17*	
Mitchel Field	43.9	22*			Taranto	94.8		18.4*	17:01*
Balboa	44.4	28			Messina	95.9	40.3*		
Bermuda	44.8	30.4*		07:11*	Wellington	97.2		22	15
San Juan	49.5	01:05		08:17	Istanbul	98.8	56.5	30	
Roosevelt Roads	50.0	11.1			Athens	99.6	06:00	34	33
Bogota	51.3	21*			Christchurch	99.9		27	41
Morne des Cadets	55.5	50*		09:36	Tamanrasset	102.1	11.1	44	
Seoresbysund	59.7	02:18*			Brisbane	103.7	18 ±	51	18:02?
Reykjavik	62.1	37		11:07	Baguio	103.8	17	57	07
Inuancayo	62.5	40½			Hongkong	103.9	23*	17:00*	
Ajpa	69.7	03:25		12:34	Manila	104.7	20		
La Paz	70.4	31.5		34*					

Table 2. Observed arrival times (min.:sec.) of longitudinal and transverse waves for main earthquake July 21, 1952. Hour (11 or 12 GCT) is omitted. An asterisk (*) indicates that times are taken from report of stations. Δ distance in degrees.—Continued.

Station	Δ	P	P'	SKS
Ksara	107.6	06:37	10:29	
Riverview	108.3	43		17:16
Helwan	109.7	44½	54	17
Chatra	113.7		57	
Calcutta	117.2			17:51
Hyderabad	125.2			18:32*
Poona	125.4		11:17.3	18:34
Bandung	128.8		27	
Djakarta	129.0		23*	
Hermanus	145.9		55	
Kimberley	148.8		58.6	
Pretoria	150.3		12:01	
Grahamstown	151.5		04	
Pietermaritzburg	153.6		04*	
Tananarive	160.1		18±	

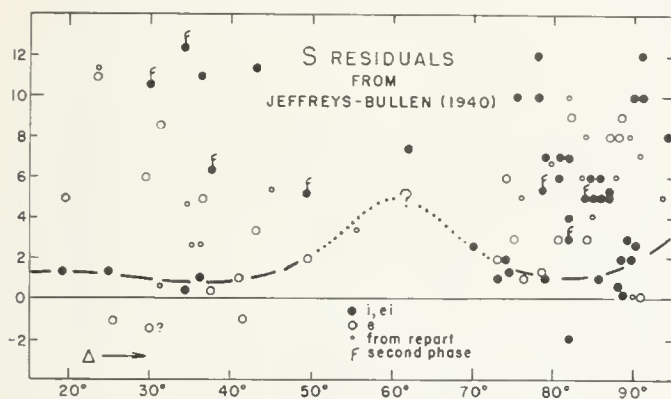


FIGURE 3. Residuals in seconds of observed travel times of transverse waves in the main shock of July 21, 1952, as function of epicentral distance. The residuals are based on the mean of the travel times of Jeffreys-Bullen (1940) for surface focus and for $h = 0.00$ (depth 33 km.).

Waves originating in a low-velocity channel are prevented from leaving this channel if they start out in a direction not too far from the direction of its axis. Paths of waves entering a low velocity layer from outside diverge inside such a channel, so that the energy flowing through a square centimeter of the wave front decreases rapidly with distance. If an earthquake originates in a low-velocity layer (as indicated in fig. 1), waves leaving the source downward cannot enter the layers with relatively high velocity above the channel and consequently cannot reach the surface of the earth unless they have reached a layer below the source with a wave velocity at least equal to the maximum velocity above the source. Thus a large fraction of the energy remains in the channel. In earthquakes with a focal depth of about 12 km or less, that is, in shocks originating above the upper channel, much more energy is transmitted to the epicentral area than in those originating at greater depth. This may contribute to the unexpectedly great damage occurring sometimes in relatively small but rather shallow shocks.

Arrival times of longitudinal and transverse waves from the main shock on July 21 and of the largest after-shock on July 29 recorded at epicentral distances of less than 18° (less than about 1,250 miles) are found to line up along complicated travel time curves as a consequence

of the peculiar ray paths produced by the low velocity layers. At epicentral distances between about 5° and 15° the first waves of the main shock arrive relatively late and show very small amplitudes; starting at about 15° or 16° the amplitudes of the first P-waves are larger than at a distance of 6°. S-waves decrease similarly at short distances; no S-waves have been found between about 10° and 18°, but at a distance of 19° they have relatively large amplitudes. The difference in distance at which the two types of waves reappear with large amplitudes is a consequence of the noticeable increase in Poisson's ratio in and below the low velocity channel at depths between about 100 and 300 km. This indicates that in this depth range the bulk modulus (resistance to compression) of the rocks increases faster (or decreases less) than their rigidity (resistance to shearing).

Residuals of observed P-waves relative to the travel times of Gutenberg-Richter (1934) and to those of Jeffreys-Bullen (1940) are reproduced in figure 2. The former are calculated for a focal depth of 25 km, the latter for 33 km. The effect of the difference in depth between the values in the tables and those for the depth of 15 km (considered to be the best approximation for the main shock) is indicated in the figure. The residuals indicated in figure 2 have been combined with similar residuals observed in longitudinal waves from Pacific surface foci (Gutenberg, 1953). The resulting corrections have been applied to travel times for continental surface foci by Gutenberg and Richter (1939, Table 1, p. 97). By subtracting from these travel times the time difference corresponding to a difference in depth between zero and 25 km, new tables for travel times of P for a focal depth of 25 km have been calculated by Mr. John Nordquist, and a new table was set up to give epicentral

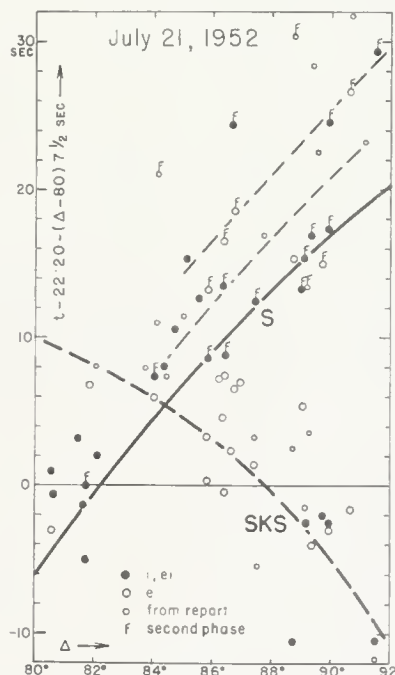


FIGURE 4. Observed travel time of S and SKS in the main shock of July 21, 1952, minus 22 minutes and 20 seconds and minus 7½ times distance in degrees beyond 80 degrees as function of distance. The figure shows the intersection of the travel time curve for S with that for SKS.

Table 3. Epicentral distances for given travel times of P and focal depth of 25 km. 1953 revision.

P-O (min. sec.)	0	1	2	3	4	5	6	7	8	9	Diff. in Δ for $\Delta h = +10$ km.
0.00					0.0	0.1	0.1	0.2	0.3	0.4	-.1
10	0.4	0.5	0.6	0.6	0.7	0.8	0.9	0.9	1.0	1.1	-.05
20	1.1	1.2	1.3	1.4	1.4	1.5	1.6	1.6	1.7	1.8	+.02
30	1.9	1.9	2.0	2.1	2.1	2.2	2.3	2.4	2.4	2.5	+.04
40	2.6	2.6	2.7	2.8	2.9	2.9	3.0	3.1	3.1	3.2	+.05
50	3.3	3.4	3.4	3.5	3.6	3.6	3.7	3.8	3.9	4.0	+.06
1.00	4.1	4.1	4.2	4.3	4.4	4.4	4.5	4.6	4.6	4.7	+.06
10	4.8	4.9	4.9	5.0	5.1	5.1	5.2	5.3	5.4	5.4	.06
20	5.5	5.6	5.6	5.7	5.8	5.9	5.9	6.0	6.1	6.1	.06
30	6.2	6.3	6.3	6.4	6.5	6.5	6.6	6.7	6.7	6.8	.06
40	6.9	6.9	7.0	7.1	7.1	7.2	7.3	7.3	7.4	7.5	.06
50	7.5	7.6	7.7	7.7	7.8	7.9	7.9	8.0	8.1	8.1	.06
2.00	8.2	8.3	8.3	8.4	8.5	8.5	8.6	8.7	8.7	8.8	+.06
10	8.9	8.9	9.0	9.1	9.1	9.2	9.3	9.3	9.4	9.4	.07
20	9.5	9.6	9.7	9.7	9.8	9.8	9.9	9.9	10.0	10.1	.07
30	10.1	10.2	10.3	10.3	10.4	10.5	10.5	10.6	10.7	10.7	.07
40	10.8	10.9	10.9	11.0	11.1	11.2	11.2	11.3	11.4	11.5	.07
50	11.5	11.6	11.7	11.8	11.8	11.9	12.0	12.1	12.2	12.2	.07
3.00	12.3	12.4	12.5	12.5	12.6	12.7	12.8	12.8	12.9	13.0	+.07
10	13.1	13.2	13.2	13.3	13.4	13.5	13.5	13.6	13.7	13.8	.07
20	13.8	13.9	14.0	14.1	14.2	14.2	14.3	14.4	14.5	14.6	.07
30	14.7	14.7	14.8	14.9	15.0	15.1	15.2	15.2	15.3	15.4	.07
40	15.5	15.5	15.6	15.7	15.8	15.9	15.9	16.0	16.1	16.2	.08
50	16.2	16.3	16.4	16.5	16.6	16.7	16.7	16.8	16.9	17.0	.08
4.00	17.1	17.2	17.2	17.3	17.4	17.5	17.6	17.7	17.8	17.9	+.08
10	17.9	18.0	18.1	18.2	18.3	18.3	18.5	18.5	18.6	18.7	.08
20	18.8	18.9	19.0	19.1	19.2	19.2	19.3	19.4	19.5	19.6	.08
30	19.7	19.7	19.8	19.9	20.0	20.1	20.2	20.3	20.4	20.5	.09
40	20.5	20.6	20.7	20.8	20.9	21.0	21.1	21.2	21.3	21.4	.09
50	21.5	21.6	21.7	21.8	21.9	22.0	22.1	22.2	22.3	22.4	.09
5.00	22.5	22.6	22.7	22.8	22.9	23.0	23.1	23.2	23.3	23.4	+.09
10	23.5	23.5	23.6	23.7	23.8	23.9	24.0	24.1	24.2	24.3	.09
20	24.4	24.5	24.6	24.7	24.8	24.9	25.0	25.1	25.2	25.3	.10
30	25.4	25.6	25.7	25.8	25.9	26.0	26.1	26.2	26.3	26.4	.10
40	26.6	26.7	26.8	26.9	27.0	27.1	27.2	27.3	27.4	27.6	.10
50	27.7	27.8	27.9	28.0	28.1	28.2	28.3	28.4	28.6	28.7	.10
6.00	28.8	28.9	29.0	29.1	29.2	29.3	29.4	29.6	29.7	29.8	+.10
10	29.9	30.0	30.1	30.2	30.3	30.4	30.6	30.7	30.8	30.9	.10
20	31.0	31.1	31.2	31.3	31.4	31.6	31.7	31.8	31.9	32.0	.10
30	32.1	32.2	32.3	32.4	32.6	32.7	32.8	32.9	33.0	33.1	.10
40	33.2	33.4	33.5	33.6	33.8	33.9	34.0	34.1	34.2	34.3	.11
50	34.4	34.6	34.7	34.8	34.9	35.0	35.1	35.2	35.4	35.5	.11
7.00	35.6	35.8	35.9	36.0	36.1	36.2	36.4	36.5	36.6	36.8	+.12
10	36.9	37.0	37.1	37.2	37.4	37.5	37.6	37.8	37.9	38.0	.12
20	38.1	38.2	38.3	38.4	38.6	38.7	38.8	38.9	39.0	39.1	.12
30	39.2	39.4	39.5	39.6	39.8	39.9	40.0	40.1	40.2	40.4	.12
40	40.5	40.6	40.8	40.9	41.0	41.1	41.2	41.4	41.5	41.6	.13
50	41.8	41.9	42.0	42.1	42.2	42.3	42.4	42.6	42.7	42.8	.13
8.00	42.9	43.0	43.1	43.2	43.4	43.5	43.6	43.8	43.9	44.0	+.14
10	44.1	44.2	44.4	44.5	44.6	44.8	44.9	45.0	45.1	45.2	.14
20	45.4	45.5	45.6	45.8	45.9	46.0	46.1	46.3	46.4	46.6	.15
30	46.7	46.9	47.0	47.1	47.2	47.4	47.5	47.6	47.8	47.9	.15
40	48.0	48.1	48.3	48.4	48.6	48.7	48.9	49.0	49.1	49.2	.15
50	49.4	49.5	49.6	49.7	49.9	50.0	50.1	50.3	50.4	50.6	.16
9.00	50.7	50.9	51.0	51.1	51.2	51.4	51.5	51.6	51.8	51.9	+.16
10	52.0	52.1	52.3	52.4	52.6	52.7	52.9	53.0	53.1	53.3	.17
20	53.4	53.6	53.7	53.9	54.0	54.1	54.3	54.4	54.6	54.7	.17
30	54.9	55.0	55.1	55.3	55.4	55.6	55.7	55.9	56.0	56.1	.18
40	56.3	56.4	56.6	56.7	56.9	57.0	57.1	57.3	57.4	57.6	.18
50	57.7	57.9	58.0	58.1	58.3	58.4	58.6	58.7	58.9	59.0	.18
10.00	59.1	59.3	59.4	59.6	59.7	59.9	60.0	60.1	60.3	60.4	+.18
10	60.6	60.7	60.9	61.0	61.1	61.3	61.4	61.6	61.7	61.9	.18
20	62.0	62.1	62.3	62.4	62.6	62.7	62.9	63.0	63.1	63.3	.18
30	63.4	63.6	63.7	63.9	64.0	64.2	64.3	64.5	64.7	64.8	.18
40	65.0	65.1	65.3	65.4	65.6	65.7	65.9	66.0	66.2	66.3	.18
50	66.5	66.7	66.8	67.0	67.1	67.3	67.4	67.6	67.7	67.9	.18
11.00	68.0	68.2	68.3	68.5	68.7	68.8	69.0	69.2	69.3	69.5	+.18
10	69.7	69.8	70.0	70.2	70.3	70.5	70.7	70.8	71.0	71.2	.18
20	71.3	71.5	71.7	71.9	72.0	72.2	72.3	72.5	72.7	72.8	.19
30	73.0	73.2	73.3	73.5	73.7	73.8	74.0	74.2	74.3	74.5	.19
40	74.7	74.8	75.0	75.2	75.3	75.5	75.7	75.8	76.0	76.2	.20
50	76.3	76.5	76.7	76.8	77.0	77.2	77.3	77.5	77.7	77.8	.20

Table 3. Epicentral distances for given travel times of *P* and focal depth of 25 km. 1953 revision.—Continued.

P-O (min. sec.)	0	1	2	3	4	5	6	7	8	9	Diff. in Δ for $\Delta h = +10$ km.
12.00	78.0	78.2	78.4	78.6	78.8	79.0	79.2	79.3	79.5	79.7	+ .20
10	79.8	80.0	80.2	80.4	80.6	80.8	81.0	81.2	81.3	81.5	.20
20	81.7	81.8	82.0	82.2	82.4	82.6	82.8	83.0	83.2	83.4	.21
30	83.6	83.8	84.0	84.2	84.4	84.6	84.8	85.0	85.2	85.4	.22
40	85.6	85.8	86.0	86.2	86.4	86.6	86.8	87.0	87.2	87.5	.23
50	87.8	88.0	88.2	88.4	88.6	88.8	89.0	89.2	89.5	89.8	.24
13.00	90.0	90.2	90.4	90.6	90.8	91.0	91.2	91.4	91.6	91.8	+ .25
10	92.0	92.2	92.5	92.8	93.0	93.2	93.4	93.6	93.8	94.0	.25
20	94.2	94.5	94.8	95.0	95.2	95.4	95.6	95.8	96.0	96.2	.26
30	96.5	96.8	97.0	97.2	97.4	97.6	97.8	98.0	98.2	98.5	.26
40	98.8	99.0	99.2	99.4	99.6	99.8	100.0	100.2	100.5	100.8	.27
50	101.0	101.2	101.4	101.6	101.8	102.0	102.2	102.5	102.8	103.0	.28
14.00	103.2	103.4	103.6	103.8	104.0	104.2	104.5	104.8	105.0	105.2	+ .28
10	105.4	105.6	105.8	106.0	106.2	106.5	106.8	107.0	107.2	107.4	.28
20	107.6	107.8	108.0	108.2	108.5	108.8	109.0	109.2	109.5	109.7	.28
30	109.9	110.1	110.3	110.6	110.8	111.0	111.2	111.4	111.7	111.9	.28
40	112.1	112.3	112.6	112.8	113.1	113.3	113.5	113.7	114.0	114.2	.29
50	114.4	114.6	114.8	115.1	115.3	115.5	115.7	115.9	116.2	116.4	.30
15.00	116.6	116.8	117.0	117.3	117.5	117.7	117.9	118.1	118.4	118.6	.30

distances corresponding to a given travel time of *P* in a continental shock with a focal depth of 25 km. These values which are needed to locate earthquakes, if travel times of *P* from various stations are known for a given shallow shock of average depth, are reproduced in table 3.

Residuals of the observed travel times of S-waves from the travel time curves of Jeffreys-Bullen (1940) are shown in figure 3. It is assumed that averages between the travel times for surface focus and those given for a depth of 33 km—marked by 0.00 in the tables—correspond to the depth of focus of the main shock. The resulting residuals are relatively small. At most distances the first S-waves seem to arrive 1 to 2 seconds later than given by the tables, but on account of the possible error in the focal depth and of the scattering of the residuals no attempt has been made to improve the existing tables.

Of special interest are the observed times of the phases S and SKS at epicentral distances near 84° where the travel time curves of these two phases intersect. SKS waves are transverse in the mantle, longitudinal in the earth's core (see figure 7, Part II-1, in *General introduction to seismology*). At distances greater than about 84°, the SKS waves precede the S-waves which have travelled over less curved paths through the mantle only. In figure 4 the observed travel times of both phases are plotted after deduction of the quantity 22^{min}20^{sec} — 7.5 (Δ -80) to permit use of a larger scale. Δ is here the epicentral distance of the station in degrees. Travel times found by Nelson (1953) for SKS agree with those indicated by the curve in figure 4 within ± 2 seconds.

Observed travel times for *P'*, the longitudinal wave through mantle and core, are given in table 4. The residuals refer to the travel times given by Gutenberg and Richter (1939, Table 19, p. 115) for surface focus diminished by 4 seconds for focal depth. The residuals are within the limits of error.

The phase SKP (first path through mantle transverse, path through core and second through mantle longitudinal) is recorded with large amplitudes at Kodai-

kaual ($\Delta=132.4^\circ$) near its focal point. At Perth ($\Delta=134.6^\circ$) the amplitudes are still rather large. The observed travel times of 22^{min}:41^{sec} and 22:56 respectively agree with those calculated from the tables within the accuracy with which Milne-Shaw records (1 mm on the trace corresponds to 7½ sec) can be read. Travel times of "channel waves" are discussed in a special study by Gutenberg (1955). No travel times of body waves other than those mentioned or of surface waves have been investigated thus far. The records of the earthquake are an extremely valuable source of research material for the future. However, periods of the longest surface waves (G) have been measured. At a few stations the longest recorded G-waves had periods of about 1 minute, although maximum periods of about ¾ minute were observed more frequently.

Amplitudes of *P*, *PP*, *S* and of surface waves have been used to determine the magnitude *M* of the shock. Results are given in table 2 of Part II-8 *Magnitude determination for larger Kern County shocks* and are discussed there. The deviations from the average do not exceed the limits of error by amounts large enough to indicate significant corrections to the tables and graphs which are based on the amplitudes of body waves at different distances from a given source and are used to determine the magnitude of a shock on the basis of observed amplitudes and periods of *P*, *PP* and *S* at a given distance.

Table 4. Observed residuals of *P'*.

Station	Δ degrees	Travel time min:sec	Residuals sec
Helwan.....	109.7	18:40	+8
Chatra.....	113.7	18:43	+2
Poona.....	125.4	19:03	-2
Bandung.....	128.8	19:13	+1
Djakarta.....	129.0	19:09?	-3?
Hermanus.....	145.9	19:42	+2
Kimberley.....	148.8	19:45	-1
Pretoria.....	150.3	19:47	+2
Grahamstown.....	151.5	19:50	+2
Pietermaritzburg.....	153.6	19:50?	-2?
Tananarive.....	160.1	20:04±	+3±

7. THE FIRST MOTION IN LONGITUDINAL AND TRANSVERSE WAVES OF THE MAIN SHOCK AND THE DIRECTION OF SLIP

BY B. GUTENBERG

ABSTRACT

Data on compressions and dilatations in the direct longitudinal waves are given and used for the determination of the fault plane at the starting point of the earthquake and for the finding of the direction of slip. A method is developed to get similar information from the first motion in transverse waves recorded at stations in the hemisphere around the epicenter and is applied to observed amplitudes which are listed. The final results are: at the depth of the source (about 10 miles) the fault plane has a dip of about 60° to 66° towards E 50° S; the slip along the fault at this depth was roughly up towards north in the upper (southeastern) block relative to the lower (northwestern) block; the vertical component of the slip was about 1.4 times that of the horizontal; the horizontal component corresponds to a relative movement north-eastward in the upper block (southeast of the fault), southwestward in the lower block.

Important information concerning the mechanism of faulting can frequently be obtained from studies of the direction of first motion in longitudinal (P) and transverse (S) waves at a sufficient number of well distributed stations.

For a study of compressions and dilatations as indicated by the first onset of longitudinal waves in earthquake records the direct p (epicentral distances less than about 140 km) can be used, the wave P_n (see fig. 1, Part II-6.) where it is clearly recorded, that is, at distances not over about 600 km, the wave P at epicentral distances between about 16° and 100° , and P' (through the core). In the main shock of July 21 p and P_n started with a dilatation at all stations, except perhaps for Riverside, where the first very short motion is small and possibly a compression. At the Big Bear station, about 50 km northeast of Riverside, the beginning is small, but a clear dilatation. At epicentral distances of about 600 to 1600 km there is a shadow zone for longitudinal waves (see fig. 1, Part II-6). It is not known how the first waves arriving in this zone have traveled; if they have been reflected somewhere, compressions may have been changed to dilatations, and vice versa. For this reason, waves arriving in the shadow zone around the epicenter are not used for determination of compressions and dilatations even in the rare instances where the first wave in the seismogram is large enough to permit the finding of the direction beyond reasonable doubt.

Contrasting with the dilatations at the near-by stations, the onset of P at 62 stations beyond the shadow zone corresponds to a compression and at 6 additional stations probably to a compression. Scattered among these compressions are dilatations at Tortosa and at Tamarrasset and a doubtful beginning at Cartuja which reports a dilatation. All records beginning with a clear P' (longitudinal wave through the earth's core) indicate compression.

Clear dilatations in the first P-wave were recorded at Whiting Field, Swan Island and Miami; these stations are under the supervision of the U. S. Fleet Weather Central at Miami and have been equipped with very sensitive instruments by the U. S. Navy Department, for the investigation of microseisms in the Caribbean area. The records written at Guantanamo Bay and Roosevelt Roads by similar instruments begin with a clear compression. At the U. S. Coast and Geodetic

Survey station at San Juan the first motion is probably a small compression followed by a large dilatation; however, the first half wave is scarcely larger than the background of microseisms. The first longitudinal waves on the records of the Mexican stations are rather small, but all seem to correspond to dilatations. At Saskatoon the records seem to begin with a small dilatation, followed by a large compression.

Data for compressions and dilatations in the aftershocks are much more scanty and, with few exceptions, are limited to near-by stations. They will be discussed by C. F. Richter in Part II-9.

A given motion at the source produces a unique pattern of compressions and dilatations at the surface of the earth. Our problem is to deduce the direction of this motion from the observed pattern of compressions and dilatations. There are two difficulties involved in this task. One is that the observations are limited to certain spots scattered over the surface of the earth and separated by large areas of oceans, by regions which have no stations or do not give out information, and by "shadow zones." The other is a consequence of the fact that relatively simple assumptions have to be made to make a theoretical treatment possible. For example, it is generally assumed that the fault is a plane. Actually, in many instances there is good evidence that the dip of the fault surface changes with depth; if it changes along the fault, the intersection of the fault surface with the horizontal plane through the focus is not parallel to the surface trace. In any case, direction of motion calculated from the pattern of compressions and dilatations corresponds approximately to the direction of motion at the point at depth where fracturing has started.

If we assume dip slip motion along a plane fault having a dip angle δ (fig. 1), we should observe at the earth's surface two sectors with compressions and two with dilatations. These four sectors are then separated by the fault plane and an auxiliary plane perpendicular to it through the earthquake focus as indicated in figure 1. The width of the zone near the epicenter E exhibiting compressions in figure 1 is given by $2h/\sin 2\delta$, if h is the focal depth, and the curvature of the earth can be neglected. If h is small, this zone is usually rather narrow. However, the curvature of the

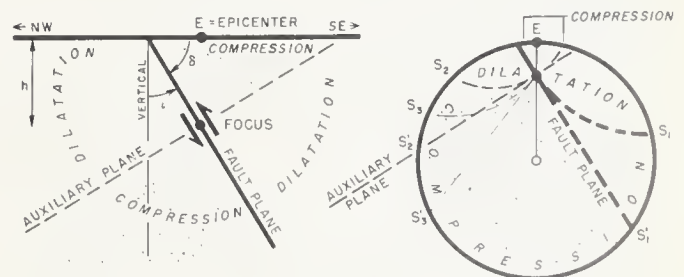


FIGURE 1. Sketch of distribution of compressions and dilatations in an earthquake.



FIGURE 2. Observed compressions and dilatations in the main earthquake of July 21, 1952. For the projection, see text. The shadow zone for longitudinal waves is indicated by shading.

rays has always to be considered. Nearly all rays of seismic waves emanating from the source intersect the earth's surface at shorter distances than the straight lines tangent to them at the source. Thus, the ray leaving the focus downward along the fault surface in figure 1 and forming the boundary between compressions and dilatations arrives at the surface at a point S_1 much closer to the epicenter than the point S_1' on the straight line extending the fault plane. In order to find in which quadrant of dilatations or compressions at the source a ray starts which arrives at a station S_3 (fig. 1) one cannot use the location of S_3 relative to the straight lines (planes) in the figure, but must find the direction at which the ray leaves the source. This is given by the tangent to the ray at the source which, in the figure, intersects the surface of the earth at the point S_3' ; this point has been called "extended position" of S_3 by Byerly (1922). Tables for the "extended distances" (e.g. arc $S_3' - E$) of these extended positions from the epicenter, if the actual distances (e.g. $S_3 - E$) are given, have been calculated by Hodgson and Storey

(1953). For the reasons given above, distances between 6° and 16° should not be used; Hodgson and Storey have already realized that difficulties arise for small distances. For distances less than 6° the vertical distribution of wave velocities near the source and the depth of focus produce considerable differences.

Use of stereographic projection simplifies the study of compressions and dilatations. The tables of Hodgson-Storey include the transformation of distances along the earth's surface to those in a stereographic projection; the unit of length used in these tables is the radius of the earth. Hodgson and Milne (1951) have summarized earlier work, especially results of Byerly and of Adkins, and have improved the method. For details of the theory and its application to observations, the references should be consulted.

In figure 2 compressions and dilatations are plotted for the main shock of July 21. The location of the points is given by the station azimuths, taken at the epicenter and the extended distances of the stations. For conversion of the epicentral distances into extended distances,

the Hodgson-Storey tables are used. It should be kept in mind that these tables are based on certain assumptions concerning the velocities of longitudinal waves in the earth's interior (which are considered to be good approximations for most distances) and that figure 2 is a stereographic projection of the "extended distances" and thus distorted in a way depending on the change of longitudinal velocity with depth. The intersections of the fault plane and of the auxiliary plane with the earth's surface remain circles in the projection.

Frequently, nothing is known about the dip and direction of motion in an earthquake to be investigated, and the circles separating compressions and dilatations on the projection may be drawn in a variety of ways. Fortunately, in our case it is known from geological investigations that the strike of the White Wolf fault is approximately towards N. 50° E. In addition, the main shock and all larger aftershocks during the first 36 hours which have been located are southeast of the fault trace at a distance from it which is smaller than the focal depth. Consequently, it can be assumed that the fault dips rather steeply, approximately towards southeast, and that in the projection the center of the circle corresponding to the intersection of the fault plane with the earth's surface is about southeast of the epicenter. In the projection this circle should be tangent to the fault trace. There is little choice to draw a circle which fulfills these requirements and, in addition, includes only dilatations. The fault plane circle indicated in figure 2, consequently, can be assumed to be with good approximation the projection of the intersection of the fault plane with the earth's surface. Since its diameter d in the units used by Hodgson-Storey is about 1.9 and $\tan \delta = d$, it follows that the dip angle δ of the fault plane with a horizontal plane is about 63° (with an estimated error of less than $\pm 5^\circ$). This would not disagree with the geological evidence and would correspond to the estimate based on the location of epicenters relative to the fault trace. The resulting relative motion is downward in the lower block, upward in the upper block, as indicated in figure 1.

In case of dip-slip, the maximum width of the zone with compressions surrounding the epicenter was found above to be given by $2h/\sin 2\delta$. With $h = 15$ km and $\delta = 63^\circ$ this gives about 37 km. There was no station at so short a distance from the epicenter. However, the result would be different if the motion had a component in the direction of the strike. This can be found theoretically from the second circle which separates compressions and dilatations. This auxiliary circle is the intersection of the auxiliary plane (figure 1) with the earth's surface. Our data for constructing the projection of this circle in figure 2 are less complete than those for the projection of the fault plane circle, partly as a consequence of the shadow zone which is marked in the figure, partly due to the lack of not too distant stations (except for Honolulu) in the southwestern half of the map. In case of dip-slip the fault plane and the auxiliary plane are perpendicular to each other, and the dip of the auxiliary plane and the fault plane dip must add up to 90° . In the projection, the centers of the two circles and the epicenter are then on one line, and the diameter of the auxiliary circle in the units used is given by \cot

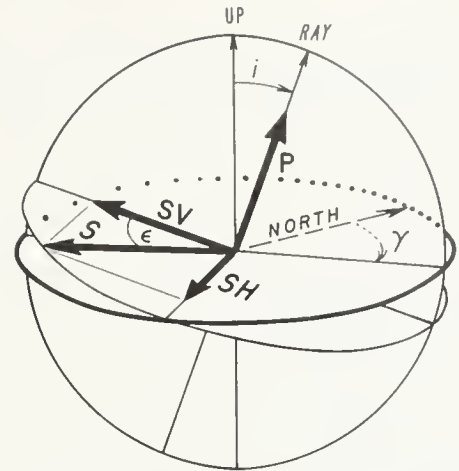


FIGURE 3. Sketch of relationship between the direction of P , S , SV , and SH . The azimuth of the plane of propagation is indicated by γ , the polarisation angle of S by ϵ , the angle of incidence of the ray by i .

$63^\circ = 0.51$. The auxiliary circle marked a) in figure 2 fulfills these requirements. It includes all dilatations established beyond reasonable doubt northwest of the fault trace and no compressions and, therefore, represents a possible solution.

If the direction of slip has a component in the direction of the fault strike, the center of the auxiliary circle is not on a line perpendicular to the direction of the strike, but, in the projection, the auxiliary circle still must pass through the two points indicated in figure 2. The circles b), c) and d) in figure 2 with the centers B, C and D respectively represent possible solutions. If the Saskatoon record starts with a small dilatation, a circle slightly larger than d would be most likely. In this case the motion along the fault surface at the source would have been almost south-north in the upper block, that is, it would have had a strike component north-eastward. However, the data for compressions and dilatations in P do not permit finding the orientation of the auxiliary circle relative to the fault more accurately. For the location of the fault circle, the recorded S -waves give additional information.

The use of transverse waves (S) in finding the direction of motion in slip is more complicated than that of longitudinal waves (P). The vibrations for P are theoretically in the direction of the ray which can be established theoretically with fair approximation, if focus and station are given, whereas those of S may be in any direction perpendicular to the ray. For calculations concerning amplitudes of S , the motion in S is usually separated into two components which are respectively in the plane of propagation (SV) and perpendicular to it (SH) (fig. 3). The motion in SV is perpendicular to the motion of P . SV has a horizontal component in the same azimuth as P and a vertical component; one of the two has a direction opposite to the corresponding component in P . SH has only a horizontal component in a direction perpendicular to that in the horizontal component of SV or P . For certain angles of incidence, the SV component arriving at the surface of the earth is totally reflected. In this case the ground moves theoret-

Table 1. Amplitude of *S*-waves and angle of polarisation (ϵ).

N, *E* are north-south and east-west components of the ground motion in *S*; *a* and *b* are calculated ground amplitudes of *SV* and *SH* respectively, all rounded off and in microns except for values indicated by *, which are given in arbitrary units. Δ = epicentral distance in degrees, α = azimuth at the epicenter towards the station, γ = azimuth at the station towards the epicenter; both are counted from north towards east.

Station	Δ degr.	α degr.	γ degr.	<i>N</i>	<i>E</i>	<i>a</i>	<i>b</i>	ϵ degr.
Ottawa	34.3	50	265	-25	+25	-14	-13	43
Pahsades	35.7	67	275	+25*	-20*	+13*	+11*	41
Honolulu	36.6	262	60	-16	+12	+1½	+10	-98
Weston	37.6	65	270	-5*	+30*	-18*	-2½*	9
San Juan	49.5	96	60	+5	+12½	-5	+5½	132
Reykjavik	62.1	28	295	-10	+4	+4¼	+3¾	37
Kiruna	73.1	10	-30	-22	+4	-11½	-3¾	18
Sapporo	73.3	313	58	-2	-2	-1½	+¼	-12
Aberdeen	71.0	30	48	-3½	+7	-4¾	+1	-11
Bergen	74.6	24	-53	-5	+4	-3½	-¾	8
Sandai	76.2	310	56	-4	0±	+1½	-1¾	-53
Tokyo CMO	78.3	307	54	-10	0±	+3¼	-4	-52
Kew	78.5	33	-43	-25	+17	-16½	-5	16
Uppsala	78.9	20	36	+10	-7½	+7	0	0
Matsushiro	78.9	310	54	-30	-30	-24	+3	-8
De Bilt	80.5	27	47	40	+44	-33	0	0
Copenhagen	80.6	24	-41	-8½	+4	-5¼	-1¼	13
Hamburg	81.4	31	-41	-20	+14	-13½	-¾	4
Coimbra	81.6	45	-52	-10	+15	-10	+¾	-4
Eva Peron	89.9	135	-45	-3	+2	-2	+1¾	-43
Christchurch	99.9	223	58	+9	-15	-4½	-8	-120

ically in ellipses. This theoretically disagreeable condition occurs in shallow shocks roughly at distances of between 30 and 3000 km (about 20 and 2000 miles) from the epicenter. For more details, see Gutenberg (1952). *S*-waves recorded at short distances from sources in southern California have been used by Dehlinger (1952) to study the ground motion in a number of earthquakes.

In the main earthquake of July 21 the motion at short distances was too large on the records to find *S*. Consequently, our investigation of recorded *S*-waves is limited to epicentral distances greater than about 35°. Another distance range which has to be excluded is between about 82° and 88° where *SKS* follows *S* immediately or precedes it by less than 25 seconds (figure 4 in Part II-6) and affects the amplitudes of *S* too much for practical use. Unfortunately, many European stations with excellent records are in this range of distances. Even beyond 88°, *S* is frequently affected by *SKS*, *SKKS* and related phases. Finally, at distances beyond about 110° *S* gradually fades out. In the remaining range of distances, all available records of stations with two horizontal components having instrumental constants not too different from each other and known relationship between direction of ground motion and direction of recorded waves were carefully studied. Theoretically, vertical components can be used, too, but instances of well recorded *S* waves on vertical records are rare on account of the usually small periods for which most vertical instruments have their maximum magnification, and the frequently small amplitudes of the vertical component of *S*.

In table 1, amplitudes of the two horizontal components *N* and *E* of *S* (positive towards north and east respectively) are entered for those stations for which the records fulfill the conditions mentioned above. If the magnification factors of the seismograph are not known, amplitudes are given in arbitrary units and are marked by "*". Otherwise, they are roughly ground motions in microns in the first clear half *S*-wave. The theory (Gutenberg, 1952) gives for the amplitudes *a* of *SV* and *b* of *SH* in the incident *S*-wave

$$\begin{aligned} a &= (N \cos \gamma + E \sin \gamma) / u = Z' / w \\ b &= (E \cos \gamma - N \sin \gamma) / 2 \end{aligned} \quad (1)$$

where γ = azimuth at the station towards the epicenter counted from north towards east; *Z* = vertical component (usually not used here). *u* and *w* are constants

Table 2. Approximate values used for quantities in equation (1).

Distance Δ	40	50	60	70	80	90	100 degrees
<i>i</i>	30	25	22	20	20	19	18 degrees
<i>u</i>	1.7	1.8	1.8	1.8	1.8	1.8	1.9
<i>w</i>	1.0	0.9	0.8	0.7	0.7	0.7	0.7

depending on the angle of incidence *i* for a given ratio of the wave velocities in *P* and *S* at the earth's surface. Approximate values of these quantities as function of the distance Δ in degrees are given in table 2 on the basis of averages found previously (Gutenberg 1952).

The polarization angle ϵ (called "Schwingungswinkel" by Galitzin, 1911) is the angle between *S* and its component *SV*. From this definition it follows (fig. 3) that

$$\tan \epsilon = SH / SV = b / a \quad (2)$$

For earlier investigations see Galitzin (1911), Gutenberg (1952) and Ingram (1953). If it is not certain whether the first or a later half wave of *S* has been measured, it may be preferable to count ϵ from +90° to -90°, otherwise it may be counted from +180° to -180°. However, the same procedure should be used for observations and calculations. If *SV* = 0, *a* = 0 and $\epsilon = \pm 90^\circ$; if *SH* = 0, *b* = 0 and $\epsilon = 0$ or $\pm 180^\circ$. Since ϵ does not depend on the individual values of *a* and *b*, but only on their ratio, absolute values of the ground motion are not required for its calculation and the data marked with asterisks in table 1 are just as useful as the others provided that the instrumental constants do not differ too much. The values of *a* and *b* in

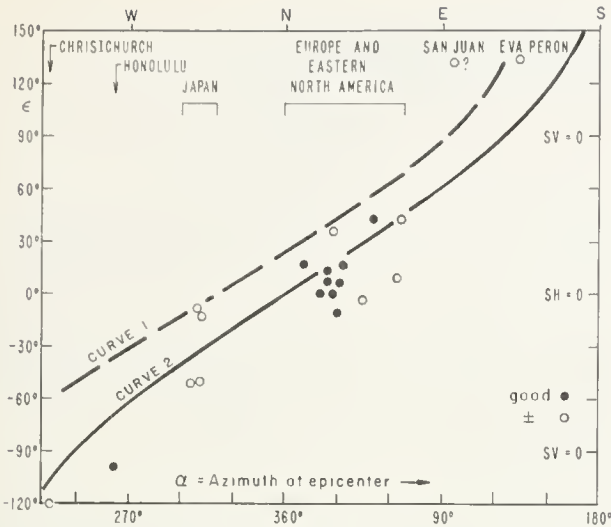


FIGURE 4. Observed angles of polarisation ϵ as a function of the azimuth towards the station at the epicenter in the main shock of July 21, 1952. Curve 1 is calculated on the assumption of dip-slip along the fault, curve 2 on the assumption that the slip was towards the north in the upper block, towards the south in the lower block, separated by the White Wolf fault.

table I are supposed to give the ground motion of the first half *SV* and *SH* wave respectively in microns, except for the values indicated by asterisks. a is positive if the horizontal component of *SV* is towards the epicenter and its vertical component upward; b is positive if its direction is to the right of the ray, looking from above. ϵ is calculated from equations (2) and (1) or directly from the ratio $r = E/N$ of the ground amplitudes of the east-west and north-south components of *S*:

$$\tan \epsilon = \frac{u}{2} \frac{r \cot \gamma - 1}{r + \cot \gamma} \quad (3)$$

The azimuth γ of the ray at the station and its azimuth α at the epicenter are measured on a globe; u is taken from table 2.

It is usually assumed (Gutenberg 1952; Ingram 1953) that the polarization angle ϵ does not change during the propagation of an S-wave, or that the change in amplitudes of *SV* and *SH* is the same, percentagewise. It is then possible to plot ϵ as a function of the azimuth α at the epicenter for stations at about the same distance in various azimuths. However, since the accuracy of the observations is not very high, and since the distance enters only through the angle of incidence i , which changes relatively little in the range of distances involved (see table 2), all results for ϵ are plotted together in figure 4 as function of α regardless of the value of i .

Apparently thus far no equations have been developed to calculate ϵ if the necessary quantities concerning the fault and the direction of slip are given. Such equations can be found by use of trigonometry. A more elegant method is the following, given by Mr. John M. Nordquist:

The amplitudes of (1) *P*, (2) *SH*, and (3) *SV* as they leave the source along a ray are assumed to be proportional to the components of the displacement of the fault in the direction of (1) the ray, (2) a horizontal line perpendicular to the ray, and (3) a line perpendicu-

lar to the ray and to (2) respectively. The direction of the ray is specified by the azimuth α of its vertical plane and the angle of incidence i (measured from the vertical). Let ϕ and ψ be the corresponding angles for the fault displacement.

In vector notation, the component of the vector *Cc* in the direction of the unit vector **d** is the scalar product

$$C(\mathbf{c} \cdot \mathbf{d}) = C(c_x d_x + c_y d_y + c_z d_z) \quad (4)$$

where the subscripts x, y, z indicate components of the unit vectors **c** and **d** in a rectangular coordinate system (x, y, z). Choosing coordinate axes pointing to the north, east, and down, we obtain the following schedule of components:

Unit vectors in direction of	Amplitude factor	Angle of		Components		
		azim.	incid.	North	East	Down
Fault motion	A	ϕ	ψ	$\sin \psi \cos \phi$	$\sin \psi \sin \phi$	$\cos \psi$
<i>P</i>	p	α	i	$\sin i \cos \alpha$	$\sin i \sin \alpha$	$\cos i$
ray.....	f					
<i>SH</i>	b	$\alpha - 90^\circ$	90°	$\sin \alpha$	$-\cos \alpha$	0
<i>SV</i>	a	α	$i + 90^\circ$	$\cos i \cos \alpha$	$\cos i \sin \alpha$	$-\sin i$

Substitution in equation (4) and collection of similar terms lead to

$$p = A [\sin \psi \sin i \cos (\alpha - \phi) + \cos \psi \cos i] \quad (5)$$

$$b = A \sin \psi \sin (\alpha - \phi) \quad (6)$$

$$a = A [\sin \psi \cos i \cos (\alpha - \phi) - \cos \psi \sin i] \quad (7)$$

All these equations of Mr. Nordquist are based on the assumption that the amplitudes of *P* and *S* generated at the source depend only on the amplitude of the displacement A on one side of the fault. Actually, the opposite motion of the other block enters also. However, if the ray starts in a direction which forms not too small an angle with the fault surface at the source, the effect of the other side upon the first motion in *S* or *P* can be neglected in a first approximation, that is, equations (5) to (7) can be used if the station is far enough from the fault plane circle in figure 2. This requirement is fulfilled for all stations in table I with the exception of San Juan, as may be seen from figure 2. For this reason the point indicating the value of ϵ for San Juan in figure 4 has been marked by ?. It also has to be considered that other factors, for example the period of the generated wave, affect the amplitudes of *P* and *S*. However, since *SV* and *SH* are components of the same S-wave, it may be assumed that $SV:SH = a:b$.

Mr. Nordquist's equations lead to

$$\cot \epsilon = \cos i \cot (\alpha - \phi) - \frac{\cot \psi \sin i}{\sin (\alpha - \phi)} \quad (8)$$

For its application the various angles must be known. For the angle of incidence of the rays an average of $i = 22^\circ$ is taken (see table 2). The only other quantities which have to be assumed for the calculation of a and b from equations (6) and (7) are the dip and strike of the direction of motion. It was assumed first that the motion was a pure dip-slip, and that the angles ϕ and ψ are given by the investigation of the compressions and dilatations. Consequently, it was assumed that in the lower block (in which all rays to the stations in table I start) $\psi = 30^\circ$ (more accurately, it should be $90 - 63 = 27^\circ$)

and $\phi = 90 + 50 = 140^\circ$ considering that the azimuth of the fault trace is about 50° . The curve 1 is indicated in figure 4. It is definitely too high.

There are various ways to calculate first approximations of the quantities involved. From equations (6) and (7) quadratic equations for $\cos(\alpha - \phi)$ or $\sin(\alpha - \phi)$ can be derived which can be used to calculate ϕ from the data of each station. The equation for $x = \sin(\alpha - \phi)$ is of the form $ax^2 + bx + c = 0$, where

$$\begin{aligned} a &= \sin^2 \psi (y^2 + \cos^2 i) \\ b &= y \sin^2 \psi \sin i \\ c &= \sin^2 i - \sin^2 \psi, \end{aligned}$$

if $y = \cot \epsilon$. For calculations, it was assumed that $\psi = 34^\circ$ and $i = 22^\circ$. ϵ was taken from table I for each station. The resulting values of $\alpha - \phi$ together with the values of a to the respective stations give $\phi = 11 \pm 24^\circ$.

Some special values of ϵ can be used to find approximations for ϕ and ψ and, in addition, give information on the way in which ϕ , ψ and i affect the curve showing ϵ as a function of α . If $b = 0$, $\epsilon = 0$ and $\phi = \alpha_0$. Figure 4 shows that $\epsilon = 0$, if α is slightly over 0° . This ϵ indicates that ϕ is slightly greater than zero, thus confirming the calculations. For $a = 0$, $\epsilon = 90^\circ$ and equation (7) gives

$$\cot \psi = \cot i \cos(\alpha_{90} - \alpha_0)$$

Figure 4 shows that $\alpha_{90} - \alpha_0$ is about 120° . This gives $\psi = 39^\circ \pm$. However, in our case the cosine changes rapidly with changing argument, so that this equation gives rather rough results for ψ ; it may be of greater value in other instances.

From equation (8) we find by differentiation

$$\frac{d\epsilon}{d\alpha} = \sin^2 \epsilon \left\{ \frac{\cos i - \cot \psi \sin i \cos(\alpha - \phi)}{\sin^2(\alpha - \phi)} \right\} \quad (8a)$$

$$\text{or } \frac{d\epsilon}{d\alpha} = \frac{\cos^2 \epsilon [\cos i - \cot \psi \sin i \cos(\alpha - \phi)]}{[\cos i \cos(\alpha - \phi) - \cot \psi \sin i]^2} \quad (8b)$$

For $\epsilon = 0$ and $(\alpha - \phi) = 0$, equation (8b) gives

$$\cot \psi = \cot i - \frac{1}{\sin i (d\epsilon / d\alpha)_0} \quad (8c)$$

This may be useful for a rough determination of ψ . Figure 4 shows that for $\epsilon = 0$, approximately $(d\epsilon / d\alpha)_0$

$= 0.7$, which gives $\cot \psi = 1\frac{1}{2} \pm$, $\psi = 34^\circ \pm$. For $\epsilon = 90^\circ$, equation (8a) leads to $(d\epsilon / d\alpha)_{90} = \cos i$.

On the other hand, for a given azimuth σ of the strike of the fault, the angle ψ depends on the angle ϕ . If the dip of the fault (counted from the horizontal plane, as usual) is indicated by δ , it is found that

$$\tan \psi = (\cot \delta) / \sin(\phi - \sigma) \quad (9)$$

The angle β between the direction of actual motion in the fault plane and that for dip-slip is found from

$$\sin \beta = \cos(\phi - \sigma) \sin \psi \quad (10)$$

Finally, curve 2 in figure 4 was calculated for $\phi = 180^\circ$ (or zero) and $\phi - \sigma = 180 - 50 = 130^\circ$. With $\delta = 63^\circ$, equation (9) then gives $\psi = 34^\circ$, as found above from $(d\epsilon / d\alpha)_0$. Curve 2 is then given by

$$\cot \epsilon = 0.93 \cot(\alpha - \phi) - 0.55 / \sin(\alpha - \phi) \quad (11)$$

The resulting curve 2 in figure 4 fits the observations beyond expectation considering the theoretical assumptions and the errors involved in the calculation of the ratio of the *EW*— to the *NS* components of the ground motion in *S* at the various stations. Before other investigations of this type produce similar good agreement as that in the present investigation, there is the danger of over-confidence in the results of this new method.

Equation (10) gives $\beta = 21^\circ$. Thus the observed compressions and dilatations as well as the observed displacements in the transverse waves combined with the assumption that the strike of the White Wolf fault is in an azimuth of about 50° from north towards east lead to the following results: the fault plane has a dip of between about 60° and 66° towards southeast (*S* 40° *E*) at the depth of the source (about 10 miles); the slip along the fault was roughly up towards north in the upper block, down towards south in the lower; the angle between the direction of slip and the direction of dip is about 20° ; thus the motion was much closer to dip-slip than to strike-slip; the vertical component of the slip was about 1.4 times that of the horizontal; the horizontal component produced a relative movement northeastward in the upper block (southeast of the fault), southwestward in the lower (northwest of the fault).

8. MAGNITUDE DETERMINATION FOR LARGER KERN COUNTY SHOCKS, 1952; EFFECTS OF STATION AZIMUTH AND CALCULATION METHODS

BY B. GUTENBERG

ABSTRACT

Methods for magnitude determination are summarized. Values for the magnitude of the main shock are listed on the basis of wave amplitudes measured on seismograms of individual stations. About 200 data from body wave amplitudes result in a magnitude of 7.6 with only slight variation in azimuth. However, amplitudes of surface waves at a given distance show a clear variation with the azimuth in which they start with a maximum towards northeast (in the direction of the fault) about 10 times the minimum which is found in waves starting towards southwest. This is considered to be a consequence of the fact that in the main shock the breaking proceeded northeastward from the neighborhood of the southwest end of the active fault segment. In the largest aftershocks there was no appreciable difference in the amplitudes of surface waves in those azimuths for which data are available. The magnitude of the main shock determined from surface waves is 7.6 to 7.7.

Magnitudes of the largest aftershocks are listed. They are calculated from maximum amplitudes at near-by stations, from amplitudes of body waves at distant stations, and from surface waves. The differences between the various results for a given shock are relatively small.

The magnitude of an earthquake was originally defined by Richter (1935) for shallow shocks in southern California as the logarithm of the maximum trace amplitude expressed in thousandths of a millimeter with which the standard short-period torsion seismometer (period 0.8 sec., magnification 2800, damping nearly critical) would register that earthquake at an epicentral distance of 100 kilometers. In southern California shocks with focal depths of about 16 km, magnitude 2 corresponds usually to the smallest earthquakes which are felt; average shallow shocks of magnitude $4\frac{1}{2}$ to 5 may produce small damage, magnitude $5\frac{1}{2}$ to 6 may cause an acceleration of one tenth of gravity; shocks of magnitude 7 or more are called major earthquakes, those of $7\frac{3}{4}$ or more, great earthquakes. The largest magnitude found thus far for earthquakes since 1904 (when sufficient instruments for the determination became available) is 8.6. However, there is indication that the Lisbon earthquake of 1755 may have had a magnitude of about $8\frac{3}{4}$ or even slightly more.

Gutenberg and Richter (1936) extended the magnitude scale to apply to shallow earthquakes occurring elsewhere and recorded on other types of instruments. The physical meaning of the scale was discussed, improvements were introduced and a nomogram for its application (drafted by Mr. J. M. Nordquist) was presented by Gutenberg and Richter (1942). If u is the horizontal component of the ground amplitude of the largest surface waves with periods of about 20 seconds in shallow shocks of average focal depth (15 to 30 km), then

$$M = F + S + \log u \quad (1)$$

where S is a small constant, different for each station, to correct for local conditions, and F depends only on the epicentral distance. Revised tabulations for F as a function of distance, and values of S for a number of stations were given by Gutenberg (1945a). Magnitudes of shallow earthquakes were then correlated with amplitudes and periods of waves through the earth recorded

at distances of over 1,000 miles (Gutenberg, 1945b). Consequently, P , PP and S are now also available for magnitude determination. For a discussion of the relationship between magnitude M and energy E of an earthquake, see Part II-1.*

For the calculation of the magnitude M from records written at distances of less than 1,000 miles the original Richter method still has to be used: that is, trace maxima on standard Wood-Anderson seismographs have to be measured and the magnitude then is found from a table or the Nordquist nomogram. For distances greater than about 1,000 miles either the maximum ground motion in surface waves with periods of about 20 seconds is determined and a nomogram or tables for F in equation (1) are used (Gutenberg, 1945a, p. 7), or values of ground amplitudes a in microns of body waves having periods T are inserted in the equation

$$M = \log (a T) + A + B + C. \quad (2)$$

A is a function of the distance and may be taken from Gutenberg (1945b, table 4, p. 65) for the various types of waves or from corresponding graphs (Gutenberg, 1945c.). B is a station correction (usually not much different from S in equation 1; see e.g., Gutenberg, 1945c, table 1). C is an empirical correction to be applied for shocks of magnitude over 7; it is about 0.2 for the main shock of July 21 and zero for all others. No correction corresponding to C is used if the calculation of M is based on amplitudes of surface waves.

If horizontal ground amplitudes u (given in microns) of surface waves over the greater arc (W_2 , across the antipodal point of the epicenter; see figure 7 in Part II-1.), with periods T of about 20 sec are known, the magnitude M is given by equation (1) where F (for a given distance Δ) is taken from table 1. These values

Table 1. Average values of F in equation (1) for W_2 -waves. Δ = distance in degrees over the shorter arc from epicenter to station.

Δ	20	40	60	80	100	120	140	160
F	6.9	6.8	6.7	6.6	6.4	6.2	5.9	5.4

of F are based on earlier research of Gutenberg and Richter (1936, p. 120) and are rough approximations since with increasing length of the wave paths the effects of variations in structure of the earth's crust accumulate.

Records of the main shock written at distances less than 18° were too large for measurement of amplitudes on torsion seismographs and, consequently, all magnitude determinations for the main shock are based on ground amplitudes calculated from records at distances over 20° . Results are given in table 2. A sign " \pm " indicates that the constants of the instruments were not well known, or that the trace amplitude was in doubt, or

* In a letter to *Nature* (1955) Gutenberg and Richter have re-discussed the definition of magnitude. For the main shock the new magnitude M is 7.4 from body waves as well as from surface waves. Revised equations and calculations give a corresponding energy release of 4×10^{23} ergs. The correction C in equation (2) is no longer added, but a correction has to be used if M is calculated from surface waves.

Table 2.

Magnitudes determined for main shock, July 21, 1952, from direct longitudinal waves (P), longitudinal waves reflected once at the earth's surface (PP), direct transverse waves (S), maxima of direct surface waves (Max) and maxima of surface waves over the greater arc (W2). H = horizontal component, Z = vertical component. Corrections B and C in equation (2) are added. Δ = epicentral distance in degrees. An asterisk (*) indicates use of reported amplitudes.

Station	Δ	Magnitude determined from						
		PZ	PH	PPZ	PPH	SH	Max H	W2H
Lincoln	18.6		7½				8	
Saskatoon	19.3		8.1				7.5	
Guadalajara	19.8		7.3±					
Tacubaya	23.4	7.9	7.4			7.4		
Puebla	24.4		7½			7½		
Sitka	25.1		7.8			7.4		
Chicago USCGS	25.4		7.8			7.8		
Veracruz	25.7		8±					
Cleveland	30.0	7.6	7.6			7.3±		
Ottawa	34.3		7.4			7.3		
Palisades	35.7	7.5*						
Honolulu	36.6		7.6			7.3	7½±	8±
Seven Falls	37.7		7¾		8	7¾		
Kingston	41.1		7.6±			7½		
Resolute Bay	41.5		7.6±			7.4±		
Halifax	42.9		7.8			7.5		
Reykjavik	62.1	7.7	7.7	7½		7.5	7.4±	
Huancayo	62.5	7.6±		7.4±				7.6
Apia	69.7		7.7		7.3			
La Paz	70.4	7.8	7.5	7.9		7.4	7.5	7.7
Angra do H.	70.4		7¾			7½		
Kiruna	73.0	7.2	7.5	7.3	7.4	7.6		
Sapporo	73.3	7.6±	8.0±			7.4±		
Aberdeen	74.0		7.5		7.4	7.6	7.8	6.9±
Edinburgh	74.3		7.3		7.6	7.3	7.7	6.6±
Rathfarnham	74.6	7.4±						
Bergen	74.6		7.4±		7.2±	7.6±	7.7±	6¾±
Durham	75.7						7.9*	
Sendai	76.1	7.8	8.1			7.3	7.2	
Tokyo ER1	78.3		8.0			7.9	7.5	7.5±
Tokyo CMO	78.3	7.9	7.9			7.9	7.4	
Kew	78.5	7.3	7.2	7.2	7.1	7.8	7.6	7.1±
Uppsala	78.9		7.0			7.1	7.9	6.8
Matsushiro	78.9		7.6				7¾	
Nagoya	80.5		7.8					
De Bilt	80.5	7.3	7.4	7.7	7.6	7.8		7¼±
Copenhagen	80.6	7.2	7.3		7.4	7.4	7.9	
Hamburg	81.4		7.4			8.1	7.8	
Coimbra	81.6		7.5			7.9	8.0	
Paris	81.7	7.5	7.6			7.9	7.8	
Osaka	81.8	7.7	7.6					
Santa Lucia	81.8		7½			7.3±		
Lisbon	82.1	8.0	8.1			7.9	7.8	
Concepcion	82.3		7½			7.3±		
Jena	84.0	7.4	7.3	7±	7.0	7.6	7.9	6.8±
Collnberg	84.3		7.3		7.0	7.3	7.8±	6.7±
Strasbourg	84.3	7.5	7.7	7.6	7.3	7.6	7.8	7.0±
Stuttgart	84.4	7.5	7.8	7.4	7.5		7.9	7.1±
Cheb.	85.0		7.7*					
Neuchatel	85.1	7.0±	7.4±			7.4±		
Zurich	85.5	7.2±	7.5					
Praha	85.8		7.6	7.3	7.6	7.1	7.9	6.7±
Tortosa	86.3		7.8±			7.8±	8.0±	
Chur	86.3	7.1±				7.1±		
Cartuja	86.4		8.1±			7.9±	7.6±	
Averroes	86.6		8.0		7.3	7.6	7.9±	
Barcelona	86.7		8.1		7.2	7.9	7.9	
Milano	86.9					7.8±		
Stara Dala	87.3		7.9*				7.9*	
Pavia	87.4	7.4	7.6	7.4	7.6	7.3		6.9
Skalnate Pleso	88.7		7.7*			7.7*	7.7*	
Trieste	89.1	7.4	7.0	7.1			7.9±	6.9
Ilurbanovo	89.1						7.9*	
Prato	89.3		7.4					
Budapest	89.7		7.7		7.6	8.17	7.9	
Eva Peron (La Plata)	89.9		7.7		7.8		7.6	7.4±
Zagreb	89.9	7.3	7.6	7.2	7.8	7.6	7.9	7.4±
Roma	91.5	7.5	7.6	7.1	7.3	7.5±		7.2±
Beograd	92.5	7.2	7.3			7.3±	7.9	7.2±
Wellington	97.2				7.3	7.3	7.4	8.8
Athens	99.6				7.2	7.2±	8.0	
Christchurch	99.9		7.4			7.8	7.1	8.2
Brisbane	103.7				7.6	7.2±	6.8	8.3
Riverview	108.3			7.2			7.0	8.4
Helwan	109.7	7.4±		7.4	7.3		7.7	7½±
Melbourne	114.6						6.9±	8.0±
Quetta	114.9				7.5		7.5	7.5±
Calcutta	117.2				8.0±		7.9±	7.8±
Hyderabad	125.2				7.3		7.6	7.3±
Bombay	125.2				7.5		7.5	7.1
Poona	125.4				7.3±		7.6±	
Kodaikanal	132.4				8.0±		7.4	
Perth	134.6						7.2	7.8
Tananarive	160.1				7.3±		7.8±	

(especially for *S* near 84° and for *W2*) that there was doubt about the proper identification of the phase. The resulting values of *M* depend to some extent on local conditions at the source and the station (unless corrected for), and on the wave path. For *PP*, the longitudinal wave reflected at the earth's surface (or at the Mohorovičić discontinuity) about half way between source and station, conditions at the point of reflection also affect the recorded amplitude; there is good indication that reflections under the bottom of the Pacific Basin result in smaller energy for *PP* and probably correspondingly greater energy in *PS* than those under continents. No corrections for these effects are applied in table 2 and, consequently, magnitudes calculated from *PP* may be expected to be too small in instances of reflections under the Pacific Basin.

Average magnitudes calculated from amplitudes of the vertical (*Z*) and horizontal (*H*) components of the phases *P*, *PP* and *S* are listed in table 3. The differences between the results given in the five columns are rather small. In finding the most likely value of *M* we have to consider that the magnitude resulting from *PP* is probably slightly too small since no correction was applied for reflections in the Pacific Basin that usually lead to relatively small amplitudes of *PP*. In addition, the magnification of many old vertical instruments is likely to be smaller than given by the stations (Gutenberg, 1945c, p. 119), and consequently slightly too small calculated values of *M* are to be expected if *PZ* and *PPZ* are used. Thus we may conclude that the magnitude indicated by the body waves of the main shock on July 21 is near 7.6.

Table 3. Magnitude *M* of main shock on July 21, calculated from amplitudes of body waves. *n* = number of stations.

	Phase and component				
	PZ	PH	PPZ	PPH	SH
<i>M</i>	7.5	7.6	7.4	7.5	7.6
<i>n</i>	29	62	16	34	53

The average magnitude calculated from *P* on records of stations in the azimuth towards Japan is 7.8, whereas the corresponding value of *M* found from records at stations in the direction towards northern Europe is only 7.4 to 7.5. Magnitudes calculated from *PP* show a distribution in azimuth similar to that in *P*: 7.6 in the azimuth towards Japan and 7.4 towards Europe. Probably these differences are mainly a consequence of effects already mentioned, but, in addition, may be expected to include a term produced by the distribution of energy with azimuth at the source which depends on the direction of strike and dip of the fault surface at the depth of focus, on the direction in which the faulting proceeded and on the direction of motion along the fault surface, and is different for longitudinal and transverse waves.

Magnitudes calculated from *SH* (table 2) show a relatively high average of 7.7 in the direction towards southern Europe, 7.6 towards northern Europe and Japan, and only 7.4 towards South America.

While the azimuthal differences in the magnitude calculated from *P*, *PP* and *S*, though fairly consistent, are

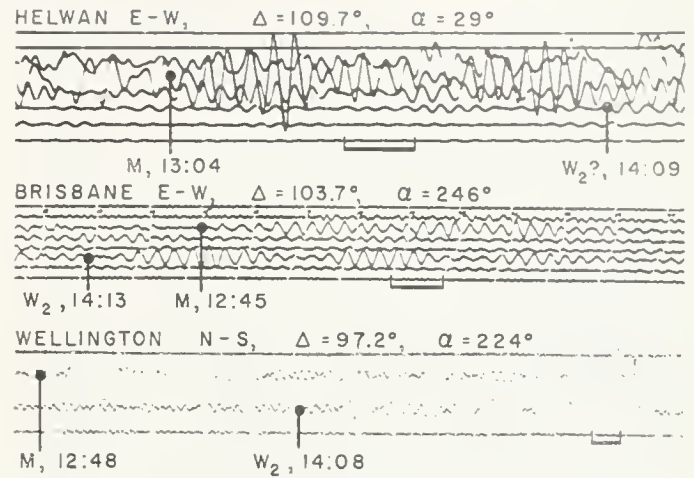


FIGURE 1. Parts of Milne-Shaw records of main shock July 21, showing maxima of direct surface waves *M* and of *W2*. The length of 1 minute is indicated in each record. All instruments have the same free period (12 sec.) and the same magnification (250).

rather small and may be produced by accidental accumulation of errors, the surface wave maxima show a very strong dependence on the azimuth of the station. Whereas maxima recorded in Europe lead to a magnitude of 7.9 ± 0.1 , those recorded in New Zealand and Australia give only about 7.1. About fifty times as much energy was radiated in the surface waves towards northeast than towards southwest. This is confirmed by the fact that on all records of the main shock written in New Zealand and Australia the largest surface waves over the greater arc (*W2*; see Fig. 7, Part II-1) have amplitudes as great or greater than the largest direct surface waves (examples in figure 1) although the paths of the *W2*-waves to these stations are about twice to three times as long as those of the direct surface waves. On the other hand, *W2*-waves cannot be identified on most European records, since in Europe their amplitudes are not significantly larger and possibly even smaller than those of late direct surface waves arriving simultaneously with *W2*, 1½ to 2 hours after the maximum of the direct surface waves (depending on the epicentral distance of the station). Most magnitudes calculated from *W2* for European stations are marked "±" in table 2 since there was doubt whether the corresponding waves were actually *W2*-waves or late direct waves.

Figure 2 shows calculated magnitudes *M*, and amplitudes a_{s4} of surface wave maxima which would have been observed at a distance of 84° (at 84°, $\log a = M - 5.0$) as a function of the azimuth towards the stations. No correction was made for the effect of wave paths (see e.g. Gutenberg, 1945a, p. 9); these would increase the values of *M* and *a* for Japanese and South American stations (azimuths near 310° and 130° respectively).

From fig. 2a average values of *a* were calculated for nine different azimuths, and the method of least squares was applied to calculate a sinusoidal curve fitting the data best. The resulting curve for the amplitude a_{s4} in microns (including standard errors) is given as function of the azimuth α by

$$a_{s4} = (417.8 \pm 20.3) + (342.2 \pm 23.7) \sin(\alpha - 54.8^\circ \pm 5.8^\circ). \quad (3)$$

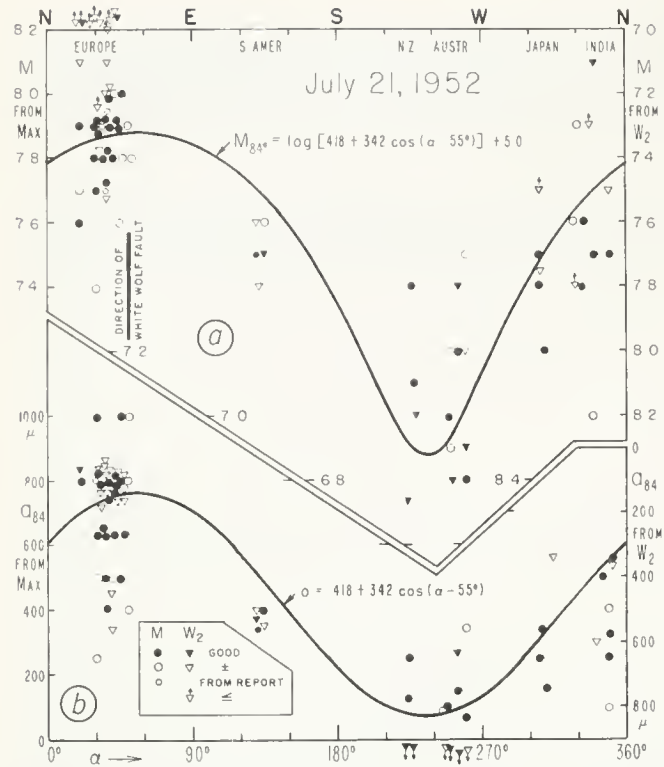
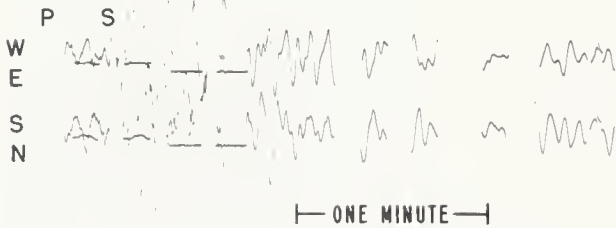


FIGURE 2. a, Calculated magnitudes of the main shock, and b, calculated amplitudes at 84° epicentral distance; both are based on maxima of surface waves (left scale) and of W₂ waves (scale at right) and plotted as function of azimuth α at the epicenter towards the station from north (0°) towards east (90°).

The magnitude corresponding to the average amplitude of 417.8 microns at a distance of 84° is 7.62 ± 0.02, the magnitude corresponding to the average energy is 7.68 ± 0.03. Thus, the recorded amplitudes of the surface waves indicate that the magnitude of the main earthquake was between 7.6 and 7.7.



PASADENA STRONG MOTION, V = 4, 1952 JULY 21

FIGURE 3. Portion of record of strong-motion seismographs at Pasadena on July 21, 1952. Epicentral distance is 124 km. Recording becomes visible when trigger device intensifies light. Small aftershocks produced short almost straight lines about 15 minutes after main shock (line below main seismogram) and 30 minutes after main shock (second line below shock). Length of 1 minute on original seismograms is 60 mm.

Table 4. Selected values of the magnitude *M*, calculated from surface wave maxima for the aftershock of July 29, 7^h.

Direction from epicenter							
Northeast		Southeast		Southwest		Northwest	
Copenhagen	6.3	La Paz	6.1	Christchurch	5.9	Matsushiro	5.8
De Bilt	6.2	Huancayo	5.6	Wellington	6.1	Bombay	6.2
Kew	5.9	Puebla	6.2	Riverview	6.0	Sitka	6.0
Durham	6.1	Veraacruz	6.2				
Uppsala	6.0	San Juan	5.7				
Praba	6.1						
Aberdeen	6.1						
Stuttgart	6.3						
Kiruna	6.2						
Roma	6.2						
Hamburg	6.4						

The trace amplitudes recorded by the WE and SN components of the strong motion instrument at Pasadena (fig. 3) are 70 and 50 mm respectively. Using calibration data found by Gutenberg and Richter (1942, p. 167) this gives a magnitude of 7.5 ± (log average trace amplitude mm + log b = 1.8 + 5.7, corresponding to Δ = 124 km). The corresponding maximum horizontal ground motion at the Seismological Laboratory is of the order of 20,000 microns with a period of about 10 seconds. These waves are superposed by smaller motion with shorter periods.

The azimuth 55 ± 6 degrees in which according to equation (3) the largest surface waves were recorded, agrees with the strike of the White Wolf fault (α = 50°) within the limits of error; the location of the aftershocks relative to the main shock (fig. 1, Part II-6A) indicates that the breaking was propagated roughly towards northeast. The fact that in this direction the surface wave maxima were roughly ten times the maxima in the opposite direction (azimuth 230° ±) may be considered to indicate that the speed of propagation of the fracturing was not much less than the wave velocity, so that it was possible for each wave to increase along the line of breaking which probably measured several tens of wave lengths. However, it is difficult to develop a detailed quantitative theory, since surface waves are formed by a variety of complicated processes. A qualitative discussion of these phenomena is given by H. Benioff in his section, *Mechanism and Strain Characteristics*.

The more or less horizontal direction towards northeast in which the faulting process proceeded should have influenced the amplitudes of P and S as function of azimuth much less than those of the maxima at distant stations, since the rays of the body waves arriving at distant stations form angles of 50° or more with horizontal direction.

In the aftershocks the faulting can be assumed to have proceeded along much shorter distances than in the main shock, and consequently no appreciably greater amplitudes of surface waves in the direction of faulting can be expected than in the opposite direction. Unfortunately, records for the surface waves at distant stations are available in a variety of azimuths for the shock of July 29, 7^h only. Characteristic values of *M* calculated from surface wave maxima for this shock are given in table 4; the average of all calculations is 6.1 (table 5). The calculated magnitudes show no difference in azimuth

Table 5.

Magnitudes M of largest aftershocks in Kern County, 1952. (a) averages calculated from trace amplitudes recorded by standard torsion seismographs at near-by stations; (b) calculated from amplitude of body waves, and (c) from amplitudes of surface wave maxima at distant stations; (d) averages from all data for the shock. n = number of data.

Date	hour:min.	a)		b)		c)		d)	
		M	n	M	n	M	n	M	n
July 21	12:02	5.6	7	-	0	5.6	1	5.6	8
	12:05	6.2	6	6.6	6	-	0	6.4	12
	12:19	5.3	5	-	0	-	0	5.3	5
23	19:41	5.6	7	-	0	5.5	7	5.5	14
	00:39	6.1	5	6.2	14	6.0	34	6.1	53
	03:19	5.3	6	-	0	4.9	12	5.0	18
	07:53	5.7	7	-	0	5.2	21	5.4	28
	13:17	5.6	6	5.9	4	5.7	19	5.7	29
25	18:14	5.3	7	-	0	4.6±	2	5.2	9
	13:13	5.1	7	-	0	4.6	3	5.0	10
	19:10	5.8	8	5.7	7	5.8	32	5.7	47
	19:43	5.9	8	5.8	2	5.6	29	5.7	39
	20:06	5.1	7	-	0	4.6	8	4.8	15
29	07:04	6.2	7	6.0	11	6.1	40	6.1	58
	08:02	5.3	7	-	0	4.9	7	5.1	14
31	15:49	5.1	7	-	0	4.4	4	4.9	11
	12:09	6.0	7	5.5	1	5.5	3	5.8	11
Aug. 1	13:04	5.1	5	-	0	-	0	5.1	5
	22:41	6.0	7	5.9	1	5.5	30	5.8	38

beyond the expected effects of wave paths. This proves also that the variation of M with azimuth in figure 2 is not a consequence of wave paths. In the shock of July 29, 7^h, no clear W2-waves were recorded, and, contrasting with the main shock, they must have been much smaller everywhere than the direct surface waves. For the shock near Bakersfield on August 22, 22^h, no records of maxima are available for the southwest sector, but in other directions the recorded maxima of surface waves give the same magnitude within the limits of error.

Magnitudes of the largest aftershocks (about magnitude 5 and over) are listed in table 5. This offers the first opportunity to compare directly a greater number of values of M calculated by the original Richter method with those found from body or surface waves at distant stations. Considering the systematic errors, the agreement is good. This is especially true for the best observed shocks, those of July 23, 0^h, of July 25, 19^h, and of July 29, 7^h. In the average there is no difference between magnitude calculated from nearby maxima and those found from body waves at distant stations. In some instances, mainly small shocks, the magnitude calculated from surface waves at distant stations is about 0.5 smaller than the corresponding value found from near-by stations. The greatest difference, 0.7, is listed for the earthquake of July 29, 15^h; in this shock the values found from the surface waves are 4.2, 4.3, 4.5 and 4.7, while those calculated from the records at near-by stations are 4.9, 4.9, 4.9, 5.0, 5.3, 5.3, 5.4. In the shocks near Bakersfield on August 22, all differences are relatively large. Values for M calculated from the near-by stations are between $5.7 \pm$ at Riverside (possibly maximum on one component too dim to be found) and at Pasadena, and 6.4 at Mineral; values from distant stations are between 5.2 at Aberdeen, College, and Sitka and 6.1 at Cleveland and Bombay. However, magnitudes calculated from surface waves at distant stations are prevailingly smaller than magnitudes found from records at nearby stations and those calculated from amplitudes of body waves at distant stations. This later was found to be due to a general phenomenon.

Magnitudes for smaller shocks ($M < 5$) have been determined in the usual way from maximum amplitudes at near-by stations by Dr. Richter. All results are entered in table 1, Part II-6A.

9. FORESHOCKS AND AFTERSHOCKS

BY C. F. RICHTER

ABSTRACT

There was little prelude to the major earthquake of July 21, 1952. Small shocks had occurred sporadically in the area. The one true foreshock occurred 2 hours earlier.

Aftershocks were studied using seismograms from stations previously existing, from new stations set up in Kern County, and from portable seismographs operating at numerous locations for short intervals. On September 3-5, 1952, three portable units were in the field.

Epicenter locations were begun assuming wave speeds determined in earlier investigations. These are consistent with the new data, so that epicenters are accurate in general within about 2 miles. However, the assumed velocities can be improved, especially at short distances.

For the first 36 hours all located epicenters lie on or south of the White Wolf fault, tending to diverge from it toward Tehachapi. This agrees with the known dip of the fault. Beginning with a large aftershock after 36^h 46^m, aftershocks occurred both north and south of the White Wolf fault. Two large ones on July 25 northeast of Caliente were followed by many small ones from the same point, continuing for months. On the night of July 28-29 a large shock and several small ones occurred along a line parallel to the White Wolf fault but passing near Bakersfield; this is almost exactly transverse to the known surface structures there. On August 22, 1952, a shock of comparatively minor magnitude (5.8) on this line added greatly to the damage at Bakersfield.

Even considering smaller shocks, epicenters of the group are confined to an area with sharp straight boundaries on at least three sides; these boundaries presumably indicate faults. To the south, the boundary runs appreciably north of the Garlock fault; westward, it lies only a few miles west of the epicenter of the main earthquake, so that the activity nowhere gets near the San Andreas fault; to the north it is marked by the line near Bakersfield.

The complexity of this distribution in space and time is probably not exceptional; but on this occasion the data are better than for any preceding major event, so that the details are established with unprecedented clearness.

The mechanical unity of the whole phenomenon is indicated by a tendency for successive shocks to occur in different parts of the active area, rather than repeating from the same point; this is illustrated by a special type of scatter plot.

The effect of the root of the Sierra Nevada in modifying the paths of seismic waves is shown clearly, especially in the times of arrival at the Tinemaha station.

Most of the shocks have been assigned to a depth of 16 kilometers (10 miles); a large fraction, especially to the northeast, having been worked out for a depth of 10 kilometers, and others, mostly small, are still shallower. Depth determination is less accurate than epicenter location.

One hundred ninety-nine shocks of magnitude 4.0 and over are listed to the end of June, 1953. Location for these is incomplete, since overlapping recording presents difficulties in the first few hours. Additional smaller shocks which have been investigated are also catalogued, bringing the listed total to 267. Twenty-one further shocks of magnitude 4.0 and over occurred to the end of June 1955 (table I).

Study of these earthquakes has been directed largely toward determining their distribution geographically and in time, with a view to conclusions as to the mechanical processes which caused them. Even in a year's work it has been possible to carry this out only for a selection from the extremely numerous instrumental records, including the shocks of magnitude 4.0 or over, with a few smaller shocks favorably located near the temporary installations. The results are catalogued in table 1, and mapped on figures 1, 2.

Condition of the Stations. Stations and instruments are described in Part II-5 and Part II-4, respectively.

Noteworthy circumstances of recording are the following:

Pasadena: One short-period torsion seismometer had its suspension broken during the main shock. Other instruments were undamaged. The strong-motion unit functioned, but recorded the main shocks and immediate aftershocks only when the flasher unit was triggered. After about an hour the unit was put to recording uninterruptedly, and has remained so to this writing. A microbarograph, responding mechanically, acted as an additional strong-motion seismograph.

Mt. Wilson: Recording failed July 27-28. In February, 1953 a new installation developed trouble which was not corrected for several weeks.

Riverside: Vertical component out of order July 21-23; readings from the much less sensitive torsion seismometers, may not represent the first seismic waves for the smaller shocks.

Santa Barbara: Both N-S torsion seismometers put out of order by the main shock; E-W and vertical components continued recording. 24 hours recording July 30/31 lost.

La Jolla: No records July 20/21. Some later gaps. Time determination very inaccurate; records chiefly useful for magnitudes of the aftershocks. Station abandoned on July 30.

Palomar: Recording satisfactory July 21-August 15. Clocks out of order August 15-28, and no time for most shocks. Barograph responded mechanically to main shock and aftershocks. Drums operating on two independent drives, which gives an additional check on time, particularly valuable for the main shock.

China Lake: Vertical pendulum put out of order by main shock; galvanometer continued responding mechanically, but times of first motion from this record may be slightly late, until repairs on August 13. Horizontal components in good order throughout.

Haiwee: Vertical pendulum usually against the stop, until adjusted in February 1953. Times mostly read from the torsion instruments; often somewhat late, since this station has a high level of background disturbance.

Tinemaha: Mostly in good order. All records September 16/17 lost, due to a short-circuit during a storm. Drums mostly out of gear October 21-24.

Barrett: No timing available July 23-30 or August 15-27. No shocks recorded (pendulum on stop) during November. Station out of commission December 21, 1952 to February 3, 1953.

Dalton: Clock not running July 19-23. Some loss of recording July 24/25. Principal instrument disturbed, records difficult to read, July 25-August 9. Low sensitivity vertical-component instrument wrote clear records throughout.

Big Bear: Recorded throughout with no deficiencies.

Shortage of personnel, especially during the vacation season, made it necessary to postpone repairs and adjustments to instruments not essential to the principal program. Imperfections which left the records at all usable often were allowed to persist; this sometimes added greatly to the expenditure of time in reading the records, so that some data absent from the accompanying tabulations are actually available, and will be added to the files in due course.

We have borrowed the entire seismogram file for stations of the University of California group, from July 20 through August 1, and for August 22-23. Most of these records are excellent and of the highest value. It is planned to study at least selected records of later date. The most important of these stations for locating the Kern County earthquakes are Fresno and Mt. Hamilton. Copies of the records at Boulder City, July 20-August 1, are also available.

The Chuchupate station operated as a strong-motion installation without absolute time July 21-23. Thereafter there were numerous interruptions, due to failure

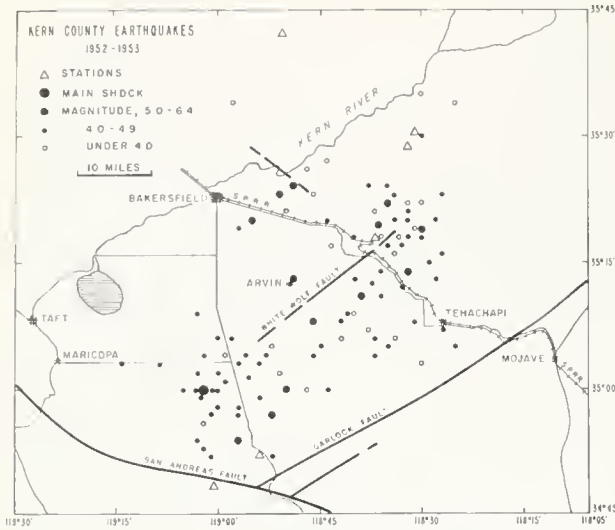


FIGURE 1. Epicenters of located shocks, July 21, 1952 through June 30, 1953. Coordinates as given in Table 1.

of the drive motor. After transfer to Fort Tejon in November the equipment functioned almost perfectly.

The Havilah station began recording on July 25, several hours after the large shocks of that date. The drum was out of gear July 26 for 6 hours, and on July 28/29 for 24 hours. Timing is uncertain for several days following August 13. The seismometer was disconnected from August 22 to August 29.

Recording at Knox Ranch was satisfactory except for much partial fogging of the records due to prolonged exposure to red light. There were no such difficulties with the same equipment at Williams Ranch, where only a few records were lost.

Recording at King Ranch was satisfactory for October 16-November 13. A rainstorm on November 15 caused trouble which lasted until December 2. The seismometer was on the stop January 15-February 19, 1953, and there was some defective recording in March.

The first location for the portable unit, designated BED, was about 200 yards northeast of a triangulation point so marked on the Tehachapi quadrangle, U.S.G.S. Records were run from July 21, 18:57 to July 22, 01:50, G.C.T. At White Oak Lodge, records were run from 04:57 to 15:00 July 22, G.C.T. At White Wolf recording began at 01:03 July 24, G.C.T.; at this location many valuable times were determined, but there was intermittent trouble of all kinds, and finally the recorder was overturned by an inquisitive horse. After this accident the unit was not again in service until August 13. The earlier of the two runs at Walker Dump (August 14/15) and the run in Kern Gorge (August 28) were only partially useful, since no radio signals were received and there is no absolute time.

Operation of the several portable units on September 4-6 and November 12-14 is discussed in reporting the special recording programs on those dates.

Location of Epicenters, Methods and Procedure. Preliminary epicenter determinations for most of these shocks were necessarily based on incomplete data. Determining times for a given shock at all stations is about an hour's work under favorable circumstances, and may take several times as long if, as usual, the registration

of earthquake motion or of time signals is imperfect. Subsequent careful location may easily consume a half day. To organize the data, first locations were made by Mr. G. G. Shor, working largely with time-differences among a few selected stations for each shock. Most of these locations provided good first-approximation solutions for further refinement. Exceptions were chiefly in the northeastern part of the affected area; these were studied in close correlation with records of small shocks in the same vicinity during the special program in September, and corrected epicenters were derived early in the investigation.

Revised epicenters (table 1, figs. 1, 2) have been calculated assuming that times of recorded first motion (table 2) are generally given either by

$$p - O = D/6.34, D^2 = \Delta^2 + h^2$$

or by

$$P_n - O = K + \Delta/8.2$$

where p and P_n represent the measured time of arrival at the station of the first longitudinal seismic wave, direct and refracted horizontally below the continental structure respectively (see fig. (1), section on the main shock).

O = instant of occurrence of the earthquake (origin time)

Δ = distance from epicenter to station (in kilometers)

h = depth of the earthquake source (hypocenter) below the epicenter

6.34 and 8.2, in units of kilometers per second, are the mean values for the two principal velocities, as found from previous studies in this area.

K is a time interval, generally about 5 to 6 seconds, which varies somewhat, both for different stations and for different epicenters. If the depth h increases, the epicenter remaining the same, K should decrease at all stations by approximately the same amount; that is, the wave P_n should arrive earlier at all stations.

In preliminary calculation the depth h has usually been taken as 16 km., an average depth for southern California found in previous investigations (Gutenberg, 1951; Richter, 1950). Some shocks have been worked out for $h = 10$ km. A few, mostly small, have been calculated for $h = 0$ ($p - O = \Delta/6.34$); this is a partly artificial assumption, since the recorded times of actual surface disturbances such as quarry blasts do not fit it.

Thus the epicenters of table 1 constitute a second approximation, based chiefly on simplifying assumptions which are uniform for the whole region. Local variations undoubtedly exist; these have been allowed for by varying the choice of h , and by identifying the first motion as either p or P_n (which partly takes care of the effect of the root of the Sierra Nevada). For short distances, the first recorded arrival must be taken as p ; at larger distances, it is P_n (unless the shock is small and the first motion has failed to record clearly). The critical distance Δ^* , at which p and P_n arrive simultaneously, using the velocities 6.34 and 8.2, is given very closely by

$$\Delta^* = 27.9 K - 0.079 h^2/K$$

Calculated values of Δ^* (km.)

$K =$	5	6	7	8 sec.
$h =$				
10	133	166	194	222
16	131	164	192	221

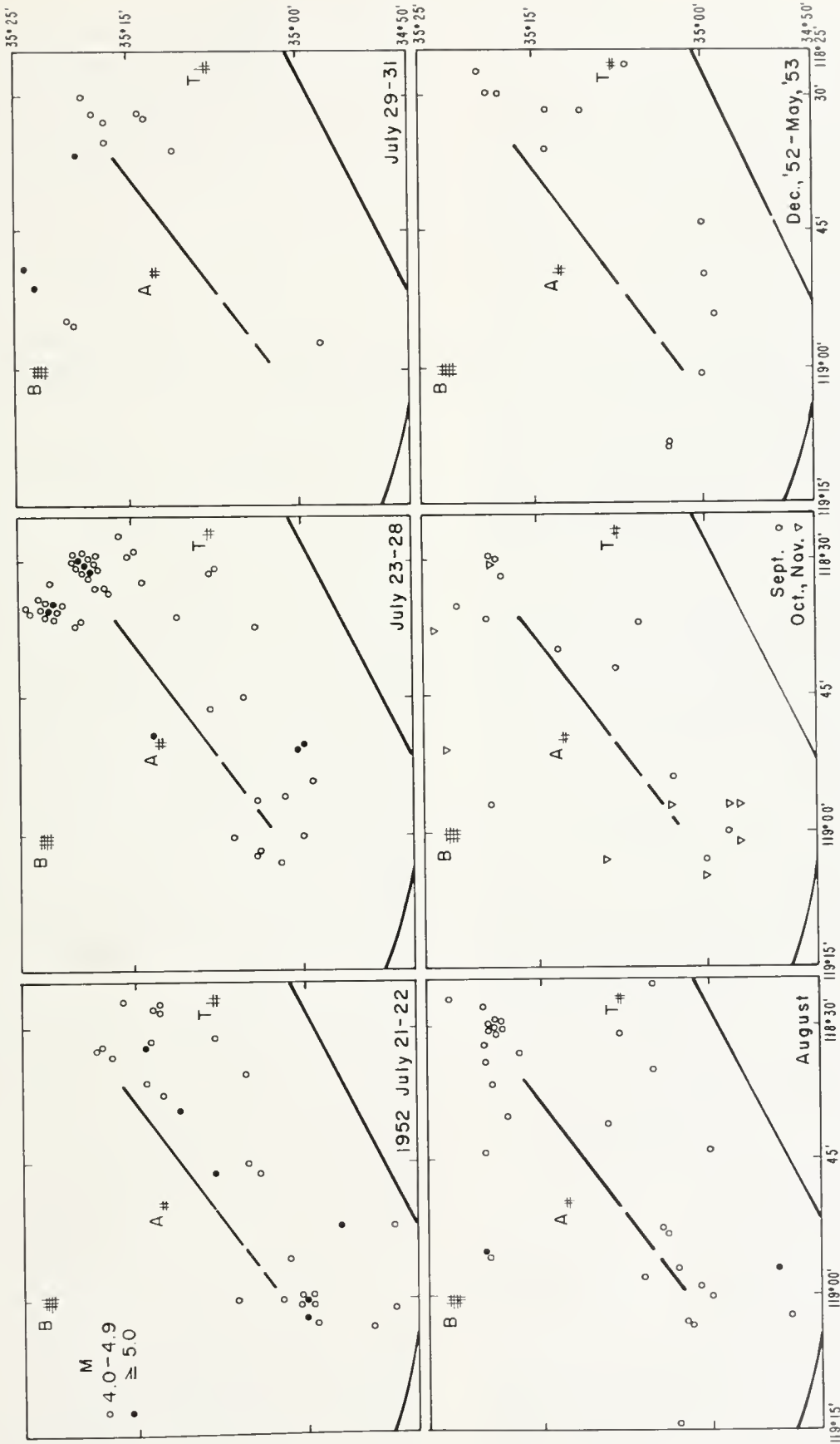


FIGURE 2. Epicenters of located shocks of magnitude 4.0 and over: (a) 1952 July 21 11:52-119°00'-July 23 00°; (b) July 23 00°-July 29 00°; (c) July 29-31; (d) August; (e) September, October, November; (f) December 1952 through June 1953.

At distances slightly shorter than Δ^* the direct wave p is often small, and may be missed or obscured in the records of small shocks.

Revised epicenters have been controlled by comparing the shocks with each other. There are many instances of shocks on different dates which agree so closely that they are clearly assignable to a common hypocenter. A not exceptionally good example is the following:

1952	Hav	Chu	II	SB	CL
July 29—19:51	38.9	41.4	53.2	52.9	53.9
July 31—19:53	21.1	23.3	34.8	34.5	35.3
Time difference 2 ⁰⁰ h02 ^m :	42.2	41.9	41.6	41.6	41.4

Errors of measurement can readily account for the slight variations shown by this tabulation. Time determination at each station involves two independent measurements, one for the time of P referred to the station clock and one for the clock correction. Each of these measurements is made to the nearest tenth of a second on a scale of one millimeter per second; each may easily be in error by 0.1 second, so that the resulting time may be 0.2 sec. in error. In comparing two shocks on different dates, one subtracts two numbers each of which may be in error by this amount.

It frequently happens that several shocks which agree in this fashion have been recorded at different temporary stations; the epicenter chosen to represent the group then is made to fit all these data as closely as possible. A number of aftershocks in the general vicinity of the epicenter of the main earthquake were recorded by the portable units and at Chuchupate, Fort Tejon, King Ranch, etc.; study of their data confirms the location for the main shock.

In some instances, where the first motion is obscured by preceding small shocks or other disturbances, location has been accomplished by comparing times of later phases.

Shocks differing slightly in epicenter can be compared most readily by plotting time differences (usually of first motions) against azimuth for the recording stations. On a rectangular plot the points are then fitted to a sine curve which establishes the amount and direction of shift from one epicenter to the other. Solutions for individual epicenters and origin times have been worked out and recorded in the following form:

Shock of 1952 October 28, 20:52:50.4 referred to 35° 22' N 118° 30' W, h = 10 km.

Station	Time of P 20:52	Δ km.	p-O h=10	O 20:52	Δ / 8.2	P- Δ / 8.2	K (July 25)	O
Knox Ranch.....	52.7	12.9	02.6	50.1				
Woody.....	58.0	48.4	07.8	50.2				
Chuchupate.....	02.9	77.6	12.3	50.6				
China Lake.....	05.3	95.9	15.2	50.1				
Haiwee.....	06.8	98.7	15.6	51.2				
King Ranch.....	08.4	111.7	18.0	50.4				
Mt. Wilson.....	12.0	133.0	21.1	50.9				
Pasadena.....	12.4	138.5	23.3	50.5				
Santa Barbara.....	15.6	151.3	24.0	51.6	18.5	57.1	6.3	50.8
Riverside.....	18.5	184.9			22.4	56.1	6.1	50.0
Big Bear.....	19.6	191.7			23.4	56.2	6.0	50.2
Tinemaha.....	21.0	193.0	30.6	50.4	23.5	57.5	6.9	50.6
Palomar.....	29.3	269.9			32.9	56.4	6.1	50.3
Barrett.....	39.3	342.5			41.8	57.5	7.1	50.4

This solution is slightly better than average. It will serve to illustrate a number of points. This epicenter, like most of those tabulated, has been worked out to the nearest whole minutes of latitude and longitude which best suit the data. Considering possible systematic errors in the velocities, local differences, etc., the placing of these epicenters individually should be considered as possibly in error by 1 minute. This means between 1.5

P	MW	F	R	T	BB	Pr
55.7	56.0	58.9	63.1	64.8	65.5	73.7
37.6	37.6	40.9	44.7	46.3	47.0	55.6
41.9	41.6	42.0	41.4	41.5	41.5	41.9 sec.

and 2 kilometers (or about 1 mile) in any direction. Relative placing of the shocks is more accurate, since the whole epicenter pattern is tied together by systematic intercomparison.

The adopted origin time is the mean of those derived from the direct wave in the third column of the table, omitting Santa Barbara and Haiwee.

The depth h has been taken at 10 km. rather than 16 km., largely in order to fit the reading at Knox Ranch. With $h = 16$ km. and $\Delta = 12.9$ km., the time $p - O$ should be 3.3 seconds rather than 2.6 seconds.

Tabulated values of Δ are calculated accurately from the coordinates of epicenter and station. The third column contains the corresponding values of $p - O$ calculated with the standard velocity of 6.34 km/sec; the origin times in the fourth column follow on subtracting these from the times of P . The values of K in the next to last column are those found for the large shocks of July 25, placed at 35°19' N 118°30' W (except that for Barrett, which is taken from the data of a shock with the same epicenter on August 30). In the last column are origin times calculated as $P - \Delta 8.2 - K$. These should compare directly with those in the third column; the agreement is close. This procedure is equivalent to taking time differences between the tabulated shock and those of July 25, correcting them by dividing the difference in distances of the given station from the two epicenters by 8.2, and inferring the origin time.

With $h = 10$ and $K = 6$, p and Pn should arrive simultaneously at $\Delta = 166$ km. However, p either does not arrive or is delayed at Santa Barbara, distant 151 km. This may be connected with the fact that the direct path from hypocenter to Santa Barbara crosses the White Wolf fault at a low angle. On the other hand, p appears to reach Tinemaha at 193 km. Tinemaha apparently records p for most of the Kern County shocks, except those farthest southwest, in the vicinity of the epicenter of the main shock; this is useful in locating trial epicenters, but care has been taken not to force the epicenters in order to bring Tinemaha readings into line. The circumstances will be discussed more fully in connection with the effect of the Sierra Nevada structures.

Readings at Haiwee tend to be slightly late relative to the other stations; this is in part due to the high level of background disturbance at Haiwee.

Assignment of magnitudes for all except the larger shocks is a routine matter; the following is an example.

Shock of 1952 October 28, 20:52:50.4.

Station	A (amplitude, mm.)		Δ (km.)	log A	log A ₀	Station correction	Magnitude
	N	E					
Haiwee.....	10.5	9.9	98.7	1.0	-3.0	0.0	4.0
Pasadena.....	1.7	4.1	138.5	0.5	-3.2	+0.2	3.9
Santa Barbara.....	2.6	2.7	151.3	0.4	-3.3	-0.2	3.5
Riverside.....	1.1	1.1	184.9	0.0	-3.5	+0.2	3.7
Tinemaha.....	2.4	3.7	193.0	0.5	-3.5	-0.2	3.8

Adopted mean magnitude, 3.8. Only amplitudes recorded by the short-period torsion seismometers are used. These are tabulated in millimeters of trace for the N-S and E-W components at each station. Distances are as given for this shock on a previous page. Log A, taken from the original publication on the magnitude scale (Richter, 1935), is the logarithm of the amplitude for the standard shock (magnitude 0) at the given distance. (The whole logarithm is negative; -3.5 means just that, and not -3 + 0.5.) The station corrections to magnitudes representing combined departure of instrument and ground conditions from the mean, are as re-determined by Gutenberg. The individual station data then yield magnitude = log A - log A₀ + station correction.

In this work much use has been made of magnitudes reported in regular bulletins from the Berkeley station. These were determined by the workers at Berkeley from their torsion seismometer records, using the same method and materials. They proved invaluable in setting up preliminary listing of the larger shocks of the group (down to magnitude 4); and the numbers have been included as of equal weight in determining adopted magnitudes. These data, together with readings from the strong-motion instruments at Pasadena, the barograph at Palomar, and the torsion seismometers, were correlated by Mr. J. M. Nordquist to provide the initial basis for table 1.

For shocks of magnitude 5 and over the maximum on the torsion seismograms is off the paper or underexposed at the nearer stations, so that more use must be made of the records written at larger distances. (See the appropriate section on magnitudes of the larger shocks.)

Data for the best recorded aftershock, to this writing, to be located at an epicenter indistinguishable from that of the main shock, have been analyzed as follows:

Shock of 1953 May 25, 03:24:00.8, referred to 35° 00' N 119° 01' W, h = 16 km.

Station	Time of P 03:24	P-O (main shock) 03:24:	Re-sult-ing 0=	Δ km.	P-O h=16	O 03:24:	$\Delta/8.2$	P- $\Delta/8.2$ 03:24:
Fort Tejon.....	04.3	xxx	xxx	17.9	03.8	00.5		
King Ranch.....	13.1	xxx	xxx	75.6	12.2	00.9		
Woody.....	13.4	xxx	xxx	79.1	12.7	00.7		
Santa Barbara.....	14.9	14.4	00.5	89.1	14.3	00.6		
Pasadena.....	20.2	19.4	00.8	122.2	19.4	00.8		
Dalton.....	23.5	xxx	xxx	144.0	22.9	00.6		
China Lake.....	26.0	24.9	01.1	157.6	25.0	01.0	19.2	06.8
Haiwee.....	27.3	26.6	00.7	158.1	25.1		19.3	08.0
Riverside.....	29.5	28.6	00.9	187.7			22.9	06.8
Tinemaha.....	37.7	36.6	01.1	242.3	38.3		29.5	08.2
Barrett.....	48.0	e45.8 146.8	01.2	336.6			41.1	06.9

P = O for the main shock of July 21 is tabulated assuming O = 11:52:14.3. This, subtracted from the arrival time of P on May 25, gives the comparison origin times in the next column. Slightly late resulting times may be due to later reading for the smaller shock. At Barrett it has been supposed that the proper correlative time for the main shock is the large impulse and not the earlier emergence. Records at Mt. Wilson, Big Bear and Palomar were defective on May 25. On the other hand, the three nearest stations and Dalton were not available for the main shock. The latter columns on the table show the solution calculated for all stations using 35° 00' N 119° 01' W. P_n arrives at China Lake, Riverside and Barrett with K = 6.0, 6.0, 6.1. Haiwee and Tinemaha show nearly identical delays due to the root of the Sierra Nevada. Possibly the epicenter for the main shock should be slightly east of 119° 01' W.

Special Recording Programs. On September 3-5 portable units were operated simultaneously at Parker Creek, Piute Ranch and Clear Creek Ranch. The intention was to record at short distances some of the numerous shocks in the vicinity of Lat. 35° 19' N. Long. 118° 30' W. Surrounding of this area was completed to the north by the station previously established at Havilah, which was shifted to Knox Ranch during the program. Reording extended from September 4 00h to September 6 00h (G.C.T.); but owing to various interruptions and accidents shocks were recorded with good timing at all four named stations only for about 11 hours of the 48. Many shocks at other hours were recorded at three stations of the four. Many shocks, including some small ones, were recorded clearly at Woody; and several of the larger shocks were recorded at the more distant stations of the network, including Chuchupate.

A similar program was undertaken on November 12-13 with two portable units in the region of the epicenter of the main shocks. One unit (Elkhorn) proved ineffective; the other, at San Emigdio Ranch, recorded several shocks, two of which were adequately recorded at Chuchupate and more distant stations. Of these two shocks, one was near the far end of the active area; the other (No. 247, at 12:04) was near by, but so small (magnitude 2.3±) that the recording is of very limited usefulness.

The most significant data obtained in these special programs were the times of the shock at 15:14 on September 4 (No. 210). At the nearer stations, S as well as P phases were recorded, and used to approximate the origin time as follows:

Station	P= 15:15:	S-P (sec.)	P-O (sec.)	O= 15:14:
Clear Creek Ranch.....	00.1	01.1	01.5	58.6
Piute Ranch.....	00.4	02.0	02.7	57.7
Havilah.....	01.8	02.8	03.8	58.0
Parker Creek.....	02.1	03.1	04.3	57.9
Woody.....	06.4	06.1	08.4	58.0
Chuchupate.....	10.0	10.1	17.8	56.2
China Lake.....	14.3	11.9	16.3	58.0

Here $S - P = (P - O) \times 1.37$. This assumes that the velocities of the longitudinal and transverse waves are in the constant ratio 1.732 (equivalent to taking Poisson's constant as 0.25); however, the two velocities need

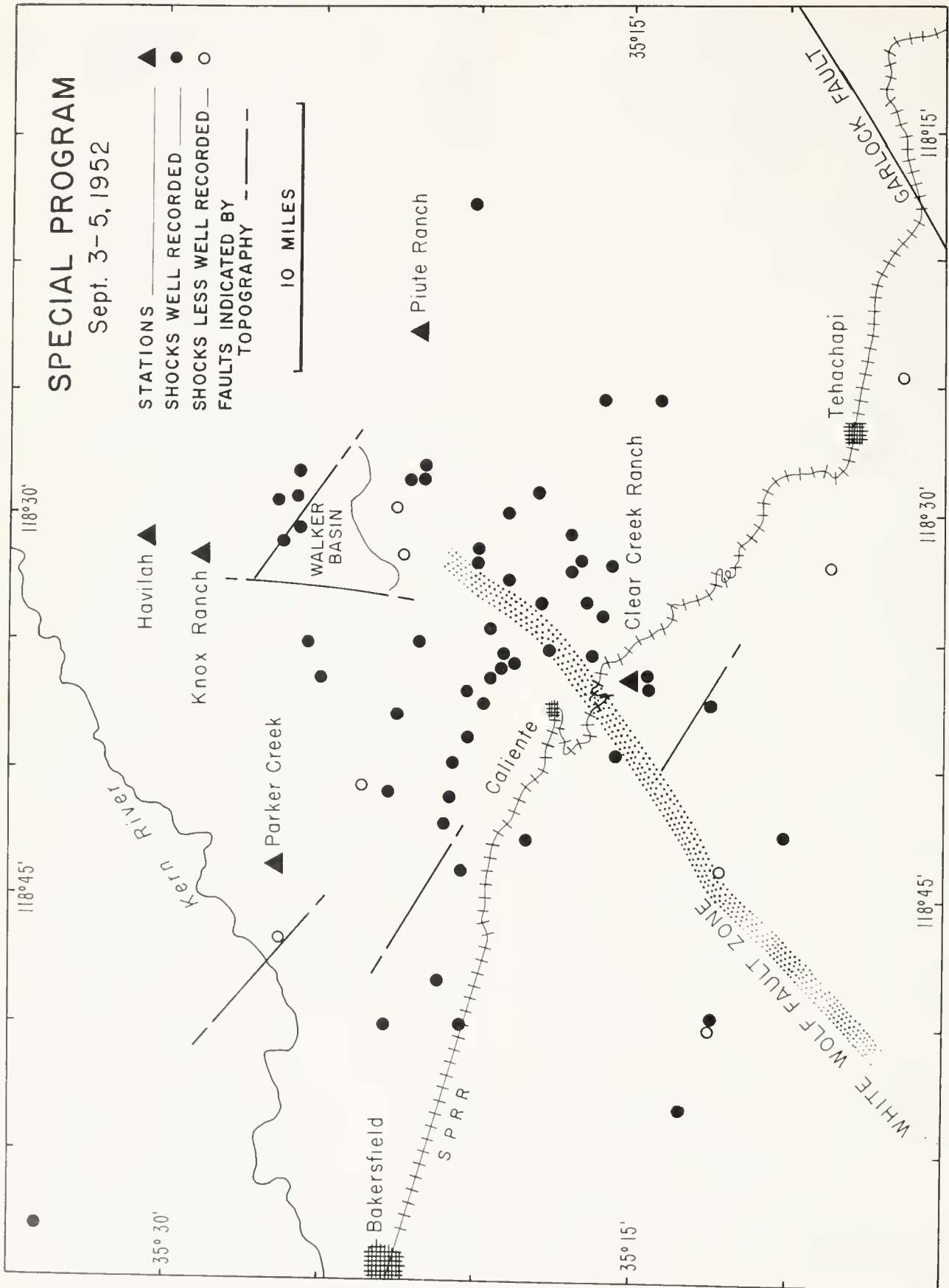


FIGURE 3. Epicenters of small shocks in the region of Caliente, recorded during the special program September 4-5, 1952.

not be individually constant. The transit time of P ($P - O$) is then subtracted from the arrival time of P at the corresponding station to give the origin time O . The agreement is close, except for Clear Creek Ranch and Chuchupate.

The result at Clear Creek Ranch is similar to observations made on former occasions with portable instruments recording at very short epicentral distances—particularly when recording the vertical component. A large sharp wave, which is naturally interpreted as S , arrives 1.0 to 1.5 seconds after P , implying an improbably small depth, or a very high velocity. Not infrequently, if the recorded shock is small or the magnification low, a later smaller impulse arrives more nearly at the time when the transverse wave would be expected. Among the shocks recorded during the special program were several (including No. 210) for which the times of P at Piute Ranch and Clear Creek Ranch differed by only a few tenths of a second, while a clearly legible S arrived at Piute Ranch about one second later than the apparent S at Clear Creek Ranch. The two instruments recorded horizontal and vertical motion, respectively. Perhaps the early apparent S , particularly in the vertical component, is due to a shallow reflection of P , a change of phase on refraction, or the like. On the other hand, a few small shocks with evidence of shallow origin have been recorded, for which there appears to be a true $S - P$ interval between 1 and 2 seconds.

Times read for S at Chuchupate are frequently later than those expected from other evidence. This is a not very sensitive vertical-component instrument, in this as in other instances recording at a distance where the true S is often readily found only on horizontal-component seismograms. No special explanation is needed to account for the early calculated origin time at this station.

From the above data a preliminary origin time was taken as 15:14:57.9. This was employed in various graphical and other trial methods to arrive at an approximate epicenter, $35^\circ 19' N 118^\circ 30' W$, and depth ($h = 10$ km.). The final calculation takes the following form:

	P= 15:15:	Δ km.	D km.	P-O (sec.)	O= 15:14:	Δ /8.2	P- Δ / 8.2 15:15:	K (sec.)
Clear Creek Ranch	00.1	12.5	16.5	02.6	57.5			
Piute Ranch	00.4	12.1	16.4	02.6	57.8			
Havilah	01.8	21.4	24.1	03.8	58.0			
Parker Creek	02.1	25.1	27.3	04.3	57.8			
Woody	06.4	52.7	53.8	08.5	57.9			
Chuchupate	10.0	73.2	74.1	11.7	58.3			
China Lake	14.3	98.9	99.5	15.7	58.6			
Haiwee	15.3	103.1	103.6	16.3	59.0			
Mount Wilson	18.6	127.7	128.3	20.2	58.6			
Pasadena	19.1	133.0	133.5	21.1	58.0			
Dalton	21.3	142.0	142.4	22.5	58.8	17.3	04.0	6.2
Santa Barbara	22.8	147.5	147.8	23.3	59.5	18.0	04.8	7.0
Riverside	25.8	179.4				21.9	03.9	6.1
Big Bear	27.0	188.2				23.0	04.0	6.2
Tinemaha	29.4	198.6	198.8	31.4	58.0	24.2	05.2	7.4
Barrett	45.9	337.7				41.2	04.7	6.9

No time is available at Palomar; the clock had stopped. Because of the high background and low magnification at Haiwee and Santa Barbara the readings there may not represent the first arrivals.

The values of Δ are calculated from the coordinates; for the nearer stations they have been checked on large

scale maps (1/62500). $D^2 = \Delta^2 + (h + H)^2$, where $h = 10$ km, is the assumed depth of the hypocenter below sea level, and H is the elevation of the station above sea level (in kilometers). The choice of h was made principally to suit the two nearest stations, and can be improved slightly by decreasing h . Using $P - O = D/6.34$ as tabulated gives the values of O in the following column. Their correspondence with the time taken from $S - P$, namely 15:14:57.9, is close except for Haiwee and Santa Barbara, and excluding Dalton and other stations where the first motion is P_n . The agreement at Tinemaha in spite of the large distance is usual for shocks in this area.

The last column tabulates $K = P - \Delta/8.2 - O$, with $O = 15:14:57.9$. The agreement at Dalton, Riverside and Big Bear is excellent. The value $K = 6.2$ is fairly consistent with the assumed $h = 10$ km.; for the representative value of K for southern California, derived by Gutenberg (1951) in previous studies is 5.1. This is believed to correspond to a usual depth $h = 16$ km.; and on reasonable assumptions K should increase about 0.13 sec. if h decreases by 1 km. and other conditions are equal. Structural differences will affect K in addition to difference in depth.

The first recorded motion at Santa Barbara and Haiwee may be P_y , for which Gutenberg (1951) found $P_y - O = 1.2 + \Delta/6.21$. For Santa Barbara this yields $P_y - O = 24.9$, whence $O = 15:14:57.9$; for Haiwee the result is $P_y - O = 17.8$, $O = 57.5$.

The relatively shallow depth helps to account for the fit for direct p at Tinemaha. The "root" of the Sierra Nevada projects downward and interferes with the propagation of the refracted P_n , which along other paths arrives ahead of p at this distance. Alternatively, the first arrival may actually be P_n delayed by an increased path through the "root" material until it coincidentally arrives at the time calculated for p . This alternative will be discussed further on.

The relatively late arrival at Barrett is probably connected with structure along that particular path, since Barrett P is similarly late for shocks too large for the first motion to have been missed.

The data of this shock may profitably be compared directly with those of others in the same area. Such comparison for three shocks appears in the following tabulation:

Station	P-O Sept. 4	July 25 19:09:		July 25 19:43:		July 26 01:02:	
	15:14:57.9	P	O	P	O	P	O
Havilah	03.9	x	x	x	x	24.3	20.4
Chuchupate	12.1	57.0	44.9	35.4	23.3	32.4	20.3
China Lake	16.4	61.1	44.7	39.6	23.2	36.4	20.0
Haiwee	17.4	61.3	44.9	40.4	23.0	38.1?	—
Mt. Wilson	20.7	65.9	45.2	?	—	41.3	20.6
Pasadena	21.2	66.2	45.0	44.5	23.3	41.4	20.2
Dalton	23.4	x	x	x	x	43.2	20.8
Santa Barbara	24.9	69.9	45.0	47.7	22.8	44.9	20.0
Riverside	27.9	73.0	45.1	51.3	23.4	48.1	20.2
Big Bear	29.1	74.7	45.6	52.0	22.9	49.5	20.4
Tinemaha	31.5	76.1	44.6	54.4	22.9	52.2	20.7

Here the first column gives the actual travel times for the first arrivals in the shock on September 4. These are

Table 1. Kern County earthquakes, July 21, 1952-June 30, 1955, including all of magnitude 4.0 or over, and all for which epicenters have been determined.

No.	Date	Time G.C.T.	Lat.N.	Long.W.	Mag.	No.	Date	Time G.C.T.	Lat.N.	Long.W.	Mag.
	(1952)						(1952)				
1	July 21	09:43:03	35 00?	119 05	3.1	82	July 23-----	06:10:45.8	35 16	118 27	4.2
2		11:52:14.3	35 00	119 02	7.7	83		06:26:28.4	35 22	118 35	4.0
3		11:54			4.5±	84		06:53:42.3	35 22	118 35	4.2
4		11:55			4.5±	85		07:37:00.2	35 17	118 33	4.8
5		11:57			4.5	86		07:53:18.7	35 00	118 50	5.4
6		11:58			4.6±	87		09:38:42.3	35 15	118 29	4.2
7		11:59			4.5±	88		10:54:13.4	35 19	118 30	4.1
8		12:02			5.6	89		13:17:05.2	35 13	118 49	5.7
9		12:05:31	35.0	119.0	6.4	90		13:30:03.8	35 15	118 29	4.4
10		12:06			4.8±	91		15:25:24.1	35 08	118 31	4.0
11		12:07			4.7±	92		16:18:37.8	35 19.5	118 36.5	4.5
12		12:10			4.5±	93		16:48:53.0	35 19.5	118 36.5	4.5
13		12:12			4.6±	94		17:22:24.0	35 19	118 30	4.5+
14		12:18			4.4	95		17:53:29.2	35 04	119 02	4.1
15		12:19:36.5	34 57	118 52	5.3	96		18:03:27.6	35 19	118 30	4.0
16		12:22			4.9	97		18:13:50.9	35 00	118 50	5.2
17		12:25			4.7	98		19:51:33.8	35 22	118 32	4.2
18		12:28			4.2	99		21:16:58.5	35 01.5	118 55.5	4.1
19		12:39			4.2	100		22:32:20.1	35 04	118 56	4.1
20		12:40			4.9	101		23:51:35.8	35 04	118 37	4.0
21		12:59			4.2	102	July 24-----	03:11:07.2	35 06	119 00	4.1
22		13:08			4.5	103		03:28:26.5	35 14	118 32	3.3
23		13:11			4.1	104		03:29:27.5	35 00	119 05	3.6
24		13:13			4.5	105		05:02:50.0	35 19	118 30	4.5
25		13:17			4.0	106		09:50:32.3	34 59	118 54	4.3
26		13:25:11.6	35 00	119 00	4.5	107		11:47:55.8	35 24	118 35	4.4
27		13:36			4.1	108		12:07:56.7	35 19	118 30	4.1
28		13:59			4.6	109		14:05:26.3	35 19	118 30	4.3
29		14:06			4.2	110		14:10:12.8	35 19	118 30	4.0
30		14:15			4.4	111		17:35:06.0	35 14	118 32	4.2
31		14:17			4.1	112	July 25-----	00:03			4.0
32		14:42			4.2	113		07:03:51.4	35 24	118 35	4.1
33		14:51			4.2	114		10:22:53.6	34 56	119 02	3.3
34		15:13:58.7	35 11	118 39	5.1	115		13:13:08.6	35 19	118 30	5.0
35		15:36			4.2	116		14:34:42.0	35 08	118 46	4.4
36		15:42			4.2	117		19:09:45.0	35 19	118 30	5.7
37		15:53*			4.5	118		19:43:23.3	35 19	118 30	5.7
38		16:17			4.1	119		20:06:05.7	35 19	118 30	4.8
39		16:38			4.5	120	July 26-----	01:02:20.6	35 19	118 30	4.2
40		17:42:44.0±	35 14	118 32	5.1	121		01:04:45.5	35 22	118 32	3.5
41		18:00			4.5	121a		06:38:50.1	35 11	118 36	4.0
42		18:23:38.5	35 18	118 32	4.5	122		09:22:06.5	35 17	118 33	4.3
43		18:26:27.5	35 18	118 32	4.1	122a		15:08:30.9	35 05	118 45	4.4
44		19:12:08.6	35 13	118 28	4.3	123		18:02:43.6	35 05	118 45	4.0
45		19:16:19.2	35 16	118 27	4.3	124		19:51:19.6	35 22	118 32	3±
46		19:41:22.3	35 08	118 46	5.5	125		22:28:21.5	34 54	118 57	3.4
47		20:21:05.9	35 13	118 28	4.2	126		22:41:03.1	35 11	118 36	4.6
48		21:51:46.9	35 06	118 42	3.6	127		22:58:56.5	35 19	118 30	4.3
49		21:53:09.3	34 52	119 01	4.3	127a	July 27-----	00:09:15.8	35 19	118 30	4.2
50		23:11:44.0	35 18	118 32	3.9	127b		02:49:11.6	35 30	118 30	4.0
51		23:53:28.1	34 59	119 02.5	4.5	128		07:16:11.3	35 02	119 03	4.1
52	July 22	01:00:58.3	35 11	118 36	3.2	129		07:35:39.3	35 22	118 35	4.2
53		01:10:43.0	35 11	118 36	3.9	130		11:34:38.4	35 04	119 02	4.1
54		01:13:14.3	35 00	118 47	3.6	131		16:18:07.5	35 22	118 35	3.8
55		01:41:02.0	35 08	118 31	4.5	132		16:26:43.9	35 08	118 46	3.9
56		01:46:08.8	35 14	118 32	3	133		17:37:43.3	35 19	118 31	3.8
57		01:51:50.8	35 17	118 33	4.4	134		18:56:23.6	35 18	118 36	3.9
58		03:21:04.8	35 12.5	118 37.5	4.4	135	July 28-----	02:21:04.4	35 06	118 34	3.9
59		07:44:55.4	34 52	118 52	4.1	136		05:45:54.0	35 08	118 31	4.2
60		08:16:23.7	35 05	118 35	4.4	137		07:29:02.7	35 05	118 52	3.7
61		08:21:21.7	35 00	119 00	4.1	138		15:41:19.7	35 22	118 35	4.0
62		08:47:34.3	35 05	118 45	4.7	139		15:43:11.7	35 22	118 35	3.7
63		09:10:25.1	35 14	118 36	4.5	140	July 29-----	05:56:23.4	35 23	118 51	3.9
64		10:19:38.6	35 02	119 00	4.1	141		07:03:46.8	35 23	118 51	6.1
65		10:44:05.7	35 03	118 30	3.8	142		07:56:23.1	35 23	118 46	3.8
66		13:31:42.9	35 00	119 00	4.8	143		08:01:46.4	35 24	118 49	5.1
67		14:05:11.1	35 06?	119 00?	4.3	144		08:07:49.5	35 26	118 47	3.8
68		14:30:18.3	34 54	119 03	4.3	145		09:37:38.0	35 07	118 38	3.9
69		15:03:14.4	35 14	118 32	4.2	146		10:19:32.7	35 21	118 32	3.7
70		17:52:36.3	35 00	119 00	4.1	147		12:50:37.2	35 20	118 44	3.5
71		19:08:59.3	35 13	118 28	4.3	148		15:49:50.3	35 11	118 36	4.9
72		19:10.4			4.1	149		17:36:43.0	35 14	118 32	4.4
73		21:02:10.8	35 04	118 46	4.2	150		19:51:32.4	35 20	118 55	4.5
74		22:31:33.4	35 01.5	118 55.5	4.7	151	July 30-----	09:59:28.9	35 18	118 32	4.0
75	July 23	00:38:32.0	35 22	118 35	6.1	152		11:02:55.0	34 58	118 57	4.1
76		00:43:08	35 0	119.0	4.4	153		14:46:50.1	35 14	118 32	4.1
77		00:47:38.0	35 22	118 35	4.6	154	July 31-----	04:10:21.7	35 17	118 33	4.2
78		03:19:23.1	35 22	118 35	5.0	155		12:09:08.8	35 19.5	118 36.5	5.8
79		03:49:27.5	35 17	118 33	4.7	156		17:19:08.2	35 17	118 35	4.5+
80		04:01:39.6	35 22	118 35	4.7	157		19:05:14.8	35 19	118 30	4.0
81		05:46:02.7	35 23	118 34	4.7	158		19:53:14.0	35 20	118 55	4.5

* Preceded by shock at 15:51 in Owens Valley region.

Table 1. Kern County earthquakes, July 21, 1952-June 30, 1955, including all of magnitude 4.0 or over, and all for which epicenters have been determined.—Continued

No.	Date	Time G.C.T.	Lat.N.	Long.W.	Mag.	No.	Date	Time G.C.T.	Lat.N.	Long.W.	Mag.
(1952)						(1952)					
159	Aug. 1	03:16:11.6	35 17	118 33	4.5+	226	Sept. 22	13:15:10.3	35 21	118 37	3.9
160		10:35:55.8	35 20	118 32	4.0	227	Sept. 25	16:21:35.5	35 03	118 54	4.1-
161		13:04:30.0	34 54	118 57	5.1	228	Sept. 26	03:51:50.0	35 08	118 46	3.9+
162		21:35:22.4	35 19	118 30	4.0	229		20:21:20.0	35 06	118 37	4.0+
163	Aug. 2	05:39:15.1	35 06	118 42	3.8	230	Oct. 2	23:10:20.6	35 24	118 38	4.2
164		19:09:19.8	35 22	118 35	3.9+	231	Oct. 6	07:51:06.6	35 09	118 40	3.6+
165	Aug. 3	01:51:56.2	35 23	118 27	4.1	232	Oct. 13	22:20:35.1	35 23	118 51	4.0+
166	Aug. 4	05:34:59.8	35 05	118 35	4+	233	Oct. 16	12:22:07.3	34 57	118 57	4.3
167		19:47:22.4	35 04	118 59	3.8	234	Oct. 20	18:14:43.2	35 19	118 30	4.3
167a		19:47:50±	?	?	4.0	235	Oct. 21	11:44:16.7	35 04	118 59	3.8+
168	Aug. 5	06:50:10.4	35 20	118 44	4.4	236	Oct. 22	20:03:28.3	35 20	118 55	3.9
169	Aug. 6	03:46:23.4	35 19	118 30	4.3	237	Oct. 23	05:33:33.7	35 35	118 30	3.8
170		22:46:13.7	35 20	118 55	3.8	238	Oct. 28	20:52:50.4	35 22	118 30	3.8
171	Aug. 7	16:31:51.2	35 02	119 03	4.9	239	Oct. 31	15:04:00.1	35 27	118 44	3.9+
172		19:19:07.0	35 20	118 55	4.2	240	Nov. 7	07:15:27.5	35 17	118 43.5	3.6
173	Aug. 8	05:17:17.6	35 20	118 34	4.0	241		08:55:35.0	35 00	119 05	4.6
174	Aug. 9	10:07:32.1	35 20	118 28	4.2	242	Nov. 9	18:41:02.0	35 34	118 25	3.5+
175	Aug. 10	06:01:18.0	35 19.5	118 36.5	4.0	243	Nov. 11	17:22:07.8	35 09	119 03	4.2
176		12:23:16.8	35 19	118 30	4.6	244		18:12:25.2	34 57	119 01	4.1
177		19:44:23.6	35 00	119 00	4.1	245	Nov. 12	04:16:30.7	34 58	119 00	3.9+
178	Aug. 11	13:21:48.8	35 19	118 30	4.4	246	Nov. 13	07:00:56.6	35 14	118 36	3.3
179	Aug. 13	04:29:39.0	35 19	118 30	4.6+	247		12:04:39.2	35 06	119 00	2.3±
180		17:39:25.1	35 09	118 41	4.7	248	Nov. 14	23:34:01.4	35 03	118 57	4.0
181		21:25:48.3	35 18	118 40	4.1	249	Nov. 27	15:36:41.1	34 58	118 57	4.0
182	Aug. 14	07:28:21.8	35 08	118 31	4.1	250	Nov. 28	16:22:29.3	35 03	118 57	3.8
183		11:41:46.1	35 04	118 53	4.2	251	Dec. 1	05:26:10.3	35 00	118 50	4.4
184	Aug. 16	05:57:23.7	35 08	118 31	3.9	252	Dec. 5	04:01:09.0	35 03	119 08.5	3.8
185	Aug. 17	06:14:03.7	35 03	118 57	4.0	253		05:02:28.2	35 04	118 59	3.6
186		09:09:06.9	35 01	118 59	4.1	254	Dec. 18	20:40:19.6	35 21	118 50	3.8+
187		11:10:26.6	35 01	118 59	3.9-	255	Dec. 21	08:38:02.4	35 05	118 45	3.6+
188		21:04:41.6	35 04	118 53	4.3	256	Dec. 25	05:56:33.4	35 20	118 28	4.1
189	Aug. 18	04:40:10.4	35 02	119 03	4.7	257	Dec. 26	18:09:38.3	35 03	118 54	3.6
190		07:16:42.8	35 02	118 51	3.9+						
191	Aug. 19	09:01:31.8	35 17	118 35	3.8		(1953)				
192		19:12:26.3	35 03	119 14	4.5	258	Jan. 10	22:17:38.4	35 14	118 36	4.0
193	Aug. 20	08:47:47.1	34 53	119 02	4.2	259	Jan. 20	08:13:22.2	35 19	118 30	4.0
194	Aug. 22	22:41:23.8	35 20	118 55	5.8	260	Feb. 19	08:12:06.4	35 18	118 30	4.4
195	Aug. 23	06:03:03.2	35 00	118 44	4.3	261	Mar. 17	16:15:16.7	35 14	118 32	4.0
196	Aug. 24	23:11:48.3	34 59	118 54	3.7	262	Mar. 23	17:06:36.6	34 59	118 54	4.0
197	Aug. 25	06:20:26.1	35 06	118 58	4.7	263	Apr. 29	12:47:45.3	35 00	118 44	4.7
198	Aug. 26	20:56:40.7	35 05	118 25	4.4	264	May 1	06:48:21.6	35 07	118 27	4.1
199	Aug. 28	07:48:41.5	35 21	118 32	3.7	265	May 23	07:52:54.8	35 03	119 08.5	4.2
200	Aug. 30	04:56:00.0	35 19	118 30	4.7	266	May 25	03:24:00.8	35 00	119 01	4.8
201		04:59:55.0	35 19	118 30	4.0	267	June 20	23:18:51.8	35 22	118 30	4.4
202	Sept. 1	10:38:59.8	35 19	118 57	4.1	268	Aug. 5	12:20:59.5	35 01	119 03	4.3
203	Sept. 2	09:06:15.3	35 06	118 58	3.8	269	Aug. 6	11:20:03.7	35 03	119 08	4.4
204		12:41:32.5	35 08	118 42	4.6	270	Sept. 2	15:27:55.6	35 02	119 06	4.0
205		16:38:08.7	35 18	118 32	4.0	271	Sept. 5	19:24:36.2	35 11	118 37	4.1
206		20:45:56.4	34 58	119 00	4.7	272	Sept. 12	06:41:16.0	35 22	118 53	4.1
207	Sept. 4	13:45:43.8	35 12.5	118 37.5	2±	273	Oct. 7	14:59:21.3	35 02	118 51	4.9
208		13:51:36.7	35 20	118 32	3.2	274	Nov. 23	20:39:01.0	35 28	118 27	4.4
208a		13:59:09.8	35 20	118 32	2.5	275	Dec. 15	12:44:35.7	35 13	118 49	4.6
209		15:05:03.2	35 22	118 35	2.6						
210		15:14:57.9	35 19	118 30	3.2		(1954)				
211		18:06:49.5	35 19	118 30	4.4	276	Jan. 12	23:33:48.6	35 00	119 01	5.9
212	Sept. 5	04:46:43.1	35 21	118 50	2.6	277	Jan. 12	23:40:37.7	35 02	119 06	4.1
213		05:18:03.0	35 19.5	118 36.5	2.8	278	Jan. 13	01:45:31.1	35 02	119 06	4.4
214	Sept. 5	06:17:10.0	35 34	118 58	1.5±	279	Jan. 27	14:19:48.0	35 09	118 38	5.0
215		06:26:11.1	35 18	118 33.5	1.5±	280	Feb. 4	20:48:41.7	35 21	118 50	4.0
215a		07:03:23.1	35 16	118 34	2+	281	Feb. 7	00:09:53	35 02	119 06	4.4
216	Sept. 12	10:35:25.1	35 00	119 03	4.5	282	Feb. 10	23:58:38.5	34 56	119 04	4.5
217	Sept. 14	20:43:23.5	35 13	118 40	4.1	283	Feb. 24	22:30:22.5	35 04	119 04	4.5
218	Sept. 15	04:40:13.3	35 19	118 30	4.9-	284	May 1	22:04:39.1	35 26	118 42	4.2
219	Sept. 16	14:23:53.0	35 19.5	118 36.5	3.4	285	May 23	23:52:43.2	34 59	118 59	5.1
220		14:24:11.1	35 22	118 35	3.8						
221		14:24:53.5	35 19.5	118 36.5	4.0+		(1955)				
222		15:21:70.6	35 22	118 35	4.3+	286	Jan. 15	11:03:06.9	34 57	118 58	4.3
223		15:36:50.7	35 22	118 35	3.4	287	Feb. 11	19:44:30.0	35 24	118 31	4.5
224		19:37:47.3	35 22	118 35	3.2	288	May 28	19:44:20.0	35 34	118 14	4.5
225	Sept. 20	08:13:51.9	35 19	118 30	3.6-						

Table 2. Recorded times of first motion.†

		SB	P	MW	CL	H	R	F	BB	T	Pr	Bt	MH	BC	a
1952 July 21															
1	09:43	17.1	22.3	23.3	29.1	31.9	34.1		37.4	41.4	40.6	49.3			
* 2	11:52	28.7	33.7	34.3	39.2	40.9	42.9	44.4	46.1	50.9	52.2	60.1?	61.7	69.0	
* 9	12:05	45.2±	50.4		57.4?	57.2	60.2		62.8	68.2			85.4		
15	12:19	52.2	53.0		60.2	60.5±	62.4		65.8±	71			87		
26	13:25	26.7	30.2			35.9	39.5			48.4					
34	15:14	20.2	18.2			17.9	25.8	28.2	27.1±	32.5		46.0	47.4	48.8	
* 40	17:43	08.5	03.8			02.6	11.3		13.5	16.9			34.9	32.7	
42	18:23	62.4	59.6		55.4	56.1	66.9	68.4	67.2	70.6	77.1	86.5	89.3	86.8	
* 43	18:26	50.8	49.6?			45.2				59.6					
44	19:12	31.0	28.0		25.0	26.7	36.2		38.4	40.6	46.1	55.0	59.3	56.1	10.6
45	19:16	42.4	39.2		35.0	36.1	46.1	50.2	47.1	50.5		66.3	68.9	66.5	22.6
46	19:41	40.8	41.8		44.7±	46.5	50.1	52.2	52.2	57.0	62.3	69.3	69.9	74.2	28.2
47	20:21	27.9	25.6			23.5	33.2		35.7	37.9			55.0	53.7	08.0
48	21:51	65.9	65.0	65.2	67.4	70.2	74.2	77.1	76.5	82.9	84.8	93.6			51.7
* 49	21:53	22.3	27.0	27.3	35.8	35.4	36.3	40.8	39.6	48.0	46.3	54.1	57.4		19.1
50	23:11	68.0	64.8	64.2		61.2	72.0		75.4	75.8		92.5	96.3		48.2
51	23:53	41.9	47.6	47.5	53.8	54.6	56.4	57.5	59.1	65.8	66.8	74.4	74.9	81.8	37.6
July 22															
* 52	01:01	19.3	17.4		16.2										02.2
53	01:10	65.1	62.8	62.5		62.1	72.2		74.1	76.7	81.4	90.7	92.8		46.7
* 54	01:13	31.1	31.8						45.9	51.5					20.8
55	01:41	24.9	20.3	20.4	20.1	22.2	28.4	34.4	30.0	36.3	38.8	48.1	54.1	50.6	04.1
* 56	01:46	31.5	28.5	28.5	26.5		37.3			42.4	49.6				12.5
57	01:52	14.8	11.5	11.4		08.5	19.9	21.9	19.5	23.1	29.0	38.1	41.7	38.7	
58	03:21	27.2	25.0	24.6	23.2	23.6	32.6	35.9	33.3	37.9	42.2	52.7	54.0		
		SB	P	MW	CL	H	R	F	BB	T	Pr	Bt	MH	BC	b
July 22															
59	07:45	10.2	11.5	11.8	19.6	21.9	21.4	27.8	24.6	35.0	30.7	39.4	46.5	48.4	02.2
60	08:16	43.4	41.9	41.2	42.4	44.4	49.2	55.0	51.1	55.2	59.6	68.9	74.7	72.8	26.5
61	08:21	36.1	41.0	41.4	47.7	45.8	49.5	50.2	51.9	57.2	59.4	69.2±	70.8		28.7
62	08:47	52.5	53.0	52.9	55.7	57.0	60.8	64.8	63.0	69.9	71.0	80.1	84.3	84.3	38.5
63	09:10	47.2	45.3	45.2	42.8	44.3	52.2	55.2	53.4	57.5	62.5	72.2	75.1	73.4	29.9
64	10:19	52.4	58.8	59.7?	63.7	65.3	68.0	69.3	71.2	76.3	77.3	86.2	86.9	46.3	46.3
65	10:44	28.3	22.2	21.9	24.3	27.0	30.5	41.2	32.1	43.0?	40.9	50.2	61.3	63.5	06.9
66	13:31	57.3	62.1	62.3	67.7	69.8	71.1	75.0	74.0	82.2	80.5	88.9	91.8	97.3	51.5
* 67	14:05	26.9	31.1	31.1	33.1	39.4	39.6	42.1	46.0	49.7	58.2	56.8			19.0
68	14:30	31.6	36.7	36.9	43.2	45.0	45.9	48.5		56.8	56.0	62.3	66.4	72.1	26.5
69	15:03	36.8	34.6	34.1	31.7	33.3	42.2	43.7	43.4	47.2	52.3	61.6	65.3	62.8	
70	17:52	48.9	55.3	56.3	61.4		64.7	65.8?	67.3	72.5	75.0	83.1	82.5		
* 71	19:09	21.8	16.8	16.7	15.5	17.4	24.7	28.2	26.7	30.4	36.1	45.5	48.7	46.8	
* 72	19:10		38.7			54.6?			43.4?	56.8					
73	21:02	28.4	29.2	29.3	32.2	32.9	37.8	40.6	41.4	46.4	48.7	57.9	58.9	63.3	
74	22:31	48.9	52.4	52.6	57.0	59.1	60.2	64.4	64.0	69.4	70.9	79.6	82.3	89.6	
July 23															
75	00:38	55.5	54.6	53.9	48.1	48.8	61.2	60.7	61.4	62.7	72.0	81.8	81.3	81.4	
76	00:43	23.1	26.5		33.6?	33.6	35.7		41.5	46.1		55.0			
77	00:47	60.7	60.5	59.7	54.5	54.6	66.2	65.9	67.4	68.4	76.5	86.7	85.9	86.4	
78	03:19	46.1	45.4	44.7	39.3	39.4	51.7	50.2	53.0	52.7	61.0	71.2	71.0	71.6	
79	03:49	50.1	48.7	47.5	44	45.5	55.1	55.8	56.4	57.7	66.9	75.4	75.4	75.5	
80	04:01	62.7	61.1	60.7	55.8	56.1	67.6	67.4	69.1	70.1	78.4	87.8	88.5	88.1	
		Ch	SB	P	MW	CL	H	R	F	BB	T	Pr	Bt	MH	BC
July 23															
81	05:46		26.3	25.0	24.4	18.8	20.4		31.0	32.6	33.4	42.7	51.2	51.8	50.9
82	06:11		08.7	05.7	05.0	01.9	03.0	12.6	16.3	13.3	17.3	23.1	32.1	36.0	33.3
83	06:26		52.9	50.1	50.1	44.5	44.8	59.0	56.4	57.9	58.7	68.4	77.6	77.9	77.0
84	06:53		65.1	64.2	64.1	58.6	58.6	67.2?	70.4	71.4	72.5	81.0	89.8	91.1	90.4
85	07:37		22.7	20.9	20.6	16.4	17.9	27.3	29.1	28.9	31.9	38.3	46.8	50.3	48.3
86	07:53		34.9	36.5	36.6	40.1	42.7	44.3	48.1	47.0	54.2?	54.9	62.6	67.0	69.5
87	09:38	25.4?	65.3	62.2	61.7	58.4	59.6	69.3	73.6	69.3	74.7	79.4	88.7±	92.4	90.2
88	10:54	26.5±	36.9	34.3	33.9	29.0	30.1	40.4	42.5	41.5	44.6	51.2	60.5±	63.3	60.9
89	13:17	13.4	24.1	26.3	25.8	26.1	27.0	33.7	34.3	36.0	39.4	45.2	52.7±	53.7	57.6
90	13:30	15.9	26.5	23.9	23.7	20.1	21.8	31.0	33.3	31.2	36.0	41.1	50.1±	53.9	51.8
91	15:25	34.5	46.9	42.3	42.0	42.1	43.6	50.1	56.4	51.1	58.3	60.8	69.7±	75.7	
92	16:18	49.4	60.2	58.9	58.7	55.1	55.8	65.8	66.5	67.5	69.3	77.3	85.7±	87.0	87.1
93	16:49	04.5	16.0	14.5	14.3	09.9	10.6	21.2	21.7	23.1	24.5	33.8	40.6±	41.0	
		Ch	SB	P	MW	D	CL	II	R	F	BB	T	Pr	MH	BC
July 23															
94	17:22	36.6	49.2	44.9	45.1	46.4	39.0	40.9	51.8	54.5	52.6	55.1	63.5	74.3	71.8
95	17:53	35.7	43.8	49.5	50.2	52.3	53.7	55.1	57.6	59.4	60.6	66.8	69.0	77.2	
96	18:03	40.6	52.2	50.4		50.5		45.1	55.6		55.6	60.2	66.4	73.7	
97	18:13	54.7	66.7	68.7	69.0	71.7	73.8	74.7	76.6	80.8	80.1	85.1	88.4	99.0	102.4
98	19:51	45.9	57.6	55.6	54.5	56.8	49.8	50.9	61.7	62.0	63.2	64.4	74.0	83.1	
99	21:17		13.9	17.5	17.9	20.9	22.1	23.3	25.9	28.8	29.7	33.9	36.6	47.2	
100	22:32	24.9	35.9	39.8	40.2	43.1	43.2	43.8	47.7	49.3	50.3	55.7	58.6	66.6	
101	23:51	42.7	55.1	53.3	53.3	56.0	55.8	58.6	61.0	67.4	62.8	69.1	71.9	88.6	

Table 2. Recorded times of first motion.†—Continued.

		Ch	SB	P	MW	D	CL	H	R	F	BB	T	Pr	MH	BC	c	
No. July 24																	
102	03:11	11.9	22.5	27.8	27.6	30.9	31.4	32.4	36.1	36.2	39.2	43.8	45.9	54.0		13.5	
103	03:28	36.1	49.0	46.4	46.0	48.2	44.2	46.1	55.3	58.1	57.5		67.0			28.0	
104	03:29	31.3	41.5	47.1	47.5	51.2		57.2	56.0	60.2	61.9	68.1				36.7	
105	05:02	61.8	74.9	71.5	70.9	73.2	65.4	67.1	78.1	80.4	78.7	81.5	89.1	100.5	97.7	52.8	
106	09:50	36.3	47.4	50.7	50.2	53.9	55.8	58.5	59.4	62.6	62.3	69.7	69.2	80.5		38.8	
107	11:47	67.8	79.1	78.6	78.6	80.6	71.6	71.8	85.4	82.5	86.4	85.3	95.3	103.1	105.7	58.4	
108	12:07	68.8	81.3	77.9	77.7	79.8	72.8	74.4	83.9	87.1	85.0	88.4	94.7	107.6	104.8	59.5	
*109	14:05		50.9	47.5	47.0	49.0	42.0	43.7	54.0	56.6	54.5	58.1	65.2	77.0	74.3	28.8	
110	14:10		37.1	33.7	33.3	35.6	28.7	30.0				44.8	51.5	63.0	61.7	15.1	
111	17:35		28.5	26.1	25.7	27.7	23.1	25.0	32.9	36.7	33.9	39.3	43.0	56.3		08.0	
No. July 25																	
*112	00:04		07.7												93.1		
113	07:03	62.2	76.2	74.7	73.5		67.8	67.4	81.0	77.9	81.9	81.2	91.9	99.4	100.6	53.6	
114	10:22	55.8	68.5	72.3	72.6											61.1	
115	13:13	20.3	33.0	29.8	29.2		24.2	25.4	36.5	38.6	37.7	40.2	47.4	59.3	56.8	10.9	
116	14:34	49.3	60.5	61.1	61.5		64.1	65.0	69.8	72.9	72.1	77.6	80.3	91.7	94.1	45.7	
117	19:09	57.0	69.9	66.2	65.9		61.1	61.3	73.0	75.3	74.7	76.1	83.9	94.3	93.0	47.3	
118	19:43	35.4	47.7	44.5			39.6	40.4	51.3	53.3	52.0	54.4	62.0	73.4	71.3	25.7	
*119	20:06	17.8	30.2	27.7?			21.3	22.3	33.7	34.8	34.6	36.7	45.2	56.1	53.6	08.1	
		Ch	Hv	SB	P	MW	D	CL	H	R	F	BB	T	Pr	MH	BC	c
No. July 26																	
120	01:02	32.4	24.3	44.9	41.4	41.3	43.2	36.4	38.1	48.1	51.9	49.5	52.2	58.7	72.0	69.4	
121	01:04	57.6	47.4	70.1	67.1	66.9	69.2	61.0	62.2	73.7			76.5	85.2			
121a	06:38	58.7	55.9	72.7	70.0	69.2	72.0	68.6	69.7	77.0	81.2	78.4	83.2	87.8	100.6		55.2
122	09:22	17.3	10.6	31.8	28.7	28.1	30.1	23.3	24.7	35.0	36.9	36.3	38.8	45.3	57.9	55.4	10.5±
122a	15:08	37.0		49.7	49.4	49.1	52.0	52.7	52.7	57.3	61.3	59.0	65.3	67.5	80.2		34.5
123	18:02	49.1		61.7	62.5	62.5	65.4	64.0	65.3	70.5	72.1	73.2	77.1	81.0	92.2	94.8	47.7±
124	19:51	30.7		43.6	41.3	40.8	43.3	35.1	36.1	47.9		51.2	50.4	58.2			21.3
125	22:28	23.8	33.0	34.9	39.0	40.1	42.4	47.8	48.1	47.6	53.0	59.5	59.2	70.8			40.3
126	22:41	11.3	09.6	24.0	22.4	22.1	24.0	20.9	23.2	29.1	34.0	31.6	36.8	41.6	53.8	52.4	22.6
*127	22:59	07.8	00.3	19.8	17.4	16.9	19.1	11.0	13.9	23.9	26.1	25.5	28.2	35.8	47.3	44.5	17.8
No. July 27																	
127a	00:09	27.8	19.0	40.7	37.1	36.5	38.4	32.3	32.9	44.0	45.7	45.3	47.2	52.5	67.0	63.9	
127b	02:49	25.7	10.0	37.6	35.9	34.9	36.8	25.7	25.4	41.5	38.9	41.6	39.0	51.8	60.4	58.4	
128	07:16	16.2	23.0	25.1	31.1	31.6	34.7	36.1	38.1	40.4	40.0	43.6	48.3	50.7	57.7		
129	07:35	50.7	41.6	62.4	61.4	61.0	63.1	55.7	56.1	68.3	66.6	69.3	69.2	78.5		87.5	
130	11:34	43.7	49.2	53.3	58.8	59.2	62.3	62.9	63.5	67.4	66.6	70.3	74.3	77.2	85.8		
131	16:18	18.9	10.0	30.9	29.6	28.9	31.7	23.8	24.3	36.0	36.0	37.4	38.1	47.2	56.5?	55.6?	
132	16:26	51.4	51.4	64.3	63.6	62.8	65.9	64.8	66.0	71.8	74.7	74.5	79.2	82.4	93.5	94.6	
133	17:37	55.0	46.9	67.5	64.1	63.9	66.0	59.0	61.0	71.3	73.6	72.4	74.7	81.6	93.8	91.4	
134	18:56	34.6	27.5	46.6	44.8	44.2	46.5	40.8	41.8	51.3	52.8	52.9	55.5	62.3	74.0	72.1	
No. July 28																	
135	02:21		11.5	26.5	22.3	23.9	23.7	24.8	29.6	38.0	32.2	39.5	40.5	57.9	53.4		
136	05:45		00.6	16.6	12.4	14.5	12.5	14.7	20.0	27.7	21.9	28.1	30.6	47.4	43.5		
137	07:29		12.0	19.4	22.2	25.3	25.1	26.2	30.2	30.8	33.7	37.8	40.6	50.2			
		Ch	Hv	SB	P	MW	D	CL	H	R	F	BB	T	Pr	Bt	MH	BC
No. July 28																	
138	15:41		22.1	43.2	41.6	43.2	36.2	36.5	48.0	48.9	49.5	50.3	58.6		68.2		
*139	15:43		14.0	35.7	34.0	37.0	28.2	28.1	41.4		44.2	42.2	54.9				
No. July 29																	
140	05:56	33.0		44.4	46.8	46.5	49.2	42.9	43.0	53.7	50.1	56.0	54.9	64.8	72.9±	69.5	75.3
*141	07:03	56.8		68.0	70.0	70.2	72.0	66.5	66.0	77.2	73.2	79.1	78.3	88.1	92.7	98.5	
142	07:56	33.0		44.6	46.5	46.2	48.8	41.5	53.7				54.2	64.4	72.5±	70.0	
*143	08:01	57.1		68.2	69.9	69.7	72.3	65.8	64.6	76.7	73.2	78.4	77.4	87.9	96.0±	93.1	97.8
144	08:08	00.0		11.4	12.8	12.5	14.5	07.5	07.7	20.1	16.1	21.7	20.8	30.7	38.6±	35.9±	40.1
145	09:37	45.9		58.7	56.6	56.5	58.4	57.1	58.9	64.1	68.9	65.7	73.1	74.1	82.7±	88.0	
146	10:19	44.5		57.0	54.2	53.9	55.9	48.5	49.2	60.5	61.7	61.9	63.4	71.3	80.6±	83.5	80.2
*147	12:50	46.5		57.4	59.8	60.1	62.7	55.8	55.6	66.9	62.9	68.8	68.0	77.8	86.0±	83.0	
148	15:49	59.3		72.5	69.6	69.6	72.1	68.5	70.1	77.1	80.6	79.0	83.9	88.3	96.5±	101.4	99.8
149	17:36	53.1	47.2	65.5	62.7	62.7	64.8	60.0	61.7	69.6	72.8	71.9	75.7	80.5	89.6±	92.9	91.7
150	19:51	41.4	38.9	52.9	55.7	56.0	58.2	53.9	53.2	63.1	58.9	65.5	64.8	73.7	82.2±	78.7	85.9
No. July 30																	
*151	09:59	39.8	32.8	53.0	50.0	49.5	51.8	44.9	46.5	56.5	59.0	54.9	60.5	66.9		79.5	77.0
152	11:02	57.8	67.2	69.5	73.1	73.5	76.5	79.7	82.4	82.4	85.3	85.4	93.0	92.1	103.3	108.6	
153	14:46	60.1	54.4	72.0	69.9	69.6	71.8	67.5	68.6	76.6	80.0	80.6	82.6	87.2	100.0	101.0	
No. July 31																	
154	04:10	32.5	25.7	42.4	41.9	44.0	38.3	39.3	48.6	51.3	50.0	52.5	59.3	69.0	71.6	69.5	
155	12:09	20.9	13.8	30.5	30.2	32.1	25.8	27.0	36.2	39.3	38.0	41.1	47.1	56.7	59.6	57.6	
156	17:19	18.9	12.6	31.5	28.9	28.5	30.6	25.4	26.0	35.2	38.3	36.6	40.9	45.8	55.3	58.6	56.1
157	19:05	26.9	18.7	39.9	36.0	35.6	37.9	31.3	32.2	41.8	46.6	43.6	46.7	52.8	62.8	65.7	62.6
158	19:53	23.3	21.1	34.5	37.6	37.6	40.2	35.3	34.8	44.7	40.9	47.0	46.3	55.6	65.0	59.6	66.7

Table 2. Recorded times of first motion.†—Continued.

		Ch	Hv	SB	P	MW	D	CL	H	R	F	BB	T	Pr	Bt	MH	BC	
No.	Aug.																	
159	1 03:16		15.5	35.7	32.9	32.2	34.2	28.1	29.0	38.8	41.5	39.8	42.8	48.7	59.3	62.2	59.4	
160	1 10:35		59.5	80.1	76.5	76.4	78.4	72.7	72.8	82.8	86.1	84.7	87.1	93.2	103.5	105.7	103.6	
161	1 13:04		42.6	43.6	47.7	48.0	51.1	54.5	55.9	56.9	61.0	60.2	67.1	66.0	75.1	77.6	83.3	
162	1 21:35	34.1	26.2	47.4	43.6	43.1	45.2	38.1	39.8	50.9		51.4	53.8	61.3	61.3	73.1		
163	2 05:39	21.0	22.8	34.1	33.4	33.2	35.9	35.7	37.3	41.7		43.8	50.8	52.3	61.5	65.1		
164	2 19:09	29.7	22.1	43.1	41.8	41.5	43.3	36.2	36.1	48.3		49.8	50.1	58.6?	69.4			
165	3 01:51	69.2	59.3	81.5	78.2	77.9	79.7	70.8	72.3	84.2		85.5	86.8	94.7	104.7			
166	4 05:35	08.7	07.8	19.4	17.9	17.5	20.2	19.1	20.4	24.8		27.6	33.9	35.7	44.0			
167	4 19:47			37.9	42.5	42.6	45.4	46.4	47.0	50.7		53.6	58.3		68.9			
167a	4 19:47			66.0	71.8													
168	5 06:50	19.6		31.7	33.4	33.1	35.7	29.1	28.5	40.3		41.6	40.3					
		Ch	Hv	W	SB	P	MW	D	CL	H	R	BB	T	Pr	Bt			
No.	August																	
169	6 03:46				32.2	47.5	44.6	44.4	46.1	39.6	41.1	51.5	52.0	54.5			71.3	
170	6 22:46			20.3	20.2	34.2	37.2	37.3	39.5	35.2	34.7	44.9	47.2	46.1			68.3	
171	7 16:32			02.9	03.2	05.1	11.4	11.8	15.0	15.9	16.5	20.0	26.5	26.5			38.8	
172	7 19:19			14.1	13.8	27.6	30.4	30.2	32.8	28.6	27.6	37.6	40.0	39.4				
173	8 05:17			22.1	25.3	40.5	38.8	38.6	39.8		35.9	46.1	47.0	49.4	57.0		65.5	
174	9 10:07			35.8	41.1	56.4	53.6	53.1	55.2		49.8	59.8	61.0	63.6	75.8		79.7	
175	10 06:01			21.7		42.1	40.6	40.7	42.7	35.7	35.5	47.4	48.8	49.2	57.5		67.5	
176	10 12:23			19.7		41.9	38.0	37.9	39.6	33.1	34.1	44.0	45.3	48.3	55.1		65.0	
177	10 19:44			35.1		37.9	43.2	43.0	46.4	48.3	49.5	51.9	55.1	61.0	63.5		70.8	
		d	Ch	Hv	W	SB	P	MW	D	CL	H	R	BB	T	Pr	Bt		
No.	August																	
178	11 13:21			51.8		73.4	72.1	70.1	72.9	65.2	66.1	78.2	78.6	80.2	87.2			
179	13 04:29			42.7		63.1	60.0	60.0	62.3	55.7	56.4	66.7	68.0	70.9	77.0			86.6
180	13 17:39			32.3		44.7	44.4	44.0	46.7		46.7	52.4	54.8	59.8	63.3			72.7
181	13 21:25			52.1		72.0	69.9	69.6	71.4	66.6	66.6	76.3	78.2	80.0	86.8			97.0
182	14 07:28	31.9		28.6		43.2	39.0?	39.3	41.6	40.4	42.1	47.7	52.4	56.4				
183	14 11:41	58.8		55.8		62.3	65.1	65.4	68.0	69.5	70.1	73.1	76.1	81.7	83.3			92.0
184	16 05:57			29.3		44.6	42.0	41.8	44.2	41.8	43.7	49.3	51.0	56.6				69.6
185	17 06:14			15.0		19.3	23.3	23.6	26.6	27.3	28.7	31.6	34.5	40.6				49.2
186	17 09:09		10.6	17.7		22.0	26.4	26.9	29.9	31.2	32.0	35.3	38.3	43.6				52.4
187	17 11:10		30.4	37.4		41.4	46.5	46.4	49.4	50.7	52.7	54.8	57.5	63.6				72.2
188	17 21:04		46.0	51.6		58.1	60.6	60.9	63.1	64.8	65.6	68.8	71.5	78.3				
189	18 04:40		15.1	22.1 ±		24.3	30.3	30.8	33.9	34.9	35.5	38.7	41.9	47.1				
190	18 07:16		47.6	53.1 ±		59.7	61.2	61.3	64.8	65.8	68.3	69.3	72.0	79.9				
191	19 09:01		41.6			54.4	52.4	52.2		48.9	49.3	59.4	60.6	63.2				
*192	19 19:12		31.6			39.2	49.0	49.1	52.3	53.4	54.6	57.7	61.1	64.2				
193	20 08:47	*59.6				59.9	65.2	65.3	66.6	72.1	74.0	74.4	77.7	86.3				
*194	22 22:41	*29.0		33.8		30.3	43.6	47.1	47.5	49.4	45.3	44.8	54.5	56.8	56.2			
*195	23 06:03		08.0			14.7	20.5	20.3	20.4	24.8	25.1	26.7	28.8	31.0	40.4			
196	24 23:12			01.1		03.0	06.8	07.2	10.1	11.9	13.8	15.4	19.2	25.7				
197	25 06:20			37.4		42.0	46.2	46.7	49.2	49.8	50.6	54.4	57.5	61.8				74.0
		i	Ch	Hv	W	SB	P	MW	D	CL	H	R	BB	T	Pr	Bt		
No.	August																	
198	26 20:56					62.8	57.6	57.3	59.7	58.5	61.2		67.5	75.5				86.0
199	28 07:48				49.1	66.0	63.1	62.7	64.8	57.3	57.9	69.2	71.0	72.1				89.6
200	30 04:56		12.1	03.2		24.1	21.4	21.0	23.0	15.6	17.2	27.9	28.8	30.5				48.3
201	30 04:59		67.0	58.0		79.0	76.4	76.2	77.9	70.9	72.0	83.0	86.0	86.4				103.4
		i	Ch	Kx	W	SB	P	MW	D	CL	H	R	BB	T	Pr	Bt		
No.	September																	
202	1 10:39			06.8		19.5	23.0	22.9	25.4	21.1	20.6	29.8	32.7	32.6				49.7
203	2 09:06					31.3	35.6	35.7	38.1	38.7	39.4	43.2	45.7	50.7				62.5
204	2 12:41		38.4			52.0	51.3	51.0	53.5	52.9	54.7	58.4	60.6	67.4				78.4
205	2 16:38		19.8			32.0	29.5	29.2	31.2	25.1	26.2	36.0	37.4	40.2	45.2			56.8
206	2 20:45		59.8	69.0		70.4	75.5	76.0	79.0	81.4	83.5	84.1	87.7	94.6	94.0			102.7
*207	4 13:45	48.3	53.3	49.5	52.7	64.7	63.0	66.1	62.3	62.3	64.8	64.8	64.8	77.3				
*208	4 13:51	40.1	48.5	40.3	45.0	62.0	57.3	57.3	59.3	53.3	53.7	63.8	65.2	68.3				74.5
*208a	4 13:59	13.3	21.6	13.5	17.6	31.2	30.4	32.3	26.3	26.8				41.6				57.9
*209	4 15:05	06.3	15.5	06.8	10.7	27.3	24.7	28.4	20.5			34.9		35.2				
*210	4 15:15	02.1	10.0	01.8	06.4	22.8	19.1	18.6	21.3	14.3	15.3	25.8	27.0	29.4				45.9
*211	4 18:06	53.5	61.1		58.4	74.3	70.4	70.3	72.3	65.5	66.9	76.7	78.0	81.0	87.8			97.0
		i	Ch	Kx	W	SB	P	MW	D	CL	H	R	BB	T	Pr	Bt		
No.	September																	
*212	5 04:16		45.3	53.3	48.5	49.1	67.4	66.1	69.4	62.2		74.8		75.2				
*213	5 05:18		05.7	15.4	06.1	10.4	26.2	27.0	27.9	19.9		34.4	35.9	34.7				
*214	5 06:17		14.0		16.6	12.9				30.7								
*215	5 06:26		14.7	23.5	14.5	19.3				27.6								
*215a	5 07:03		26.7	34.5	26.8	31.1	46.1	43.6	47.2	40.1			52.5	55.0	55.5	81.7		

Table 2. Recorded times of first motion.†—Continued.

			Ch	Kx	W	SB	P	MW	D	CL	H	R	BB	T	Pr	Bt	
No.	September																
216	12	10:35	28.4	37.0		38.7	44.8	45.3	49.1	50.1	51.3	53.7	57.0	61.3			
217	14	20:43		29.4	32.7	45.7	43.7	43.5	45.7	42.3	43.8	50.6	52.7	56.9		71.2	
218	15	04:40		16.8	21.9	38.2	34.4	34.4	35.9	29.2	30.3	40.6	42.1	44.5		61.2	
*219	16	14:23	65.4	55.9	60.3	77.5	77.1	76.0	78.1	69.9	71.2	82.5	86.4	84.8			
*220	16	14:24	22.7	12.8	18.2	34.7			33.2				44.9				
*221	16	14:24	65.9	56.2	61.2	77.9	77.7	76.3		70.9				85.7			
222	16	15:21	18.9	09.2	14.7	30.5	29.0	28.9	30.6	23.7	24.6	35.1	37.2	38.2			
223	16	15:36	62.2	52.4	57.8			72.1	74.2	66.7	67.6	79.0	82.8	81.2			
224	16	19:37	60.1	49.6	54.6	70.5	69.2	68.3	71.0	63.5	64.0	76.0	79.2				
225	20	08:13	63.3	54.6	60.7	76.0	72.5	71.9	74.1	68.1	69.1	79.3	80.4	83.4		99.1	
226	22	13:15		12.7	16.6	32.8	32.1	32.1	34.3	27.1	27.4	38.8	40.3	41.2		58.3	
227	25	16:21	40.2	45.2	47.0	52.4	54.9	55.3	59.1	59.6	63.3	66.6	72.1	72.1	14.1	81.8	
228	26	03:51	56.7	58.3	60.8	69.0	69.0	69.2		72.0	72.8	77.4	79.9	85.2			
229	26	20:21	27.6	26.6	30.7	40.9	38.2	38.0	40.7	39.7	41.0	45.3		55.5	56.2	65.0	
	October																
230	2	23:10	32.2	22.5	26.0	44.6	43.8	43.1		37.5	37.0	50.6	51.5	50.5	60.6	71.3	
231	6	07:51	13.6	12.0		27.2	25.9	25.3	28.0	26.0	27.5	33.4	35.5	41.3		53.3	
232	13	22:20	45.5		41.0	56.1	58.6	58.5	61.2	54.7	54.0	66.0	67.1	66.3		85.9	
233	16	12:22	10.0	19.6	20.1	21.8	25.6	25.8	28.9	32.3	34.4	34.8	38.3	45.9			
			Ch	Kx	Kg	W	SB	P	MW	D	CL	H	R	BB	T	Pr	Bt
No.	October																
234	20	18:14	55.0		61.1		67.3	64.3	63.9	66.0	59.6	60.4	70.1	72.0	74.2	81.0	
235	21	11:44	21.3	27.5	28.9		32.4	37.2	37.5	39.8	40.2	41.8	45.3	48.5	53.0	57.6	
236	22	20:03	37.4	35.4	40.7	34.7	47.8	51.7	52.3		48.5	48.8	59.1	61.2	70.5		
237	23	05:33	49.3	34.7	52.6	38.5	60.6	59.1	58.8		46.9	46.9	65.0	65.6	77.0		
238	28	20:52	62.9	52.7	68.4	58.0	75.1	72.4	72.0	73.8	65.3	66.8	78.5	79.6	81.0	89.3	
239	31	15:04	10.7	02.8	12.8		22.0	24.5	23.8	26.2	17.8	16.6	31.2	32.2	28.8	42.3	
	November																
240	7	07:15	36.2	32.1	41.7		47.4	49.2	48.5	51.1	46.4	46.4	56.5	58.3	59.5		
241	7	08:55	39.4	47.7	46.6		48.1	54.8	55.0	58.0	60.7	62.0	63.8	67.2	72.1		
242	9	18:41		04.0	21.6	08.8	30.7	27.1	26.0	27.9	14.6	14.1	31.5	34.6	29.0	43.1	
			Ch	Wm	Kg	W	SB	P	MW	D	CL	H	R	BB	T	Pr	Bt
No.	November																
243	11	17:22	14.1±			18.3	23.6	29.0	29.4	31.3	31.8	32.7	37.1	39.6	43.7	48.0	
244	11	18:12	35.3±			39.2	38.7	44.1	44.5	47.2	50.4	52.5	53.1	56.8	64.6	64.2	
245	12	04:16				44.8	44.6	49.7	49.9	52.7	55.9	58.2	58.4	61.9	69.2	69.7	
*246	13	07:00	66.4	58.1	73.6	63.3	79.1	76.7	76.2	78.8	74.3	75.7	83.2	84.9	89.9		
*247	13	12:04	43.9	46.1	50.2		55.4	59.9	59.9	63.3	64.7		70.3		75.0		
248	14	23:34	05.1	08.8	13.5	12.8	16.5	21.1	21.6	24.4	25.9	27.3	29.8	32.9	37.9	40.3	
			FT	Wm	Kg	W	SB	P	MW	D	CL	H	R	BB	T	Pr	Bt
No.	November																
249	27	15:36	44.8			55.8	59.5	59.6	63.2	65.6	67.6	68.2	71.5	79.7			
250	28	16:22		37.1		44.7	49.1	49.6	51.7	53.1	55.6	57.9	60.7	66.1			
	December																
251	1	05:26	12.4	16.9		26.4	28.3	28.3	30.9	33.3	34.5	37.0	39.2	47.9	47.1	56.1	
252	5	04:01	14.3	18.7	19.4	22.7	30.4	30.7	32.9	35.1	37.0	38.7	42.0	47.0	48.8	57.1	
253	5	05:02	32.5	35.2		44.0	48.8	49.3	51.3	51.8	53.6	56.7	59.7	63.8	67.3	76.1	
254	18	20:40	27.6			32.1	40.7	43.6	42.7	44.6	40.0	39.4	49.9	51.9	51.1	60.5	
255	21	08:38		07.1	17.3	12.9	21.4	21.3	21.2	23.9	23.3	25.7	29.4	31.6	38.5	40.1	
256	25	05:56	43.6	35.7	52.1	41.1	58.2	55.0	54.5	56.1	48.5	49.7	62.5	64.6	72.3		
257	26	18:09	42.0	44.9	51.2	48.8	54.5	57.8	58.1	60.4	61.4	62.5	68.2	74.3	75.8		
	January																
258	10	22:17	45.5	40.1	56.1		60.8	58.0	57.7	60.1	56.6		65.0	67.2	71.6	75.8	
259	20	08:13	32.2			30.9	47.0	43.9	43.1	45.2	38.1	38.9	50.2	51.5	53.0	61.2	
	February																
260	19	08:12	15.7	07.5	24.1	14.7	31.3	27.4	26.9	28.5	22.7	24.0	33.9	35.1	38.2	45.0	58.7
	March																
261	17	16:15	24.9				39.2	36.8		38.6	34.1	35.3	42.9	44.4	48.8	54.5	
262	23	17:06	39.9			48.3	52.1	55.5		59.5	60.6	61.4	64.0	67.1	73.8	75.1	83.4
	April																
263	29	12:47	48.7		61.3	58.2	63.4	62.5		65.1	67.4	69.1	70.5	73.7	82.2	81.3	90.5
	May																
264	1	06:48	28.2		40.5	33.0	43.8	39.4		41.0	38.9	41.3	46.9	49.0	55.9	57.7	67.3
265	23	07:52	59.7		65.4	67.5	68.4	76.4		78.6	81.0	82.4	85.4	91.9	95.6	103.2	
266	25	03:24	04.3		13.1	13.4	14.9	20.2		23.5	26.0	27.3	29.5	37.7		48.0	

†Table 2 shows times of recorded first motions for those shocks whose epicenters are given in Table 1, and a few others which remain unlocated. These times normally refer to the direct *p* or to *Pn*. Generally, when the first legible motion is a later wave it is not reported here; it is included in a few instances of doubt or of special interest. A few readings of later arrivals, and first motions for stations not in the column headings, will be found in the notes to the individual shocks. Presence of such a note is indicated by an asterisk (*) to the left of the serial number.

All times are Greenwich Civil Time. Seconds are run beyond 60 to save space. The order of stations, left to right, is generally that of distance from 35° N 119° W.

Station abbreviations in the column headings are:

BB	Big Bear	MH	Mt. Hamilton	a	BED
BC	Boulder City	MW	Mt. Wilson	b	White Oak
Bt	Barrett	P	Pasadena	c	White Wolf
Ch	Chuchupate	Pr	Palomar	d	Shirley Meadow
CL	China Lake	R	Riverside	e	Walker Dump
D	Dalton	SB	Santa Barbara	f	Piute Ranch
F	Fresno	T	Tinemaha	g	Clear Creek
FT	Fort Tejon	W	Woody	h	Kern Gorge
H	Haiwee	Wm	Williams Ranch	i	Parker Creek
Hv	Havilah			j	Clear Creek Ranch
Kg	King Ranch			k	Elkhorn
Kx	Knox Ranch			l	San Emigdio
				a	Santa Anita Dam

- *Notes for individual shocks (as indicated by asterisks in the table)
- No. 2—Main shock. The time given for Barrett, 60.1, is clear but relatively early. A much larger impulse at 61.0 agrees better with the readings of some later shocks of the series.
 - No. 9—First large aftershock. Readings difficult because of overlapping records. Additional times: Mt. Hamilton 12:06:25.4, Palo Alto 21.9, Berkeley 31.3. Times read by Dr. Gutenberg from very distant stations suggest origin time 12:05:29±. Overlap of seismograms continues serious from this time, and practically invalidates Mt. Wilson down to No. 48.
 - No. 40—Badly confused by preceding smaller shocks, consequently not so well located as subsequent comparable shocks.
 - No. 43—Confused by No. 42. Some readings, clearly not first motion, check well against later arrivals recorded for No. 42.
 - No. 49—Confused by No. 48. At Haiwee, the emergence at 35.4 fits *Pn* at $\Delta = 170.2$ km., while a sharp impulse at 36.2 fits direct *p*.
 - No. 52—Small shock. *S - P* interval at BED (= a), 2.5 sec. Compare No. 53.
 - No. 54—Chuchupate *S - P* = 4.3 sec.
 - No. 56—*R* and *Pr* times are not *Pn*, but check with second arrivals in other shocks.
 - No. 67—Probably at least two shocks. Santa Barbara has a doubtful earlier reading (25.2). China Lake first motion at 31.6 is also unexpectedly early. Solution unsatisfactory.
 - No. 70—Not well located. Santa Barbara: small first motion 48.9, larger arrival at 51.0.
 - No. 72—Confused by No. 71, but still more by an intervening shock of magnitude 3.5±.
 - No. 109—There is a dubious earlier reading at Santa Barbara: 50.1.
 - No. 112—An earlier time at Chuchupate—47.0—does not fit.
 - No. 119—Partly confused by an earlier small shock from a different epicenter.
 - No. 126—Small earlier shock recorded at Hv 22:41:07.9, Ch 09.5, MW 20.0, T 35.6.
 - No. 139—Confused by No. 138; some tabulated times are late arrivals.
 - No. 141—La Jolla 07:04:30.7.
 - No. 143—La Jolla 08:02:31.3.
 - No. 147—Fresno 62.9; sharp impulse 65.6.
 - No. 151—BB 54.97 possibly an earlier shock. Impulse at 57.8.
 - No. 192—Pasadena 49.0, a clear impulse; but a preceding doubtful emergence at 48.4 fits the given solution better.
 - No. 194—The shock of the series causing most of the damage at Bakersfield. Additional readings: F 22:41:50.5, MH 68.5, Berkeley 79.2, Tucson 131.3.
 - No. 195—F 06:03:33.9, MH 52.3.
 - No. 207 ff. Shocks on Sept. 4-5 were recorded during the special program.
- For further details and some readings for *S* see text. Table 2 lists *P* for station *i* (Parker Creek). The following are for stations *f* (Piute Ranch) and *j* (Clear Creek Ranch).

No.	Sept. 4	f	j
207	13:45	48.4	45.5
208	13:51	39.2	38.7
208a	13:59	12.2	11.8
209	15:05	06.6	05.6
210	15:15	00.4	00.1
211	18:06	----	51.5
No.	Sept. 5		
212	04:46	50.0	46.9
213	05:18	06.2	04.7
215	06:26	14.1	12.9
215a	07:03	26.7	24.0

Nos. 219, 220, 221. Three shocks in close succession. Clearly separable at the nearer stations. Locations completed using times of *S*, especially at the more distant stations.

No. 246—San Emigdio 07:01:07.1
 No. 247—San Emigdio 12:04:41.7

subtracted from the tabulated times of *P* for the other three shocks to give the immediately following times of origin. While the two shocks on July 25 are among the largest of the series, their recording shows evidence of complication, and the first motion is often difficult to read precisely; so that it is a little surprising that the agreement is so good. For the smaller shock on July 26 it is evident that the fluctuations in the calculated times of *O* are within the limits set by errors of measurement, considering that those of September 4 and of July 26 are here combined.

The three July shocks also show closely the same time differences for *P* at stations not available on September 4, such as Palomar, Fresno, Boulder, and Mt. Hamilton.

The two larger shocks were recorded at White Wolf, with *P* at 19:09:47.3 and 19:43:25.7. The distance to 35° 19' N 118° 30' W is 16.7 km.; with *h* = 10 km. this gives *D* = 19.8 km., when *D*/6.34 = 3.1 sec. This would give origin times 19:09:44.2 and 19:43:22.6. Especially the first appears rather early; this may be due to complexity of the shock, or to a circumstant affecting other recording in this area, discussed on a later page.

Mr. Shigegi Suyehiro and Mr. G. G. Shor took up the data of the September 4 shock, applying the method of least squares as used by Richter (1950) to determine the mean velocity of the direct *P* wave of southern California. Assuming only the origin time 15:14:57.9 and rectilinear propagation with constant velocity *v*, this method sets up a system of equations which are linear in *v*² and the coordinates of the epicenter. In this instance the result was *v*² = 40.01, with a standard error of ±0.080. This corresponds to *v* = 6.33, with limits corresponding to standard error at 6.26 and 6.38. Since the 1949 investigation yielded *v* = 6.34, the agreement is satisfactory.

Attempts to use the least-square method to improve epicenter and depth led to no material change.

Shock No. 213 (Sept. 5, 05:18:03.0) was the next best recorded on this program. Origin time was determined from the following:

	P	S-P	P-O	O
Clear Creek Ranch	05:18:04.7	00.7		05:18:
Parker Creek	05.7	01.1?		
		02.0	2.7	03.0
Knox Ranch.....	06.1	02.1	2.9	03.2
Piute Ranch.....	06.2	02.0	2.7	03.5
Woody.....	10.4	05.5	7.5	02.9
Chuehupate.....	15.4	09.4	12.9	02.5
China Lake.....	19.9	12.4	17.0	02.9

Here Clear Creek Ranch and Parker Creek both recorded a wave too early to be *S*.

Trial led to the epicenter 35° 19.5' N 118° 36.5' W with a close fit for *P - O* = $\Delta/6.34$ (nominally *h* = *O*) at all the nearer stations except Chuchupate (where the well observed first motion is unaccountably late). The distant stations recording *Pn* are Pasadena, Dalton and Riverside, yielding *K* = 6.6, 6.9, 6.6; this large value of *K* is consistent with small *h*.

The largest shock on September 4-5 was No. 211, at 18:06. This was recorded at Clear Creek Ranch and Parker Creek, but not at the other near-by stations. Its times check well with those of No. 210 (at 15:14) and the large shocks referred to the same epicenter. Other shocks recorded were all small. The epicenter of No. 214 is interesting, being northwest of the general active area (Woody was the nearest recording station); a shock of magnitude 3.8 originated in the same vicinity on May 21, 1953.

Mr. St. Amand has constructed a chart (figure 3) on which the small shocks of these 2 days are located using the differences in times at the four nearest stations, assuming a depth of 10 kilometers. The general scatter is probably not significant; but the roughly east-west alignment near Lat. 35° 20' north is confirmed by epicenters of larger shocks on other dates; this suggests a transverse structure which bounds the active area in this direction

(except for the line extending northeast from Bakersfield).

Geographical Sequence of Foreshocks and Aftershocks. Since 1857 major crustal strains have not been relieved in southern California, as would normally be expected, along the major faults such as the San Andreas or Garlock faults. Moderate shocks have originated at relatively unexpected points—among them the Walker Pass earthquake of 1946 (Chakrabarty and Richter, 1949), within the Sierra Nevada, and the Manix earthquake of 1947 (Richter, 1947; Richter and Nordquist, 1951), originating in the central Mojave Desert on a fault apparently without surface expression. The occurrence of a major earthquake on the White Wolf fault, as distinguished from a moderate earthquake comparable to those just named, is a similarly unexpected event pointing to a persistent and probably increasing condition of unusual strain.

The previous seismic history of the region of Kern County affected by the 1952 earthquakes is summarized in Part II-3. Like most parts of southern California, this area has been subject to geographically scattered and moderately frequent minor shocks (see fig. 1 of Part II-3). The last of these prior to July 21, 1952, was on June 14.

Table 3.

Located earthquakes in southern California and adjacent areas, June 1-July 20, 1952. Times are Greenwich Civil Time; for Pacific Daylight-Saving Time subtract 7 hours, which may alter the date. Letters A, B, C, D indicate decreasing quality of determination. M = magnitude.

1952		Lat. N.	Long. W.		M	
June	2	04:19:18	34° 00'	117° 37'	A	2.2
	4	18:29.0	32 ?	115 ?	D	3.6
	5	09:38:12	33 17	116 42	C	3.3
	11	08:01:57	32 45	117 20	C	3.0
	12	12:45:42	32 34	117. 16	C	3.4
	12	12:54:38	32 34	117 16	C	2.6
	14	16:54:50	34 55	118 50	C	2.7
	14	21:28.3	33.7	120.7	D	2.8
	16	08:34:49	33 14	115 58	C	3.5
	27	11:04.3	32.0	115.5	D	3.6
	29	06:22:14	32 50	118 16	B	2.5
	29	06:22:25	32 50	118 16	B	3.2
	29	07:06:17	34 00	117 12	B	2.6
	July	1	16:29:24	34.3	119.8	D
10		08:45:52	33 55	118 11	C	3.7
13		01:15	32 ?	117 ?	D	3.9
14		09:51:33	34.2	115.4	D	3.5
14		20:15.2	32.5	115.4	D	3.8
14		21:52.2	32.2	116.4	D	3.4
15		06:21	34 ?	121 ?	D	3.0
17		03:17:02	34.4	118.9	D	2.5
19		09:24:42	33 30	118 33	C	2.3
19		21:33:09	35 24	117 16	C	2.8
20		08:21:11	33 49	118 09	C	1.9

There was nothing identifiable as a specific prelude to the events of July, 1952. In fact, there is only a limited basis for the idea, still in circulation in technical literature, that a large earthquake is generally preceded by an increase of minor local activity in its area. This is the exception, not the rule. The earthquakes at Helena, Montana, in October, 1935 began with small shocks followed by larger ones over about 3 weeks, culminating in the destructive earthquakes of October 18 and October 31. Similar instances have been reported from Japan and elsewhere; but at least some of these are only apparent, and due to handling the data uncritically. In

volcanic regions there is commonly an increase of small local shocks before an eruption; but this is due to different conditions than where earthquakes are non-volcanic and presumably due to faulting.

Table 3 gives a complete list of those shocks in southern California and vicinity during June and the first 3 weeks of July, 1952 well enough recorded to permit assigning an epicenter (even of the lowest accuracy, D). In addition, there were a usual number of very small shocks near enough one station or another to be recorded there only, and a sprinkling of shocks in northern Mexico, probably in the very active area near the head of the Gulf of California. The small shock on July 10 in the Los Angeles metropolitan area naturally attracted disproportionately more journalistic attention than most of the others. These few weeks were a period of rather less than average activity locally.

The change in regional activity on July 21 was very marked. Beginning about 10h G.C.T., and continuing into July 22, there were a series of shocks in northern Mexico, some of which were reported felt and thereby tended to confuse information as to the extent of perceptibility of the Kern County earthquakes. As the table shows, similar shocks had been occurring for some time; but the same is not true of the following, especially with reference to occurrence in swarms within a few

July 21	14:20	Small shock near Haiwee
	15:51:39	Near Coso Junction (not far from Haiwee); magnitude 3.8
	17:12	Near Riverside
	17:14	Near Riverside
	17:28	Near Riverside
July 23	21:57	Near Tinemaha
	12:51	Near Santa Barbara
	18:59	Near Big Bear
July 24	19:06	Near Big Bear
	19:08	Near Big Bear
	19:25	Near Big Bear
	11:15	Near Santa Barbara
	11:16	Near Santa Barbara
July 27	18:15	Near Santa Barbara
	20:20	Near Santa Barbara
	20:30	Near Santa Barbara

hours. During August an increasing number of shocks from epicenters not in Kern County began to be recorded. One of these has been tentatively placed as follows:

August 23 10:09:07. Lat. 34° 30' N. Long. 118° 13' W. Magnitude 5.0. This shock was rather sharply felt in the Los Angeles metropolitan area. The epicenter is near the town of Acton, not far south of the San Andreas fault zone; this led to spectacular newspaper stories to the effect that the great fault was "waking up." If, as commonly supposed, the San Andreas fault dips nearly vertically, this earthquake is not directly associated with it. Note also: August 20 15:25:04. Lat. 43½ N. Long. 126½ W. Magnitude 6.5 and November 22 07:46:38. Lat. 35.8 N. Long. 121.2 W. Magnitude 6.1±.

The earthquakes of November 21-22 and following, were also associated in the popular mind with the San Andreas fault, although the epicenter is much farther west, near the small community of Bryson, and probably on the Nacimiento fault.

The history of the principal series of earthquakes begins (table 1) with the one indubitable foreshock at 09:43 on July 21. This shock, of the small magnitude

3.1, cannot be located with the same accuracy as most of the earthquakes tabulated; its epicenter appears to have been slightly west of that of the main shock. As in some earlier known instances, such as the Long Beach earthquake of 1933, the foreshock thus is close to the point of initial rupture at which the extended faulting began.

As indicated in other sections, a major change occurred with the large aftershock on the afternoon of July 22 (July 23, 00:38, G.C.T.). Figure 2a shows all the epicenters determined for aftershocks preceding this time. All of them lie on the southeast side of the surface trace of the White Wolf fault. Beginning about 19h on July 21 this includes practically all shocks of magnitude 4 and over. In the preceding 7 hours only five epicenters can be specified; those for 4 of the 5 aftershocks of magnitude 5 and over in the interval, and one for a shock of magnitude 4.5 at 13:25, which happened to be preceded by a short interval of quiet. Otherwise, the seismograms at all stations in the first 7 hours show such continuous overlapping of the records of successive earthquakes that the times of first motion cannot be identified, and precise location is impracticable. (See fig. 9, Part II-1.) The known geographical restriction applies strictly only to the subsequent interval of 29 hours. Very small shocks may of course have been occurring in other parts of the area even at this time, since they were originating simultaneously at distant points in southern California.

Since the above was written, Mr. A. Sanford has obtained approximate epicenters for the shocks of magnitude 4 and over from 12:18 through 16:38 on July 21. These all are also on the southeast side of the surface fault trace.

Epicenters in this first interval show some concentration along a zone diverging eastward from the trace of the White Wolf fault, passing under Bear Mountain and Woodford. This may represent the course of rupture in the main shock, proceeding at roughly constant depth of the order of 16 kilometers (9 miles) from the hypocenter near Wheeler Ridge along a fault surface dipping steeply eastward. This brings Tehachapi and Cummings Valley more nearly above the actual rupture than might otherwise be thought, and helps to explain the observed intensity of shaking at those places.

The earthquake at 00:38 on July 23, from an epicenter north of the White Wolf fault line, was followed by many aftershocks of its own, from nearly the same source. These can be picked out readily on the records of several stations, since they have a characteristic appearance. Consequently, it has been easy to search the same records for small shocks of the same group during the immediately preceding hours, on July 22; none have been found.

Figure 2b shows epicenters located from July 23, 00:38 through July 28. During this interval shocks continued on the southeast side of the White Wolf fault. In addition to aftershocks of July 23, 00:38, shocks occurred at other points to the northwest—notably July 23, 13:17, with epicenter practically at the town of Arvin, where it was strong enough to add to the damage.

Two of the larger aftershocks originated at 19:09 and 19:43 on July 25. Their epicenter (Lat. $35^{\circ} 19' N$.

Long. $118^{\circ} 30' W$.) is rather closely fixed, especially since later shocks from the same source were recorded during the special program on September 5-6. It is slightly east of the projected strike of the White Wolf surface trace. As table 1 shows, shocks referable to this epicenter began at least as early as July 23, 10:54. Especially if records are disturbed or imperfect, it is often difficult to separate these from shocks near Lat. $35^{\circ} 16' N$. Long. $118^{\circ} 27' W$., such as were already occurring on July 21; but when recording is good there is no serious doubt. The shocks at Lat. $35^{\circ} 19' N$. Long. $118^{\circ} 30' W$. were numerous; after an increasing foreshock series, and the culminating shocks on July 25, aftershocks of all sizes continued there through the entire period of investigation. For some months these shocks were more frequent than any others in Kern County.

The following chart (fig. 2c) shows aftershock epicenters from July 29 through July 31. In the upper part of this chart appears a line of epicenters for shocks most of which occurred in the early hours of July 29. The largest of these, at 07:04, added somewhat to the damage at Bakersfield and caused some alarm there; this is natural, since the epicenter was only a few miles from the city. The consequences of the similar shock on August 22 were more serious. The alignment of adjacent epicenters roughly northeast-southwest suggests an active fault as roughly parallel to the White Wolf fault. On the other hand, the surface structures in the vicinity of Bakersfield strike generally northwest—except for the canyon of the lower Kern River, which cuts across the Sierra Nevada block not far from the line of epicenters.

The last chart of the series (fig. 2) shows what may be termed a gradual spreading of the activity over the surrounding area in subsequent months. This can be interpreted in part as a return to normal minor activity in the whole of southern California, with occasional epicenters just outside the boundaries of the area most disturbed in July.

The distribution of epicenters has bearing on the question of relation of the White Wolf fault to the north-south Kern Canyon fault described by Lawson (1902-04) in the upper canyon of the Kern River. From these data there is no support for a connection between the two faults. The stations at Havilah and Knox Ranch recorded many small shocks at apparently very short distances. Most of these, however, could be referred to the nearest epicenters southward shown on the figures just cited. The remainder may be ascribed mostly to the general sporadic seismicity which resulted in small shocks being recorded near every station in operation. However, the shocks in October and November north of Havilah and close to the Kern River are closely aligned with the epicenters near Bakersfield. This alignment, if projected, would pass near the epicenters of the Walker Pass shocks of 1946, which accordingly lie north of the strike of the White Wolf fault.

The general map (fig. 1) shows that the epicenters southeast of the White Wolf fault are distributed over a roughly rectangular area not extending quite to the Garlock fault, and terminating rather definitely both northeastward and southwestward. This suggests a rectangular outline in plan for the crustal block displaced in the main event; if so, the sharp boundary to the

southwest near the main epicenter looks suspiciously like the trace of a cross fault.

The two conspicuously distinct epicenters westward from that for the main shock, corresponding to shocks on August 19 and December 5, and May 23, are well determined, the latter especially so. They conform to the generally wider extent of activity northwest of the White Wolf fault. The rather isolated shock on July 22, 13:30 at Lat. $35^{\circ} 03' N.$, Long. $118^{\circ} 30' W.$, not far from the White Oak temporary station, is well located but has a magnitude of only 3.8.

Data bearing on the depths of these shocks will be discussed on another page. Even relative depths are reasonably well determined only for a small percentage of these earthquakes, excluding most of the more important ones. There is no clear indication of regular increase in depth on receding from the White Wolf fault southeastward, as might be expected if the hypocenters were following the dip of the main fault downward. This presumably means that, in the first 36 hours as well as later, fractures were occurring not merely at the base of the upper or southeastern block, but throughout its thickness up to the vicinity of the surface. It is noteworthy that most of the epicenters near the White Wolf trace but southeast of it correspond to shocks of relatively late date; those of early date, at least those large enough to be well located, leave a considerable space vacant between epicenter and fault trace (see fig. 2). In other words, supposing a general tendency of shocks to occur at a critical depth near 16 km., none are known to have occurred in the lower (northwestern) block in the first 36 hours. The shock with epicenter at Arvin (July 23, 13:17) and the larger of the shocks near Bakersfield, appear to have originated near the normal critical depth.

Considering the data presented in this section, the following description applies to the mechanism of the entire series of events.

On July 21 a roughly rectangular crustal block was thrust relatively upward and northwest along the steeply dipping White Wolf fault, fracturing internally at the same time. On July 23 shocks began occurring (apparently at normal depth) near the margin of the relatively downthrown block, perhaps extending somewhat beneath the relatively upthrown block. Strong activity on July 25 suggests extension of faulting to a northeast terminal point, which thereafter long remained a more important center of readjustment of strain than the vicinity of the epicenter of the main shock.

On July 29 the readjustment of strain, progressing gradually outward from the original rupture, sufficed to cause an extended fracture along a deep-lying fault zone striking northeast roughly at right angles to the known surface structures (except the gorge of the Kern River). This occurrence presents an interesting parallel to the Manix earthquake of 1947. On that occasion instrumentally located epicenters (Richter and Nordquist, 1951) clearly indicated displacement on a fault striking northwest. This is roughly at right angles to the surface structure, including the Manix fault along which minor trace effects were developed, probably as a secondary effect of the larger and different displacement in the basement rocks. This instrumentally established line in

the Manix region is roughly parallel to a number of important faults traversing the area immediately to the southwest. Similarly, the instrumentally established line in the Bakersfield area is roughly parallel to the White Wolf and Garlock faults.

The complexity of the earthquake series in 1952 is probably in no way unusual for seismic events of equal consequence. This happens merely to be one of a very few instances where the data are at all adequate for detailed analysis.

Evidence of the mechanical interrelationship of the entire group of Kern County shocks is the tendency for shocks to occur close together in different parts of the active area. It was soon noticed that it was nearly always wrong to assume that two successive shocks were from the same source. This was investigated more precisely in the following manner.

Epicenters of all the well located shocks beginning about 18h July 21 were assigned serial numbers in geographical order, approximately southwest to northeast along the trend of the White Wolf fault. These numbers ran from 1 to 82. Serial numbers 82 to 92 were assigned to epicenters in the outlying zone near Bakersfield, also from southwest to northeast. A scatter plot (fig. 4) was then constructed, in which the abscissa of each point is the serial number of the epicenter of a given shock, while the ordinate is the corresponding serial number for the next consecutive shock of magnitude 4 or over in the chronological list (table 1). Some shocks of magnitude near 4 were added to the list after the plot was constructed; but this introduces no more arbitrariness than the omission of the very numerous shocks of smaller magnitude.

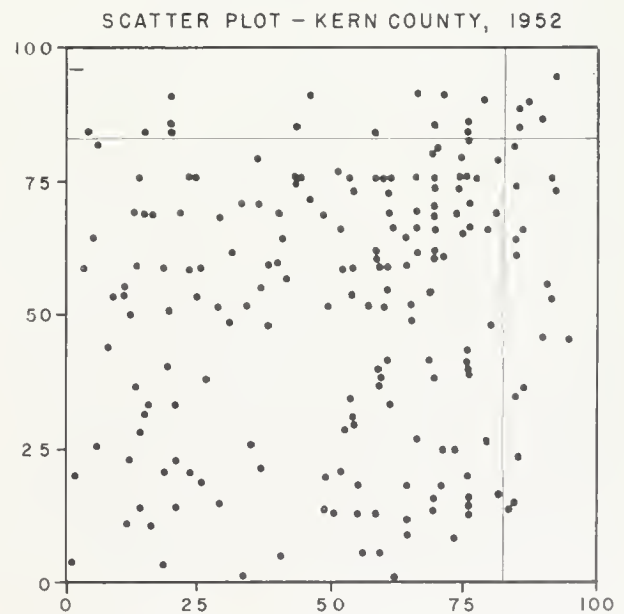


FIGURE 4. Scatter plot, showing tendency not to repeat from the same epicenter. Coordinates are serial numbers assigned to epicenters in geographical order.

On the scatter plot, repetition from the same vicinity should lead to concentration near the central diagonal. This is true only near the two corners, which represent the two extremes of the active area and the Bakersfield

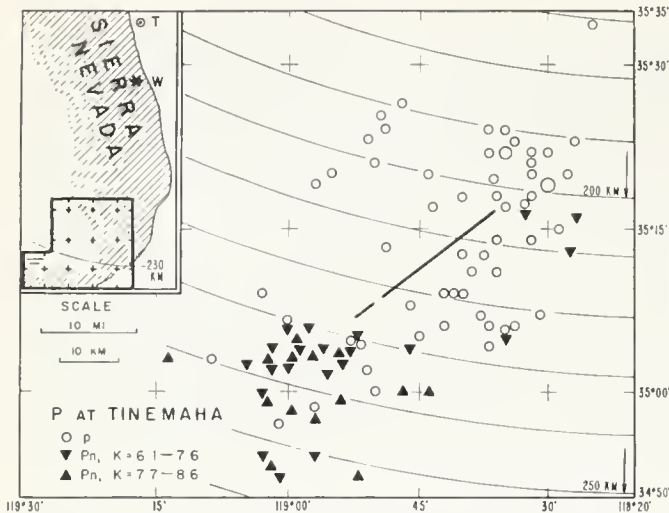


FIGURE 5. Nature of direct wave recorded at Tinemaha from indicated epicenters, showing effect of the Sierra Nevada. On the inset, T indicates Tinemaha, and W Mount Whitney.

zone. Clustering near the other two corners indicates tendency for a shock near one extreme to be followed by a shock near the other extreme. The conspicuous absence of points in the center of the plot does not indicate a geographical gap, because of the serial-number system of plotting. This is evident from the number of points with corresponding abscissa or ordinate. Merely two successive shocks rarely had epicenters with serial numbers from 25 to 50; these epicenters cover the White Wolf zone except for its terminal portions.

Direct and Refracted P. Root of the Sierra Nevada. The refracted wave Pn should precede the direct wave p (fig. 1 in section II-6) at distances ranging from 130 to 200 km. or over, depending chiefly on the value of the constant K . The variations in this critical distance Δ^* and in K are largely determined by the "root" of the Sierra Nevada. This is particularly clear for first motions recorded at the Tinemaha station. Figure 5 shows the nature of the first motion there in relation to epicentral location. Interpretation naturally depends closely on the determination of both epicenter and origin time, so that a single observation cannot be given much weight. On the figure, points have been duplicated and displaced slightly to denote different shocks at the same location. A few epicenters in the northern part of the plot, to which unusually many shocks are assigned, have been indicated by larger spots. For the main shock $K = 7.1$. Three signatures have been used, indicating (1) time fitting $p - O = D/6.34$ with $h = 16$ km, or slightly later; (2) times representing Pn with $K = 7.7-8.6$; (3) Pn with $K = 6.1-7.6$. Distance from Tinemaha is indicated by arcs numbered in kilometers. Locations of Tinemaha (T) and Mt. Whitney (W) appear on the small-scale inset.

The geographical boundary between p and Pn on this chart is evidently between 220 and 230 km. This would correspond to $K = 8+$, which represents much of the data; but, especially in the vicinity of the principal epicenter, prevailing values of K are much lower. They are still higher than the general value for southern California. In other words, Pn arriving at Tinemaha from

the southwestern San Joaquin Valley is delayed by the conditions of the Sierra Nevada structure, presumably involving a greater depth of the Mohorovičić discontinuity along these profiles. This delay is less for the region of the principal epicenter than a little farther east—which is to be expected, since the eastern profiles pass for a longer distance through the most elevated part of the Sierra Nevada block. For the long sub-Sierran path from the main epicenter to the station at Reno, the effect is even greater, with $K = 8.8$ for the very large and clear first recorded motion.

Corresponding results for the other recording stations may be summarized as follows.

Haiwee readings are questionable as probably not representing the first motion except for the largest shocks. At distances under about 150 km. the travel times usually fit fairly well for the direct wave, p . Beyond 150 km. they either fit quite closely to $Py - O = 0.1610\Delta + 1.2$ (this includes the main shock), or to Pn with $K = 6 \pm$, these times being earlier than those calculated for Py .

China Lake times, with very few exceptions, agree closely with those calculated for the direct waves, even at distances out to 171 km. (this includes the main shock, at a distance of 157 km.). This suggests values of Δ^* and K comparable with those found for Tinemaha.

At Boulder City, Pn times are available for about 45 shocks. The corresponding values of K are less than 5.7 for only five of these—Numbers 51, 86, 97, 156 and 161 of table 1. Except No. 156, these are in the southwestern part of the active area. For the main shock $K = 6.6$, which is near the mean value for the remaining observations at Boulder City.

Over 70 times of Pn are available for Fresno. In the southwestern part of the area the corresponding values of K are systematically lower than for most other stations; for the main shock Fresno has $K = 4.5$. In the northeastern section, and in the vicinity of Bakersfield, there is no such systematic difference; occasional low values of K occur, but on the whole Pn arrives later for the more eastern epicenters, suggesting a small delay due to the Sierra structure. The maximum K for Fresno is about 6.5—except for numbers 135 and 136, where the first arrival is so late that it nearly fits for the direct p at the large distance of 215 km. (these epicenters are near Tehachapi).

The analogous data for Santa Barbara must be interpreted cautiously. Because of high background and low magnification, small first motions tend to be missed, and even larger arrivals may be read a few tenths of a second late. The direct wave, usually fitting well for $h = 16$ km., is recorded consistently to about 120 km. At that distance it begins to be preceded by Pn with K about 5. For the shocks near $35^\circ 19' N, 118^\circ 30' W$, K is about 6.3, consistent with their shallower depth, possibly plus some delay due to the Sierran structures.

For Dalton Δ^* is between 140 and 150 km. Many excellent records of shocks in this range show p clearly as a small long-period phase immediately followed by larger short-period motion. The only shocks of this series recorded at Dalton with Pn clearly in advance of p are those near Bakersfield, at distances near 165 km., with K about 5.7.

Values of K for Riverside are entered numerically on figure 6. A separate signature indicates data for

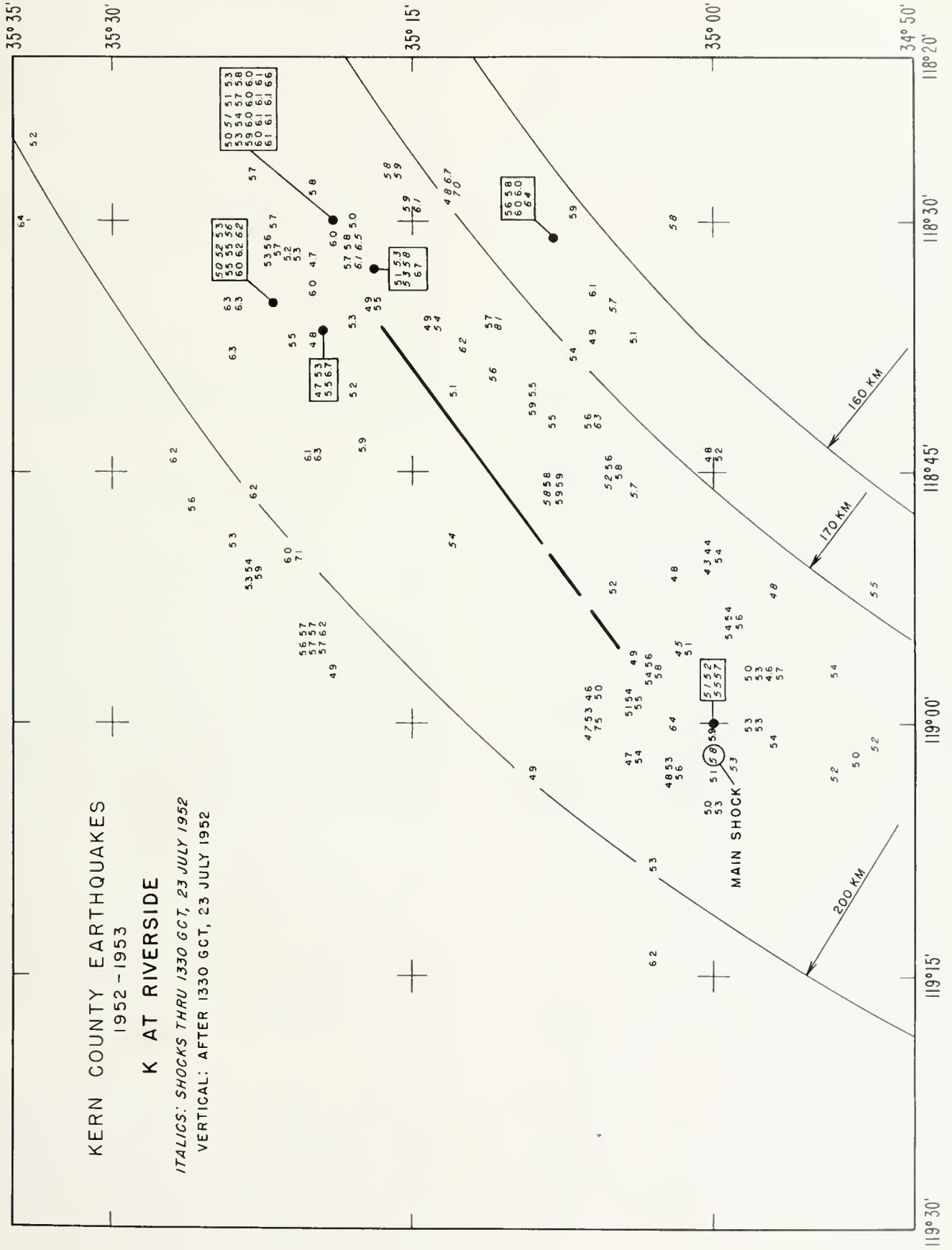


FIGURE 6. Values at Riverside, for indicated epicenters, of the quantity $K = P - O - \Delta/S.2$. Data for July 21-22 are from horizontal-component records only.

Table 4. Compressions and dilatations.

	P	MW	R	Pr	SB	CL	H	T	BB	BC	F	Chuchupate
July 21.....11:52	—	—	+?	—	—	—	—	—	—	—	—	—
21.....19:41	+	—	+	+	+	—	—	—	+?	+	—	—
23.....00:38	+	-?	-?	±	+	+?	+?	—	—	—	—	—
23.....03:19	—	—	—	-?	+	—	—	+	—	+	+	—
23.....07:53	—	—	+	—	+	+	±	—	+	+	—	—
23.....13:17	+	-?	—	+	+	—	—	—	+	—	—	—
23.....18:14	+	—	—	—	+	—	+	+?	—	—	—	—
25.....13:13	—	—	—	+	±	—	±	—	—	—	±	—
25.....19:09	—	—	—	—	+	—	-?	—	—	—	±	+
25.....19:43	—	—	+	+	+	—	+?	—	+	+	—	+
29.....07:04	+	+	+	—	+	—	—	+	—	+	—	—
29.....08:02	—	—	—	—	+	+	—	+	—	—	—	—
29.....15:49	+	+	+	+	—	—	+	—	+	—	—	—
31.....12:09	—	—	—	—	—	—	—	—	+	+	—	+
Aug. 1.....13:04	—	—	+	+	+	+	±	±	—	—	—	—
22.....22:41	+	+	+	+	+	—	—	+	+	—	+	—

July 21-23, when the vertical-component instrument was not recording and times of *Pn*, read from the horizontal-component records, may be slightly late for all but the largest shocks. Values of *K* less than 5 occur chiefly in the southwest area (although the main shock gives *K* = 5.8). The shallow shocks near 35° 19' 118° 30' have *K* near 6. Variations otherwise are generally rather small, and within the limits of error. Direct *p* is recorded for a few epicenters to the southeast.

One shock is close enough to Big Bear to have recorded the direct wave. This is No. 198, with epicenter distant 166.7 km. The calculated *P* — *O* is 26.5 sec., which would give an origin time of 20:56:41.0, only 0.3 seconds later than the adopted mean value. The remaining shocks show *Pn*, with *K* generally near 6.

Early P at Very Short Distances. About a dozen shocks are recorded at distances less than 20 kilometers with times of first motion 1 to 2 seconds earlier than those calculated from the direct wave at more distant stations, with *V* = 6.34. These observations are chiefly at Havilah, Knox Ranch, and White Wolf. A local cause is suggested; this may be a limited region in which the prevailing velocity is somewhat lower (not higher!) than average. Seismic waves emerging from this region will arrive systematically late at large distances. Consequently the origin time extrapolated back to the source will be determined as later than its true value, and the arrivals at short distances will appear relatively early. With reasonably favorable distribution of the distant stations in different directions, no serious error in locating the epicenter is likely.

Some of these early observations may be due to smaller shocks immediately preceding the one recorded at distant stations. This is almost certainly the case for No. 127b (July 27, 02:49:11.6), with epicenter about 2 kilometers from Havilah, apparently recorded at that station 1.6 seconds earlier than the calculated origin time.

Other Seismic Waves Recorded. Transverse waves (*S*) are regularly recorded. For the larger shocks, especially at short distances, they are hard to read because of unmanageably large trace amplitudes. The smaller shocks of the catalogue will provide ample data for a future investigation of *S*. Thus far, times of *S* have been used only to fix the origin times, as described for the special program.

Especially at Big Bear and Riverside, numerous readings of sharp later phases of the *P* group have been made. For Big Bear, most of these have a travel time well represented by $\Delta/6 - 0.4$; for Riverside, $\Delta/6 - 0.7$ seems better.

Waves arriving between the *P* and *S* groups, considered to be reflected from the base of the continental rocks, are being investigated by Mr. G. G. Shor.

Depth of the Shocks. The best established determinations of depth are for the shocks of the special recording program, especially No. 210 discussed elsewhere, for which the best value seems to be close to *h* = 9 km. (below sea level). This result is then almost equally valid for the larger shocks originating near the same point. Comparison with the main shock, and the large shocks near Bakersfield, then confirms that these are deeper, with a depth near that (16 km.) previously taken as standard. Many small shocks appear to have very shallow depth of origin. One large shock (No. 155, July 31, 12:09:08.8) shows systematic early arrival at distant stations with respect to near stations, leading to the approximate result *h* = 23 km.

Relatively small values of *K* at several stations for a number of shocks in the southwestern part of the active area implies that these are deeper than the average; deeper, in particular, than the main shock. The alternative would be some systematic cause for taking the origin late—late, that is, relative to the arrival of *Pn* at distant stations. Rejecting this, it should be noted that these epicenters are chiefly southeast and east of that for the main shock, and the greater associated depths are therefore consistent with the southeast dip of the White Wolf fault.

The probably reflected waves mentioned above promise to improve estimates of at least relative depth of the various shocks.

Statistics. Table 1 is only partly statistical in purpose. It lists, as completely as possible, all known shocks of the series assigned magnitude 4.0 or over, from July 21, 1952 through June, 1953. Where possible, epicenter and origin time have been determined for each of these.

The same table includes other shocks selected for study, for all of which epicenter, origin time and magnitude are given. Some of these, especially those for the special program on September 4-5 are very small.

Total numbers are as follows (through June, 1953):

Magnitude	Number
Over 7	1
6.5 - 6.9	0
6.0 - 6.4	3
5.5 - 5.9	8
5.0 - 5.4	6
4.5 - 4.9	58
4.0 - 4.4	125

Only two shocks over magnitude 4.9 occurred in August 1952, and none thereafter. Month by month totals, magnitude 4.0 and over, are:

1952 July	135
August	32
September	12
October	4
November	5
December	2
1953 January	2
February	1
March	2
April	1
May	3
June	1

Data of this kind have occasionally been reported in the press as "total numbers" of shocks. This is nonsensical. As a partial check on the frequency of smaller earthquakes, a count was run during September on shocks of magnitude 3.0 to 3.9, as estimated from the Pasadena seismograms. These numbered 90, while those from 4.0 to 4.9 number 12 in the same month. This proportion would indicate well over 1000 shocks of magnitude 3.0-3.9 in 1952. Smaller shocks were of course still more numerous; for 24 hours on September 4-5 30 shocks were easily counted on the Mt. Wilson seismogram, while during the same hours at least 158 were clearly recorded at Knox Ranch. (The special program was operated at this time.) Persistence of general activity may be illustrated by noting that on one of the last days of recording at Williams Ranch, March 14/15, 1953, about 20 small near-by earthquakes were recorded.

Listing is certainly incomplete for the first few hours on July 21. Only shocks clearly distinguishable as individuals are listed. Many shocks of magnitude over 4.0 must have escaped attention immediately following larger ones; in the first few minutes following the main shock, shocks of magnitude 4.5 and perhaps even 5 may have been missed.

Compressions and Dilatations. Table 4 gives available data for initial compressions (+) and dilatations (—) at various stations for the shocks of magnitude 5 and over; \pm indicates a clearly recorded motion in which the direction of initial displacement is indeterminate. Blank entries are chiefly due to smaller shocks. The seismograms of the larger aftershocks frequently begin with a small, slow motion which rapidly increases. If smaller shocks precede, it is sometimes not possible to tell the direction of first motion for the larger shock.

The general recording of initial dilatation for the main shock, consistent with thrust faulting, is not duplicated in any of the other tabulated shocks. Most of them show a distribution of compressions and dilatations in different directions which calls for a considerable strike-slip component. The pair of shocks from nearly the same epicenter at 07:04 and 08:02 on July 29 are particularly striking, since on many seismograms their first displacements are sharply opposite, while on others they are in the same direction.

The shock of magnitude 4.8 on May 25, 1953, compared on a previous page with the main shock, appears to conform approximately with the main shock in its pattern of first motions.

First motions were noted for a number of the best recorded smaller shocks, and investigated with reference to epicentral location. At Santa Barbara initial compressions were recorded from most of the epicenters except those near that of the main shock. At Mt. Wilson and Pasadena initial dilatations are in the majority, except for prevailing compressions at the most distant epicenters of the group, near Bakersfield, and the nearest, near Tehachapi.

10. MECHANISM AND STRAIN CHARACTERISTICS OF THE WHITE WOLF FAULT AS INDICATED BY THE AFTERSHOCK SEQUENCE

BY HUGO BENIOFF

ABSTRACT

The strain rebound characteristics of the aftershock sequence of the Kern County earthquake of 1952 indicated that the aftershocks southeast of the fault were generated by compressional strains whereas those on the northwest side were produced by shearing strains. Assuming that the original strain zone is outlined by the aftershocks spatial pattern, values for the strain characteristics of the strain zone preceding the earthquake can be computed as follows: volume of strained rock = 7.3×10^{10} cm³; average strain = 8.7×10^{-3} ; average stress = 26 kg/cm²; purely elastic strain energy density = 6.6×10^2 erg/cm³; creep strain energy density roughly 5×10^2 ergs/cm³.

Although the results are not as precise as might be desired (owing to the small number of available portable seismographs and to uncertainties of wave transmission in the vicinity of faults) the instrumental observations of the aftershock sequence, reported in the preceding papers by Gutenberg and by Richter, have provided information as to magnitudes, epicenters, and foci, hitherto not available for any earthquake. Thus the approximate distribution of aftershock foci around a seismic source has been determined for the first time.

With this information and the elastic strain rebound characteristic of the sequence it has been possible to derive additional conclusions as to the mechanism and strain characteristics of the fault. Figure 1 is a map showing the locations of all epicenters determined to date by Professor Richter. Assuming that the fault segment which was active in the production of the principal shock is effectively defined by the distribution of aftershock epicenters in a direction parallel to the fault, it may be concluded that slipping extended approximately from a few kilometers southwest of the principal epicenter to the vicinity of Caliente, a total distance of 60

kilometers. In the past the writer has assumed that the foci of aftershocks occurred on or very near the active fault segment. It is clear from the distribution of epicenters in this series, however, that the foci occupy a zone extending some 22 kilometers from the fault on the northwest side to some 16 kilometers on the southeast side. In an earlier paper (Benioff, 1951a) the writer concluded that in the 1906 San Francisco earthquake the observed ground displacement, the length of active segment, together with reasonable calculations of energy from the magnitude, indicated that the major proportion of the elastic strain which generated the earthquake was necessarily confined to a narrow strain zone some 20 kilometers wide. Moreover, one of the conditions for this concentration of strain energy was shown to be a reduced effective elastic coefficient of the rock in this zone in comparison with that of the surrounding rock. The occurrence of the Kern County aftershocks within a limited zone on either side of the fault suggests that this zone is in fact the strain zone and that the reduced effective elastic coefficient is perhaps brought about by the many fractures or minor faults on which these aftershocks occurred. The crosshatching in figure 1 indicates roughly the horizontal area of the strain zone as given by the epicenters. The portion southeast of the fault is very nearly rectangular whereas the northwest portion approximates a trapezoid in shape. The observed data are not sufficiently precise for accurate focal depth measurements, but in so far as they can be relied upon, they suggest that most of the foci are situated at the common depth of roughly 16 kilometers with some at shallower depths and a few somewhat deeper. It should be emphasized, however, that the position of a focus refers solely to the point at which faulting is initiated. In any earthquake the seismic energy is radiated from a moving area of slip extending generally from the focus upwards and downwards as well as horizontally. Consequently, except for very small shocks, the position of the effective source does not coincide with the focus. A transverse, vertical section through the fault zone with a composite projection of the foci is shown in figure 2. The 62° dip of the fault shown in the vicinity of the focus is taken from Gutenberg's calculation reported elsewhere in this publication. The increase of the angle of dip near the surface is required by the nearness of the epicenter to the surface trace of the fault.

Since in this series of shocks we have no way of determining the depth to which faulting extends, it is assumed here that the lower limit extends to the Mohorovičić discontinuity (HM in the figure) at approximately 35 kilometers from the surface. In constructing this projection of the foci it has been assumed that all occur at a depth of 16 kilometers. However, wherever several occurred together they are shown displaced vertically from each other. The vertical spread in the figure is thus a matter of drafting convenience and has no other significance. The common 16 kilometer focal depth corresponds roughly with Gutenberg's low velocity layer where, in addition to a reduced wave velocity, one may expect also a reduced strength.

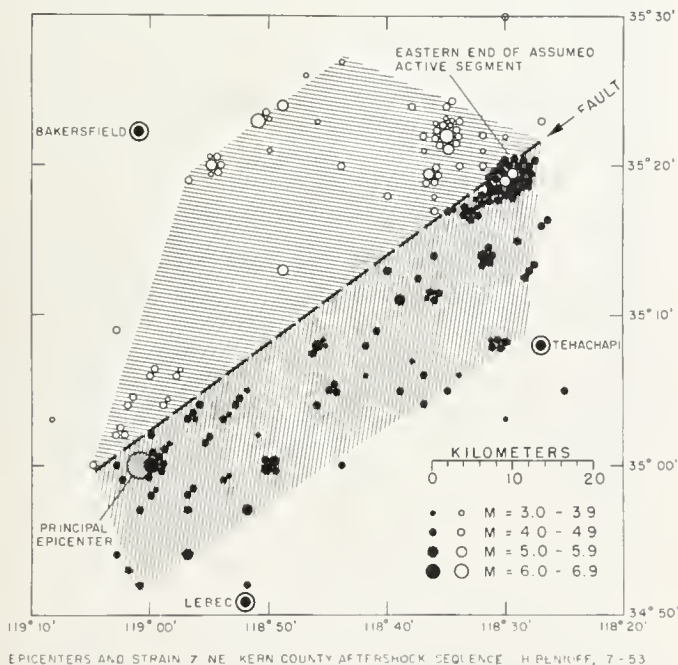


FIGURE 1.

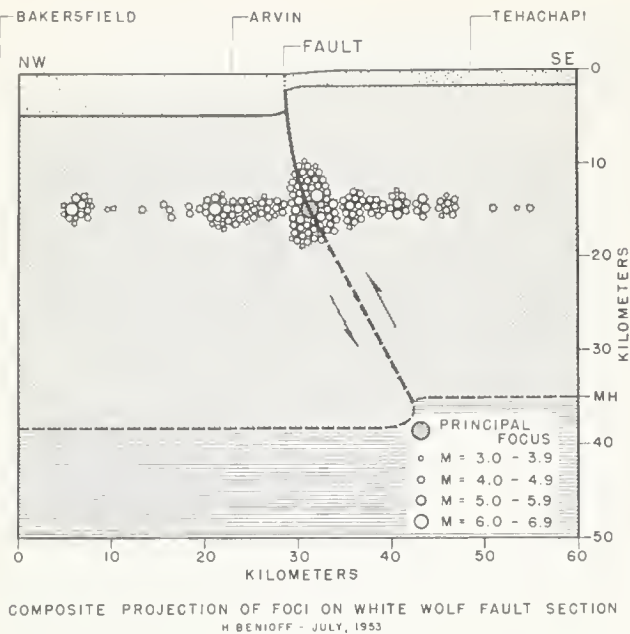


FIGURE 2.

For the first day or so following the principal shock the aftershocks occurred so frequently that a large proportion cannot be located owing to overlapping on the seismograms. Of those which have been located by Richter to date, it appears that during the first 36.7 hours (1.53 days) all aftershock foci were situated within the southeast block of the strain zone only. Thereafter the northwest block became active and foci then continued to occur throughout the whole strain zone with minor fluctuations or concentrations in position and time. The elastic strain rebound characteristic of all aftershocks presumed to originate in the southeast section of the strain zone is represented by the upper curve in figure 3. Except for an interval of a few minutes following the principal shock, this characteristic has the form $S = a + b \log t$, which, according to the writer's theory of aftershock generation (Benioff, 1951b), is produced by elastic afterworking resulting from a compressional strain of the rock in the strain zone. Epicenters of the shocks used in making this curve are shown as filled circles in figure 1. The lower curve in figure 3 is the elastic strain rebound characteristic of all shocks with foci in the northwest section of the strain zone. The shocks used for this curve are shown as open circles in figure 1. This sequence began 1.37 days after the time of beginning of the southeast sequence and has the form $S = A + B [T - (\exp - \alpha T^{1/2})]$, representing elastic afterworking of a shearing strain in this section of the strain zone. The dual form of aftershock activity was first observed in the 1933 Long Beach earthquake aftershock sequence (Benioff, 1951b). In this earlier observation, no information was available as to the distribution of aftershock epicenters and it was therefore assumed that the dual activity existed within the whole strain zone on both sides of the fault—an assumption which raised difficult problems. The present finding, in which the two components of creep occur in different sections of the strain zone situated on opposite sides of the fault,

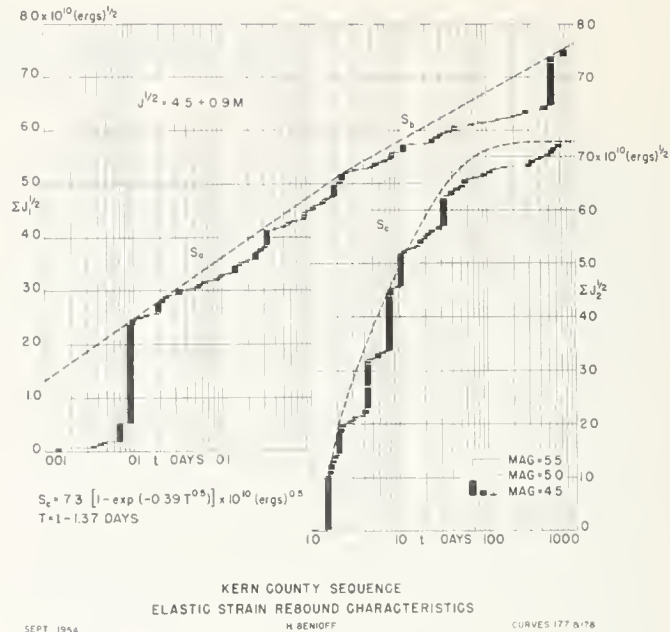


FIGURE 3.

is much more satisfying, although by no means without problems of interpretation. Thus it is difficult to account for shearing strain on one side of the fault with a compression on the other side without resorting to a complicated mechanical configuration. The delay in onset of the shearing creep recovery which was observed also in the Long Beach series and in the Hawke's Bay sequence of 1931 still remains obscure. The delay in the case of the Hawke's Bay earthquake (Benioff, 1951b), which was of the same magnitude (7.6) as the Kern County shock, was 2.4 days, whereas in the Long Beach earthquake (magnitude 6.4) the delay was only 0.135 days. It would thus appear on the basis of these three observations that the delay may be greater the larger the principal earthquake. Moreover, in all three earthquakes the compressional sequence was made up of a large number of relatively small shocks, whereas the shearing sequence was composed of a relatively smaller number of larger shocks.

The surface areas of the portions of the strain zone northwest and southeast of the fault trace are each approximately 1050 km². Assuming the depth of the strain zone to be 35 kilometers, the total volume of rock in the strain zone is 2100 × 35 = 7.3 × 10⁴ km³ = 7.3 × 10¹⁹ cm³. Taking the energy of the principal shock as 4.8 × 10²² ergs * the average energy density stored in the rocks before the earthquake in the form of purely elastic strain was 6.6 × 10² ergs/cm³. The energy J , stored in a volume V of rock having an elastic constant μ and an average elastic strain ϵ is

$$J = \frac{1}{2} \mu V \epsilon^2$$

from which one obtains the relation

$$\epsilon^2 = \frac{2J}{\mu V}$$

* On the basis of $M = 7.6$ and an energy conversion equation of the form $\log J = 9.0 + 1.8 M$.

Assuming a value of $\mu = 5 \times 10^{11}$ and substituting the values of J and V for this shock in the above equation we have

$$\epsilon^2 = 2.7 \times 10^{-9}$$

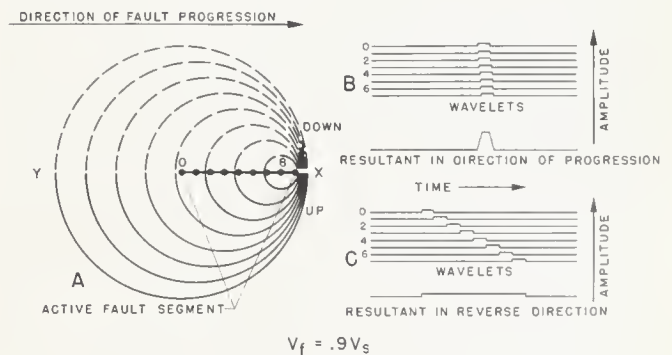
and the purely elastic strain preceding the earthquake is thus $\epsilon = 5.2 \times 10^{-5}$, on the assumption that the efficiency of conversion of elastic energy to wave energy is 1—which cannot be far wrong. In addition to the purely elastic strain there was an additional creep strain of the rock which was the source of the aftershock energy. The amount of the creep strain can be estimated as follows (see Benioff, 1951b): The sum of the strain release increments ($\Sigma J_i^{1/2}$) of the compressional series of aftershocks is 7.5×10^{10} (ergs)^{1/2} and that of the shearing series is 7.3×10^{10} . Thus the total strain release in the aftershocks was $(7.3 + 7.5) \times 10^{10} = 1.5 \times 10^{11}$ (ergs)^{1/2}. The corresponding value for the principal earthquake was 2.2×10^{11} . Thus assuming that the creep elastic constant is equal to the purely elastic constant and that the volume of rock involved is the same for the two types of strain, the elastic creep strain was approximately equal to the purely elastic strain. The total strain of the rock just preceding the earthquake was thus 8.7×10^{-5} . The average elastic stress borne by the rocks just before fracture is

$$\sigma = \epsilon\mu = 5.2 \times 10^{-5} \times 5 \times 10^{11} = 2.6 \times 10^7 \text{ dynes/cm}^2 = 26 \text{ kg/cm}^2.$$

Taking the total width W of the strain zone as 36 kilometers the total relative slip y , of the two fault surfaces, during the principal shock is thus $y = \epsilon W = 5.2 \times 10^{-5} \times 3.6 \times 10^6 \text{ cm} = 190 \text{ cm} = 1.9 \text{ meters}$. This, of course, is a very rough approximation and depends entirely upon the constants chosen for the magnitude-energy equation.

For a dip slip fault such as this one, faulting in the direction of slip is propagated by compressional and tensional strain increments initiated on opposite sides of the fault by the progressing slip area. The speed in this direction is thus less than average compressional wave speed in the medium. Hence in the principal shock the time required for the faulting to reach the surface from the focus was greater than $18.5/6.5 = 2.8$ seconds. Likewise faulting in the direction of strike is propagated by shearing increments of opposite sign on the two sides of the fault and must proceed with a speed less than the average transverse wave speed. The time required for faulting to progress horizontally from the focus to the end point in the vicinity of Caliente was therefore greater than $60/3.8 = 16$ seconds. In an earlier paper (Benioff, 1951a) the writer showed that the finite speed of fault propagation resulted in an unsymmetrical radiation pattern for the seismic wave energy. Thus referring to figure 4, which is a slight modification of one shown in that paper, the line 0-8 represents the total horizontal extent of faulting assumed to originate at 0 and terminate at 8. The drawing shows the configuration of a group of wavelets originating at points 0, 1, 2, 3, etc. along the fault at the moment when the slip progression has reached point 8. The largest circle represents the position of the wavelet which began at the point 0 when faulting was initiated. The next smaller circle represents the position of the wavelet

propagated from point 1 which started later than the wavelet from point 0. In like manner the remaining circles show the positions of wavelets originating at points 2, 3, 4, etc. as the faulting progressed. It is clear that the contributions from each of the numbered point sources are concentrated in the direction of faulting and are dispersed in the reverse direction. The combined effect at a point such as X in the direction of faulting is shown roughly at B . We assume that the slip displacement at any point along the fault has the form of a ramp function. The corresponding slip velocity is a rectangular function. The wave motion at X is thus composed of the resultant of each of the wavelets generated at the numbered points as shown. The resultant wave in the direction Y , away from the direction of faulting progression, is shown at C . The resultant in B has a larger amplitude than the one in C and in addition is of shorter duration. Since the power in a pulse varies with the square of the velocity amplitude, it is clear that the wave travelling in the direction of the faulting progression will have much more power than the wave propagated in the opposite direction. Actually, the wavelet contributions from the two sides of the fault are opposite in phase as indicated by dashed lines for one and continuous lines for the other and consequently, in the general direction of the fault plane, they form an interference pattern having amplitudes which vary with azimuth. The large values of shear wave power in the forward faulting direction is thus very likely a contributing cause of the relatively large destruction at Tehachapi. Although we have no precise information as to the speed of faulting, we know that it must have been less than the shear wave speed but not much less, since if it were, the wavelets from the extremes would be out of phase with each other and the consequent reduced total strain increment would be insufficient to propagate the slip. It is thus very likely that the progression speed is in the neighborhood of the speed of the Rayleigh waves— $0.9V_s$ —where V_s is the transverse wave speed. Under these conditions the wavelet augmented vertical component of the progressing slip should be tightly coupled to the Rayleigh wave mode with consequent generation along the fault of strong Rayleigh waves in the general direction of faulting progression. This generation would take place directly without the commonly assumed transformation from body waves. In the reverse direction the wavelet resultant amplitude is



EFFECTS OF SLIP PROGRESSION ON WAVE AMPLITUDES AND SHAPES
H. BENIOFF · JULY, 1953

FIGURE 4.

small and the direction of travel of the waves is opposite to that of the fault progression. Consequently in this direction the coupling is very weak and the generated Rayleigh waves are quite small in amplitude. Thus Gutenberg's observations of a strong asymmetry in the azimuthal distribution of Rayleigh wave energy, reported in an accompanying paper of this series, may be

taken as independent evidence that, in this earthquake, faulting progressed a substantial distance in the north-east direction from the focus. Observations of unsymmetrical surface wave radiation patterns have been made by Ewing and Press on the Assam earthquake of August 1950 and by them and the writer on the Rayleigh waves of the Kamchatka shock of November 4, 1952.

11. RELATION OF THE WHITE WOLF FAULT TO THE REGIONAL TECTONIC PATTERN

BY HUGO BENIOFF

ABSTRACT

For a large and old fault system such as the San Andreas it is not safe to attempt to determine the configuration of the stress pattern now active from the geometry of the break. The easterly deviation of the fault in the vicinity of the Garlock intersection together with the left strike-slip displacements on the Garlock fault indicate that in addition to the regional movements parallel to the San Andreas fault there is a regional movement parallel to the Garlock fault. These two movements are eventually incompatible and it appears that the White Wolf fault is an expression of this incompatibility.

The White Wolf seismic activity is related to or derived from the general regional tectonic pattern. Unfortunately, our knowledge of the latter is not in a satisfactory state. The principal observational data bearing on the problem are provided by the geometric relations of the active faults, their slip characteristics and the secular block movements which produce the slips. In general, the relation between the stresses which produce motion on a fault and its geometric configuration is not always as simple as we should wish. Thus, for example, the application of stress to a rock mass having a structural weakness such as a contact or other defect produces a fracture which does not necessarily follow the geometry of fractures in a homogenous medium. Likewise, once a fracture has occurred, movements will continue on it even though the stress pattern is greatly altered from the original form which produced the fracture. Moreover, if the writer's conclusion regarding the concentration of strain in relatively narrow strain zones along faults is correct, the stress interpretation of the pattern is still more troublesome. On this hypothesis the major portions of the blocks between faults, in a seismically active region, are relatively unstrained and so act principally as stress transmitting members to the narrow strain zones at their margins, where the strain is secularly accumulated for intermittent release in earthquakes. Another difficulty arises from the fact that we do not know the nature of the forces which produce the stresses. Thus the interpretation of a pattern of fault movements in terms of stress is affected by one's basic assumptions as to whether or not the forces originate within the whole block masses as body forces, or are applied horizontally from outside the affected region, or are generated by coupling to moving structures below. The nature of these forces can be determined only after measurements of the small residual strain variations occurring within the blocks at a large number of points are available for a substantial interval of time. Another difficulty arises from our ignorance as to the depth to which the faults and their strain zones extend. In the California region it is commonly assumed that they extend to not more than ± 35 kilometers—the depth of the Mohorovičić discontinuity. However, nearly all of the continental margins of the Pacific Ocean except the coast of North America from Mexico to Alaska have deep focus earthquakes, indicating that the seismically active structures of the continents extend to depths of 150 to 300 kilometers (Benioff, 1949, 1953). The line of volcanoes and the parallel mountain ranges of the western coast of North America are evidence that the structure of this

region is perhaps similar to the rest of the Pacific continental margins except that the deep activity here has subsided. We cannot, therefore, rule out the possibility that the faults producing our shallow earthquakes may extend to great depths or may be coupled to the deeper structures which could react either as passive or active members of the stress-strain complex. Even though the foci are shallow, slip may thus extend to greater depths. However, even if it may not be possible at this time to determine the nature of the regional tectonic stress pattern, something can be done in the way of describing the general dynamic behavior of the region as exhibited by the geometry and known movements of the faults. The San Andreas fault is, of course, the dominating structure in this region. As pointed out earlier by Gutenberg, the seismic evidence in the form of the distribution of epicenters indicates that this fault extends from a point off the coast of Oregon to the lower reaches of the Gulf of California as shown on the map, figure 1, a total length of 3,000 kilometers. The epicenters are taken from Gutenberg and Richter (1950) and represent all earthquakes to 1948 which exhibited P phases beyond an epicentral distance of 20° . The linear distribution of shocks parallel to the known surface expression of the fault includes those known to be on the fault, such as the 1906 San Francisco earthquake, and a number of smaller shocks located in the vicinity of the fault. These latter are presumed to represent auxiliary strain relief accompanying the principal activity of the fault. The epicenters continue along the north and south extensions of the fault without significant change at the points where the visible trace enters the ocean and it is therefore assumed that the fault segment extends to the end points of the epicenter distribution. The term "fault" is used here in the megaseopic sense denoting a region of contact between two great blocks moving relative to each other. The position of the slip surfaces at any given time varies with the strength, friction and cementing in the contact region and consequently the fault is, in effect, a zone of fracture and not a single surface. The movement on this San Andreas fault is of the right-lateral strike-slip type in which the oceanic block is moving northwest relative to the continental block as shown by the solid arrows in figure 2. In view of the profound discontinuity between the Pacific continental margins and the adjacent oceanic masses, it is not unreasonable to assume that the San Andreas fault represents movement along or guided by continental-oceanic contact. The fault is fairly straight from the northern terminus to the region of the San Emigdio Mountains where it is deflected sharply eastward some 35° . From this point south it has the form of an arc concave toward the Pacific and thus becomes nearly parallel to the northern straight segment in the vicinity of Whitewater. From there it continues southeast in a roughly straight line. In the vicinity of the sharp bend, the Garlock and Big Pine faults intersect the San Andreas fault at angles of approximately 40° . These faults (Garlock and Big Pine) are both of the left-lateral strike-slip type. It has been argued that the

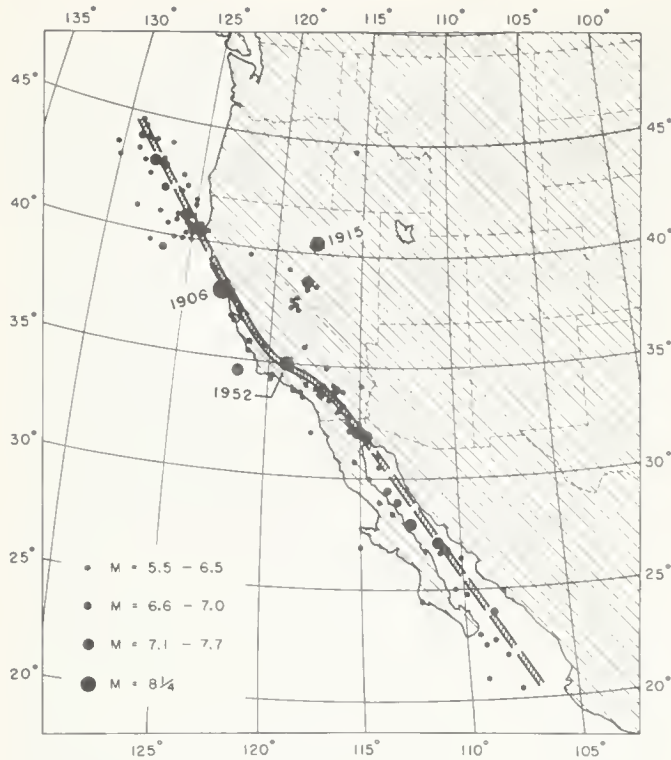


FIGURE 1. San Andreas fault zone as defined by earthquake epicenters.

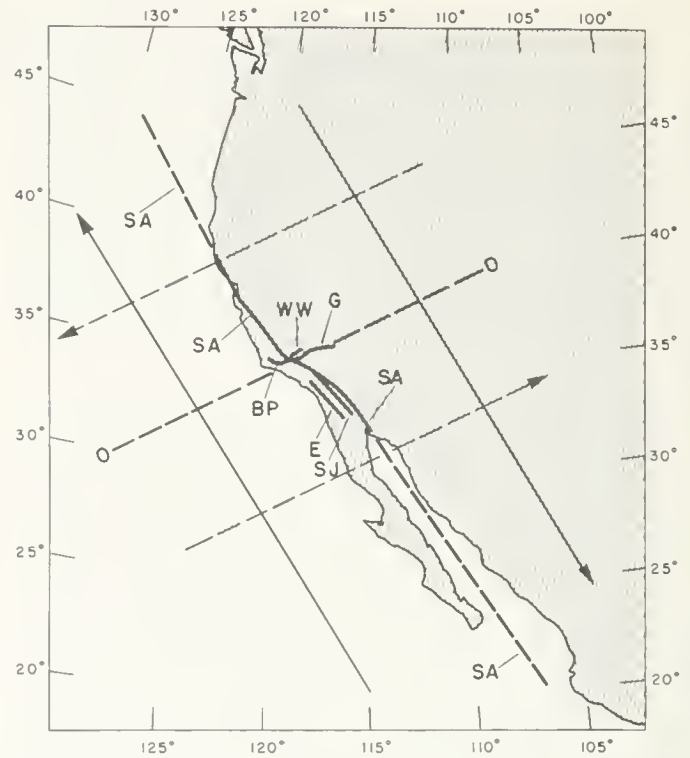


FIGURE 2. Dynamics of the San Andreas-Garlock fault system. S.A., San Andreas fault; G., Garlock fault; B.P., Big Pine fault; W.W., White Wolf fault; E., Elsinore fault; S.J., San Jacinto fault.

Garlock-Big Pine faults are conjugate fractures with the San Andreas fault resulting from a north-south linear horizontal stress or a horizontal shearing couple oriented north-east-southwest counter clockwise. However, this concept meets with difficulties. Thus at shallow depths (less than 50 km or so) fractures occur at angles less than 45° with the direction of the greatest principal stress whereas in the San Andreas-Garlock intersection the angle is greater than 45° . Moreover, conjugate fractures must occur nearly simultaneously; otherwise, the occurrence of the first break alters the stress pattern in such a way as to prevent the second fracture from developing. If the San Andreas fault has undergone the large (350 mile) total displacement posited by Hill and Dibblee (1953) (a not unreasonable assumption) then the Big Pine-Garlock component is of later origin and must therefore have developed in response to a later and different stress system from that which produced the San Andreas fracture. The bend in the San Andreas fault together with directions of slip of the Big Pine-Garlock fractures suggests that these are expressions of

a movement of the mass north of the Garlock fault in a westerly direction relative to the southern mass, as shown by the dashed arrows in figure 2, and that this movement started after the San Andreas fault was developed. The region in the vicinity of the Garlock-San Andreas intersection is thus one of severe distortion since the two fault movements being nearly at right angles to each other must ultimately be incompatible if they both continue without reversals.

The existence of the San Jacinto and Elsinore faults aligned approximately along the southern projection of the northern segment of the San Andreas fault may thus be evidence that this primary incompatibility is being resolved by the production of new fractures capable of taking over the linear San Andreas movement.

The distortion of that portion of the eastern block of the San Andreas fault moving southward along the curved restraint of the great bend must be principally of the form of a compression oriented approximately north-south. The White Wolf fault is thus a mechanism for relief of this localized stress.

12. STRONG-MOTION RECORDS OF THE KERN COUNTY EARTHQUAKES

BY FRANK NEUMANN AND WILLIAM K. CLOUD

ABSTRACT

The U. S. Coast and Geodetic Survey program of earthquake investigation is outlined and some results from the July 21, 1952 Kern County earthquake are given. Distribution of intensity in the 160,000-square-mile felt area of the shock is discussed and is summarized by an isoseismal map. Strong-motion seismograph results are indicated, and the relationship between acceleration, intensity, and distance examined. Damage due to permanent shifting of the ground is mentioned and possible causes suggested. The paper concludes with a comparison between the July 21 earthquake and the August 22 aftershock.

The Coast and Geodetic Survey's program of earthquake investigation consists in collecting descriptive and statistical information on earthquakes, in measuring destructive earthquake motions with special seismographs, and in analyzing the data for information of scientific and engineering value. In the Pacific Coast area, the field work and preliminary processing of records is conducted by the Seismological Field Survey which is a branch office of the bureau. The Washington Office further analyzes the material thus obtained, conducts research and development programs and publishes final results.

The two principal functions of the Seismological Field Survey are to collect descriptive information on earthquakes of all types, both large and small, and to maintain a network of strong-motion seismograph stations that operate only when strong seismic motion automatically triggers the instruments. The descriptive information serves to furnish a comprehensive picture of the intensity distribution throughout a shaken area. A good idea is thus obtained of the varied response characteristics of different types of soils and rocks to earthquake vibrations. It is found, for instance, that damage is generally minimum on outcrops of basement rock, and that the maximum damage occurs on unconsolidated soils with high water tables. While it is known that a great difference may exist between the motion of basement rock outcrop and an adjoining area of unconsolidated soil—as much as a 10- or 15-fold difference in acceleration—no effective effort has yet been made to correlate, in a comprehensive way, the elastic properties of various rocks and soils with their geological and dimensional characteristics. It is very probably a complex relationship. The descriptive information collected in this phase of the program is published in unabridged form in the quarterly Abstracts of Earthquake Reports prepared in the San Francisco Office and in abridged form in the annual seismological reports of the bureau—The U. S. Earthquake series.

The Seismological Field Survey supervises the operation of strong-motion seismographs in California and other western states and in Central and South American countries. These instruments register the ground motions automatically on photographic paper whenever the motion becomes strong enough to close an operating circuit through actuating a pendulum starting device. The ground motion is most often measured in the form of acceleration. In order to convert such records to displacement and thus reveal the longer period waves that are in the motion, the records of strong disturbances are

generally double-integrated. These data are used to correlate the actual ground motion with the various degrees of intensity reported at or near the stations, and to furnish the structural engineer precise data that can be used in estimating earthquake stresses in buildings and other structures. The instrument data are published in the quarterly Engineering Seismology Bulletin of the bureau and in its annual seismological report.

Modified Mercalli Intensity Scale of 1931 (abridged)

- I. Not felt except by a very few under especially favorable circumstances. (I Rossi-Forel Scale)
- II. Felt only by a few persons at rest, especially on upper floors of buildings. Delicately suspended objects may swing. (I to II Rossi-Forel Scale)
- III. Felt quite noticeably indoors, especially on upper floors of buildings, but many people do not recognize it as an earthquake. Standing motor cars may rock slightly. Vibration like passing truck. Duration estimated. (III Rossi-Forel Scale)
- IV. During the day felt indoors by many, outdoors by few. At night some awakened. Dishes, windows, doors disturbed; walls made creaking sound. Sensation like heavy truck striking building. Standing motor cars rocked noticeably. (IV to V Rossi-Forel Scale)
- V. Felt by nearly everyone; many awakened. Some dishes, windows, etc. broken; a few instances of cracked plaster; unstable objects overturned. Disturbances of trees, poles, and other tall objects sometimes noticed. Pendulum clocks may stop. (V to VI Rossi-Forel Scale)
- VI. Felt by all; many frightened and run outdoors. Some heavy furniture moved; a few instances of fallen plaster or damaged chimneys. Damage slight. (VI to VII Rossi-Forel Scale)
- VII. Everybody runs outdoors. Damage negligible in buildings of good design and construction; slight to moderate in well-built ordinary structures; considerable in poorly built or badly designed structures; some chimneys broken. Noticed by persons driving motor cars. (VII Rossi-Forel Scale)
- VIII. Damage slight in specially designed structures; considerable in ordinary substantial buildings with partial collapse; great in poorly built structures. Panel walls thrown out of frame structures. Fall of chimneys, factory stacks, columns, monuments, walls. Heavy furniture overturned. Sand and mud ejected in small amounts. Changes in well water. Disturbed persons driving motor cars. (VIII+ to IX Rossi-Forel Scale)
- IX. Damage considerable in, specially designed structures; well designed frame structures thrown out of plumb; great in substantial buildings with partial collapse. Buildings shifted off foundations. Ground cracked conspicuously. Underground pipes broken. (IX+ Rossi-Forel Scale)
- X. Some well-built wooden structures destroyed; most masonry and frame structures destroyed with foundations; ground badly cracked. Rails bent. Landslides considerable from river banks and steep slopes. Shifted sand and mud. Water splashed (slopped) over banks. (X Rossi-Forel Scale)
- XI. Few, if any, (masonry) structures remain standing. Bridges destroyed. Broad fissures in ground. Underground pipe lines completely out of service. Earth slumps and land slips in soft ground. Rails bent greatly.
- XII. Damage total. Waves seen on ground surfaces. Lines of sight and level distorted. Objects thrown upward into the air.

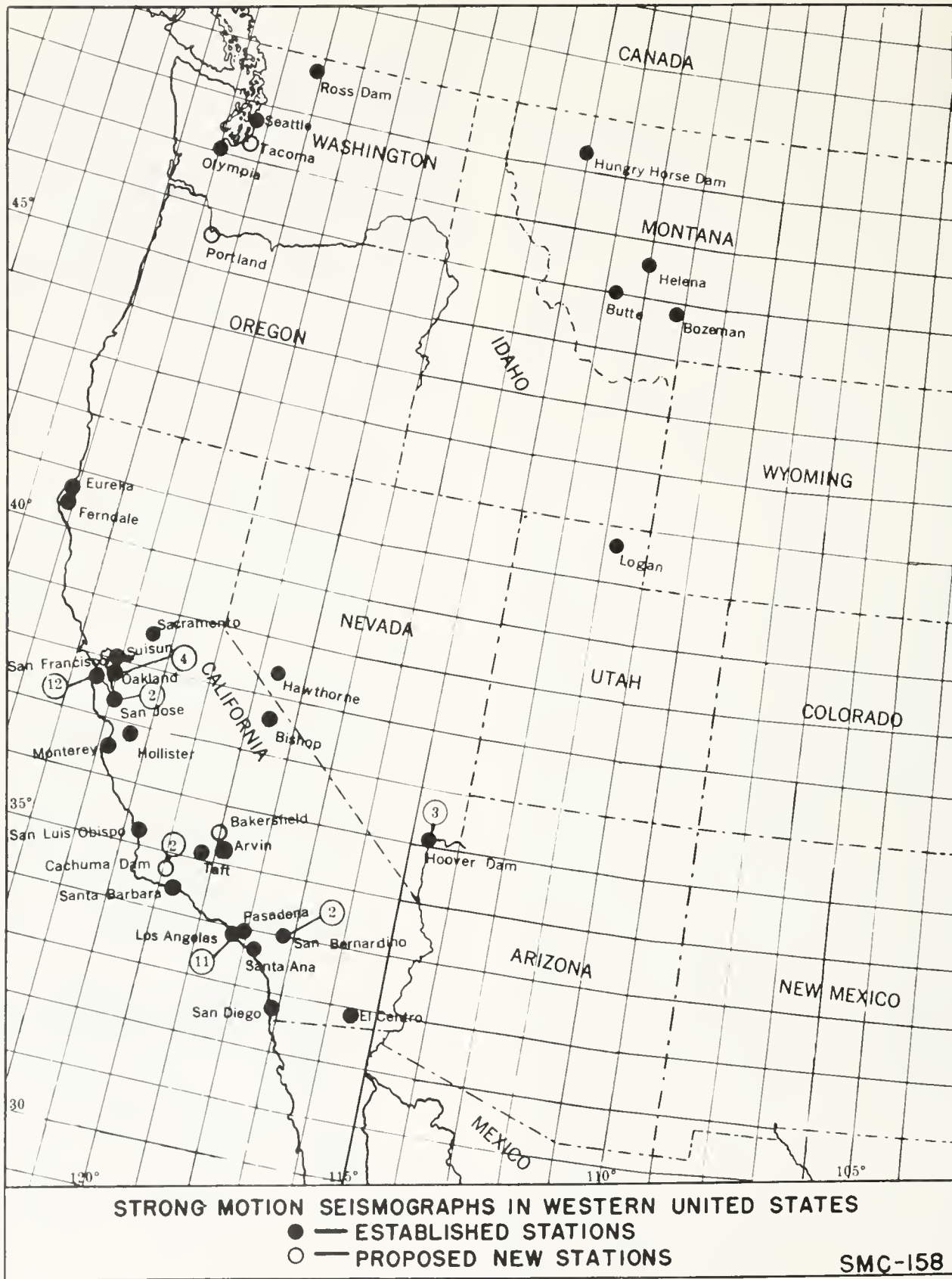


FIGURE 1.



FIGURE 2.

Intensity Distribution. The intensity scale used in the study of all U. S. earthquakes is the Modified Mercalli Intensity Scale of 1931 described in volume 21 of the Bulletin of the Seismological Society of America. It has been difficult to assign a specific maximum intensity to the central area of the Kern County earthquake because of the sparsity of population there and the resulting uncertainty inherent in making appraisals solely on the basis of ground disturbances such as cracks, rock slides, dust clouds, etc. Such intensity appraisals are made with much greater assurance when the earthquake effects on buildings and other structures are available for study. If one used only the vibrational effects on buildings as a measure of intensity there would be difficulty in assigning MM intensity 9 to any more than a very few points in the central area of the shock. Within a radius of 10 or 15 miles of the area of greatest structural damage intensity 8 would be a more representative value. This means broadly that damage to well-designed structures was slight or negligible; it was considerable in substantially built structures; and serious in poor masonry structures—some of which completely collapsed.

With reference to the intensities 10 and 11 found on the isoseismal map, they may be considered consistent with a rigid interpretation of the intensity scale, especially if one leans toward a higher rating when such choice might exist. This is ordinarily considered legitimate practice since all isoseismal maps aim to show the maximum intensity in an area—not the average nor minimum. In the Kern County shock, however, many of

the higher intensities in the central area were based on the cracking and permanent shifting of the ground. This might be classed as indirect damage and is not a legitimate index of the vibrational intensity of the ground motion. Then again, too little is known of the response characteristics of different types of soil safely to consider disturbances in such soils as measures of MM intensity. It will be recalled that, in his investigation of ground coefficients, H. O. Wood, in his study of the great 1906 earthquake, estimated that there was a 10-fold variation in ground acceleration on different formations in San Francisco alone. In view of these considerations it seems best to adhere to structural effects insofar as possible in appraising earthquake intensity.

The isoseismal map constructed by the Seismological Field Survey shows many features in common with similar maps for other shocks. It has special interest in showing the intensity distribution for the second largest shock to occur in California since 1900, and because of the information program developed in California over the past 20 years, the overall intensity distribution picture is perhaps one of the best yet obtained for any strong shock. The irregularity of the isoseismal lines reveals in a broad way the anomalous character of the surface and subsoil structure at the hundreds of cities and towns reporting intensity. Recent studies of intensity distribution have indicated that at localities which are resting for all practical purposes on outcrops of basement rock, the intensities are minimum (all other factors such as epicentral distance being the same) and that at such localities the decrease in intensity with increase of epicentral distance is surprisingly uniform and generally the same for all shocks. The isoseismal map should therefore be interpreted as showing the anomalous response of the many kinds of surface formations to the earthquake vibrations transmitted through the underlying basement rock. Outside the immediate epicentral area it is common experience to find the intensities reported at a given epicentral distance covering a range of 4 or 5 grades. It is in accord with past experience, too, to find certain sensitive spots as far as 100 miles from the epicenter reporting intensities as high as found in the epicentral area itself. It is not until these ranges are exceeded, that one would be justified in questioning the authenticity of the data on the score of the wide ranges of intensity reported.

Strong-Motion Seismograph Results. Because of the limited distribution of strong-motion accelerographs, no record was obtained of the stronger ground motions in the central area. The nearest station was at Taft, roughly 35 miles from the area of greatest intensity, and there the maximum resultant acceleration was .22 g (gravity) for a wave of .22-second period. A portion of this record is shown as figure 4. In the Imperial Valley earthquake of 1940, an acceleration of .34 g was registered at El Centro 4 miles from the area of maximum intensity; and in the Puget Sound shock of 1949, .20 g was registered at Olympia, 13 miles from the epicenter. From a study of past records it is estimated that the maximum accelerations in the central area of the July 21 shock may have been .35 to .5 g at points where intensity 9 is indicated on the strength of damage to buildings, and .20 to .35 g where intensity 8 is indicated. At Taft

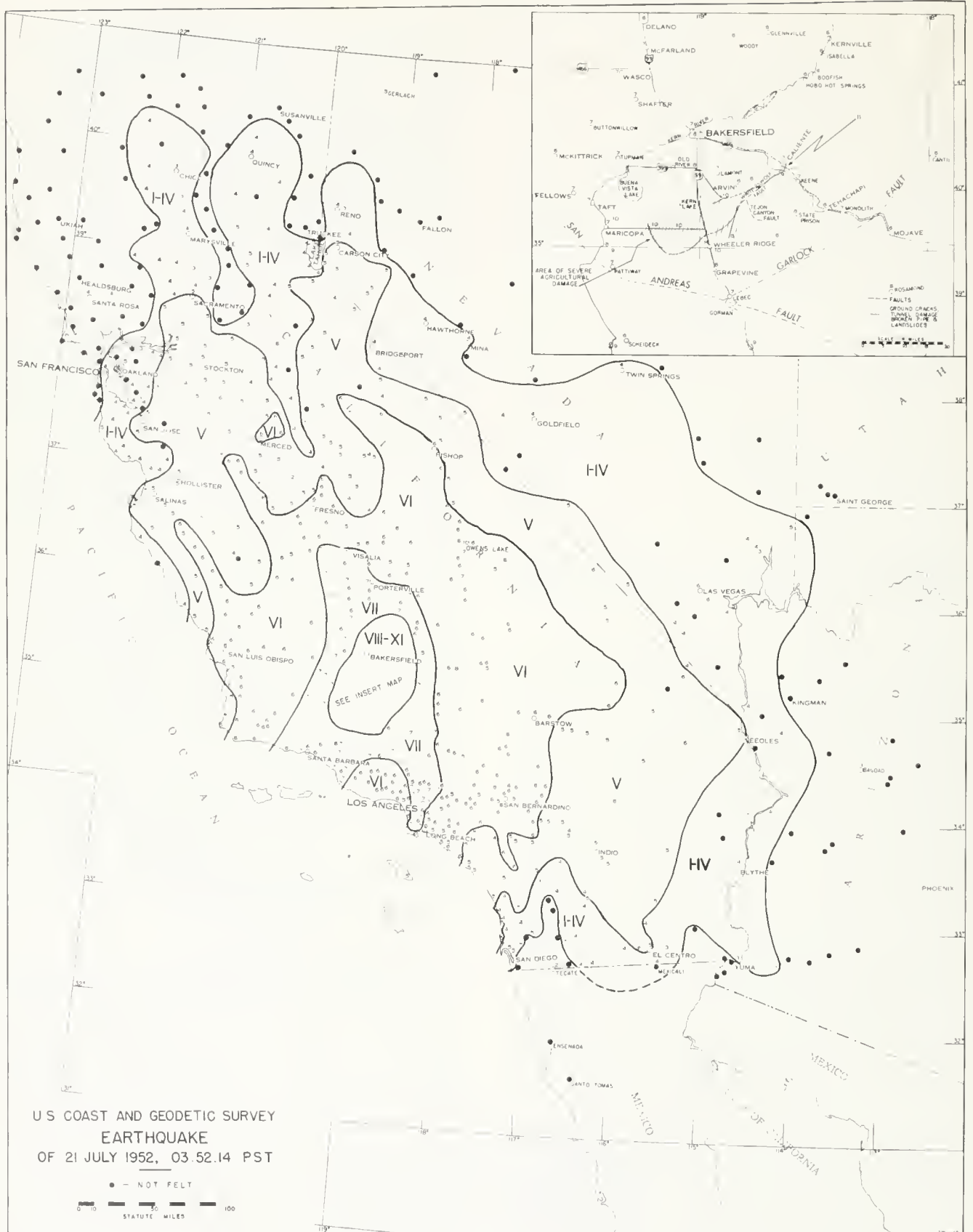


FIGURE 3.

the instrument registered an expectable acceleration for the intensity 7 actually experienced there.

Although no unusually high accelerations were recorded instrumentally the data obtained at 22 strong-motion stations furnished some of the best information yet available on the ground motions associated with various grades of intensity at different epicentral distances. It was found for instance that, while intensity 6 connotes a certain maximum acceleration when observed in epicentral areas, considerably lower accelerations were registered 100 miles or more from the epicenter for that same intensity. It appears, therefore, that any forcefulness that the ground motion loses at the greater distances because of its lower acceleration is compensated for by the longer duration of the disturbance. It was found in the Kern County earthquake that, within the limits of the data obtained, the acceleration associated with a given intensity was reduced to roughly one-half when that same intensity was registered instrumentally 100 miles from the epicenter, and approximately one-fourth at 200 miles, the reduction in acceleration for a given intensity being of exponential character.

Damage. Over most of the shaken area the damage to buildings, elevated water tanks and other structures followed the usual pattern. In general, structures stood up well when earthquake provisions were incorporated in their design. Poorly designed and constructed buildings were, as usual, the first to collapse. The unusual feature of the Kern County shock was the great damage due to permanent shifting or distortion of the ground. This sometimes took the form of settling or slumping of great masses of earth, especially in the hill areas. This was in evidence over a great length of the White Wolf fault and apparently reached its peak along the Southern Pacific Railroad in the vicinity of Bealville, a point somewhat remote from the epicentral area. It would be difficult to decide whether the permanent ground movements here were solely the result of a readjustment along the White Wolf fault, a re-settling or slumping of the hills or portions of them as a result of such movement, or the breaking of another fault lock in this area that could have released a vast amount of vibrational energy practically beneath the railroad bed. Fault lock may be described as points where the fault surfaces are locked together and release a great amount of potential energy when finally forced to yield to the stresses accumulating along the fault.

The other type of ground disturbance that attests to the unconsolidated nature of the terrain was the wrecking of miles of underground concrete irrigation pipes, the furrowing of fields and the appearance of innumerable ground cracks. These, it appears, were the result of the violence of the ground vibrations which could have represented possibly a 10- or 15-fold amplification of the vibrations in the basement rock. Little has been done, however, as previously stated, to distinguish between the elastic constants of different types of soils so that it is difficult to know what amplifications of basement rock should be expected or what the effects of mass vibratory movement might be on the soil in this area. A great variety of reactions in various types of soil might be expected to result from the same magnitude of basement rock disturbance.

Epicenter. The epicenter of the July 21 shock as located from sensitive seismograph data by the Pasadena Laboratory was Lat. $35^{\circ}00'$ north, Long. $119^{\circ}02'$ west. This is about 4 miles west of Wheeler Ridge. For some time such epicenters have been recognized as representing merely the location of the first break in what might be a complex series of fault breaks, especially in the case of very strong shocks. The theory that a fault movement represents the successive breaking of a number of locks, or strong points, along a fault finds credence in the character of the intensity distribution in many shaken areas. At this writing, with some of the available information still to be processed, there is some indication that the major break in the White Wolf fault may have occurred due south or southeast of Arvin in the region of the Tejon Canyon fault. The location of the major break is best obtained from the pattern of the intensity distribution in the epicentral area, but unfortunately, as previously stated, accurate appraisals of intensity in the epicentral area are difficult to make because of the sparsely settled nature of the area. As previously suggested there is also the possibility that a secondary break may have occurred near Bealville or the Southern Pacific Railroad.

The Bakersfield Shock. Since the seismographic evidence obtained by the Seismological Laboratory of the California Institute of Technology reveals the widespread nature of the aftershocks, it is clear that Bakersfield was within range of the readjustments taking place

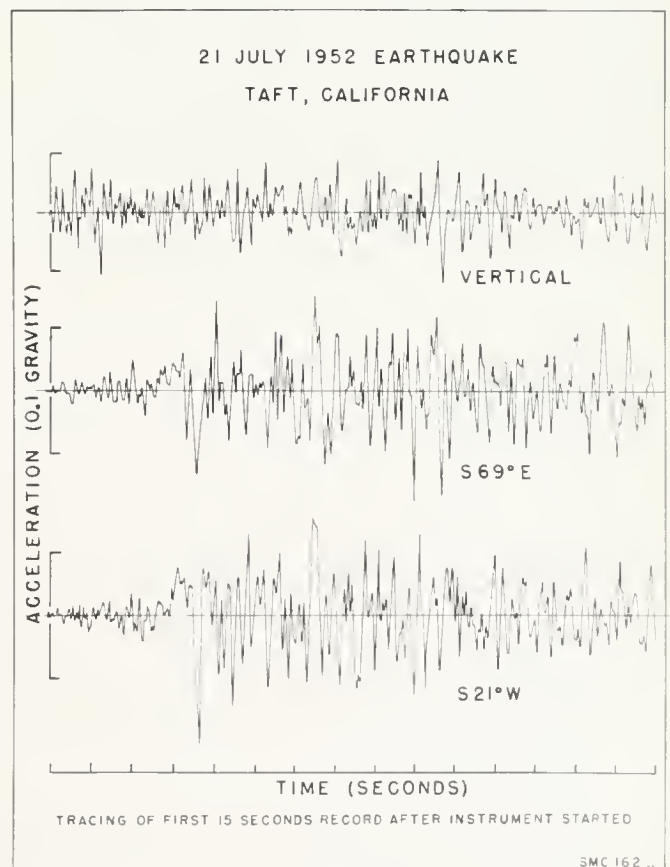


FIGURE 4.

in the deep rock structure around the epicentral area. On August 22, one of these strong aftershocks struck close to Bakersfield, roughly 5 miles southeast of the center of the city, according to the Pasadena Laboratory. This aftershock, according to the Gutenberg-Richter magnitude rating, released only about 1/1000 of the energy involved in the principal shock of July 21; but the latter epicenter was 20 miles or more further away. During the earlier shock the intensity in Bakersfield was a weak 8. When the aftershock of August 22 struck with an apparently greater intensity—a full 8—the damage in Bakersfield rose to an unofficially estimated \$20,000,000. There seems no doubt that the weakening of

many structures in the first shock was responsible for much of the aftershock damage.

Compared with the total damage of \$60,000,000 reported by the press for all shocks of the Kern County series, the \$20,000,000 damage at Bakersfield represents a third. It is clear that the earthquake risk in an urban area is largely a function of its distance from a fault lock, or plug, at which a great quantity of energy may be stored up in the form of stress in the deep basement rock. With respect to the relative areas shaken by the two earthquakes, the main shock of July 21 was felt over approximately 160,000 square miles while the Bakersfield shock covered only one-fourth that area.

PART III—STRUCTURAL DAMAGE

INTRODUCTION

PART III deals with the effects of the earthquakes on man-made structures and installations. The first paper (Part III-1) relates damage in some of the buildings examined to geologic factors. It is followed by a series of short papers (Part III-2 to 8) summarizing damage to oil fields, a refinery, highways and bridges, water works, electrical installations, railroad tunnels and right-of-way, elevated tanks, and to agriculture.

The Kern County earthquakes afforded structural engineers an excellent opportunity to re-examine the performance of buildings subjected to earthquake shocks. *Structural damage to buildings* (Part III-9) by Karl V. Steinbrugge and Donald F. Moran is an analysis, by two

structural engineers of the Pacific Fire Rating Bureau, of the damage to buildings based on extended field work in Kern and Los Angeles Counties. The pattern of damage to all types of buildings, including public schools, is discussed and the effectiveness of current earthquake resistive design practice is evaluated. Financial losses are estimated and an earthquake insurance classification of buildings is included. Part II closes with a paper by G. W. Housner on *The design of structures to resist earthquakes*, in which a short description of current methods of design of earthquake-resistant buildings is presented, based on measured and analyzed behavior of a structure when subjected to ground motion.

CONTENTS

	Page
1. Arvin-Tehachapi earthquake—structural damage as related to geology, by J. Schlocker and Dorothy H. Radbruch.....	213
2. Earthquake damage to oil fields and to the Paloma cycling plant in the San Joaquin Valley, by Robert L. Johnston.....	221
3. Highway damage resulting from the Kern County earthquakes, by O. W. Perry, with supplement, Bridge earthquake report, Arvin-Tehachapi earthquake, by Stewart Mitchell.....	227
4. Damage to water works systems, Arvin-Tehachapi earthquake, by H. B. Hemborg.....	235
5. Damage to electrical equipment caused by Arvin-Tehachapi earthquake, by G. A. Peers.....	237
6. Earthquake damage to railroads in Tehachapi Pass, by Southern Pacific Company.....	241
7. Earthquake damage to elevated water tanks, by Karl V. Steinbrugge and Donald F. Moran.....	249
8. Earthquake damage to California crops, by Karl V. Steinbrugge and Donald F. Moran.....	257
9. Structural damage to buildings, by Karl V. Steinbrugge and Donald F. Moran.....	259
10. The design of structures to resist earthquakes, by G. W. Housner.....	271

1. ARVIN-TEHACHAPI EARTHQUAKE—STRUCTURAL DAMAGE AS RELATED TO GEOLOGY¹

BY J. SCHLOCKER AND DOROTHY H. RADBRUCH²

INTRODUCTION

The effects of the Tehachapi earthquake of July 21, 1952, add new evidence to substantiate the long-held belief that structural damage is greatest in areas underlain by thick unconsolidated sediments and least in areas underlain by rock. This earthquake was one of the most severe ever recorded in California. In intensity it ranked between the weaker Long Beach earthquake of March 10, 1933, and the more severe San Francisco earthquake of April 18, 1906. Magnitude on the Gutenberg-Richter scale as determined in Pasadena, California, was 7.7. The provisional location of the epicenter, determined by the U. S. Coast and Geodetic Survey in cooperation with the Science Service and the Jesuit Seismological Association, is 35.1° N. latitude, 118.9° W. longitude; this was later corrected to 35° 00' and 119° 00'. The time of the initial shock was 4 hours, 52 minutes, 11 seconds A.M. Pacific Daylight Saving Time.

Early newspaper and radio reports received in San Francisco, California, on July 21, 1952, indicated that the earthquake had caused considerable damage to man-made structures in the town of Tehachapi. Subsequent reports showed that damage was widespread in the southern end of the San Joaquin Valley, approximately 25 miles west of Tehachapi. Inasmuch as the earthquake presented a valuable opportunity to gather first-hand information on the geologic control of damage, the writers, assisted by A. P. Cerkel, of the Engineering Geology Branch of the U. S. Geological Survey, spent 3 days, July 22 to 24, in the Bakersfield-Arvin-Tehachapi area. Part of their time was devoted to an examination of cracks and fissures in the surficial material that were apparently related to fault movement in the underlying bedrock; such features are described in more detail elsewhere in this volume. This paper is confined to the results of a brief examination of another noteworthy feature of this earthquake—the relationship between damage to man-made structures and the type of material upon which the structures were erected. For each building studied, the type of construction, the extent of damage, and the geologic setting were observed, and a photograph was taken. Detailed investigation of the method of construction was not made. For example, certain earthquake-resistant features may have been incorporated in the design of some structures; these features could not be easily determined by the writers, who are geologists untrained in the evaluation of building design.

Through the kindness of A. D. Edmonston, State Engineer, valuable information was obtained from an unpublished report on the geology of the Cummings Valley area prepared by the California State Division of Water Resources. K. V. Steinbrugge, structural engineer with the Pacific Fire Rating Bureau, furnished information on the damage to the California Institution for Women and the Cummings Valley School. C. S. Chitwood, Tehachapi City Engineer, furnished information on the subsurface conditions in Tehachapi.

GEOLOGIC SETTING

Most of the observations were made in the towns of Arvin and Tehachapi, and in Cummings Valley. The mountainous eastern part of this area is underlain by ancient granitic and metamorphic rocks. These rocks are exposed at the surface on the steeper slopes, but in several intermontane basins they are covered by varying thicknesses of alluvium. The mountains slope westward toward the broad San Joaquin Valley, whose alluvial sediments cover the crystalline rocks to great depths in the western third of the area shown in figure 1.

Arvin is on the thick alluvium of the San Joaquin Valley. The character of this alluvium is shown by the log of a well approximately 12 miles south of Arvin; this well penetrated 625 feet of sand, clay, and gravel before reaching bedrock.

Tehachapi is on thick alluvium in the central part of Tehachapi Valley, an intermontane valley of 36 square miles that lies between the Tehachapi Mountains and the southern end of the Sierra Nevada. Only the uppermost few feet of this alluvium is known in any detail. In the northern part of Tehachapi, 800 feet north of the Southern Pacific Railroad track, it consists of 2 to 3 feet of light olive-gray calcareous sandy clayey silt that overlies about 4 feet of greenish-white calcareous sandy clay. Both the silt and the underlying clay are plastic when wetted with water, the clay becoming more plastic than the silt. C. S. Chitwood, Tehachapi City Engineer, reports that the surficial silt becomes thicker southward and reaches a thickness of 6 to 10 feet along the southern border of the town. He also reports that sandy clay and gravel beds underlie the greenish-white clay. The water table appears to lie a considerable distance below the surface. An old stream channel, 5 to 10 feet deep and approximately 10 feet wide, is reported to have trended northwest across Tehachapi, crossing G Street at the



FIGURE 1. Index map of the Bakersfield-Arvin-Tehachapi area.

¹ Publication authorized by the Director, U. S. Geological Survey.

² Geologists, U. S. Geological Survey.

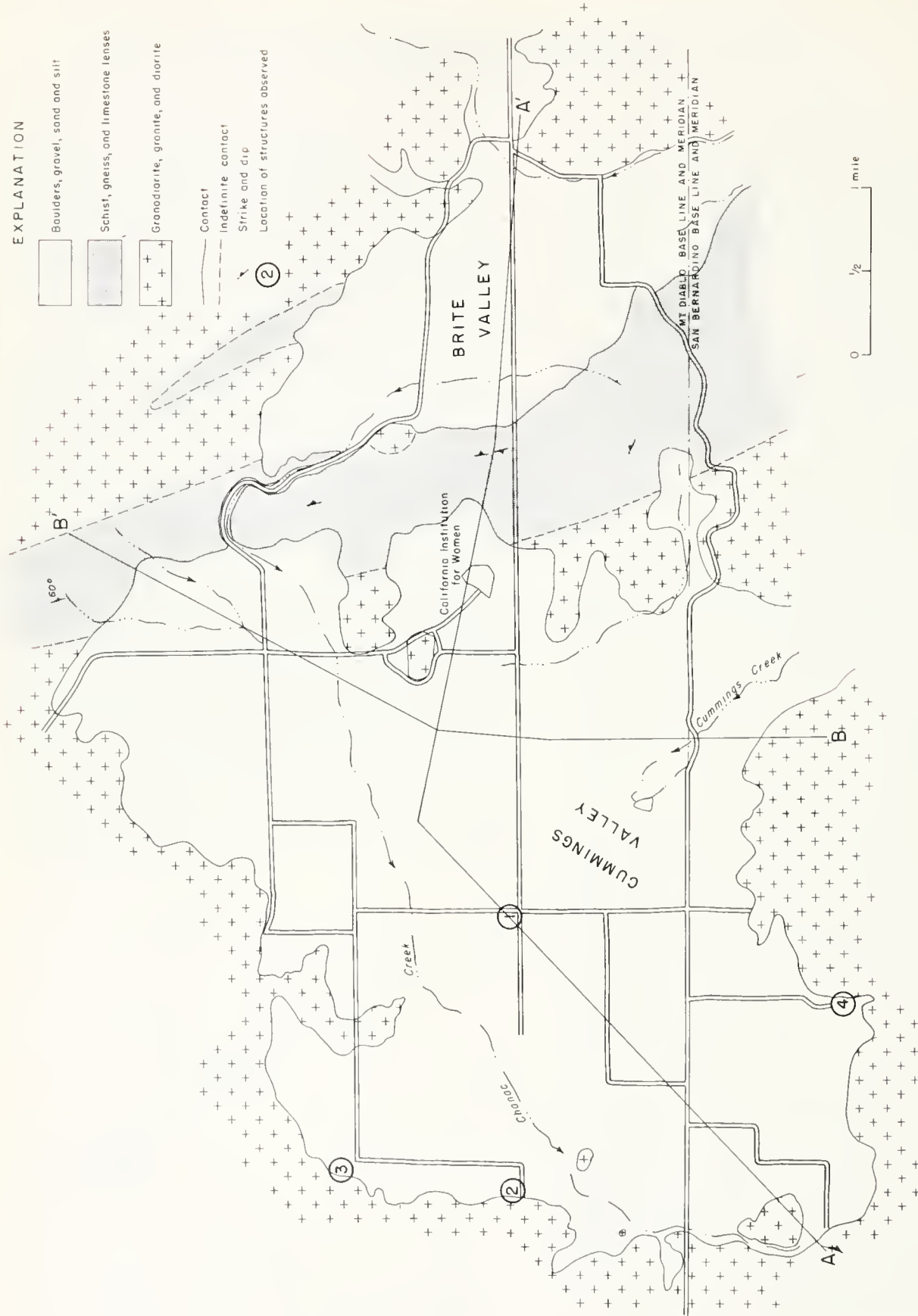


FIGURE 2. Geologic map of Cummings Valley area.

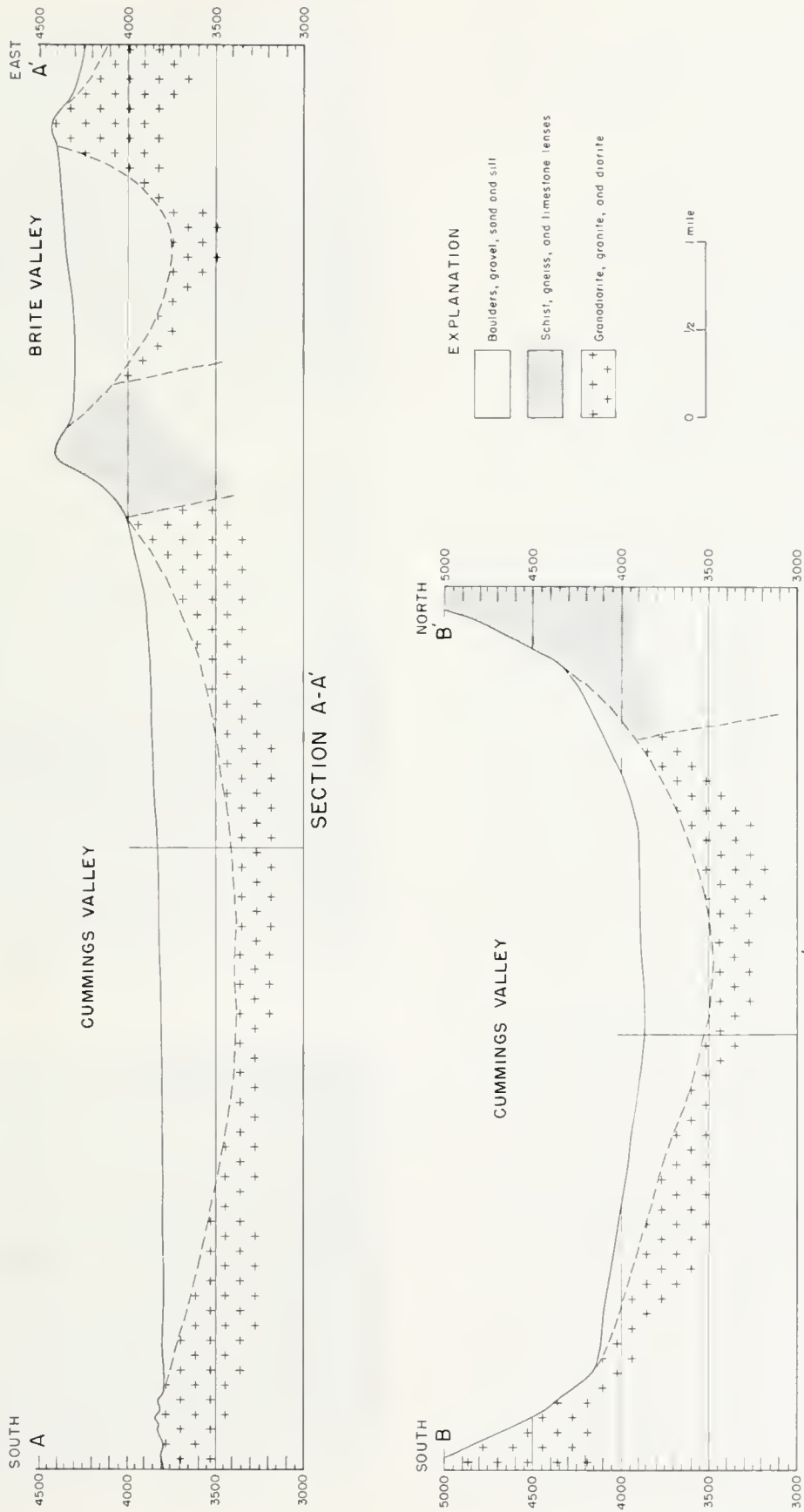


FIGURE 3. Geologic sections through Cummings Valley area.

Type of structure	Foundation material	Damage	Figure number	Figure 2 location number
Steel	Thick alluvium	None		
Reinforced concrete	Thick alluvium	None		
Brick	Thick alluvium	Extensive damage or collapse	4-7	
Reinforced concrete block	Thick alluvium	Little or no damage except for cracking of unsupported facade	8-9	
Unreinforced concrete	Thick alluvium	Collapse	10, 11	1
Adobe	Thick alluvium	Collapse	12	
	10 ± feet fill over rock	Extensive cracking	15	2, 3
	Few inches of fill over rock	Slight cracking or no damage	13-14	4
Frame	Thick alluvium	Slight or no damage	16-17	
	10 ± feet fill over rock	Slight or no damage	18	3
Stone masonry	Thick alluvium	Moderate damage to collapse	12	
	Few inches fill over rock	No damage	--	4

intersection with Davis Street, two blocks east of the center of the row of business establishments that were damaged severely. Structures built on man-made fill now occupying the channel were damaged to about the same degree as those built on the adjoining alluvium.

Cummings Valley is a high-level, oval-shaped intermontane basin between Tehachapi and Arvin, north of the Tehachapi Mountains and southeast of Bear Mountain. As indicated on the geologic map, figure 2, hills of granitic and metamorphic rocks rise on all sides of the valley. The valley itself has been filled with unconsolidated alluvium by gently sloping, coalescing alluvial fans. The unconsolidated sediments consist of boulders and coarse gravel in the upper parts of the alluvial fans, and fine gravel, sand, silt, and clay at lower elevations. The alluvium thickens towards the center of the valley, where it reaches a maximum thickness of about 450 feet. Depth to ground water in the central part of Cummings Valley was 35 feet or more in June 1950.

INFLUENCE OF GROUND WATER

The influence of ground water on the shearing strength of sediments and on the amount of earth movement and consequent damage was not investigated in detail. Studies of other earthquakes (Collins and Foster, 1949) indicate that upheaval of earth commonly occurs in areas where the water table is high. In most places in the Bakersfield-Arvin-Tehachapi area the water table was too far below the surface to cause surface phenomena such as sand boils; approximately 3 miles southwest of Arvin, however, where the water table is reported to be about 6 feet below the surface, mud boils and extensive surface cracking developed.

RELATIONS BETWEEN GEOLOGY, TYPE OF CONSTRUCTION, AND DAMAGE

Buildings representative of several different types of construction were studied, including those built of steel, reinforced concrete, unreinforced concrete, concrete block with various amounts of reinforcing, brick, wood frame, stone masonry, and adobe. Because examples of the first five types were found only on alluvium, comparative data on them are lacking. Examples of the last



FIGURE 4. Brick construction on alluvium. Damaged building in business district of Arvin. Other buildings, of reinforced concrete, were undamaged.



FIGURE 5. Brick construction on alluvium. Damaged buildings in business district of Tehachapi. Much damage caused by roof falling into building when brick walls collapsed. Undamaged reinforced-concrete theater building at right.

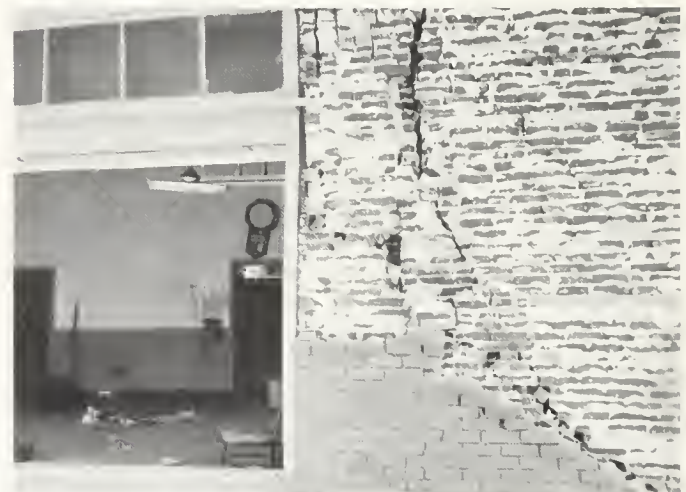


FIGURE 6. Detail of damaged brick building in business district of Tehachapi. Same building is shown at left in figure 5.



FIGURE 7. Brick construction on alluvium. Badly damaged building in business district of Tehachapi. Undamaged frame building at left.



FIGURE 8. Reinforced concrete-block construction on alluvium. Slightly damaged building in Tehachapi.



FIGURE 9. Detail of building shown in figure 8. Slight damage—one roof tile shaken off, stucco finish cracked.

three types were found on several different natural materials, hence the amount of damage to structures on one kind of ground can be compared with damage to similar structures on other kinds of ground. It was found that the condition of adobe structures was one of the most sensitive indications of the kind of foundation material.

Data gathered on damage to structures, as related to the type of earth material on which the structures were built, are summarized in the table below and are given in somewhat more detail in the following paragraphs.

Steel. An undamaged service station of steel construction is across the street from the center of the greatest concentration of damaged structures in Tehachapi.

Reinforced Concrete. Reinforced-concrete buildings were constructed on thick alluvium in the towns of Tehachapi and Arvin, and in Cummings Valley. All such buildings were undamaged by the earthquake, with the exception of those at the California Institution for Women, in Cummings Valley. Close observation could not be made at the Institution, but damage to its buildings was reported to consist of shifting of the heavy wood and slate roofs and collapse of some of the hollow-tile interior walls. The outer walls, which were constructed of reinforced concrete, as well as interior walls of reinforced-concrete construction, were little damaged, but some damage did occur to concrete walls in one building. The bulk of the damage, however, was in the roof structure and partitions. The alluvium, upon which the Institution buildings stand, is approximately 150 feet thick; the water table in June 1950 was at a depth of approximately 25 feet.

Brick. Brick buildings in the business districts of Arvin and Tehachapi were severely damaged by the earthquake, except for the modern one-story brick building of Safeway Stores in Arvin. Figures 4-7 show damaged brick structures in these two communities. Some brick walls collapsed completely; the outer veneer cracked away from other walls two or more bricks thick; some of the walls stood, but were so badly cracked that they were unsafe. In most places, collapse was caused by individual bricks breaking loose from mortar; where all the bricks broke loose along the mortar joints, walls were reduced to rubble. Many brick chimneys on frame buildings were destroyed, although the frame buildings remained relatively undamaged.

Reinforced Concrete Block. Reinforced concrete-block buildings in Tehachapi were damaged slightly or not at all, as shown by figures 8-9. The façade that fell from one of the concrete buildings was constructed of concrete blocks lightly reinforced. The façade was added after the building was completed, and the reinforcing was apparently not tied securely to the main part of the building.

Unreinforced Concrete. The Cummings Valley School, according to K. V. Steinbrugge, structural engineer, was built of concrete with only a few widely spaced reinforcing rods, which did not overlap. The concrete fractured between the ends of the reinforcing rods. Cummings Valley School is near the center of the valley, on



FIGURE 10. Improperly built concrete construction on thick alluvium. Damaged schoolhouse in Cummings Valley.



FIGURE 11. Detail of damaged schoolhouse shown in figure 10.



FIGURE 12. Adobe and stone-masonry construction on alluvium. Completely demolished building in Tehachapi.



FIGURE 13. Adobe construction on a few inches of fill overlying rock. Undamaged building on south side of Cummings Valley.

thick alluvium. The demolished schoolhouse is shown in figures 10 and 11.

Adobe. Adobe buildings in Tehachapi, built on thick alluvium, were demolished by the earthquake. At the northwest edge of Cummings Valley, adobe buildings were built on approximately 10 feet of natural and artificial fill, predominantly of sand-, silt-, and clay-size alluvium, overlying rock. Walls of some adobe buildings were only slightly cracked along the adobe-mortar joints; walls of other buildings were badly cracked along these joints. Frame buildings at this site were almost undamaged. On the south side of Cummings Valley, adobe buildings, some as much as 50 years old, were built on a few inches to a few feet of fill overlying bedrock. The buildings were undamaged except for a few slight cracks in the adobe walls. Adobe structures in Tehachapi and Cummings Valley are shown in figures 12-15.

Frame. Frame structures, mostly private dwellings, built on thick alluvium in Tehachapi, Arvin, and Cummings Valley, withstood the earthquake quite well. Tilting and sagging took place in some of the buildings in Tehachapi, throwing doors and windows somewhat out of line; some windows were broken; but, with a few exceptions, no badly damaged frame structures were seen. A rather high, wooden lagged foundation frame supporting an old frame house in Tehachapi was deflected from the



FIGURE 14. Adobe construction on a few inches of fill overlying rock. Undamaged building on south side of Cummings Valley. Building is very old; cracks are not due to earthquake but are old cracks with edges rounded by rainwash.

vertical by the earthquake, so that the weight of the house caused the formerly vertical lagging to collapse, several days after the strongest shock. Brick chimneys on frame buildings were loosened or destroyed, and in some places fireplace chimneys pulled free from the frame structure and collapsed. On the northwest side of Cummings Valley, frame buildings on approximately 10 feet of fill overlying rock were undamaged or only slightly damaged. Figures 16-18 show frame structures in Tehachapi and Cummings Valley.

Stone. In Tehachapi and Cummings Valley, buildings made of field stone or rubble held together with mortar were found in conditions ranging from slightly damaged, in which only the rubble pieces had fallen out, to demolished. On the south edge of Cummings Valley, a structure whose walls consist of stone masonry to a height of about 6 feet and adobe above, rested on a small amount of alluvium or artificial fill overlying bedrock. The stone masonry was undamaged; the adobe portion of the walls cracked around window and door openings, and some adobe blocks fell out from the area under the point of the roof. An adobe and rubble-masonry building in Tehachapi, on thick alluvium, was demolished.



FIGURE 15. Part adobe, part frame construction on approximately 10 feet of fill. Damaged building on northwest side of Cummings Valley. Adobe wall is cracked, but frame portion of building is intact.

SUMMARY AND CONCLUSIONS

Steel and properly reinforced concrete or concrete-block structures erected on thick alluvium (with a relatively deep water table) in Tehachapi, Arvin, and Cummings Valley withstood the Tehachapi earthquake with little or no damage. No data are available regarding such structures built on other foundation materials. Brick buildings, with some exceptions, and unreinforced or inadequately reinforced concrete buildings erected on alluvium were severely damaged by the earthquake; no data are available regarding damage to such structures built on other foundation materials such as fill or rock. Most wood-frame buildings in good structural condition withstood earthquake shocks with very little damage, regardless of the foundation material on which they were



FIGURE 16. Frame construction on alluvium. Undamaged building in Tehachapi. Adjacent adobe structure was extensively damaged.



FIGURE 17. Frame construction on alluvium. Damaged dwelling in residential district of Tehachapi. Frame portion only slightly damaged; brick chimney pulled away from frame.



FIGURE 18. Adobe and frame construction on approximately 10 feet of fill overlying rock. Slightly damaged building on northwest side of Cummings Valley. Adobe portion of building is cracked; frame portion is undamaged.

built. Stone-masonry and adobe buildings built on rock or on a very small amount of natural or artificial fill overlying rock were undamaged or only slightly damaged by earthquake shocks; the extent of damage for

those built on fill overlying rock varied with the thickness of the fill, the damage increasing with increasing depth of fill. Adobe buildings on thick alluvium were badly damaged or demolished.

2. EARTHQUAKE DAMAGE TO OIL FIELDS AND TO THE PALOMA CYCLING PLANT IN THE SAN JOAQUIN VALLEY

BY ROBERT L. JOHNSTON

ABSTRACT

The Arvin-Tehachapi earthquake of July 21, 1952, caused a decided change in the daily production of several oil fields in the San Joaquin Valley. The fields exhibiting the most noticeable effects of the earthquake were Tejon Ranch, Kern River and Fruitvale. In general, production variations consisted of a sharp rise in casing pressure, accompanied by a slight decline in daily production of oil and water. Nearly all the affected wells had returned to normal production within a period of 2 to 3 weeks. It is significant to note that these fields produce from relatively shallow and unconsolidated formations. No evidence of actual fault movement was detected in any of the wells although a number of casing failures at shallow depths were reported in the Tejon Ranch area. Fire resulting from the earthquake caused approximately 2 million dollars worth of damage to the Paloma Unit Cycling Plant operated by the Western Gulf Oil Company.

As might well be expected, all companies were immediately concerned as to the damaging effect to subsurface installations such as casings, liners, tubing and pumping units following the Arvin-Tehachapi earthquake of July 21, 1952. The effect of the shock at the surface was only too apparent in the open fractures in the valley floor, cracked and crumbled buildings, broken pipe lines and the oily mess left by the miniature earthquake waves that splashed a good deal of oil out of numerous sumps throughout the area. It appeared possible that a significant amount of subsurface damage might be expected. A quick survey, however, showed that none of the oil fields has sustained losses of major consequence to subsurface equipment. Detailed surveys were not attempted until about 10 days after the earthquake when the reports from several fields began to show some noticeable changes had taken place in the rates of daily production. Greatest variations in production as a result of the earthquake were demonstrated in the Tejon Ranch, Kern River and Fruitvale fields.

Although data are still being gathered, enough information has been obtained to give a fair summary of the earthquake disturbance for the various fields in the San Joaquin Valley. At the south end of the valley in the Wheeler Ridge field relatively little effect of the shock could be detected in any of the wells. The only perceptible change in the immediate area was a slight settling of the surface of the ground around the well installations. The ground slumping resulted in a great deal of pump trouble which was easily adjusted by mechanical means. Production was off slightly for a few days but has since returned to normal with no permanent effects. In view of the proximity of the Wheeler Ridge field to the trace of the White Wolf fault, it seems rather unusual that the wells were not damaged to a much greater extent.

The Tejon Ranch area seems to have suffered the greatest amount of damage to subsurface equipment. Several of the shallow wells were found with casing collapsed or tubing kinked as shown in the photograph (fig. 2). In six wells the tubing could not be pulled and it was necessary to drill a twin well in each case. A decided variation in casing pressures was recorded in certain parts of the Tejon Ranch area. Several of the wells showed an increased casing pressure many times above normal in the first few days after the earthquake. There were instances

where the casing pressure rose from 50 pounds per square inch to 320 pounds per square inch, from 30 pounds per square inch to 300 pounds per square inch, and from 15 pounds per square inch to 195 pounds per square inch. The exact time at which the casing pressures reached their highest readings differed in the various wells; some showed highest readings on the second day after the earthquake, while others showed highest readings on the third or fourth day. Following the initial fast rise in casing pressures was a period of slow but steady decline lasting about 2 weeks which brought the pressures to about 20 percent below normal. The pressures have since returned to nearly pre-earthquake conditions after a long period of slow build-up.

Variations in the daily production of oil and gas were usually associated with the fluctuations in gas pressures. For example, in one small portion of the Tejon Ranch field one well jumped from 20 barrels per day to 34 barrels per day while a nearby producer dropped from 54 barrels per day to 6 barrels per day. As yet, those wells showing extreme production changes or in which the casings have collapsed do not seem to form any pattern which might be construed as falling along fault lines.

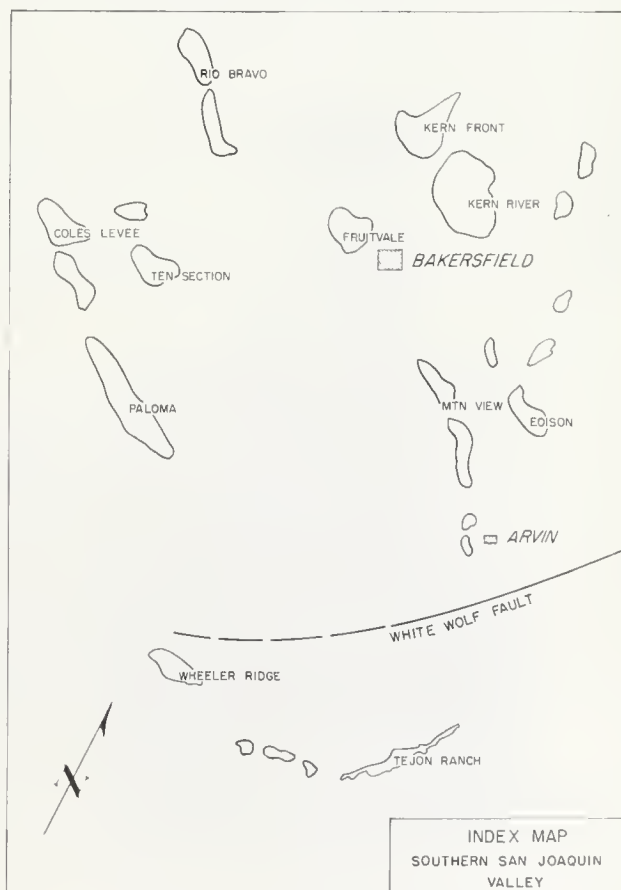


FIGURE 1. Index map showing major oil fields in the vicinity of the White Wolf fault.



FIGURE 2. Twisted tubing pulled from a well where the casing had collapsed following the Arvin-Tehachapi earthquake of July 21, 1952.

Although many storage tanks skidded slightly on their foundations, only very few actually collapsed as did the one shown in figure 3. It was one of a battery of three 1500-barrel tanks in the Tejon Ranch area. The other two tanks suffered relatively minor damage.

Further north along the east side of the San Joaquin Valley in the Arvin, Mountain View, Edison and Race Track areas, comparatively little production variation was observed. Here and there wells did show a slight build-up in casing pressure which then dropped below normal after a few days time but they soon returned to their original status. A temporary decline in oil production over a period of about 10 days was noticed but production is now also back to normal. It may be well to emphasize that in the Arvin-Edison locality, which lies very close to the White Wolf fault, the deeper



FIGURE 3. This storage tank was one of a battery of three. It collapsed, spilling 800 barrels of oil, but the two adjacent tanks were relatively undamaged.



FIGURE 4. A mass of butane which escaped from these 2500-barrel spheres became ignited by an electrical spark, causing the initial explosion and resultant fire at the Paloma cycling plant.



FIGURE 5. A closeup of the fiercely blazing skeletal remnants of one of the large cooling towers. A gigantic blowtorch effect was caused by the ignited gases which are normally being cooled beneath the towers.

wells experienced only insignificant production changes with no evidence of subsurface damage. Even those wells completed barefoot in the Edison field suffered no loss in production or damage to subsurface installations.

In the Kern River-Kern Front fields, 150 wells were found to be sanded up as a result of the July 21st earthquake. In spite of the amount of sand caving throughout the field, in no wells were the casings found to be collapsed or sheared. A temporary although slight increase in gas pressures was noted and was accompanied by a minor drop in daily production. All the wells are now back to normal daily output.

A rather decided fluctuation in gas pressures was recorded in the Fruitvale field, although very few of the wells became sanded up. Several of the wells showed a sharp build-up from approximately 150 to about 800 pounds per square inch of casing pressure. A steady decline, however, was noted approximately a week after



FIGURE 6. A general view of the Paloma cycling plant showing the blackened area of explosion and fire. The spherical butane storage tanks are at the left, remaining cooling towers and tall vessels in the center, and compressor plant at the extreme upper right.

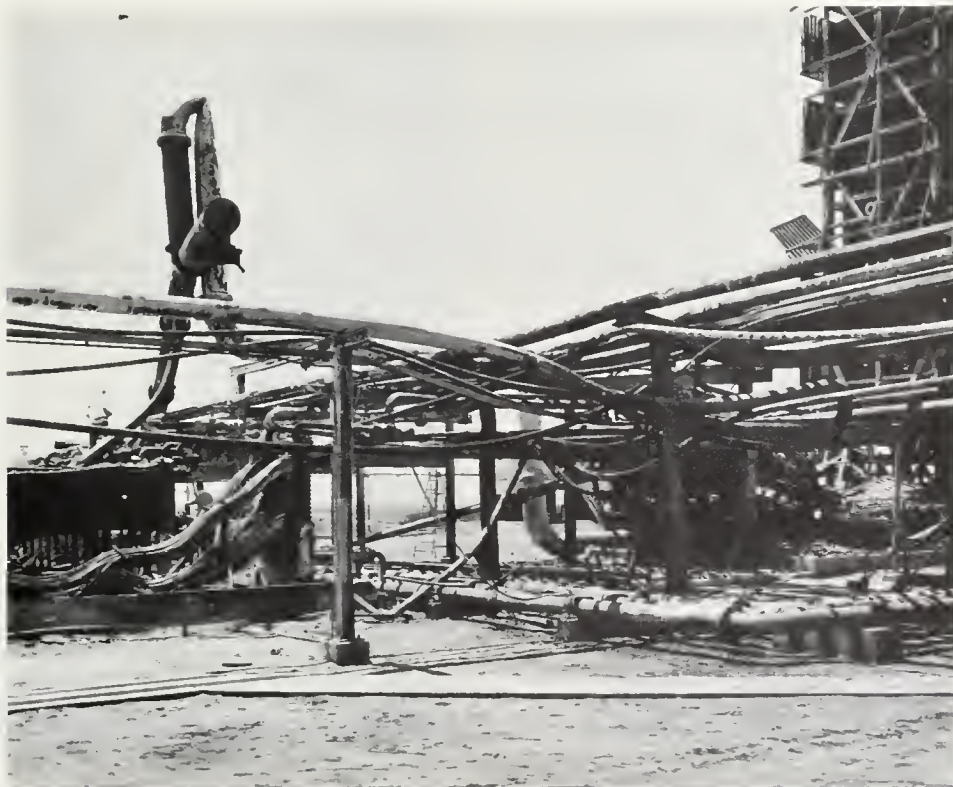


FIGURE 7. Heavy steel beams and pipes were warped into a maze of grotesque shapes by the intensity of the fire at the Paloma cycling plant.



FIGURE 8. These thick steel bolts were stretched $1\frac{1}{2}$ inches as the tall 100-ton absorber rocked back and forth on its concrete base during the quake of July 21, 1952.

the earthquake and at the end of a 2-week period the pressures had decreased steadily to below normal. Daily production of oil and water dropped rapidly to approximately 25 percent below normal. Although the gas pressures as well as the production figures increased steadily, average daily output was not reached until about 5 months later.

Only very insignificant production changes were noted in the central valley fields: Paloma, Greeley, Rio Bravo, Coles Levee and Trico fields. One example of casing collapse at 9000 feet occurred in the South Coles Levee field. On pulling the casing, however, it was evident that the failure was due largely to previous corrosion and that the earthquake merely caused the final collapse. Other similar casing failures were discovered in the valley where the bad pipe was found to have been corroded rather than sheared by earth movements.

Numerous wells along the west side of the San Joaquin Valley also became sanded up as a result of the earthquake. The sanded wells were scattered from the south end of the Midway-Sunset field north through the South Belridge and Los Hills fields and as far north as the Coalinga area. Again there was the characteristic slight rise in gas pressure and a slight loss in daily production. Nearly all the wells have returned to their previous normal capacity.

The fields showing the greatest effects of the earthquake, such as fluctuation in production, had sanding conditions, kinked tubing, and casing collapse are those producing from soft unconsolidated formations. From general observation it appears that the earthquake shocks set up a jelly-like motion in the soft sediments



FIGURE 9. A strong westerly component of movement is indicated by the slippage of this tank along its fractured concrete base. A similar direction of movement was noticed in other storage tanks throughout the San Joaquin Valley.

which resulted in no definite pattern of well damage—even in the Tejon Ranch area. Although investigations were made of all wells reportedly affected by the earthquake, no actual slippage or movement along a fault plane could be established. Knowing the very small amount of displacement necessary to cause a casing break (as has been demonstrated in the Ventura Avenue field), it seems quite surprising that there were not a considerable number of wells so affected.

The second major earthquake of August 22nd brought about only slight changes in the daily production of oil and gas in scattered areas but did not inflict any further damage to oil well installations.

In direct contrast to the minor losses sustained in subsurface installations was the spectacular and costly fire at the Paloma Cycling plant on the morning of July 21, 1952. The plant is located about 16 miles southwest of Bakersfield at the south end of the San Joaquin Valley. The raw condensate from the wells in the Paloma field is separated into propane, butane and natural gas, and the residual dry gas is pumped back down into the reservoir sand at pressures of 4500 pounds per square inch. Damage to this plant which resulted from a combination of earthquake, explosion and fire is estimated at \$1,800,000.00.

The shock of the earthquake caused two of the large spherical butane storage tanks to collapse, thereby rupturing lead-in lines and releasing quantities of highly volatile material. The gaseous material spread out over the surrounding area and was ignited after one and a

half minutes by electrical flashes from a transformer bank almost 3 blocks away. Of such force was this initial explosion that it stripped 80 percent of the covering material from the 2-block long compressor house and crumpled walls and instrument control shelters in the main plant.

Following the explosion, the entire area in the vicinity of the damaged spherical storage tanks was engulfed in an inferno of flames which consumed two huge motor-driven cooling towers and a portion of a large stationary cooling tower, as well as starting many other minor fires throughout the plant.

Evidence of a strong rocking motion during the earthquake was indicated by the stretching of steel foundation bolts on one of the large absorbers. The vessel stands 60 feet high and weighs approximately 100 tons. As may be seen in the photographs, figure 8, the heavy steel bolts were stretched about $1\frac{1}{2}$ inches. It has been estimated that the top of the absorber must have swung over an arc of 3 feet to account for the stretch of the bolts at the base.

It was indeed fortunate that none of the 14 men on duty at the time of the earthquake was seriously injured or killed during the explosion and fire. Prompt action in shutting-in all key valves in the high pressure system saved possible destruction of much more of the plant facilities. The herculean task of tearing out and replacing damaged equipment and getting the Paloma Cycling Plant back into normal production required about four and a half months.

3. HIGHWAY DAMAGE RESULTING FROM THE KERN COUNTY EARTHQUAKES

By O. W. PERRY •

The major Arvin-Tehachapi earthquake occurring at 4:52 a.m. (PDT) on July 21, 1952, centering at Wheeler Ridge just west of U. S. Highway 99, caused the greatest damage to the highways. Except for a few locations, the aftershocks appeared to cause little increased damage. This is understandable as the major earthquake with a magnitude of $7\frac{1}{2}$ released about 60 times the total energy of the greatest aftershock which had a magnitude of $6\frac{1}{2}$ (July 29). Damage, although very extensive, was found not as severe as first reported, after maintenance crews had had time to verify. When movement along the White Wolf fault took place, initiating the earthquakes, severe lurching of large masses of rock and earth, accentuated in alluvium, fill, and loose ground, developed surface cracks and disturbed loose surface materials over an area of many square miles. The damage to highways was largely the direct result of: (1), settlement of fill; (2), landslides, rock falls, and slumping of cut slopes and steep natural slopes; and (3), changes in the amount of flow and course of running water.



FIGURE 1. Landslide cracks along trace of White Wolf fault 300 feet north of Highway 466.

State Route 140, east of Arvin, known locally as the White Wolf grade, roughly parallels the northeast-trending White Wolf fault along the lower slopes of Bear Mountain. The fault crosses U. S. Highway 466 north of Bear Mountain. Most of the damage to Route 140, and other highways in this area, resulted from fill settlement and was scattered for several miles. Although both transverse and longitudinal cracks developed in the pavement, the most serious cracking was along the margins of the pavement in filled sections of the highway, resulting in loss of roadway width. One of the unusual results of the earthquake is that streams which usually only flowed during winter storms and were dry most of the year started flowing good volumes of water right after the first quake on July 21 and have continued to flow since. In many cases vertical displacement of the old stream beds caused the streams to create new channels and intercept the highway at locations where there was no pro-



FIGURE 2. Transverse cracking on Highway 466 resulting from slumping of fill about a quarter of a mile west of trace of White Wolf fault.

vision for them. The resulting extensive roadside erosion is shown in two of the photographs of Highway 140.

Most of the damage to the more important U. S. Highway 466, while it cost much less to repair, was similar to that of State Route 140. The structures did not appear to suffer much but there was fill settlement at most of the approaches. For example, settlement at the Tehachapi Overhead was about 8 inches at the west end of the bridge. One of the peculiar aspects of this approach settlement is that in no case could any displacement or movement be discerned along the side slopes or toes of the fills.

Probably the most spectacular damage was to U. S. Highway 99. This highway was closed for a few hours



FIGURE 3. Horizontal displacement of highway shown by center line. View east on Highway 466. Not on trace of White Wolf fault.

• District VI Maintenance Engineer, California Division of Highways.



FIGURE 4. Bridge over Walker Basin Creek showing cracking resulting from settlement of fill at the approach.



FIGURE 5. Cracks on Highway 466 resulting from settling of marginal fill.

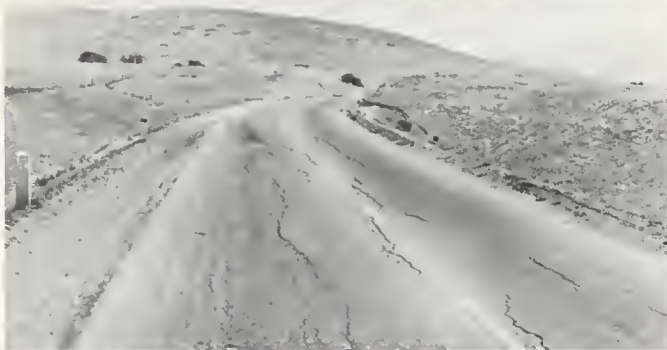


FIGURE 6. Center cracking in pavement in filled area, Highway 466.

because of a slide near the Ridge Maintenance Station in Los Angeles County. The southbound lanes of this four-lane highway were soon cleared and were used for two-way traffic around the slide. In the vicinity of Grapevine Station, there was considerable horizontal displacement and settlement on the fill sections which caused adjacent concrete slabs, which were not held together with tie bolts, to spread apart, resulting in deep, wide cracks in the traveled way. The reinforced concrete center barrier had a section broken out by a rolling granite boulder and developed an uneven crest because of differential movement in the pavement. Just north of Grapevine Station the last construction project called for about 3 feet of new fill on the old fill and also con-

siderable widening of the downhill side. The entire fill slid continuously after the first earthquake on July 21, 1952, so that it was impossible to make permanent repairs for some time. The maintenance crews endeavored to keep the cracks filled in order to keep water out of the subgrade. An attempt was made to eliminate much of the vertical displacement in the traveled way by filling in with oil-mixed material. On U. S. 99 as well as on U. S. 466 there was not as much damage at the place where the White Wolf fault crossed the highway as there was at location some distance away; most of the damage was a considerable distance from the actual fault. A very interesting phenomenon occurred at two locations on U. S. 99 about 11 miles south of Bakersfield. Water-saturated silty sand was erupted along cracks as a result of the earth movements. In some places ground water, which is very close to the surface in this vicinity, was evidently pumped out, resulting in voids and subsequent settlement. The maximum settlement of 11 inches was confined to the easterly lane. However, the movement continued throughout the remainder of the month of July and the settled areas eventually extended across the southbound lanes into the westerly shoulder.

The effects of the July 21 earthquake and numerous aftershocks on the Kern Canyon road (Route 178) have been very damaging and costly. A rock slide on the morning of July 21 closed the road. However, there were many minor rock slides and many places in which large fragments of granitic rock in the region fell onto the highway. The extremely steep natural slopes in lower Kern Canyon facilitated rock falls. The slopes in the slide area are made up of loose, shattered, fractured, and jointed granitic rock. The sequence of aftershocks between the Arvin-Tehachapi earthquake of July 21 and the Bakersfield earthquake of August 22 made it impossible to keep this roadway clear. It was also extremely dangerous for men working in the area and even if the roadway could have been cleared it would have been very hazardous to public traffic. Consequently it was not open to traffic until September 19, 1952. Inspection of the steep natural mountain slopes adjacent to the highway made it apparent that the slides would have to be contended with until nature stabilized the slope. Numbers of fissures developed by sliding on the



FIGURE 7. Transverse and longitudinal cracking of pavement in filled area, Highway 466.



FIGURE 8. Cracks in pavement in filled area east of sand cut, Highway 466, opened up by severe aftershock of July 29, 1952.

steep slopes, which allowed storm water to enter the sub-surface material and facilitate sliding. There was a continual dropping of rocks ever since the first earthquake. On December 20, 1952, a storm loosened so many rocks throughout the length of the slide area that it was considered advisable to close the road during the hours of



FIGURE 9. Marginal cracking in filled area of Highway 466, opened up in aftershocks.



FIGURE 10. Damage to pavement on State Route 140, White Wolf grade. This highway roughly parallels the White Wolf fault for several miles.

darkness. The following morning it was discovered that a slide during the night had closed the road. This was removed and a third slide occurred on December 22.

With the exception of the Kern Canyon road and U. S. 99 south of Bakersfield, highway damage had been repaired and most of the evidence erased by December 1952. These two exceptions required constant watching and continual maintenance. For several months two locations on Highway 99 were subsiding, and until the earth's surface became stabilized, it was possible only to relieve the hazards to traffic temporarily, as it was in lower Kern Canyon.



FIGURE 11. Marginal cracking in filled area, and minor landslide in cut slope. White Wolf fault at break in slope at top margin of photograph. View southwest along State Route 140.

BRIDGE EARTHQUAKE REPORT, ARVIN-TEHACHAPI EARTHQUAKE

BY STEWART MITCHELL *

One of the most interesting facts regarding damage to the highway bridges is the small amount of damage to the structures themselves. Following is a tabular description of the bridges on U. S. Highway 466 and U. S. Highway 99 with the bridges listed, whether or not they were damaged. Figure 28 shows the location of bridges listed.

Structure Along U. S. 466

Bridge 50-38, Walker Basin Creek, Road VI-Ker-58-D

Location—14.6 miles southeast of Bakersfield.

Description—Two lane timber trestle with RC deck; 4 spans at 19 feet.

Damage—Nothing significant; slight movement in approach fills.

Bridge 50-39, Walker Basin Creek, Road VI-Ker-58-D

Location—14.8 miles southeast of Bakersfield.

Description—Two lane timber trestle with RC deck; 13 spans at 19 feet.

Damage—Approach fill settled 4 inches at bridge ends. East abutment piles shifted channelward $\frac{3}{4}$ inch under cap, bent 8 piles moved laterally $\frac{1}{2}$ inch under cap.

Bridge 50-40, Caliente Creek, Road VI-Ker-58-D

Location—16.2 miles southeast of Bakersfield.

Description—Two lane timber trestle with RC deck; 11 spans at 19 feet.

Damage—No appreciable movement recorded.

Bridge 50-63, Bena Cattlepass, Road VI-Ker-58-D

Location—18.1 miles southeast of Bakersfield.

Description—Two lane timber span under shallow fill. Timber abutments on timber sills. One span at 9 feet.

Damage—None.

* Bridge engineer, State Division of Highways.



FIGURE 12. Erosion on margin of pavement, State Route 140, resulting from diversion and increased flow of minor stream after earthquake of July 21, 1952.



FIGURE 15. Shoulder settlement in fill, with a resulting step-off at edge of concrete pavement, U. S. 99, near Grapevine.



FIGURE 13. Longitudinal cracking in pavement of northbound lane of U. S. Highway 99 near Grapevine. This type of cracking took place in filled sections where adjacent concrete slabs were not held together with tie bolts.



FIGURE 16. Sloughing and slumping on cut slope, Highway 99, near Grapevine.



FIGURE 14. Boulder trail on hill slope and broken center line barrier, U. S. Highway 99, near Grapevine.



FIGURE 17. Cracking on upper side of fill, Highway 99, north of Grapevine station. Continued slumping in this filled section long delayed permanent repairs.



FIGURE 18. Wavy top line of center barrier, Highway 99, near Grapevine, showing irregular settlement of pavement.



FIGURE 21. Settlement of shoulder surfacing amounting to maximum of 11 inches, east lane of U. S. 99, near Wheeler Ridge.

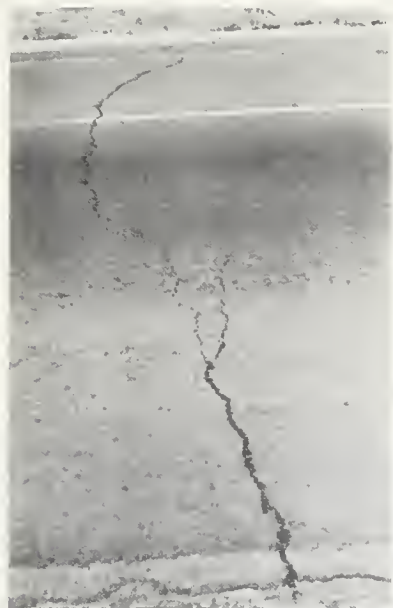


FIGURE 19. Transverse cracks, resulting from lurching in alluvium, in pavement of the northbound lanes of U. S. 99, about a mile north of junction with Maricopa highway.



FIGURE 22. Main rock slide of granitic fragments closing Kern Canyon road (Route 178) after July 21 earthquake.



FIGURE 20. Fissure eruptions of mud along lurch cracks in soil about 11 miles south of Bakersfield adjacent to U. S. 99.



FIGURE 23. Boulder of granitic rock on pavement, Kern Canyon road.

Bridge 50-158, Loch Cattlepass, Road VI-Ker-58-D
Location—18.4 miles southeast of Bakersfield.
Description—Two lane timber span under shallow fill. Timber abutments on timber sills. One span at 9 feet.
Damage—None.

Bridge 50-159, Lomond Cattlepass, Road VI-Ker-58-D
Location—18.7 miles southeast of Bakersfield.
Description—Two lane timber span under shallow fill. Timber abutments on timber sills. One span at 9 feet.
Damage—None.

Bridge 50-160 Dip Cattlepass, Road VI-Ker-58-D
Location—18.8 miles southeast of Bakersfield.
Description—Two lane timber span under shallow fill. Timber abutments on timber sills. One span at 9 feet.
Damage—None.

Bridge 50-161 Gila Cattlepass, Road VI-Ker-58-D
Location—19.9 miles southeast of Bakersfield.
Description—Two lane timber span under shallow fill. Timber abutments on timber sills. One span at 9 feet.
Damage—None.

Bridge 50-162 Bug Cattlepass, Road VI-Ker-58-D
Location—20.2 miles southeast of Bakersfield.
Description—Two lane timber span under shallow fill. Timber abutments on timber sills. One span at 19 feet.
Damage—None.

Bridge 50-163 Haypress Creek Cattlepass, Road VI-Ker-58-D
Location—20.5 miles southeast of Bakersfield.
Description—Two lane timber span under shallow earth fill. Timber posts on timber sills. One span at 12 feet.
Damage—Large cracks in fill along each abutment. Top of west end tipped 6 inches north and top of east end tipped 6 inches south.

Bridge 50-164 Pertshire Cattlepass, Road VI-Ker-58-D
Location—21.4 miles southeast of Bakersfield.
Description—Two lane timber span under shallow fill. Timber abutments on timber sills. One span at 9 feet.
Damage—None.

Bridge 50-165 Lyctus Cattlepass Road VI-Ker-58-D
Location—22.3 miles southeast of Bakersfield.
Description—Two lane timber span under shallow fill. Timber abutments on timber sills. One span at 9 feet.
Damage—None.

Bridge 50-166 Dog Cattlepass, Road VI-Ker-58-D
Location—22.7 miles southeast of Bakersfield.
Description—Two lane timber span under shallow fill. Timber abutments on timber sills. One span at 9 feet.
Damage—None.

Bridge 50-168 Meadow Cattlepass, Road VI-Ker-58-D
Location—23.8 miles southeast of Bakersfield
Description—Two lane span of 90 inch multiplate pipe under shallow fill.
Damage—None.



FIGURE 25. Granitic boulder on Kern Canyon road.

Bridge 50-169 Barley Cattlepass, Road VI-Ker-58-D
Location—24.0 miles southeast of Bakersfield.
Description—Two lane timber span under shallow fill. Timber abutments on timber sills. One span at 11 feet.
Damage—None.

Bridge 50-44 Tehachapi Creek Bridge and Overhead IX-Ker-58-E
Location—31.5 miles southeast of Bakersfield.
Description—Two lane continuous plate girder spans with RC deck on steel towers and rubble-masonry piers. Spans: one at 60 feet, one at 67.5 feet, one at 93 feet, one at 70 feet, one at 75 feet (S).

Damage—
Approaches—fills settled slightly three feet from abutments; cracked slightly parallel to road at fill tops. One-half inch crack in surfacing between bridge ends and fill.



FIGURE 26. Natural hill slope above rock slides on highway in Kern Canyon, showing loose and fragmented granitic rock.



FIGURE 24. Slab of granitic rock two-thirds buried beneath pavement of Kern Canyon road. Result of a rock fall.



FIGURE 27. Landslide cracks on slopes above Kern Canyon road. These allow entry of storm water and bring constantly renewed slides and rock falls.

Bearings—girder sole plates at both abutments moved slightly on bottom flanges. South abutment masonry plate shifted $\frac{1}{2}$ inch toward midspan; anchor bolts here possibly partly sheared.

Deck-slab—slab soffit spalled along edges of top flange for 10 feet length over south abutment; no displacement.

Bridge 50-171 Tehachapi Creek Bridge Road IX-Ker-58-E
Location—37.1 miles southeast of Bakersfield.

Description—Two lane simple plate girder spans with RC deck on rubble masonry—concrete piers and abutments. Spans: one at 79 feet, one at 80 feet, one at 66 feet, one at 61 feet (S).

Damage—

Bearings—grout pads cracked at pier 3 and abutment 5. Right girder sole plate moved $\frac{1}{16}$ inch on bottom flange abutment 6; left girder sole plate abutment 1 moved $\frac{1}{32}$ inch on bottom flange.

Bridge deck—right curb spalled slightly at pier 2 expansion joint.

Bridge 50-172 Tehachapi Creek Bridge Road IX-Ker-58-E
Location—37.2 miles southeast of Bakersfield.

Description—Two lane simple plate girder span with RC deck on rubble masonry abutments. Spans: one at 91 feet.



FIGURE 28. Location of bridges listed.

Damage—

Approach—fills separated $\frac{1}{2}$ inch from south abutment wings; no similar gap at end of deck. Both approaches cracked parallel to road at top of fill slope for a 15 foot distance beyond wing ends.

Bridge—No damage.

Bridge 50-173 Branch Tehachapi Creek IX-Ker-58-E

Location—37.5 miles southeast of Bakersfield.

Description—Two lane RC slab span on RC abutments. Span: one at 21 feet.

Damage—None.

Bridge 50-149 Tehachapi Creek Bridge and Overhead IX-Ker-58-F

Location—40 miles southeast of Bakersfield.

Description—Two lane continuous plate girder spans with RC deck on concrete piers and abutments. Spans: five at 92 feet.

Damage—

Approaches—settled 8 inches behind north abutment, 5 inches behind south abutment. Fills spread laterally for 50 foot distance beyond bridge ends. Fill height about 30 feet. Cracks opened 1 inch longitudinally along top edge. Two inch gap between bridge end and fill and $\frac{3}{4}$ inch gaps between fill slope and wingwall outer faces.

Bearings—right girder anchor bolts at north abutment completely sheared off, at south abutment only one anchor bolt completely sheared under right girder. Other appears undamaged. Abutment bearing grout pads cracked and spalled; worst under right girder. At intermediate piers spalling of grout pads was minor but indicated slight lateral movement of base plates.

Substructure—vertical cracks through lateral concrete struts at top of columns about 12 inches from column faces. Similar cracks collision walls between columns at railroad track. Open $\frac{1}{16}$ inch to $\frac{1}{8}$ inch.

Bridge Roadway—concrete deck edge spalled at contact with south abutment face. Expansion joint sleeve of tubular steel rail on right at south abutment disengaged and fouled. Other rail and deck joints normal.

Bridge 50-99 Tehachapi Storm Drain IX-Ker-58-F

Location—42 miles southeast of Bakersfield; also 1 mile east of Tehachapi.

Description—Two lane standard RC box culvert. Spans: three at 10.5 feet.

Damage—None visible.

Structures Along U. S. Highway 99

Bridge 50-48 R, Cuddy Creek, Road VI-Ker-4-A

Location—40 miles south of Bakersfield.

Description—2 lane RC simple girder bridge on RC column bents and abutments. Spans: 4 at 33 feet.

Damage—None.

Bridge 50-48 L, Cuddy Creek, VI-Ker-4-A

Location—40 miles south of Bakersfield.

Description—2 lanes continuous RC slab span bridge on RC column bents and abutments. Spans: 4 at 32 feet.

Damage—None.

Bridge 50-157 R&L, Cressy Cattlepass, VI-Ker-4-A

Location—38 miles south of Bakersfield.

Description—RC rigid frame flat slab span on RC abutments.

Span: 1 at 15 feet. Two separate structures on divided highway.

Damage—None.

Bridge 50-128 R&L, Grapevine Creek, VI-Ker-4-A

Location—36 miles south of Bakersfield.

Description—Standard RC double box culverts. Spans: 2 at 12 feet. Two separate structures on divided highway.

Damage—None.

Bridge 50-36 Grapevine Creek, road VI-Ker-4-A

Location—35 miles south of Bakersfield.

Description—4 lane divided simple plate girder spans with RC deck on RC piers and abutments. Spans: 3 at 65 feet.

Damage—None. Old cracks in grout pads at north abutment bearings unchanged. Slight abutment settlement.

Bridge 50-190 R&L New Rim Canal, road VI-Ker-4-B

Location—18 miles south of Bakersfield.

Description—Standard RC box culverts. Spans: 5 at 6 feet. Two separate structures on divided highway.

Damage—None.

Bridge 50-191R, Copper Creek, Road VI-Ker-4-B

Location—15 miles south of Bakersfield.

Description—Standard RC triple box culverts. Spans: 3 at 7 feet, for north bound traffic only.

Damage—None.

Bridge 50-192 East Branch Canal, Road VI-Ker-4-C

Location—3 miles south of Bakersfield.

Description—Standard Triple RC box culvert. Spans: 3 at 8 feet.

Damage—None.

Bridge 50-33 Kern River, Road VI-Ker-4-G

Location—1 $\frac{1}{2}$ miles north of Bakersfield.

Description—4 lane steel girder spans on RC piers plus timber trestle spans on piles all with RC deck.

Damage—No earthquake damage found on this 2292 foot-long structure.

Forty-seven bridges were examined immediately after the earthquake, and no damage attributable to the quake was found, although buildings in Bakersfield were seriously affected.

The 47 structures were in the immediate vicinity of Bakersfield on US 99, SSR 178 and US 466, and north a distance of 25 miles on US 99, SSR 65 & SHR 142.

4. DAMAGE TO WATER WORKS SYSTEMS, ARVIN-TEHACHAPI EARTHQUAKE *

BY HAROLD B. HEMBORG

The following is a summary of the detailed reports, prepared by the Seismological Forces Subcommittee of the American Society of Civil Engineers, describing the damage and effect caused by the Arvin-Tehachapi Earthquake of July 21, 1952, to the waterworks structures and to the distribution systems serving the cities of Arvin, Bakersfield, and Los Angeles and damage to the facilities which serve the Kern Delta and adjacent rim land areas.

The Los Angeles Distribution System. The water distribution facilities of the Department of Water and Power, City of Los Angeles, include 5023.6 miles of main pipe, 464,025 active services, 39 distribution reservoirs and 44 distribution tanks.

Immediately following the earthquake a check was made of the distribution facilities in all districts as to the extent of damage to the reservoirs, tanks, pumping plants and other miscellaneous structures but no evidence of any damage was reported.

A check of the cast iron and steel pipe in the Distribution System disclosed a total of 67 leaks which were reported on July 21 and 22. Of this number it was estimated that 35 were caused by the earthquake.

The following is a tabulation of leaks in both cast iron and steel mains:

Leaks—cast iron pipe				
Size	Graphitization	Round crack	Split	Joint
2"	1			
4"	1		1	
6"		1	4	2
Leaks—steel pipe				
Size	Rust hole		Split	
1½"	1			
2"	2			1
3"	1			
4"	10			1
6"	21			
8"	14			
10"	1			
14"	2			
20"	1			
30"	1			
39"	1			
Total 67				

Not included in the above tabulation were approximately 15 leaks in 2-inch cast iron service pipe. All of such leaks occurred in the southern portion of the Metropolitan area of the City and examination of the pipe showed it to be moderately graphitized. The pipe was approximately 25 years old. Practically all of the breaks in the cast iron pipe also occurred in the southern portion of the City in that all of the pipe in this general area is about 25 years old and shows the effect of graphitization. There was no evidence of damage to any recently installed cast iron pipe.

* A summary of the American Society of Civil Engineers Seismological Forces Subcommittee report: Samuel B. Morris, Chairman, General Manager and Chief Engineer, Department of Water and Power, City of Los Angeles; Richard E. Hemborg, Member, Distribution Engineer, Water Distribution Division, Department of Water and Power, City of Los Angeles; George L. Henderson, Member, Chief Engineer, Kern County Land Company, Bakersfield, California; A. Vernon Lynn, Member, Chief Engineer, California Water Service Company, San Jose, California; Alfred L. Trowbridge, Member, Chief Engineer, North Kern Water Storage District, Bakersfield, California; Harold B. Hemborg, Secretary, Executive Engineer, Water System, Department of Water and Power, City of Los Angeles.

The leaks reported in the steel pipe were found to be caused from rust holes in the steel pipe and since the pressure regulators indicated considerable surge in the trunk lines it was thought that the resulting increase of pressure accelerated the break-through of rust holes which were close to normal failure.

It does not appear that the azimuth of the broken pipe lines had any connection with the extent of damage, in that the number of leaks in the north-south lines and east-west lines were about evenly divided. It can therefore be concluded that the main reason for the leaks was the pressure surge created by the shock and not due to the direction of the shock waves. Also of note is the evidence that there were only two joint leaks in spite of the fact that practically all joints in the cast iron pipe lines are made with portland cement. A few calls were received from consumers to shut off their water supply due to broken house plumbing.

There was very little damage to the Los Angeles Aqueduct which is surprising considering that much of it is located approximately 25 miles from the epicentral region of the earthquake. No indication of damage to tunnels and conduit sections of the aqueduct was found throughout its entire length. The only damage reported was the development of cracks in the crests of Dry Canyon Dam and Haiwee Dam.

The Haiwee Dam and Reservoir, which is part of the Aqueduct System, is approximately 14 miles north of Little Lake, approximately 90 miles from the epicentral area at Wheeler Ridge. The Haiwee dam is of hydraulic fill construction and was completed in February, 1913. The inspection of this structure after the earthquake disclosed the presence of numerous small cracks along a 250-foot section of the crest at the maximum section of the dam. This cracking was in an arc pattern beginning at the upstream edge of the crest and extending downstream an external distance of approximately 40 feet.

The Dry Canyon Dam and Reservoir is 6 miles north of Saugus, approximately 50 miles from the earthquake epicenter. The Dry Canyon Dam is a smaller dam but of similar construction to Haiwee and was completed in 1912. The earthquake damage to this dam consisted of several continuous cracks parallel to the axis along the entire crest and located approximately 5 feet from the downstream edge of crest. These cracks had a maximum opening of 1½ inches and were found to extend down into the hydraulic fill core. Result of check surveys of the dam showed a horizontal displacement of 0.21 foot towards the reservoir and settlement of 0.18 foot. The Bouquet Dam, constructed in 1932-33, is located the same distance from the epicentral area as the Dry Canyon Dam but is of rolled filled construction where the moisture content of the soil material and rolling operations were under strict laboratory control. There was no evidence of any damage to this structure.

The Arvin Distribution System. There is no detailed report of damage to the Arvin System. Mr. McElroy, System Operator, Arvin Water Company, furnished the following data:

The Arvin Distribution System consists of approximately 8 miles of street main, 1100 services, pumping

plant and elevated steel tank of 75,000 gallon capacity with high water 87 feet above ground. Approximately 4 miles of 10 inch steel pipe conducts water from the pumping plant to the steel tank with normal pressure of 47 lbs. sq. in. The pressure charts indicated a surge effect resulting in a maximum pressure of 65 lbs. sq. in. The elevated steel tank suffered no damage except for sag in the sway bracing rods.

There was a total of 25 leaks in the wood and steel mains of 3 and 4 inch diameter, mostly due to joint failure. There was one joint failure in the cast iron pipe and one service leak. There were no breaks or leaks in the Transite pipe.

Taft, Maricopa and West Side Oil Fields Served by Western Water Company. The only damage to facilities serving Taft, Maricopa, and the West Side oil fields was the partial failure of a longitudinal welded seam of a 30-inch pipe line. The total length of cracking was about 4 feet, not continuous, but made of a number of short cracks separated by portions of the weld which remained intact. There was no report of any earthquake damage to the distribution systems serving these communities.

Kern Delta and Adjacent Rim Land Areas. There are five timber diversion weirs located along the channel of the Kern River, each of which is several hundred feet in length, with the superstructure from 10 to 15 feet in height erected above a substructure consisting of 2-inch plank deck supported by anchor and sheet piling 16 feet in length. Only one of these weirs was damaged by the earthquake shock; it was buckled upward to a height of about 3 feet at the midpoint along approximately 50 feet of its transverse length. The deck separated from the piling and the stream flow of between 300 and 400 second feet passed beneath the deck along the eastern bulkhead.

Subsequent examination revealed that the upper part of the piling was "punky" and it seemed evident that the failure was caused by the deteriorated condition of the piling of the substructure rather than a weakness in design.

The effect of the earthquake upon the water section of the canal was to cause waves several feet in height which broke on the top of the canal bank. In receding, these waves brought all loose debris into the canal section and it accumulated on the structure next downstream to an extent which, in some places, caused bank overflow.

Damage to the canal section was evidenced by longitudinal cracks in embankments above the water line, apparently due to slump of saturated material.

The Kern Lake area has been under almost complete irrigation by the use of surface water for many years. The damage in this area consisted of settlement of soil surfaces and damage to the domestic water installations of ranch headquarters as listed below.

- 12—500-gallon light steel tanks mounted on timber towers were destroyed.
- 6—Pumping units were destroyed due to these tanks falling upon them.
- 1—6500-gallon tank and tower of recent fabricated steel construction was destroyed.

The East Levee of Buena Vista Lake is a 5-mile-long embankment constructed about 60 years ago. The earthquake damage to this structure took the forms of longi-

tudinal cracking, settlement and subsidence on both water and land sides of the levee. Along a 200-foot length of the levee, a settlement of over 2 feet was noted and it is thought that the degree of damage suffered during the earthquake was aggravated by the solution of gypsum beds underlying the foundation.

For almost 20 miles along the approximate location of the trace of the White Wolf fault and for a distance of several miles on each side is an area under the highest type of irrigation development, with water pumped from ground water sources. This zone experienced violent surface disturbance due to the earthquake and damage to irrigated crop areas and physical works was extensive.

The damage to the electrical power installations at individual pumping plants took the form of the dismounting of the transformer banks from the pole-supported overhead platforms. A total number of 838 single units so installed were dismounted and fell to the ground.

Throughout the area the destruction of farm distribution systems constructed in the usual manner of plain concrete pipe was general. Pipes were broken and concrete standpipes thrown to the ground. Damage to the farm supply reservoirs took the form of longitudinal cracks in the embankments with settlement and slump on the water side.

The amount of damage apparently varied with the degree of embankment saturation and, in some instances, with water in the reservoir the embankments gradually slumped to ground level and filled the reservoir depressions.

Many of the wells within the zone of surface disturbance were damaged due to lateral displacement of the upper end of the casing. In all cases this displacement was found to terminate at depths of from 30 to 40 feet below ground surface. A successful method of correcting this condition was to excavate with a clam shell digger around the casing to such depths as above indicated, which removed the strain from the casing and allowed it to spring back to a vertical position.

Damage to crops resulted from fissures and surface disturbance due to both lateral and vertical movement. Major crop damage, however, was due to lack of water on account of failure of the distribution systems, damage to wells and loss of transformers.

Bakersfield's Distribution System. The water distribution facilities for the City of Bakersfield include 313 miles of mains, 25,908 services, 3 elevated tanks and 16 steel flat bottom surface tanks. Two of the elevated water tanks erected in 1928 and 1929 collapsed as a result of the earthquake of July 21, 1952. One of these tanks, known as the "A" Street Tank, was of 250,000-gallon capacity, had a height of 95 feet from ground to overflow and was constructed with 6 supporting columns. The other tank, known as the Bernard Tank, was of 150,000-gallon capacity, had a height of 80 feet from ground to overflow and also was constructed with 6 supporting columns. The third elevated tank, of recent construction, was designed with the horizontal force factor of 8 percent and was not damaged by either the earthquake of July 21 or the Bakersfield earthquake in August.

The damage to the distribution system consisted of two breaks in 4-inch mains, one in the 12-inch main and five services broken at the corporation cock.

5. DAMAGE TO ELECTRICAL EQUIPMENT CAUSED BY ARVIN-TEHACHAPI EARTHQUAKE

By G. A. PEERS *

Electrical installations in the Arvin-Tehachapi-Bakersfield area were damaged in the Arvin-Tehachapi earthquake of July 21, 1952, but no damage of consequence occurred on August 22. Most of the area was serviced by the Pacific Gas and Electric Company but some by Southern California Edison Company. Much of the damage was to platform-type pole transformers, 846 of which toppled. Very fast restoration of service by power companies prevented agricultural losses due to power failure. The heaviest substation damage was at Weedpatch where 4 rail-mounted transformers broke their restraining chocks and moved south to fall off their rails. Such damage can be reduced materially by larger chocks positively anchored to the rails.

Steam Plants. The Kern Steam Plant, 4 miles west of Bakersfield between the Rosedale Highway and the Santa Fe Railroad, was built in 1947-1948 and has a capacity of 175,000 kw in two units. The building is constructed with a steel frame and concrete walls. The damage to the building was negligible, there being only a slight spalling of concrete in one very small spot on the east wall adjacent to a steel beam and one break in the bond between the face of a column and the west-end wall. The oil storage tanks in the yard were slightly damaged. The floating roof of Tank No. 3, which was three-quarters filled at the time of the earthquake, rotated about 15 degrees counter-clockwise breaking the ladder that leads from the side of the tank to the roof. About 500 barrels were spilled on the roof and on the ground on the northwest and southeast sides of the tank. Tank No. 4 had a small amount of oil on the roof, sustained slight damage to the seals and was rotated about 15 degrees clockwise. All of the structures including the building and the plant were designed for a lateral force of 20 percent gravity. There were no cracks in partition walls including those that were constructed of tile. The thrust bearing in the No. 2 house turbine wiped and one boiler feed pump lost its suction.

Midway Steam Plant is a steel frame, concrete building, containing two 12,500 kw generators and associated equipment located in the southeast quarter of section 13, T. 29 S., R. 23 E., MDB&M adjacent to the community of Buttonwillow. In this plant some windows were broken, and the control room partitions were cracked. The west partition wall cracked so badly it had to be replaced. This is a concrete wall about 6 inches thick without reinforcement. A 10,000-gallon elevated water tank at this plant collapsed and fell towards the east.

Kern Canyon Hydro Plant has one 10,600 kva vertical unit housed in a reinforced concrete building located in the northeast quarter of section 6, T. 29 S., R. 30 E., MDB&M. There was no damage to the power house building or equipment, but at the diversion dam, about 3 miles upstream in the Kern River, a rock slide badly damaged the dam and gate control equipment.

Substations. The substations mentioned below are all shown on the map, figure 1.

At Weedpatch Substation four 6,000 kva transformers on tracks tipped over to the south breaking the bus

structure. The tracks were in a north and south direction. The wheels of the transformer trucks were lightly wedged.

None of the transformers mentioned below were in any way tied down to the foundation.

At San Bernard Substation one 5,000 kva transformer tipped over to the south, two other similar transformers shifted slightly on their concrete foundations. The transformer section of a 6667 unit type substation shifted south 3 feet, one oil circuit breaker in a cell flew out and landed a few feet away to the south.

At Wheeler Ridge Substation three 5,000 kva transformers shifted to the south leaning up against the columns supporting the bus. A pipe frame structure supporting the bus for the distribution regulator and breaker was slightly deformed.

At Old River Substation three 3,900 kva transformers shifted south to the edge of the foundation but did not fall. There was some damage to the electrical connections.

At Paloma Substation supplying the Paloma Refinery the earthquake damage was negligible but fire from the refinery fire did considerable damage. The transformers had moved slightly.

At Lakeview Substation the six 1,250 kva transformers moved south slightly. There were some ground cracks in the substation yard and a 10 x 10-foot control house on concrete foundation moved a few inches. Cyclone fence along the north line was moved out of line.

The P.G.&E. Office Building at Taft is a hollow clay tile building with a brick facing; the parapet cracked about 30 feet and the interior had minor plaster cracks.

At the Bakersfield Office and the garage there was no appreciable damage other than minor cracking due to the earthquake, but after the earthquake of August 22 the building had to be abandoned. This was the only damage of any consequence resulting from the Bakersfield earthquake of August 22, 1952.

Damage to Transmission and Distribution System. There were only two cases of 70 kv transmission line trouble. One was due to a pole falling over as the result of the earth opening up and one to conductors swinging together and burning the line down.

Distribution circuits themselves had a great many minor troubles, principally on spans that were designed to be slack for guying reasons. These slack spans were almost universally wrapped together in the area where the map shows transformer damage. There was, however, one circuit of normal span length running south of Panama Substation in which the wires were wrapped together in the middle of the spans. While all of these cases of the conductors being wrapped together would normally have caused a great many burn-downs, there were very few because the transmission lines serving this area were de-energized automatically by protective equipment before the distribution lines were actually shorted.

The greatest damage to the distribution system came about through platform mounted transformers. In the area affected there were two general designs. The older design consisted of two 6 x 8-foot timber struts installed between two poles, the transformers set without any

* General superintendent of transmission and distribution, Pacific Gas and Electric Company.

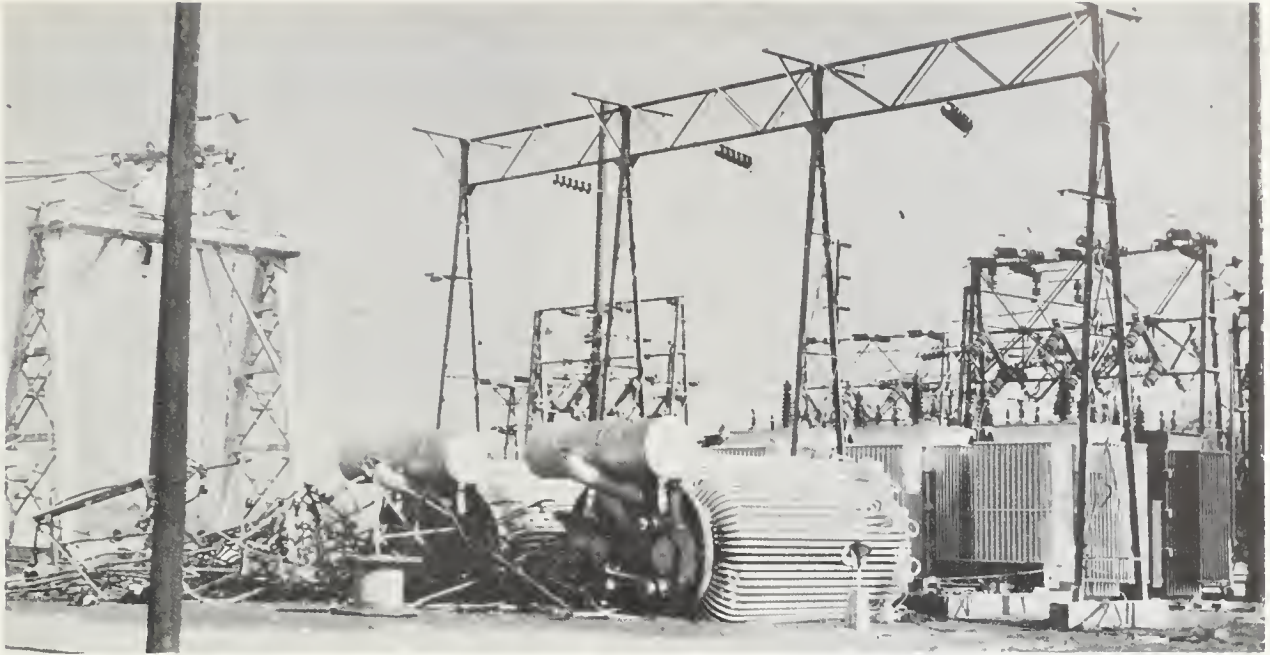


FIGURE 2. Overturned transformers at Weedpatch substation of Pacific Gas and Electric Company. *Photo by Archer Warne.*



FIGURE 3. Detail of transformer damage at Weedpatch substation. View north. *Photo courtesy Pacific Gas and Electric Company.*



FIGURE 4. Damage to platform-mounted pole transformers. Long way of structure east-west. *Photo courtesy Pacific Gas and Electric Company.*

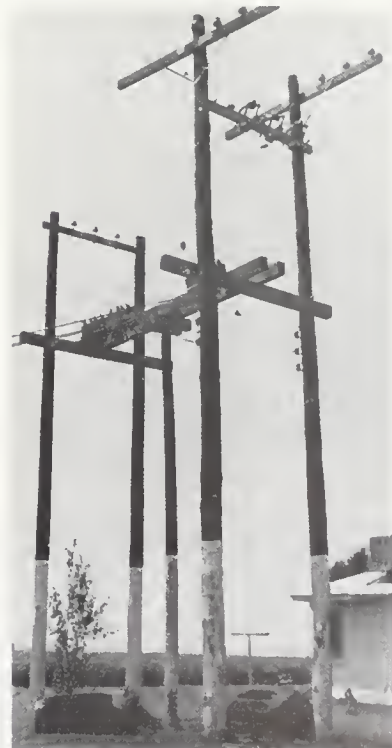


FIGURE 5. Pole transformers toppled to ground. *Photo courtesy Pacific Gas and Electric Company.*

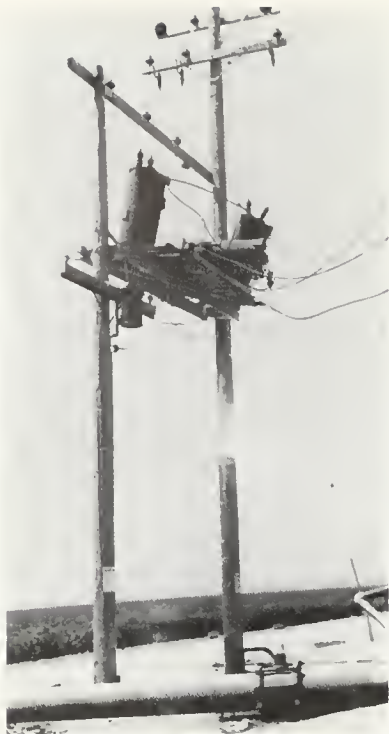


FIGURE 6. Damage to platform-mounted pole transformers. Long way of structure north-south. *Photo courtesy Pacific Gas and Electric Company.*

attachments on these timbers. In some larger transformers a third pole was added at the center. The more recently designed transformer platforms consisted of steel struts between poles with a wood platform approximately 5 feet wide with 4 x 6's running lengthwise of the platform on either side of the transformers. In general, the center of gravity of these distribution transformers was about one-third of the height of the tank. Apparently due to the length of the earthquake these transformers rocked; some of them apparently fell off the platform directly and some apparently rolled off. It is difficult to know just the exact way in which they fell; apparently the oil slopping around inside greatly influenced the result.

No transformers which were mounted on single poles by hangers or the more modern type bolted directly to the pole fell off, though the poles on which they were mounted showed evidence of rotating around in the



FIGURE 7. San Bernard substation, transformer damage. *Photo courtesy Pacific Gas and Electric Company.*

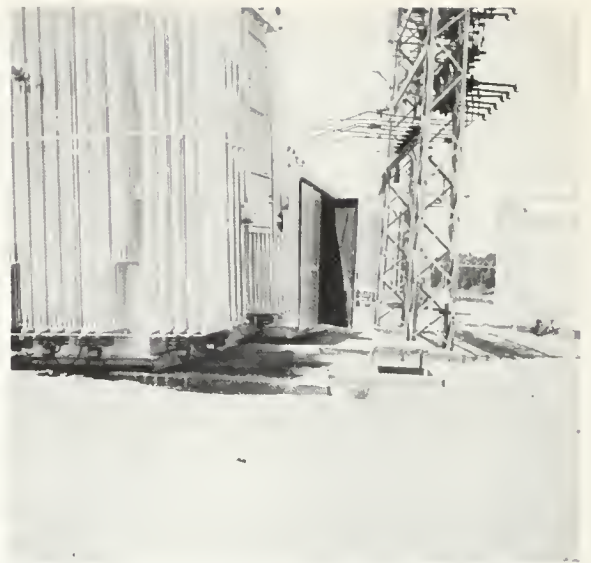


FIGURE 8. San Bernard substation, transformer damage. *Photo courtesy Pacific Gas and Electric Company.*

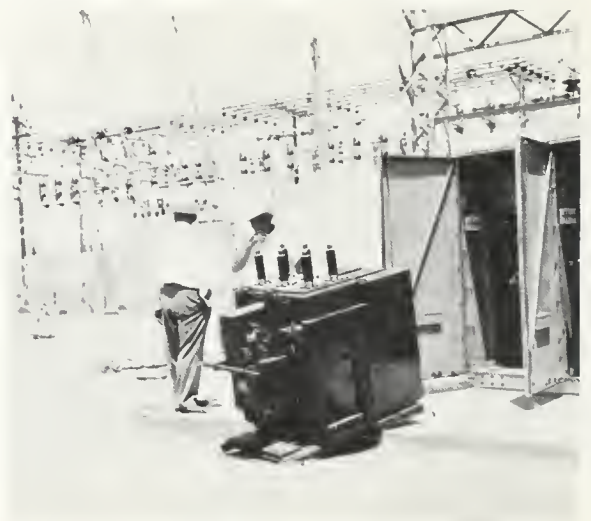


FIGURE 9. San Bernard substation, transformer damage. *Photo courtesy Pacific Gas and Electric Company.*

earth leaving an annular space from $\frac{1}{2}$ inch to $1\frac{1}{2}$ inches between the pole and the displaced ground.

There were approximately 846 transformers displaced on the structures during this earthquake, 246 of which suffered very minor damage or none. About 100 transformers were scrapped due to age or condition, and the remaining 500 needed bushing and tank repairs; about 50 of these had repairs to their core and coil.

In the area of greatest earthquake force the orientation of the long axis of the transformer platform appeared to make no difference, but in the areas of less severity it appeared that those structures with the long axis north and south lost fewer transformers. The newer structures were also somewhat better able to retain the transformers.

Throughout the area where the transformers left the structures there were scattered transformer installations which suffered no damage.

6. EARTHQUAKE DAMAGE TO RAILROADS IN TEHACHAPI PASS *

The damage. The Arvin-Tehachapi earthquake, on the morning of July 21, 1952, did major damage to 11 miles of railroad on the western approach to Tehachapi Pass, part of the major freight link between northern and southern California operated by the Southern Pacific Company and used also by the Santa Fe Railway Company. In this major damage area on the railroad, between Caliente and Rowen, four tunnels were badly shattered, and linings of four more were cracked. Early inspection parties found three water tanks overturned, including the 350,000-gallon tank at Tehachapi station; rails were out of alinement, and a water line running down the mountain as far as Bena was broken.

Near Tunnel 1, above Caliente, 100 feet of fill had dropped away from the rails, leaving them suspended 4 feet in the air. At tunnel 3, 700 feet long, near Bealville, the east 200 feet was badly damaged. The side walls of the tunnel, of heavily reinforced concrete 23 inches thick, were pushed in and the arch was broken in places. One rail was found twisted into an S-shape with one of the curves pushed under the wall of the tunnel; yet neither the wall nor the rail was broken.

the rails were 4 feet above the floor. Long jagged fissures several hundred yards long zigzagged along the earth's surface 160 to 190 feet above the roofs of the tunnels. These fissures were developed on, or close to, the trace of the White Wolf fault near its northeastern extremity.

The track between Tunnels 4 and 5 was covered with slides in several places. Where the line curved over a fill across Clear Creek canyon between the two tunnels, the earth from the ballast line outward had been shaken down about 3 feet. The west portal of Tunnel 5 was broken up and, for 600 feet inside, the walls and arches were damaged to varying degrees. Beyond that point, and about 360 feet apart, two plugs completely blocked the tunnel. The concrete lining between the plugs was damaged beyond repair. The east 200 feet of the bore was only slightly damaged. Tunnel No. 6, 300 feet long, was partially blocked by a cave-in, and the track between it and Tunnel 5 was twisted up and down and sideways.

From Tehachapi down past the base of the mountain, the earth beside the tracks in cuts and fills had been shaken down from a few inches to several feet from the ballast line outward. Engineers think that the ground directly under the tracks had been compacted by the weight of trains over the decades, while that outside was less firm so that it shook down during the earthquake.

The Railroad West of Tehachapi Pass. A description of the terrain and the line helps in understanding the problem faced in the wake of the disaster. Construction of a railroad over the Tehachapi mountains in 1875-76 involved a climb of 2,734 feet from the base of the mountains, in the San Joaquin Valley, to top the 4,025-foot Tehachapi Pass about 16 air miles away to the east. This was done by laying 28 miles of track on a winding alinement extending through 18 tunnels and around the Tehachapi Loop where long trains gain 77 feet in elevation by climbing over their own tails in ascending the mountains.

Longest of the tunnels was Number 5 which was completed about March 10, 1876. It was 1,169.6 feet from portal to portal. The tunnels originally were wood lined. They were increased to standard clearances and given concrete linings by 1921. Of the original 18 tunnels, two were bypassed by line changes in 1921, and one was daylighted in 1943.

The ruling grade throughout the area is 2.2 percent. The line is single track, with the exception of sidings, and is regulated by centralized traffic control.

Reconstruction. Within a few hours after the main shock, officials of the Southern Pacific Company had inspected the damage and decided on a swift-moving course of action for restoring the line to use. Briefly put, the plan contemplating the daylighting of the east end of Tunnel 3, the complete daylighting of Tunnels 4 and 6, and the repair and reconstruction of Tunnel 5 at the damaged points. To help implement its plan the road called on the services of the Morrison-Knudsen Company, contractor on many of the largest construction



FIGURE 1. Map of a portion of the Southern Pacific lines in California.

Tunnel 4, originally 300 feet east of Tunnel 3, was several feet closer due to the earth's movement (See Part I-7). As a result the connecting rails between the tunnels had been pushed into sharp curves. Throughout its 334.4 feet, Tunnel 4 was badly cracked; at one place

* Adapted from articles by Southern Pacific Company (How the SP repaired earthquake damage: *Railway Age*, Sept. 22, 1952, pp. 54-59; Earthquake rocks San Joaquin Division: *Southern Pacific Bull.*, Aug. 1952, pp. 7-9; Tehachapi earthquake clean-up: *Southern Pacific Bull.*, Sept. 1952, pp. 3-7) and information and photographs furnished by J. W. Corbett, Vice-President in charge of operations, E. E. Mayo, Chief Engineer, and C. J. Astrue, Assistant Chief Engineer, all of the Southern Pacific Company.

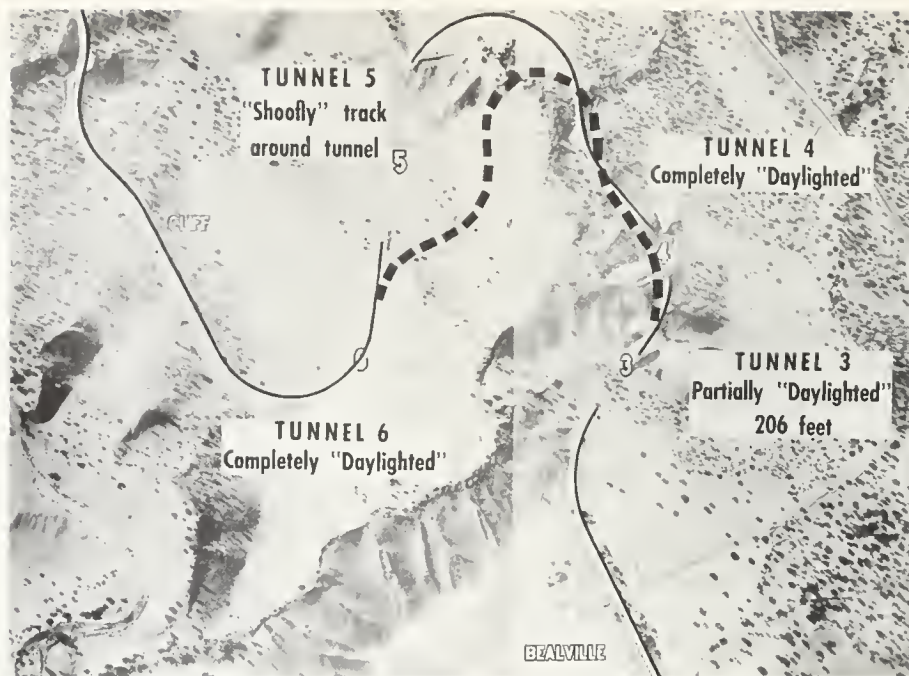


FIGURE 2. Aerial view showing topography and railroad alignment in the earthquake area.



FIGURE 3. Tank cars overturned on Oil City Branch by earthquake.



FIGURE 4. Track east of Tunnel 1. View west from north side of track.

projects in the nation. Early the following morning, the contractor had bulldozers on the scene slicing away at the top of the mountain over Tunnel 3. The emergency reconstruction task was primarily a matter of daylighting all or portions of the damaged tunnels and of constructing a long shoofly around one of them. To move the vast amount of earth required by this work (1,090,700 cubic yards) the railroad and contractors amassed more than 1,000 men and about 175 pieces of heavy earth-moving units. Estimated total cost of reconstruction in the 11-mile distance from Caliente to Rowen exceeded \$2,500,000.

Working on an around-the-clock schedule the railroad and contractor completed the emergency repair work in

time to permit traffic to be resumed at the end of 25 days. While the engineering forces of the road were thus engaged in repairing the damage caused by the second most severe earthquake in recorded California history, the operating department was doing its part by solving the problems involved in diverting traffic over the Coast route, the Southern Pacific Company's other main north-south line in California.

Men and machinery were mobilized from all over the West by the railroad and the contractor. The railroad company brought in six extra track gangs and six bridge and building gangs. In addition, the Santa Fe provided an extra track gang and three bridge and building gangs. The Morrison-Knudsen Company brought men by air-



FIGURE 5. Track east of Tunnel 1, from south side of track.

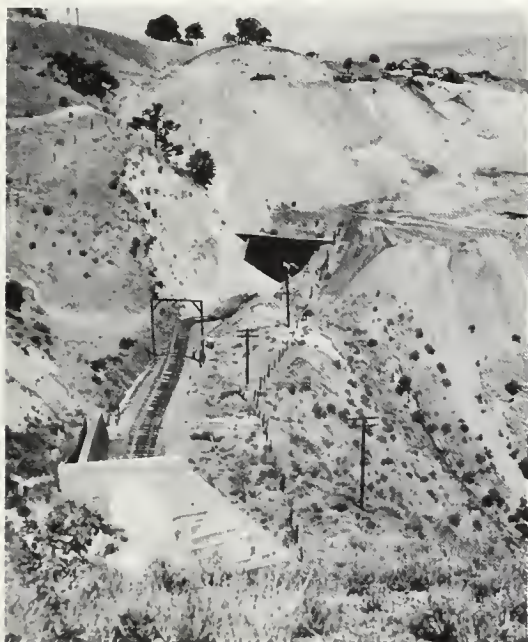


FIGURE 6. Equipment daylighting and removing 250 feet of east end of Tunnel 3. Slide at entrance caused by bulldozing. This picture taken 36 hours after Arvin-Tehachapi earthquake.

plane from as far as points in Idaho and Oregon; eventually it had 500 men on the job. Bulldozers, scrapers and other construction equipment were subcontracted from eight construction firms in the general vicinity, and the Santa Fe Railway ran a special train from Albuquerque, New Mexico, to speed the contractor's equipment from that area to the scene. Within hours after the first shock, extra gangs, diner cars, and outfit cars began moving toward the emergency zone from the Western, Shasta, Sacramento, Los Angeles, and Coast Divisions of the Southern Pacific Company.

By the morning of July 22, scores of cars of ballast, water, bridge timbers, signal equipment and other materials were rolling toward the earthquake-wracked area.



FIGURE 7. East portal of Tunnel 3 seen from top of Tunnel 4, showing daylighting in progress over Tunnel 3.



FIGURE 8. View east from east end of Tunnel 3; Tunnel 4 in background.

An emergency supply of water in tank cars was made available to the community of Tehachapi, where the business district had been demolished and 11 persons killed, and the Southern Pacific station in the town was made an emergency post office. Within 36 hours, bulldozers had carved out more than 5 miles of winding but serviceable access roads over the rugged terrain around the area, thus speeding the flow of men and materials.

The use of radio played an important part in expediting the project. An emergency radio communications center was set up in a caboose in Bealville. Men out on the job communicated with it by use of 15 walkie-talkie sets. Instructions and messages were relayed to and from Bakersfield, the nerve center, through the caboose.



FIGURE 9. Looking west toward Tunnel 3 from position above Tunnel 4.



FIGURE 11. Earthquake fault above Tunnel 4.



FIGURE 10. Earthquake fault above Tunnel 4.



FIGURE 12. Crack in knoll east of Tunnel 4.



FIGURE 13. Work in progress between Tunnels 3 and 4, August 1, 1952.



FIGURE 14. Dragline working at west portal of Tunnel 4, August 3, 1952.



FIGURE 15. Looking east from position above west end of old Tunnel 4, toward new fill, August 12, 1952.



FIGURE 16. Excavating for footings and reconstruction of west portal of Tunnel 5, left side, August 5, 1952.

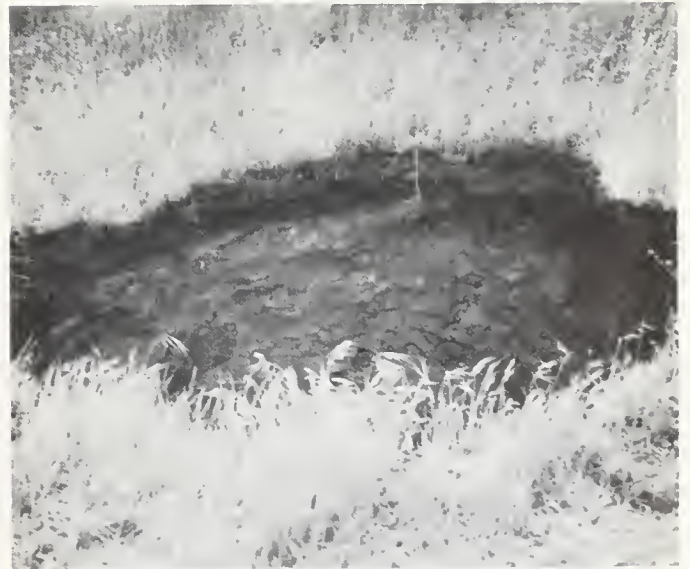


FIGURE 17. Large hole over Tunnel 5, July 30, 1952.



FIGURE 18. Broken fill between Tunnels 6 and 7.

The tremendous concentration of men, equipment, and materials immediately started to work on the plan of repair. Crews were split into two 10½-hour shifts. The other 3 hours of the day were devoted to the maintenance and repair of equipment. Twelve to fifteen 1,500-1,800-watt portable light plants allowed night-time operation at the same pace set during daylight hours. Except for the battle against time, no major construction problems were found.

In daylighting the east end of Tunnel 3 its concrete shell was pounded into rubble with three-ton steel balls swung from cranes. A 206-foot length of this tunnel was



FIGURE 20. Crack in hill on ridge between Caliente and Tehachapi Creeks. Elevation 3000 feet. President Russe's inspection party, Southern Pacific Company, in background.



FIGURE 19. Crack in hill on ridge between Caliente and Tehachapi Creeks. Crack at widest point 59 inches, depth 6 feet. Elevation approximately 3000 feet. August 9, 1952.



FIGURE 21. Crack in hill between Caliente and Tehachapi Creeks. Elevation approximately 3000 feet. August 9, 1952.

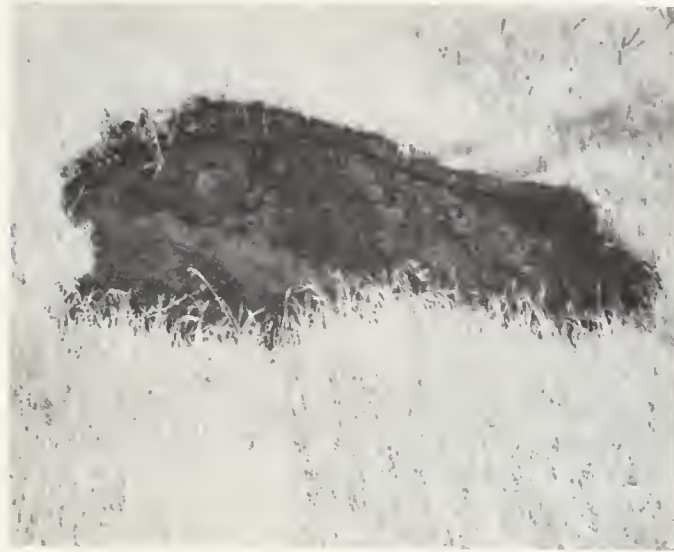


FIGURE 22. Hole highest on hill above Tunnel 5.

daylighted, leaving a 494-foot tunnel. The new cut at the east end of the tunnel is 147 feet deep. The daylighting of Tunnel 4 created a cut 181 feet deep. The old walls of the bore were left in place to serve as retaining walls. The cut that replaces Tunnel 6 has a depth of 140 feet.

It had become apparent, by August 2, that the damage to Tunnel 5 exceeded the original appraisal. Hence, after working on the bore for 10 days, it was decided to build a shoo-fly around the tunnel so that traffic could be restored while work on the tunnel continued. To construct the shoo-fly, Morrison-Knudsen hauled 250,000 cubic yards of earth in 150 hours from two giant cuts to make a new fill on the curve between Tunnels 4 and 5. Part of the earth came from a cut about 100 feet into the mountain alongside Tunnel 4 to make room for the curve leading into the shoo-fly; the remainder came from the shoo-fly cut in the same mountain in which Tunnel 5 was located. Before the fill was begun, 480 feet of 72-inch diameter corrugated steel drainage pipe was laid. A joint where the pipe made a change in grade was secured with a shot-creted collar and intermediate joints were connected by standard corrugated collars. The fill material was laid in 6-inch lifts. With up to 50 diesel tractors and scrapers working the major fill area simultaneously, the compaction went ahead steadily, with water sprayed on continuously. This grading job was the most spectacular operation of the entire project. The finished fill is 460 feet across at the bottom, 50 feet at the top, and is 132 feet high. The shoo-fly is 690 feet shorter than the original line through Tunnel 5; grade on the shoo-fly is 2.37 percent. The 15-degree curve leads into it over the fill.

The repairs to Tunnel 5 required 3 to 4 months to complete. In breaking through the tunnel's cave-ins, a top drift was first bored, and the sagging arch supported with 4-inch spiling. After that, the drift was winged out and steel segment wallplates set, with steel posts under them. A shotcrete lining was constructed inside the plates to provide a temporary finish.

About 1.75 miles of new track had to be laid. Long tangents of track had to be resurfaced and lined because of small irregularities. Because of countless aftershocks in the days following the first earthquake, the water line from Tehachapi Springs to Caliente, broken in hundreds of places, continued to pull apart for a couple of weeks.

Rocks, some of them the size of automobiles, had to be removed from the tracks. Because of the deeply weathered granitic rock in the tunnel area, the only dynamite needed during the entire project was used to break fallen rocks into pieces that could be handled. All cuts were sealed by bridge and building gangs before traffic was resumed. Berms 20 feet wide were cut in the slopes of the daylighted sections.

Maintenance of Passenger and Freight Services. While repair crews sweated and strained to repair the damage quickly, operating personnel performed the momentous task of diverting north-south freight traffic over the railroad's Coast route. Westbound trains were routed over the Santa Paula branch between Montalvo and Burbank, via Saugus. Eastbounds ran over the regular Coast route through Chatsworth Junction. This set-up gave the railroad the equivalent of double track through that area. Trains were limited to 75 cars or the tonnage equivalent as far northward as Watsonville Junction.

Two new telegraph offices went into operation and schedules were lengthened, sometimes to 24 hours, at others. Emergency diesel facilities were pressed into service at San Luis Obispo. Diesels from the blocked San Joaquin Valley route augmented the motive power pool on the Coast route. Also, the Santa Fe Railway loaned seven diesel locomotives, and steam locomotives from several other divisions were added to the power supply.

Meanwhile, 145 brakemen and firemen from other divisions moved over to other duties on the Coast route at the peak; these included 29 men from the Santa Fe Railway Company. The remainder were from the Southern Pacific Company's Rio Grande, Tueson and San Joaquin Divisions.

During the height of the emergency, the Coast route handled a daily average of 24 trains compared to 8 before, and 1,702 cars compared to 651. The peak was reached on August 10 when 1,886 cars travelled the Coast route. These figures do not include 8 scheduled passenger trains, an extra passenger train, and local freight service.

The emergency did not halt passenger service on the San Joaquin route. Only one train, the "West Coast," Nos. 59 and 60, a night passenger train between Sacramento and Los Angeles, was annulled. The San Joaquin-Sacramento "Daylights," the overnight "Owls," and passenger trains Nos. 55 and 56, ran on regular sched-

ules north of Bakersfield. Passengers, baggage, mail and express were shuttled between Bakersfield and Los Angeles by bus and truck. The regular schedule of departures and arrivals at the Los Angeles Union Passenger Terminal was maintained.

On August 15, the twenty-sixth day after the earthquake struck, a Southern Pacific freight train consisting of 100 empties wound slowly down the mountains out of Tehachapi. Two days later the Los Angeles-bound "San Joaquin Daylight" snaked up the mountain, the first passenger train to make the trip since early on July 21.

7. EARTHQUAKE DAMAGE TO ELEVATED WATER TANKS *

BY KARL V. STEINBRUGGE ** AND DONALD F. MORAN **

ABSTRACT

Elevated tanks with no lateral force design were badly damaged. The performance of earthquake-resistive tanks was far superior to that of wind-braced tanks. A common type of tower failure resulted in the tank resting upside down and almost within its own base. Rod and rod connection detail failures were common primary causes of tank failure. Tower-type structures have little reserve strength when compared to a typical building, and lateral force coefficients and allowable stresses should be arrived at after due consideration of this fact.

Wind Braced Tanks. Elevated tanks with no lateral force design, other than for wind, were badly damaged as they always have been in past severe shocks. Of the 12 wind designed tanks in the area, two collapsed, seven had broken or stretched rods and three were not damaged after July 21, 1952.

Tower failures wherein the tank rests upside down and almost within its own base are common. One explanation is that when a rod or rod detail failure occurs in the top panel, the tank starts to rotate and descend. However, the large diameter riser acting as a column picks up the load immediately and the tank turns over and comes down in an inverted position inside the tower. Several tanks showed effects of punching action of the riser on the bottom. A graphic explanation of this type of failure is shown in the diagram (fig. 2).

No foundation movement was noted. Nearly all of the foregoing tanks had some anchor-bolt stretching and of those that collapsed, some anchors were necked-down and failed in tension. This tension failure was probably due to prying action of the falling columns and not to direct uplift. Incipient or actual column failure due to direct compression was not noted. However, where the tower completely failed this would be difficult to verify. Tank No. 16 located at Maricopa Seed Farms had paint flaked just above the welded column splices on the tubular legs but only where the plate thicknesses changed.

There was damage to wind braced tanks in Lancaster, El Monte and Los Angeles—the latter two approximately 70 miles south of the epicenter.

Earthquake Braced Tanks. The behavior of wind braced tanks was interesting, but the important lessons are to be learned from the performance of earthquake resistive tanks. Performance of earthquake resistive tanks was so much superior to that of the wind designed tanks that there is no doubt that present design methods are in the right direction.

Tank No. 11 (see accompanying table), which was an old wind designed tank brought into the area and reinforced for 10 percent gravity in accordance with the Uniform Building Code, failed. The columns were reinforced in the two lower panels and new rods and gusset plates were used. A serious deficiency was the use of cotter keys to secure the elevis pins. Numerous cotter keys were sheared off and many pins had fallen out.

* Data in this paper are condensed from *An engineering study of the southern California earthquake of July 21, 1952 and its aftershocks*, published in the Bulletin of the Seismological Society of America, vol. 44, no. 2B.

** Structural Engineers, Pacific Fire Rating Bureau, San Francisco and Los Angeles.

Some elevises spread to as much as 4 or 5 inches, allowing the pins to drop out. No rods were broken. Two gusset plates were torn around the reinforcing pad plate. There was no evidence of initial column failure and the foundations were not disturbed. The consensus of engineers who examined the structure was that the failure of the cotter keys was the primary cause of collapse. In 1933, the Board of Fire Underwriters of the Pacific prohibited the use of cotter keys in tanks erected under their jurisdiction.

Tank No. 16 was slightly damaged although there were indications that this particular area was severely shaken. Two adjacent steel buildings had their bracing rods stretched and broken, indicating a maximum calculated acceleration approaching 50 percent gravity. Soil conditions at the site are very poor and piling was used for the foundation. Reinforced concrete struts were used around the base and diagonally. Rods in all panels of the tank tower were tightened after the shock. The takeup was greatest at the bottom and decreased toward the top. All bases moved inward (approximately $\frac{1}{2}$ inch at maximum); this would contribute to the loosening of rods, particularly in the lower panel. There is some evidence that the bracing rods were somewhat loose prior to the shock. Grout beneath the base plates and beside the shear fins was shattered and large portions of the pier caps were spalled.

On January 12, 1954, a strong aftershock caused damage in the vicinity of Maricopa Seed Farms. Tank No. 16 again stretched its anchor bolts, although in this shock anchor bolts at the southeast and northwest column legs were stretched while the anchor bolts on the other axis were damaged in the July 21, 1952 shock. No appreciable rod stretching was noted after the January 12th shock, although paint flaking on the rods indicated unit stresses of a high order. Temporary plates placed under the nuts of the anchor bolts after July 21st were found bent and also rusted where the nut indented the plate. This indicated that between the two previously mentioned shocks an aftershock occurred sufficiently strong to stress the anchor bolts again.

Tank No. 1 stretched its anchor bolts about three-sixteenth of an inch after the July 21st shock and cracked the tops of the pile caps. The pattern of cracking was similar to tank No. 16, but no concrete spalled. Steel reinforcing hoop ties were used in the tops of the piers. This tank also was on piling and had reinforced concrete ties around the base and diagonally.

Damage. The use of ties in poor soil areas undoubtedly played an important part in holding the damage to a minimum. No foundation movement was noted.

Anchor bolt stretching was noted on tanks Nos. 1, 2, 13, 14 and 16. This stretching of anchor bolts indicates the possibility of a deficiency in present coefficients or stresses. For example, a typical 100M gallon tank on 100 foot tower with battered legs, when designed for a lateral force of 10 percent G, has practically no anchor bolt stress. However, if subjected to a lateral force of 20 percent the anchor tension becomes approximately 43,000

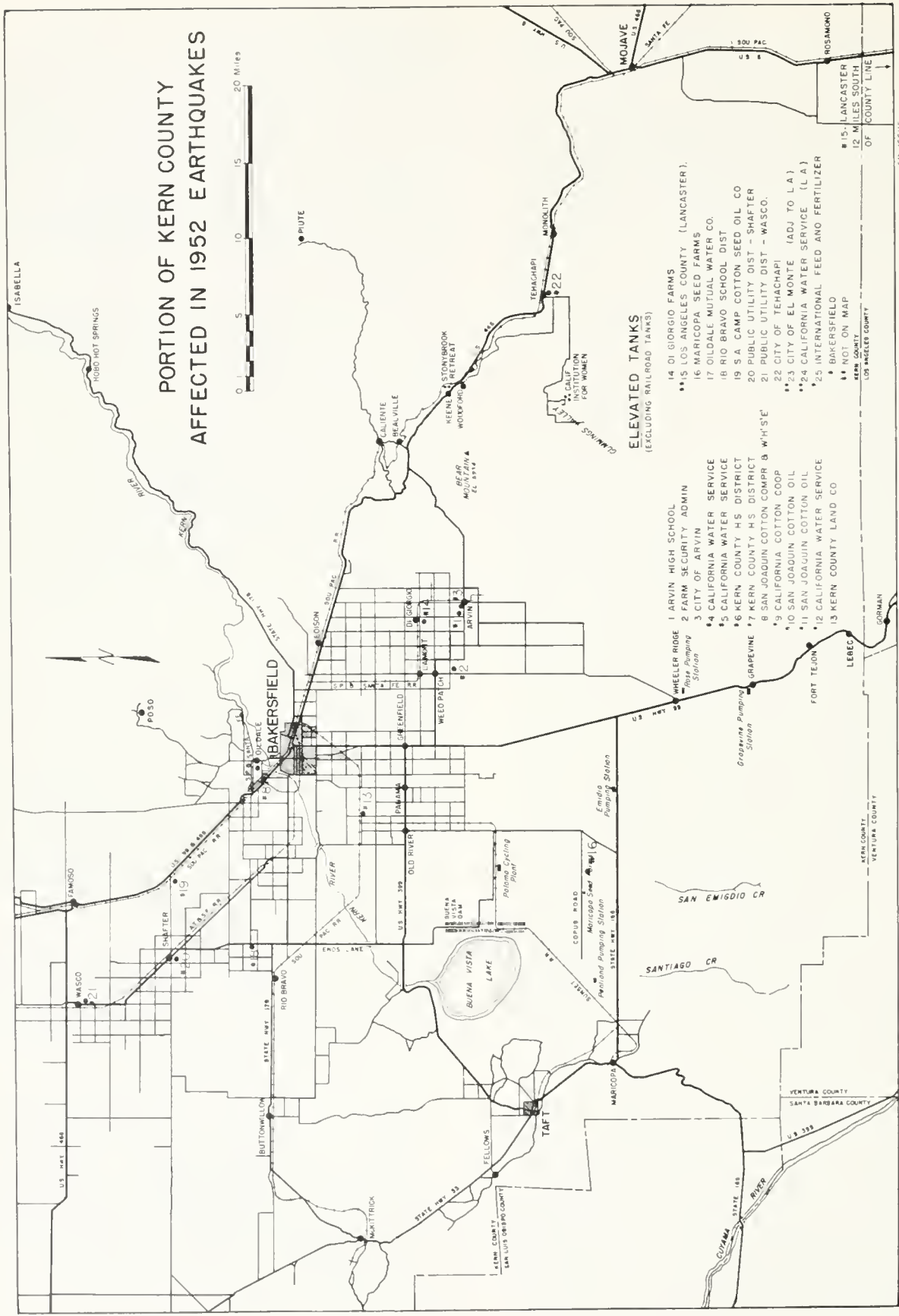
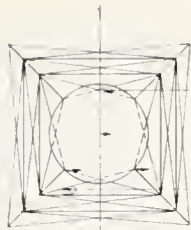


FIGURE 1.



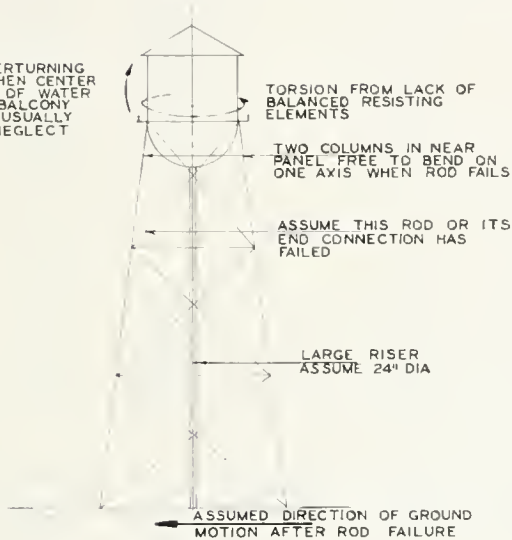
THIS UNDATED PANEL REMAINS RIGID - BECOMES APPROXIMATE CENTER OF ROTATION

ASSUME THIS ROD OR ITS END CONNECTION HAS FAILED

PLAN

- 1 SECONDARY DEFLECTIONS DUE TO ROD ELONGATIONS NOT CONSIDERED, ALTHOUGH IMPORTANT IN SOME CASES
- 2 BREAKAGE OF RODS IN UPPER PANEL IS COMMON OBSERVATION ON DAMAGED TANKS AND BUCKLED BOTTOMS ON COLLAPSED TANKS

SOME OVERTURNING EXISTS WHEN CENTER OF MASS OF WATER IS ABOVE BALCONY GIRDER USUALLY SMALL NEGLECT



TORSION FROM LACK OF BALANCED RESISTING ELEMENTS

TWO COLUMNS IN NEAR PANEL FREE TO BEND ON ONE AXIS WHEN ROD FAILS

ASSUME THIS ROD OR ITS END CONNECTION HAS FAILED

LARGE RISER ASSUME 24" DIA

ASSUMED DIRECTION OF GROUND MOTION AFTER ROD FAILURE

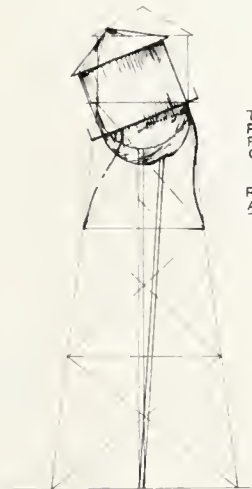
ELEVATION I



COLUMN FAILS, PROBABLY DUE MAINLY TO BENDING

SLACK ROD

ELEVATION II



TANK TOPPLES ABOUT RISER. PROBABLY TOWARDS FIRST OF TWO FRONT COLUMNS TO FAIL

RISER ACTS AS COLUMN AND OFTEN BUCKLES BOTTOM OF THE TANK.

ELEVATION III



IV

AS A RESULT TANK TOWER DOES NOT OVERTURN BUT THE TANK USUALLY FALLS WITHIN ITS COLUMN BASES, AND THE BOTTOM OF THE TANK IS UP

PROBABLE FAILURE SEQUENCE OF FOUR COLUMN WINDBRACED ELEVATED TANK

FIGURE 2.

Tank number	Location and contractor date	Etlip. design	Code	Capacity (gal.)	Dia. (ft.)	Constr.	Tower height	Panels	Physical characteristics		Damage in July 21, 1952 earthquake	Status since earthquake	Remarks
									No.	Type			
1	Arvin High School Pittsburgh-Des Moines Co.—1948	12%	Title 21 California Division of Architecture	100,000	30'-6"	Steel welded	100'	4	4	Wide flange	Drilled piles. Concrete struts, diagonal & perimeter.	Anchor bolts tightened. Additional concrete poured around the piers.	Hoop ties were in the tops of piers.
2	Arvin 5 miles W. of Arvin, Farm Security Admin. Pittsburgh-Des Moines Co.—1940	10%	Board of Fire Underwriters of the Pacific	30,000	15'	Steel riveted	75'	3	4	2 channels back to back —with lacing.	Spread footings. No struts.	Anchor bolts not tightened 6-8-53.	Some evidence that rods had been tightened.
3	Arvin City of Arvin Chicago Bridge and Iron Co.—1945	None	-----	75,000	26'	Steel riveted	65'-6"	2	4	2 channels back to back —with lacing.	Spread footings. No struts.	New rods for 10% earthquake per Uniform Building Code. Rod connections and tower not reinforced.	Tank partially emptied after first shock.
4	Bakersfield 3d & A Sts., California Water Service Co. Pittsburgh-Des Moines Co.—1929	None	-----	250,000	40'	Steel riveted	65'	2	6	2 channels back to back —with lacing.	Spread footings. No struts.	No damage observed.	Tank probably full at time of earthquake. Tank fell generally southwest on its side.
5	Bakersfield Northwest Bakersfield California Water Service Co. Pittsburgh-Des Moines Co.—1948	8%	Uniform Building Code	500,000	50'	Steel riveted	95'	2	10	2 channels back to back —with lacing.	Spread footings. No struts.	Loose rods tightened by other than original contractor.	
6	Bakersfield SE. corner 14th & "C" Kern Co. High School Dist. Pittsburgh-Des Moines Co.—1932	None	-----	25,000	15'	Steel riveted	62'	3	4	2 channels back to back —with lacing.	Spread footings. No struts.		
7	Bakersfield S-S College, between Cora Lane and Corrientes, Kern Co. High School Dist. Pittsburgh-Des Moines Co.—1938	20%	-----	30,000	15'	Steel riveted	80'	4	4	Wide flange.	Spread footings. No struts.		
8	Bakersfield 4 mi. N. of Bakersfield San Joaquin Cotton Company and Warehouse Company Pittsburgh-Des Moines Co.—1925	None	-----	100,000	24'	Steel riveted	100'	3	4	2 channels back to back —with lacing.	Spread footings. No struts.	Reinforced for 10% earthquake per Pacific Fire Rating Bureau specifications. Steel struts installed around base.	Broke rod showed signs of flaw at break near forged end.
9	Bakersfield SE. Bakersfield, Brandage Lane, California Cotton Coop. Pittsburgh-Des Moines Co.—1947	10%	Board of Fire Underwriters of the Pacific	100,000	24'	Steel riveted	100'		4	2 channels back to back —with lacing.	Spread footings. Reinforced concrete perimeter struts.	Repaired by other than original contractor.	
10	Bakersfield NW. corner, California & Washington, San Joaquin Cotton Oil Co. Pittsburgh-Des Moines Co.—1933	8%	Board of Fire Underwriters of the Pacific	50,000	19'	Steel riveted	100'	3	4	2 channels back to back —with lacing.	Spread footings. Reinforced concrete perimeter struts.	No damage observed.	Tower reinforced for 8% gravity after 1933 earthquake.

Tank number	Location and contractor date	Ehho. design	Code	Physical characteristics						Damage in July 21, 1952 earthquake	Status since earthquake	Remarks	
				Capacity (gal.)	Dia. (ft.)	Tower height	Legs		Foundations				
							No.	Type					
11	Bakersfield SW. corner, California & Washington, San Joaquin Cotton Oil Co. Consolidated-Western Steel Corp.—1949	12%	Uniform Building Code	100,000	24'	100'	3	4	2 channels back to back —with lacing.	Spread footings. No struts.	Collapsed. Some gusset plates torn. Cotter pins sheared. No rods broken. Foundations not disturbed.	Replaced with new tank by Chicago Bridge and Iron Company per Pacific Fire Rating Bureau revised specifications.	Tank was originally a Cole Company tank and brought in from East. Reinforced by Consolidated-Western Steel Corp. for 12% ⁴ . Tank overturned and fell inside base.
12	Bakersfield Bernard and Elmira Sts., California Water Service Co., Chicago Bridge and Iron Co.—1928	None	-----	150,000	28'	55'	2	6	2 channels back to back —with lacing.	Spread footings. No struts.	Collapsed. Several rods broke. Anchor bolts failed. Foundations not disturbed.		Probably full at time of earthquake. Tank overturned and fell within base.
13	Bakersfield Gostord Rd. at railroad Kern County Land Co., Chicago Bridge and Iron Co.—1949	10%	Uniform Building Code	100,000	28'	50'	2	4	Welded tubular	Piling. Reinforced concrete struts diagonally and around perimeter.	Plate beneath anchor bolt nut was bent slightly. Some cracking of piers and grout. Movement in slots.	Anchor bolts appear to have been tightened.	
14	Di Giorgio Farms NW. of Arvin, Di Giorgio Farms Chicago Bridge & Iron Co.—1951	12%	Uniform Building Code	100,000	28'	100'	3	4	Welded tubular	Spread footings. Reinforced concrete struts around perimeter.	Rods elongated slightly. Anchor bolts elongated slightly and plate beneath anchor bolt nut was bent.	Rods adjusted. Anchor bolts tightened.	
15	Lancaster County of Los Angeles Chicago Bridge & Iron Co.—1921	None	-----	75,000	22'	70'-6"	3	4	2 channels back to back —with lacing.	Spread footings. No struts.	5 diagonal rods broke; 3 in top panel and 2 in center panel. 4 breaks at forge welds and one 1" away. One radial riser rod broke and rivets leaked on riser.	Will strengthen to 10% G per Los Angeles County Building Code.	Strain cracks in several places of top 2 panel rods. Looped ends stretched.
16	Maricopa Seed Farms SW. of Bakersfield Maricopa Seed Farms, Chicago Bridge & Iron Co.—1951	10%	Pacific Fire Rating Bureau	100,000	28'	100'	3	4	Welded tubular	Drilled piles. Reinforced concrete struts diagonally and around perimeter.	1" takeup in bottom panel turnbuckles due to rod stretching. Base movement, and pinhole stretching. Elongation also occurred in upper panels. Grout loosened. * (See remarks.)	Rods adjusted. Anchor bolts tightened. Concrete piers repaired. Steel struts installed around base.	See text for more details. *All bases moved inward slightly.
17	Oldale SE. corner Wells & Miner Aves. Oldale Mutual Water Co., Pittsburgh-Des Moines Co.—1924	None	-----	75,000	21'	50'	2	4	2 channels back to back —with lacing.	Spread footings. No struts.	No damage observed.	Reinforced for 10% Uniform Building Code.	
18	Rio Bravo Rio Bravo School District Pittsburgh-Des Moines Co.—1951	12%	Title 21 California Division of Architecture	25,000	18'	80'	4	4	Wide flange	Spread footings. Struts.	No damage observed.		
19	Shafter S. A. Camp Cotton Seed Oil Co., Pittsburgh-Des Moines Co.—1951	12%	Uniform Building Code	100,000	24'	100'	4	4	2 channels back to back —with lacing.	Spread footings. Struts around perimeter.	No damage observed.		Rebuilt and re-erected from San Leandro, Calif.
20	Shafter Public Utility District Pittsburgh-Des Moines Co.—1930	None	-----	75,000	21'	75'	3	4	2 channels back to back —with lacing.	Spread footings. No struts.	No damage observed.	Rods appear to have been tightened.	

Tank number	Location and contractor date	Etha. design	Code	Capacity (gal.)	Dia. (ft.)	Constr.	Tower height	Physical characteristics		Damage in July 21, 1952 earthquake	Status since earthquake	Remarks	
								No.	Type				
21	Wasco Public Utility District Pittsburgh-Des Moines Co., 1926	None	-----	100,000	24'	Steel riveted	92'	3	2 channels back to back —with lacing.	Spread foot- ings. No struts.	No damage observed.		
22	Tehachapi West of "D" St., N. of Mojave St., City of Tehachapi Unknown—1906(?)	None	-----	45,000		Steel riveted	40'	2	2 channels back to back —with lacing.	Spread foot- ings. No struts.	Rods welded and tightened. Columns partially straightened and reinforced.	Tank full at time of shock.	
23	El Monte City of El Monte Chicago Bridge and Iron Co.—1914	None	-----	60,000	19'	Steel riveted	90'- 7"	3	2 channels back to back —with lacing.	Spread foot- ings. No struts.	All rods on north and east sides stretched. One middle panel rod broke in forged weld.	Rods taken up and broken rod butt welded.	Approximately 70 miles south of epicenter.
24	Los Angeles Stringer Ave., California Water Service Chicago Bridge & Iron Co.—1925	None	-----	50,000	19'	Steel riveted	40'	2	2 channels back to back —with lacing.		One top panel rod broke.	Broken rod removed and re- placed with new one.	Approximately 70 miles south of epicenter.
25	Bakersfield Southwest Bakersfield, In- ternational Feed & Ferti- lizer Co.—U. S. Govern- ment—1945	---	-----	20,000		Wood	40'±	4	Wood posts	Wood struts around base.	No damage observed.		Tank is always about 2/3 full.

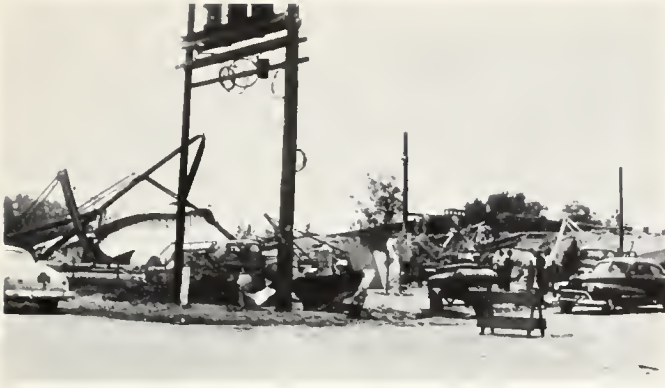


FIGURE 3. Elevated water tank that collapsed during July 21, 1952, earthquake. Bernard and Elmira Streets, Bakersfield. *Photo by Gordon B. Oakeshott.*

pounds per square inch. The possibility of stretching due to rocking about the rigid column base should not be overlooked.

It is known, from instrumental records of this shock, that large vertical accelerations accompanied the horizontal movement. These acting together could add to the theoretical stress by reducing the dead loads.

An analysis of the Taft accelerogram records by the Earthquake Research Laboratory of the California Institute of Technology indicates that for a typical earthquake braced tank at Taft the probable actual lateral force would have been approximately equivalent to 20 to 25 percent *G*. Analysis of other accelerogram records indicates that structures with low damping characteristics, such as tank towers, must be designed with caution.



FIGURE 4. Elevated water tank that collapsed during July 21, 1952, earthquake. Third and A streets, Bakersfield. *Photo by Gordon B. Oakeshott.*

Tower-type structures have little reserve strength when compared to a typical building, and the computation of lateral force co-efficients as well as allowable stresses should consider it.

Stretching of bracing rods was fairly common in wind braced tanks, possibly due in part to the rods being somewhat slack before the shock. However, since the bracing rods are primary lateral force-resisting members and a defect in material or construction can bring collapse, their unit stresses should be kept to a moderate level and the construction carefully inspected. Also, conservative stresses reduce the possibility of permanent elongation which could have a serious effect due to impact in strong aftershocks or shocks of long duration.

8. EARTHQUAKE DAMAGE TO CALIFORNIA CROPS *

BY KARL V. STEINBRUGGE ** AND DONALD F. MORAN **

A number of statements have appeared regarding the extensive agricultural losses from the July 21, 1952 earthquake. While this was no doubt true in localized areas, observations by the authors would indicate that ranchers were able to improvise and were usually able to irrigate without major crop losses. Power was restored quickly and thereby undamaged wells could be pumped again. Only a few wells were unusable as the result of shock. Damage was usually noted in the upper 40 feet, but wells were from 600 feet to 1500 feet deep. The writers have no record of wells which were total losses.

Concrete irrigation systems were damaged over large areas, but rarely destroyed. To repair this damage, pipe layers and crews from all parts of California and neighboring states were called in. The pipe was usually tongue and groove, and was not reinforced. Breaks were found as close together as 3 feet to 6 feet in some areas. Vertical standpipes were generally damaged in the heaviest hit areas.



FIGURE 1. Cotton rows offset by lurch fracture, July 21, 1952, near Arvin. Photo by Lauren A. Wright.

Many miles of earth irrigation canals and also concrete lined canals were reported to have sustained minor damage in the form of sloughing of their banks, but none were known to have had a major break.

Water levels in some wells rose markedly after the main shock. (See Part I—10). This could be partly attributed to the cessation of pumping due to power failures but possibly was primarily due to consolidation of the soil. The California Division of Water Resources reported one 100-foot well became artesian for 2 days after the shock.

* Data in this paper are from *An engineering study of the southern California earthquake of July 21, 1952, and its aftershocks*, published in the *Bulletin of the Seismological Society of America*, vol. 44, no. 2B.
 ** Structural Engineers, Pacific Fire Rating Bureau, San Francisco and Los Angeles.



FIGURE 2. Offset cotton rows half a mile east of U. S. Highway 99 and northeast of Mettler. View west. Photo courtesy California Division of Water Resources.

Accurate determination of earthquake loss to agriculture is difficult, although data have been published or are available in reports. Probably the most detailed study to date has been made by a representative of the Kern County Agricultural Department. Following is a tabulated summary of the findings which were prepared in 1952.

Agricultural losses.

Arvin-Wheeler Ridge Area:

A. Crop losses:

Peas: Loss of second crop and fertilization	_____	\$90,000
Grape: Damage to plants in 16,500 acres	_____	1,550,000
Cotton: Includes pipe damage: 91,920 acres	_____	7,000,000
Alfalfa hay: 10,000 acres lost 1 cutting	_____	330,000
Alfalfa seed: 17,000 acres	_____	2,500,000

Potatoes:

Arvin-Wheeler Ridge: Loss of one of the double crop	_____	\$70,000
Cummings Valley: Quality lower	_____	75,000
Wheat, milo, corn, onions, pears	_____	None

B. Releveling: Bulk of it reported above. Probable that total damage will not be known for several years

750,000

C. Irrigation pipe and ditches:

113,000 acres under irrigation _____ 5,000,000

D. Water supply: Well failures and water tank failures

150,000

Edison Area: Estimated A-D above _____ 3,500,000

Shafter-Wasco-Delano: Estimated A-D above _____ 1,800,000

Total Agricultural Loss _____ \$23,595,000

Accuracy of the above estimate is subject to wide variation. Witnesses cannot always be relied upon, because of hysteria, inaccurate records, and possibly tax considerations. In one instance in the foregoing loss summary, the analysis was based on one property which was presumed to have suffered a loss of over \$1,000,000. The actual total loss, including damage to buildings is now estimated at \$40,000 up to the time of this report. A spot



FIGURE 3. Northwest-trending cracks 1 mile west of U. S. Highway 99 and 7.5 miles south of McKittrick Road. Note damage to farm reservoir. Cracks vary in direction; trend of those in photo N. 60° W. View southeast. *Photo courtesy California Division of Water Resources.*

check of several large cotton gins would indicate that cotton losses may also be considerably less than reported. Lastly, all estimates include the cost of leveling of the ground which is the result of slumping, etc., and this leveling work may continue for a year or two.



FIGURE 4. Buena Vista dam, east levee; view south. Subsidence and cracking of the fill caused by earthquake. Maximum settlement shown in photo is 2 feet. *Photo courtesy California Division of Water Resources.*

Based on unofficial data and the authors' observations, it is likely that the total agricultural loss will actually be \$5,000,000 to \$7,000,000.

Aftershocks caused some additional damage to underground piping. Negligible damage occurred from the August 22nd shock. Some additional damage was reported about 25 miles southwest of Bakersfield after the January 12, 1954 aftershock.

9. STRUCTURAL DAMAGE TO BUILDINGS *

BY KARL V. STEINBRUGGE ** AND DONALD F. MORAN **

ABSTRACT

The Kern County earthquakes of July 21 and August 22, 1952 afforded structural engineers an opportunity to re-examine the performance of man-made structures when subjected to earthquake shocks. The July 21 shock, felt over an area of 160,000 square miles, produced some building damage as far away as San Diego and San Francisco, but major damage was in Arvin and Tehachapi where 12 people were killed. Building damage in Bakersfield on July 21 was principally confined to isolated parapet failure and to loosening and cracking in older structures and those not designed as earthquake resistant. Damage on August 22 was largely restricted to Bakersfield, with 2 people killed, 35 injured, and over 400 earthquake-damaged buildings. Total building damage—Kern County, Los Angeles, Long Beach, Pasadena, Santa Barbara—is estimated at \$37,650,000. Total damage, including Paloma refinery (\$2,000,000 ±), agriculture (over \$6,000,000) was between \$48- and \$55,000,000.

Damage to masonry structures and those of large mass was significantly different for buildings without specific lateral force bracing systems as compared to those with lateral force bracing systems. Most of the materials and types of construction generally considered hazardous in an earthquake can be made earthquake resistant by intelligent design and good construction. The effect of the two major earthquakes, plus aftershocks, produced cumulative damage. Damage in the more distant cities—Los Angeles, Long Beach, and Santa Barbara—was generally confined to the older, taller buildings, in part, the result of longer periods of vibration farther from the epicenter. The newer earthquake resistive structures behaved well except for some damage to interior partitions and trim.

The pattern of severe damage to public schools was similar to that of other types of structures and, in general, followed the pattern of previous earthquakes. School buildings constructed under the controls of the State Field Act of 1933 were practically undamaged whereas the older buildings were seriously affected. In Bakersfield City School District alone, replacement cost of damaged school buildings is estimated at \$6,191,000, while the cost in the rest of Kern County is placed at \$6,663,000. Cost of repairs to the "Field-Act" schools which were damaged was always less than 1 percent of the value of the structures but to "non-Field-Act" schools damage ranged from small up to total loss.

INTRODUCTION

The southern California earthquakes of 1952 have afforded an excellent opportunity to re-examine the performance of man-made structures when subjected to earthquake shocks. Two principal shocks, from the damage standpoint, occurred on July 21, 1952, and on August 22, 1952. The first was a great earthquake, widely felt, but probably not as great as three other well known shocks in California: 1906 at San Francisco, 1857 at Fort Tejon and 1872 at Owens Valley. The August 22, 1952 Bakersfield earthquake was a moderate shock with its epicenter close to a populated area already "loosened-up" by previous shocks.

The authors, through the Earthquake Department of the Pacific Fire Rating Bureau, made a detailed study of these earthquakes with the following objectives in mind:

1. To review earthquake insurance rating practice, and compile data helpful to earthquake insurance underwriting.
2. To evaluate the effectiveness of current earthquake resistive design practice, and
3. To contribute material for future earthquake research.

* Data in this paper are condensed from *An engineering study of the southern California earthquake of July 21, 1952, and its aftershocks*, published in the Bulletin of the Seismological Society of America, volume 44, number 2B.

** Structural Engineers, Pacific Fire Rating Bureau, San Francisco and Los Angeles.

All of the above objectives are interrelated and a study of one must include some if not all of the others.

Unfortunately, many areas in California and other western states still do not have adequate building laws requiring that new buildings be designed to resist strong earthquake forces. Others that have adopted good building codes do not have effective enforcement and judging the probable earthquake behavior of buildings on the basis of local codes may be dangerous.

Accurate reporting of facts requires considerable time and the careful checking of reports from untrained observers. The spectacular is often newsworthy and misleading; these earthquakes were another example of this. The headline "Tehachapi Levelled" was common in the newspapers after the July 21, 1952 shock, but accompanying photos were often taken from undamaged structures. More than one illustration so captioned had in the background a two story structure (concrete walls, wood roof and wood floors) which had slight damage. The extent of misinformation regarding damage within Los Angeles may be seen from the following extracts from a bulletin published in Los Angeles by and for building owners and managers. It was released shortly after the July 21st shock.

"Older Buildings erected prior to 1933 evidently built so well they withstood the shake 'even-Stephen' with some of the newer buildings 'scientifically' engineered to resist lateral (earthquake) forces."

"Old Adobe Buildings reported erected more than 125 years ago, weathered all earthquakes, including the last one, without a crack."

The inference from the last extract would be that adobe structures are "safe" in an earthquake. Even a casual knowledge of the history of California Missions should dispel this.

GENERAL EFFECTS

Intensities of the July 21, 1952, and August 22, 1952 earthquakes are found on isoseismal maps published by the U. S. Coast and Geodetic Survey (Part II—12). These maps are the product of their detailed report published as "Abstracts of Earthquake Reports for the Pacific Coast and Western Mountain Region," MSA-75. A brief description of the shaken area for both shocks and some of their effects follows:

July 21, 1952 Earthquake. The July 21, 1952 shock was felt over an area of 160,000 square miles according to the U. S. Coast and Geodetic Survey study (Part II—12). In Las Vegas, it was reported that a building under construction required realigning of the structural steel. In San Francisco, approximately 275 airline miles from Tehachapi, the authors have record of 12 pressure tanks, located on the roofs of buildings, which turned in signals due to the water within them moving up and down through a range of at least 6 inches. It is probable that other unrecorded instances occurred. In San Francisco the press recorded that the shock was primarily felt by persons in the upper stories of the multistory buildings. The Coast Survey reported that windows rat-



FIGURE 1. Lerner's store, 19th Street, just off Chester Avenue, downtown Bakersfield. Photo by *Bakersfield Californian*, courtesy State Division of Water Resources.

tled in such far away places as Quincy, northern California, Reno, Nevada, and San Diego, California, near the Mexican border. At least one building was damaged in San Diego.

Salt beds at Owens Lake moved horizontally and probably settled somewhat, and caused damage to surface installations. The salt beds are usually 60 inches to 70 inches deep in the areas which are being mined. Two-inch sample pipes, going through the salt beds, were bent, and indicated movement between various horizontal layers of salt beds. Not only was there movement between the layers, but the beds moved against each other causing 18 inch-high windrows on the surface. Salt beds rest on mud, and this mud was forced to the surface in several places. Structures located outside of the salt bed area were not damaged, except for cracks appearing in a brick boiler. The foregoing information is from Columbia-Southern Chemical Corporation at Bartlett, California, William K. Cloud of the U. S. Coast and Geodetic Survey and the authors' observations.

Metropolitan Los Angeles (some 70 to 80 miles south of the epicenter) suffered extensive non-structural building damage in the taller structures. Numerous power failures occurred and burglar alarms went off. Sixty-eight earthquake gas shutoff valves functioned (approximately 10 percent of the total) in the Los Angeles City School District. It was stated regarding the Prudential Insurance Building on Wilshire Boulevard, "literally miles of fluorescent light fixtures fell." Water sloshed out of many private swimming pools, and piping was broken in at least one location. Plate glass windows were broken at numerous locations. Structures in Long Beach and Santa Barbara were also affected.

In Kern County the shaken area can be divided into the effects in mountainous regions and in the alluvial San Joaquin Valley. Tehachapi is located in a relatively small alluvial basin as compared to the Bakersfield-Arvin area. Tehachapi was essentially an older town, the construction of the business district being primarily unreinforced brick with sand-lime mortar. Brick and adobe buildings suffered extensively. The town is not

large, for the report of safety inspection issued the day after the shock lists 37 inspected locations which covered practically the entire business area. While structural damage was severe, structural engineers who had studied the Long Beach, Helena, Santa Barbara, and other earthquakes, generally came to the conclusion that the degree of structural damage in Tehachapi relatively did not exceed that in Long Beach in 1933. The fact that 10 of the 12 deaths occurred in this community may have created an unwarranted assumption regarding building damage.

It is the authors' opinion that the Modified Mercalli Scale should be interpreted differently at the damaged railroad tunnels than that shown on the isoseismal map (Part II-12). The isoseismal map lists an intensity of XI at the tunnels, and damage was great. However, any man-made structure astride the surface dislocation of a fault will be seriously damaged. This applies equally to high-value tunnels or to low-value fences. Value of a particular structure should not determine earthquake intensity. To assign a single damage item with a high intensity rating is also questionable when one considers that various types of neighboring structures, not highly earthquake resistant, generally did not suffer material damage. A similar parallel can be drawn to oil well damage in Terminal Island. For further information regarding earthquake intensities as related to faulting, see pages 313-316 of the "Bulletin of the Seismological Society" for October, 1942.

Bakersfield is located on the delta of the Kern River. This river drains into Buena Vista Lake, which normally has no natural outlet. Large areas of marshland have been reclaimed from the Buena Vista Lake region, and much of this ground requires piling for any substantial structure.

Areas of filled or other than firm natural ground have always been identified with intensified earthquake effects. This was clearly noted in the San Francisco 1906 shock as well as in other earthquakes. In the 1952 earthquakes it was not possible to draw a sharp distinction



FIGURE 2. Old mill of Kern County Land Company destroyed in August 22 earthquake. Photo by *Bakersfield Californian*, courtesy State Division of Water Resources.



FIGURE 3. Looking southwest across Main Street, Tehachapi; undamaged reinforced concrete building, left center. *Wide World Photos.*

between damage to buildings on rock and those on poor ground due to the relatively few structures in areas which would allow such a comparison. However, damage at the Paloma Oil Refinery and at the Maricopa Seed Farm, located on former marsh and lake beds, was heavier than at the cities of Taft and Maricopa, on the Coast Range foothills. This becomes more significant when one considers that the steel structures being on the marshlands and having some earthquake bracing were damaged, while unreinforced lime-mortar brick buildings at Taft and Maricopa were only moderately damaged.

The present trend in building codes to ignore the intensified severity in saturated ground areas is not warranted by observed effects in the major shocks on record.

Arvin is partly old construction with unreinforced brick and concrete block; structural damage was severe in this older area. However, the performance of the reinforced concrete block and reinforced grouted brick in the newer section was good. The casual or inexperienced observer could be led to believe the earthquake intensity here was moderate compared to Tehachapi.

Damage in Bakersfield as a result of the July 21st shock was generally light and confined to isolated parapet failure. Numerous brick buildings were "loosened up" and cracks were apparent. Older public schools, not designed to resist shock, showed evidence of damage. In contrast to this general pattern was the severe damage to the Kern General Hospital. Another major structure

notably loosened up was the County Court House. Multi-story steel and concrete structures had minor damage generally confined to the first story, although some pounding was noted between wings in upper stories of El Tejon Hotel. It is reported that municipal swimming pools lost 25 percent of their water due to sloshing. Water from a 20-foot-wide canal spilled over its 4-foot embankment according to the Bakersfield Fire Department.

August 22, 1952 Earthquake. The earthquake of August 22 was relatively a local shock and damage was restricted to Bakersfield and immediate vicinity, although it was felt over an area of 40,000 square miles according to the U. S. Coast and Geodetic Survey. A comparison of isoseismal maps indicates the smaller scope.

Two people were killed and 35 injured in Bakersfield, and the small life loss is somewhat surprising for a metropolitan area with 75,000 population. Damage was principally confined to brick buildings within a 64 block area in downtown Bakersfield. Building collapses were few, but the extent of damage may be seen from the following data, correct to June 9, 1953:

* Status of damaged buildings	
Total earthquake damaged buildings	396 Structures
Torn down buildings	90 Structures
Repaired or being repaired	210 Structures
** Decision pending	96 Structures

* Does not include schools or other public buildings.
 ** At least nine of these probably will be torn down.

This list, of course, has changed since that date. Dwellings and a few commercial establishments were wood frame. Masonry structures were primarily confined to the downtown or commercial areas. Where structural damage occurred, buildings were repaired to their original condition or improved. In general, rehabilitation work in the Kern County area has been better than that following any previous shock. Kern County is in contrast to the "paint and plaster" repairs in San Francisco after 1906, and the superficial repair noted after the Santa Barbara and Long Beach shocks.

One point not generally appreciated is the cumulative effect of earthquake damage. One often hears statements to the effect that a structure came through one earthquake and "therefore" will come through the next one. Buildings in Bakersfield suffered progressive damage in shocks from July 21st on, and judgment on the severity of the August 22nd shock must be tempered with the fact that considerable damage already existed in many buildings. Kern General Hospital, however, had been temporarily strengthened after the July 21st shock and these strengthened areas suffered little or no additional damage.

Larger multistory concrete and steel frame buildings again suffered relatively light damage on August 22nd, although the damage was probably somewhat heavier than July 21st. One three-story reinforced concrete structure (Brook's Department Store) suffered serious structural damage. The August 22nd shock had predominantly higher frequencies which adversely affected the low rigid buildings.

The authors saw no evidence of transformer damage although isolated cases of toppling may have occurred. No damage was reported to elevated tanks; oil wells were again affected with production in some cases increasing and in others decreasing.

The following summary has been compiled from official city and county records, insurance company records, building owners' records, and personal estimates by the authors. The estimate is only of earthquake property damage, and thus does not include loss of revenue

from these properties. It is based on actual losses and excludes improvements and betterments often made during rehabilitation. The summary includes damage from the July 21st and August 22nd shocks, and also small aftershocks.

Building damage:	
Bakersfield	\$23,000,000
Kern county, except Bakersfield	4,250,000
Los Angeles, Long Beach, Pasadena	10,000,000
Santa Barbara	400,000
Total building damage	\$37,650,000
* Oil wells and refineries	2,000,000
Agriculture	6,000,000
Public Utilities	600,000
Dams, Roads and Bridges	100,000
Railroad	2,300,000
Total earthquake damage	\$48,650,000

* Probably over 75% of this fire damage at Paloma Refinery. No other significant fire losses occurred.

Damage to Structures. Structures can be grouped into two general categories according to their performance in earthquakes:

- A. Buildings without specific lateral force bracing systems: Structures of this type have been classed according to their materials of construction, as brick, wood frame, etc. For earthquake insurance purposes this has been broken into Classes I through VIII. Structures in classes I, II, and III generally have fair lateral force resistance.
- B. Buildings with specific lateral force bracing systems: Structures of this type possess a logical lateral force bracing system capable of resisting a high degree of shock. This system may be incorporated unknowingly but usually is specifically designed. For earthquake insurance purposes, structures in this category are termed class "Special Rate."

These two categories have significantly different performance records in severe earthquakes, especially for masonry and structures of large mass. However, the distinction between the two greatly diminishes for light structures such as wood dwellings and steel gasoline tanks.

Most of the materials and types of constructions generally considered hazardous in an earthquake can be



FIGURE 4. Looking east along Main Street, Tehachapi. Photo by Gordon B. Oakeshott.

made earthquake resistant by intelligent design and good construction. Structures of this type enjoy lower insurance rates and deductibles, and are usually rated as class "Special Rate."

Damage patterns of the 1952 shocks fall into two area divisions. In the July 21st shock, the areas of violent ground motion (Tehachapi, Arvin, etc.) experienced considerable damage to old unit masonry structures, but in distant cities such as Los Angeles, damage was principally to multistory structures. The August 22nd shock, being essentially local in character, caused damage in Bakersfield primarily to masonry structures.

The effects of these two earthquakes, plus the many aftershocks, are considered together, for the damage was cumulative in areas of strong ground motion.

*Abridged earthquake insurance classification
Pacific Fire Rating Bureau.*

Category	Earthquake class	Relative damage-ability	Simplified description of structures in this class
"A" Generally without specific lateral force bracing systems.	I	1.	Small wood frame structures, as dwellings not over 3000 square feet and not over 3 stories.
	II	1.5	One story all steel. Single or multistory steel frame, concrete fire-proofed concrete exterior panel walls, concrete floors and roof—moderate wall openings, otherwise Class V.
	III	2.	Single or multistory concrete frame, concrete walls, floors and roof—moderate wall openings, otherwise Class VI.
	IV	4.	Large area wood frames and other wood frames not falling in Class I.
	V	4.	Single or multistory steel frame, unreinforced masonry exterior panel walls, concrete floors and roof.
	VI	5.	Single or multistory concrete frame, unreinforced masonry exterior panel walls, concrete floors and roof.
	VII, Reduced base rate.	5.	Walls of cast in place or precast reinforced concrete, reinforced brick, reinforced concrete block, or reinforced brick, with floors and/or roof other than reinforced concrete. Reinforcing must be adequate.
	VII	7. up	Building with unreinforced brick bearing walls with lime mortar. Certain multistory steel or concrete frame structures with wood floors or unusually poor design features.
"B" E. Q. resistant	Special rate	VIII	Bearing walls of unreinforced adobe, hollow clay tile, or unreinforced hollow concrete block.
		0.5 to 2.	Buildings which can resist earthquake of 1906 type with minimum to slight property damage.

Note: Unfavorable foundation conditions and/or hazardous roof tanks can increase the earthquake hazard greatly.

Classes I and IV—Kern County. The relatively few wood frame structures seriously damaged was interesting. In 1933 in Long Beach, a large number of wood dwellings were thrown off their foundations. The authors, who spent many weeks in the Kern County area, saw scarcely ten off their foundations.

After the July 21st shock, dwellings in Tehachapi usually had plaster cracks and brick chimneys generally were down. Dwellings at General Petroleum's Rose and Emidio Pumping Stations were thrown off their founda-

tions. Inspection of dwellings thrown off their foundations usually revealed a complete lack of bracing or bolting to foundation walls. One dwelling southwest of Arvin slid off its foundation due to the lack of anchor bolts. This particular structure was located in an area of extensive ground fracturing.

One example of stone veneer on wood frame was noted at Wheeler Ridge, where the unanchored stone veneer collapsed on parked cars. One instance of veneered wood frame dwelling damage was reported in Bakersfield, but no damage was detected in the veneer.

Large wood frames, including iron clad, performed well in Kern County. Glass in markets and other large glass areas was broken. Because of the relatively light weight, comparative wind and earthquake calculations indicate that if most of these can safely withstand a strong wind, they can withstand severe shocks with minor to moderate damage.

Classes II and V, and Class "Special Rate"—Kern County. All steel gasoline service stations came through without damage. The wind versus earthquake analysis for wood frame warehouses also holds true here. Gasoline service stations generally qualify for the lowest earthquake insurance rates.

Prefabricated all steel warehouses were inspected at two locations. One in Bakersfield (at the San Joaquin Tractor Company) had stretched bracing rods after the August 22 shock. The other had no damage.

Few multistory steel frame structures are found in Bakersfield. One such structure, the Haberfelde Building, is discussed below under *Exposure*.

Classes III and VI, and Class "Special Rate"—Kern County. The July 21st earthquake damaged several multistory reinforced concrete structures in Kern County. The Paek House at the Monolith Cement Company received damage. The concrete panel walls were found to be not truly monolithic with the concrete frame but damage was moderate.

Tehachapi State Prison for Women, located in Cummings Valley, has been considerably misrepresented by the press. The several two story detention cottages have reinforced concrete walls, floors, and ceilings partially of reinforced concrete. Roofs are slate on steeply pitched wood framing. Built just prior to the 1933 Long Beach shock, they were not specifically designed to resist shock. Some evidences of faulty concrete construction have been found, but by and large the concrete appeared to be sound. The wood roof framing was somewhat illogical as well as deficient in detail. In addition to chimney failures, the roof tended to flatten due to the weight of the slate roofing and failure of the roof sill plates.

The structures were relatively long as compared to their width, and also of relatively rigid construction. However, numerous non-structural hollow clay tile partitions fractured indicating that even with the relatively slight amplitudes which occur in relatively rigid buildings this material may be damaged. Over-all damage to all structures at the prison was moderate.

Another rigid reinforced concrete structure is the Main Fire Station in Bakersfield. Designed to resist shock, damage was negligible. After serious damage occurred to the City Hall in the August 22nd shock, city officials moved their offices to this place of relative secu-



FIGURE 5. Looking at south side of Main Street, Tehachapi; Juanita Hotel at left. Photo by Gordon B. Oakeshott.

ity. Brock's Department Store, on the other hand, suffered heavy damage in the August 22nd shock. Earthquake resisting elements were unbalanced and resulted in a twisting motion (torsion). The south wall took most of the earthquake loads. This wall, poorly reinforced by today's standards and having poor quality concrete, cracked seriously but did not collapse.

The spectacular nature of fire damage is obvious, but earthquake losses sometimes are difficult to evaluate except by trained engineers. "Paint and plaster" structural repairs could have completely hidden this type of damage; this practice has been common in previous California earthquakes. "Paint and plaster" repairs after the 1925, 1926 and 1941 shocks in Santa Barbara fell apart during the July 21, 1952 shock.

Class VII and Class "Special Rate" with Reinforced Concrete Walls and Wood Roof—Kern County. The inherent resistance of structures with reinforced concrete walls and wood floors and roof, as compared to those with unreinforced brick walls and wood roof and floors, often has been noted. When well designed to resist shock and when well built, a high degree of earth-

quake resistance may be obtained in this type of structure. The July 21st earthquake was a clear indication of the variable performance of this type of construction. In Tehachapi, the Beekay Theatre, while not having a complete and logical bracing system, possessed inherent strength because of the few wall openings, low ceiling height, and small ground floor area (about 50 feet x 75 feet). It lost only one piece of acoustic ceiling tile in the shock. Performance of the Catholic Youth Center in Tehachapi was even more outstanding. It is a two-story structure with wood second floor and roof, and concrete walls. The only damage was a plaster crack all around at the ceiling-to-wall juncture. This structure was often seen in the background of press photos showing "Tehachapi Flattened." The Bank of Tehachapi, designed to resist shock, performed well except for the poorly constructed hollow concrete block parapets.

Cummings Valley School, a classic in poor design, poor material and poor workmanship, collapsed. The Shafter School, south of Bakersfield, suffered serious structural damage to the concrete walls and wood roof. This damage was due to subsidence of the foundation



FIGURE 6. Roundup Cafe at a Main Street corner, Tehachapi. Photo by Gordon B. Oakeshott.

material under a portion of it. See section on public schools below for further data.

The August 22nd shock caused no notable damage to this class.

Class VII and Class "Special Rate" with Reinforced Brick Walls—Kern County. A good example of brick designed to resist shock is the Arvin High School. It cost approximately \$3,800,000 to build and was constructed in stages by various contractors. Damage in the July 21st shock plus numerous strong aftershocks was less than 1 percent. No life hazard was involved. Details are found in the Public School Section below.

The Safeway Store in Arvin was constructed following the Store's current trend of very few wall openings. One story with wood roof, the walls are of reinforced brick masonry. Negligible damage was reported after the July 21st shock.

After the August 22nd earthquake the authors found no evidence in Bakersfield of any reinforced grouted brick masonry structure suffering damage, although it is probable that minor instances occurred. Further information on reported damage is being sought.

Class VII with Unreinforced Brick Bearing Walls and Wood Interiors—Kern County. The brick structures in this class are those with lime mortar and are generally lacking in earthquake resistance. Lime mortar possesses little structural strength and, as has been observed in all previous shocks, damage to this class of structure is generally serious.

A study has been made of the performance records of all brick structures in Bakersfield constructed prior to 1903, and which were in existence at the time of the 1952 shocks. The following is a summary, correct to November, 1952, of 71 structures:

Type of damage	Number of structures	percent
Heavy damage—torn down -----	14	20
* Heavy damage—repaired -----	19	27
Heavy damage—decision pending -----	2	3
Moderate damage—torn down -----	1	1
* Moderate damage—repaired -----	21	30
Moderate damage—decision pending ---	7	10
Slight damage—repaired -----	6	8
No damage -----	1	1
	71	100

* Of these, 16 had one or more of the upper stories removed

The statement sometimes made that the "older structures are substantial because they have stood the test of time" is a fallacy.

The performance of unreinforced brick built after 1903 is in no way different than that prior to 1903. Structures in Arvin and Tehachapi damaged in the July 21st shock showed similar effects to those in Bakersfield after August 22nd, and in most cases with more spectacular results. Performance of unreinforced stone buildings was not particularly different from brick.

Class VIII with Unreinforced Brick Bearing Walls and Interior Steel Frames—Kern County. Structures having concrete floors, steel beams and steel interior columns, but with exterior bearing walls of unreinforced brick with lime mortar performed in a fashion similar to conventional brick-joisted construction. These usually are not earthquake resistant and are not given Class "Special Rate." The principal damage in Bakersfield

from the July 21st shock occurred to the Kern General Hospital. On August 22nd serious damage was suffered by the Kern County Court House. It is similar in construction to the Hospital, except that the footings were reported to be of brick instead of concrete and more hollow clay tile partitions were used. The Court House was immediately abandoned.

The *Bakersfield Californian* newspaper building is the only one in this class known to have experienced only slight damage. Evidence of movement of the north wall with respect to the roof and floors was detected after August 22nd.

Class VII and Class "Special Rate" with Metal Roofs and Masonry Walls—Kern County. Two examples of this class in Bakersfield were studied in detail; both of these suffered slight damage in the August 22nd shock.

The Fox Theater in Bakersfield dropped the metal roof where it joined the proscenium wall. This failure was due to the steel purlins (having no anchor bolts) pulling out of the concrete wall. Anchorage specified on the original drawings was not complied with. This structure was not specifically designed to resist shock. Considering that the metal roof deck was held in place by light sheet metal clips and that it had none of the characteristics of a structural diaphragm, it is surprising that more damage did not occur. Over-all damage must be classed as slight.

The San Joaquin Tractor Company in Bakersfield is another example of a one story structure with a metal roof. A moderate amount of earthquake bracing exists. Front and side walls are of reinforced concrete, while the rear wall was hollow concrete block panels. Built about 1949, the walls are well reinforced. While rod bracing exists in the roof, it was so constructed as to be largely ineffectual. As the result of the July 21st shock, glass in the northeast wall broke and the construction joints showed signs of movement. The August 22nd shock loosened the roof to wall connection by pulling out anchor bolts. Of further interest is the lack of damage to the metal deck not specifically designed to resist shock. Overall damage was slight.

Also of interest is the Simpson Motors structure at the corner of 3rd Street and Hill in Arvin. One story in height, it has a metal roof supported by steel beams and light steel trusses. Walls are 8 inch reinforced hollow concrete block and are load bearing. Designed to resist shock, although having what would normally be considered excessive openings and glass areas, damage was negligible. Damage was primarily confined to glass breakage, and it has been reported that one minor wall crack appeared. Ground motion was strong enough to throw the roofing gravel off the roof. The hollow concrete block walls act as shear walls to take the earthquake forces to the ground. The earthquake bracing in the roof is by means of a system of steel flat bars used as X-bracing, and the metal deck was not used as a diaphragm.

Class VIII and Class "Special Rate" with Hollow Concrete Block Bearing Walls and with Wood Floors and/or Roofs—Kern County. Concrete block is a relatively new material as far as general structural use is concerned; it has been principally used in the last 20 years. Its earthquake performance record is short and



FIGURE 7. Looking south at west end of Main Street, Tehachapi. Photo by Gordon B. Oakeshott.

virtually non-existent for reinforced block prior to this shock.

Performance of concrete block structures in these earthquakes was as variable as other unit masonry types. The degree of damage decreased as the degree of earthquake bracing increased. Structures with well reinforced hollow concrete block and lacking other strong earthquake bracing (as roof ties) followed a pattern similar to structures with reinforced concrete walls.

Hollow concrete block buildings designed to resist heavy shock, such as the Bank of America in Arvin, had slight damage, while non-reinforced or poorly reinforced hollow concrete block buildings were seriously damaged.

The relatively few hollow concrete block failures has caused some unwarranted comparison with unreinforced brick. The bulk of the damage in Kern County was to the large number of buildings of unreinforced brick, while it was the authors' observation that most of the hollow concrete block was reinforced. This can be attributed to the fact that hollow concrete block has been used as a building material primarily in recent years and it has been in this period that earthquake bracing in the form of reinforced unit masonry walls has become generally accepted. The policy of the Pacific Fire Rating Bureau is to give equally low earthquake insurance rates to buildings of both materials, provided the same degree of earthquake resistance exists in both.

Class VIII, Adobe Bearing Walls — Kern County. Wherever inspected, unreinforced adobe was seriously damaged or destroyed. No attempt was made to make a complete survey of this type of construction. Damage was general to practically all adobe dwellings in Tehachapi. The use of a concrete bond beam in one structure was not adequate. The July 23, 1953, special edition of the Tehachapi News stated that "every adobe house was either completely demolished or damaged beyond repair."

At Grapevine, an adobe motel collapsed. All adobe structures of which the authors have record on the large Tejon Ranch and also on the Karpe Ranch were damaged and were torn down. The Kern County Fire House at Keene was seriously damaged and not safe for use.

One reinforced adobe dwelling located on hospital premises in Taft was slightly cracked. The one story county offices in Bakersfield (on U. S. Highway 99) are reported to be reinforced; only minor cracking was noted.

Special Structures — Kern County. Precast reinforced concrete has been developed considerably in recent years. Usually the strength of each individual panel of concrete is not in question, but rather the method of interconnection (or "joining") of these panels. Panels may weigh only a few pounds or as much as 8 to 10 tons. The most common type in this class is the so-called "tilt-up." These are usually one story, with wood roof and precast reinforced concrete walls. A number are found in the Bakersfield area. Practically all of these have been constructed to resist some degree of earthquake and some would qualify for Class "Special Rate." The main damage at one location may have been the result of misapplication of building code provisions. In order to keep the end walls "non-bearing" and thus thinner (less concrete to be placed and lifted), roof joists parallel to the wall were anchored only to their supporting beams, but not to the adjoining wall. Movements between the walls and the roof diaphragm was sufficient to tear the roofing.

The Lockheed plant in Bakersfield sustained major damage in the August 22nd shock. Its roof and walls are of precast concrete. The design drawings were not followed in many important respects and much earthquake resistance was lost. The Di Giorgio Winery southeast of Bakersfield has one structure with a precast roof. Despite the heavy shaking, the roof system stayed together.

Cement silos at Monolith had negligible damage, but eight silos at Karpe Ranch (on Highway 99, south of Greenfield) were damaged. The latter were conventional poured-in-place construction instead of the "slip-form" process, and damage was noted at the construction joints. No masonry stack failures were reported but Monolith Stack No. 1 was later torn down, primarily due to its weakened condition and potential earthquake hazard to the adjacent kilns in the event of collapse.

The old sewage disposal plant at Bakersfield was damaged while the new plant was not. Wave action (not unlike that which damaged steel oil tanks) working against the steel baffles caused damage.

Exposure — Kern County. Two types of building damage can occur owing to exposure to hazards outside of the building: pounding and failure of overhanging structures.

Two structures, built with no, or inadequate free space between, can pound together in an earthquake. A good example of this in Bakersfield was the Haberfelde Building in the August 22nd shock. The building is structurally two independent units, this being the result of a major addition made shortly after the original building was built. From appearance, occupancy, and fire standpoints they are one. These two units pounded together causing considerable nonstructural damage. Two adjoining buildings also pounded this structure. Not commonly realized is the fact that this pounding also occurs to smaller structures. The Brower Building had considerable structural damage and the pile of dust at the foot of the junction between it and the adjoining building is an indication of the motion. The Brower Building is brick joisted, except that steel beams and east iron columns exist along both street fronts.

Earthquake separation between Brock's Main Store and its Addition was satisfactory just as it was at Kern General Hospital between the 1938 Addition and the 1929 Wing.

Overhanging parapets are a serious life as well as property hazard. When parapets fall on adjoining buildings, as they did in numerous instances in Bakersfield, both life and property are in danger. Parapets usually are the first to fail, and in the July 21st shock caused serious structural damage. Also, we note with interest that the same shock caused damage to at least two structures in distant Santa Barbara when parapets from adjoining buildings fell.

Bakersfield—Summary of Building Damage. Damage to fire resistive multistory structures has already been discussed. The following tabulation was made from Bakersfield Building Department and the Pacific Fire Rating Bureau's records in conjunction with maps of the Sanborn Map Company. The tabulation is correct to July 1953. Kern General Hospital and public schools are excluded.

*Floor Areas of Structures with Masonry Walls,
Wood Floors and Roofs.*

	Torn down (pet.)	Repaired (pet.)	Repair or demolition undecided (pet.)	In- damaged (pet.)	Total (pet.)
Brick	16	42	20	22	100 (2,717,410 s.f.)
Concrete brick	20	40	36	4	100 (230,950 s.f.)
Concrete	6	12	6	76	100 (1,186,680 s.f.)
Hollow concrete block	2	6	*	92	100 (488,525 s.f.)

* Negligible.

The percentages in the table are based on floor areas, and the total is the total floor area involved excluding basements. In some instances damage may be partly or entirely from outside hazards such as overhanging parapets or the building pounding against the adjacent struc-

ture. Repaired structures include those which have had their upper stories removed due to shock damage.

No attempt was made to segregate structures by degree of lateral force resistance. However, inspection of numerous structures and examination of many plans indicates that the conventional brick and concrete brick were by and large of lime mortar and without reinforcing steel. The walls of concrete and hollow concrete block, however, were usually reinforced and the average mortar in the hollow concrete block was better than that of the brick. The variation in earthquake performance has been explained previously in this paper. When specifically designed to resist a high degree of shock, little loss should be expected and each type of construction should give approximately equal performance.

Los Angeles—Summary of Building Damage. Damage in Los Angeles as a result of the July 21, 1952, shock was generally confined to fire resistive structures over five or six stories high. A few isolated instances of minor damage to one and two story non-fire resistive buildings were noted but they are not significant.



FIGURE 8. Grapevine Motel, U. S. Highway 99. Photo courtesy Chief, Seismological Field Survey, U. S. Coast & Geodetic Survey.

This pattern of damage is in contrast to that which was experienced in Kern County on July 21st and in Bakersfield on August 22, 1952, in that the one and two story brick bearing wall buildings were most affected as compared to the taller fire resistive type such as the Hotel Padre and the Haberfelde buildings. One explanation for this difference is that the earth motion in the Los Angeles area was generally of longer periods which adversely affect taller buildings with corresponding longer natural periods. In other words, the motion some 70-80 miles from the epicenter was such as to excite vibrations of crack-producing magnitudes in tall structures while not affecting the lower more rigid buildings. Another contributing factor is the previous damage to these tall buildings in past shocks, particularly the Long Beach shock of 1933. It is known that effective repairs were generally not made after these shocks or even after the July 21, 1952, shock for that matter. No cases of structural damage were noted and principal damage was to partitions, masonry filler walls, ceilings, marble trim, veneer and exterior facing. Considering the relative value of these items as compared to the structural frame and floors it can be seen, and has been proven in past shocks, that non-structural damage can amount to 50 percent or more of the value of the building.



FIGURE 9. Frame house in Bakersfield after the earthquake of August 22, 1952. Photo courtesy *The San Francisco Examiner*.

It should be added that the buildings under discussion above are the older ones without adequate earthquake bracing. The newer earthquake resistive structures behaved well with the exception of one of relatively flexible design which suffered damage to interior partitions and trim. Unfortunately, the number of tall earthquake resistive structures, even in Los Angeles, is still a very small percentage of the total and the over-all behavior in a future shock would still be poor.

Long Beach—Summary of Damage. Behavior of tall buildings in Long Beach was similar to that in Los Angeles. However, it is disquieting to note rather extensive damage to major structures in some cases when one considers that they were located some 100 miles south of the epicenter. Again damage was confined to partitions, unreinforced masonry panel walls, and other non-structural items. In the 1933 shock these buildings in general suffered more extensive damage than those in Los Angeles, and the methods of repair were often equally ineffective. The Pacific Fire Rating Bureau's files contain damage reports on the taller buildings which are practically identical for 1933 and 1952 and there is no reason to believe that a future shock would produce any different results.

Santa Barbara—Summary of Building Damage. The damage pattern in Santa Barbara was similar to that in Los Angeles and Long Beach except that somewhat more damage was suffered by several one and two story masonry structures. Three taller buildings suffered varying degrees of damage and again this could be attributed to previous poorly repaired earthquake damage in 1925, 1926 and 1941. Severe structural damage was suffered

by at least one of these tall structures. It should be noted that there are few buildings over three or four stories in Santa Barbara.

PUBLIC SCHOOLS

The design standards or building code for public school construction in California have been substantially the same since 1933, although details of the code have been revised several times. It was adopted after the passage of the so-called "Field Act" which regulates design and construction of public schoolhouses throughout the state. This Act was passed as a result of the poor structural behavior of existing school buildings in the shock of March 10, 1933. The code was under revision at the time of the subject 1952 earthquakes.

In general, this code (known as Title 21, California Administrative Code) covers standards of earthquake resistant design and construction. One important requirement is for continuous resident inspection during construction. Also general construction supervision is required by a licensed architect or structural engineer, and engineering supervision by the Division of Architecture. Altogether, this inspection and supervision provides excellent construction control for public school buildings. The earthquake bracing provisions of Title 21 are designed to prevent life loss in an earthquake of the intensity of the San Francisco 1906 shock, and in such a shock to keep property damage to a minimum. The law, however, contained no retroactive provisions and therefore the earthquake bracing provisions of Title 21 are not mandatory in structures built prior to the Act.

Earthquake requirements of the Division of Architecture did not materially differ from the recommendations of the Pacific Fire Rating Bureau.

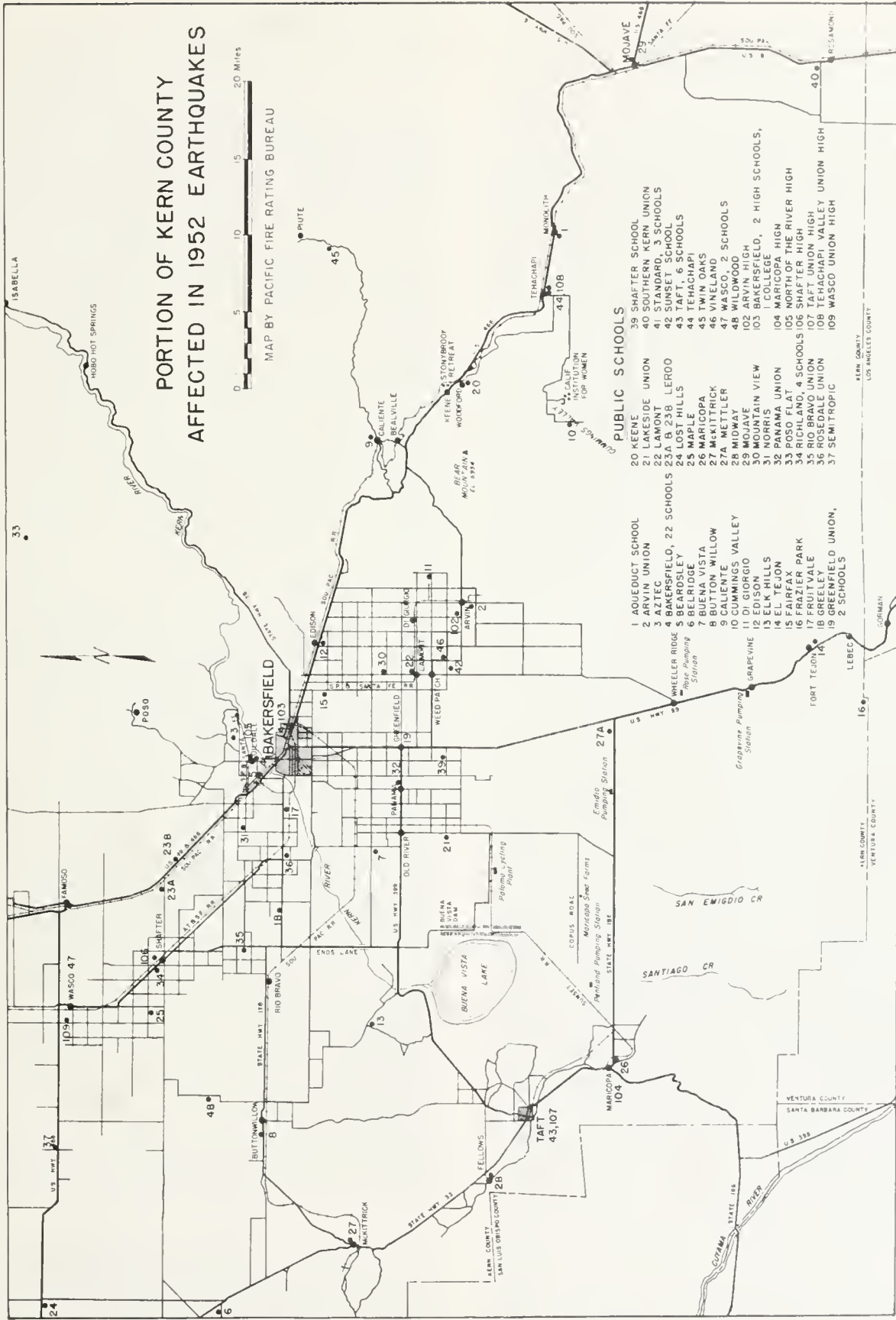


FIGURE 10.

Damage to the schools in the area affected by the earthquakes was considerable and confined to the older masonry structures, with certain exceptions. Complete damage data for the area as a whole are not available at this time but an idea can be had from the Bakersfield City School District where building areas totaling about 288,000 square feet were damaged so severely, after the August 22nd shock, as to require their removal from service. This involves about 175 classrooms serving slightly less than 6,500 pupils. Of these buildings about 16,000 square feet can possibly be rehabilitated. The total replacement cost is estimated to be \$6,191,000 in this one district. An unofficial estimate of the replacement costs of schools in Kern County, exclusive of the Bakersfield City School District, is \$6,663,000. This latter figure is the result primarily of July 21st damage.

The pattern of severe damage in the schools was similar to that of other types of structures, and in general followed the pattern of previous earthquakes. The buildings constructed under the controls of the Field Act were practically undamaged, whereas the older buildings were seriously affected. At some schools, the contrast between the condition of buildings constructed before 1933 and the later buildings was impressive.

There was some slight damage to school buildings constructed under the Field Act, and in general the damage furnished valuable information to structural engineers. The most extensive damage in a "Field Act" school occurred at the Arvin High School. This plant consists of a number of buildings nearly all of which have reinforced grouted brick exterior walls to provide the necessary earthquake resistance. One of these walls at the west end of the Administration Building in the second story cracked in the first shock. While there was no collapse, the wall was so weakened in the aftershocks that damage to the side wall columns and interior plaster partitions resulted. Inspection showed that the construction of this wall was not good. Adhesion was imperfect between the brick and mortar and the reinforcing steel was not thoroughly embedded in grout. It is probable that damage was caused by this faulty construction. There would have been no injuries or lives lost in this building even if it had been occupied at the time of the earthquake. There was no damage in the reinforced brick walls of the one story classroom buildings although there was minor damage in particular details in some of the other buildings. The total cost of repairs at this high school plant was less than one percent of the total value of the plant. The contrast is noticeable between this loss and the losses ranging up to 100 percent to unbraced buildings in downtown Arvin.

Another example of faulty construction is the defective bracing system in the Tehachapi High School gymnasium. Fortunately there was sufficient reserve of strength in this building to prevent all but slight damage although the shock was severe as evidenced by overturned shop equipment. There was some plaster damage in the older non-conforming portions of this school plant but no other damage in the modern portions.

An example of the poorest of the older non-conforming buildings is the Cummings Valley School which was built about 1910. This was a small, one-story unit with

concrete walls and a wood-framed, shingle-covered roof. There was a little reinforcement in the walls but this was ineffective since there were no lapped splices in the bars either in the walls or at the corners. Neither were there dowels at the bases of the piers. The concrete was made from excessively fine materials and had little strength. The building collapsed.

The damage to the old Vineland School represents typical damage to non-earthquake resistant school houses with brick bearing walls. The collapse of the brickwork over the main exit ways from the building and the progressive loosening up of the building during the aftershocks has been observed in past earthquakes. The severe damage to this building was in contrast to the new wing, constructed under the Field Act, which suffered no damage.

Shafter School, located south of Bakersfield, has concrete walls and wood roof framing. Located in the Kern River delta area, it is probable that many years ago a part of the school property was the river bed. All of this land has since been leveled either by natural means or by farmers for irrigation purposes. In the July 21st shock the portion of the building resting over the poorest ground of the old river bed settled as much as several feet. The result of this subsidence was the breaking of the concrete walls, rendering the building unsafe for use.

There were seven additions to the Tehachapi Elementary School constructed under the Field Act. Several were of reinforced concrete frames and walls, one of steel and concrete "tilt-up" construction and one of wood frame and stucco. There was some plaster cracking and spalling but no structural damage. Plaster cracks were pronounced where the ceiling metal lath was turned down along sides of concrete roof or ceiling beams. In the latest addition (wood frame) cracks and spalls occurred at window sills and heads adjacent to narrow plywood shear panels in the exterior walls. Similar slight damage occurred at bottoms of architectural fins. Sash putty was badly macerated. In the assembly unit the roofing was cracked sufficiently to cause leaks during a rain on July 29th. Many of the reflectors from the lights in the classroom units had fallen to the floors. Books slid from cases and shelves. Probably most of this damage can be attributed to the flexibility of the construction, due to the large glass areas and the difficulty of inserting stiff bracing panels in the walls. The cost of repairs was reported to be about \$600. Considering the extensive damage to masonry commercial buildings two blocks distant, it is gratifying to note the excellent behavior of this school plant under these conditions.

The failures in these earthquakes emphasize the need for competent and continuous inspection during construction. This is not intended to infer that contractors are unwilling to construct buildings in accordance with plans and specifications, but competent inspection is an added factor in accomplishing the desired result. In fact good inspection is an aid to the conscientious builder.

ACKNOWLEDGMENT

The authors would like to acknowledge the considerable work and research done by the California State Division of Architecture, in particular Mr. M. A. Ewing, in order to make this section on public schools complete.

10. THE DESIGN OF STRUCTURES TO RESIST EARTHQUAKES

BY G. W. HOUSNER *

ABSTRACT

A discussion is presented of special structural behavior, observed to have taken place during the Arvin-Tehachapi earthquake, whose implications are of interest in the design of structures. Some experimental data are presented on the measured behavior of a structure when subjected to ground motion, and the effect of mass, stiffness and damping on the response of the structure is discussed. A short description is presented of current methods of design to resist earthquakes.

INTRODUCTION

The occurrence of a strong earthquake focuses attention on the importance of designing structures to withstand the stresses produced by the motion of the ground. The majority of the existing structures in the western United States were not designed to resist earthquakes, and hence are particularly susceptible to damage. This was true of those structures in the vicinity of the epicenter of the Arvin-Tehachapi shock, for only a small percentage were of modern earthquake-resistant design. None of the severely damaged structures had been designed to resist earthquakes, so that it is not surprising that they suffered damage. The chief lesson to be learned from the behavior of these structures is that buildings, water tanks, etc., that are not designed to resist earthquakes should not be erected in localities that are subject to earthquakes.

The damage to the poorly designed buildings did bring out one significant fact, namely, that a shock may damage a structure to a greater degree than is superficially apparent. The Arvin-Tehachapi shock of 21 July caused a moderate amount of readily observable damage in the city of Bakersfield, chiefly toppling of parapets and cracking of walls. Some buildings suffered damage which was not so obvious but could be described as a general loosening. This was sufficiently disturbing so that steps were taken to tighten up and tie together quite a number of these buildings. However, the general feeling was that the city of Bakersfield had not suffered very severely, but when the city was shaken by the after-shock a month later widespread damage appeared. The visible damage was disproportionately great when compared to that caused by the original shock. There was no doubt that the first shock had weakened many buildings to the point where the second shock could easily produce serious visible damage. A similar instance was that of Helena, Montana in 1935. This city was shaken by two earthquakes with approximately the same intensity; the second shock produced much greater, severe, visible damage than the first shock. The lesson to be learned from this is that an earthquake may cause internal damage and weakening of buildings that is not readily apparent but which has appreciably reduced the ability of the buildings to resist earthquakes. In this way a series of shocks, none of which is sufficiently strong to cause serious damage by itself, may by a cumulative effect produce severe damage.

A simple example of the cumulative effect of earthquakes is the behavior of an elevated water tank. It is often observed that after an earthquake the steel cross-

bracing rods, which give the structure its strength to resist lateral forces, have been elongated. When the rods have been retightened by means of the turnbuckles the tank has been restored superficially to its original condition. However, there is a limit to the total elongation that a rod can undergo without breaking. If this ultimate elongation of the rod is 4 inches, and the earthquake elongated the rod 2 inches, then after the rod is retightened it is in a condition where it can withstand only an additional 2 inches of elongation. A second or third earthquake may thus collapse the tank.

BEHAVIOR OF WELL-DESIGNED STRUCTURES

A well-designed structure is one for which the design has taken into account the stresses that may be produced by an earthquake and structural members are incorporated having the requisite strength to resist these stresses. In order to accomplish this it is essential to have an understanding of how structures behave during an earthquake. The slipping along an earthquake fault releases stress waves which travel through the earth's crust. When they reach a point on the surface of the earth a vibratory motion is experienced during the passage of the waves. The motion of the ground will induce oscillatory stresses and strains in a structure. The characteristics of vibratory motion of a structure will depend upon the characteristics of the ground motion and also upon the properties of the structure, such as size, shape, mass, stiffness, damping, etc.

The building vibration induced by ground motion is illustrated in figures 1 and 2. Figure 1 is the measured horizontal ground acceleration (Hudson et al. 1952), and figure 2 is the measured horizontal acceleration of the second floor of the building. The ground motion was produced by the detonation of 370,000 lbs. of buried explosive at a distance of approximately 1000 feet from the building. The ground acceleration (figure 1) was measured on the floor of the sub-basement of the building and it is very similar to the ground motion of a moderately strong but very short duration earthquake. The building is a steel-frame mill building with corrugated-iron siding and roofing. The building motion (figure 2) was measured on a 6-inch thick concrete floor slab that was 45 feet above the ground floor and was restrained laterally by vertical cross-bracing in the walls. The building had been designed to resist earthquakes and it had a period of vibration of approximately $\frac{1}{3}$ sec.

The oscillatory motion of the building is clearly exhibited by figure 2. It is seen that there were 12 reversals of stresses during the more violent motion of the building. The strong ground motion had a duration of 1 second and during this time there was an increase in the motion of the building which was then followed by a gradual decay of the vibrations. The maximum ground acceleration was 8 percent of gravity and the maximum building acceleration was 10.5 percent of gravity. Had the duration of the strong ground motion been 5 seconds instead of 1 second, appreciably higher building accelerations would have been experienced.

* Division of Engineering, California Institute of Technology.

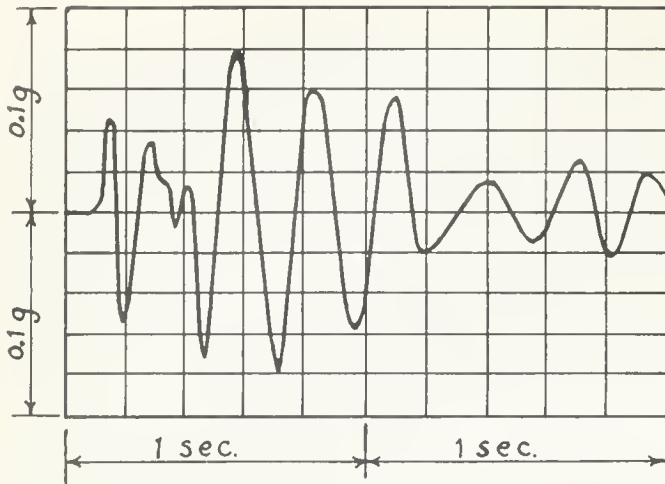


FIGURE 1. Recorded ground acceleration of explosive-generated ground shock.

If the mass, stiffness, or damping of the building were different, the building motion would be different from that shown in figure 2. In particular, the maximum building acceleration would be different. Figure 3 shows the effect of building properties upon the maximum building acceleration. The curves of figure 3 are the computed maximum accelerations of the building corresponding to the ground motion of figure 1 for various combinations of mass, stiffness, and damping. The mass and stiffness are reflected only in the period of vibration of the building, for example, the actual building had a period of vibration of $\frac{1}{3}$ of a second but if either the mass were decreased or the stiffness increased the period would be shortened, and vice-versa. A significant feature of figure 3 is that it shows that buildings that are identical in every respect except in stiffness will experience quite different building accelerations. It also shows that damping may have marked effect upon the building response. The curves shown are for 0.02, 0.05, and 0.10 of critical damping.

The curves shown in figure 3 characterize the ground motion of figure 1 but they are not typical of earthquake ground motion. Corresponding curves have been computed for various strong earthquake ground motions and these have been published in the Bulletin of the Seismological Society of America (Housner et al. 1953).

As can be seen from the foregoing, a structure will undergo a complicated vibratory motion during an earth-

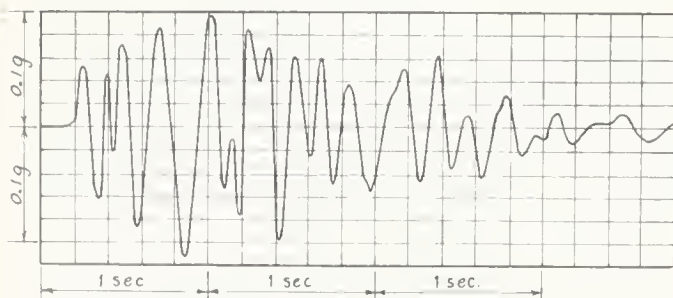


FIGURE 2. Recorded acceleration of upper floor of mill building.

quake. The strong ground motion during the Arvin-Tehachapi shock had a duration of approximately 10 seconds and a maximum ground acceleration of approximately 18 percent g was recorded 30 miles from the epicenter, at Taft. These ground accelerations were thus more than twice as great and were 10 times the duration of the ground motion shown in figure 1. The motion of structures during the Arvin-Tehachapi shock were thus appreciably more severe than would be experienced from the explosive-generated ground shock. In view of this, it is clearly impossible to reconstruct the motion of a structure from an examination of its condition after the earthquake.

When trying to evaluate the behavior of those structures that had been designed to resist earthquakes it must be borne in mind that they underwent a severe vibration whose intensity and characteristics depended upon the size, shape, mass, stiffness, damping, etc., as well as upon the ground motion itself. With so many factors involved it is not possible to draw general conclusions from isolated specific instances; however, there is valuable information to be derived from an examina-

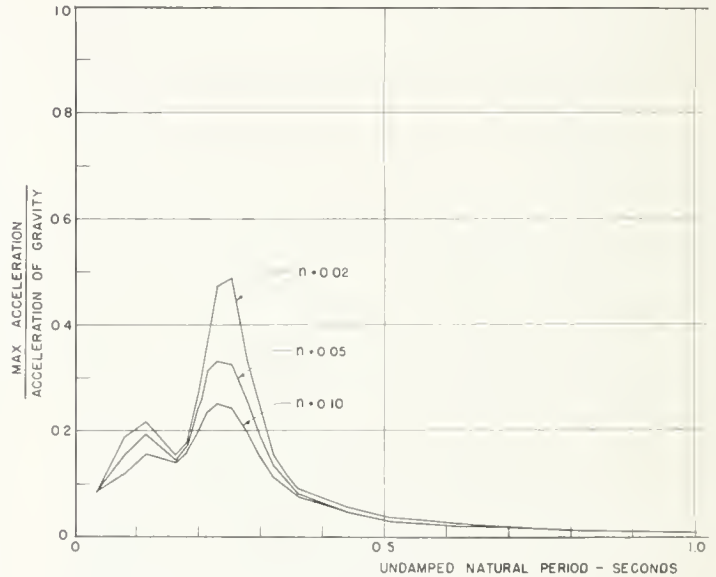


FIGURE 3. Maximum acceleration for various periods of vibration and damping.

tion of damaged structures. A number of structures in the Arvin-Tehachapi area that had been designed to resist earthquakes did show evidence of having been overstressed. There were several elevated water tanks (10 percent g design) whose bracing rods had been stretched thus showing that the actual stresses had been greater than those which would be produced by a static lateral force equal to 10 percent of the weight of the tank. A number of tall cantilever oil refinery columns whose anchor bolts had been designed for 12 percent g at 15,000 p.s.i. had vibrated sufficiently to stretch the anchor bolts. This would indicate stresses greater than those produced by a static lateral load of approximately 36 percent g. A reinforced brick shear wall in a new school building was diagonally cracked, indicating stresses greater than those for which the wall had been designed. In addition to the foregoing, there was some

overstressing of connections, cracking of the walls of a small reinforced concrete-block building, wracking of a precast concrete roof slab, etc. It is true that it is invariably the weakest part of a structure that is damaged first, and the initial reaction is to consider that an error has been made in design which, if corrected, would give a completely sound building. Sometimes it is true that the weakness did result from an error in design or construction but in many instances the weakness should not be attributed to an error, due to the fact that every structure has a weakest part. At the present technological level the best that can be done is to make all of the parts have approximately the same strength and the factors of safety used in the design are intended to provide a tolerance that will take care of the unavoidable differences in strength.

From this point of view, it must be concluded that the intensity of the Arvin-Tehachapi shock was of such a magnitude that it was just at the threshold of damaging structures that had been designed to resist earthquakes. Except for isolated cases of damage, such as those mentioned above, the well designed buildings survived the shock with no apparent damage. If the intensity of the ground motion had been greater there would undoubtedly have been more damage to earthquake-resistant designed buildings. The recorded ground motion at Taft (30 miles from the epicenter at Wheeler Ridge) had an intensity approximately half as great as that at the town of El Centro during the May 1940, El Centro shock, and perhaps half as great as that in the Long Beach-Compton area during the March 1933 Long Beach shock. It is estimated that the intensity of ground motion just north of Wheeler Ridge was of the same order of magnitude as that at El Centro during the 1940 shock.

From the observed damage it can also be concluded that special structures such as the oil refinery columns, elevated water tanks, etc., are likely to experience greater stresses than ordinary buildings. These special structures are of a type that has very low damping and thus will experience relatively large vibratory motion during an earthquake. In addition, structures of this type have no sources of strength other than the structural elements provided to resist earthquake stresses. For example, the cross-bracing on an elevated water tank is the only element resisting lateral forces, whereas in a building there are often other sources of strength such as interior partitions, concrete fireproofing of steel beams and columns, etc. Although such elements are not taken into account when making the design, they do contribute to the ultimate strength. Also, buildings that use the exterior walls for the main lateral load carrying elements will often be much stronger than the nominal design values if the walls have a few window and door openings. For special structures of the aforementioned type it thus appears advisable to use somewhat larger lateral load factors in the design than for ordinary buildings.

CURRENT METHODS OF DESIGN

During an earthquake a structure is excited into a more or less violent vibration, with resulting oscillatory stresses, which depend both upon the ground motion and the physical properties of the structure. This is such a complex dynamic problem that it does not appear feasi-

ble to make a precise dynamic stress analysis of the problem, particularly inasmuch as it is not possible to foretell the precise nature of future earthquake ground motion nor to compute precisely all of the physical properties of a structure before it is built. The present methods of design are based upon a static rather than a dynamic approach, the structure being designed to resist certain static lateral forces. The static lateral forces are intended to produce stresses of the same order of magnitude as the maximum dynamic stresses likely to be experienced during an earthquake. Because of the complexity of the vibration problem and the various factors influencing the dynamic behavior of a structure, it is not possible to state with certainty the correct static loads that should be used in all instances, so that the loads used in present design methods must be considered as approximations which will be improved as additional knowledge is gained. To indicate the nature of the current methods of designing against earthquakes the following outline is given.

DESIGN LOADS

The Structure as a Whole. The structure as a whole, that is, the main load-resisting system, is designed to withstand a specified static, lateral load. Each element of mass of the structure is assumed to exert a lateral force of intensity $F_L = CW$, where W is the weight of the element of mass and C is a specified seismic coefficient. The structure is designed to resist the lateral load for any possible horizontal direction of F_L . The tributary loads induced by F_L are apportioned to the main lateral-load-bearing elements in accordance with analysis which take into consideration the relative rigidities of the different parts of the structure.

As for the direction of application of the horizontal load, it is customary to analyze only two cases, namely, with the lateral forces applied separately, parallel to the two principal axes of the structure. In apportioning the tributary loads to the main lateral-load-bearing members, it is not customary to make a refined analysis. An accuracy of ± 10 percent is considered satisfactory. The labor involved in making a more exact analysis is not warranted because application of static instead of dynamic lateral loads very likely introduces an error in load distribution of at least that magnitude.

The main lateral-load-resisting system may be a steel, concrete, or wood frame; or it may consist only of the walls and floors of a building, which then are designed as structural elements; or it may consist of a system of vertical and lateral trussing. In framed structures having rigid concrete floors or rigid masonry walls, the floors and walls are considered to be parts of the lateral-load-carrying system.

The coefficient C in the formula for lateral forces has magnitude which is intended to give a static lateral load which will produce stresses in the main structural elements of approximately the same order of magnitude as would be produced by severe earthquakes. At present the magnitudes of the coefficient C used in different regions of the state reflect the opinion and judgment of the engineers and officials who have written the design specifications which are incorporated in the various building ordinances and laws. In the light of this fact the regional

variations in the values of C may be taken to represent opinions concerning seismicity of the various regions. Furthermore, the values of C may depend upon the height of the structure and may vary along the height, the variations reflecting the results of experience and research concerning equivalent static loads. The magnitude of C may also vary with subsoil conditions such as the static and dynamic load-bearing capacities of the foundation material, and with the type of foundation used to support the structure. The magnitude of C may also vary with the function of the structure. For example, school buildings, important elements in electric-power systems, and other structures, damage to which might cause serious public hazard, may be designed to resist larger than usual lateral loads, whereas some structures such as light frame dwellings are often designed to resist smaller than usual lateral loads. Such variations reflect a weighing of costs against possibility of future losses. Current practice in regard to the magnitudes of the coefficient C is exemplified by the building codes in use in California. Pertinent excerpts from building codes are given further on.

Studies have shown that for a given earthquake the appropriate value of C to be used depends upon the type of structure under consideration. Not enough information is at present available to permit assigning values of C which are known to be the most suitable. As a consequence, engineers are not in complete agreement concerning the values of C which should be used. However, as additional knowledge is built up, it should become possible to assign proper values to C for earthquakes of specified intensity. It is, of course, not possible to predict the maximum intensity of future earthquakes.

Experience has shown that the requirements for earthquake-resistant design increase very little the cost of the ordinary small structure, but that when they are applied to large structures the increase in cost is more appreciable. For example, the design requirements when applied to a twelve-story building are difficult to meet. Although it is a simple matter to design a parapet wall for a seismic coefficient $C = 1.00$, it is not easy to construct a twelve-story building to resist a seismic coefficient $C = 0.10$. The difficulties encountered in designing large structures make it important to know the proper values of the seismic coefficients, and it is with regard to this question that most of the disagreement among engineers exists. The problem may be stated thus: For an earthquake of specified intensity, how should the seismic coefficient vary along the height of the structure? Analysis of earthquake records and the response of structures to ground motion has thrown some light on this question, and the information thus obtained is reflected to some degree in building ordinances.* However, more records of earthquakes must be obtained and analyzed, and more information must be obtained about the dynamic properties of structures, before this question can be given a final answer.

Parts of a Structure. Each part of a structure is designed to withstand a lateral load $F_L = CW$ (as defined above). The coefficient C for a part of the structure is not necessarily the same as the coefficient C for the structure as a whole. For example, the values

of C for filler wall panels and for parapet walls are customarily larger than the values of C used for the structure as a whole. The lateral loads specified for parts of a structure are used only in designing those parts and their connections, and are not used in the design of the structure as a whole. The relatively large values of C used for parts of a structure apply in general to such parts as have suffered severe damage in past earthquakes and the failure of which is a special hazard to the public—for example, parapet walls falling to the ground. (For current practice as exemplified by building codes, see below, VI.) To design parts of a structure using larger values of C than are used for the structure as a whole is an apparent inconsistency when static loads are used. However, the actual deformations and stresses during an earthquake are dynamic, and the static lateral loads are intended to approximate the dynamic stress condition.

Foundations. The foundation of a structure is designed to resist the action of lateral loads, $F_L = CW$. The lateral load is applied to the structure as a whole and the foundation is designed to keep the maximum soil-bearing pressure within the allowable magnitude and to prevent uplift of a footing. The magnitude of the coefficient C and the magnitude of the allowable soil pressure vary with the type of foundation material. These variations reflect the ability of different soils to withstand dynamic loading, as well as their ability to withstand static loading.

At present it is not known how the behavior of a structure during an earthquake is modified by the properties of the soil upon which it rests. It is possible that soils of certain types may have an appreciable influence upon the response of a structure to ground motion. This is a question which must be answered by future investigations. It is also possible that the intensity of the ground motion during an earthquake may be modified by the local properties of the soil. This question will be answered as additional strong-motion earthquake records are obtained.

Dead and Live Load. When the formula $F_L = CW$ is applied, the entire dead-load mass of the structure plus some specified percentage of the live load is used in computing the magnitude of the lateral load. The percentage of live load used varies with the estimated actual live-load mass that can be expected, on the average, in structures of different types. There is general agreement that the total dead load should be used, but agreement is not unanimous regarding the percentage of live load to be used. It is rather common to use dead load plus one-half live load for ordinary occupancy and dead load plus full live load for storage occupancy.

GENERAL FEATURES OF DESIGN

The Structure as a Whole. The tributary lateral loads are apportioned to the elements of the main load-carrying system on the basis of an analysis which takes into consideration the relative rigidities of the elements and the rigidity and continuity of the tributary parts of the structure. For example, in a framed structure with concrete floors, the rigidity of the floors is taken into account in apportioning loads to the vertical frames.

* See references 1 and 2, at end of paper.

The use of floors and roofs as lateral-load-carrying structural members is probably a distinctive feature of California practice. In a steel-frame building with concrete floor slabs the columns are restrained by the floors, that is, so long as the floor remains monolithic the lateral motion of every column is determined at every floor level by the lateral displacements of the floors. The floors must distribute the lateral loads to the column bents in accordance with their relative rigidities; hence, if fracture of the floor is to be prevented, it must be designed as a lateral beam strong enough to withstand the stresses imposed upon it.

In general, the pattern of deformation is prescribed by the type of construction, and this determines the deformation of the parts. If it is desired to prevent fracture of a part, that part must be designed to withstand the stresses imposed upon it even if its action is not required to resist lateral loads. Sometimes it is not possible to design the part so as to prevent failure, and the possibility of fracture must then be accepted. For example, a steel-frame building which has interior partition walls will, upon lateral deformation, stress the walls, since they usually are much more rigid than the steel columns. Usually it is not feasible, however, to design the interior partitions to carry their share of the lateral loads. It is recognized that during a strong earthquake the partition walls will probably fracture; but the walls are designed in such a way that their fracture will not precipitate their collapse. For this reason, unreinforced hollow-tile partition walls are not used.

The design of the main load-carrying structural elements is based on a thorough stress analysis. In framed structures the frame is designed in accordance with the principles of rigid-frame analysis. As for nonsymmetrical structures in which the center of mass does not coincide with the center of rigidity, the rotational deformation of the structure is considered in the analysis. In general, the framing of a structure is made as simple and symmetrical as possible, in order to avoid complicated dynamic behavior during an earthquake.

The degree of refinement used in an analysis depends in part upon the type of structure. For example, a beam-and-column frame is analyzed by any of the standard methods of rigid-frame analysis, whereas a structure the framing of which is not straightforward is usually analyzed by more approximate methods. The time required to make a detailed analysis of the latter type of structure is very considerable, and experience has shown that for certain types of structures the increased accuracy obtained with a more exact analysis does not justify the time required.

Structures in which a rigid frame is not incorporated, such as certain types of bearing-wall buildings, are provided with positive lateral-load-carrying elements. Either the floors and roof are designed as lateral beams, or lateral trussing is provided to serve this function. The walls are designed as vertical beams. Structures other than buildings are provided with positive lateral-load-carrying systems which consist of rigid frames, trussing, guying, etc.

The procedures in this respect are not stereotyped. It is generally agreed that if the structure is not overstressed when the stresses are determined by the prin-

ciples of mechanics the method of framing is satisfactory. This provides ample opportunity for the designer to use his ingenuity. Care is taken, however, to avoid the use of brittle materials for main lateral-load-resisting members, that is, materials are not used whose brittle fracture might cause collapse. Care is also taken to avoid the use of combinations of members made of materials with widely differing moduli of elasticity.

An illustration of aseismic design and analysis is presented in *Analysis of small reinforced concrete buildings for earthquake forces*, published by the Portland Cement Association.

Parts of a Structure. All parts of a structure are designed to carry the specified lateral loads. The design is based on an analysis which considers the relative rigidities of the parts as well as the method of framing.

All points of connection tying together parts of a structure or connecting parts to the structural frame are analyzed and designed to withstand the stresses imposed by the lateral loads.

The walls of a building customarily are utilized as lateral-load-carrying elements of a structure. When they are so utilized, they are designed as vertical frames or beams taking into account the relative rigidities of the walls and any other vertical elements acting with them.

The floors of a building customarily are utilized as lateral-load-carrying elements of a structure. When they are so utilized, they are designed as horizontal beams taking into account the relative rigidities of the vertical structural elements which restrain their horizontal motion.

The foundation of a structure is designed so that there can be no shifting of the structure with respect to the foundations and no shifting of one part of the foundation with respect to other parts.

Tall, slender structures are designed to be stable against overturning under the specified static lateral load. This feature of the design is intended chiefly to insure against excessive soil pressures rather than as a precaution against actual overturning during an earthquake.

In designing parts of a structure, use is made of typical details. Considerable time is required to make analyses of structural details, and hence it has often been customary to utilize typical details which have been designed to carry known loads.

ALLOWABLE STRESSES USED IN A SEISMIC DESIGN

It is customary to design a structure so that the stress resulting from the combined actions of the lateral and vertical loads does not exceed $1\frac{1}{3}$ times the allowable stress for vertical loads only.

A structure is analyzed separately for wind load and for seismic load. The stresses must be within the allowable values for each type of loading.

PREPARATION OF PLANS

Damage suffered by structures in past earthquakes has shown that connections fastening the parts of a structure together are often the weakest elements. This weakness has sometimes been ascribable to inadequately detailed structural drawings. It is now customary for

the engineer to show on the plans carefully detailed drawings of structural connections and joints. When masonry walls are used as lateral-load-carrying elements, elevations of the walls are shown on the plans with the size, length, and location of the reinforcing bars clearly designated. In general, those features of the structural framing which are required to resist lateral forces are detailed on the working drawings.

SUPERVISION OF CONSTRUCTION

Damage suffered by structures in past earthquakes has shown that improper methods of construction were in some instances the causes of serious weaknesses. To overcome this, more rigid inspection procedures have been introduced to ensure that the structures are erected in accordance with the plans and specifications.

MAGNITUDES OF SEISMIC COEFFICIENT

To illustrate the magnitudes of the seismic coefficients currently being used in the regions of greatest seismic activity, excerpts from three building codes are presented. The values of the seismic coefficients are understood to be subject to revision as increased knowledge and experience are accumulated.

Building Code A. Any story of a building, $C = \frac{60}{N + 4.5}$, where N is the number of stories above the story under consideration, and the factor shall be applied to the summation of all required loads above the story under consideration.

Bearing partitions and walls and shaft-enclosure walls and exterior walls	$C = 0.20$
Cantilever walls, projections	$C = 1.00$
Roof structures and chimneys, smokestacks and towers, and tanks attached to or part of a building	$C = 0.20$
Isolated structures, stacks and towers, plus tank and contents	$C = 0.20$

Building Code B. The structure as a whole, and every portion not itemized in this table $C = 0.08$ on soil over 2,000 lbs.; $C = 0.16$ on soil under 2,000 lbs.

Bearing walls, nonbearing walls, partitions, curtain walls, enclosure walls, panel walls	$C = 0.20$
Cantilever parapet walls and other cantilever walls, except retaining walls	$C = 1.00$
Exterior and interior ornamentation and appendages	$C = 1.00$
Towers, tanks, towers and tanks plus contents, chimneys, smokestacks, and penthouses when connected to or a part of a building	$C = 0.20$

Building Code C. Considering the combination of vertical loads and horizontal forces, the following reductions in live loads are permissible.

Not less than 60 percent of the unit roof and floor loads may be used in design when the stresses due to vertical loads are combined with those due to horizontal forces.

Unit-storage live loads may be reduced 25 percent when stresses due to vertical loads and horizontal forces are combined.

Whenever connections are designed and constructed to resist moments, such connections and members connected thereto shall be designed for moments and shears resulting from vertical loads as well as horizontal forces.

In designing buildings or structures to resist overturning, the dead-load-resisting moment shall be not less than $1\frac{1}{2}$ times the overturning moment due to horizontal forces. For seismic forces, this factor shall apply only to the building or building unit as a whole.

The amount of earthquake force shall be considered to be applied in any direction and shall not be less than that given by the formula $F = CW_{D,L}$. When allowable soil-bearing pressure is less than two tons per square foot, $C = 0.10$; when more than two tons, $C = 0.08$; when more than four tons, $C = 0.06$.

In calculating maximum tensile fiber stresses due to wind forces, it is permissible to deduct the direct dead-load compression due to gravity from the tension due to bending. However, in considering seismic forces, the maximum tensile fiber stresses may be reduced by not more than 75 percent of the direct stress due to vertical dead loads.

Tank towers, tanks, chimneys, smokestacks, and marquees attached to a building shall be designed to resist a lateral force of 20 percent of the dead and live loads. Parapet walls, cantilever walls above roofs, exterior ornamentation and appendages shall be designed to resist a lateral force of 100 percent of their weight. The structural members of the building supporting the special structures named above need only be designed to resist a lateral force based upon the value of coefficient C applicable to the building in general.

For buildings supported on piling, the coefficient C shall be the same as that for a soil having a resistance not greater than two tons.

The vertical structural units of the building which resist the force of the earthquake shall be so arranged that in any horizontal plane the centroid of such resisting structural units is coincident with the center of gravity of the weight of the building, or else proper provision shall be made for the resulting torsional moment on the building.

The total horizontal shear at any level shall be distributed to the various resisting units at that level in proportion to their rigidities, giving due consideration to the distortion of the horizontal distributing elements.

Reinforced concrete or masonry walls with all permanent structural elements capable of providing resistance shall be assumed to act integrally with structural frames in resisting shears and moments due to horizontal forces, unless specifically designed and constructed to act independently from the said structural frames.

SELECTED BIBLIOGRAPHY

1. Los Angeles City Building Code, R. C. Colling, publisher, 124 West Fourth Street, Los Angeles, California.
2. Uniform Building Code, R. C. Colling, publisher, 124 West Fourth Street, Los Angeles, California.
3. Rules and Regulations Relating to the Safety of Design and Construction of Public School Buildings, State Division of Architecture, Sacramento, California.
4. Earthquake Resistant Buildings, S. I. Crookes, Leighton's Ltd., New Zealand, 1940.
5. Analysis of Small Reinforced Concrete Buildings for Earthquake Forces, Portland Cement Association, 33 West Grand Street, Chicago, Ill.
6. Continuity in Concrete Building Frames, Portland Cement Association, 33 West Grand Street, Chicago, Ill.
7. Earthquakes, N. H. Heck, Princeton University Press, 1936.

8. Earthquake Damage and Earthquake Insurance, J. R. Freeman, McGraw-Hill, 1932.
9. Engineering Seismology, K. Suyehiro, Proceedings of the American Society of Civil Engineers, May, 1932.
10. Earthquake Hazards and Earthquake Insurance, F. L. Hoffman, The Spectator Co., New York, 1928.
11. The California Earthquake of April 18, 1906, Carnegie Institution of Washington, Vol. 1, 1908.
12. The San Francisco Earthquake and Fire of April 18, 1906, U. S. Geological Survey, Government Printing Office, 1907.
13. Earthquake Investigations in California 1934-1935, U. S. Coast and Geodetic Survey Special Publication No. 201, Government Printing Office, Washington, D.C., 1936.
14. Earthquake History of the United States, U. S. Coast and Geodetic Survey, Serial No. 609, Government Printing Office, Washington, D.C., 1941.
15. Destructive and Near-Destructive Earthquakes in California and Nevada, 1769-1933, U. S. Coast and Geodetic Survey, Serial No. 191, Government Printing Office, Washington, D.C., 1934.
16. United States Earthquakes 1933, U. S. Coast and Geodetic Survey, Serial No. 579, Government Printing Office, Washington, D.C., 1935.
17. United States Earthquakes 1934, Serial No. 593, 1936.
18. United States Earthquakes 1935, Serial No. 600, 1937.
19. United States Earthquakes 1940, Serial No. 647, 1942.
20. Scientific and Technical Papers of K. Suyehiro, Tokyo, 1934.
21. The Japanese Earthquake of 1923, C. Davison, T. Murby and Co., London, 1931.
22. The Great Earthquake of 1923 in Japan, Bureau of Social Affairs, Japan, 1926.
23. The Outline of Reconstruction Work in Tokyo and Yokohama, Bureau of Reconstruction, Japan, 1929.

REFERENCES CITED IN BULLETIN 171
FINDING LISTS

REFERENCES

- Anderson, J. A., and Wood, H. O., 1925, Description and theory of the torsion seismometer: *Seismol. Soc. America Bull.*, vol. 15, pp. 1-72.
- Bear, T. L., and Vidos, A., 1952, San Emigdio foothills: *Am. Assoc. Petroleum Geologists et al., Guidebook, Joint Ann. Meeting AAPG, SEPM, SEG, Los Angeles, March 1952*, p. 279.
- Benioff, Hugo, 1932, A new vertical seismograph: *Seismol. Soc. America Bull.*, vol. 22, pp. 155-169.
- Benioff, Hugo, 1934, A new electro-magnetic seismograph: *Sixth Pacific Sci. Cong., Proc. 1933*, pp. 2443-2450.
- Benioff, Hugo, 1935, A linear strain seismograph: *Seismol. Soc. America Bull.*, vol. 25, pp. 283-309.
- Benioff, Hugo, 1949, Seismic evidence for the fault origin of oceanic deeps: *Geol. Soc. America Bull.*, vol. 60, p. 1837.
- Benioff, Hugo, 1951, Global strain accumulation and release as revealed by great earthquakes: *Geol. Soc. America Bull.*, vol. 62, pp. 331-338.
- Benioff, Hugo, 1951a, The mechanism of earthquake generation. Paper read at the meeting of the Seismol. Soc. America, Univ. Southern California, March 23-24, 1951.
- Benioff, Hugo, 1951b, Earthquakes and rock creep. Part 1: Creep characteristics of rocks and the origin of aftershocks: *Seismol. Soc. America Bull.*, vol. 41, pp. 31-62.
- Benioff, Hugo, 1954, Orogenesis and deep crustal structure—additional evidence from seismology: *Geol. Soc. America Bull.*, vol. 65, pp. 385-400.
- Benioff, H., Buwalda, J. P., Gutenberg, B., and Richter, C. F., 1952, The Arvin earthquake of July 21, 1952: *California Div. Mines Min. Inf. Service*, vol. 5, no. 9, pp. 4-7.
- Blanchard, F. B., and Byerly, Perry, 1935, A study of a well gauge as a seismograph: *Seismol. Soc. America Bull.*, vol. 25, pp. 313-321.
- Buwalda, J. P., 1920, Fault system at the southern end of the Sierra Nevada, California (abstract): *Geol. Soc. America Bull.*, vol. 31, p. 127.
- Buwalda, J. P., 1952, Recent California earthquakes—geology: *Am. Assoc. Petroleum Geologists Pacific Section, Program*, p. 3.
- Buwalda, J. P., and St. Amand, P., 1952, The recent Arvin-Tehachapi, southern California, earthquake: *Science*, vol. 116, pp. 645-650.
- Byerly, P., 1928, The nature of the first motion in the Chilean earthquake of November 11, 1922: *Am. Jour. Sci.*, vol. 16, pp. 232-236.
- California Division of Mines, 1952, Arvin-Tehachapi earthquake: *California Div. Mines Min. Inf. Service*, vol. 5, no. 9, pp. 1-4.
- Chakrabarty, S. K., and Richter, C. F., 1949, The Walker Pass earthquakes and structure of the southern Sierra Nevada: *Seismol. Soc. America Bull.*, vol. 39, pp. 93-107.
- Collins, J. J., and Foster, H. L., 1949, The Fukui earthquake, Hokuriku region, Japan; vol. 1, *Geology: Office of the Engineer, General Headquarters, Far East Command, Tokyo, February 1949*.
- Craig, A. W., 1952, Mountain View—Arvin District: *Am. Assoc. Petroleum Geologists et al., Guidebook, Joint Ann. Meeting AAPG, SEPM, SEG, Los Angeles, March 1952*, pp. 138-139.
- Crowell, J. C., 1952, Geology of the Lebec quadrangle, California: *California Div. Mines Special Rept. 24*, 23 pp., map.
- Crowell, J. C., 1952a, Probable large lateral displacement on San Gabriel fault, southern California: *Am. Assoc. Petroleum Geologists Bull.*, vol. 36, pp. 2026-2035.
- Day, A. L., 1938, An adventure in scientific collaboration: *Carnegie Inst. Washington Pub. 501*, pp. 3-35.
- Dehlinger, P., 1952, Shear-wave vibrational directions and related fault movements in southern California earthquakes: *Seismol. Soc. America Bull.*, vol. 42, pp. 155-173.
- Dibblee, T. W. Jr., and Chesterman, C. W., 1953, Geology of the Breckenridge Mountain quadrangle, California: *California Div. Mines Bull. 168*, 56 pp., map.
- Doell, E. C., 1943, Trico gas field: *California Div. Mines Bull. 118*, pp. 551-552.
- Durrell, C., 1940, Metamorphism in the southern Sierra Nevada northeast of Visalia, California: *Univ. California, Dept. Geol. Sci. Bull.*, vol. 25, 100 pp.
- Erickson, E. L., 1948, Wasco oil field, Kern County: *Soc. Exploration Geophysicists, Geophys. Case Histories*, vol. 1.
- Ferguson, G. C., 1943, Correlation of oil field formations on east side San Joaquin Valley: *California Div. Mines Bull. 118*, pp. 239-246.
- Galitzin, B., 1911, Ueber die Schwingungsrichtung eines Bodenteilchens in den transversalen Wellen der zweiten Vorphase . . . : *Acad. Petersburg Bull.*, pp. 1019-1028.
- Gutenberg, B., 1943, Earthquakes and structure in southern California: *Geol. Soc. America Bull.*, vol. 54, pp. 499-526.
- Gutenberg, B., 1944, Travel times of principal P and S phases over small distances in southern California: *Seismol. Soc. America Bull.*, vol. 34, pp. 13-32.
- Gutenberg, B., 1945a, Amplitudes of surface waves and magnitudes of shallow earthquakes: *Seismol. Soc. America Bull.*, vol. 35, pp. 3-12.
- Gutenberg, B., 1945b, Amplitudes of P, PP, and S and magnitudes of shallow earthquakes: *Seismol. Soc. America Bull.*, vol. 35, pp. 57-69.
- Gutenberg, B., 1945c, Magnitude determination for deep-focus earthquakes: *Seismol. Soc. America Bull.*, vol. 35, pp. 117-130.
- Gutenberg, B., 1951, Revised travel times in southern California: *Seismol. Soc. America Bull.*, vol. 41, pp. 143-163.
- Gutenberg, B., 1952, SV and SH: *Am. Geophys. Union Trans.*, vol. 33, pp. 573-584.
- Gutenberg, B., 1953, Travel times of longitudinal waves from surface foci: *Nat. Acad. Sci. Proc.*, vol. 39, pp. 849-853.
- Gutenberg, B., 1954, Low-velocity layers in the earth's mantle: *Geol. Soc. America Bull.*, vol. 65, pp. 337-348.
- Gutenberg, B., 1955, Channel waves in the earth's crust: *Geophysics*, vol. 20.
- Gutenberg, B., and Richter, C. F., 1934, On seismic waves (first paper): *Gerlands Beitr. z. Geophysik*, vol. 43, pp. 56-133.
- Gutenberg, B., and Richter, C. F., 1936, On seismic waves (third paper): *Gerlands Beitr. z. Geophysik*, vol. 47, pp. 73-131.
- Gutenberg, B., and Richter, C. F., 1939, On seismic waves (fourth paper): *Gerlands Beitr. z. Geophysik*, vol. 54, pp. 94-136.
- Gutenberg, B., and Richter, C. F., 1942, Earthquake magnitude, intensity, energy, and acceleration: *Seismol. Soc. America Bull.*, vol. 32, pp. 163-191.
- Gutenberg, B., and Richter, C. F., 1954, *Seismicity of the earth*, Princeton University Press, Princeton, N. J. (revised ed.).
- Hake, Benjamin F., 1928, Scarps of the southwestern Sierra Nevada, California: *Geol. Soc. America Bull.*, vol. 39, pp. 1017-1030.
- Hanna, G. D., 1930, Geology of the Sharktooth Hill area, Kern County, California: *California Acad. Sci. Proc. Dec. 15, 1930*.
- Hill, M. L., 1947, Classification of faults: *Am. Assoc. Petroleum Geologists Bull.*, vol. 31, pp. 1669-1673.
- Hill, M. L., and Dibblee, T. W. Jr., 1953, San Andreas, Garlock and Big Pine faults, California: *Geol. Soc. America Bull.*, vol. 64, pp. 443-458.
- Hodgson, J. H., and Milne, W. G., 1951, Direction of faulting in certain earthquakes of the North Pacific: *Seismol. Soc. America Bull.*, vol. 41, pp. 221-242.
- Hodgson, J. H., and Storey, R. S., 1953, Tables extending Byerly's fault-plane techniques to earthquakes of any focal depth: *Seismol. Soc. America Bull.*, vol. 43, pp. 49-61.
- Hoots, H. W., 1930, Geology and oil resources along the southern border of San Joaquin Valley: *U. S. Geol. Survey Bull. 812D*, pp. 243-332.
- Housner, G. W., Martel, R. R., and Alford, J. L., 1953, Spectrum analysis of strong-motion earthquakes: *Seismol. Soc. America Bull.*, vol. 43, no. 2.
- Hudson, D. E., Alford, J. L., and Housner, G. W., 1952, Response of a structure to an explosive-generated ground shock: *California Inst. Technology, ONR Rept.*, September 1952.
- Hughes, D. S., and Cross, J. H., 1951, Elastic wave velocities at high pressure and temperatures: *Geophysics*, vol. 16, pp. 577-593.
- Ingram, R. E., 1953, Vibration angle of S wave: *Seismol. Soc. America Bull.*, vol. 43, pp. 145-151.
- Jacob, C. E., 1941, On the flow of water in an elastic artesian aquifer: *Am. Geophys. Union, Trans.*, 1941, p. 577.
- Jeffreys, H., and Bullen, K. E., 1940, *Seismological tables*: *British Assoc. for the Advancement of Sci.*, 48 pp.
- Jenkins, Olaf P., 1938, *Geologic map of California*, scale 1:500,000, California Div. Mines.

- La Rocque, G. A. Jr., 1941, Fluctuations of water level in wells in the Los Angeles Basin, California, during five strong earthquakes, 1933-1940: *Am. Geophys. Union Trans.* 1941, pp. 374-386.
- Lavery, J. R., 1952, Tejon embayment: *Am. Assoc. Petroleum Geologists et al., Guidebook, Joint Ann. Meeting AAPG, SEG, Los Angeles, March 1952*, p. 277.
- Lawson, A. C., 1904, Geomorphology of the upper Kern basin: *Univ. California, Dept. Geol. Sci. Bull.*, vol. 3, pp. 291-386.
- Lawson, A. C., 1906, The geomorphic features of the middle Kern, California: *Univ. California, Dept. Geol. Sci. Bull.*, vol. 4, pp. 397-409 (1904-1906).
- Lawson, A. C., 1906a, The geomorphology of the Tehachapi Valley system: *Univ. California, Dept. Geol. Sci. Bull.*, vol. 4, pp. 431-463.
- Leggett, R. M., and Taylor, G. H., 1935, Earthquake instrumentally recorded in artesian wells: *Seismol. Soc. America Bull.*, vol. 25, pp. 169-175.
- Louderback, G. D., 1942, History of the University of California seismograph stations and related activities: *Seismol. Soc. America Bull.*, vol. 32, pp. 205-229.
- Marks, J. G., 1941, Stratigraphy of Tejon formation in its type area, Kern County, California (abstract): *Geol. Soc. America Bull.*, vol. 52, p. 1922.
- Marliave, E. C., et al., 1952, Report on physical effects of Arvin earthquake of July 21, 1952, 16 pp., 5 pls., 38 photos, California Div. Water Resources.
- Marliave, Chester, 1938, Geological reconnaissance report on Isabella dam sites situated on Kern River in Kern County, State of California, 23 pp., California Div. Water Resources.
- May, J. C., and Hewitt, R. L., 1948, The basement complex in well samples from the Sacramento and San Joaquin Valleys, California: *California Jour. Mines and Geology*, vol. 44, pp. 129-158.
- Miller, W. J., 1931, Geologic sections across the southern Sierra Nevada of California: *Univ. California, Dept. Geol. Sci. Bull.*, vol. 20, pp. 331-360.
- Miller, W. J., and Webb, R. W., 1940, Descriptive geology of the Kernville quadrangle, California: *California Jour. Mines and Geology*, vol. 36, pp. 343-378.
- Nelson, R. L., 1953, A study of the seismic waves SKS and SKKS: Ph.D. thesis, California Inst. Technology, 1952.
- Nugent, L. E. Jr., 1942, The genesis of subordinate conjugate faulting in the Kern River salient: *Jour. Geology*, vol. 50, pp. 900-913.
- Parker, G. G., and Stringfield, V. T., 1950, Effects of earthquakes, trains, tides, winds, and atmospheric pressure changes on water in the geologic formations of southern Florida: *Econ. Geology*, vol. 45, pp. 441-460.
- Prout, John W. Jr., 1940, Geology of the Big Blue group of mines, Kernville, California: *California Jour. Mines and Geology*, vol. 36, pp. 379-421.
- Reid, H. F., 1910, Report on the mechanics of the California earthquake of 1906: *Carnegie Inst. Washington Pub.* 87, 11.
- Richter, C. F., 1935, An instrumental earthquake magnitude scale: *Seismol. Soc. America Bull.*, vol. 25, pp. 1-32.
- Rieber, Frank, 1930, Results of elastic-wave surveys in California and elsewhere: *Am. Assoc. Petroleum Geologists Bull.*, vol. 14, pp. 1557-1571.
- Salvatori, Henry, 1948, Early reflection seismograph exploration in California: *Soc. Exploration Geophysicists, Geophys. Case Histories*, vol. 1, pp. 529-543.
- Schriever, William, 1952, Reflection seismograph prospecting—how it started: *Geophysics*, vol. 17, pp. 936-942.
- Seismological Society of America, 1922, Fault map of the State of California.
- Simpson, E. C., 1934, Geology and mineral deposits of the Elizabeth Lake quadrangle, California: *California Jour. Mines and Geology*, vol. 30, pp. 371-415, map.
- Slout, John, 1948, Geophysical history of the Rio Bravo field, California: *Soc. Exploration Geophysicists, Geophys. Case Histories*, vol. 1, pp. 569-585.
- Terzaghi, Karl, and Peck, R. B., 1948, Soil mechanics in engineering practice, pp. 57-61, New York, Wiley & Sons.
- Thomas, H. E., 1940, Fluctuations in ground-water levels: *Seismol. Soc. America Bull.*, vol. 30, pp. 93-97.
- Townley, Sidney D., and Allen, Maxwell W., 1939, Descriptive catalog of earthquakes of the Pacific Coast of the United States, 1769 to 1928: *Seismol. Soc. America Bull.*, vol. 29, pp. 1-297.
- Treasher, Raymond C., 1949a, Engineering geology of the Isabella project, California (abstract): *Geol. Soc. America Bull.*, vol. 60, p. 1946.
- Treasher, Raymond C., 1949, Kern Canyon fault, Kern County, California (abstract): *Geol. Soc. America Bull.*, vol. 60, p. 1958.
- Vaughan, F. E., 1943, Geophysical studies in California: *California Div. Mines Bull.* 118, pp. 67-70.
- Warne, A. H., 1953, Evidence of extensive lateral faulting in the Bakersfield area, Kern County, California (abstract): *Am. Assoc. Petroleum Geologists*, vol. 37, p. 183.
- Waterman, J. C., 1948, Geophysical history of the Ten Section oil field: *Soc. Exploration Geophysicists, Geophys. Case Histories*, vol. 1, pp. 551-553.
- Weatherly, B. B., 1948, The history and development of seismic prospecting: *Soc. Exploration Geophysicists, Geophys. Case Histories*, vol. 1, pp. 7-20.
- Weatherly, B. B., 1948a, Early seismic discoveries in Oklahoma: *Soc. Exploration Geophysicists, Geophys. Case Histories*, vol. 1, pp. 283-302.
- Webb, Robert W., 1936, Kern Canyon fault, southern Sierra Nevada: *Jour. Geology*, vol. 44, pp. 631-638, 1936.
- Webb, Robert W., 1946, Geomorphology of the Middle Kern River basin, southern Sierra Nevada, California: *Geol. Soc. America Bull.*, vol. 57, pp. 355-382.
- Wiese, J. H., 1950, Geology of the Neenach quadrangle: *California Div. Mines Bull.* 153, pp. 5-50, map.
- Wiese, J. H., and Fine, S. F., 1950, Structural features of western Antelope Valley, California: *Am. Assoc. Petroleum Geologists Bull.*, vol. 34, pp. 1647-1658.
- Wood, H. O., 1916, The earthquake problem in the western United States: *Seismol. Soc. America Bull.*, vol. 6, pp. 181-217.

FINDING LIST OF AUTHORS

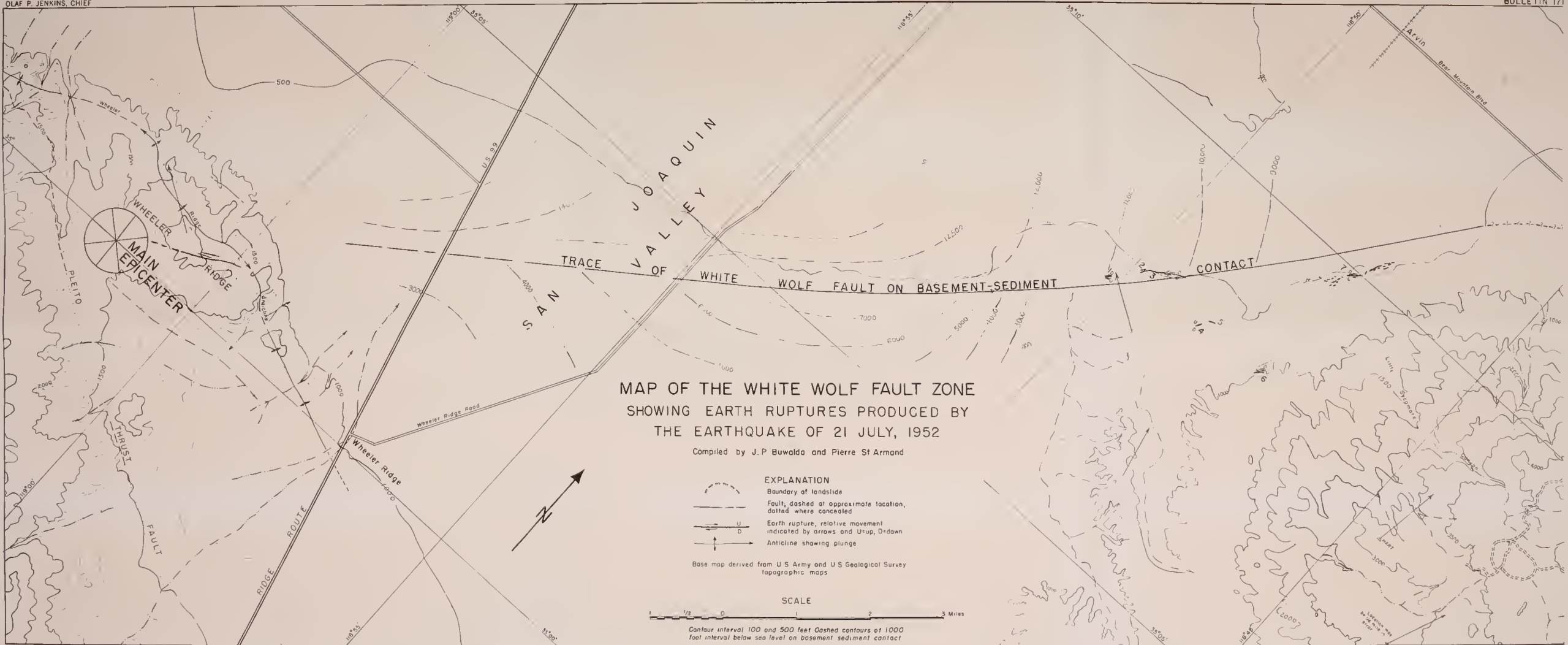
- Benioff, Hugo, *Mechanism and strain characteristics of the White Wolf fault as indicated by the aftershock sequence*: 199-202
- Benioff, Hugo, *Relation of the White Wolf fault to the regional tectonic pattern*: 203-204
- Benioff, Hugo, *Seismograph development in California*: 147-151
- Benioff, Hugo, and Gutenberg, B., *General introduction to seismology*: 131-135
- Briggs, Revoc C., and Troxell, Harold C., *Effect of Arvin-Tehachapi earthquake on spring and stream flow*: 81-97
- Buwalda, John P., and St. Amand, Pierre, *Geological effects of the Arvin-Tehachapi earthquake*: 41-56
- Cloud, William K., Neumann, Frank and, *Strong-motion records of the Kern County earthquakes*: 205-210
- Davis, G. H., Worts, G. F., Jr., and Wilson, H. D., Jr., *Water-level fluctuations in wells*: 99-106
- Dibblee, T. W., Jr., *Geology of the southeastern margin of the San Joaquin Valley, California*: 23-31
- Gutenberg, B., *Epicenter and origin time of the main shock on July 21 and travel times of major phases*: 157-163
- Gutenberg, B., *Magnitude determination for larger Kern County shocks, 1952; effects of station azimuth and calculation methods*: 171-175
- Gutenberg, B., *Seismograph stations in California*: 153-156
- Gutenberg, B., *The first motion in longitudinal and transverse waves of the main shock and the direction of slip*: 165-170
- Gutenberg, B., Benioff, H. and, *General introduction to seismology*: 131-135
- Hemborg, Harold B., *Damage to water-works systems, Arvin-Tehachapi earthquake*: 235-236
- Hill, Mason L., *Nature of movements on active faults in southern California*: 37-40
- Housner, G. W., *The design of structures to resist earthquakes*: 271-277
- Johnston, Robert L., *Earthquake damage to oil fields and to the Paloma cycling plant in the San Joaquin Valley*: 221-225
- Kuper, Donald H., Muessig, Siegfried, Smith, George I., and White, George N., *Arvin-Tehachapi earthquake damage along the Southern Pacific Railroad near Bealville, California*: 67-74

- Mitchell, Stewart, *Bridge earthquake report, Arvin-Tehachapi earthquake*: 229-234
- Moran, Donald F., Steinbrugge, Karl V. and, *Structural damage to buildings*: 259-270
- Moran, Donald F., Steinbrugge, Karl V. and, *Earthquake damage to California crops*: 257-258
- Moran, Donald F., Steinbrugge, Karl V. and, *Earthquake damage to elevated water tanks*: 249-255
- Muessig, Siegfried et al., *Arvin-Tehachapi earthquake damage along the Southern Pacific Railroad near Bealville, California*: 67-74
- Neumann, Frank, and Cloud, William K., *Strong-motion records of the Kern County earthquakes*: 205-210
- Oakeshott, Gordon B., *Preface*: 11-12
- Oakeshott, Gordon B., *The Kern County earthquakes in California's geologic history*: 15-22
- Peers, G. A., *Damage to electrical equipment caused by the Arvin-Tehachapi earthquake*: 237-240
- Perry, O. W., *Highway damage resulting from the Kern County earthquakes*: 227-229
- Radbruch, Dorothy H., Schloeker J. and, *Arvin-Tehachapi earthquake—structural damage as related to geology*: 213-220
- Richter, C. F., *Foreshocks and aftershocks*: 177-197
- Richter, C. F., *Seismic history in the San Joaquin Valley*: 143-146
- St. Amand, Pierre, Buwalda, John P. and, *Geological effects of the Arvin-Tehachapi earthquake*: 41-56
- Schloeker, J., and Radbruch, Dorothy H., *Arvin-Tehachapi earthquake—structural damage as related to geology*: 213-220
- Sklar, Maurice, *Application of seismic methods to petroleum exploration in the San Joaquin Valley*: 119-127
- Smith, George I. et al., *Arvin-Tehachapi earthquake damage along the Southern Pacific Railroad near Bealville, California*: 67-74
- Soske, Joshua L., *Seismic prospecting for petroleum and natural gas in the Great Valley of California*: 107-118
- Southern Pacific Company, *Earthquake damage to railroads in Tehachapi Pass*: 241-248
- Steinbrugge, Karl V., and Moran, Donald F., *Earthquake damage to California crops*: 257-258
- Steinbrugge, Karl V., and Moran, Donald F., *Earthquake damage to elevated water tanks*: 249-255
- Steinbrugge, Karl V., and Moran, Donald F., *Structural damage to buildings*: 259-270
- Troxell, Harold C., Briggs, Revoe C. and, *Effect of Arvin-Tehachapi earthquake on spring and stream flow*: 81-97
- VanderHoof, V. L., *The major earthquakes of California: a historical summary*: 137-141
- Warne, Archer H., *Ground fracture patterns in the southern San Joaquin Valley resulting from the Arvin-Tehachapi earthquake*: 57-66
- Webb, Robert W., *Kern Canyon lineament*: 35-36
- White, George N. et al., *Arvin-Tehachapi earthquake damage along the Southern Pacific Railroad near Bealville, California*: 67-74
- Whitten, C. A., *Measurements of earth movements in California*: 75-80
- Wilson, H. D., Jr. et al., *Water-level fluctuations in wells*: 99-106
- Worts, G. F., Jr. et al., *Water-level fluctuations in wells*: 99-106

FINDING LIST OF TITLES




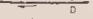
- Aftershock sequence: 199-202
- Aftershocks, foreshocks and: 177-197
- Application of seismic methods to petroleum exploration: 119-127
- Bridge earthquake report: 229-234
- Buildings, damage to: 259-270
- Crops, damage to: 257-258
- Damage, related to geology: 213-220
- Damage, to buildings: 259-270
- Damage, to crops: 257-258
- Damage, to electrical equipment: 237-240
- Damage, to highways: 227-229
- Damage, to oil fields: 221-225
- Damage, to Paloma cycling plant: 221-225
- Damage, to railroads: 67-74; 241-248
- Damage, to water tanks: 249-255
- Damage, to water-works systems: 235-236
- Design of structures to resist earthquakes: 271-277
- Earth movements, measurements of: 75-80
- Earthquake damage to crops: 257-258
- Earthquake damage to oil fields and Paloma cycling plant: 221-225
- Earthquake damage to railroads: 67-74; 241-248
- Earthquake damage to water tanks: 249-255
- Earthquakes, historical summary: 137-141
- Effect on spring and stream flow: 81-97
- Electrical equipment, damage to: 237-240
- Epicenter and origin time, main shock: 157-163
- Faults, lineament: 35-36
- Faults, movements on: 37-40
- First motion, main shock: 165-170
- Fluctuations, water-level in wells: 99-106
- Foreshocks and aftershocks: 177-197
- Fracture patterns, ground: 57-66
- Geologic history, Kern County earthquakes in: 15-22
- Geological effects: 41-56
- Geology, related to structural damage: 213-220
- Geology, San Joaquin Valley: 23-34
- Great Valley, seismic prospecting in: 107-118
- Ground-fracture patterns: 57-66
- Highway damage: 227-229
- Historical summary of earthquakes: 137-141
- Kern County earthquakes in geologic history: 15-22
- Kern County lineament: 35-36
- Magnitude determination: 171-175
- Measurements of earth movements: 75-80
- Mechanism and strain characteristics of White Wolf fault: 199-202
- Movements, measurements of: 75-80
- Movements on faults: 37-40
- Oil fields, damage to: 221-225
- Paloma cycling plant, damage to: 221-225
- Petroleum exploration, application of seismic methods to: 119-127
- Preface: 11-12
- Prospecting, seismic: 107-118
- Railroads, damage to: 67-74; 241-248
- Relation of White Wolf fault to regional tectonic pattern: 203-204
- San Joaquin Valley, application of seismic methods to petroleum exploration in: 119-127
- San Joaquin Valley, geology of: 23-34
- San Joaquin Valley, seismic history: 143-146
- Seismic history, San Joaquin Valley: 143-146
- Seismic methods, application to petroleum exploration: 119-127
- Seismic prospecting in Great Valley: 107-118
- Seismograph development in California: 147-151
- Seismograph stations in California: 153-156
- Seismology, introduction to: 131-135
- Slip, direction of: 165-170
- Spring and stream flow, effect on: 81-97
- Strain characteristics, White Wolf fault: 199-202
- Stream and spring flow, effect on: 81-97
- Strong-motion records: 205-210
- Structural damage as related to geology: 213-220
- Structural damage to buildings: 259-270
- Tanks, damage to: 249-255
- Tectonic pattern, relation of White Wolf fault to: 203-204
- Tehachapi Pass, damage to railroads in: 241-248
- Time, main shock: 157-163
- Travel time, major phases: 157-163
- Water tanks, damage to: 249-255
- Water-level fluctuations in wells: 99-106
- Water-works systems, damage to: 235-236
- Wells, fluctuation of water-level in: 99-106
- White Wolf fault, mechanism and strain characteristics: 199-202
- White Wolf fault, relation to regional tectonic pattern: 203-204

O



MAP OF THE WHITE WOLF FAULT ZONE
SHOWING EARTH RUPTURES PRODUCED BY
THE EARTHQUAKE OF 21 JULY, 1952

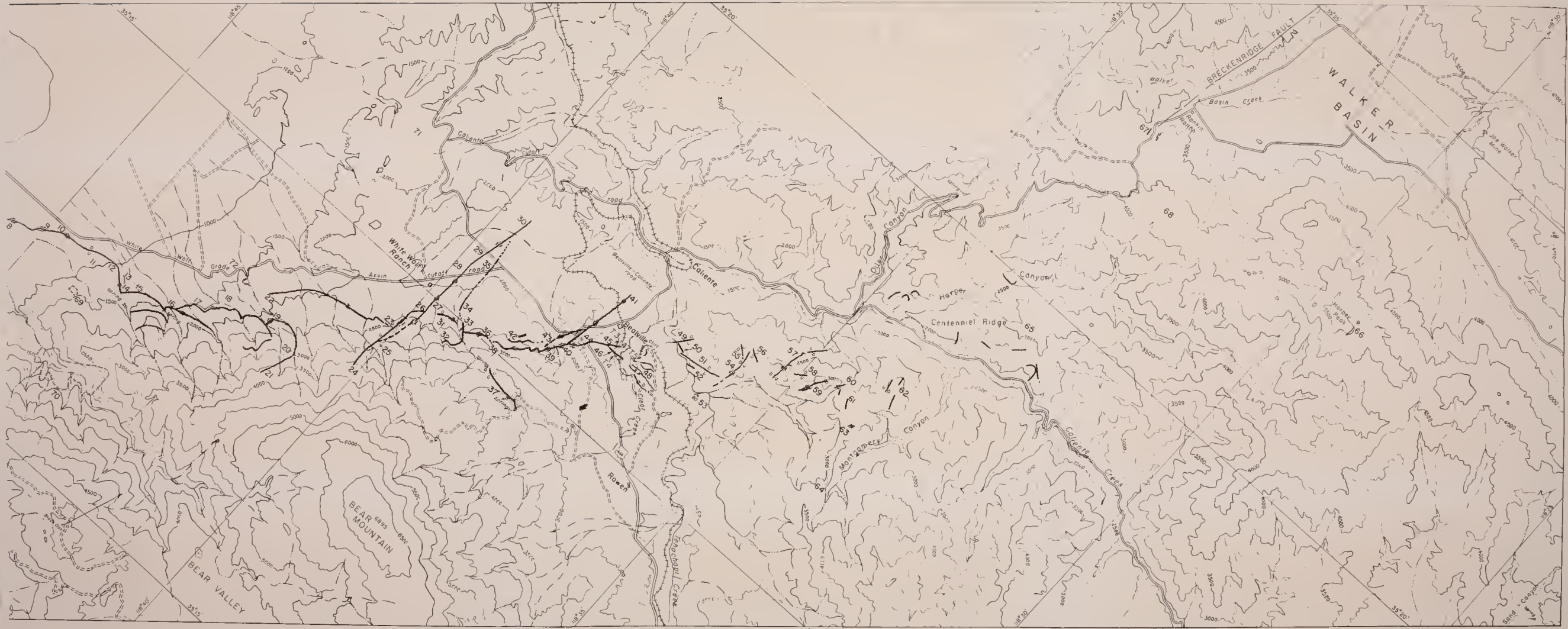
Compiled by J. P. Buwalda and Pierre St Armand

- EXPLANATION**
-  Boundary of landslide
 -  Fault, dashed at approximate location, dotted where concealed
 -  Earth rupture, relative movement indicated by arrows and Up, D, down
 -  Anticline showing plunge

Base map derived from U S Army and U S Geological Survey topographic maps



Contour interval 100 and 500 feet Dashed contours of 1000 foot interval below sea level on basement sediment contact



EXPLANATION

- Quaternary landslides
- Plio-Pleistocene Kern River and Tulare fms. continental sediments
- Mio-Pliocene Chonaco and Bena fms. continental sediments
- Miocene marine sediments (Santa Margarita sand, Moricopa shale, Round Mountain silt, Olcese ss., Temblor fm., Freeman sh., Pyramid Hills and Vedder sands)
- Oligocene(?) Walker fm., continental sands and gravels, including Bealville fanglomerate and Tecuya fm.
- Eocene Tejon fm.; moraine
- Jurassic(?) hornblende-biotite quartz diorite, inclusions of Paleozoic-Triassic(?) kernville & Pampa biotite schists, limestone
- Pre-Cambrian(?) Pelona schist

5 MILES
SCALE

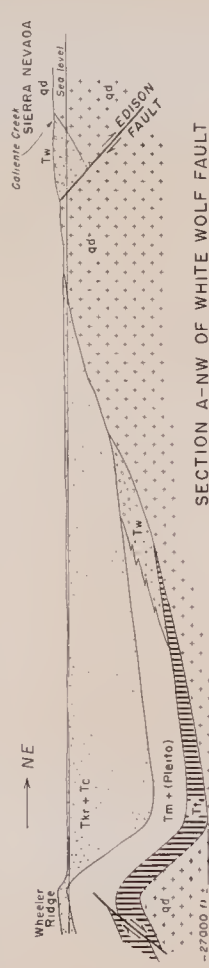
..... Fault-vertical or near vertical
 - - - - - Fault-normal (hachures indicate down thrust black)
 - - - - - Fault-reverse or thrust (▼ toward upthrust black)

Faults solid where accurately located, dashed where inferred, dotted where concealed. Arrows indicate strike-slip or lateral movement

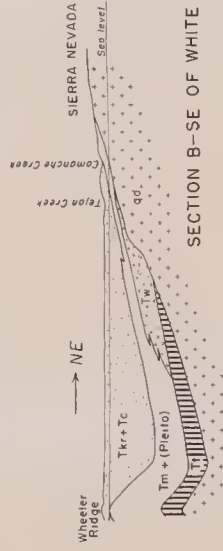
Geology generalized by T. W. Dibblee Jr.

GEOLOGIC MAP
 OF THE
 SOUTHERN SIERRA NEVADA,
 TEHACHAPI
 AND
 SAN JOAQUIN VALLEY

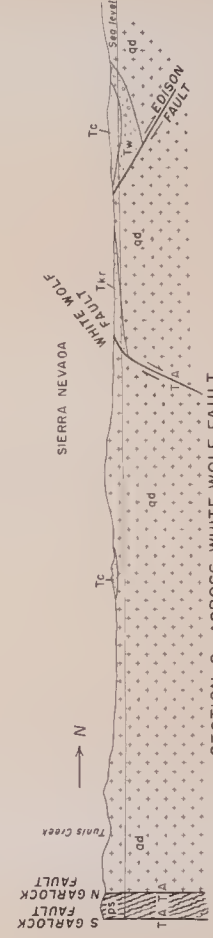
LIBRARY
 UNIVERSITY OF CALIFORNIA
 DAVIS



SECTION A-NW OF WHITE WOLF FAULT



SECTION B-SE OF WHITE WOLF FAULT



SECTION C--ACROSS WHITE WOLF FAULT

